NASA/TM–2014-218266

Maneuver Acoustic Flight Test of the Bell 430 Helicopter Data Report

Michael E. Watts and Eric Greenwood
Langley Research Center, Hampton, Virginia

Charles D. Smith
Analytical Mechanics Associates, Inc., Hampton, Virginia

Royce Snider
Bell Helicopter Textron, Inc., Fort Worth, Texas

David A. Conner
U.S. Army Research, Development and Engineering Command
Aviation and Missile Research, Development and Engineering Center
Aeroflightdyamics Directorate, Langley Research Center, Hampton, Virginia

May 2014

NASA STI Program . . . in Profile

Since its founding, NASA has been dedicated to the advancement of aeronautics and space science. The NASA scientific and technical information (STI) program plays a key part in helping NASA maintain this important role.

The NASA STI program operates under the auspices of the Agency Chief Information Officer. It collects, organizes, provides for archiving, and disseminates NASA's STI. The NASA STI program provides access to the NASA Aeronautics and Space Database and its public interface, the NASA Technical Report Server, thus providing one of the largest collections of aeronautical and space science STI in the world. Results are published in both non-NASA channels and by NASA in the NASA STI Report Series, which includes the following report types:

- TECHNICAL PUBLICATION. Reports of completed research or a major significant phase of research that present the results of NASA Programs and include extensive data or theoretical analysis. Includes compilations of significant scientific and technical data and information deemed to be of continuing reference value. NASA counterpart of peer-reviewed formal professional papers, but having less stringent limitations on manuscript length and extent of graphic presentations.

- TECHNICAL MEMORANDUM. Scientific and technical findings that are preliminary or of specialized interest, e.g., quick release reports, working papers, and bibliographies that contain minimal annotation. Does not contain extensive analysis.

- CONTRACTOR REPORT. Scientific and technical findings by NASA-sponsored contractors and grantees.

- CONFERENCE PUBLICATION. Collected papers from scientific and technical conferences, symposia, seminars, or other meetings sponsored or co-sponsored by NASA.

- SPECIAL PUBLICATION. Scientific, technical, or historical information from NASA programs, projects, and missions, often concerned with subjects having substantial public interest.

- TECHNICAL TRANSLATION. English-language translations of foreign scientific and technical material pertinent to NASA's mission.

Specialized services also include organizing and publishing research results, distributing specialized research announcements and feeds, providing information desk and personal search support, and enabling data exchange services.

For more information about the NASA STI program, see the following:

- Access the NASA STI program home page at *http://www.sti.nasa.gov*

- E-mail your question to help@sti.nasa.gov

- Fax your question to the NASA STI Information Desk at 443-757-5803

- Phone the NASA STI Information Desk at 443-757-5802

- Write to:
  STI Information Desk
  NASA Center for AeroSpace Information
  7115 Standard Drive
  Hanover, MD 21076-1320

NASA/TM–2014-218266

Maneuver Acoustic Flight Test of the Bell 430 Helicopter Data Report

.
Michael E. Watts and Eric Greenwood
Langley Research Center, Hampton, Virginia

Charles D. Smith
Analytical Mechanics Associates, Inc., Hampton, Virginia

Royce Snider
Bell Helicopter Textron, Inc., Fort Worth, Texas

David A. Conner
U.S. Army Research, Development and Engineering Command
Aviation and Missile Research, Development and Engineering Center
Aeroflightdyamics Directorate, Langley Research Center, Hampton, Virginia

National Aeronautics and
Space Administration

Langley Research Center
Hampton, Virginia 23681-2199

May 2014

Acknowledgments

The test could not have been accomplished without a team of dedicated individuals. The onsite test team consisted of three NASA (Michael Watts, Eric Greenwood and Benny Cheung), two U.S. Army (David Conner and Ben Sim), ten Bell (Royce Snider, John Brieger, Joel Baden, Rick Gorton, Jay Latham, Pete Trevino, Huy K Nguyen, Luther Simmons, Terry Dalehite and Britt Jolley), three AMA (Keith Scudder, Mike Walke and Charles Smith), two U.S. Air Force (Todd Dulle and Jeremy Brown), one University of Maryland (Rick Sickenberger), and two University of Mississippi personnel (Xiaoi Di and Rommel Stribling). Numerous NASA, Bell, University of Maryland, U.S. Army and Air Force personnel also provided support before, during and after the test. The authors would like to thank their tireless effort, professionalism and dedication in making this test happen.

Available from:

NASA Center for AeroSpace Information
7115 Standard Drive
Hanover, MD 21076-1320
443-757-5802

Abstract

A cooperative flight test by NASA, Bell Helicopter and the U.S. Army to characterize the steady state acoustics and measure the maneuver noise of a Bell Helicopter 430 aircraft was accomplished. The test occurred during June/July 2011 at Eglin Air Force Base, Florida. This test gathered a total of 410 test points over 10 test days and compiled an extensive database of dynamic maneuver measurements. Three microphone arrays with up to 31 microphones in each were used to acquire acoustic data. Aircraft data included Differential Global Positioning System, aircraft state and rotor state information. This paper provides an overview of the test and documents the data acquired.

Contents

List of Tables

List of Figures

Acronyms

AGL Above Ground Level

AGLMIP Above Ground Level at the Maneuver Initiation Point

ART Acoustic Re-propagation Technique

ASCII American Standard Code for Information Interchange

BVI Blade Vortex Interaction

BVISPL Blade Vortex Interaction Sound Pressure Level

CAFTA Computer Aided Flight Test Analysis

CTR Civil Tilt Rotor

CTRDAC Civil Tiltrotor Development Advisory Committee

dB decibels

DGPS Differential Global Positioning System

FFT Fast Fourier Transform

GPS Global Positioning System

INU Inertial Navigation Unit

KIAS Knots Indicated Airspeed

LaRC Langley Research Center

MIP Maneuver Initiation Point

NetCDF Network Common Data Form

OASPL Overall Sound Pressure Level

PDU Pilot Display Unit

RH Relative Humidity

RNM Rotorcraft Noise Model

SEL Sound Exposure Level

SPL Sound Pressure Level

TALP Terminal Area Landing Point

TPP Tip-Path-Plane

UTC Coordinated Universal Time

UTM Universal Transverse Mercator

V/ESTOL Vertical/Extremely Short Take Off and Landing

WAMS Wireless Acoustic Measurement System

1 Introduction

Airport congestion and flight delays continue to increase as passenger demand continues to grow. Vertical lift aircraft can have a significant impact on reducing airport congestion and flight delays. In 1995, the Civil Tiltrotor Development Advisory Committee (CTRDAC) Final Report to Congress [1] found that Civil Tilt Rotors (CTRs) could produce significant societal benefits, reducing airport congestion, creating jobs, and having a positive impact on the balance of trade. A study in 2001 [2] showed that 26% of commercial operations from the 64 major airports had a trip length of less than 500 miles and could be offloaded from conventional aircraft with Runway Independent Aircraft. This resulted in a reduction of the projected 2017 average delay time from 86.5 minutes to 18.3 minutes, thus showing Vertical/Extremely Short Take Off and Landing (V/ESTOL) aircraft can have a significant impact on commercial operations. An even more recent study [3] focused on the three major regions of Atlanta, Las Vegas and the Northeast Corridor and found that a fleet of 90 to 120 passenger CTRs would reduce the average delays in 2025 from 60 minutes to less than a minute.

Several barriers need to be overcome before the public will accept rotorcraft for commercial scheduled operations. One of the barriers is the acoustic impact of these operations on the community in and around the terminal area. Rotorcraft noise heard on the ground is governed by three physical processes, as shown in Figure 1.

Sound from the rotorcraft is generated via several physical mechanisms across a range of frequencies and directions depending on the flight condition. This noise is propagated through the atmosphere to the receiver. The propagated noise is affected by the atmospheric conditions and the terrain. Finally, the receiver perceives the signal in a way that is dependent on individual human characteristics.

Research flight testing, such as that reported in [4, 5], has been performed by NASA and other agencies to gather data used to validate acoustic codes such as the Rotorcraft Noise Model (RNM) [4] that are designed to predict the noise footprint on the ground. However, these codes currently use steady linear segments for their flight paths. Previous testing has shown an acoustic impact when the helicopter turns [6–8] or maneuvers aggressively [9] but these data sets were either limited in scope or were acquired in less than ideal weather conditions. A detailed set of maneuvering helicopter acoustic measurements is needed to better understand and incorporate these unsteady flight effects into ground footprint prediction codes.

2 Technical Approach

The NASA Langley Research Center (LaRC), Bell Helicopter Textron and the U.S. Army Aeroflightdynamics Directorate conducted a joint flight test to investigate the steady and maneuvering acoustics of a Bell 430 helicopter, shown in Figure 2. This Maneuver Acoustic Flight Test was performed at Eglin Air Force Base, Test Area B-75, in June/July 2011. The primary purpose for this flight test was to obtain a benchmark database of detailed acoustic source noise characteristics for a maneuvering helicopter. This database is intended to be used to predict ground noise footprints due to vehicle operations, to develop low noise operations, and for the development and validation of acoustic prediction methods. Figure 3 shows the B-75 test range with the control area, reference locations and weather balloon systems indicated. The blue lines indicate the two different flight paths used.

3 Test Aircraft

The acoustic test was conducted using a Bell Model 430, Serial Number 49001, equipped with retractable wheel landing gear (Figure 2), owned and operated by Bell Helicopter Textron per an experimental airworthiness certificate for research and development. The Bell Model 430 is an intermediate sized 10-place twin-turbine-engine helicopter incorporating a four-bladed main rotor and two-bladed tail rotor configuration. The engines are Allison 250-C40B turboshaft with Full Authority Digital Engine Control. The main transmission is rated at 870 shaft horsepower for single engine operation (30 second rating) and 1311 shaft horsepower for twin engine operation. Maximum gross weight is 9300 pounds (4218 kilograms). Bell Model 430 specifications are shown in Table 1 and key locations on the aircraft are shown in Table 2 in units of inches. The helicopter was externally configured as a standard Model 430 with the following exceptions: a flight test airspeed boom installed with angle of attack and angle of side slip vanes, NASA provided Tip-Path-Plane (TPP) data acquisition cameras mounted on the top of the left and right stub-wings, and small blade tracking tabs installed on the tips of the main rotor blades. The TPP measurement system was removed for the last day of testing.

4 Aircraft Measurements

The aircraft was fitted with a customized version of the Micro Airborne Data Acquisition System (μADAS, Figure 4), including a Pilot Display Unit (PDU). The data acquisition unit of the NASA TPP system was mounted to the Bell Helicopter instrumentation pallet inside the cabin. A calibration that measured the relationship between the main rotor blades geometric pitch angles and the control system positions (aircraft rigging) was performed and documented prior to testing. Several instrumentation cards were damaged during an under-voltage event that occurred during test preparation after the aircraft arrived at Eglin Air Force Base. As a result of this and other issues, not all instruments were available during the entire test. A decision was made to perform each type of testing with the minimum instrumentation required for that test phase. This decision allowed the flight test to continue and instrumentation was added as it was recovered. This reduced the programmatic risk and allowed all phases of testing to be performed. Table 3 lists the availability of the aircraft instrumentation for each flight. This table also lists the accuracy of the instrumentation.

4.1 Aircraft Position

Accurate vehicle position data are essential to not only the generation of high-quality source noise semi-spheres but also for accurate maneuver acoustics modeling. A Bell Helicopter DGPS system was used for flight path guidance as well as an accurate measure of aircraft position. This system consisted of both aircraft and ground based components. Aircraft mounted components of the DGPS included a Global Positioning System (GPS) antenna, recorder, wireless modem and modem antenna. Additional aircraft components included instrumentation to process the DGPS base station correction signal, flight guidance processing and a pilot course deviation indicator (Figure 5). The ground station consisted of a precision GPS antenna located at a pre-surveyed location, a recorder and a wireless modem transmitter to broadcast the GPS correction signal to the aircraft (Figure 6). The desired guidance course was selected via the PDU and precision flight guidance cues were provided back to the pilot in real-time during flight test via the course deviation indicator.

4.2 Control Positions

The aircraft was instrumented with collective and cyclic position measurement instrumentation. Collective and cyclic were recorded as a percent of full deflection of the controls. A static rigging calibration was performed to relate these percentage measurements to the movement of the swashplate and thus to static blade pitch angle.

4.3 Aircraft State

An on-board aircraft attitude and rate gyro was used to provide pitch, roll and yaw attitudes and rates as a function of time. Analysis of the aircraft's system attitude data indicated an intermittent and unpredictable "drift" in attitude signal. In an effort to obtain reliable aircraft attitude data, an Inertial Navigation Unit (INU) unit provided by the Army was installed during the maneuver portion of the testing. This unit recorded reliable pitch, roll and yaw attitudes and rates as a function of time. It should be noted that both the aircraft's and Army's INU systems provided consistent rate data, only the aircraft's attitude data exhibited a drift. In spite of this intermittent problem, the aircraft's system attitude data is useful in some cases, for example, when the INU data is unavailable to indicate abrupt changes in pitch, roll, and yaw attitude caused by pilot control inputs.

An instrumentation boom was installed for the test that measured angle-of-attack, sideslip as well as static and dynamic pressure. Aircraft true airspeed was derived from the measured pressures and the outside air temperature from the NASA weather balloon system described below. Torque and fuel remaining were noted on the flight card by the flight test engineer during each data acquisition run.

4.4 Tip Path Plane Orientation Measurement

The measurement of the main rotor TPP angle-of-attack is desirable to accurately estimate the mean inflow through the rotor system and serves as an experimental check of predictions for steady and quasi-steady flight. A TPP measurement system that accurately measures the location of the rotor tips at four locations around the aircraft was used during portions of this flight test. This system was developed for NASA by University of Maryland and uses lasers and cameras mounted on the aircraft as shown in Figure 7 [10]. These lasers are reflected off of retroreflective tape mounted on the rotor tips (Figure 8). The reflections are captured by the cameras at four azimuth locations. The system was installed and operated on the aircraft by a Bell/University of Maryland team. A pulse was recorded by the data acquisition system when the red (reference) blade passed over the tail of the aircraft (at the azimuth angle $\psi = 0°$). This pulse is used by the TPP measurement system for azimuthal alignment as well for deriving the rotor RPM. TPP data was recorded during two flights during the Maneuver Phase of the test. However, a maximum deviation of $0.2°$ was seen in the movement of the TPP with respect to the fuselage so the data is not presented in this report. This minimal movement is due to the stiff design of this particular rotor system. The data is not contained as part of the electronic data package but is available upon request.

5 Bell Aircraft Data Files

Following each test flight, the aircraft data were downloaded and processed using a mobile Bell Helicopter Computer Aided Flight Test Analysis (CAFTA) system. This enabled the test team to assess and validate aircraft state parameter and flight profiles performed during the same day of testing, prior to test planning for the next day. Examples of these "Quick-look" aircraft data plots used for same-day data evaluation are shown in Figures 9 to 13 for a dynamic maneuver from 6° descending flight.

Final processed and calibrated aircraft data results were provided in the following format for each flight condition performed:

1. Two CAFTA output files with aircraft position and state parameter data sampled at 125 Hz,

2. One post-processed "Track-file" with all aircraft position and state parameter data in the CAFTA output files, down-sampled to the DGPS sample rate of 5 Hz and synchronized with Coordinated Universal Time (UTC)-time, and

3. One additional CAFTA output file with rotor azimuth reference sampled at 2000 Hz per rotor revolution.

6 Microphone Instrumentation

The acoustic data were acquired using NASA's Mobile Acoustic Facility. This facility consists of two trailers, one is used to control the flight test and the other to maintain the 36 Wireless Acoustic Measurement Systems (WAMSs) used to record the acoustic signals. Each WAMS consists of a ground board, microphone, GPS receiver and antenna. UTC time obtained from the GPS was used to synchronize all microphone, aircraft and weather information together. The WAMS setup used for this test consisted of a 1/2 inch Falcon (B&K 4189) microphone inverted with the diaphragm 1/4 inch over a 15 inch round ground board, shown in Figure 14. Notice that the microphones are offset from the center of the ground board to minimize the edge effects. The acoustic signals were acquired at 25,000 samples per second at 16 bit resolution. Up to 31 of these systems were deployed in three different configurations depending on the flight conditions being tested that day.

A recent upgrade to the WAMS system had the unforeseen consequence of introducing an intermittent delay of precisely one second to the recorded acoustic data. A procedure was developed to identify these delays and correctly synchronize the measured acoustic data. Using a previously developed time-domain de-Dopplerization technique [11], the acoustic pressure time histories for all recorded signals during each run were transformed from time of observation to time of emission. A window of the transformed data was then selected for each run corresponding to a time range when the helicopter was located 3000 to 6000 feet before arriving at the microphone array. Examining the data in this way ensures that the measured signal primarily reflects the thickness noise radiated by the main and tail rotors. A cross correlation of these windows was computed for all possible channel pair combinations in the array. The cross correlations were then used to uniquely identify the channels which were offset by the intermittent one second. This analysis is possible because the main rotor and tail rotor blade passing frequencies are non-integer multiples of each other, such that the period between phase alignment of the main and tail rotor thickness signals is much greater than one second. The corrections calculated by this method were applied to the raw microphone time histories. The Sound Pressure Level (SPL) for the band pass filtered (20-100 Hz) corrected time histories were then calculated and plotted. These corrected time history plots were examined for correctness and adjustments were made to the data where applicable. Note that all data distributed has these offset corrections applied with the exception of the terminal area approaches.

6.1 Source Noise Microphone Layout

Straight line level flight and steady descents were measured using a linear array consisting of 21 microphone locations in a 3,429 foot line perpendicular to the flight path. The spacing was set such that there was a microphone approximately every 11.5° from directly below the aircraft to near in-plane of the rotor for a flyover height of 150 feet above the center microphone. Three locations (directly below and the +/- 200 foot microphone locations) had three microphone configurations; inverted over a ground board, the diaphragm flush mounted in a ground board and a microphone on a four foot tripod. These three locations will provide data that will be used to compare the effects of different microphone mounting configurations. The result was 27 microphones being deployed for this configuration. The source noise array is shown in Figures 15 and 16. Table 4 lists the microphone locations. This table contains the latitude, longitude and geoid height in meters from the GPS survey. Coordinate systems were established with the center at the microphone 11 position which is also the nominal aircraft crossing location (This microphone 11 position is referred to as the reference location for all coordinate systems in this report). The first coordinate system is a Universal Transverse Mercator (UTM) type coordinate system where UTM X is True East and UTM Y is True North. These UTM coordinates were then rotated by 123.6 Degrees in the counter clockwise direction to generate the local coordinate system where positive X is along the primary flight path, positive Y to the left of the flight path and Z is positive up. This array was also used for the steady turns portion of the test. Additionally, Table 5 lists the GPS locations and cartesian coordinates of the non-microphone key locations.

6.2 Maneuvering Noise Microphone Layout

Based on preliminary predictions of where the high levels of noise during maneuvers would be expected when the aircraft was directly over the Maneuver Initiation Point (MIP) at 150 foot altitude, a 31 microphone array was designed to capture Blade Vortex Interaction (BVI) noise and near in-plane noise directivity. Figures 17 and 18 show the microphone array and Table 6 lists the microphone locations, referenced to microphone 34 (which is the same location as microphone 11 in the source noise measurement array). The flight path is shown in blue. The coordinate system for this table is the same as that for the source noise measurement layout. Figure 19 shows the projection of the microphones on a Lambert projection of the semi-sphere to illustrate the directivity pattern to be captured when the aircraft is directly over the MIP. The Lambert projection allows a minimally distorted picture of the external noise radiation pattern. The process of projecting the hemispherical surface as a 2D image using the Lambert projection is shown in Figure 20. The center of the plot, marked with an elevation angle of -90° represents the underside of the semi-sphere. The edges with a 0° elevation represent noise radiated in the horizon plane. Azimuth angles start at 0° behind the helicopter, and progress counter-clockwise with the direction of the Bell 430 rotor rotation such that the right hand side of the plot represents the advancing side of the semi-sphere.

6.3 Terminal Area Noise Microphone Layout

A microphone array was designed to capture noise with the aircraft flying various approach flight profiles into a terminal area. This array consisted of microphones placed primarily in a rectangular grid which spanned 3,000 feet (laterally) by 6,400 feet (in the flight direction) and resulted in an array of 27 microphones. Figures 21 and 22 show the resultant array and Table 7 lists the microphone locations relative to microphone 98 location (which is the same location as microphones 11 and 34 in the previous layouts). The coordinate system for this table is the same as for the source and maneuver arrays. This coordinate system resulted in the primary flight direction being in the negative Y direction.

7 Weather Instrumentation

An extensive set of weather measurements were made throughout the test. A tethered weather balloon system was located near the control area 4750 feet from the reference microphone. This ballon was continuously traversed (1) from 0 to 300 feet Above Ground Level (AGL) during the source, steady turn, and maneuvering flight test phases and (2) from 0 to 1,000 feet AGL during the terminal area approach testing. Another tethered balloon was placed 4,750 feet from the reference microphone and was stationary at a height of 300 feet. This stationary balloon had up to five weather sondes at constant altitudes during much of the test. Up to four weather sondes were also placed around the test area. Two of these sondes were mounted on 8 foot high poles, one was mounted on a 25 foot high pole and one was mounted on a 30 foot high pole. All weather sondes recorded wind speed and direction, temperature, pressure and relative humidity. Weather sondes determine the altitude based on static pressure. However, the static pressure can change as a function of time due to things such as clouds transitioning over the sensor. To take into account the changes in ambient pressure and accurately record the altitude of the profiling balloon, the pressure altitude value was reset when the balloon was on the ground for each profile. However, the static balloon only set the pressure altitude to reference the ground at the beginning of the day. Thus to get an accurate altitude reading it must be compared to the ground static pressure at any given time. The locations of the weather instrumentation are indicated on Figure 23. Not all weather instrumentation was available during all testing. Some weather sondes acquired data even during non test days to acquire historical weather information. Table 8 shows the availability of weather instrumentation during the test. All available weather data is included in the electronic data package.

8 Flight Conditions Flown

8.1 Level Flight Source Noise Mapping

Steady flight condition data were acquired for level flight and constant descent rate for various flight speeds. Data from these "speed sweeps" are used to generate semi-spheres for the steady flight segments and are used by codes such as RNM for prediction of noise on the ground ("ground footprints"). Most of the level flight conditions were flown with the gear retracted and all descents were flown with the gear extended for safety of flight reasons. Three days of source noise mapping flights were flown. Table 9 lists the nominal level flight conditions, the condition reference code and the number of test points available for that condition in the format "L1 - 11", where L1 is the condition code and 11 is the number of verified test points acquired and contained in the distributed data set. All test condition tables provided use this format. Note that there can be several test points for the same flight condition as each condition was repeated several times.

Often in flight testing, a "housekeeping" flight condition is flown at certain intervals during the test to give an indication of the repeatability of the data. For this portion of the testing, a level flight housekeeping condition was flown at a flight speed of 80 knots. OASPL values for the reference microphone as a function of distance along the flight track are shown in Figure 24 for seven housekeeping runs flown during the three days of source noise mapping. These repeated runs show a 3 dB scatter when the aircraft was at a location 850 feet before arriving at the center microphone. This level of scatter is considered normal for this type of testing.

Sound semi-spheres were created using the Acoustic Re-propagation Technique (ART) methodology contained within RNM. ART captures the noise spectra from all microphones at specific time intervals (typically every 0.5 seconds) along the flight profile and relates these spectra to the aircraft position, thus providing noise levels as a function of noise emission angle. These measured noise levels are then de-propagated to a semi-sphere of a specified semi-sphere radius, centered at the aircraft GPS receiver. The semi-sphere radius used here is 100 feet. Atmospheric and speed effects are accounted for during this de-propagation process. For more details, the de-propagation process is described more fully in [4]. Figures 25, 26 and 27 present Lambert projections of the OASPL semi-spheres as a function of true airspeed during level flight. The circles in these figures represent data points acquired. The acoustic pressures were averaged over more than one data run as indicated by the brackets where appropriate to represent one true airspeed for the semi-spheres. The general trend of increasing noise levels as a function of true airspeed is as expected. However, at the low airspeeds there is a slight decrease in OASPL on the retreating side with increasing airspeed until approximately 105 knots.

8.2 Steady Descent Source Noise Mapping

Steady descents were performed to investigate the BVI noise as a function of airspeed and descent angle. Table 10 lists the constant descent flight conditions flown, the condition reference code, and the number of points for that condition. BVISPL is the integrated sound pressure level over the 5th thru 50th blade passage frequencies (116 to 1,160 Hz) which are the frequencies of interest for investigating BVI. The level flight semi-spheres for the BVISPL are shown in Figures 28, 29 and 30 to compare the level flight with the descent conditions. Figure 31 shows the actual descent angle as a function of true airspeed for each point along with that data run's number. The scatter seen in this plot is attributed to the pilot flying indicated airspeed by using the aircraft internal instrumentation and a visual system for flight path guidance. As indicated in Table 3, the indicated airspeed instrument for the source portion of the testing was not functional. Because of this, the true airspeed was derived from combining the GPS derived groundspeed with the wind direction and wind velocity as measured by the NASA weather balloon. Figures 32 thru 80 show the OASPL and the BVISPL hemispheres for each of the descent points shown in Figure 31 in run number order. To better visualize the BVISPL trends, Figure 81 was generated and shows the descent angle as a function of true airspeed with the points color coded with the maximum BVISPL level seen in each of the BVISPL hemispheres presented in Figures 32 thru 80. This figure shows the expected trend of increasing BVI noise with increase in descent rate and true airspeed.

No groupings around the nominal points are evident so to facilitate examining trends in airspeed and descent angle, an empirical model of the helicopter's external noise radiation characteristics was generated. A four-dimensional modified Shepard's method (described in Appendix A) was used to create a model that represents the external noise radiation of the helicopter as a function of flight path angle, true airspeed, and radiation direction (azimuth and elevation) from the set of acoustic hemispheres created by the source noise characterization of the Bell 430 helicopter. The result is a model of the helicopter's external noise radiation which varies smoothly with variation in flight condition and directivity angle. By constructing a single model incorporating variations in both flight condition and directivity, more accurate noise estimates may be produced at conditions and directions which have not been directly measured. For instance, during source noise characterization of steep descent conditions over a linear array of microphones it is particularly difficult to acquire data near the plane of the horizon. The modified Shepard's method interpolation combines both noise data measured near the plane of the horizon during shallower descents with out-of-plane noise data from steeper descent conditions to provide an estimate of the in-plane noise radiation during steeper descent conditions. This model was used to generate Figure 82 and shows the semi-spheres for a flight path angle sweep at 80 knots true airspeed. Figure 83 was also generated using this model and shows the semi-spheres for a speed sweep at a flight path angle of 6 degrees.

Tables 11 thru 13 contain the test cards as recorded in the control trailer during the Level Flight and Steady Source Noise portion of the test for the data included in the electronic data distribution package.

8.2.1 Steady Turn Source Noise Mapping

Steady level flight constant bank angle turns were flown over the linear source ground array. The helicopter approached parallel to the array, but offset laterally from the array line by the distance of the radius of the turn being flown. The turn was then initiated such that it was stabilized by the time a heading 45° from the initial flight direction was obtained with the goal of crossing over the reference microphone. The pilot then maintained the designated angle of bank (either 15° or 30°) while simultaneously maintaining a constant airspeed of 60 or 80 KIAS at 200 foot AGL throughout the steady portion of the turn. The steady turn was held for at least 90 degrees of heading change with the aircraft exiting the turn parallel to the microphone array. This procedure for a right hand turn is shown in sketch form in Figure 84. Both left and right hand turns were flown with one test day devoted to acquiring this steady turn data. The left and right turn flight paths are shown in Figure 85. Table 14 lists the conditions flown, the condition reference code and the number of points collected for that condition. Steady turns were flown with gear down for safety of flight reasons. The projection of the microphone position at one-half second intervals is shown in a semi-sphere for a 30° , 80 knot right steady turn is shown in Figure 86 and shows good coverage for generating semi-spheres. It should be noted that 0° elevation on these semi-spheres is in the horizontal plane and not rotated with the helicopter. This example was a typical projection for the steady turn testing. Figure 87 shows the OASPL and Figure 88 the BVISPL semi-spheres for the steady turns performed during this test.

Table 15 contains the test cards as recorded in the control trailer during the Steady Turns portion of the test.

8.3 Maneuvers

A primary focus of this test was the acoustic characterization of maneuvers and five days of testing were devoted to these flight conditions. The dynamic maneuvers were flown with the gear down for safety of flight and using slow, medium, and fast pilot control (stick) deflection rates. Nominally the fast rate was about four times that of the slow rate. The medium rate was defined as one between the slow and fast rates. The helicopter initially established a steady flight condition along a straight line trajectory which was perpendicular to the primary linear array and passed over the MIP which was 1,500 feet before the reference microphone (X = -1,500 feet). This stabilized pre-maneuver flight condition was nominally established 500 feet before reaching the MIP (X = -2,000 feet). The pilot initiated the maneuver from this steady state flight condition just before reaching the MIP. The maneuver test plan focused on isolated pilot control inputs such as cyclic pitch, cyclic roll, and collective pull/push. More complex coordinated maneuvers were also acquired. Maneuver conditions were prioritized such that "Priority One" cases acquired at least four points and "Priority Two" cases acquired at least two points for each condition. An 80 knot level flight (L1) and 80 knot, fast cyclic pitch up at 6° descent (D12, see Section 8.3.2 below for a more detailed description) were chosen as housekeeping cases and were flown at the beginning and end of each flight. Figure 89 shows the OASPL, elevation over the reference microphone and longitudinal cyclic control inputs versus horizontal distance from reference microphone for seven cyclic pitch up housekeeping points to demonstrate the consistency of the control inputs by the pilot and that the spread of acoustic data was within 4 dB OASPL.

Data for each of the maneuver points acquired are presented in the following sections. The 80 knot level flight housekeeping conditions are shown in Figures 90 to 99. The constant speed descent cases flown over the maneuver microphone measurement array are shown in Figures 100 to 118. The acoustic pressure time histories were corrected for ground board installation effects and then de-Dopplerized in the time domain. Six contour plots for microphones 40 thru 60 are shown on the left of the figures. The flight path is indicated with a blue line with the aircraft moving from left to right. Each contour subplot shows a BVISPL noise footprint generated at 6 times of emission where the aircraft location is denoted by a symbol on the flight path. The average of three 4,096 point Fast Fourier Transforms (FFTs) (using a Hanning window) centered around each of these locations were averaged. Also shown on the right of each figure are the flight track projected to the XY coordinate plane, the altitude, the cyclic and collective control positions, the roll and pitch attitudes, and the indicated and true airspeeds. For longitudinal cyclic 0% is with the stick aft. For lateral cyclic 0% is to the stick to the left. For collective, 0% is with the collective stick down. Roll right and pitch up are the positive rotational directions. Plotting scales were kept consistent for all the figures with the exception of the altitude subfigure with the text *Scale Shifted* appearing when it is not the standard scale. All figures in the Maneuvers section are of the same format.

Tables 16 thru 20 contain the test cards as recorded in the control trailer during the maneuver noise portion of the test for the data included in the electronic data distribution package.

8.3.1 Collective Pull-Up or Push-Over

A dynamic maneuver involving the collective control was performed to measure the effect of a transient maneuver which used just a collective control input. This maneuver starting from a level flight condition where the rotor wake is expected to be near the rotor plane. The pilot initiated a constant rate ramp of the collective pull or push at the start of this maneuver, allowing flight path angle and airspeed to change freely. Only slow and fast maneuvers were executed based on emerging noise data indicating that the medium speed collective control inputs would yield little or no useful information. The maneuver was performed with cyclic control inputs primarily held fixed. The maneuver was initiated from level flight at 150 feet Above Ground Level at the Maneuver Initiation Point (AGLMIP) for positive collective inputs and 250 feet AGLMIP for negative collective inputs.

Table 21 lists the conditions flown, the condition reference code and the number of points collected for that condition. The points acquired are shown in Figures 119 to 143

8.3.2 Cyclic Pitch-Up

Cyclic pitch-up maneuvers were performed to measure the effect of a transient longitudinal cyclic control input, starting from a level flight condition or a descending flight condition (6° and 9° descent angles were used) where the rotor wake is expected to be near the rotor disk plane. At initiation of the maneuver, the pilot entered a constant rate ramp input of aft longitudinal cyclic, allowing flight path angle and airspeed to change freely. Slow, medium, and fast cyclic control input maneuvers were executed. All other controls were specified to be held fixed throughout the cyclic pitch-up maneuver. These maneuvers were initiated at 150 feet AGLMIP for cyclic inputs initiated from level flight and 250 feet AGLMIP for maneuvers initiated from a descent.

Table 22 lists the conditions flown, the condition reference code and the number of points collected for that condition. The points acquired are shown in Figures 144 to 197

8.3.3 Cyclic Roll

Maneuvers were performed to measure the effect of just using a transient lateral cyclic control input to cause an aircraft roll. These cyclic rolls were started from a level flight condition as well as a 6° descending flight condition where the rotor wake is expected to be near the rotor. At the initiation of the maneuver, the pilot entered a constant rate ramp input of lateral cyclic, allowing bank angle, flight path angle, and airspeed to change freely. Slow, medium and fast control rate maneuvers were executed by applying a lateral cyclic ramp input at a rate defined as from trimmed position towards the left or right. All other controls were specified to be held fixed throughout the maneuver. Cyclic roll maneuvers were performed from stabilized conditions of level flight and 6° descent for 60, 80 and 100 knot indicated airspeeds. Level flight maneuvers were initiated at 150 feet AGLMIP for both left and right rolls. Descending maneuvers were initiated at 250 feet AGLMIP for both left and right rolls.

Table 23 lists the conditions flown, the condition reference code and the number of points collected for that condition. The points acquired are shown in Figures 198 to 283

8.3.4 Quick Stop/Start

The quick stop/start maneuvers were flown to investigate the effect of the transition from steady constant airspeed flight to accelerating or decelerating flight. The onset of accelerating or decelerating flight changes the configuration of the rotor wake and has an effect on the radiated noise, especially during the transition to decelerating flight where the wake is expected to move closer to the rotor disk. These maneuvers were initiated from a steady flight condition of 80 KIAS in level flight at 150 feet AGLMIP. The pilot began the acceleration or deceleration at 200 feet before the MIP using 2, 4 and 6 knots per second changes in airspeed along the flight path towards the target airspeed of 60 or 100 KIAS. Collective was controlled so that altitude was maintained during the maneuver.

Table 24 lists the conditions flown, the condition reference code and the number of points collected for that condition. The points acquired are shown in Figures 284 to 300.

8.3.5 Roll Angle Changes During Climbing Flight

This maneuver is similar to the single control input cyclic descending roll maneuver, except that it is performed while the aircraft is climbing instead of descending. However, in order to initiate the roll maneuver at the desired altitude over the microphone array, the climb can only be entered just prior to the MIP. To perform this maneuver the helicopter started from steady level flight at 80 KIAS with an altitude of 150 feet AGLMIP. At 750 feet before the MIP, (2,250 feet from reference microphone) the pilot began a 6° or 9° climb at constant airspeed. At the MIP the pilot performed a cyclic roll. The roll rate was the same roll rate as the fast rate from the cyclic roll maneuvers and executed by applying a lateral cyclic ramp input from trimmed position to left or right.

Table 25 lists the conditions flown, the condition reference code and the number of points collected for that condition. The points acquired are shown in Figures 301 to 312.

8.3.6 Roll Angle Changes During Accelerating Flight

The rotor wake geometry is different in accelerating/decelerating flight than in steady level flight and provides a different initial condition for transient maneuvers. The purpose of these maneuvers is to assess the acoustic effect of decelerations or accelerations prior to entry into a turn. The maneuver was initiated from a steady flight condition of either 60 or 100 KIAS in level flight at 150 feet AGLMIP. The pilot then began to accelerate or decelerate at a rate of 4 knots per second while maintaining 150 feet AGLMIP. This acceleration or deceleration was initiated at a point such that the airspeed was approximately 80 KIAS at the MIP. Once the MIP was reached, the pilot performed a cyclic roll (left or right) while continuing to accelerate or decelerate.

Table 26 lists the conditions flown, the condition reference code and the number of points collected for that condition. The points acquired are shown in Figures 313 to 334.

8.4 Terminal Area Approaches

Terminal area approach data were acquired for use in verification of ground footprint predictions. A number of different approach and level flight profiles were flown. These profiles ranged from a constant speed profile with a single descent angle to decelerating and turning approaches. All approaches were flown with gear down for safety of flight, were started at 1,000 feet AGL over the Terminal Area Landing Point (TALP) and terminated at the TALP shown in Figure 21.

Table 27 contains the test card as recorded in the control trailer during the terminal area approach portion of the test for the data included in the electronic data distribution package and the approaches are described below:

1. Single descent angle, constant speed approaches were flown at 60 knots at descending flight path angles of 6° (T1 - 2) and 9° (T2 - 3). The airspeed was held constant during the descent until it became necessary for the pilot to terminate the approach at the TALP. These approaches are shown in Figures 335 thru 339.

2. Single descent angle, decelerating approaches were flown starting at an airspeed of 100 knots and decelerating to approximately 20 knots at the TALP while holding 6° (T3 - 2), 9° (T4 - 2) or 12° (T5 - 2) descending flight path angles. These approaches are shown in Figures 340 thru 345.

3. Complex approaches that included multiple descent angles, multiple airspeed combinations, U-shaped and spiraling descents were flown (T6 - 2, T7 - 3, T8 - 2, T9 - 4 and T10 - 1). Flying these complex pre-defined approaches proved to be problematic and beyond the capability of the guidance system but twelve attempts were made to fly the five complex approach profiles by the pilot using ground markers as guidance. These test points provide valuable information even though the actual profile flown varies from the defined profile because the aircraft information was recorded and can thus be used to predict the footprint for the actual profile flown and compared to the measured footprint. These approaches are shown in Figures 346 thru 357.

4. Three test points were taken where the pilot was asked to fly the quietest profile that he considered possible, based on his extensive piloting experience (T11 - 3). These approaches are shown in Figures 358 thru 360.

5. Several level flights were flown in the same manner and flight direction as in the source noise measurement portion of the test to acquire aircraft data for these conditions that was not available during that phase of testing due to instrumentation issues as described in Table 3. These points (L1 - 2, L6 - 1, L8 - 2 and L10 - 2) are shown in Figures 361 thru 367.

The measured Sound Exposure Level (SEL) contour for the A-weighted noise radiation during a standard 60 knot 6° approach is shown in Figure 335 and the contour for a 100 knot, 12° decelerating approach is shown in Figure 345. The higher speed, 12° , decelerating approach shows a significant decrease in SEL from the standard 6° approach and is the quietest approach profile flown during this test. This correlates with the observation made during the source noise measurements that the peak BVI descent rate is near 9° . This result is consistent with previous findings [12–14] which show that during approach, deceleration at an angle steeper than the peak BVI condition can reduce noise.

9 Electronic Data

Data described in this paper are open and available electronically upon request from Michael Watts, Aeroacoustics Branch (D314), Mail Stop 461, NASA Langley Research Center, 23681, Michael.e.watts@nasa.gov. The data are provided in standard American Standard Code for Information Interchange (ASCII) text and/or Network Common Data Form (NetCDF) formats, depending on data type. NetCDF is a "self-describing", packed binary format which is platform independent. Drivers for a multitude of platforms are available at no cost at http://www.unidata.ucar.edu/software/netcdf/. The file structure for the electronic data is shown in Figure 368. Descriptions of the contents of each file type, including file naming convention and file format, are contained in the following subsections.

9.1 Microphone Location File

The microphone GPS locations are contained in the comma delimited text file `M430MicFullList.csv`. This file has a row for each microphone which contains the microphone number, latitude and longitude in decimal degrees, orthometric height in meters and an installation type keyword. The installation types are (1) `invgb7` for inverted 7 mm over a ground board, (2) `elevtd` for elevated 4 feet on a tripod, (3) `gdbdfl` for flush mounted in a ground board with the diaphram pointed up and (4) `empty` for no microphone of this number. The commercial software package MATLAB® function `micConvert` is included and used to read this file and generate the microphone locations in a UTM Cartesian coordinate system centered at an input reference location with +X in the easterly direction and +Y in the northerly direction. The function `coordrotate` can then be used to rotate that UTM coordinate system to point the +X in the desired direction, in this case to 326.4° true. The primary installation type used in the data analysis for this paper is the `invgb7` type and has a constant installation correction of 6 dB for 0 to 10,000 Hz due to the ground plane.

9.2 Acoustic Pressure Time History Data

Acoustic pressure time history data, in units of Pascals, are in the NetCDF binary files contained in the `M430_pascals_v3` directory. This data is corrected for time offset issues but uncorrected for installation effects. There is one file per microphone per data run with the file name being the `<6 Digit NASA Run Number>_<2 Digit Microphone Number>_pascal_v3.nc`. For example, file `273100_08_pascal_v3.nc` is the file containing the acoustic pressure time history data in Pascals for NASA run number 272100, microphone number 8. Table 29 describes the variables contained in the acoustic pressure time history files. The included function `netCDFimport` is used to import the netCDF data into MATLAB®.

The acoustic pressure data has been corrected for an acquisition time alignment problem as mentioned in a previous section. The text file `all_time_offsets_v3.txt` contains the corrections applied to the baseline data to create the data marked with the v3 in the filename. This file contains one section for each data point acquired which contains a row that lists the applicable microphone number and another row that lists the offset applied for those microphones. A 0 offset is no correction, 1 is add 1 second to the start time, and a 9 is to not include the microphone in the data set.

9.3 Test Reference Data

Information about each test point is contained in the comma delimited text file `M430FullRefList.csv` and Table 28 describes the values contained within the file. The function in file `loadM430RefInfo.m` loads these variables into MATLAB® in a data structure that contains the values for the specified run number. The entire table can be read into MATLAB® using the function `csvimport`.

9.4 Aircraft Data

Low frequency, high frequency and rotor azimuth data recorded on the aircraft is contained in three comma delimited text files for each run number. The low frequency data was sampled at a rate of 5 Hz and is contained in a file with the naming convention of `<6 Digit NASA Run Number>_lfacdata.csv`. The file has two rows of header and then a row for each time step. The high frequency file name is structured the same way except that it has `_hfacdata` and the rotor azimuth data has `_azacdata`. These data files are contained within the directory `M430aircraftData`. Tables 30, 31 and 32 describe the variables contained within the files. The function `loadM430ACData` is included in the distribution which loads the aircraft data into a MATLAB® data structure.

9.5 Aircraft Tracking Data

Tracking data records the position of the GPS antenna in space as a function of time at a 5 Hz sample rate. The files are contained in the directory NASAGPS with one comma delimited file for each run number with the file name being the <6 Digit NASA Run Number>.GPS. Each file contains 5 columns that are UTC local time, seconds from midnight, latitude, longitude and orthometric height in feet. The World Geodetic System 1984 (WGS84) ellipsoid is used for all tracking calculations in this report. The GPS receiver and the longitude, buttline and waterline locations on the aircraft (in inches) are located in Table 2. Three MATLAB® functions are included in the distribution. The M430trackNASAGPS function reads in the tracking file and uses gps_to_utm to calculate the aircraft track in UTM coordinates in relation to a reference location. It then uses the coordrotate to rotate the UTM coordinates by a specified rotation as discussed previously.

9.6 Individual Semi-spheres

One-third Octave sound semi-spheres were generated for each of the steady state level and descent test points acquired during the source phase of the test. These files are included in the data distribution and are contained in a folder called M430_individual_hemispheres_v3. Each files name is of the format Be430<last 3 digits of the run number>.nc. For example, Be430100.nc is the file for run 273100. Table 33 describes the variables contained in these NetCDF files.

9.7 Averaged Semi-spheres

One-third octave band, level flight sound semi-spheres were averaged based on true airspeed as described in 8.1. These averaged semi-sphere files are included in the data distribution and are contained in a folder called M430_averaged_hemispheres_v3. Each file's name is of the format Be430<3 digit condition number>.nc where the condition numbers run from 721 to 733 and indicate increasing airspeed as shown on Figures 25 thru 27 and Figures 28 thru 30.

9.8 Weather Data

The weather data is contained in three sub-folders in the folder Weather.

9.8.1 NASA Profiling Weather Balloon

The profiling weather balloon raw data is stored in comma delimited text files within the NASA_weather_balloon folder. The naming convention is EglinSonde<date in mmddyy format>.csv. Each file contains Secs, hr, min, sec, altitude (ft), temperature (° F), relative humidity

(%), pressure (kPa), cup wind speed (kts), wind direction (mag), wind direction (true), dynamic WS (kts), ground temperature (° F), density (kg/m3). This raw data file is divided into individual profiles as designated in the MATLAB® script `M430wprofiles`. This script calls the MATLAB® functions `readRawBalloonWeather`, `loadballoonprofiles` and `weatherfitsmooth` to load the raw balloon data, separate the profiles and then curve fit the data. The results of these actions are data structures in MATLAB® that are described in the comments of the `fltwpDescription.m` file. Results of this separation and curve fitting are graphically displayed in folders within the `NASA_weather_balloon` directory. One example is shown in Figure 369.

9.8.2 NASA Stationary Weather Sensors

NASA ground weather station data is stored in files within the `NASA_weather_stations` folder. The naming convention is `SW<date in mmddyy format>_<sensor number>.txt`. The pertinent parameters in each file are time, date, temperature(° F), humidity (%Relative Humidity (RH)), pressure (kPa), wind speed (kts), wind direction (mag), wind direction (true), and dew point (° F). The MATLAB® script `readNASAWeatherStation` reads these weather weather files for the days where testing occurred and loads the data into the data structure described in the file `nwsFormat.m`.

9.8.3 Ole Miss Stationary Weather Balloon

The Ole Miss weather balloon data is stored in files within the `Ole_Miss_weather` folder. The naming convention is `OM<date in mmddyy format>_<sensor number>.txt`. The pertinent parameters in each file are time, pressure (hPa), temp(K), humidity (%RH), alt (meters), wind speed (meters per second) and wind direction (mag). The MATLAB® script `readOleMissBalloon` reads these weather weather files for the days where testing occurred and loads the data into the data structure described in the file `omwFormat.m`.

9.9 Test Cards

The directory `Test_Cards` contains two subdirectories. The `NASA_Cards` subdirectory contains Microsoft Excel formatted files containing the test cards as written in the control trailer during the testing for all data points acquired. The `Pilot_Cards` subdirectory contains scans of the notes (in pdf format) taken by the flight test engineer onboard the aircraft during testing.

10 Concluding Remarks

A cooperative flight test between NASA, Bell Helicopter, and the U.S. Army to characterize the acoustics of, and to measure maneuver noise on, a Bell Helicopter 430 aircraft was accomplished during June/July 2011 at Eglin Air Force Base in Florida. This test gathered a total of 410 test points over 10 test days and included extensive measurements with the aircraft performing dynamic maneuvers. Three microphone configurations with up to 31 microphones in each configuration were used and specifically targeted to the acoustic data type being measured. Aircraft data were acquired, including DGPS, aircraft state and rotor state information. This data set contains a complete acoustic representation of the Bell 430 aircraft for inclusion in the RNM database. The data shown demonstrates that maneuvers lead to significant increases in noise. The terminal area measurements include a variety of flight paths ranging from simple to complex and provide valuable information for the validation of ground footprint prediction tools. This extensive data set is publicly available upon request.

References

1. "CTRDAC-1995-REPORT, civil tiltrotor development advisory committee report to congress in accordance with PL102-581," December 1995.

2. J. Johnson, V. Stouffer, D. Long, and J. Gribko, "Evaluation of the national throughput benefits of the civil tilt rotor," NASA, NASA CR 2001-211055, September 2001.

3. W. W. Chung and et.al., "Modeling high-speed civil tiltrotor transports in the next generation airspace," NASA, NASA CR 2011-215960, January 2011.

4. D. A. Conner, C. L. Burley, and C. D. Smith, "Flight acoustic testing and data acquisition for the rotorcraft noise model (RNM)," in *American Helicopter Society 62nd Annual Forum*, May 2006.

5. M. E. Watts, D. A. Conner, and C. D. Smith, "Joint Eglin acoustic week III data report," NASA/TM-2010-216206, March 2010.

6. E. Greenwood, F. H. Schmitz, G. Gopalan, and B. W.-C. Sim, "Helicopter external noise radiation in turning flight: Theory and experiment," in *American Helicopter Society 63rd Annual Forum*, May 2007.

7. H. Ishi, H. Gomi, and Y. Okuno, "Helicopter flight tests for BVI noise measured using an onboard external microphone," in *AIAA*

Flight Mechanics Conference and Exhibit, San Francisco, CA, August 2005.

8. P. Speigel, H. Buchholz, and M. Pott-Pollenske, "Highly instrumented BO105 and EC135-FHS aeroacoustic flight tests including maneuver flights," in *American Helicopter Society 61st Annual Forum*, May 2005.

9. R. D. Sickenberger, G. Gopalan, and F. H. Schmitz, "Helicopter near-horizon harmonic noise radiation due to cyclic pitch transient control," in *American Helicopter Society 67th Annual Forum*, May 2011.

10. R. D. Sickenberger and F. H. Schmitz, "Longitudinal tip-path-plane measurement using an optics-based system," in *American Helicopter Society 63rd Annual Forum*, Virginia Beach, VA, May 2007.

11. E. Greenwood and F. H. Schmitz, "Separation of main and tail rotor noise ground-based acoustic measurements using time-domain de-dopplerization," in *35th European Rotorcraft Forum*, September 2009.

12. N. Lappos, J. Arnold, P. Erway, and E. McConkey, "The development of a decelerating helicopter instrument landing system using differential GPS," in *American Helicopter Society 56th Annual National Forum*, Virginia Beach, VA, May 2000.

13. F. H. Schmitz, G. Gopalan, and B. W.-C. Sim, "Flight-path management/control methodology to reduce helicopter blade–vortex interaction noise," *Journal of Aircraft*, vol. 39, no. 2, pp. 193–205, 2002.

14. F. H. Schmitz, E. Greenwood, R. D. Sickenberger, G. Gopalan, B. W.-C. S. amd David Conner, and E. M. III, "Measurement and characterization of helicopter noise in steady-state and maneuvering flight," in *American Helicopter Society 63rd Annual Forum*, Virginia Beach, VA, May 2007.

Appendix A

Empirical Noise Radiation Model

A modified Shephard's method is described by Equation A1 and was used to construct a model from the noise levels stored in the set of measured hemispheres.

$$u(\mathbf{x}) = \sum_{i=0}^{N} \frac{w_i(\mathbf{x}) u_i}{\sum_{j=0}^{N} w_j(\mathbf{x})} \tag{A1}$$

where $\mathbf{x}$ is the four-dimensional vector describing the interpolant, $u(\mathbf{x})$ the estimated noise level, N the number of measured data points, u_i the measured noise levels, and w_i the weights associated with each data point. In the standard Shepard's method these weights are the square of the inverse of the distance, d, between the interpolant and the data points:

$$w_i(\mathbf{x}) = \frac{1}{d(\mathbf{x}, \mathbf{x}_i)^2} \tag{A2}$$

The modified Shepard's method used to construct the model includes a nearby subset of the local data to estimate the noise levels at each interpolant. This is described by using the modified weights given in Equation A3. For modeling the external noise radiation, the data were scaled such that the radius, R, included radiation directions within 180°, flight path angles within 3°, and true airspeeds within 10 knots of the interpolants.

$$w_k(\mathbf{x}) = \left(\frac{R - d(\mathbf{x}, \mathbf{x}_k)}{R d(\mathbf{x}, \mathbf{x}_k)} \right)^2 \tag{A3}$$

Tables

Table 1: Bell Model 430 Specifications

Main Rotor Diameter	42 ft
Num. Main Rotor Blades	4
MR RPM, BPF	348.6 RPM, 23.2 Hz
Tail Rotor Diameter	6 ft 10.6 in
Num. Tail Rotor Blades	2
TR RPM, BPF	1880.7 RPM, 62.7 Hz
Power Plant	2- Allison 250-C40B - 783 HP ea.
Empty Weight	5,305 lb
Max Take Off GW	9,300 lb
Max Speed	143 knots

Table 2: Aircraft Locations

Position	Longitudinal, in	Butt Line, in	Water Line, in
GPS Antenna	159.5	0	93
Hub	252.5	0	142
Pilot Eye	152	16	73
IMU	216	-0.5	44
Tail Rotor	543.5	-22.5	99
Nominal CG	249.8	-0.17	70

Table 3: Data Availability

Test Phase	Source			Turns	Dynamic Maneuvers					Term Area	Accuracy
Date	6/17/11	6/18/11	6/19/11	6/22/11	6/24/11	6/25/11	6/26/11	6/28/11	6/30/11	7/1/11	
Flight Number	1273	1274	1275	1277	1278	1280	1282	1285	1287	1288	
Ind AS				x	x	x	x	x	x	x	±2 kts
AC Heading				x	x	x	x	x	x	x	±0.5°
AC AOA	x		x	x	x	x	x	x	x	x	±0.5°
AC Sideslip	x		x	x	x	x	x	x	x	x	±0.5°
AC Pitch Rate				x	x	x	x	x	x	x	±0.5° /s
AC Roll Rate				x	x	x	x	x	x	x	±0.5° /s
AC Yaw Rate				x	x	x	x	x	x	x	±0.5° /s
AC Vert Acc	x	x	x	x	x	x	x	x	x	x	±0.01 g
Long Cyclic				x	x	x	x	x	x	x	±2% range
Lat Cyclic				x	x	x	x	x	x	x	±2% range
Collective				x	x	x	x	x	x	x	±2% range
INU Pitch						x (1)	x	x	x		±0.2°
INU Roll						x (1)	x	x	x		±0.2°
INU Heading						x (1)	x	x	x		±0.5°
INU Pitch Rate						x (1)	x	x	x		±0.2° /s
INU Roll Rate						x (1)	x	x	x		±0.2° /s
INU Yaw Rate						x (1)	x	x	x		±0.2° /s
INU Long Acc						x (1)	x	x	x		±0.01 g
INU Lat Acc						x (1)	x	x	x		±0.01 g
INU Vert Acc						x (1)	x	x	x		±0.01 g
Rotor Speed		x	x	x		x (3)	x	x	x	x	±0.5 RPM
DGPS	x	x	x	x	x	x	x	x	x	x	±5 ft
TPP								x (2)	x (2)		±0.1°

(1) INU data available for acoustic runs 341 to 345 for this flight
(2) TPP data available for acoustic runs 461 to 493 and 521 to 551
(3) Rotor Speed not available for 280369 - 280401

Table 4: Source Array

Mic Number	Latitude	Longitude	Geoid Height Feet	UTM X Feet	UTM Y Feet	X Feet	Y Feet	Z Feet	Angle Deg
1	30.57110870	-86.78589432	179.2	-1428.3	-948.6	-0.1	1714.6	13.7	5.0
2	30.57170890	-86.78484675	180.5	-1098.6	-730.3	-0.6	1319.2	15.0	6.5
3	30.57242381	-86.78360749	181.7	-708.5	-470.2	0.2	850.4	16.2	10.0
4	30.57313456	-86.78236678	168.4	-318.1	-211.7	-0.4	382.1	2.9	21.4
5	30.57335828	-86.78196859	166.1	-192.7	-130.4	-2.0	232.7	0.6	32.8
6	30.57340936	-86.78188108	165.9	-165.2	-111.8	-1.7	199.5	0.5	36.9
7	30.57347578	-86.78176599	165.4	-129.0	-87.6	-1.6	155.9	-0.1	43.9
8	30.57355352	-86.78164207	165.7	-90.0	-59.4	0.3	107.8	0.2	54.3
9	30.57361506	-86.78151867	165.9	-51.1	-37.0	-2.5	63.1	0.4	67.2
10	30.57366749	-86.78143342	165.7	-24.3	-17.9	-1.5	30.2	0.2	78.6
11 (ref)	30.57371670	-86.78135616	165.5	0.0	0.0	0.0	0.0	0.0	-90.0
12	30.57375520	-86.78127846	165.4	24.5	14.0	-1.9	-28.1	-0.1	-79.4
13	30.57380798	-86.78118616	165.7	53.5	33.2	-1.9	-62.9	0.2	-67.2
14	30.57386812	-86.78108272	165.9	86.1	55.1	-1.7	-102.2	0.4	-55.7
15	30.57394608	-86.78094570	165.8	129.2	83.4	-2.0	-153.8	0.3	-44.3
16	30.57401445	-86.78082641	165.6	166.7	108.3	-2.0	-198.8	0.1	-37.0
17	30.57406597	-86.78073256	165.5	196.3	127.0	-2.7	-233.8	0.0	-32.7
18	30.57428658	-86.78034417	164.4	318.5	207.3	-3.5	-380.0	-1.1	-21.5
19	30.57500530	-86.77910116	159.0	709.7	468.7	-2.2	-850.5	-6.5	-10.0
20	30.57576255	-86.77778083	153.7	1125.2	744.1	-2.6	-1349.0	-11.8	-6.3

Continued on next page

Table 4: *continued*

Mic Number	Latitude	Longitude	Geoid Height Feet	UTM X Feet	UTM Y Feet	X Feet	Y Feet	Z Feet	Angle Deg
21	30.57631968	-86.77681516	153.7	1429.1	946.8	-1.9	-1714.3	-11.8	-5.0
22 (1)	30.57340936	-86.78188108	165.9	-165.2	-111.8	-1.7	199.5	0.5	36.9
23 (1)	30.57371670	-86.78135616	165.5	0.0	0.0	0.0	0.0	0.0	-90.0
24 (1)	30.57401445	-86.78082641	165.6	166.7	108.3	-2.0	-198.8	0.1	-37.0
25 (2)	30.57340936	-86.78188108	165.9	-165.2	-111.8	-1.7	199.5	0.5	36.9
26 (2)	30.57371670	-86.78135616	165.5	0.0	0.0	0.0	0.0	0.0	-90.0
27 (2)	30.57401445	-86.78082641	165.6	166.7	108.3	-2.0	-198.8	0.1	-37.0

1) Microphone mounted flush in ground board

2) Microphone mounted on 4' tripod

Table 5: Primary Test Site Locations

Mic Number	Latitude	Longitude	Geoid Height Feet	UTM X Feet	UTM Y Feet	X Feet	Y Feet	Z Feet
Command	30.55920632	-86.77469684	159.5	2096.1	-5277.6	-5556.1	1173.4	-6.0
NASA Balloon	30.55965011	-86.77488155	149.1	2038.8	-5116.2	-5389.4	1132.6	-16.4
Ole Miss Balloon	30.58719478	-86.77866867	173.4	8456.8	4902.2	3615.9	-3416.4	7.9
Helo Fueling Point	30.57612933	-86.78524273	188.2	-1223.1	877.5	1407.7	533.5	22.7
NASA WS 2	30.56561074	-86.79283572	186.2	-3613.1	-2948.1	-457.1	4640.8	20.7
NASA WS 3	30.57042378	-86.7785311	150.8	889.1	-1197.7	-1489.6	-78.1	-14.7
NASA WS 4	30.57725482	-86.77331893	158.4	889.1	-1197.7	-1489.6	-78.1	-14.7
Ref Mic	30.57371670	-86.78135616	165.5	0.0	0.0	0.0	0.0	0.0
MIP	30.57027433	-86.77872111	150.9	829.3	-1252.0	-1501.7	1.8	-14.6
TALP	30.57670613	-86.76845112	161.7	4061.3	1087.5	-1340.7	-3984.9	-3.8

Table 6: Maneuver Array

Mic Number	Latitude	Longitude	Geoid Height Feet	UTM X Feet	UTM Y Feet	X Feet	Y Feet	Z Feet
30	30.57596749	-86.78132113	196.1	11.0	818.7	675.9	-462.1	30.6
31	30.57242381	-86.78360749	181.7	-708.5	-470.2	0.2	850.4	16.2
32	30.57313456	-86.78236678	168.4	-318.1	-211.7	-0.4	382.1	2.9
33	30.57355352	-86.78164207	165.7	-90.0	-59.4	0.3	107.8	0.2
34 (ref)	30.57371670	-86.78135616	165.5	0.0	0.0	0.0	0.0	0.0
35	30.57386812	-86.78108272	165.9	86.1	55.1	-1.7	-102.2	0.4
36	30.57428658	-86.78034417	164.4	318.5	207.3	-3.5	-380.0	-1.1
37	30.57500530	-86.77910116	159.0	709.7	468.7	-2.2	-850.5	-6.5
38	30.57576255	-86.77778083	153.7	1125.2	744.1	-2.6	-1349.0	-11.8
39	30.57698436	-86.77565139	157.5	1795.3	1188.6	-3.1	-2153.1	-8.0
40	30.57155716	-86.77970384	156.6	520.0	-785.5	-942.0	1.3	-8.9
41	30.57129968	-86.78004863	155.1	411.5	-879.1	-960.0	143.5	-10.4
42	30.57181080	-86.77884551	151.2	790.2	-693.2	-1014.6	-274.8	-14.3
43	30.57170669	-86.77806828	148.1	1034.8	-731.1	-1181.5	-457.6	-17.4
44	30.57111041	-86.77906344	151.4	721.6	-948.0	-1188.9	-76.7	-14.1
45	30.57087364	-86.77917684	152.2	685.9	-1034.1	-1240.9	0.7	-13.3
46	30.57075619	-86.77933187	152.4	637.1	-1076.8	-1249.5	64.9	-13.1
47	30.57116577	-86.77855599	148.4	881.3	-927.8	-1260.4	-220.9	-17.1
48	30.57100087	-86.77875519	150.2	818.6	-987.8	-1275.7	-135.5	-15.3
49	30.57061904	-86.77898857	151.5	745.2	-1126.7	-1350.8	2.5	-14.0

Continued on next page

Table 6: *continued*

Mic Number	Latitude	Longitude	Geoid Height Feet	UTM X Feet	UTM Y Feet	X Feet	Y Feet	Z Feet
50	30.57029347	-86.77954704	151.6	569.4	-1245.1	-1352.2	214.5	-13.9
51	30.57095752	-86.77839517	148.6	931.9	-1003.6	-1351.5	-221.2	-16.9
52	30.57070376	-86.77872690	151.0	827.5	-1095.9	-1370.7	-83.1	-14.5
53	30.57047580	-86.77887094	151.2	782.2	-1178.8	-1414.7	0.5	-14.3
54	30.57068009	-86.77852443	150.4	891.2	-1104.5	-1413.1	-131.4	-15.1
55	30.57074055	-86.77805043	148.6	1040.4	-1082.5	-1477.3	-267.9	-16.9
56	30.57027433	-86.77872111	151.0	829.3	-1252.1	-1501.8	1.8	-14.5
57	30.56983347	-86.77936940	152.4	625.3	-1412.4	-1522.5	260.4	-13.1
58	30.57004126	-86.77877620	151.4	812.0	-1336.8	-1562.8	63.1	-14.0
59	30.57004441	-86.77863330	151.3	857.0	-1335.7	-1586.8	25.0	-14.2
60	30.57023452	-86.77788985	151.2	1091.0	-1266.5	-1658.6	-208.2	-14.3
MIP	30.57027433	-86.77872111	150.9	829.3	-1252.0	-1501.7	1.8	-14.6

Table 7: Terminal Area Array

Mic Number	Latitude	Longitude	Geoid Height Feet	UTM X Feet	UTM Y Feet	X Feet	Y Feet	Z Feet
30	30.57596749	-86.78132113	196.1	11.0	818.7	675.9	-462.1	30.6
70	30.56907604	-86.78497050	150.5	-1137.6	-1687.9	-776.8	1881.4	-15.0
71	30.56866129	-86.78864962	183.6	-2295.5	-1838.7	-261.8	2929.4	18.1
72	30.57031013	-86.78579551	168.7	-1397.2	-1239.0	-259.2	1849.4	3.2
73	30.57184176	-86.78297063	166.6	-508.1	-682.0	-287.0	800.5	1.1
74	30.57345922	-86.78017751	156.8	370.9	-93.6	-283.2	-257.2	-8.7
75	30.57498317	-86.77726758	153.7	1286.7	460.7	-328.1	-1326.8	-11.8
76	30.57656070	-86.77441894	165.0	2183.2	1034.5	-346.0	-2391.0	-0.5
77	30.56478501	-86.78978185	180.9	-2652.0	-3248.5	-1239.1	4006.3	15.4
78	30.56636239	-86.78696742	176.4	-1766.1	-2674.9	-1251.3	2951.0	11.0
79	30.56792475	-86.78425997	155.5	-913.9	-2106.6	-1249.3	1926.8	-10.0
80	30.56955622	-86.78124086	153.4	36.3	-1513.3	-1280.7	806.9	-12.1
81	30.57110422	-86.77838536	147.8	935.0	-950.2	-1308.8	-253.2	-17.7
82	30.57268267	-86.77555974	153.6	1824.3	-376.1	-1322.5	-1311.7	-11.8
83	30.57431565	-86.77271214	161.4	2720.4	218.0	-1323.4	-2386.8	-4.1
84	30.56244362	-86.78802297	178.5	-2098.4	-4100.2	-2254.8	4016.3	13.1
85	30.56394259	-86.78518121	158.0	-1203.9	-3555.0	-2295.5	2969.6	-7.5
86	30.56562396	-86.78226434	145.1	-285.8	-2943.5	-2293.9	1866.5	-20.3
87	30.56723679	-86.77955099	149.2	568.2	-2356.9	-2277.7	830.5	-16.3
88	30.56879386	-86.77671554	156.1	1460.6	-1790.5	-2299.6	-226.2	-9.4

Continued on next page

Table 7: *continued*

Mic Number	Latitude	Longitude	Geoid Height Feet	UTM X Feet	UTM Y Feet	X Feet	Y Feet	Z Feet
89	30.57051563	-86.77384063	155.2	2365.4	-1164.2	-2278.4	-1326.4	-10.3
90	30.57204661	-86.77095128	158.1	3274.7	-607.3	-2317.5	-2392.0	-7.4
91	30.56682131	-86.78324044	149.0	-593.1	-2508.0	-1761.2	1881.5	-16.5
92	30.56176285	-86.78344280	142.0	-656.8	-4347.9	-3258.6	2952.4	-23.5
93	30.56329667	-86.78054118	146.5	256.5	-3790.0	-3299.1	1882.9	-19.0
94	30.56492667	-86.77767446	154.4	1158.8	-3197.1	-3304.4	803.3	-11.1
95	30.56654073	-86.77486860	151.1	2041.9	-2610.0	-3303.8	-257.2	-14.4
96 (1)	30.57110422	-86.77838536	151.6	935.0	-950.2	-1308.8	-253.2	-13.9
97 (1)	30.56993126	-86.77751901	150.6	1207.7	-1376.8	-1815.0	-244.4	-14.9
98 (ref)	30.57371670	-86.78135616	165.5	0.0	0.0	0.0	0.0	0.0
TALP	30.57670613	-86.76845112	161.7	4061.3	1087.5	-1340.7	-3984.9	-3.8

1) Microphone mounted on 4' tripod

Table 8: Weather Instrumentation Availability

Date	Flight	Ground Station				NASA Balloon	Ole Miss Balloon
		1	2	3	4		
6/8/11		x					
6/9/11		x					
6/10/11		x					
6/11/11		x					
6/12/11		x					
6/13/11		x	x	x	x		
6/14/11		x	x	x	x		
6/15/11		x	x	x	x		
6/16/11		x	x	x	x		
6/17/11	1273	x	x	x	x	x	
6/18/11	1274	x	x	x	x	x	100, 150, 200, 250
6/19/11	1275	x	x	x	x	x	9, 100, 200, 300
6/20/11		x	x	x	x		
6/21/11		x	x	x	x		
6/22/11	1277	x	x	x	x	x	200
6/23/11		x	x	x	x		
6/24/11	1278	x	x	x	x	x	250
6/25/11	1280	x	x	x	x	x	9, 75, 150, 250, 350
6/26/11	1282	x	x	x	x	x	9, 75, 150, 250, 350
6/27/11		x	x	x	x		
6/28/11	1285	x	x	x	x	x	9, 75,150, 250, 350
6/29/11		x		x	x		
6/30/11	1287	x	x	x	x	x	
7/1/11	1288	x	x	x	x		

Table 9: Source Level Flight Test Points

KIAS	Gear Up	Gear Down
50	L2 - 1	
60	L3 - 5	
70	L4 - 2	
80	L1 - 11	L11 - 2
90	L5 - 1	
100	L6 - 2	
110	L7 - 1	L12 - 2
120	L8 - 3	
130	L9 - 4	

Table 10: Steady Descent Flight Test Points

	Airspeed, KIAS				
Angle	50	60	70	80	90
-3°		A4 - 2		A18 - 2	
-6°	A2 - 2	A6 - 4	A13 - 2	A20 - 4	A27 - 2
-7.5°		A7 - 2	A14 - 1	A21 - 4	A28 - 1
-9°	A3- 1	A8 - 3	A15 - 2	A22 - 2	A29 - 1
-10.5°		A9 - 2		A23 - 3	
-12°		A10 - 3	A17 - 2	A24 - 2	A31 - 1

Table 11: Flight 1273 Test Card, 6/17/2011, Source Array

NASA Run Num	Data On Time	Data Off Time	Cond Counter	KIAS	Cross Alt	Flight Path Angle	Ground Temp	Wind Speed	Wind Heading	Comments
901	6:21:05	6:22:07	AMB	NA	NA	NA	75.1	0.0	175	Helo entered field during ambient
100	6:30:38	6:31:41	L1	80	200	0.0	74.8	0.0	175	Housekeeping
103	6:42:52	6:43:51	A18	80	200	-3.0	75.7	0.0	175	30 ft low
104	6:46:37	6:47:36	A18	80	200	-3.0	76.1	0.0	175	Good - 5 kts slow, 215 AGL cross
105	6:50:48	6:52:05	A4	60	200	-3.0	76.5	0.0	175	Below GS - 180 AGL (left cross wind)
106	6:55:19	6:56:36	A4	60	200	-3.0	77.0	0.0	175	Good course, low
108	7:04:01	7:05:00	A13	70	200	-6.0	77.5	1.0	175	Cross high, Wind 5.6@213
109	7:07:56	7:09:00	A13	70	200	-6.0	78.0	0.0	175	2500 AGL cross, Wind 8.5@221@250 AGL
110	7:12:39	7:14:08	A2	50	200	-6.0	78.0	1.7	175	Left crab? 270 AGL cross
112	7:21:10	7:22:48	A2	50	200	-6.0	79.2	1.2	215	200 AGL cross
113	7:25:19	7:26:42	A6	60	200	-6.0	78.9	6.4	209	slight right drift - 210 AGL
114	7:29:10	7:30:28	A6	60	200	-6.0	79.7	4.2	186	
115	7:33:07	7:34:17	A6	60	200	-6.0	79.6	4.9	213	230-240 AGL
116	7:37:54	7:38:52	A20	80	200	-6.0	79.8	3.7	210	220 AGL low fuel
-	-	-	-	-	-	-	-	-	-	Refuel, Balloon profile to 1000 AGL
117	8:39:38	8:40:52	L1	80	200	0.0	83.5	6.6	204	+/- 2 kts
118	8:43:27	8:45:22	L2	50	200	0.0	80.6	5.9	206	+/- 3 kts
119	8:47:57	8:49:34	L3	60	200	0.0	80.9	4.6	214	170 AGL cross +/-1.5 kts
120	8:52:19	8:54:12	L3	60	200	0.0	82.3	3.4	220	5 kts slow
121	8:56:38	8:58:19	L3	60	200	0.0	82.6	4.2	204	
122	9:00:57	9:02:26	L4	70	200	0.0	83.0	2.9	253	stab at 1,500', 155 AGL , 6kts off
123	9:04:55	9:06:22	L4	70	200	0.0	83.1	3.7	221	155 AGL 70-65 kts
124	9:08:48	9:10:00	L1	80	200	0.0	82.8	4.2	231	190 AGL
125	9:12:25	9:13:39	L1	80	200	0.0	82.2	4.4	184	190 AGL
126	9:16:00	9:17:04	L5	90	200	0.0	81.8	5.6	201	190 AGL

Continued on next page

Table 11: *continued*

NASA Run Num	Data On Time	Data Off Time	Cond Counter	KIAS	Cross Alt	Flight Path Angle	Ground Temp	Wind Speed	Wind Heading	Comments
127	9:19:18	9:20:19	L6	100	200	0.0	81.8	-	192	+/-1 kts, 190 AGL, A/S Boom reading low
128	9:23:59	9:24:55	L7	110	200	0.0	83.4	6.5	245	+/-1 kts 115, 94 on boom
129	9:26:58	9:27:50	L8	120	200	0.0	83.0	2.7	213	+/-1 kts, 94 on boom
130	9:29:53	9:30:43	L9	130	200	0.0	83.3	6.8	240	+/-1 kts, 96 kts on boom
131	9:33:14	9:34:28	L1	80	200	0.0	83.3	6.1	256	180 AGL
902	9:41:18	9:42:18	AMB	NA	NA	NA	81.7	8.8	241	A/C +3 nm out at start

Table 12: Flight 1274 Test Card, 6/18/2011, Source Array

NASA Run Num	Data On Time	Data Off Time	Cond Counter	KIAS	Cross Alt	Flight Path Angle	Ground Temp	Wind Speed	Wind Heading	Comments
901	5:21:49	5:22:51	AMB	0	0	0.0	72.9	1.2	145	none
902	5:26:15	5:27:16	AMB	0	0	0.0	73.0	1.0	145	Increased Gains
141	6:07:43	6:08:58	L1	80	200	0.0	73.2	2.0	145	none
145	6:22:44	6:24:00	A10	60	200	-12.0	73.2	1.2	145	Poor
146	6:26:40	6:27:54	A10	60	200	-12.0	73.2	1.0	145	Good glideslope
147	6:30:52	6:32:04	A10	60	200	-12.0	73.4	0.7	145	800 AGL to 50 AGL, good glideslope
148	6:34:39	6:35:35	A24	80	200	-12.0	73.6	1.2	145	under GS, collective full down - Olemiss up
149	6:38:09	6:39:07	A24	80	200	-12.0	74.0	1.2	145	
150	6:41:47	6:42:55	A9	60	200	-10.5	74.1	0.5	145	100 AGL above path, GS good
151	6:45:32	6:46:28	A9	60	200	-10.5	74.3	0.7	145	Poor, 150 AGL above, 10 kts high
152	6:49:09	6:50:23	A9	60	200	-10.5	74.5	1.7	145	Good!
153	6:52:56	6:53:55	A23	80	200	-10.5	74.7	2.0	146	8% torque
154	6:56:20	6:57:14	A23	80	200	-10.5	74.9	0.2	146	fast and high
155	6:59:44	7:00:44	A23	80	200	-10.5	75.2	1.2	146	little slow, but good glidepath and slope
156	7:03:37	7:04:48	A8	60	200	-9.0	75.6	1.2	158	profile 4/5 mislabel?
157	7:07:24	7:08:42	A7	60	200	-7.5	75.6	0.7	158	30 AGL high
158	7:11:01	7:12:24	A7	60	200	-7.5	76.3	0.0	158	+/- 1 kts, GS good
159	7:14:36	7:15:37	A21	80	200	-7.5	76.8	0.5	158	30 AGL high, end for fuel
-	-	-	-	-	-	-	-	-	-	Refuel, Balloon profile to 1000 AGL
160	7:59:52	8:01:05	L1	80	200	0.0	73.7	6.6	222	none
161	8:04:11	8:05:48	L3	60	200	0.0	80.1	4.2	191	good a/s and altitude, but 10% Q variation
162	8:08:32	8:10:13	L3	60	200	0.0	80.6	6.6	201	4 kts decay
163	8:12:50	8:14:03	L11	80	200	0.0	80.0	3.4	192	gear down, '+/- 1 kts A/S, 10 AGL
164	8:16:45	8:17:58	L11	80	200	0.0	80.0	6.1	177	gear down
165	8:20:29	8:21:30	L12	110	200	0.0	80.4	6.4	183	gear down (100 kts actual)

Continued on next page

Table 12: *continued*

NASA Run Num	Data On Time	Data Off Time	Cond Counter	KIAS	Cross Alt	Flight Path Angle	Ground Temp	Wind Speed	Wind Heading	Comments
166	8:23:49	8:24:47	L12	110	200	0.0	80.7	4.2	207	gear down (100 kts actual)
167	8:27:06	8:28:06	L6	100	200	0.0	81.2	4.4	184	good a/s, glideslope
168	8:30:48	8:32:00	L1	80	200	0.0	82.1	4.2	184	good
169	8:34:22	8:35:17	L8	120	200	0.0	81.1	5.1	227	left of center
170	8:37:49	8:38:37	L9	130	200	0.0	81.2	9.3	196	good (134 KIAS)
171	8:41:14	8:42:01	L9	130	200	0.0	80.6	8.8	201	133-134 KIAS
172	8:44:27	8:45:19	L13	131	200	0.0	81.5	5.6	202	130-133 KIAS
177	9:00:24	9:01:22	A21	80	200	-7.5	81.8	5.4	199	260 AGL
178	9:03:41	9:04:37	A21	80	200	-7.5	81.8	9.5	203	240 AGL
179	9:07:37	9:08:53	L1	80	200	0.0	82.0	10.8	173	
903	9:16:55	9:18:06	AMB	0	0	0.0	82.1	3.7	196	gain: -107
904	9:19:50	9:20:52	AMB	0	0	0.0	81.9	4.6	185	gain: -113

Table 13: Flight 1275 Test Card, 6/19/2011, Source Array

NASA Run Num	Data On Time	Data Off Time	Cond Counter	KIAS	Cross Alt	Flight Path Angle	Ground Temp	Wind Speed	Wind Heading	Comments
901	5:23:34	5:24:32	AMB	0	0	0.0	75.8	0.2	253	ambient
181	5:54:39	5:55:29	L9	130	200	0.0	75.9	2.0	247	Stabilized glideslope at 1500’
182	5:58:29	5:59:43	A8	60	200	-9.0	76.0	0.7	247	Stabilized glideslope at 1500’
183	6:02:09	6:04:09	A8	60	200	-9.0	75.2	1.7	194	none
184	6:07:23	6:08:16	A22	80	200	-9.0	75.5	1.5	184	none
185	6:11:00	6:11:57	A22	80	200	-9.0	76.1	3.4	212	good, 180 AGL cross, getting gusty
187	6:18:39	6:19:47	A21	80	200	-7.5	75.5	1.2	278	good glideslope, 81 KIAS
188	6:22:30	6:23:24	A20	80	200	-6.0	76.0	0.2	278	81 KIAS +/-1, good course
189	6:26:09	6:27:12	A27	90	200	-6.0	76.0	1.5	253	late data stop, 92 KIAS
190	6:29:42	6:30:33	A27	90	200	-6.0	76.1	1.0	253	lots of collective motion
191	6:33:39	6:34:52	A32	60	390	-6.0	76.5	2.4	252	180 AGL cross, good glideslope, 58 KIAS
192	6:38:35	6:39:36	A17	70	200	-12.0	76.6	0.2	253	good slope, 70-61 KIAS
193	6:42:40	6:43:42	A17	70	200	-12	76.9	0.0	253	good slope, 70-71 KIAS
194	6:46:35	6:47:29	A31	90	200	-12.0	76.9	1.7	253	none
195	6:50:46	6:52:33	A3	50	200	-9.0	77.2	1.2	252	good slope, 42-47 kts
196	6:55:23	6:56:31	A15	70	200	-9.0	77.4	1.5	252	100 ft high
197	6:59:07	7:00:14	A15	70	200	-9.0	77.3	2.4	252	280 AGL high, 5 KIAS increase near end
198	7:02:37	7:03:37	A29	90	200	-9.0	77.7	2.0	252	none
199	7:06:42	7:07:38	A20	80	200	-6.0	77.9	2.0	252	roll cyclic inputs, midcourse corrections
200	7:10:26	7:11:25	A20	80	200	-6.0	78.2	0.5	228	81-81 KIAS, good
201	7:14:26	7:15:31	A14	70	200	-7.5	78.2	0.7	228	70-71 KIAS, 220 AGL cross
202	7:18:06	7:19:05	A28	90	200	-7.5	78.2	2.9	237	KIAS 92-93, 230 AGL cross
203	7:21:17	7:22:35	L1	80	200	0.0	78.2	2.0	231	housekeeping - good course
-	7:23:17	-	-	-	-	-	-	-	-	Refuel
204	8:13:14	8:14:34	L1	80	200	0.0	80.9	6.1	265	housekeeping - gusty at altitude - 82-77 KIAS

Continued on next page

Table 13: *continued*

NASA Run Num	Data On Time	Data Off Time	Cond Counter	KIAS	Cross Alt	Flight Path Angle	Ground Temp	Wind Speed	Wind Heading	Comments
205	8:20:40	8:22:26	B1	60	65	Max	80.4	7.8	253	climb - KIAS +/- 2 kts
206	8:29:41	8:31:13	B1	60	65	Max	80.6	6.6	264	55-65 KIAS
207	8:33:55	8:35:32	B1	60	65	Max	81.0	5.6	262	60-65 KIAS
208	8:38:08	8:39:29	B2	80	65	Max	81.2	8.1	279	
209	8:42:02	8:43:20	B2	80	65	Max	81.0	9.5	264	KIAS +/- 2 kts
902	9:53:48	9:54:50	AMB	0	0	0.0	83.4	9.5	251	Ambient

Table 14: Steady Turn Flight Test Points

		Bank Angle	
KIAS	Direction	15°	30°
60	Left	S1 - 2	S2 - 3
	Right	S5 - 2	S6 - 4
80	Left	S3 -1	S4 - 2
	Right	S7 - 2	S8 - 3

Table 15: Flight 1277 Test Card, 6/22/2011, Source Array

NASA Run Num	Data On Time	Data Off Time	Cond Counter	KIAS	Turn Dir	Bank Angle Angle	Ground Temp	Wind Speed	Wind Heading	Comments
901	5:01:28	5:02:30	AMB	0	0.0	0	71.0	1.0	44	ambient
241	5:52:43	5:54:01	S5	60	Right	15	71.1	0.0	44	12 deg bank crossing 200 ft south
242	5:57:02	5:58:33	S5	60	Right	15	71.1	0.0	44	200ft off center, Wind 2.5@187@200 AGL
243	6:00:39	6:01:47	S6	60	Right	30	71.3	0.0	44	20-25 deg bank, increased speed 10kts, climb
244	6:03:17	6:04:28	S6	60	Right	30	71.2	0.2	44	12 KIAS increase
245	6:06:05	6:07:08	S6	60	Right	30	71.0	2.2	62	6 KIAS increase, bank angle good
246	6:09:02	6:10:02	S6	60	Right	30	71.1	2.4	62	bank 26-30
247	6:12:20	6:13:30	S7	80	Right	15	71.0	0.7	76	KIAS '+/- 1 kts, +/- 2 deg bank
248	6:15:20	6:16:30	S7	80	Right	15	71.0	0.2	77	Good!
249	6:18:10	6:19:09	S8	80	Right	30	70.9	0.5	77	Bank shallow by 2 deg
250	6:20:42	6:21:33	S8	80	Right	30	71.0	0.0	77	25-30 deg Bank, +5 KIAS
251	6:23:23	6:24:09	S8	80	Right	30	71.2	0.0	77	Wind 5@146@200 AGL
252	6:26:38	6:27:51	S1	60	Left	15	71.1	1.2	77	Bank 12-15
253	6:30:01	6:31:08	S1	60	Left	15	71.5	0.0	77	100 ft off center
254	6:33:07	6:34:05	S2	60	Left	30	71.8	0.0	77	bad
255	6:35:46	6:36:47	S2	60	Left	30	72.0	0.0	83	+/- 1 kts, 2 deg bank, 150 ft off
256	6:38:24	6:39:22	S2	60	Left	30	71.9	0.5	83	Wind 4.5@154@200 AGL, good
257	6:41:32	6:42:42	S3	80	Left	15	72.0	0.7	84	300 ft past center
258	6:44:55	6:46:06	S3	80	Left	15	71.6	1.2	109	good - 150 ft off center
259	6:48:10	6:49:06	S4	80	Left	30	72.0	0.5	109	good
260	6:51:17	6:52:15	S4	80	Left	30	71.8	1.5	105	bank 2 deg low, 50 off center

Table 16: Flight 1278 Test Card, 6/24/2011, Maneuver Array

NASA Run Num	Data On Time	Data Off Time	Cond Counter	KIAS	Cross Alt	Flight Path Angle	Direct	Rate	Ground Temp	Wind Speed	Wind Heading	Comments
901	4:10:46	4:11:46	AMB	NA	NA	NA	NA	NA				ambient
902	5:02:40	5:03:41	AMB	NA	NA	NA	NA	NA	73.9	0.0	142	ambient
301	5:52:02	5:53:09	L1	80	200	0.0	NA	NA	73.8	2.0	43	housekeeping
302	5:56:01	5:56:55	D10	80	250	-6.0	Pitch Up	Slow	73.7	2.2	39	Wind 2@249@250 AGL, med rate actual
303	5:59:37	6:00:27	D10	80	250	-6.0	Pitch Up	Slow	73.4	2.2	15	good
304	6:02:46	6:03:41	D10	80	250	-6.0	Pitch Up	Slow	73.4	1.2	15	82 KIAS
305	6:05:54	6:06:49	D10	80	250	-6.0	Pitch Up	Slow	73.2	2.9	358	good
306	6:08:58	6:09:52	D10	80	250	-6.0	Pitch Up	Slow	73.1	2.9	2	temp inv 3 deg/300 ft
307	6:12:23	6:13:14	D12	80	250	-6.0	Pitch Up	Fast	73.1	2.4	6	240 AGL
308	6:15:21	6:16:11	D12	80	250	-6.0	Pitch Up	Fast	73.4	2.2	8	none
309	6:18:18	6:19:13	D12	80	250	-6.0	Pitch Up	Fast	73.4	1.5	15	245 AGL
310	6:21:23	6:22:18	D12	80	250	-6.0	Pitch Up	Fast	73.4	0.7	15	270 AGL
311	6:24:35	6:25:26	R12	80	250	-6.0	Roll Left	Fast	73.4	0.0	15	control rate fast
312	6:27:20	6:28:12	R12	80	250	-6.0	Roll Left	Fast	73.4	0.2	15	good rate
313	6:30:09	6:30:57	R12	80	250	-6.0	Roll Left	Fast	73.5	0.2	15	270 AGL
314	6:32:55	6:33:46	R12	80	250	-6.0	Roll Left	Fast	73.5	0.0	15	good, 280 AGL
315	6:35:40	6:36:30	R12	80	250	-6.0	Roll Left	Fast	73.8	0.0	15	250 AGL
316	6:38:17	6:39:06	R10	80	250	-6.0	Roll Left	Slow	73.9	0.0	15	control rates high
317	6:40:53	6:41:43	R10	80	250	-6.0	Roll Left	Slow	73.8	1.5	23	control rates high
318	6:43:37	6:44:29	R10	80	250	-6.0	Roll Left	Slow	73.4	1.0	110	+1 KIAS, control rate good
319	6:46:28	6:47:19	R10	80	250	-6.0	Roll Left	Slow	73.5	0.2	110	good, 81-82 KIAS, little fast controls
320	6:49:15	6:50:01	R10	80	250	-6.0	Roll Left	Slow	73.6	0.0	110	control rates medium

Continued on next page

Table 16: *continued*

NASA Run Num	Data On Time	Data Off Time	Cond Counter	KIAS	Cross Alt	Flight Path Angle	Direct	Rate	Ground Temp	Wind Speed	Wind Heading	Comments
321	6:52:02	6:52:48	R10	80	250	-6.0	Roll Left	Slow	73.5	1.0	110	245 AGL, better rates
322	6:54:52	6:55:38	R10	80	250	-6.0	Roll Left	Slow	73.7	0.0	110	250 AGL, +1 KIAS
323	6:57:47	6:58:36	R24	80	250	-6.0	Roll Right	Fast	74.0	0.7	110	control rate fast
324	7:00:39	7:01:28	R24	80	250	-6.0	Roll Right	Fast	74.0	0.0	110	low alt
325	7:03:12	7:04:02	R24	80	250	-6.0	Roll Right	Fast	74.1	0.0	111	Wind 1.6@266@260 AGL
326	7:05:41	7:06:33	R24	80	250	-6.0	Roll Right	Fast	74.3	0.0	111	good
327	7:08:11	7:09:00	R22	80	250	-6.0	Roll Right	Slow	74.5	0.0	111	light on fuel
328	7:10:43	7:11:30	R22	80	250	-6.0	Roll Right	Slow	74.7	0.0	111	medium rate
329	7:13:05	7:13:56	R22	80	250	-6.0	Roll Right	Slow	74.7	0.0	111	Wind 1.6@290@260 AGL, 230 AGL good rate
NA	NA	NA	D10	80	250	-6.0	Pitch Up	Slow	75.1	0.0	111	No data call
330	7:18:42	7:19:44	D10	80	250	-6.0	Pitch Up	Slow	75.2	0.0	111	good rate, 260 AGL
331	7:21:21	7:22:18	D10	80	250	-6.0	Pitch Up	Slow	75.4	0.0	111	good rate, 260 AGL

Table 17: Flight 1280 Test Card, 6/25/2011, Maneuver Array

NASA Run Num	Data On Time	Data Off Time	Cond Counter	KIAS	Cross Alt	Flight Path Angle	Direct	Rate	Ground Temp	Wind Speed	Wind Heading	Comments
901	4:51:41	4:52:42	AMB	NA	NA	NA	NA	NA	68.1	2.7	346	ambient
341	5:56:23	5:57:37	L1	80	200	0.0	NA	NA	68.0	1.5	82	Wind 5.7@75@200 AGL
342	6:01:51	6:02:41	D12	80	250	-6.0	Pitch Up	Fast	67.9	2.2	81	man start moved 150m back, 300 AGL
343	6:04:58	6:05:48	R22	80	250	-6.0	Roll Right	Slow	67.8	2.2	73	290 AGL, medium rate

Continued on next page

Table 17: *continued*

NASA Run Num	Data On Time	Data Off Time	Cond Counter	KIAS	Cross Alt	Flight Path Angle	Direct	Rate	Ground Temp	Wind Speed	Wind Heading	Comments
344	6:07:42	6:08:28	R22	80	250	-6.0	Roll Right	Slow	67.8	2.2	61	none
345	6:10:16	6:11:12	R22	80	250	-6.0	Roll Right	Slow	67.8	2.2	61	-1 KIAS, good rate
346	6:13:14	6:14:15	R21	60	250	-6.0	Roll Right	Fast	67.9	0.2	61	310 AGL, no Mic 40
347	6:16:11	6:17:11	R21	60	250	-6.0	Roll Right	Fast	68.1	1.5	61	315 AGL, little fast control rate
348	6:19:13	6:20:16	R21	60	250	-6.0	Roll Right	Fast	68.2	2.2	61	260 AGL
349	6:22:20	6:23:21	R21	60	250	-6.0	Roll Right	Fast	68.4	2.9	60	good rate, above path
350	6:25:35	6:26:38	D7	60	250	-6.0	Pitch Up	Slow	68.5	3.2	57	good rates
351	6:28:48	6:29:54	D7	60	250	-6.0	Pitch Up	Slow	68.8	2.2	59	good rates, on course, 1-2 KIAS slow
352	6:32:14	6:33:13	D9	60	250	-6.0	Pitch Up	Fast	69.1	2.0	61	good rates, on condition
353	6:35:30	6:36:40	D9	60	250	-6.0	Pitch Up	Fast	69.5	1.0	68	none
354	6:39:07	6:40:15	D9	60	250	-6.0	Pitch Up	Fast	69.7	1.5	68	+/- 1 KIAS, rates slow
355	6:42:21	6:43:29	D9	60	250	-6.0	Pitch Up	Fast	70.2	1.5	67	good rates, good course
356	6:45:44	6:46:21	D4	80	150	0.0	Pitch Up	Slow	70.3	1.7	67	120 AGL over MIP, good rate and course
357	6:48:17	6:49:08	D4	80	150	0.0	Pitch Up	Slow	70.7	1.0	67	rate a little faster, but still slow
358	6:50:54	6:51:45	D4	80	150	0.0	Pitch Up	Slow	71.1	1.5	67	good, slow input (4-4.5 s)
359	6:53:35	6:54:21	D6	80	150	0.0	Pitch Up	Fast	71.3	1.5	67	on condition
360	6:56:11	6:57:00	D6	80	150	0.0	Pitch Up	Fast	71.3	1.2	70	rate slightly slow
361	6:58:49	6:59:44	D6	80	150	0.0	Pitch Up	Fast	71.2	2.4	82	quick control rate
362	7:01:26	7:02:16	D6	80	150	0.0	Pitch Up	Fast	71.5	2.2	81	-1 KIAS, good rate/course
363	7:04:20	7:05:16	D3	60	150	0.0	Pitch Up	Fast	71.5	1.0	81	collective increase about 2 sec in to hold NR

Continued on next page

Table 17: *continued*

NASA Run Num	Data On Time	Data Off Time	Cond Counter	KIAS	Cross Alt	Flight Path Angle	Direct	Rate	Ground Temp	Wind Speed	Wind Heading	Comments
364	7:07:13	7:08:15	D3	60	150	0.0	Pitch Up	Fast	71.8	1.2	81	none
365	7:10:15	7:11:19	D3	60	150	0.0	Pitch Up	Fast	72.0	3.4	68	medium control rate
366	7:13:15	7:14:23	D3	60	150	0.0	Pitch Up	Fast	72.1	3.4	68	slightly high – good
367	7:16:21	7:17:27	D3	60	150	0.0	Pitch Up	Fast	76.9	2.7	77	Wind 5.6@74@200 AGL, stick bumped
368	7:20:06	7:20:51	R6	80	150	0.0	Roll Left	Fast	73.0	4.2	53	good
-	-	-	-	-	-	-	-	-	-	-	-	Refuel
369	8:02:34	8:03:22	R6	80	150	0.0	Roll Left	Fast	77.1	2.0	41	Wind 4.3@78@200 AGL, +1 KIAS
371	8:07:32	8:08:24	R6	80	150	0.0	Roll Left	Fast	77.6	2.9	36	good
372	8:10:04	8:10:50	R6	80	150	0.0	Roll Left	Fast	77.8	3.2	23	120 AGL
373	8:12:35	8:13:27	R4	80	150	0.0	Roll Left	Slow	77.5	2.2	15	good
374	8:15:09	8:15:57	R4	80	150	0.0	Roll Left	Slow	78.4	0.0	12	good rate, good course
375	8:17:45	8:18:34	R4	80	150	0.0	Roll Left	Slow	78.6	0.7	30	rate a little fast (medium)
376	8:20:21	8:21:13	R4	80	150	0.0	Roll Left	Slow	79.0	1.5	41	no mic 44
377	8:23:00	8:23:48	R4	80	150	0.0	Roll Left	Slow	78.7	1.2	18	good
378	8:25:49	8:26:34	R18	80	150	0.0	Roll Right	Fast	79.1	2.2	18	good
379	8:28:14	8:28:59	R18	80	150	0.0	Roll Right	Fast	79.0	1.0	18	good
380	8:30:39	8:31:27	R18	80	150	0.0	Roll Right	Fast	79.5	1.5	18	good
381	8:33:06	8:33:52	R18	80	150	0.0	Roll Right	Fast	79.4	2.2	29	-1 KIAS
382	8:35:36	8:36:22	R16	80	150	0.0	Roll Right	Slow	79.7	2.7	69	good
383	8:38:01	8:38:54	R16	80	150	0.0	Roll Right	Slow	80.0	2.2	43	none
384	8:40:28	8:41:18	R16	80	150	0.0	Roll Right	Slow	79.8	0.0	342	-1 KIAS, little fast rate
385	8:42:58	8:43:49	R16	80	150	0.0	Roll Right	Slow	79.8	1.5	326	none
386	8:45:25	8:46:26	R15	60	150	0.0	Roll Right	Fast	79.8	1.7	322	-1 KIAS, medium rate

Continued on next page

Table 17: *continued*

NASA Run Num	Data On Time	Data Off Time	Cond Counter	KIAS	Cross Alt	Flight Path Angle	Direct	Rate	Ground Temp	Wind Speed	Wind Heading	Comments
387	8:48:12	8:49:15	R15	60	150	0.0	Roll Right	Fast	80.9	4.2	21	50 AGL low, -2 KIAS
388	8:50:59	8:52:01	R15	60	150	0.0	Roll Right	Fast	80.3	2.2	10	1-2 KIAS slow, o.w. good
389	8:53:32	8:54:53	R15	60	150	0.0	Roll Right	Fast	79.9	2.2	351	good
390	8:56:24	8:57:12	C4	80	150	0.0	Pull Up	Slow	80.3	3.7	350	input late (100 m)
391	8:59:05	8:59:58	C4	80	150	0.0	Pull Up	Slow	80.7	1.5	358	good
392	9:02:01	9:02:52	C6	80	150	0.0	Pull Up	Fast	81.2	2.2	6	good, 1 sec to 10% rate
393	9:04:40	9:05:35	C6	80	150	0.0	Pull Up	Fast	81.6	0.0	30	late input (50 m)
394	9:07:21	9:08:12	C6	80	150	0.0	Pull Up	Fast	82.0	2.2	37	good 1 sec to 12%
395	9:10:07	9:10:57	C6	80	150	0.0	Pull Up	Fast	82.1	2.2	22	still late
396	9:12:50	9:13:14	C6	80	150	0.0	Pull Up	Fast	81.5	2.2	348	good
398	9:19:24	9:20:30	A5	60	200	-4.5	NA	NA	82.1	2.2	345	+/- 2 KIAS, +/- 30 ft
399	9:22:44	9:23:48	A12	70	200	-4.5	NA	NA	81.8	1.0	335	+1/-3 KIAS
400	9:25:57	9:26:52	A19	80	200	-4.5	NA	NA	82.2	0.0	335	+1/-2 KIAS
401	9:28:49	9:29:46	A26	90	200	-4.5	NA	NA	82.8	2.9	329	bumpy
402	9:31:57	9:32:57	A16	70	200	-10.5	NA	NA	83.0	2.7	298	bumpy
403	9:35:42	9:36:37	A16	70	200	-10.5	NA	NA	82.5	2.0	317	-4 KIAS, above glide slope
404	9:39:03	9:40:09	A16	70	200	-10.5	NA	NA	83.2	2.2	339	large control inputs
405	9:42:28	9:43:46	L1	80	200	0.0	NA	NA	83.3	5.4	243	+/- 200 FPM sink rate
406	9:46:23	9:47:13	D12	80	250	-6.0	Pitch Up	Fast	82.7	3.9	292	none
902	10:26:14	10:27:15	AMB	0	0	0.0	0.0	0	82.9	6.6	211	ambient

Table 18: Flight 1282 Test Card, 6/26/2011, Maneuver Array

NASA Run Num	Data On Time	Data Off Time	Cond Counter	KIAS	Cross Alt	Flight Path Angle	Direct	Rate	Ground Temp	Wind Speed	Wind Heading	Comments
901	5:21:05	5:22:06	AMB	NA	NA	NA	NA	NA	72.0	1.0	136	ambient
411	5:56:17	5:57:35	L1	80	200	0.0	NA	NA	72.6	1.7	136	housekeeping
412	6:00:08	6:01:01	D12	80	250	-6.0	Pitch Up	Fast	73.1	1.7	136	man housekeeping, rate a bit fast
413	6:03:20	6:04:14	D10	80	250	-6.0	Pitch Up	Slow	73.1	2.0	135	Wind 4.5@318@200 AGL, medium rate actual
414	6:06:20	6:07:15	D10	80	250	-6.0	Pitch Up	Slow	72.9	2.0	134	good
415	6:09:26	6:10:19	D10	80	250	-6.0	Pitch Up	Slow	73.7	2.0	133	rate - 4 sec (slow)
416	6:12:41	6:13:31	R12	80	250	-6.0	Roll Left	Fast	73.8	2.0	133	good rate/airspeed, glideslope 1.5 deg
417	6:15:33	6:16:23	R12	80	250	-6.0	Roll Left	Fast	73.8	1.5	133	good
418	6:18:21	6:19:10	R10	80	250	-6.0	Roll Left	Slow	73.7	1.2	133	fast rate actual
419	6:21:00	6:21:57	R10	80	250	-6.0	Roll Left	Slow	73.8	1.0	133	good, Wind 4.3@325@240
420	6:23:37	6:24:30	R10	80	250	-6.0	Roll Left	Slow	73.8	0.7	133	bumpy input
421	6:26:20	6:27:11	R10	80	250	-6.0	Roll Left	Slow	74.0	0.7	133	good
422	6:29:06	6:29:59	R24	80	250	-6.0	Roll Right	Fast	73.9	0.0	133	unsmooth input, Wind 5.8@314@240 AGL
423	6:31:46	6:32:34	R24	80	250	-6.0	Roll Right	Fast	74.0	0.0	133	rate medium actual
424	6:34:21	6:35:11	R24	80	250	-6.0	Roll Right	Fast	74.0	0.2	133	good, +/- 1 KIAS
425	6:36:50	6:37:43	R24	80	250	-6.0	Roll Right	Fast	74.1	0.5	133	+/- 1 KIAS
426	6:39:30	6:40:19	C10	80	250	0.0	Push Over	Slow	74.4	0.0	133	rate medium actual
427	6:42:10	6:43:02	C10	80	250	0.0	Push Over	Slow	74.4	0.2	133	X = MIP- 25m
428	6:45:00	6:45:48	C10	80	250	0.0	Push Over	Slow	74.3	0.0	133	3-4 sec rate actual
429	6:47:52	6:48:20	C12	80	250	0.0	Push Over	Fast	74.1	0.0	133	very fast rate
430	6:50:40	6:51:31	C12	80	250	0.0	Push Over	Fast	74.2	0.2	133	good

Continued on next page

Table 18: *continued*

NASA Run Num	Data On Time	Data Off Time	Cond Counter	KIAS	Cross Alt	Flight Path Angle	Direct	Rate	Ground Temp	Wind Speed	Wind Heading	Comments
431	6:53:54	6:54:37	C12	80	250	0.0	Push Over	Fast	74.7	1.5	93	Noticed 150 AGL for all C push overs (C10, C12)
432	6:56:25	6:56:25	C12	80	250	0.0	Push Over	Fast	74.6	1.2	93	good
433	6:59:26	7:00:17	C4	80	150	0.0	Pull Up	Slow	75.5	0.0	93	fast actual, fixed cyclic, no real airspeed change
434	7:02:10	7:03:01	C4	80	150	0.0	Pull Up	Slow	75.6	0.2	93	roll response without cyclic correction
435	7:05:04	7:06:09	C1	60	150	0.0	Pull Up	Slow	75.6	0.7	93	glideslope low
436	7:08:05	7:09:11	C1	60	150	0.0	Pull Up	Slow	75.9	1.0	93	160 AGL, little roll response
437	7:11:08	7:12:13	C3	60	150	0.0	Pull Up	Fast	75.9	2.0	62	medium rate actual
438	7:14:17	7:15:20	C3	60	150	0.0	Pull Up	Fast	76.0	1.7	22	good
439	7:17:23	7:18:36	D1	60	150	0.0	Pitch Up	Slow	75.8	2.0	8	good
-	-	-	-	-	-	-	-	-	-	-	-	Refuel
440	8:21:10	8:22:28	L1	80	200	0.0	0.0	0	80.7	5.1	333	housekeeping, +3/-2 KIAS
441	8:25:06	8:26:26	A10	60	200	-12.0	NA	NA	80.9	7.6	312	unsteady
442	8:28:48	8:30:18	A10	60	200	-12.0	NA	NA	81.1	6.1	313	unsteady
443	8:32:35	8:33:39	A24	80	200	-12.0	NA	NA	80.9	2.7	291	unsteady
444	8:36:05	8:37:25	A8	60	200	-9.0	NA	NA	81.0	3.2	307	better quality
445	8:39:46	8:40:45	A22	80	200	-9.0	NA	NA	81.6	5.1	342	better, Wind 7.2@310@300 AGL
446	8:43:17	8:44:38	A6	60	200	-6.0	NA	NA	82.0	7.1	319	glideslope unsteady
449	8:54:18	8:55:16	A18	80	200	-3.0	NA	NA	81.4	6.1	311	unsteady glideslope
450	8:57:44	8:58:35	D12	80	250	-6.0	Pitch Up	Fast	81.2	7.3	335	housekeeping, good, Wind 8.1@327@260 AGL
451	9:00:47	9:02:08	L1	80	200	0.0	NA	NA	81.9	7.8	345	housekeeping, unsteady alt

Table 19: Flight 1285 Test Card, 6/28/2011, Maneuver Array

NASA Run Num	Data On Time	Data Off Time	Cond Counter	KIAS	Cross Alt	Flight Path Angle	Direct	Rate	Ground Temp	Wind Speed	Wind Heading	Comments
901	5:02:09	5:03:10	AMB	0	0	0.0	0.0	0	74.4	0.0	322	ambient
461	5:45:10	5:46:23	L1	80	150	0.0	0.0	0	73.8	0.0	323	camera crew near ref mic position
462	5:51:01	5:52:55	D12	80	250	-6.0	Pitch Up	Fast	73.6	0.0	323	+1 KIAS, GS high
463	5:54:29	5:56:24	R15	60	150	0.0	Roll Right	Fast	73.7	0.0	323	1.5 sec rate
464	5:57:32	5:59:22	R15	60	150	0.0	Roll Right	Fast	73.4	0.0	323	+/-1 KIAS, 140 AGL
465	6:00:31	6:02:20	R3	60	150	0.0	Roll Left	Fast	73.5	0.0	323	1 sec rate, +/- 10 AGL
466	6:03:17	6:05:15	R3	60	150	0.0	Roll Left	Fast	73.7	0.0	323	good
467	6:06:21	6:07:56	R18	80	150	0.0	Roll Right	Fast	73.7	0.0	323	good
468	6:08:56	6:10:36	R18	80	150	0.0	Roll Right	Fast	73.9	0.0	323	good
469	6:11:48	6:13:49	R17	80	150	0.0	Roll Right	Med	74.0	0.0	324	good
470	6:14:35	6:16:05	R17	80	150	0.0	Roll Right	Med	74.2	0.0	324	good
471	6:17:06	6:18:43	R6	80	150	0.0	Roll Left	Fast	74.5	0.0	324	135 AGL,+/-1 KIAS, 1 sec rate, good
472	6:19:35	6:21:16	R6	80	150	0.0	Roll Left	Fast	74.6	0.0	324	good, Wind 3.5@ 294@160 AGL
473	6:22:06	6:23:47	R5	80	150	0.0	Roll Left	Med	74.5	0.0	324	+/-1 KIAS, rate slow, 2-3 sec
474	6:24:49	6:26:26	R5	80	150	0.0	Roll Left	Med	74.8	0.0	324	good
475	6:27:22	6:29:05	D5	80	150	0.0	Pitch Up	Med	75.0	0.0	324	good
476	6:30:22	6:32:07	D5	80	150	0.0	Pitch Up	Med	75.2	0.0	324	good
477	6:33:21	6:35:08	D11	80	250	-6.0	Pitch Up	Med	74.7	0.0	324	good
478	6:36:26	6:38:10	D11	80	250	-6.0	Pitch Up	Med	74.8	0.0	324	good
479	6:39:20	6:41:14	R12	80	250	-6.0	Roll Left	Fast	75.5	0.0	324	good
480	6:42:10	6:44:07	R12	80	250	-6.0	Roll Left	Fast	75.6	0.0	325	good, 79 KIAS
481	6:45:00	6:46:54	R11	80	250	-6.0	Roll Left	Med	75.7	0.0	325	good

Continued on next page

Table 19: *continued*

NASA Run Num	Data On Time	Data Off Time	Cond Counter	KIAS	Cross Alt	Flight Path Angle	Direct	Rate	Ground Temp	Wind Speed	Wind Heading	Comments
482	6:47:41	6:49:31	R11	80	250	-6.0	Roll Left	Med	75.9	0.0	327	good
483	6:50:36	6:52:31	R24	80	250	-6.0	Roll Right	Fast	76.3	0.0	327	good, 1-1.5 sec rate
484	6:53:31	6:55:19	R24	80	250	-6.0	Roll Right	Fast	76.5	0.2	327	slow rate (2 sec)
485	6:56:29	6:58:00	R24	80	250	-6.0	Roll Right	Fast	76.8	0.0	328	good
486	6:58:58	7:00:53	R23	80	250	-6.0	Roll Right	Med	77.1	0.0	328	good
487	7:01:48	7:03:33	R23	80	250	-6.0	Roll Right	Med	76.9	0.0	328	good
488	7:04:40	7:06:41	R9	60	250	-6.0	Roll Left	Fast	77.8	0.0	328	good
489	7:07:34	7:09:49	R9	60	250	-6.0	Roll Left	Fast	78.0	0.0	328	57 KIAS
490	7:12:02	7:14:03	D19	80	250	-9.0	Pitch Up	Slow	78.3	0.0	328	good
491	7:15:15	7:17:02	D19	80	250	-9.0	Pitch Up	Slow	78.5	0.0	328	good
492	7:18:54	7:20:37	D21	80	250	-9.0	Pitch Up	Fast	78.4	0.0	328	good
493	7:21:52	7:23:40	D21	80	250	-9.0	Pitch Up	Fast	78.2	0.0	328	good
-	-	-	-	-	-	-	-	-	-	-	-	Refuel
494	8:02:10	8:05:04	A10	60	200	-12.0	0.0	0	80.5	4.6	279	slope/lateral corrections
495	8:06:32	8:08:54	A10	60	200	-12.0	0.0	0	80.7	4.4	328	high (230 AGL cross)
496	8:10:31	8:12:29	A24	80	200	-12.0	0.0	0	81.0	4.4	299	+3 KIAS, 260 AGL
497	8:13:51	8:16:23	A4	60	200	-3.0	0.0	0	81.5	5.6	313	+/- 2 KIAS, 175 AGL, Wind 7@303@200 AGL
498	8:18:10	8:20:07	A18	80	200	-3.0	0.0	0	81.4	5.4	290	good
499	8:21:32	8:23:21	M2	80	200	0.0	Accel	Med	81.1	5.1	307	2 kts/s actual
500	8:24:55	8:26:35	M2	80	200	0.0	Accel	Med	81.7	3.7	340	2.5 kts/s actual
501	8:28:01	8:29:45	M3	80	200	0.0	Accel	Fast	81.7	4.9	321	accel unsure? Initiate at 2000 ft for future accel
502	8:31:56	8:33:41	M3	80	200	0.0	Accel	Fast	81.9	5.9	290	4 kts/s actual, 5 sec to get collective w/o overtorque

Continued on next page

Table 19: *continued*

NASA Run Num	Data On Time	Data Off Time	Cond Counter	KIAS	Cross Alt	Flight Path Angle	Direct	Rate	Ground Temp	Wind Speed	Wind Heading	Comments
503	8:35:05	8:36:58	M3	80	200	0.0	Accel	Fast	82.3	4.2	296	2 kts/s actual
504	8:38:17	8:40:05	M4	80	200	0.0	Decel	Slow	81.4	9.3	315	overdrive some mics, Mic 51 did not record, good cond
505	8:41:23	8:43:19	M5	80	200	0.0	Decel	Med	81.6	7.8	333	good, decel 3-3.5 kts/s
506	8:44:37	8:46:17	M6	80	200	0.0	Decel	Fast	81.6	7.3	301	good, 5 kts/s (approaching overspeed)
507	8:47:49	8:49:59	M6	80	200	0.0	Decel	Fast	82.0	5.6	313	good, 5 kts/s, 33,34,35 overdriven
508	8:51:34	8:53:20	Y6	60-80	200	0.0	Left/Accel	Fast	82.3	9.0	279	wrong maneuver
509	8:55:28	8:57:20	Y6	60-80	200	0.0	Left/Accel	Fast	82.3	7.6	313	accel 500-700m prior to roll initiation
510	8:58:47	9:00:31	Y6	60-80	200	0.0	Left/Accel	Fast	82.4	5.9	289	good! 2 kts/s accel, good timing on roll
511	9:01:36	9:03:28	Y24	60-80	200	0.0	Right/Accel	Fast	82.3	9.8	307	roll 100m too soon
512	9:04:20	9:06:17	Y24	60-80	200	0.0	Right/Accel	Fast	82.3	7.3	307	good, input at MIP
513	9:07:20	9:09:31	Z15	80	200	6.0	Right	Fast	81.9	7.3	313	climb start 300m before MIP
514	9:11:05	9:12:42	Z15	80	200	6.0	Right	Fast	82.2	8.3	281	good
515	9:13:48	9:15:21	Z15	80	200	6.0	Right	Fast	82.7	6.4	297	good
516	9:16:15	9:18:17	L1	80	150	0.0	0.0	0	83.4	6.8	304	housekeeping
517	9:20:02	9:21:55	D12	80	250	-6.0	Pitch Up	Fast	83.2	2.7	317	housekeeping

Table 20: Flight 1287 Test Card, 6/30/2011, Maneuver Array

NASA Run Num	Data On Time	Data Off Time	Cond Counter	KIAS	Cross Alt	Flight Path Angle	Direct	Rate	Ground Temp	Wind Speed	Wind Heading	Comments
901	5:24:51	5:25:51	AMB	NA	NA	NA	NA	NA	70.7	0.2	356	ambient
521	5:45:00	5:47:03	L1	80	200	0.0	NA	NA	70.7	0.0	355	housekeeping
522	5:52:13	5:53:42	R17	80	150	0.0	Roll Right	Med	70.6	1.0	355	good
523	5:54:40	5:56:04	R17	80	150	0.0	Roll Right	Med	70.5	1.5	355	good, Wind 6.4@14@160 AGL
524	5:56:57	5:58:24	R18	80	150	0.0	Roll Right	Fast	70.6	1.2	355	good
525	5:59:20	6:00:47	R18	80	150	0.0	Roll Right	Fast	70.6	0.5	355	good, Wind 7.8@19@160 AGL
526	6:01:44	6:03:03	D5	80	150	0.0	Pitch Up	Med	70.6	1.2	355	+1KIAS, good
527	6:04:01	6:05:29	D5	80	150	0.0	Pitch Up	Med	70.5	0.5	355	fast rate, other a/c
528	6:06:28	6:08:02	D5	80	150	0.0	Pitch Up	Med	70.5	1.5	355	other aircraft in area, good
529	6:08:52	6:10:22	D6	80	150	0.0	Pitch Up	Fast	70.4	1.7	356	good
530	6:11:19	6:13:03	D6	80	150	0.0	Pitch Up	Fast	70.4	1.7	356	good
531	6:14:13	6:16:15	D3	60	150	0.0	Pitch Up	Fast	70.3	1.7	356	-1 KIAS, 105 AGL
532	6:17:24	6:19:38	R21	60	250	-6.0	Roll Right	Fast	70.4	2.0	352	slope unstable, strong wind grad (4@100 ft)
533	6:20:33	6:22:41	R21	60	250	-6.0	Roll Right	Fast	70.5	2.0	343	pitch up instead of roll
534	6:23:52	6:26:01	R21	60	250	-6.0	Roll Right	Fast	70.7	1.5	344	good
535	6:27:02	6:28:36	C10	80	250	0.0	Push Over	Slow	71.0	1.0	351	33,34,35 overdriven, fast rate
536	6:29:38	6:31:19	C10	80	250	0.0	Push Over	Slow	71.0	1.0	351	good
537	6:32:36	6:34:19	C12	80	250	0.0	Push Over	Fast	71.2	2.2	348	good
538	6:35:26	6:37:00	C12	80	250	0.0	Push Over	Fast	71.3	0.7	348	190 AGL, good
539	6:38:10	6:39:50	C12	80	250	0.0	Push Over	Fast	71.5	1.5	349	good, Wind 7.2@11@160 AGL
540	6:41:07	6:42:35	M5	80	150	0.0	Decel	Med	71.8	0.7	349	100m too early
541	6:43:31	6:45:11	M5	80	150	0.0	Decel	Med	71.8	1.7	349	rate unsure

Continued on next page

Table 20: *continued*

NASA Run Num	Data On Time	Data Off Time	Cond Counter	KIAS	Cross Alt	Flight Path Angle	Direct	Rate	Ground Temp	Wind Speed	Wind Heading	Comments
542	6:46:22	6:47:57	M5	80	150	0.0	Decel	Med	71.8	1.7	349	rate a bit slower
543	6:49:17	6:50:49	M6	80	150	0.0	Decel	Fast	72.2	2.4	346	good
544	6:52:13	6:54:04	M6	80	150	0.0	Decel	Fast	72.7	1.5	337	good
545	6:55:46	6:57:23	M2	80	150	0.0	Accel	Med	72.7	2.2	343	1 kts/s
546	6:58:41	7:00:20	M3	80	150	0.0	Accel	Fast	73.0	2.4	333	2-3 kts/s
547	7:01:33	7:03:12	M3	80	150	0.0	Accel	Fast	73.0	2.4	332	2-3 kts/s
548	7:04:30	7:05:59	Z15	80	150	6.0	Roll Right	Fast	73.3	2.7	332	+/-1 KIAS, good track, shallow climb
549	7:06:51	7:08:26	Z15	80	150	6.0	Roll Right	Fast	73.6	3.9	358	+/-1 KIAS, good
550	7:09:45	7:11:29	Z6	80	150	6.0	Roll Left	Fast	73.6	3.2	340	late input
551	7:12:43	7:14:02	Z6	80	150	6.0	Roll Left	Fast	73.8	3.4	350	good, +/-1 KIAS, fast rate
-	-	-	-	-	-	-	-	-	-	-	-	Refuel
552	7:51:47	7:53:31	Z18	80	150	9.0	Roll Right	Fast	76.6	4.9	350	+/- 1 KIAS, bumped collective on climb
553	7:54:47	7:56:23	Z18	80	150	9.0	Roll Right	Fast	77.0	5.6	351	roll a bit early
554	7:57:36	7:59:32	Z18	80	150	9.0	Roll Right	Fast	77.1	4.4	353	
555	8:01:01	8:02:37	Z9	80	150	9.0	Roll Left	Fast	77.4	6.9	6	+1 KIAS
556	8:03:53	8:05:31	Z9	80	150	9.0	Roll Left	Fast	77.7	5.6	13	good (F15 over B70 @ 16000 AGL)
557	8:07:49	8:09:43	Y30	80	150	0.0	Decel/Right	Slow/Fast	77.9	3.4	345	75 KIAS at MIP, slow roll rate
558	8:11:18	8:12:55	Y30	80	150	0.0	Decel/Right	Slow/Fast	78.1	5.6	1	mic 49 overdriven
559	8:14:15	8:15:44	Y30	80	150	0.0	Decel/Right	Slow/Fast	78.5	5.4	5	83 KIAS at MIP
560	8:17:03	8:18:38	Y12	80	150	0.0	Decel/Left	Slow/Fast	78.8	5.6	13	80 KIAS at MIP

Continued on next page

Table 20: *continued*

NASA Run Num	Data On Time	Data Off Time	Cond Counter	KIAS	Cross Alt	Flight Path Angle	Direct	Rate	Ground Temp	Wind Speed	Wind Heading	Comments
561	8:19:48	8:21:45	Y12	80	150	0.0	Decel/Left	Slow/Fast	78.7	5.9	358	good
562	8:22:33	8:24:03	Y33	80	150	0.0	Decel/Right	Med/Fast	79.2	5.1	355	good
563	8:25:22	8:26:54	Y33	80	150	0.0	Decel/Right	Med/Fast	79.8	4.2	22	good
564	8:28:07	8:29:39	Y15	80	150	0.0	Decel/Left	Med/Fast	79.3	5.6	355	overdrove 41
565	8:30:45	8:32:11	Y15	80	150	0.0	Decel/Left	Med/Fast	79.4	6.4	2	good
566	8:33:31	8:35:44	Y21	80	150	0.0	Accel/Right	Slow/Fast	79.5	6.6	354	not much accel
567	8:36:35	8:38:32	Y21	80	150	0.0	Accel/Right	Slow/Fast	79.6	6.4	8	still slow accel
568	8:39:53	8:41:38	Y3	80	150	0.0	Accel/Left	Slow/Fast	80.0	5.1	360	slow accel
569	8:42:47	8:44:36	Y3	80	150	0.0	Accel/Left	Slow/Fast	80.1	6.4	2	still slow
570	8:48:34	8:50:38	Y24	80	150	0.0	Accel/Right	Med/Fast	80.4	4.4	0	good
571	8:51:43	8:53:32	Y24	80	150	0.0	Accel/Right	Med/Fast	81.6	5.9	18	Left roll actual
572	8:54:39	8:56:28	Y24	80	150	0.0	Accel/Right	Med/Fast	81.4	9.0	8	better accel
573	8:57:44	8:59:35	Y6	80	150	0.0	Accel/Left	Med/Fast	81.1	8.6	5	good
574	9:00:52	9:03:04	L1	80	150	0.0	NA	NA	81.1	9.5	10	+/- 2 KIAS
575	9:05:11	9:07:16	D12	80	150	-6.0	Pitch Up	Fast	81.5	6.1	4	good

Table 21: Collective Flight Test Points

		Rate	
KIAS	Input	Slow	Fast
60	PU	C1 - 2	C3 - 2
80	PU	C4 - 3	C6 - 6
	PO	C10 - 5	C12 -7

PU - Collective Pull

PO - Collective Drop

Table 22: Cyclic Pitch-Up Flight Test Points

		Rate		
KIAS	Angle	Slow	Medium	Fast
60	0°	D1 - 1		D3 - 6
	-6°	D7 - 2		D9 - 5
80	0°	D4 - 3	D5 - 2	D6 - 5
	-6°	D10 - 9	D11 - 2	D12 - 12
	-9°	D19 - 2		D21 - 2
100	0°		D22 - 3	D23 - 1

Table 23: Cyclic Roll Flight Test Points

			Rate		
KIAS	Angle	Input	Slow	Medium	Fast
60	0°	Left			R3 - 2
		Right			R15 - 6
	6°	Left			R9 - 2
		Right			R21 - 6
80	0°	Left	R4 - 5	R5 - 2	R6 - 7
		Right	R16 - 4	R17 - 2	R18 - 6
	6°	Left	R10 - 11	R11 - 2	R12 - 9
		Right	R22 - 6	R23 - 2	R24 - 11
100	0°	Right		R26 - 2	R25 - 2

Table 24: Quick Start, Quick Stop Flight Test Points

	Rate		
KIAS	Slow	Medium	Fast
80 to 100		M2 - 3	M3 - 5
80 to 60	M4 - 1	M5 - 4	M6 - 4

Table 25: Roll Angle Change During Climbing Flight Test Points

		Direction	
KIAS	Angle	Left	Right
80	0° to 6°	Z6 - 2	Z15 - 5
	0° to 9°	Z9 - 2	Z18 - 3

Table 26: Roll Angle Change During Accelerating/Decelerating Flight Test Points

		Cyclic Input	
KIAS	KIAS kt/s	Left	Right
60 to 80	1	Y3 - 2	Y21 - 2
	2	Y6 - 5	Y24 - 4
100 to 80	-1	Y12 - 2	Y30 - 3
	-2	Y15 - 2	Y33 - 2

Table 27: Flight 1288 Test Card, 7/1/2011, Terminal Area Array

NASA Run Num	Data On Time	Data Off Time	Cond Counter	KIAS	Cross Alt	Ground Temp	Wind Speed	Wind Heading	Comments
901	5:25:46	5:27:17	AMB	NA	NA	71.9	0.0	343	ambient
601	5:44:18	5:46:25	L1	80	150	71.4	1.0	343	housekeeping - stablized by X = -5000
602	5:50:41	5:52:54	L1	80	150	71.2	1.7	343	good
603	5:42:22	5:56:16	L6	100	150	71.1	2.4	343	good, -1 KIAS
604	5:57:37	5:59:15	L8	120	150	71.2	2.7	353	altitude unsteady until X = -1500
605	6:00:48	6:02:23	L8	120	150	71.2	2.9	353	117-118 KCAS
606	6:03:49	6:05:22	L10	140	150	71.0	2.9	355	A/S 138-140 KIAS
607	6:07:01	6:08:27	L10	140	150	71.0	2.2	3	A/S 139 KIAS, 131 KCAS
610	6:20:03	6:23:13	T2	NA	NA	71.2	0.5	3	overshoot TALP by 200 ft
611	6:25:06	6:28:26	T2	NA	NA	71.2	0.5	3	
612	6:33:46	6:35:53	T4	NA	NA	71.9	2.0	3	slightly left of course, 20-50 ft above GS
613	6:38:08	6:40:22	T4	NA	NA	72.2	1.7	3	may only slow to 20 KIAS at TALP
614	6:42:51	6:44:49	T5	NA	NA	73.2	1.2	3	approach auto
615	6:47:40	6:49:49	T5	NA	NA	73.2	1.7	3	near auto - good, wobbley course
616	6:53:11	6:55:29	T6	NA	NA	73.5	0.7	3	little low on approach, bit fast
617	6:57:52	7:00:31	T6	NA	NA	73.9	0.5	3	better
618	7:04:03	7:07:04	T7	NA	NA	74.5	1.7	13	40 ft above glideslop
619	7:10:20	7:13:29	T7	NA	NA	74.9	2.0	21	not on course
620	7:16:27	7:19:26	T7	NA	NA	75.0	3.2	11	good glideslope, constant accel
-	-	-	-	-	-	-	-	-	Refuel
621	8:19:46	8:22:44	T1	NA	NA	80.0	3.4	25	slightly under glideslope
623	8:26:53	8:30:24	T1	NA	NA	79.9	5.6	4	above glidepath, lateral deflections
624	8:33:04	8:35:35	T3	NA	NA	80.6	3.7	1	bit of course wander
625	8:38:44	8:41:30	T3	NA	NA	82.6	4.6	26	much better course

Continued on next page

Table 27: *continued*

NASA Run Num	Data On Time	Data Off Time	Cond Counter	KIAS	Cross Alt	Ground Temp	Wind Speed	Wind Heading	Comments
626	8:44:11	8:46:55	T8	NA	NA	82.4	4.4	33	good
627	8:49:22	8:52:12	T8	NA	NA	82.9	6.4	28	slowed to 95 kts early, then held on first segment
629	8:59:59	9:01:53	T9	NA	NA	84.2	4.4	29	terminated - below glidepath
630	9:04:35	9:06:59	T9	NA	NA	84.2	7.1	47	visual marker does not seem aligned with guidance
631	9:09:56	9:12:03	T9A	NA	NA	83.9	7.6	35	did not intercept flightpath at desired point
632	9:14:58	9:16:30	T9A	NA	NA	85.0	9.5	34	terminated - initial at 1,300 ft
633	9:19:19	9:22:11	T11	NA	NA	85.0	8.1	22	level 100-60 KIAS, steep descent 55 - 0
634	9:24:54	9:27:23	T11	NA	NA	86.1	4.6	19	
635	9:30:04	9:33:10	T11A	NA	NA	86.3	7.8	28	turning during approach, decelerating descending left turn
638	9:43:02	9:45:31	T10A	NA	NA	86.6	5.4	10	unguided - little fast and shallow, but closer to T10
639	9:48:34	9:50:53	T2	NA	NA	87.0	3.9	29	100 KIAS actual

Table 28: Reference File Variable Names

Column Number	Variable	Description	Units
1	test	Daily test number	
2	nasa	NASA run number	
3	bell	Bell run number	
4	utc_h_start	UTC start time hours	hours
5	utc_m_start	UTC start time minutes	minutes
6	utc_s_start	UTC start time seconds	secs
7	utc_secs_from_mid	UTC seconds from midnight	secs
8	utc_local_secs_from_mid	Local time seconds from midnight	secs
9	duration	Run length	secs
10	trfile	Bell CAFTA system file name	
11	ref_location	Reference mic description for guidance	
12	ref_mic_loc	Reference mic number for guidance	
13	ref_lat	Reference point latitude for guidance	
14	ref_lon	Reference point longitude for guidance	
15	ref_elips_ft	Reference point elipsoid height for guidance	ft
16	ref_hgt_ft	Reference point hgtm height for guidance	ft
17	test_cond	Planned test condition code	
18	overhead_time	Reference overhead time	secs
19	test_plan_ctr	Test condition counter	
20	description	Test condition description	
21	avg_grd_spd	Average ground speed	kts
22	profile_number	Bell guidance profile number	
23	true_heading	Commanded true heading	deg
24	gross_weight	Aircraft gross weight	pounds
25	target_ias	Commanded indicated airspeed	kts
26	asp_tol	Airspeed tolerance	kts
27	rtr_torque	Rotor torque	percent
28	fuel_rem	Fuel remaining	pounds
29	long_cg	Longitudinal center of gravity	in
30	fpa	Commanded flight path angle	deg
31	direction	Maneuver direction	
32	rate	Maneuver rate	
33	control_temp_F	Temperature at control van	deg F
34	control_ws_kts	Wind speed at control van	kts
35	control_wd	Wind direction at control van	deg
36	daily_weather_profile	Weather profile in structure flt*wp	
37	fwpinfo_profile_num	Weather profile number in fwpinfo	
38	comments	Comments from test cards	

Table 29: Pressure Time History File Contents

Variable Name	Description	Units
pressure	Acoustic pressure as measured	pascals
X	Mic X location in rotated coordinate frame	feet
Y	Mic Y location in rotated coordinate frame	feet
Z	Mic Z location in rotated coordinate frame	feet
overhead_time	Time that aircraft is closest to ref location	seconds
UTM_X	Mic X location in UTM coordinate frame	feet
UTM_Y	Mic Y location in UTM coordinate frame	feet
global.test	Test description	
global.location	Test location	
global.date	Date of test	
global.run_number	Run number	
global.noise_source	Aircraft type	
global.mic_number	Microphone number	
global.X	Mic X location in rotated coordinate frame	feet
global.Y	Mic Y location in rotated coordinate frame	feet
global.Z	Mic Z location in rotated coordinate frame	feet
global.sample_rate	Samples per second of pressure data	
global.start_time	Local seconds from midnight of first sample	secs
global.overhead_time	Time that aircraft is closest to ref location	seconds
global.number_samples	Number of data samples	
global.UTM_X	Mic X location in UTM coordinate frame	feet
global.UTM_Y	Mic Y location in UTM coordinate frame	feet

Table 30: Low Frequency Aircraft Data File Variables

Column Number	Variable Name	Description	Units	Source
1	timelf	UTC local seconds from midnight	secs	
2	Xlf	x coord along 326.3° flight track	ft	GPS
3	Ylf	y coord perp. to 326.3° flight track	ft	GPS
4	Zlf	elevation over microphone 11	ft	GPS
5	UTM_Xlf	x UTM coordinate + is East	ft	GPS
6	UTM_Ylf	y UTM coordinate + is North	ft	GPS
7	latlf	aircraft latitude		GPS
8	lonlf	aircraft longitude		GPS
9	geoidlf	GPS geoid height	m	GPS
10	iaslf	Indicated Airspeed	kts	VF0006
11	iasnewlf	calculated IAS	kts	
12	casnewlf	calibrated airspeed	kts	
13	gsktfltlf	ground speed	kts	GPS
14	tasnewlf	TAS using tempF and statpres	kts	
15	psidlf	Boom PSID	PSI	00VF06
16	statpreslf	Boom Static Pressure	PSI	PZ0002
17	totpreslf	Boom Total Pressure	PSI	PZ0003
18	tempFlf	° F from NASA weather balloon	F	NASA WB
19	aoalf	AC Angle of Attack	deg	00QP02
20	sidesliplf	Sideslip	deg	00QQ02
21	pitchratelf	AC Pitch Rate	deg/s	87RP01;
22	rollratelf	AC Roll Rate	deg/s	87RR01
23	yawratelf	AC Yaw Rate	deg/s	87RQ01
24	truehdnglf	true heading	deg	GPS
25	vertacclf	AC Vertical Accelerateion	G	00GV01
26	longcyclf	Longitudinal Cyclic	%	10DF04
27	latcyclf	Lateral Cyclic	%	10DL01
28	collf	Collective	%	10DF07
29	inupitchlf	INU Pitch Attitude	deg	00QP61
30	inurolllf	INU Roll Attitude	deg	00QR61
31	inuheadinglf	INU True Heading	deg	00DZ61
32	inupitchratelf	INU Pitch Rate	deg/s	00RP61
33	inurollratelf	INU Roll Rate	deg/s	00RR61
34	inuyawratelf	INU Yaw Rate	deg/s	00RQ61
35	inulongacclf	INU Longitudinal Acceleration	G	00GF10
36	inulatacclf	INU Lateral Acceleration	G	00GL10
37	inuvertacclf	INU Vertical Acceleration	G	00GV10
38	rtrspeedlf	Rotor Speed	RPM	RM3004

Table 31: High Frequency Aircraft Data File Variables

Column Number	Variable Name	Description	Units	Source
1	timelf	UTC local seconds from midnight	secs	
2	Xlf	x coord along 326.3° flight track	ft	GPS
3	Ylf	y coord perp. to 326.3° flight track	ft	GPS
4	Zlf	elevation over microphone 11	ft	GPS
5	UTM_Xlf	x UTM coordinate + is East	ft	GPS
6	UTM_Ylf	y UTM coordinate + is North	ft	GPS
7	latlf	aircraft latitude		GPS
8	lonlf	aircraft longitude		GPS
9	geoidlf	GPS geoid height	m	GPS
10	iaslf	Indicated Airspeed	kts	VF0006
11	iasnewlf	calculated IAS	kts	
12	casnewlf	calibrated airspeed	kts	
13	gsktfltlf	ground speed	kts	GPS
14	tasnewlf	TAS using tempF and statpres	kts	
15	psidlf	Boom PSID	PSI	00VF06
16	statpreslf	Boom Static Pressure	PSI	PZ0002
17	totpreslf	Boom Total Pressure	PSI	PZ0003
18	tempFlf	° F from NASA weather balloon	F	NASA WB
19	aoalf	AC Angle of Attack	deg	00QP02
20	sidesliplf	Sideslip	deg	00QQ02
21	pitchratelf	AC Pitch Rate	deg/s	87RP01;
22	rollratelf	AC Roll Rate	deg/s	87RR01
23	yawratelf	AC Yaw Rate	deg/s	87RQ01
24	truehdnglf	true heading	deg	GPS
25	vertacclf	AC Vertical Accelerateion	G	00GV01
26	longcyclf	Longitudinal Cyclic	%	10DF04
27	latcyclf	Lateral Cyclic	%	10DL01
28	collf	Collective	%	10DF07
29	inupitchlf	INU Pitch Attitude	deg	00QP61
30	inurolllf	INU Roll Attitude	deg	00QR61
31	inuheadinglf	INU True Heading	deg	00DZ61
32	inupitchratelf	INU Pitch Rate	deg/s	00RP61
33	inurollratelf	INU Roll Rate	deg/s	00RR61
34	inuyawratelf	INU Yaw Rate	deg/s	00RQ61
35	inulongacclf	INU Longitudinal Acceleration	G	00GF10
36	inulatacclf	INU Lateral Acceleration	G	00GL10
37	inuvertacclf	INU Vertical Acceleration	G	00GV10
38	rtrspeedlf	Rotor Speed	RPM	RM3004
39	redaz	azimuth angle for red blade	deg	
40	redtheta75	theta at .75 radius	deg	
41	orangeaz	azimuth angle for orange blade	deg	
42	orangetheta75	theta at .75 radius	deg	
43	blueaz	azimuth angle for blue blade	deg	
44	bluetheta75	theta at .75 radius	deg	
45	greenaz	azimuth angle for green blade	deg	
46	greentheta75	theta at .75 radius	deg	

Table 32: Azimuth Aircraft Data File Variables

Column Number	Variable Name	Description	Units
1	azsecs	UTC local seconds from midnight	sec
2	oneP	once per rev pulse 1 = red blade over tail	
3	onePaz	azimuth angle for red blade	deg

Table 33: Hemisphere File Contents

Variable Name	Description	Units
BB	Broadband data switch	
NB	Narrow-Band data switch	
PT	Pure-Tone data switch	
DOPPLER_SHIFT_REMOVED	0 = False and 1 = True	
EMPTY_WEIGHT	(not used for this test)	
FUEL_WEIGHT	(not used for this test)	
LOAD_WEIGHT	(not used for this test)	
RADIUS	Radius of Sound Sphere	ft
FLIGHT_PATH_ANGLE	Target flight path angle	deg
PYLON_ANGLE	(not used for this test)	
SPEED	True airspeed	kts
MASTTILT	(not used for this test)	
XYZ	(not used for this test)	
PHI	Spherical angle phi°	deg
THETA	Spherical angle theta	deg
FREQUENCY	Center frequencies	Hz
AMPLITUDE	Sound pressure level	dB
GROSS_WEIGHT	Aircraft gross weight	lbs
TARGET_SPEED	Commanded IAS	kts
TARGET_ANGLE	Commanded flight path angle	deg
OAT	Crossing altitude temperature	° F
CROSS_ALT	Crossing altitude at reference	ft
STAT_PRESS	Crossing altitude satic pressure	psi
WIND_SPEED	Crossing altitude wind speed	kts
WIND_DIR	Crossing altitude wind direction	deg
GROUND_SPEED	Average ground speed	kts
INDICATED_SPEED	Average IAS over processed data	kts
START_X	Processing starting X	ft
STOP_X	Processing ending X	ft
global.title	Hemisphere description	

Figures

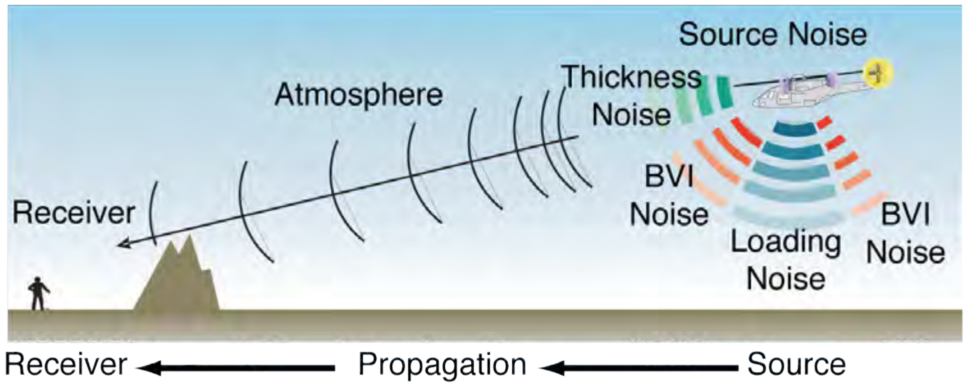

Figure 1: Rotorcraft acoustics issues.

Figure 2: Bell 430 helicopter.

Figure 3: Testing area overview.

Figure 4: MicroADAS installation in aircraft.

Figure 5: Flight course deviation indicator.

Figure 6: DGPS ground station setup.

Figure 7: TPP cameras mounted on pylon.

Figure 8: TPP reflective tape mounted on rotor tip.

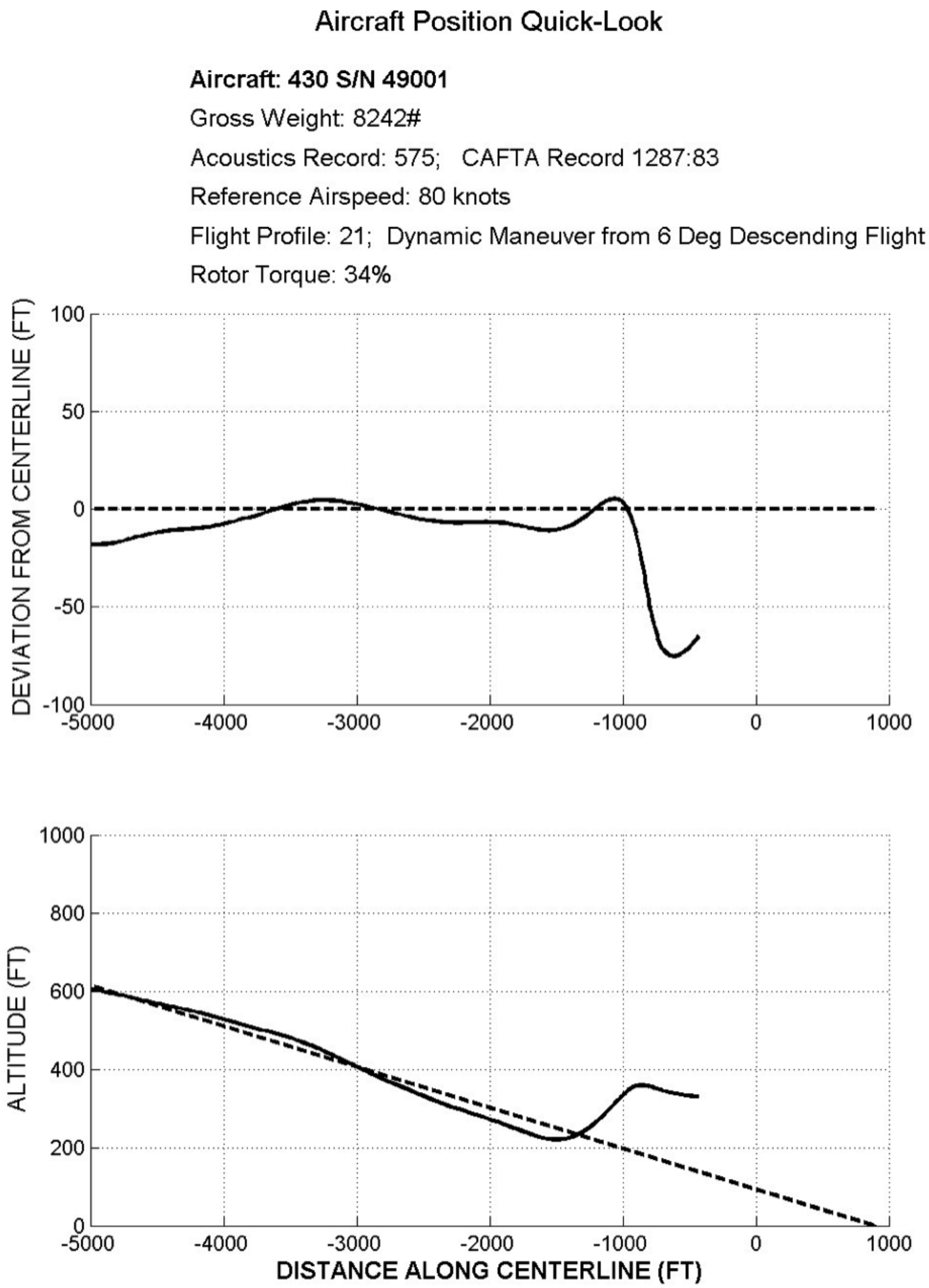

Figure 9: Quick-look aircraft position.

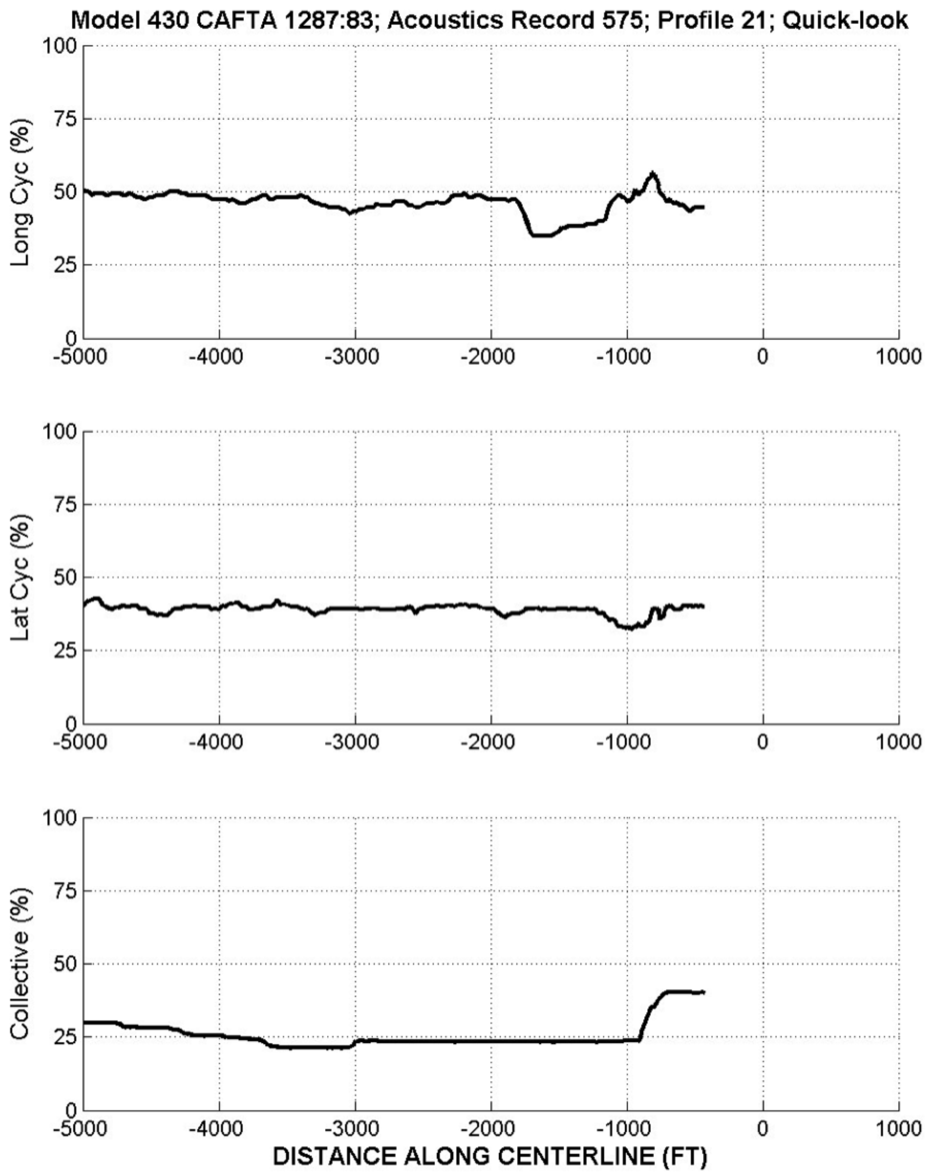

Figure 10: Quick-look aircraft control positions.

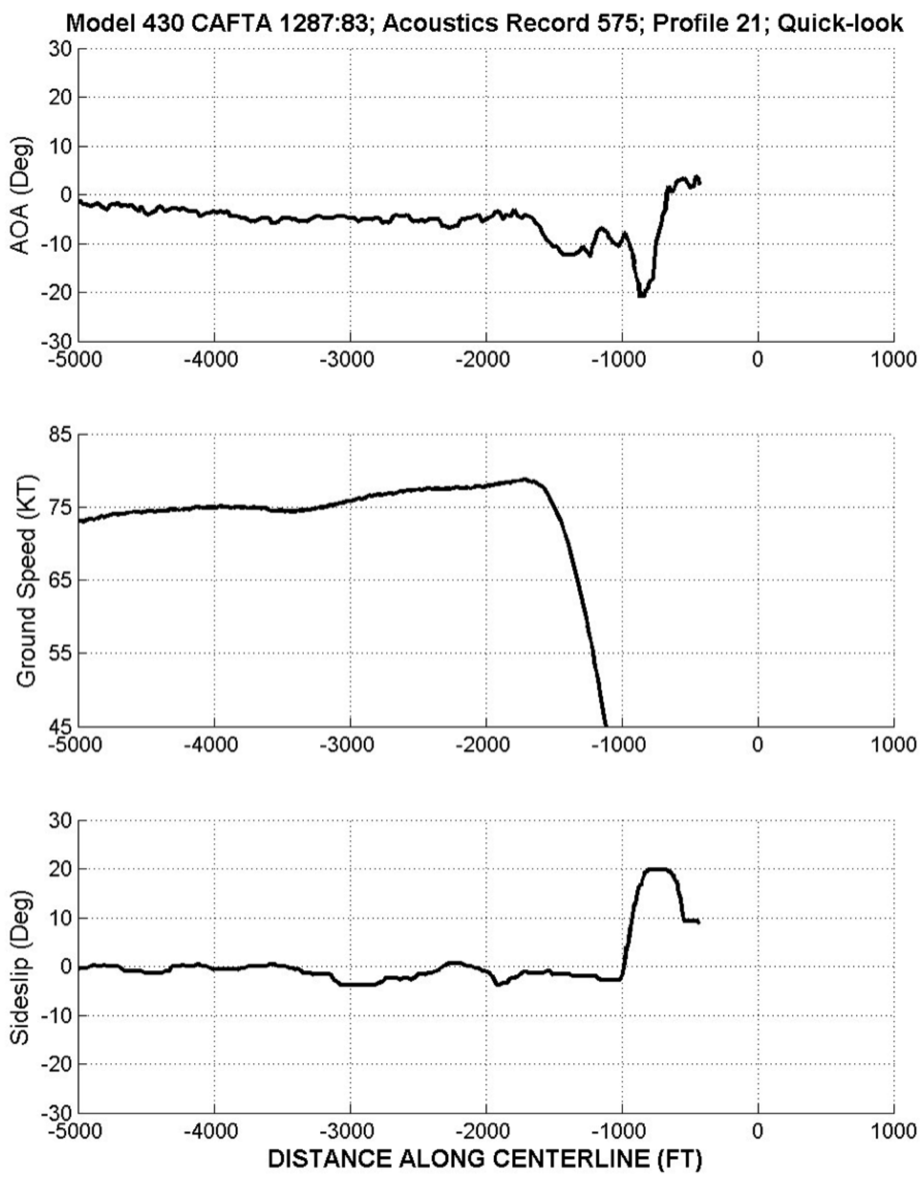

Figure 11: Quick-look aircraft state parameters.

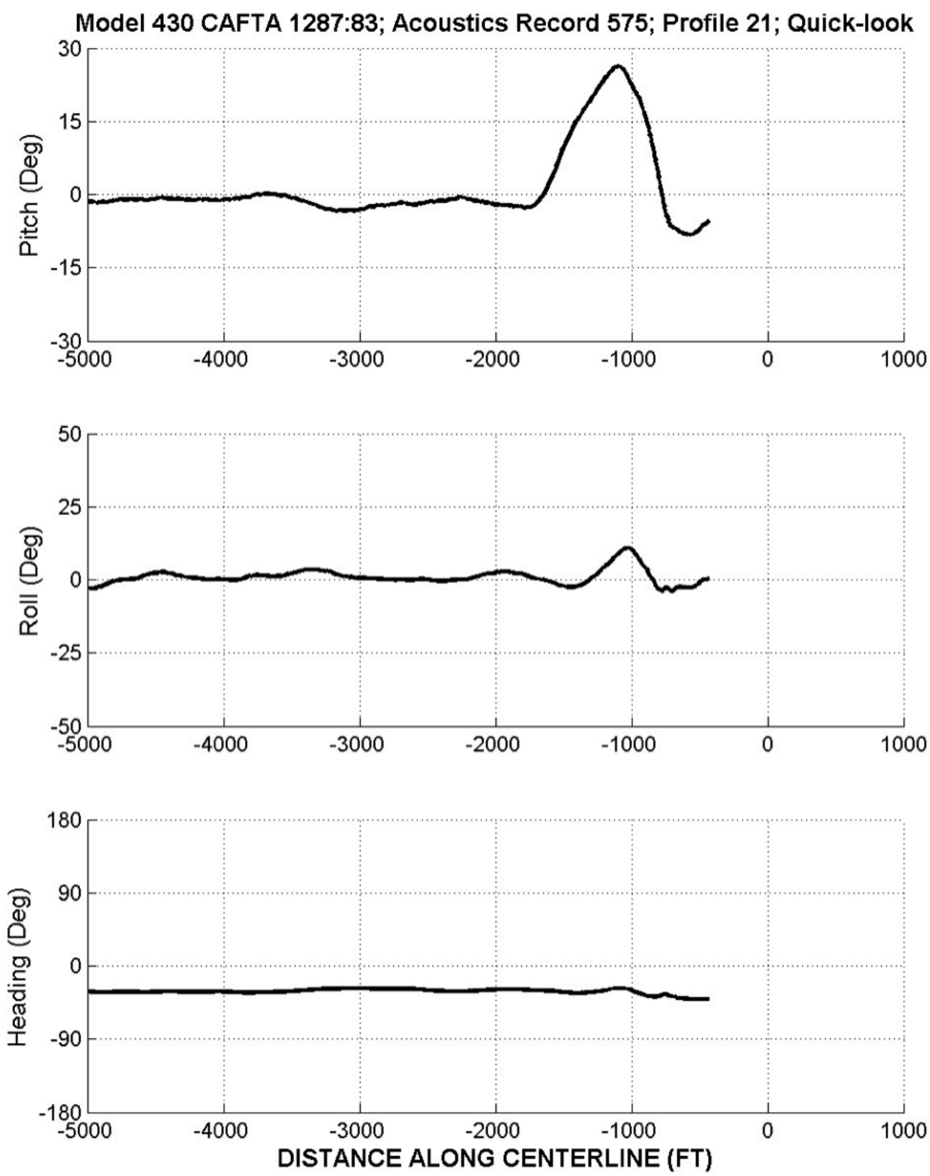

Figure 12: Quick-look aircraft control attitudes.

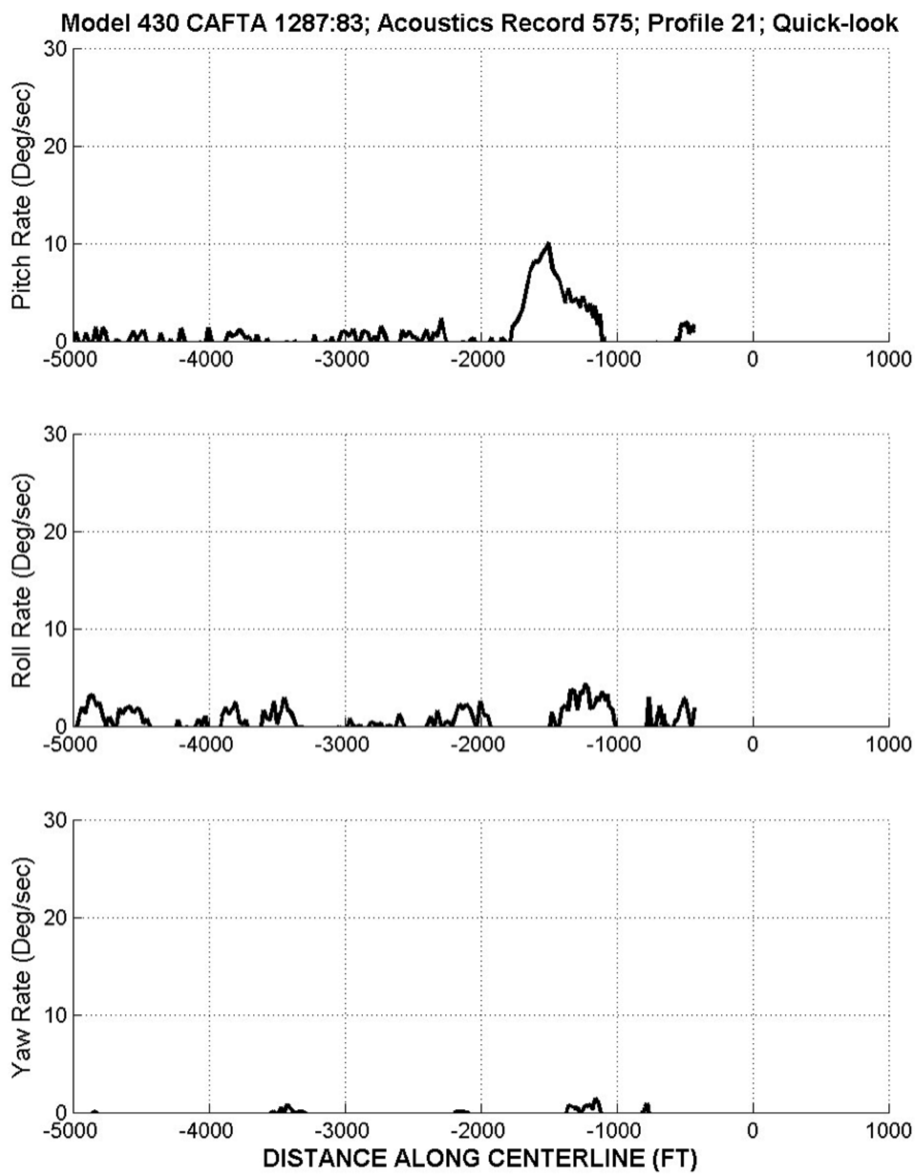

Figure 13: Quick-look aircraft attitude rates.

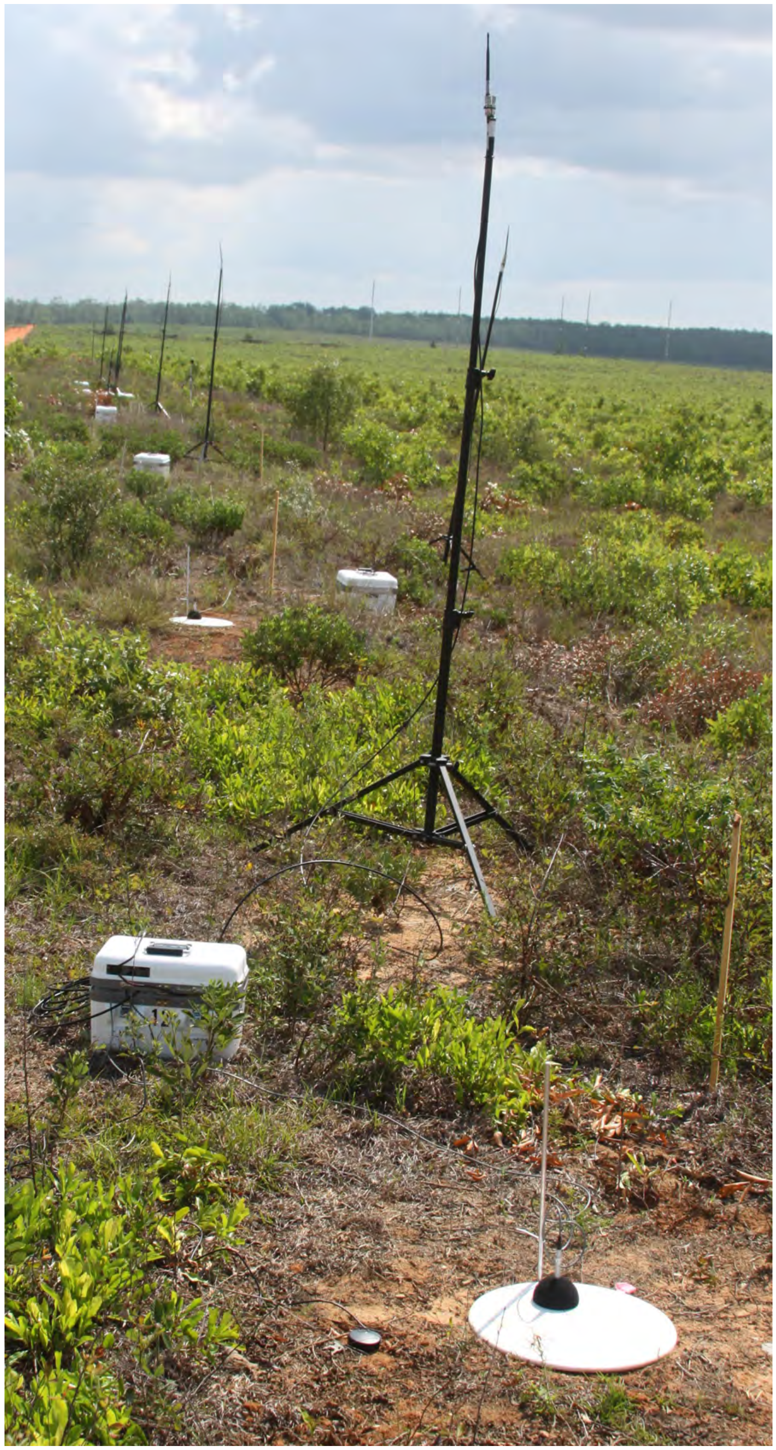

Figure 14: Wireless Acoustic Measurement System.

Figure 15: Source noise microphone array.

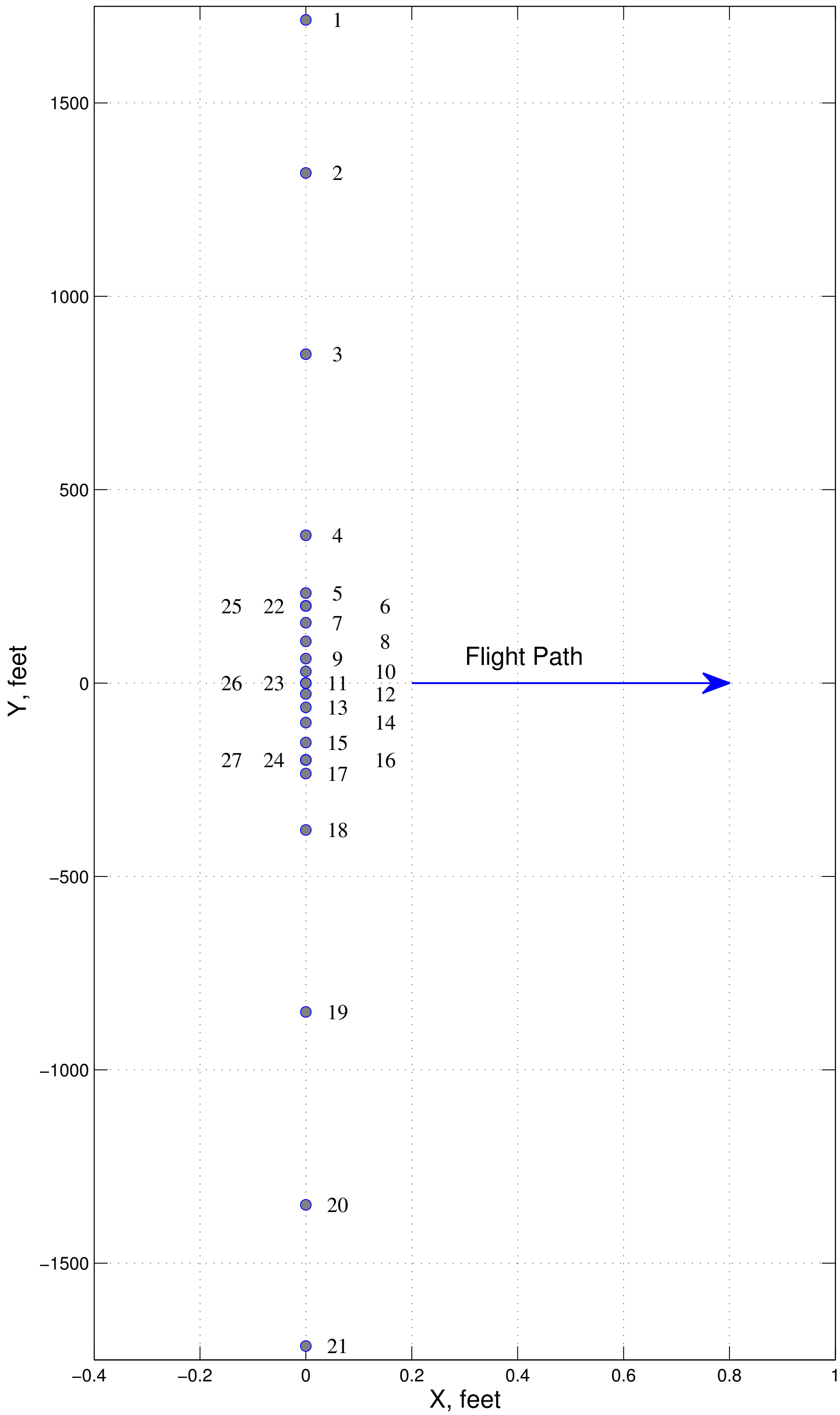

Figure 16: Source noise microphone array.

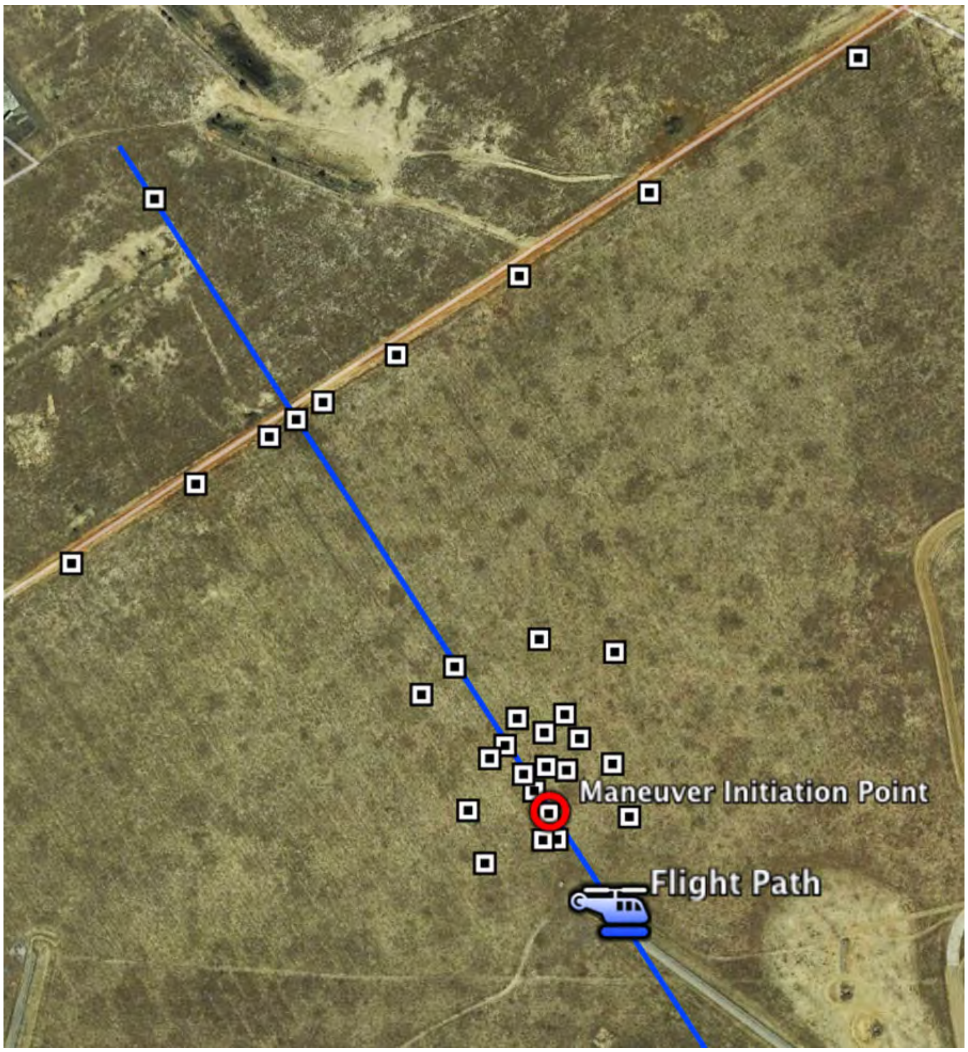

Figure 17: Maneuver microphone array.

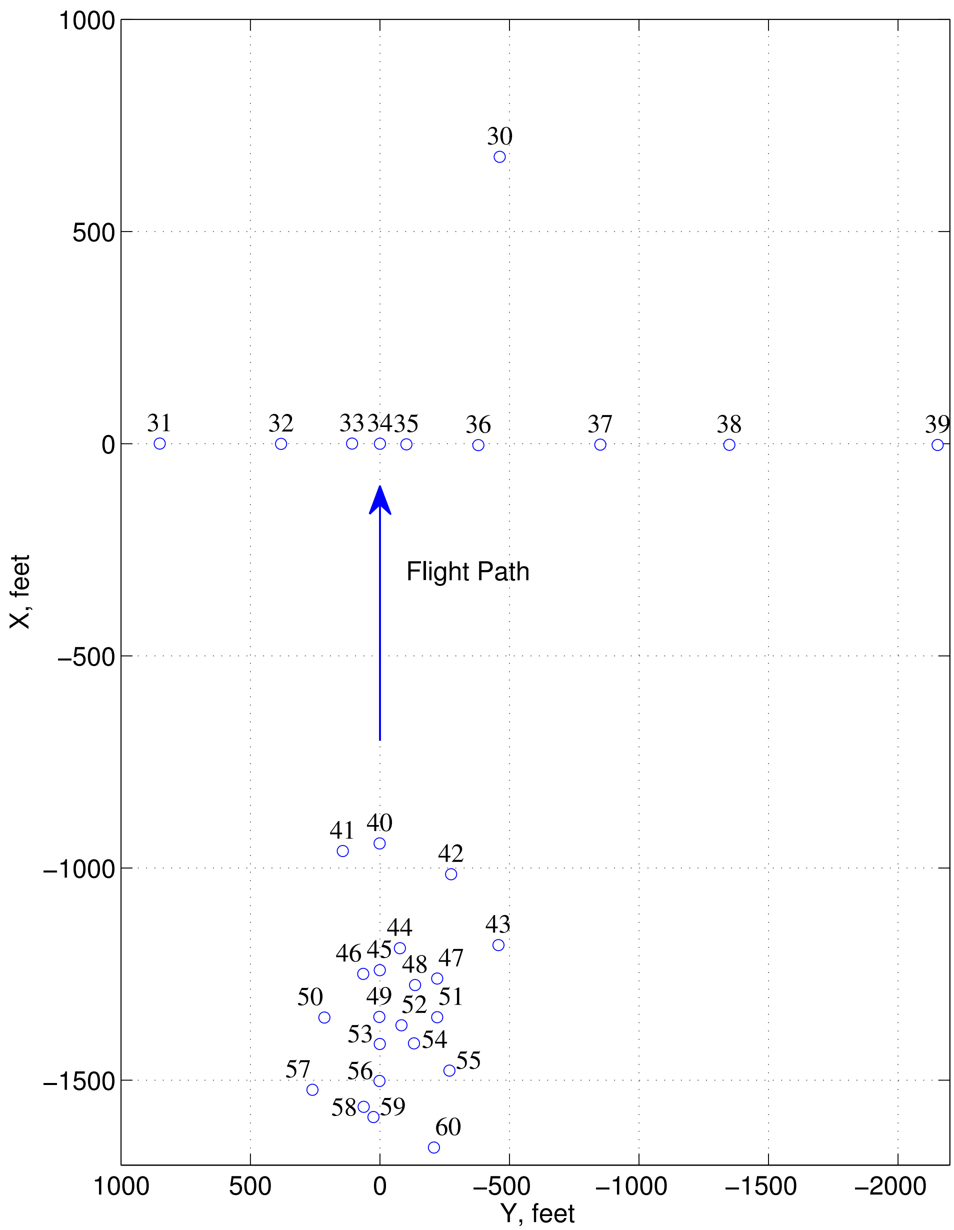

Figure 18: Maneuver microphone array.

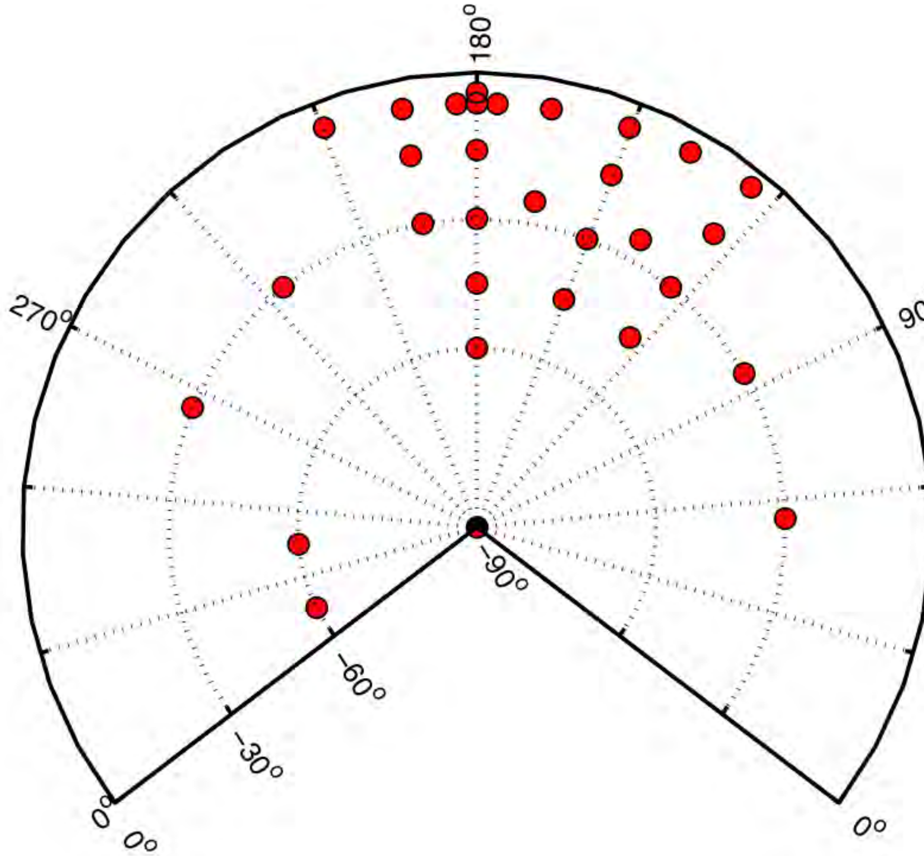

Figure 19: Maneuver microphone array projection onto semi-sphere.

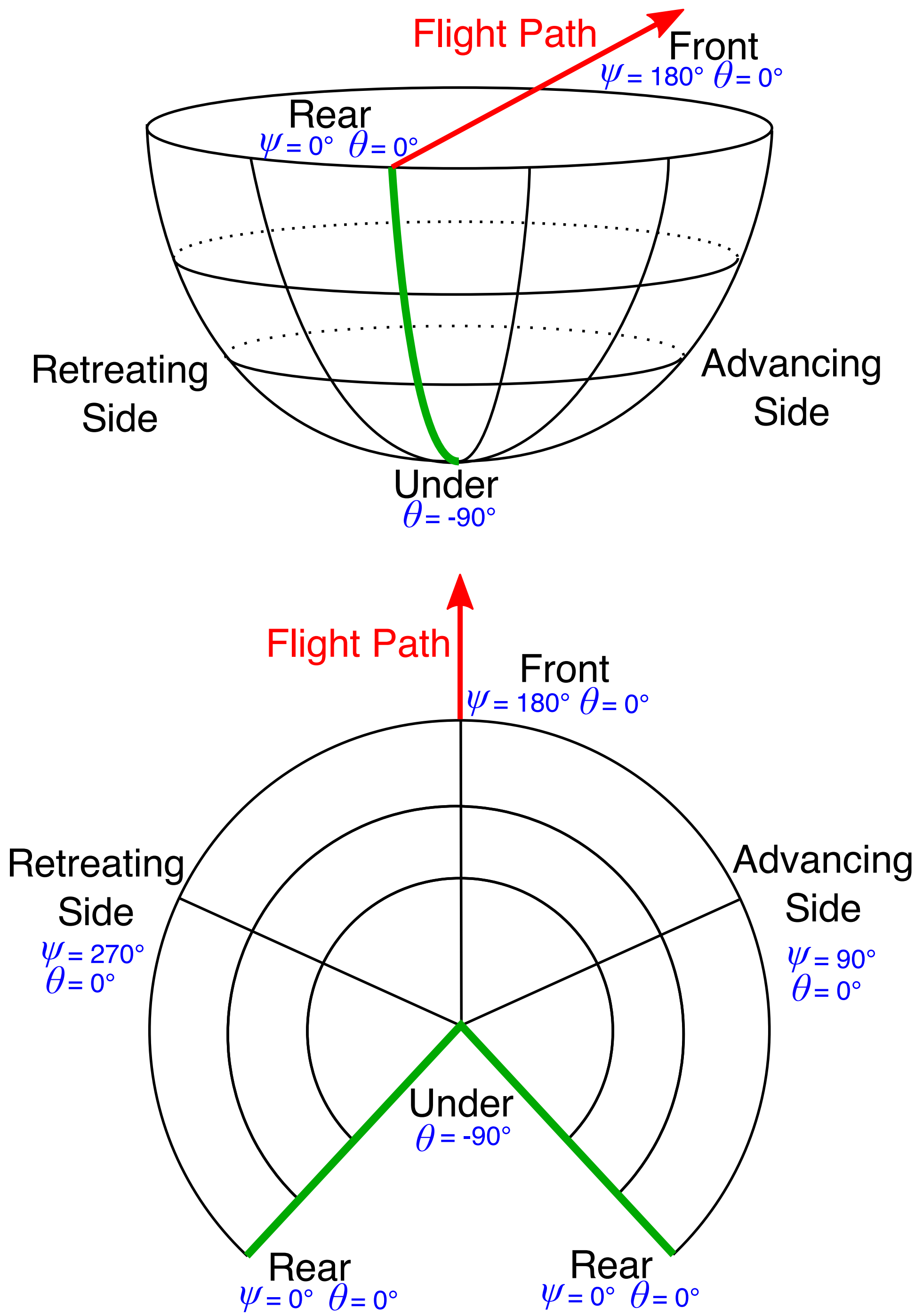

Figure 20: Lambert conformal conic projection of an acoustic radiation semi-sphere.

Figure 21: Terminal area microphone array.

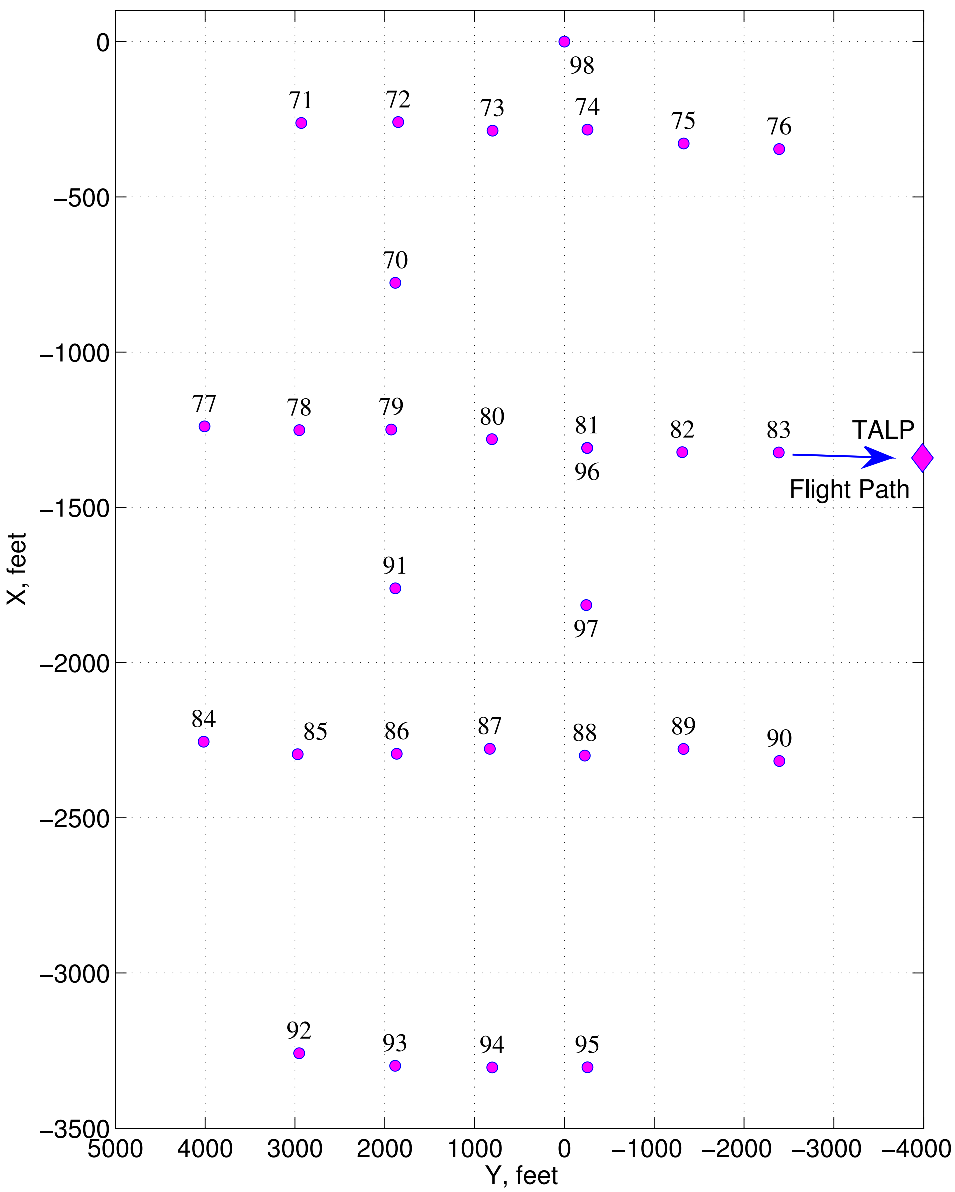

Figure 22: Terminal area microphone array.

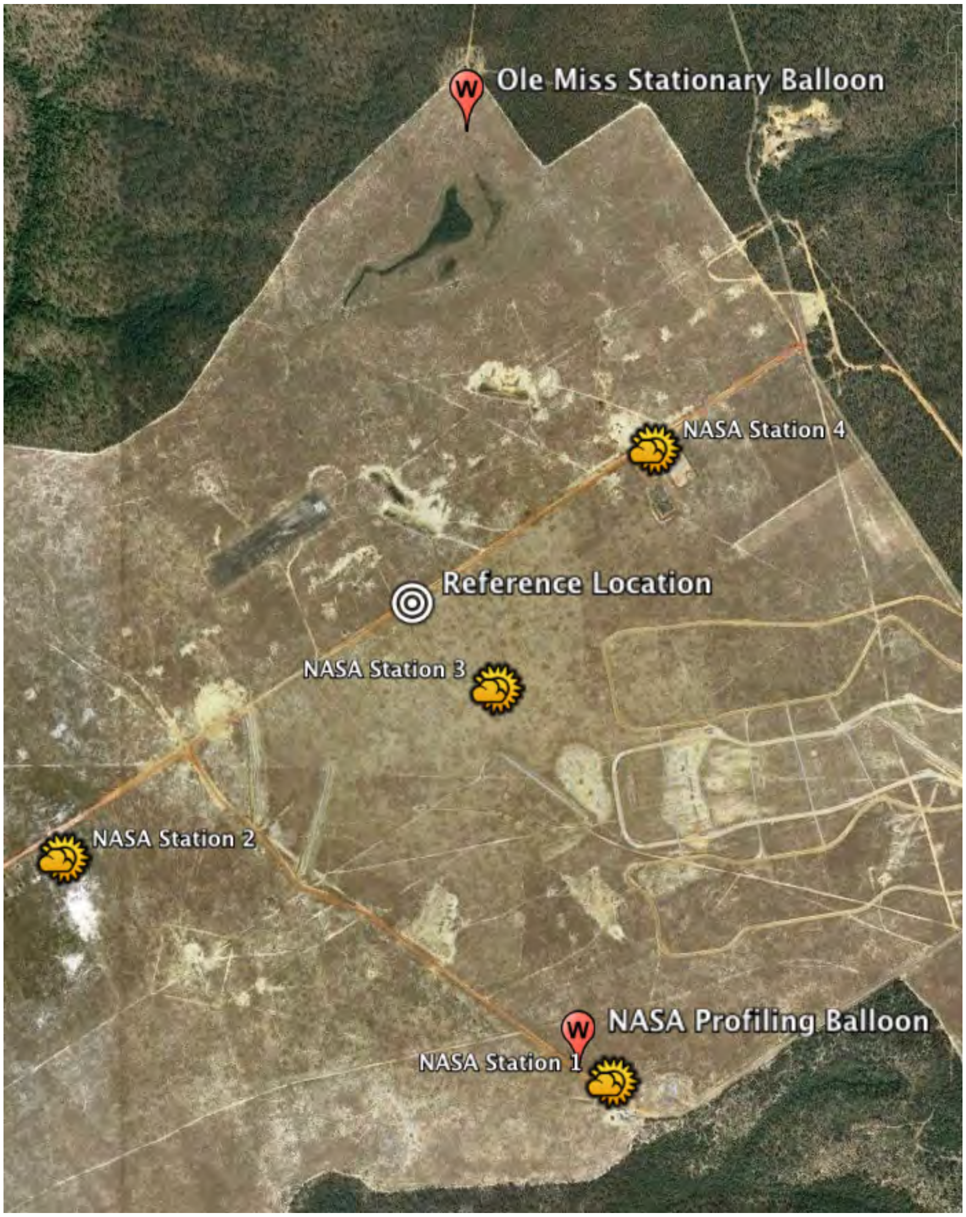

Figure 23: Weather instrumentation locations.

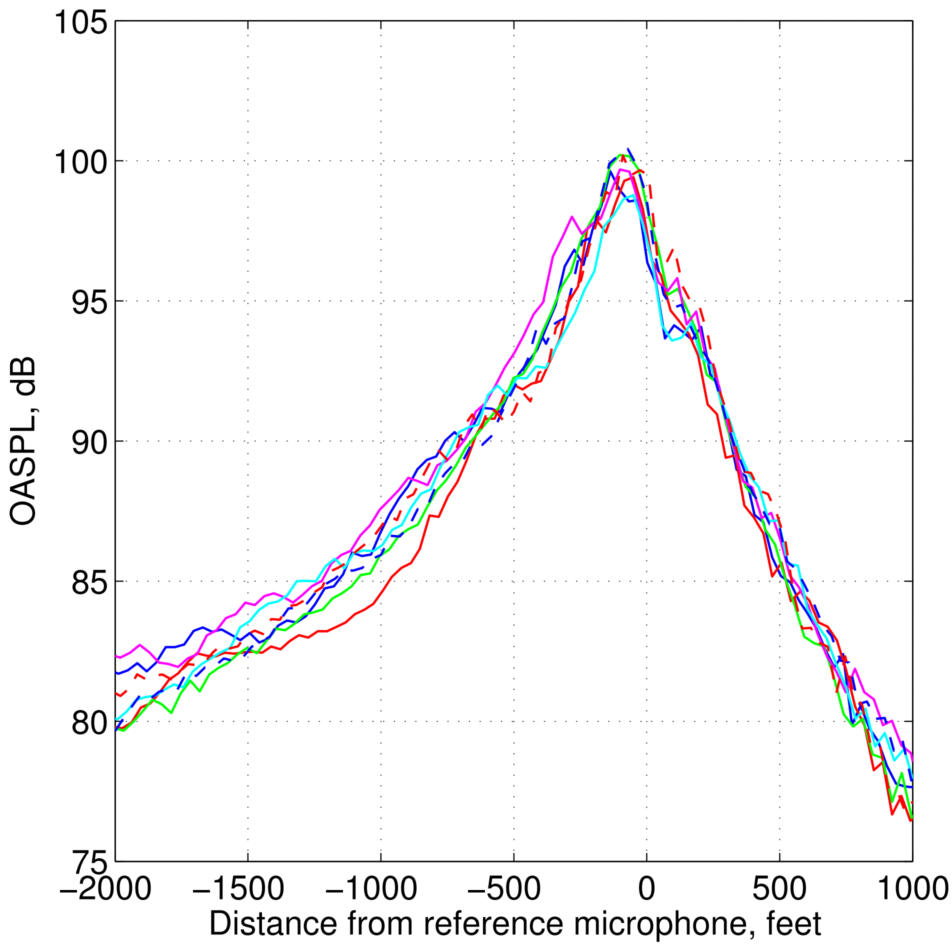

Figure 24: Level flight, 80 KIAS housekeeping runs.

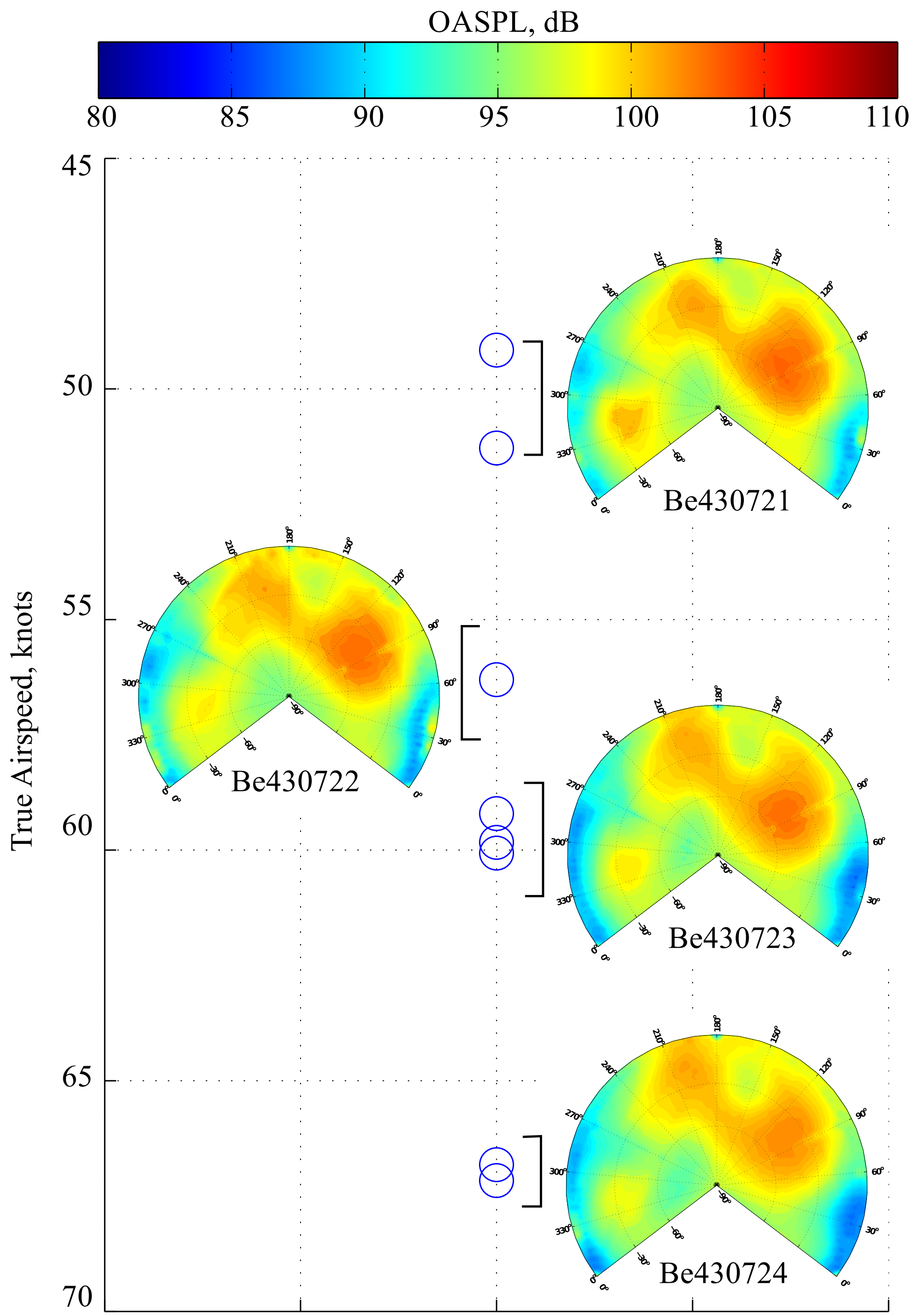

Figure 25: Semi-spheres for low speed level flight, OASPL.

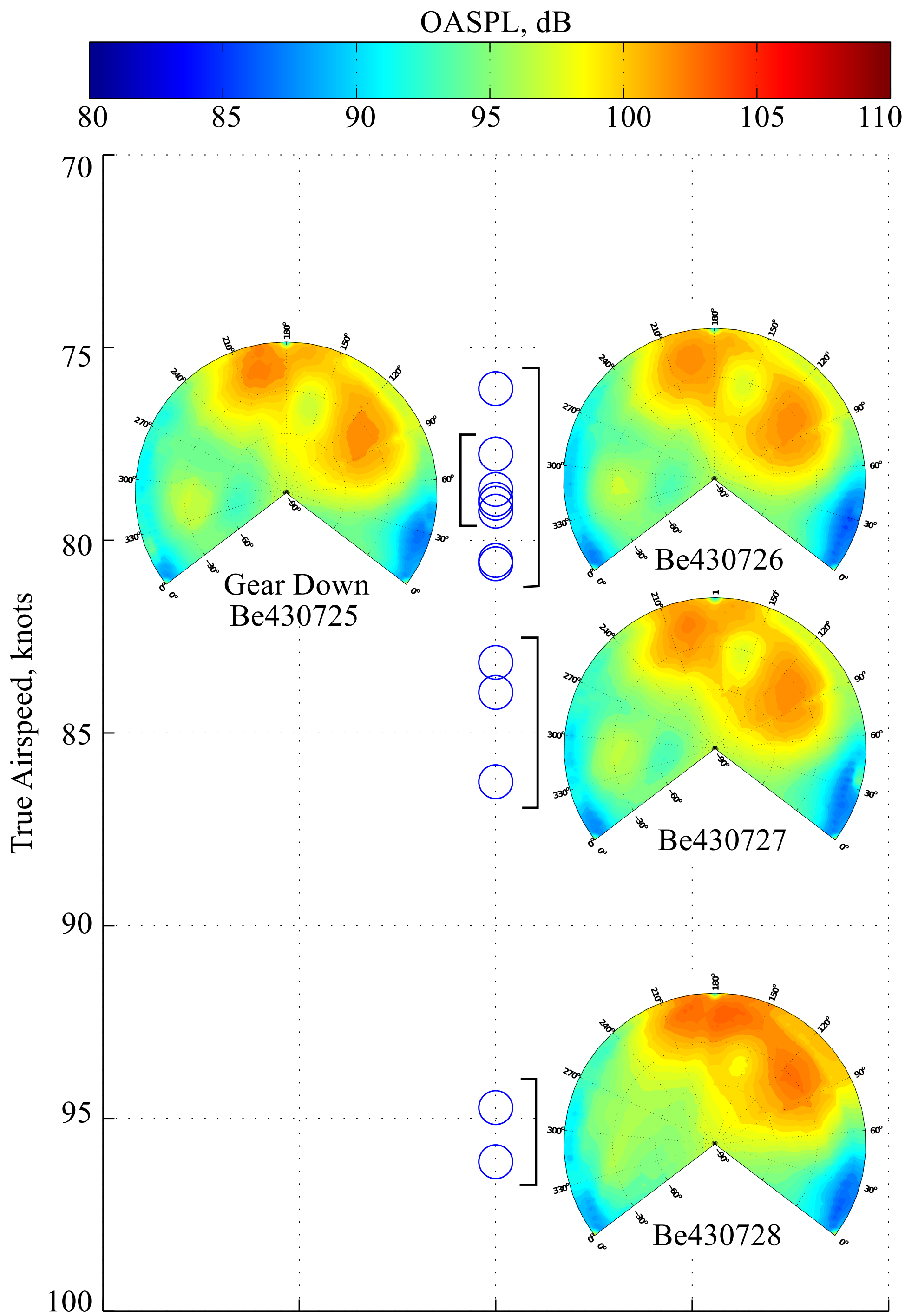

Figure 26: Semi-spheres for mid speed level flight, OASPL.

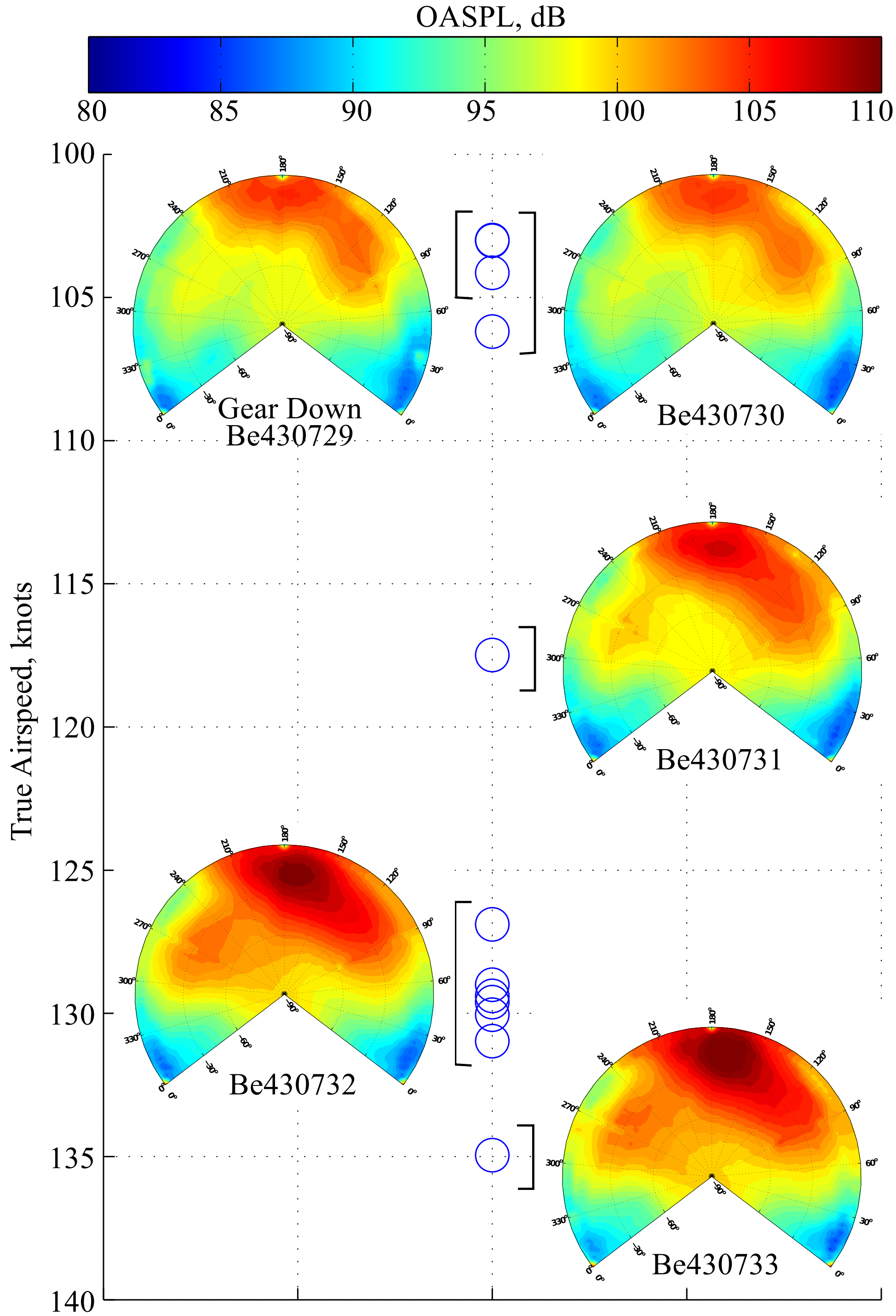

Figure 27: Semi-spheres for high speed level flight, OASPL.

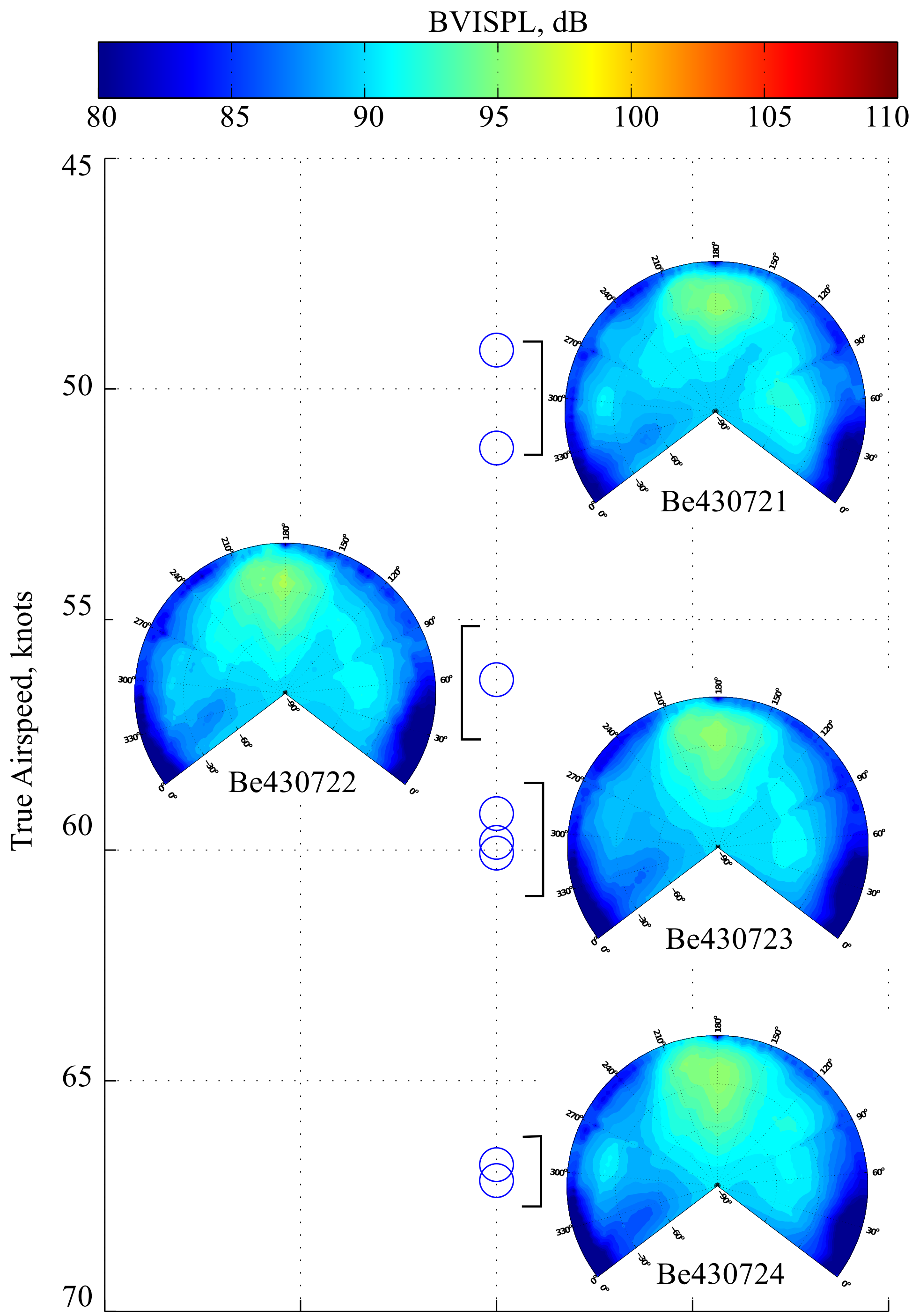

Figure 28: Semi-spheres for low speed level flight, BVISPL.

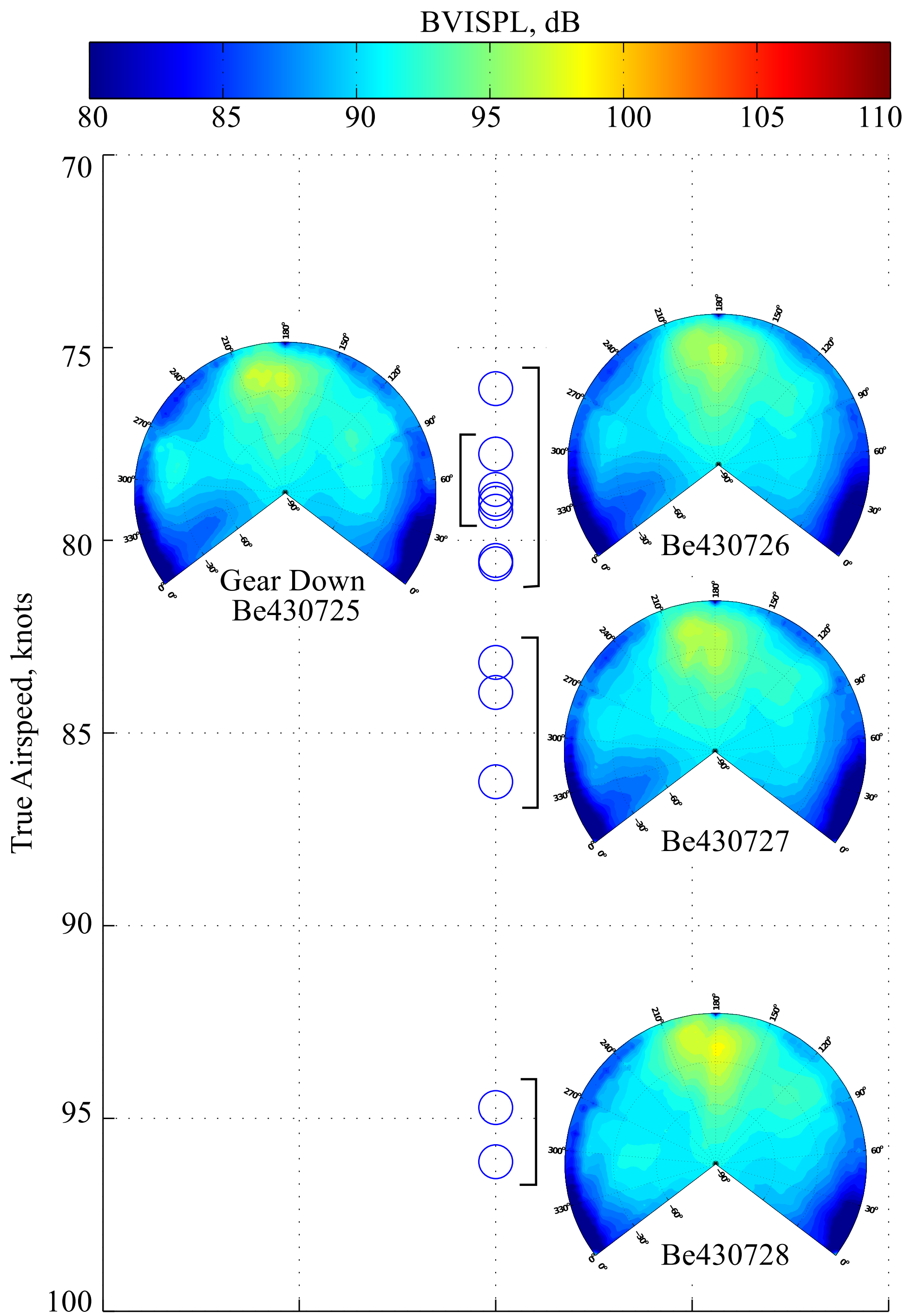

Figure 29: Semi-spheres for mid speed level flight, BVISPL.

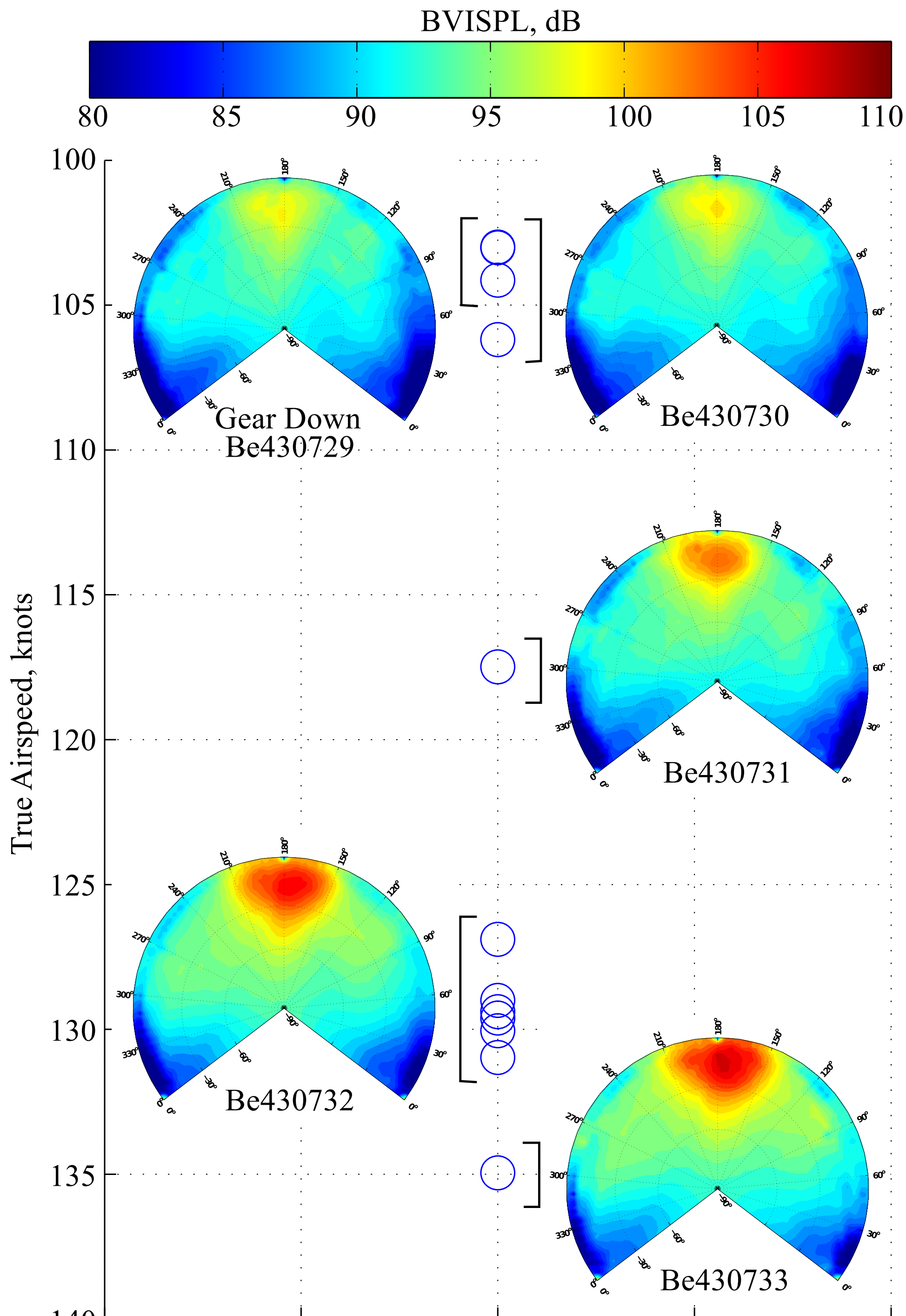

Figure 30: Semi-spheres for high speed level flight, BVISPL.

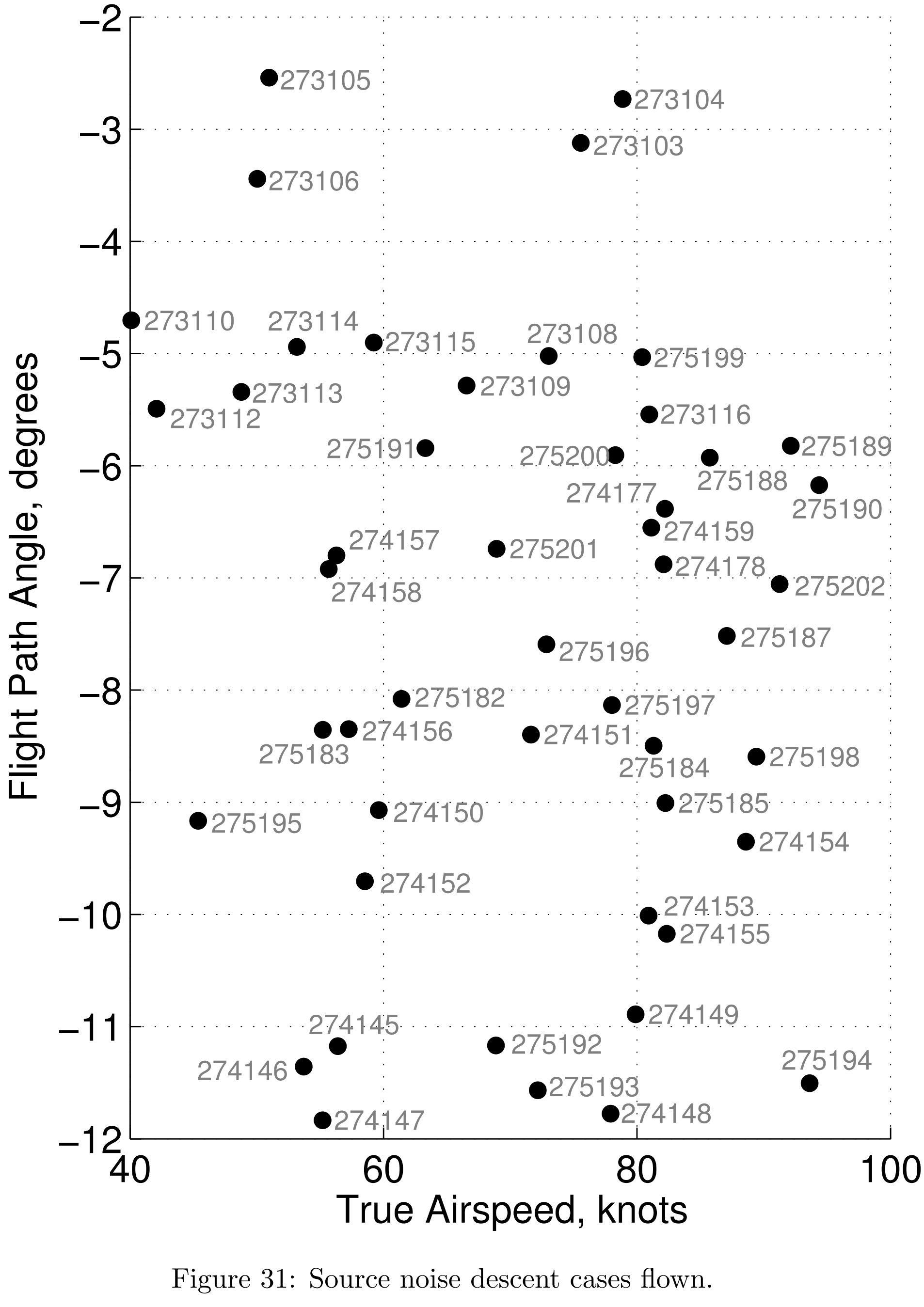

Figure 31: Source noise descent cases flown.

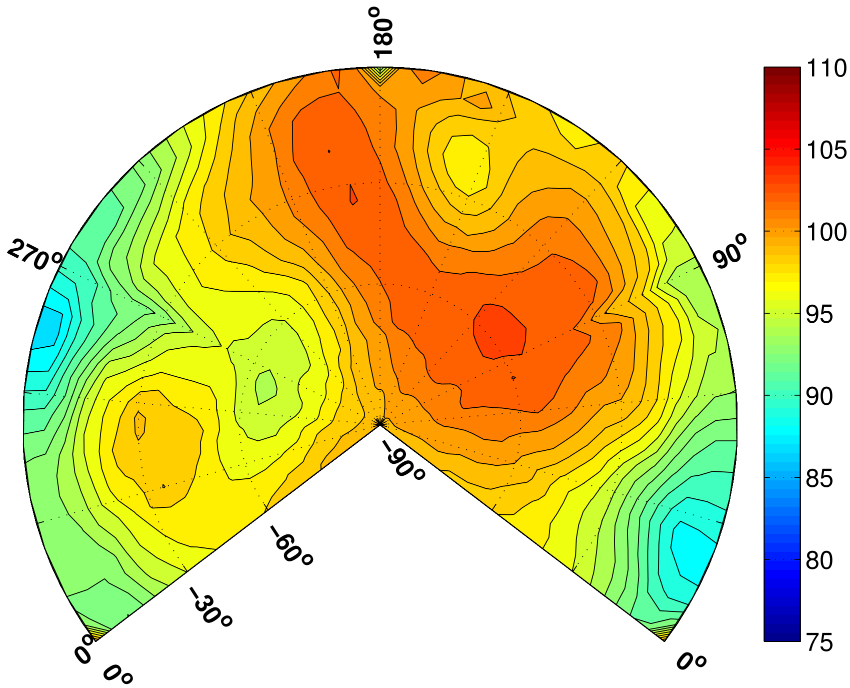

(a) OASPL, dB

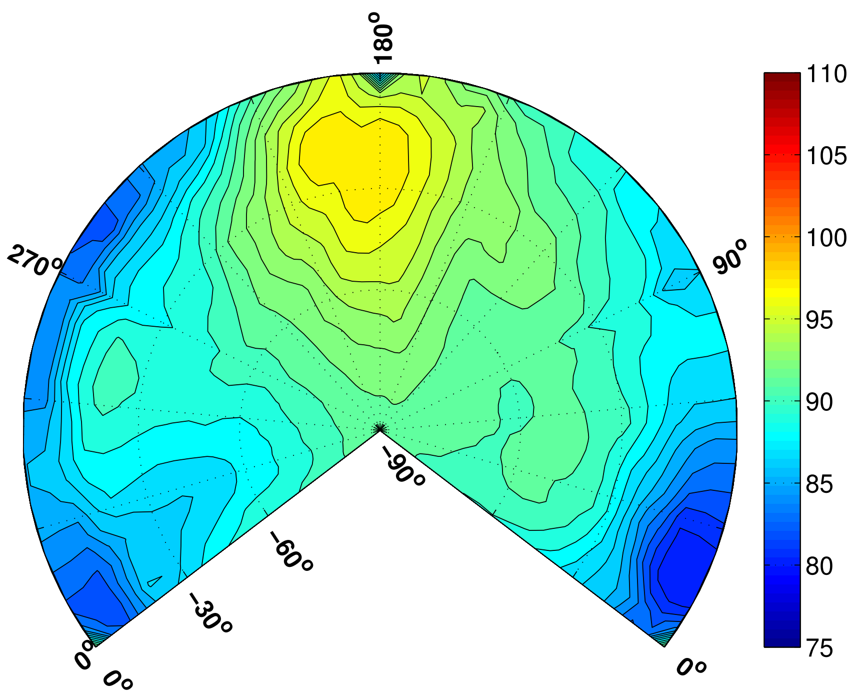

(b) BVISPL, dB

Figure 32: Descent hemi-sphere Be430103, 75.6 KTAS, -3.1°

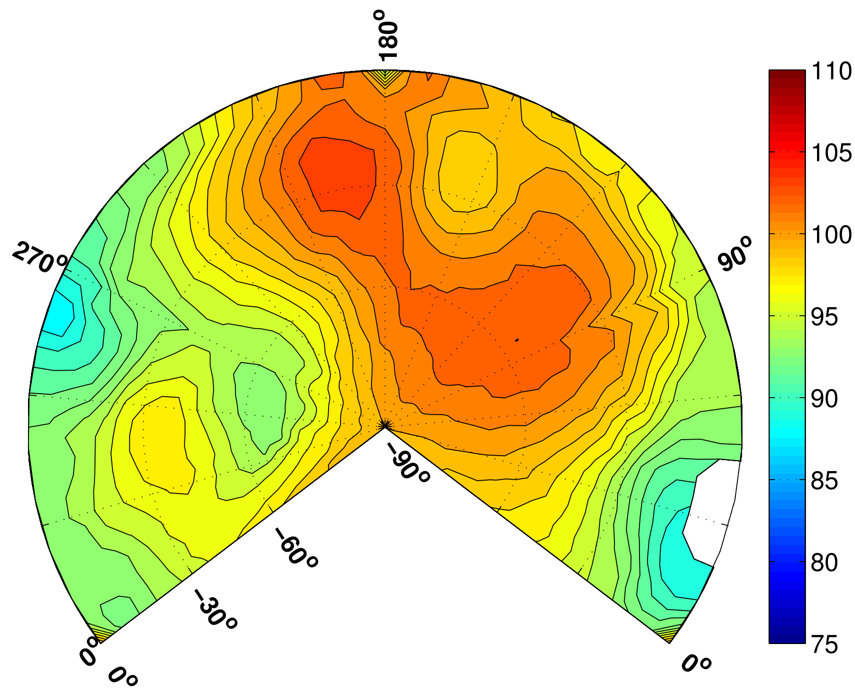

(a) OASPL, dB

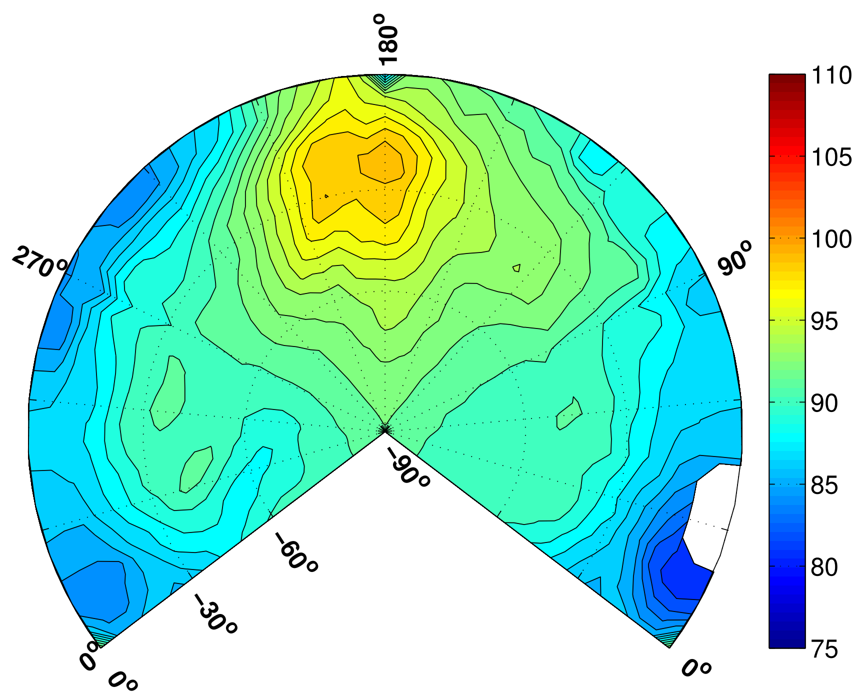

(b) BVISPL, dB

Figure 33: Descent hemi-sphere Be430104, 78.9 KTAS, -2.7°

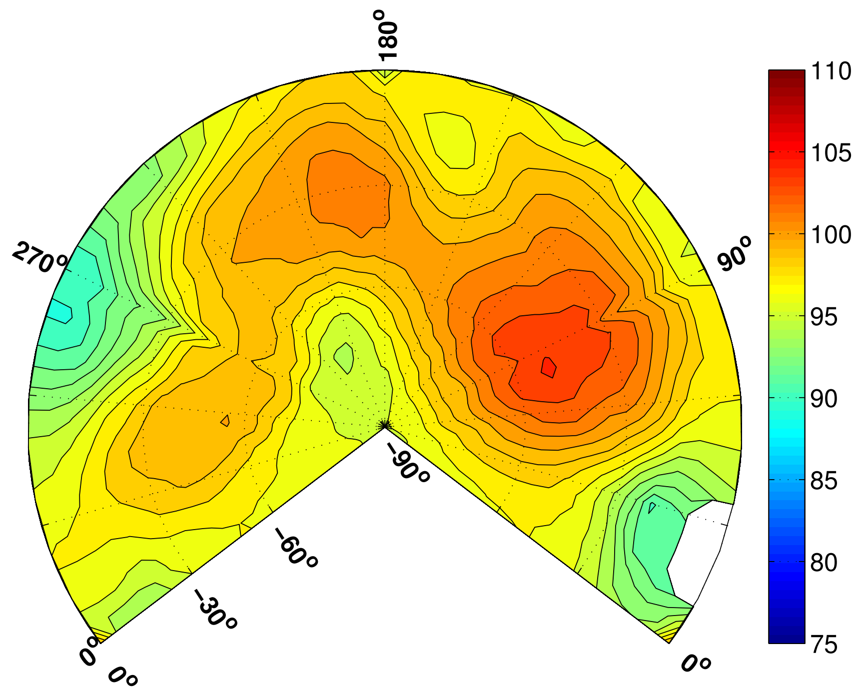

(a) OASPL, dB

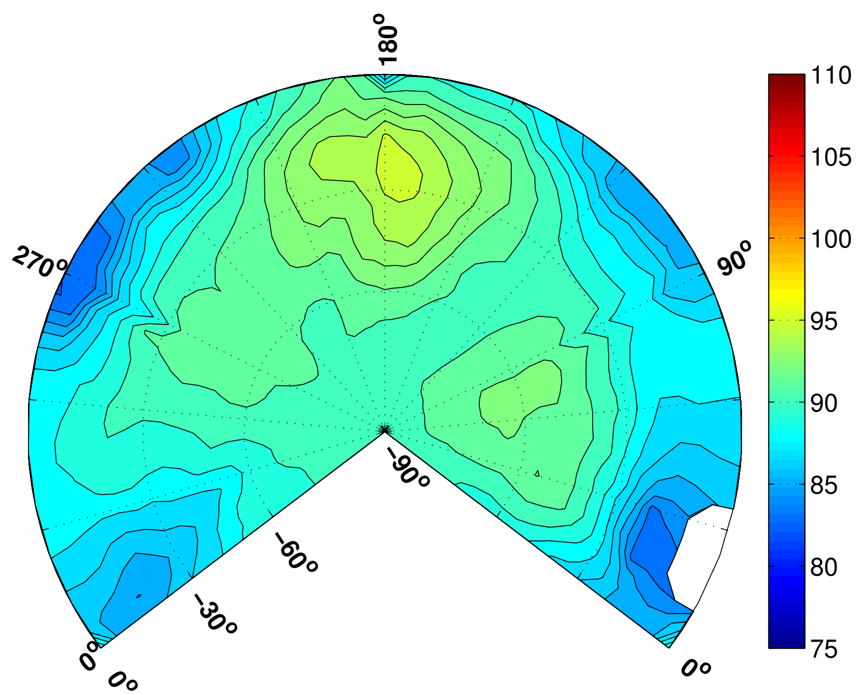

(b) BVISPL, dB

Figure 34: Descent hemi-sphere Be430105, 51.0 KTAS, -2.5°

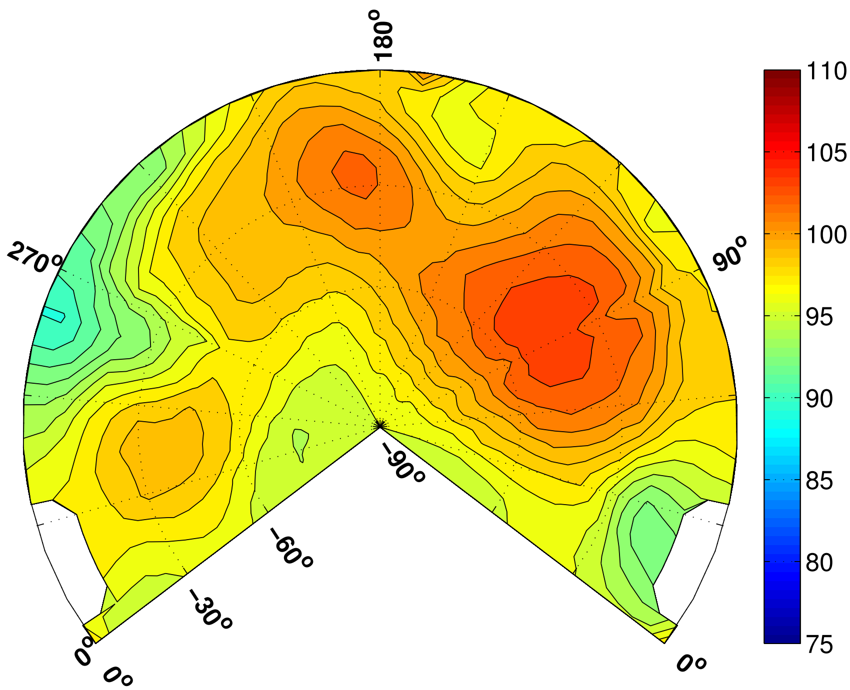

(a) OASPL, dB

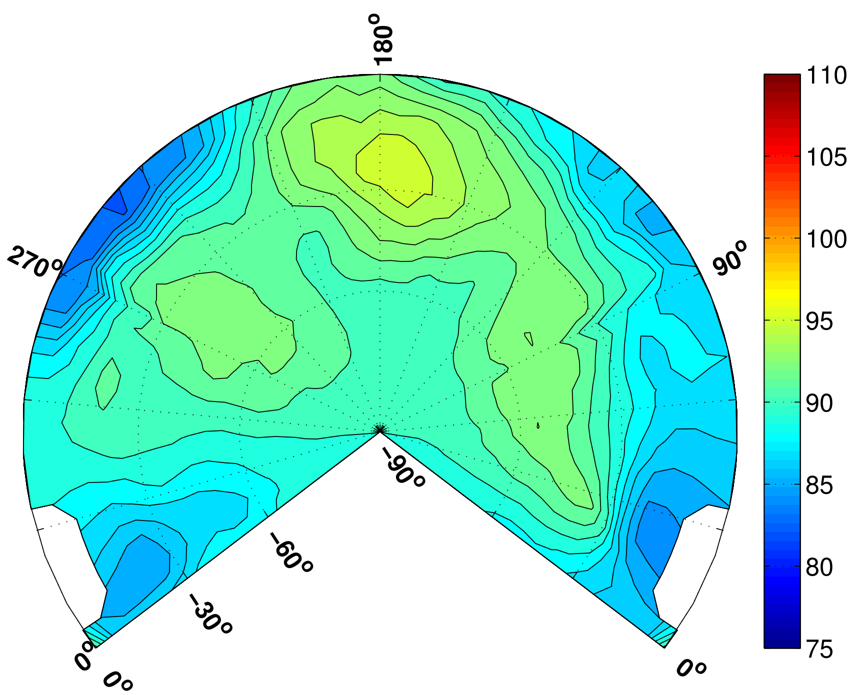

(b) BVISPL, dB

Figure 35: Descent hemi-sphere Be430106, 50.0 KTAS, -3.4°

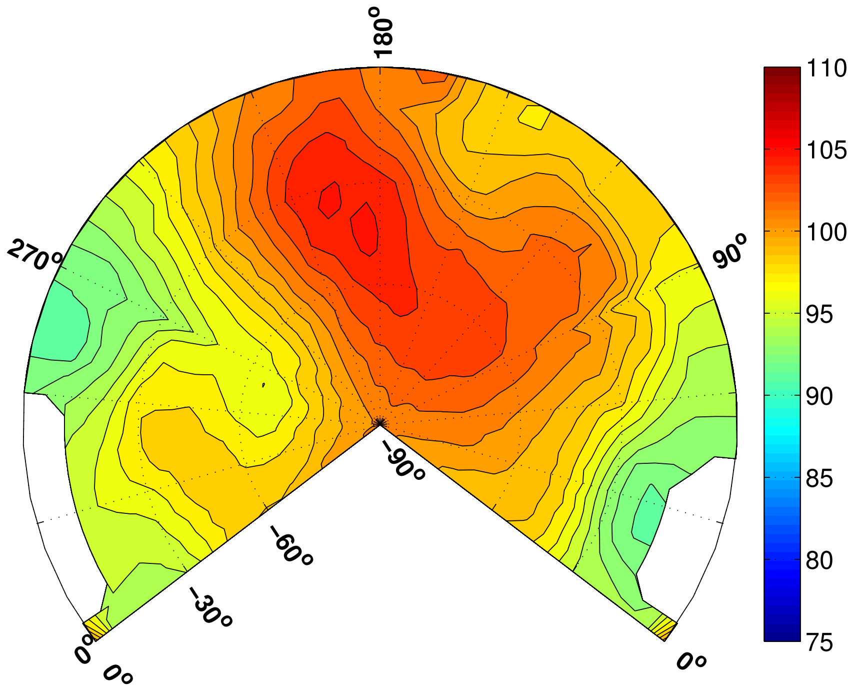

(a) OASPL, dB

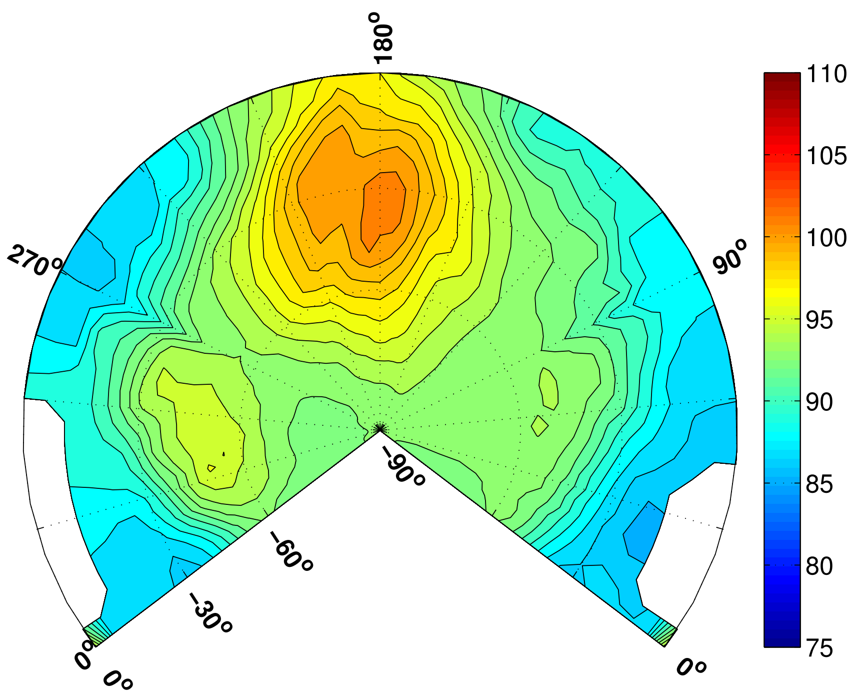

(b) BVISPL, dB

Figure 36: Descent hemi-sphere Be430108, 73.0 KTAS, -5.0°

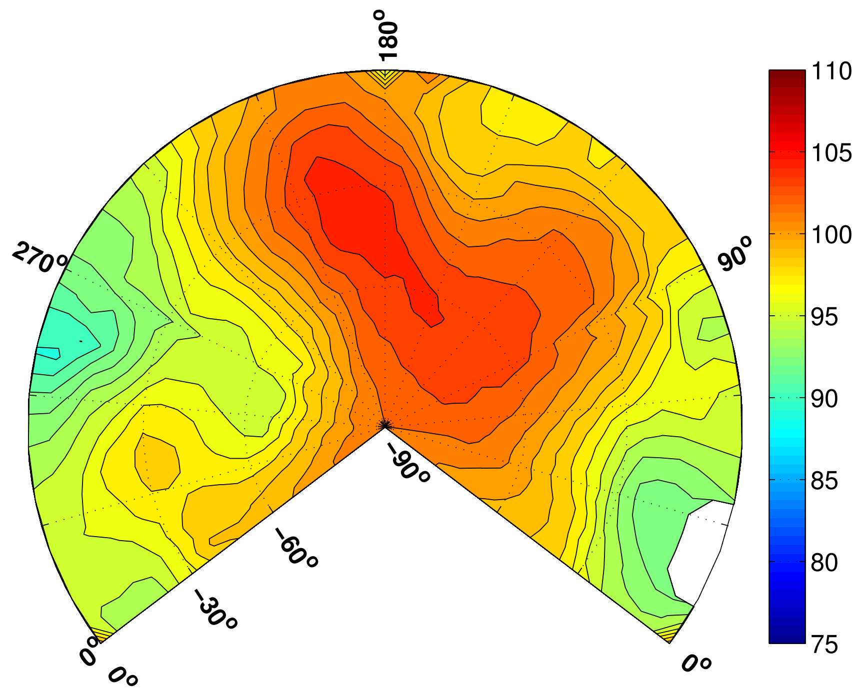

(a) OASPL, dB

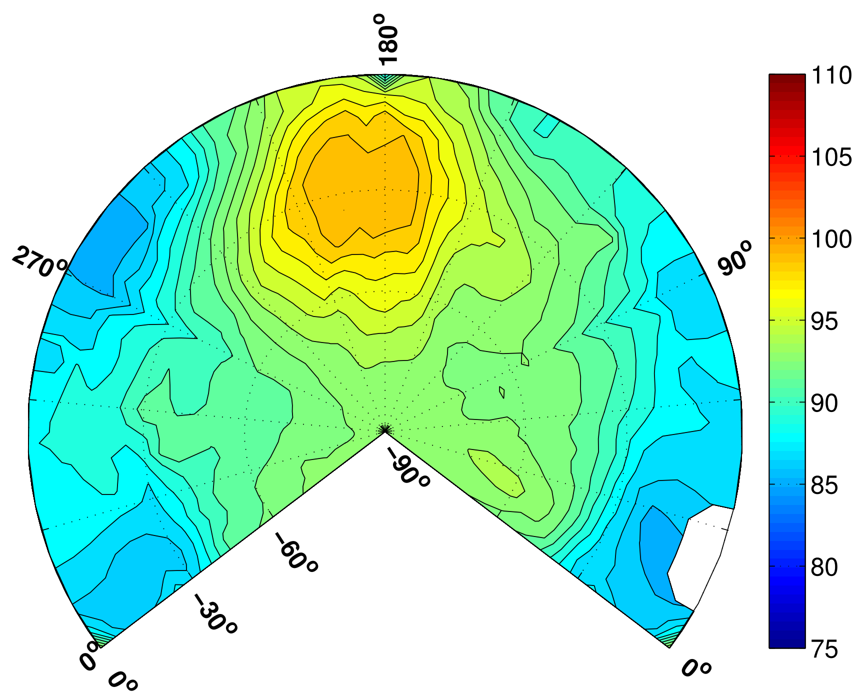

(b) BVISPL, dB

Figure 37: Descent hemi-sphere Be430109, 66.6 KTAS, -5.3°

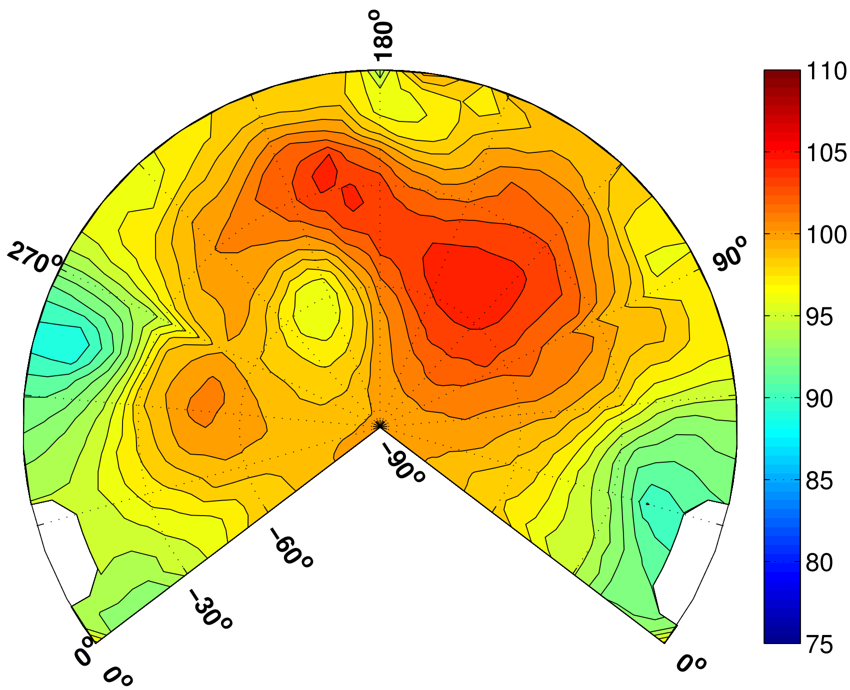

(a) OASPL, dB

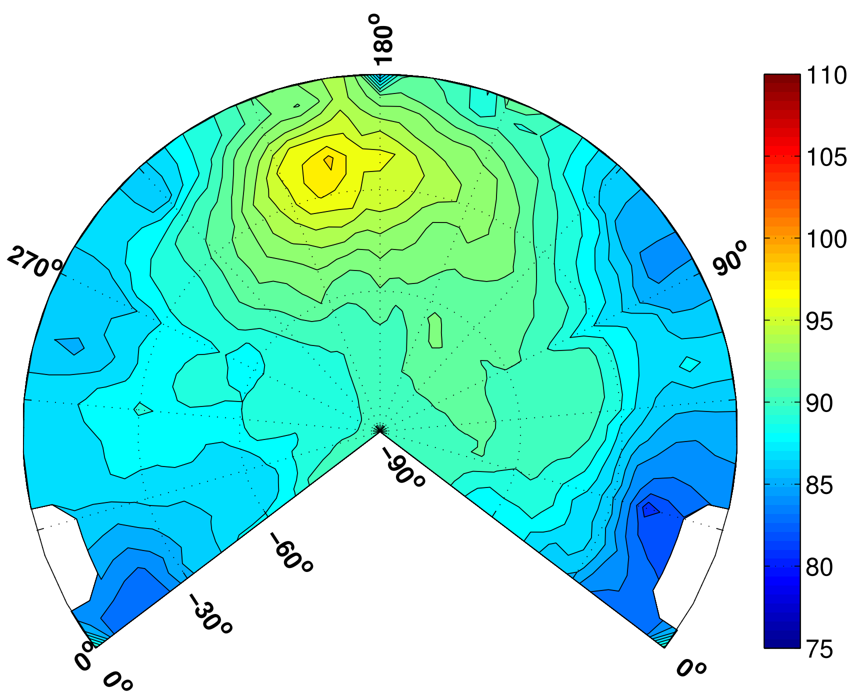

(b) BVISPL, dB

Figure 38: Descent hemi-sphere Be430110, 40.1 KTAS, -4.7°

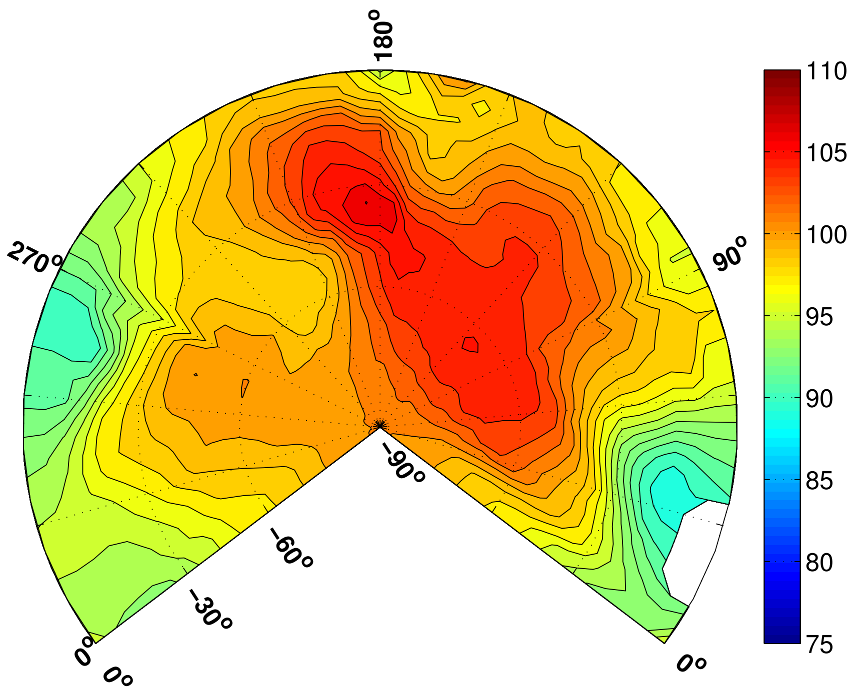

(a) OASPL, dB

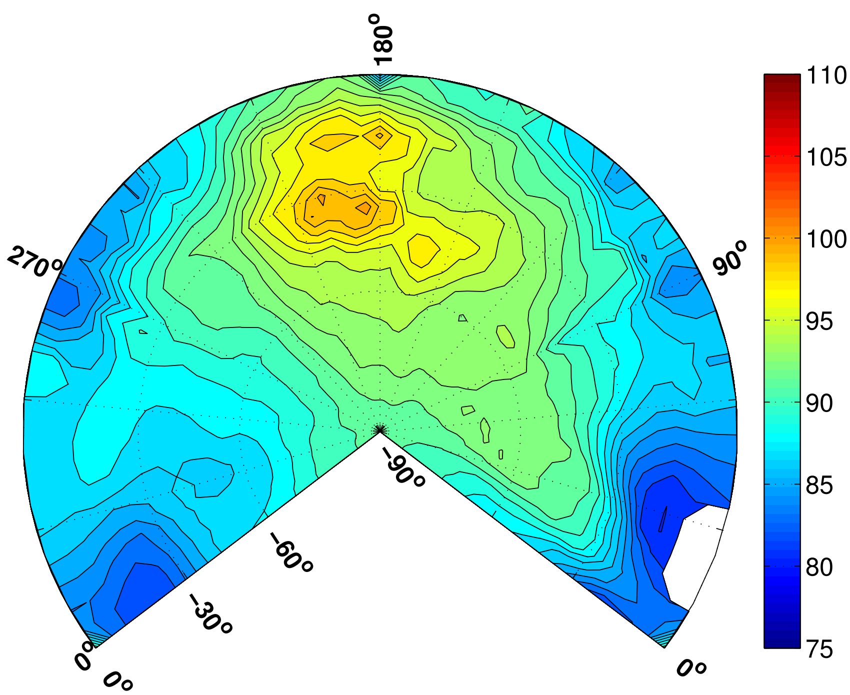

(b) BVISPL, dB

Figure 39: Descent hemi-sphere Be430112, 42.1 KTAS, -5.5°

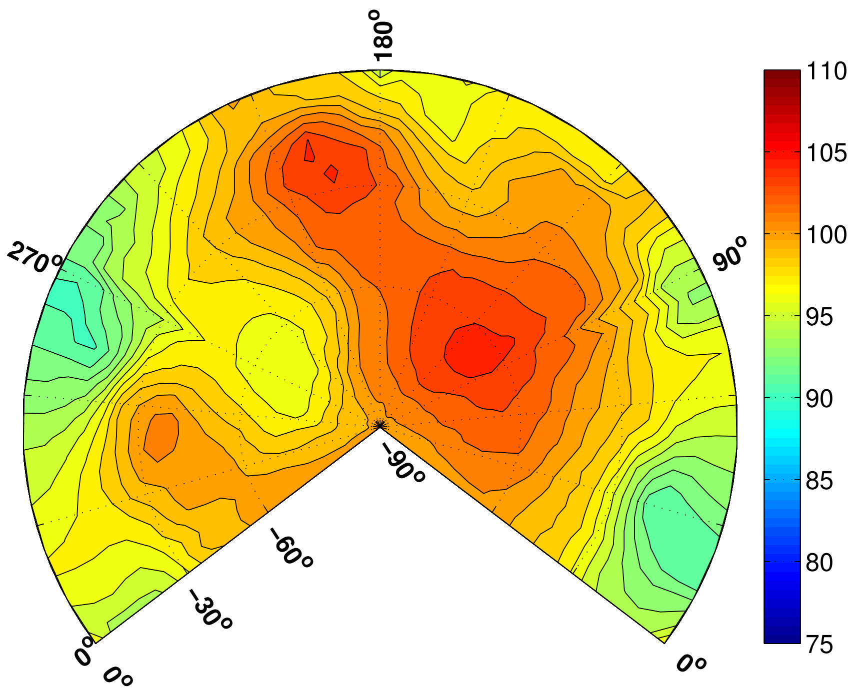

(a) OASPL, dB

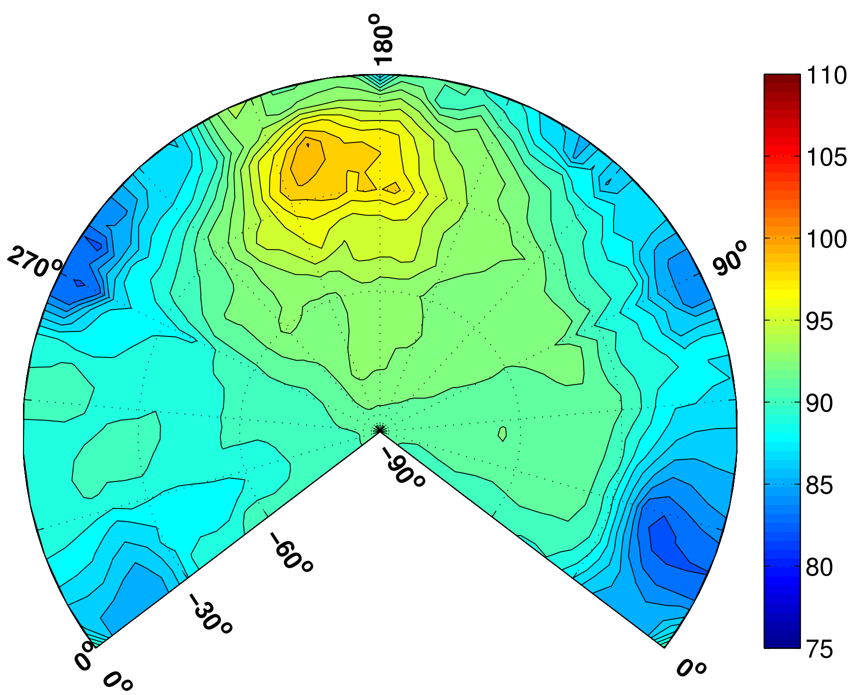

(b) BVISPL, dB

Figure 40: Descent hemi-sphere Be430113, 48.8 KTAS, -5.3°

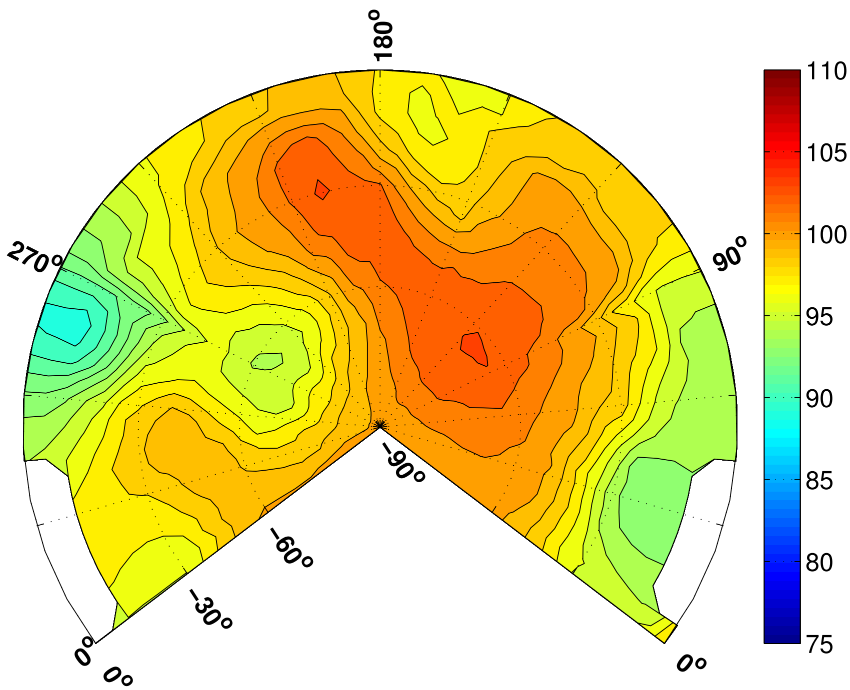

(a) OASPL, dB

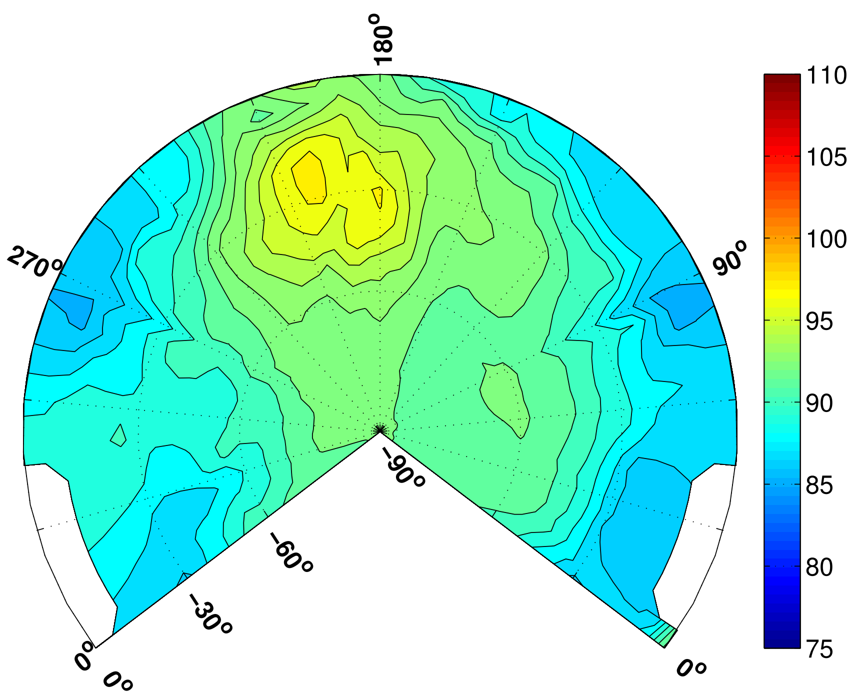

(b) BVISPL, dB

Figure 41: Descent hemi-sphere Be430114, 53.2 KTAS, -4.9°

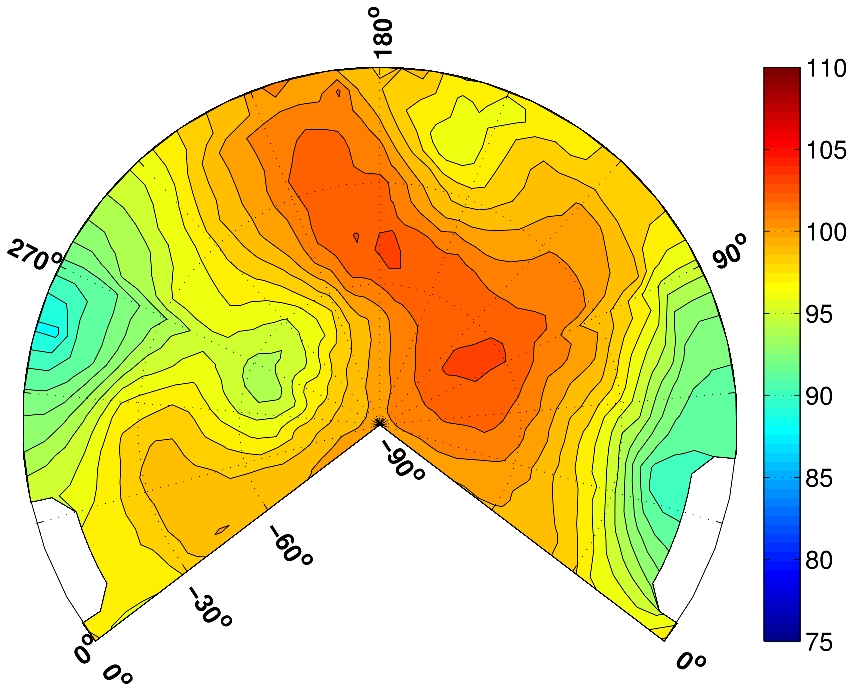

(a) OASPL, dB

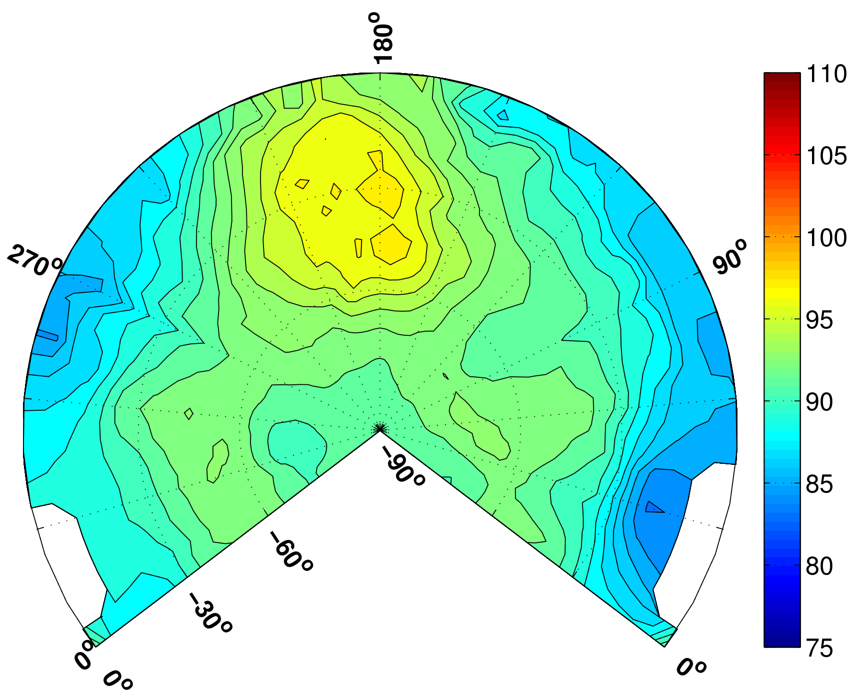

(b) BVISPL, dB

Figure 42: Descent hemi-sphere Be430115, 59.2 KTAS, -4.9°

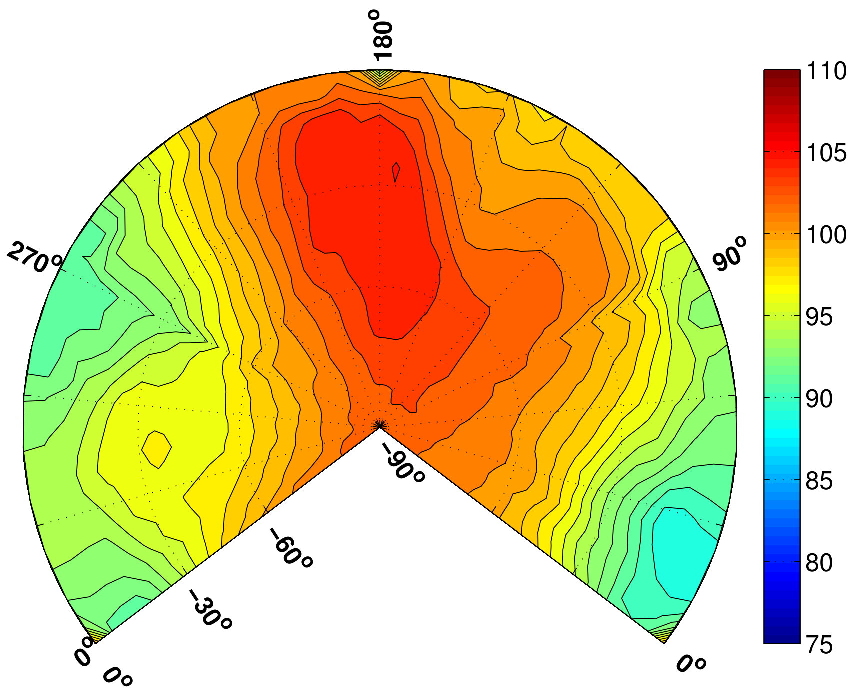

(a) OASPL, dB

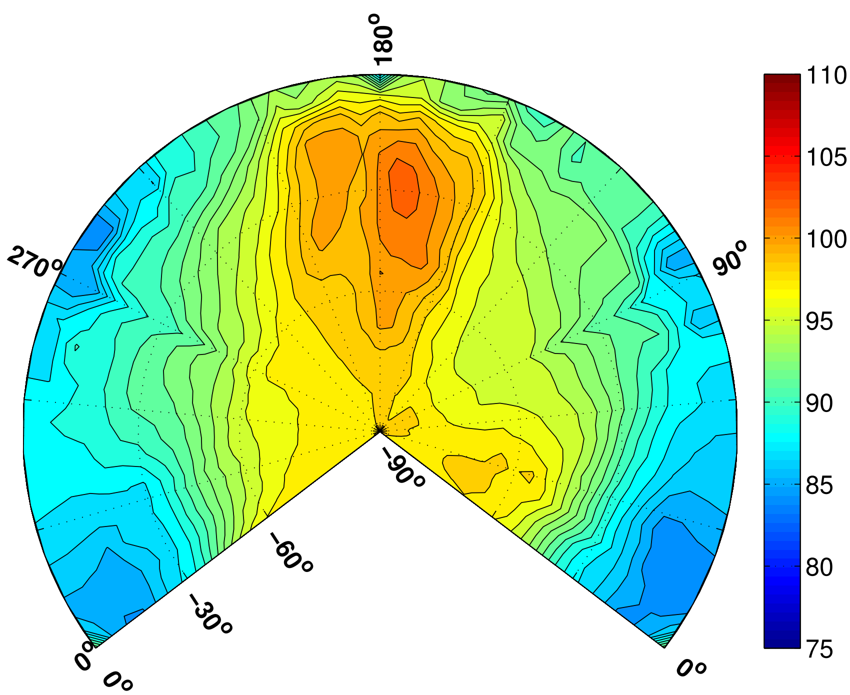

(b) BVISPL, dB

Figure 43: Descent hemi-sphere Be430116, 81.0 KTAS, -5.5°

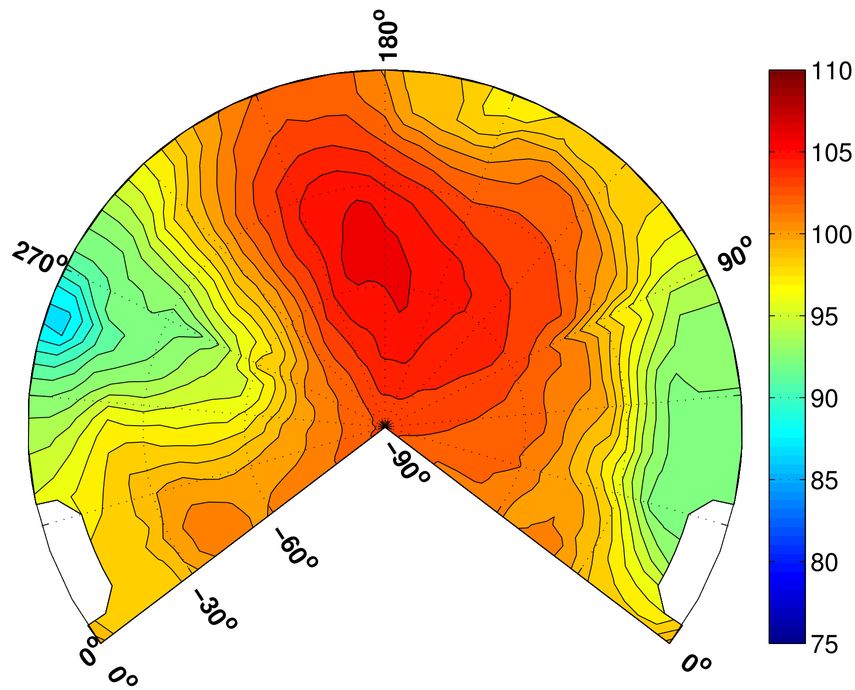

(a) OASPL, dB

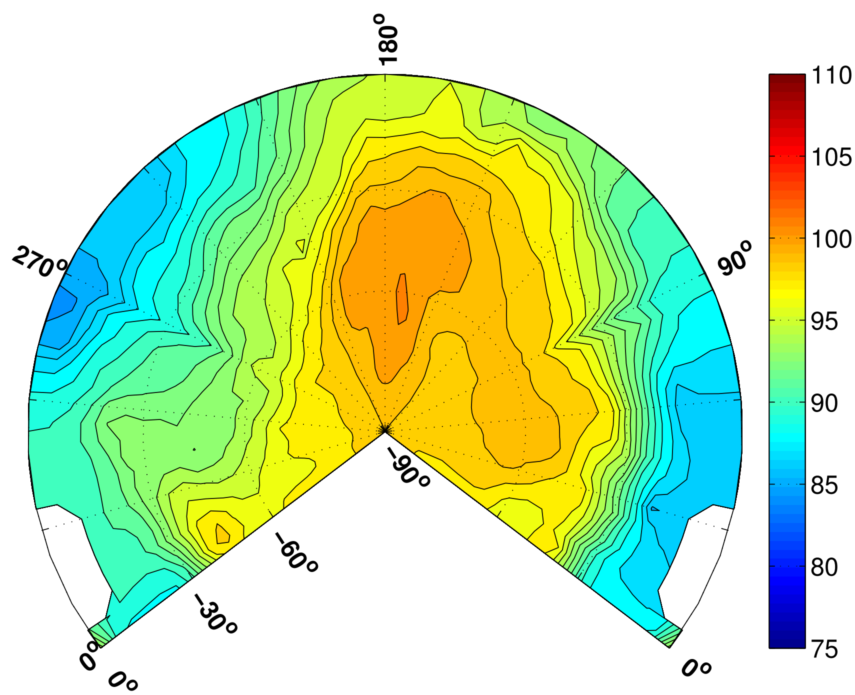

(b) BVISPL, dB

Figure 44: Descent hemi-sphere Be430145, 56.4 KTAS, -11.2°

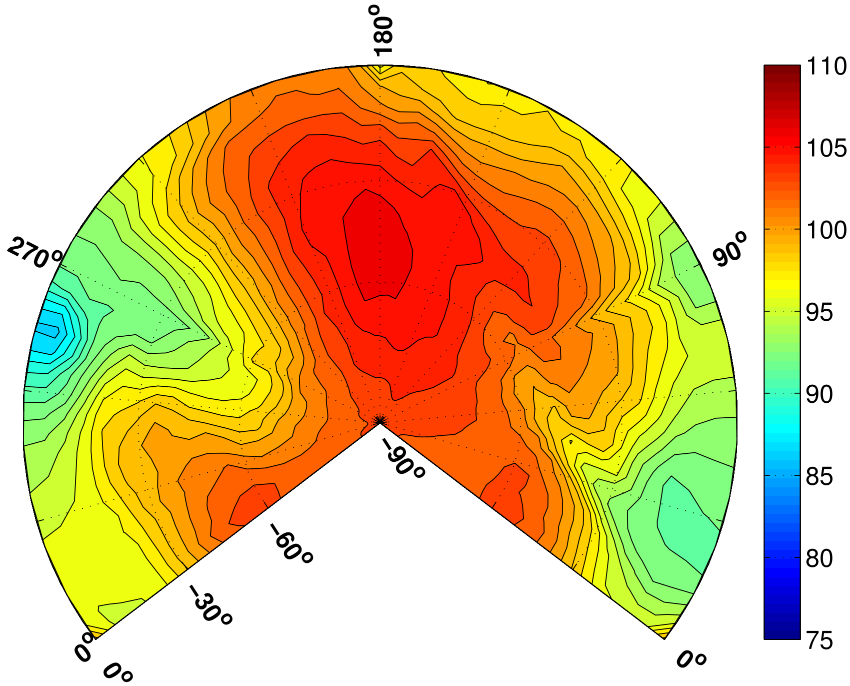

(a) OASPL, dB

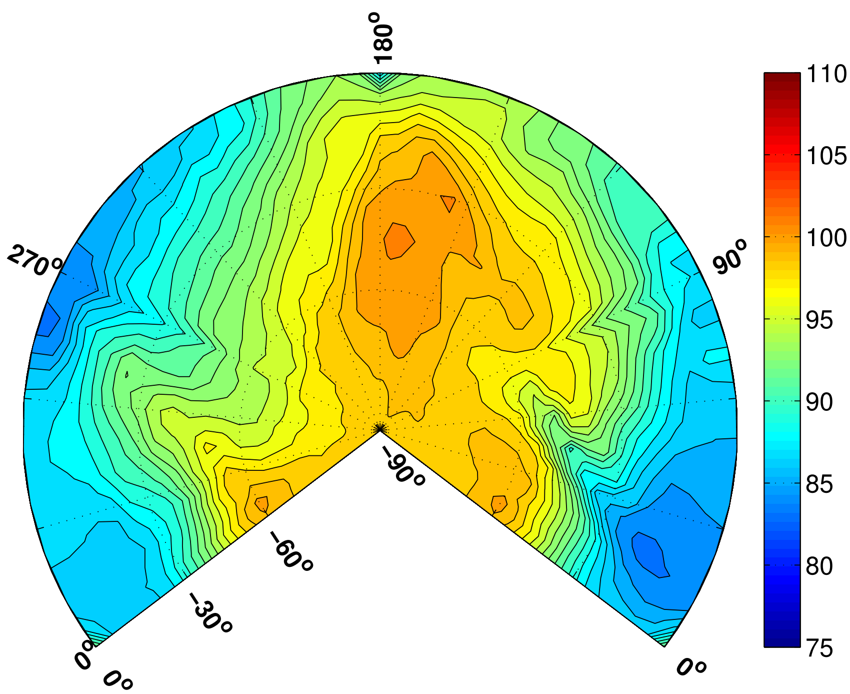

(b) BVISPL, dB

Figure 45: Descent hemi-sphere Be430146, 53.7 KTAS, -11.4°

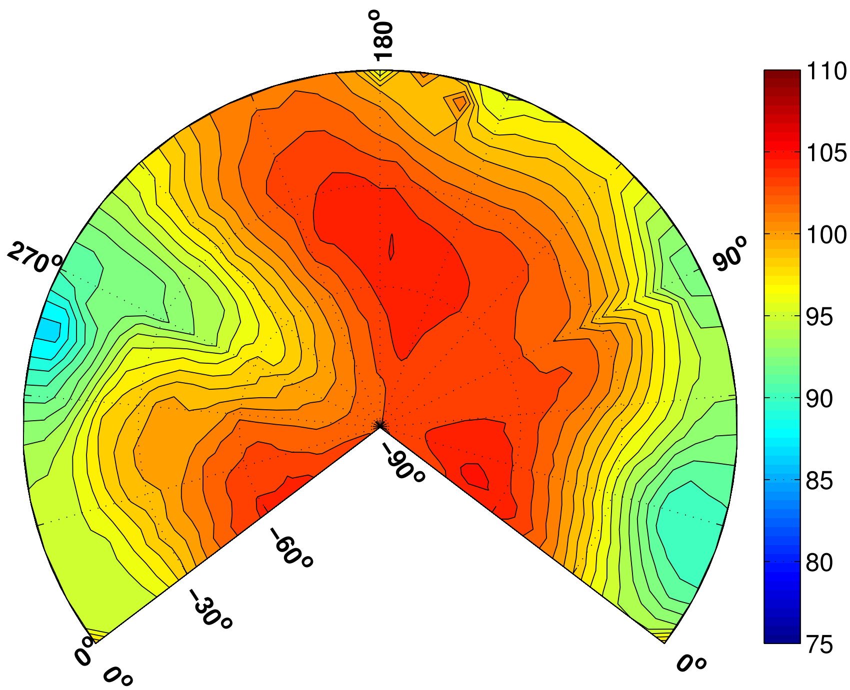

(a) OASPL, dB

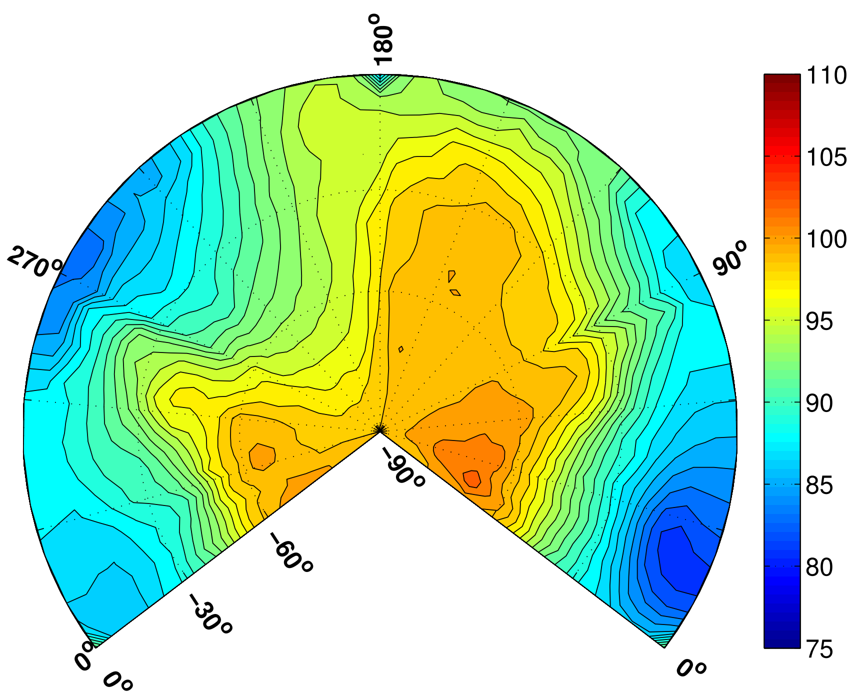

(b) BVISPL, dB

Figure 46: Descent hemi-sphere Be430147, 55.2 KTAS, -11.8°

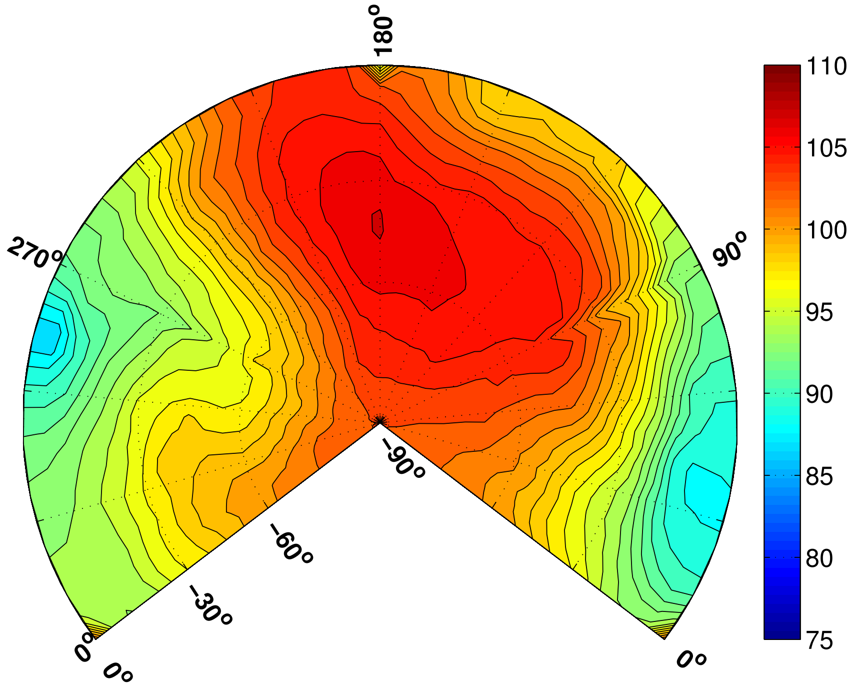

(a) OASPL, dB

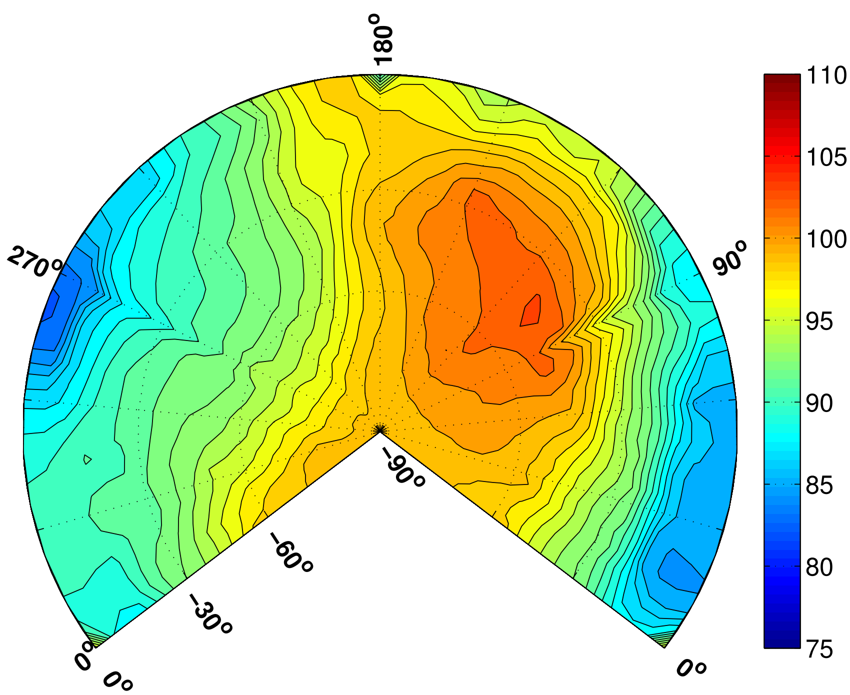

(b) BVISPL, dB

Figure 47: Descent hemi-sphere Be430148, 77.9 KTAS, -11.8°

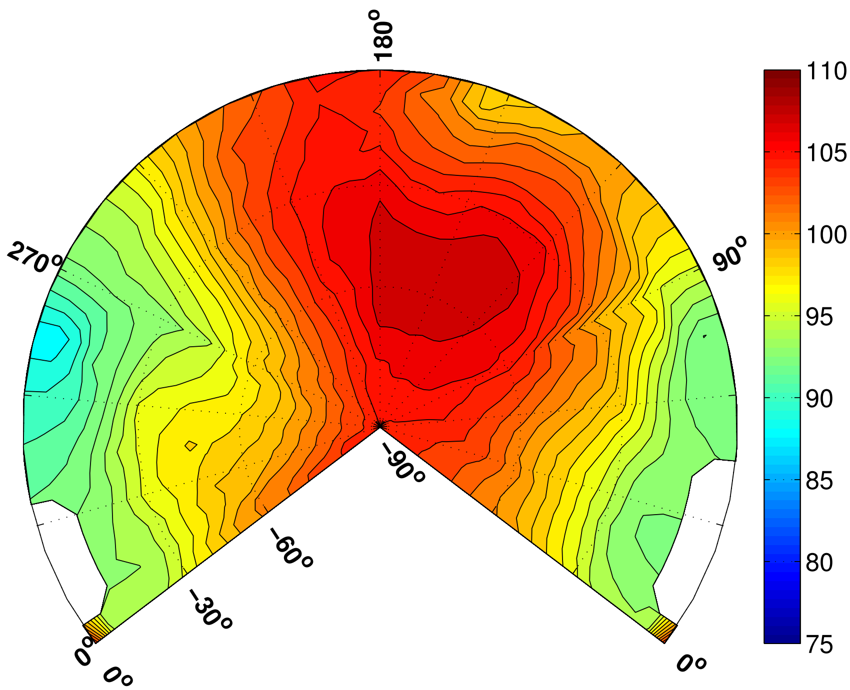

(a) OASPL, dB

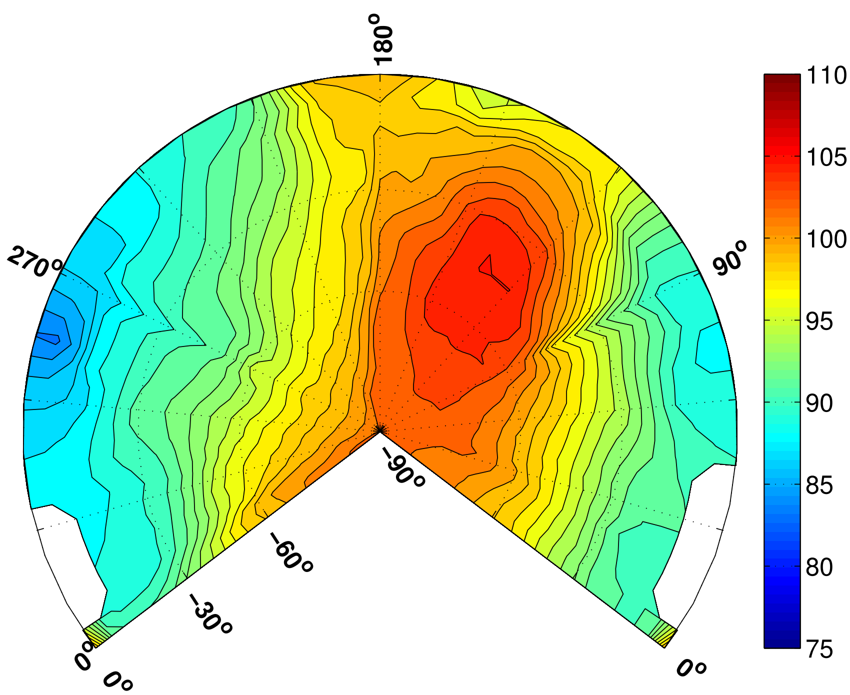

(b) BVISPL, dB

Figure 48: Descent hemi-sphere Be430149, 79.9 KTAS, -10.9°

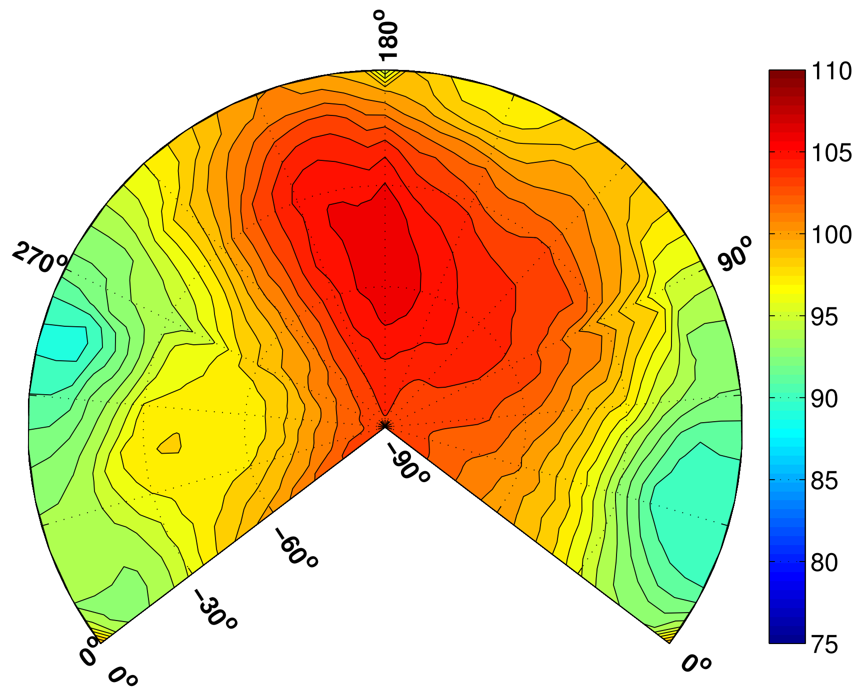

(a) OASPL, dB

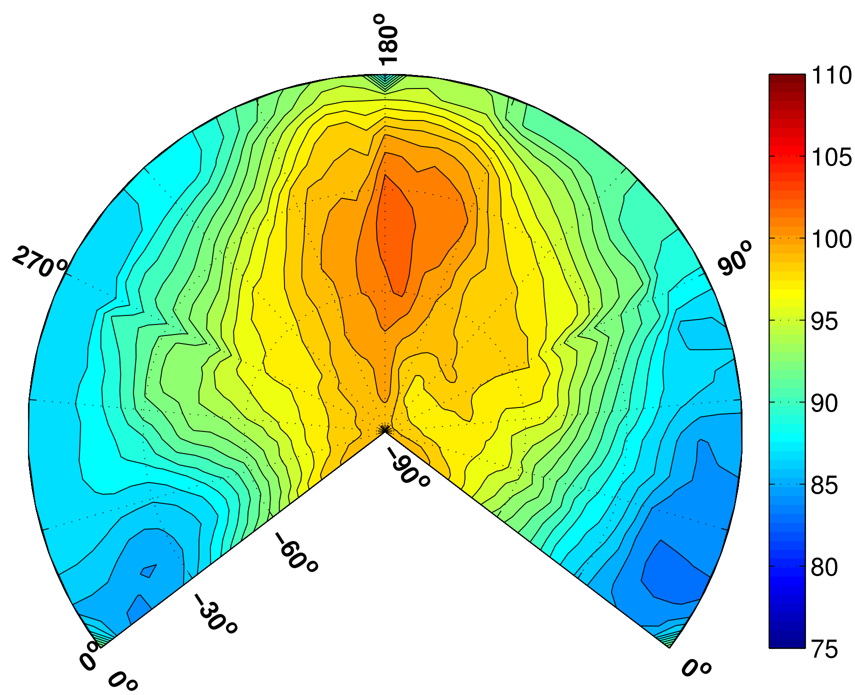

(b) BVISPL, dB

Figure 49: Descent hemi-sphere Be430150, 59.6 KTAS, -9.1°

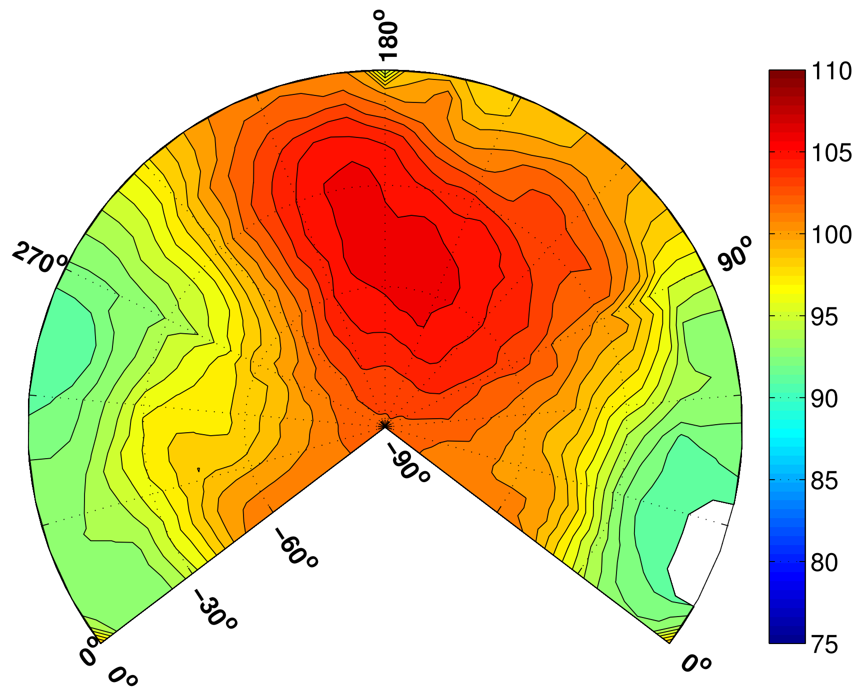

(a) OASPL, dB

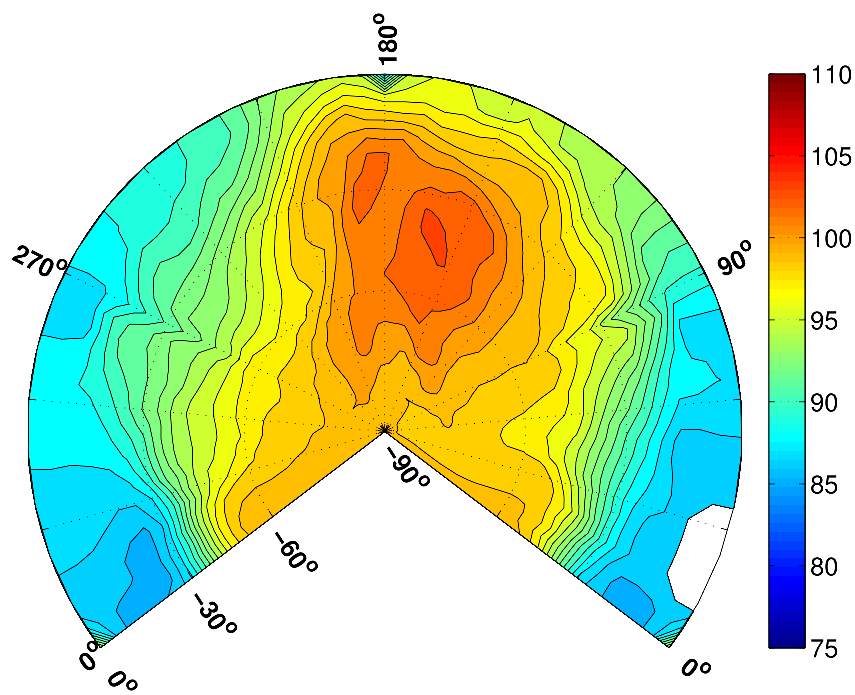

(b) BVISPL, dB

Figure 50: Descent hemi-sphere Be430151, 71.6 KTAS, -8.4°

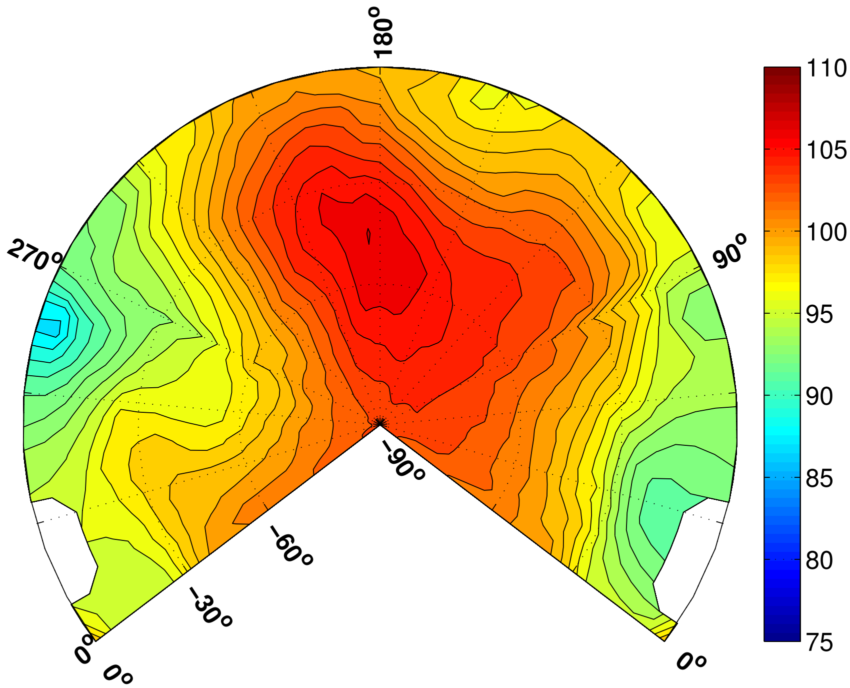

(a) OASPL, dB

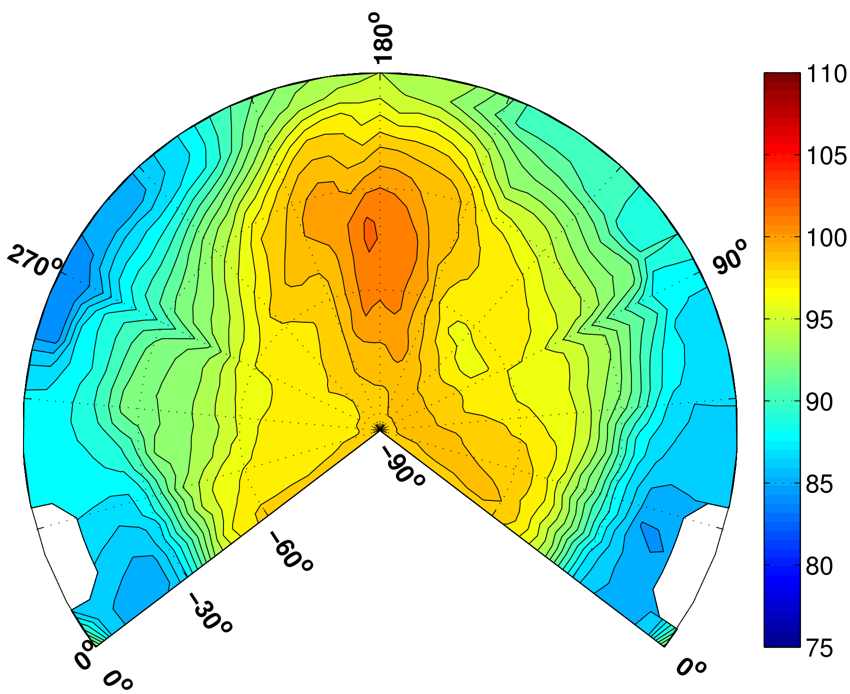

(b) BVISPL, dB

Figure 51: Descent hemi-sphere Be430152, 58.5 KTAS, -9.7°

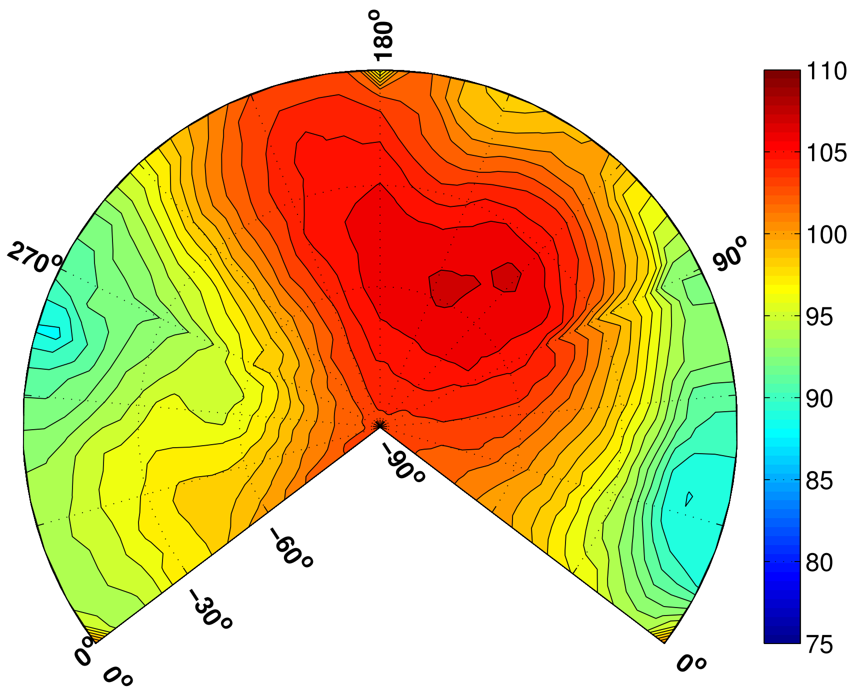

(a) OASPL, dB

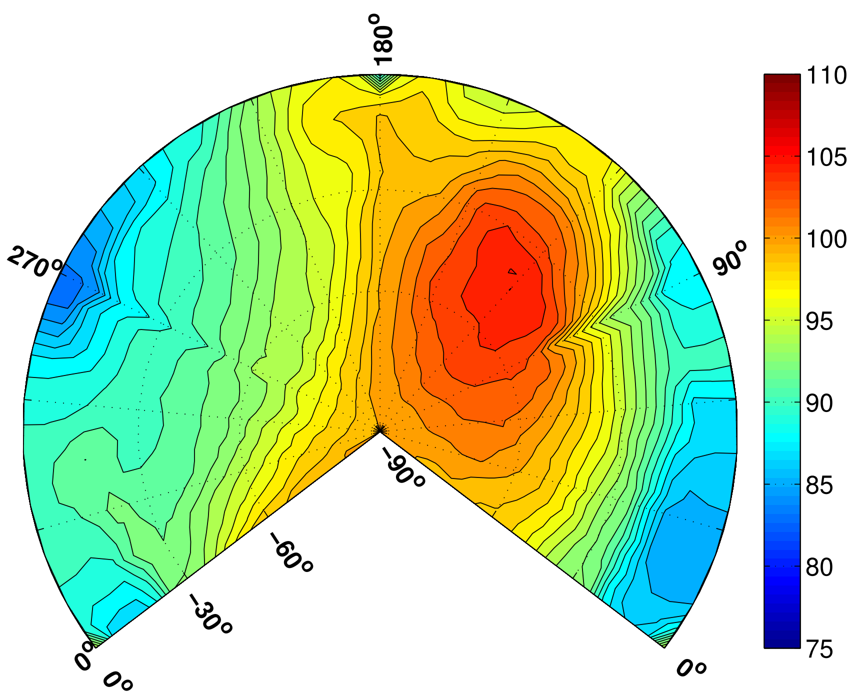

(b) BVISPL, dB

Figure 52: Descent hemi-sphere Be430153, 80.9 KTAS, -10.0°

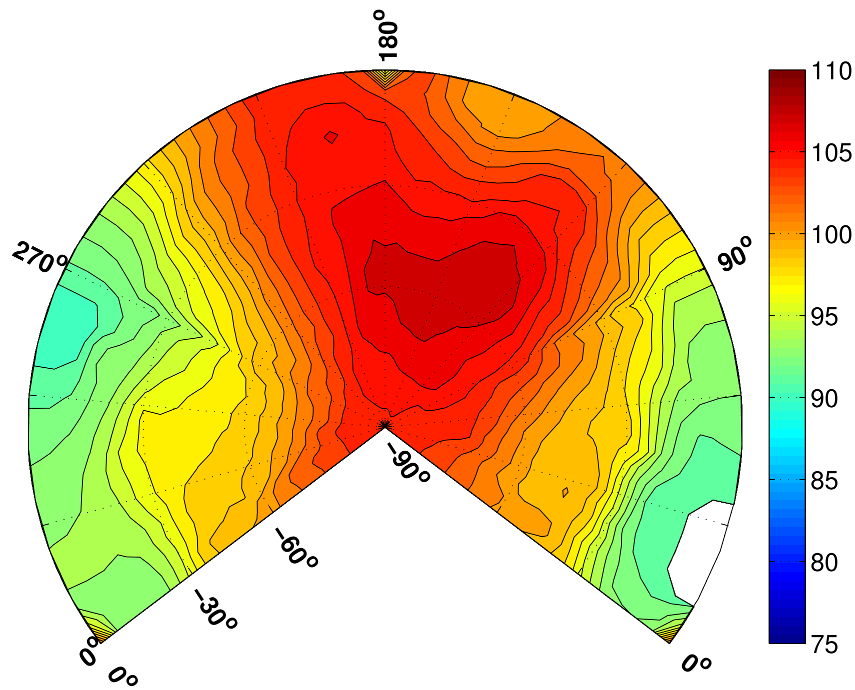

(a) OASPL, dB

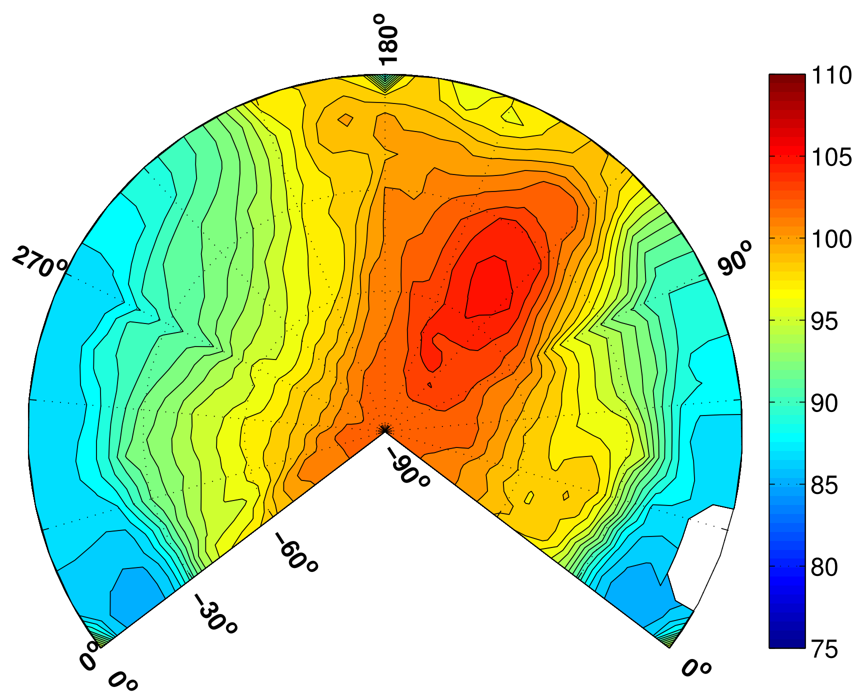

(b) BVISPL, dB

Figure 53: Descent hemi-sphere Be430154, 88.6 KTAS, -9.4°

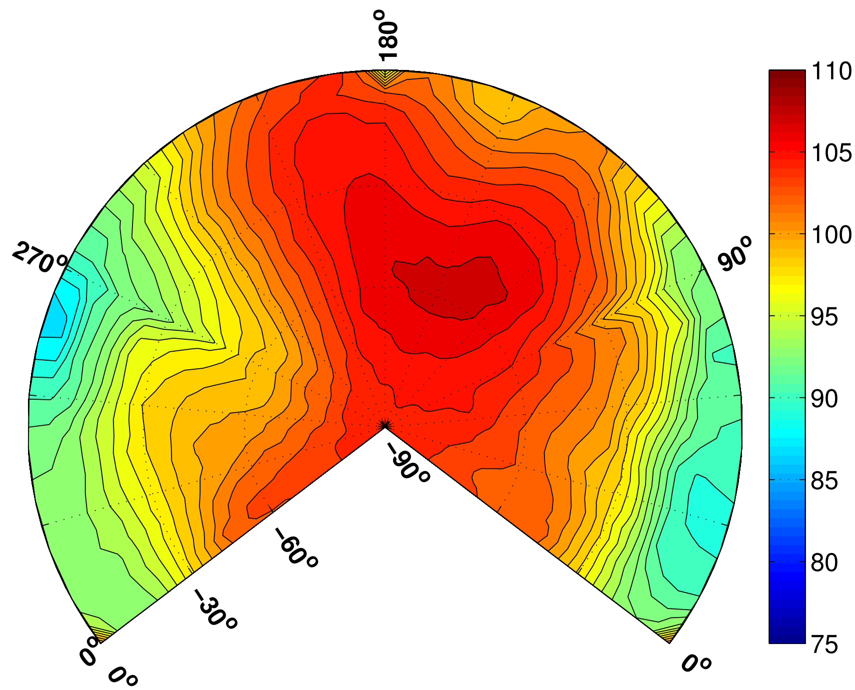

(a) OASPL, dB

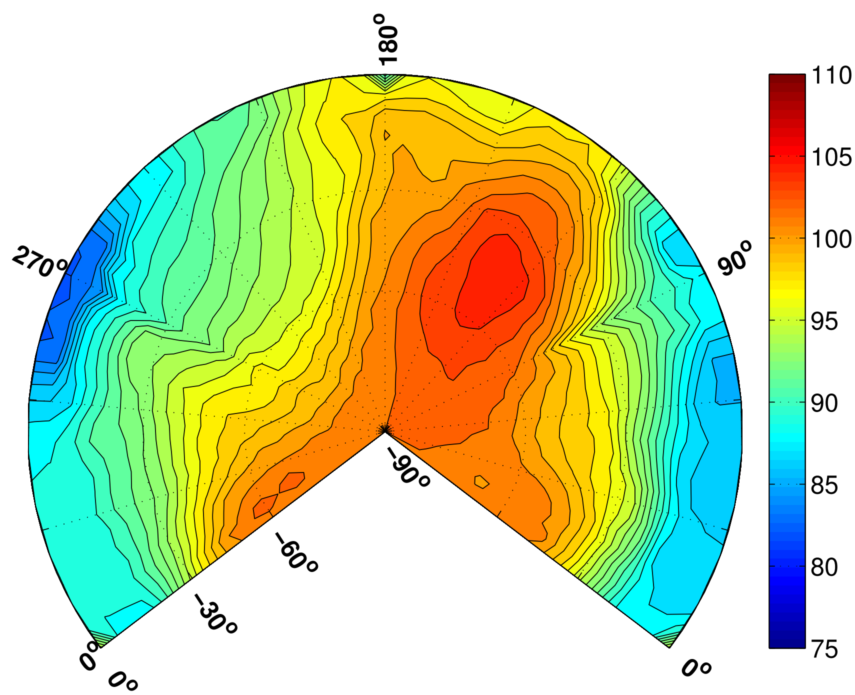

(b) BVISPL, dB

Figure 54: Descent hemi-sphere Be430155, 82.3 KTAS, -10.2°

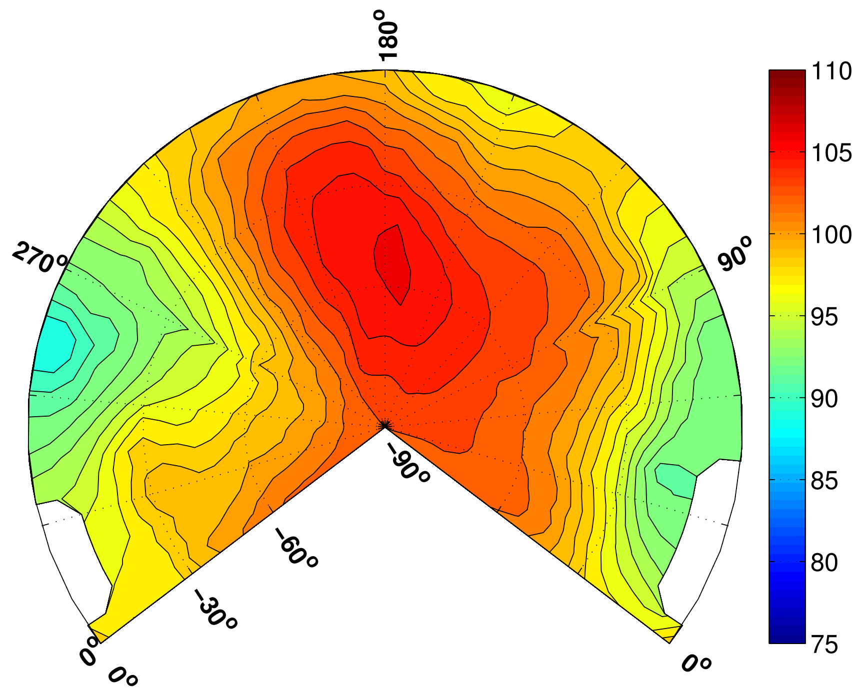

(a) OASPL, dB

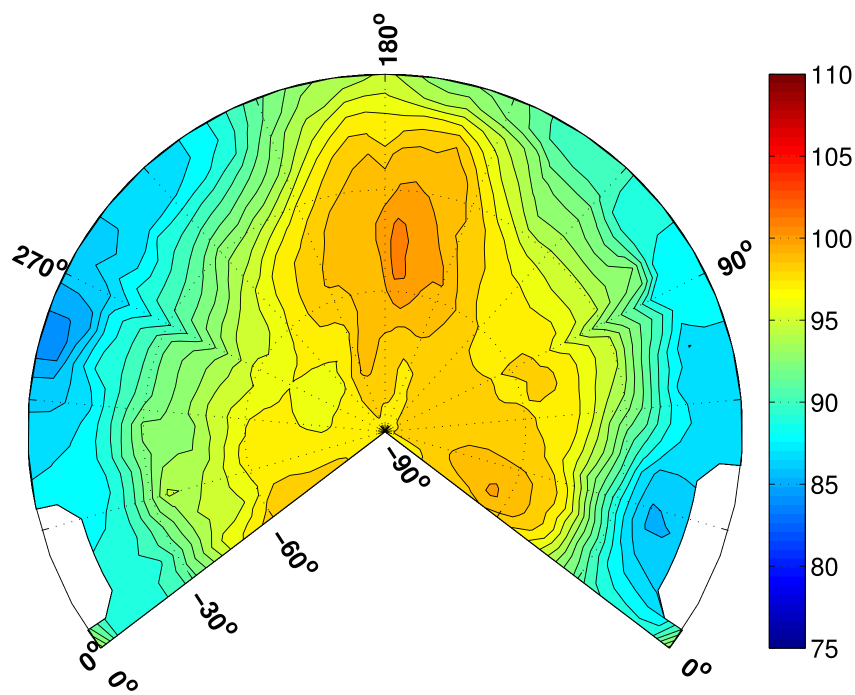

(b) BVISPL, dB

Figure 55: Descent hemi-sphere Be430156, 57.2 KTAS, -8.3°

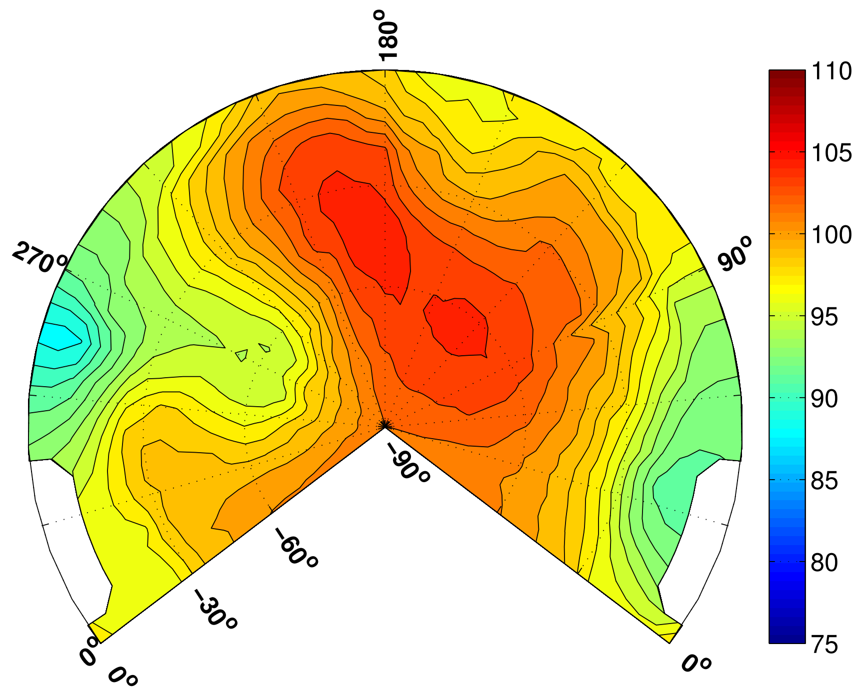

(a) OASPL, dB

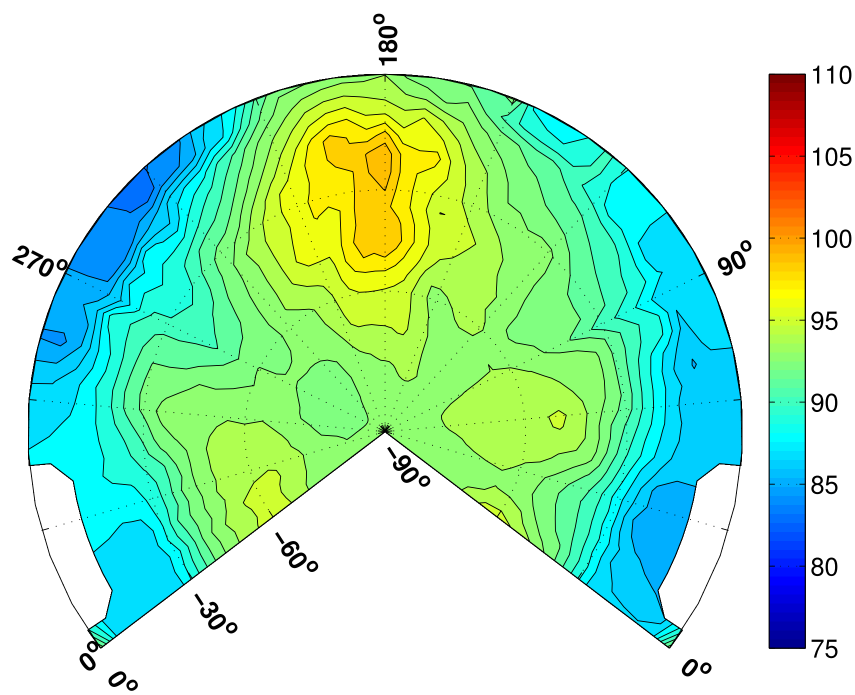

(b) BVISPL, dB

Figure 56: Descent hemi-sphere Be430157, 56.3 KTAS, -6.8°

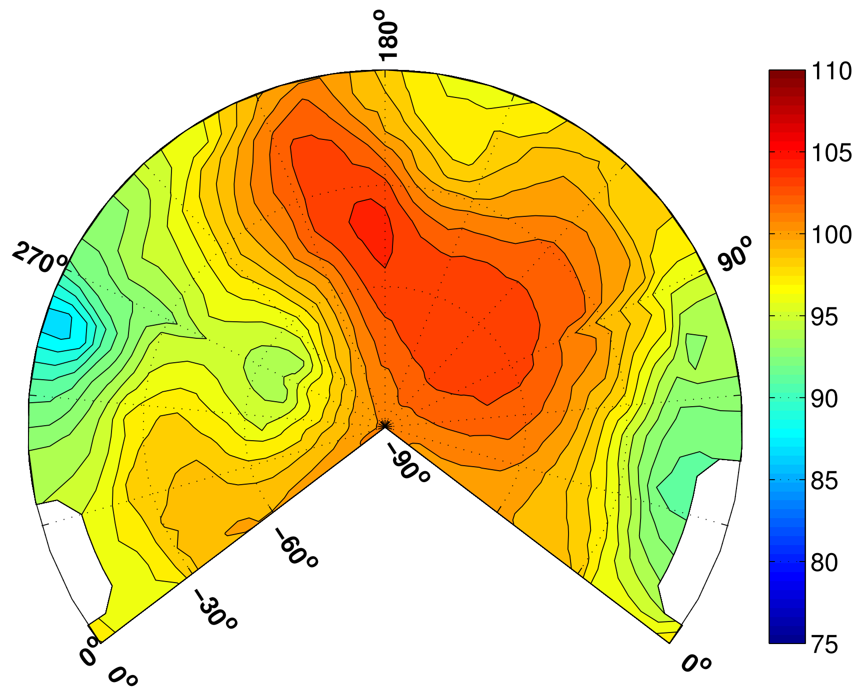

(a) OASPL, dB

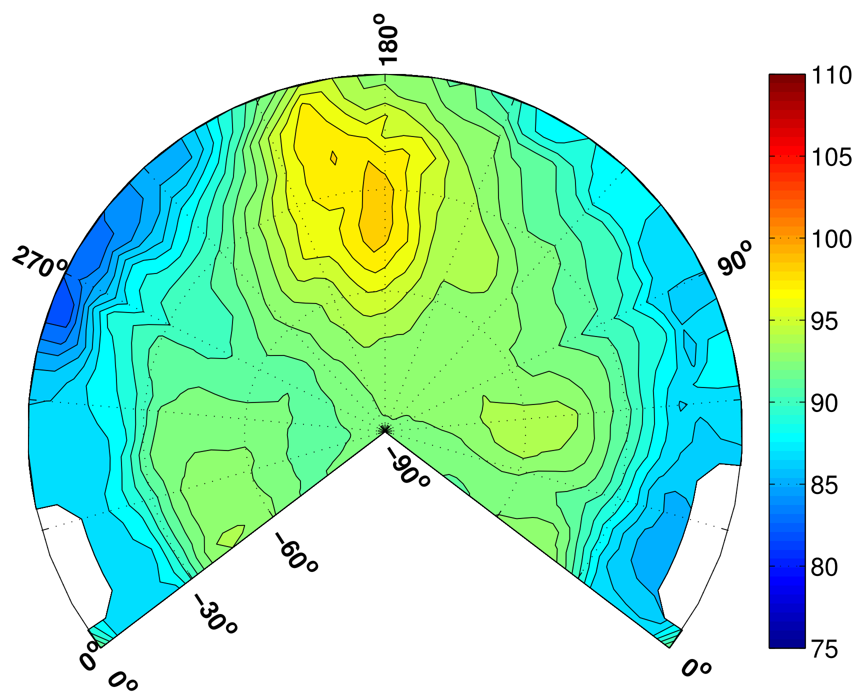

(b) BVISPL, dB

Figure 57: Descent hemi-sphere Be430158, 55.7 KTAS, -6.9°

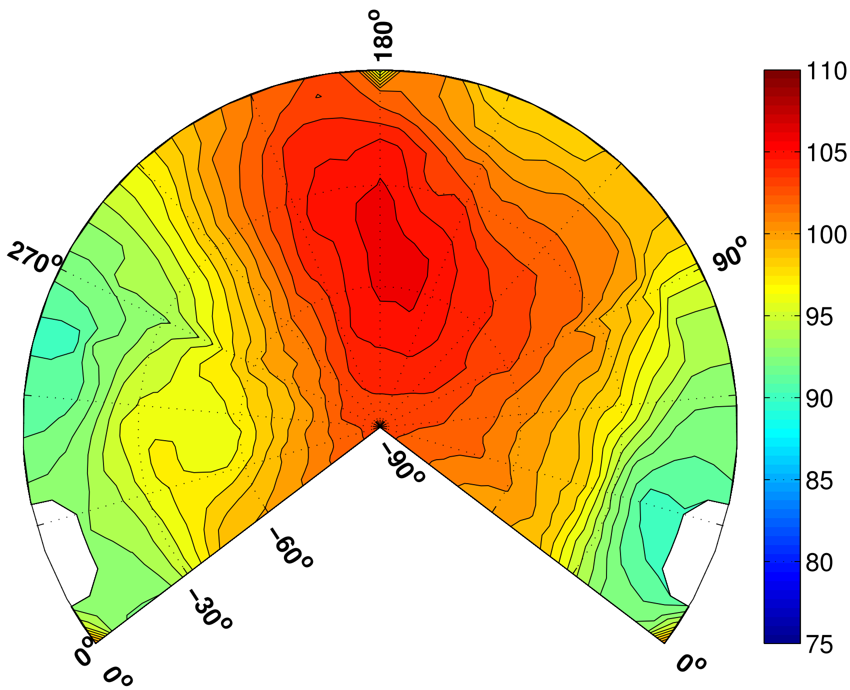

(a) OASPL, dB

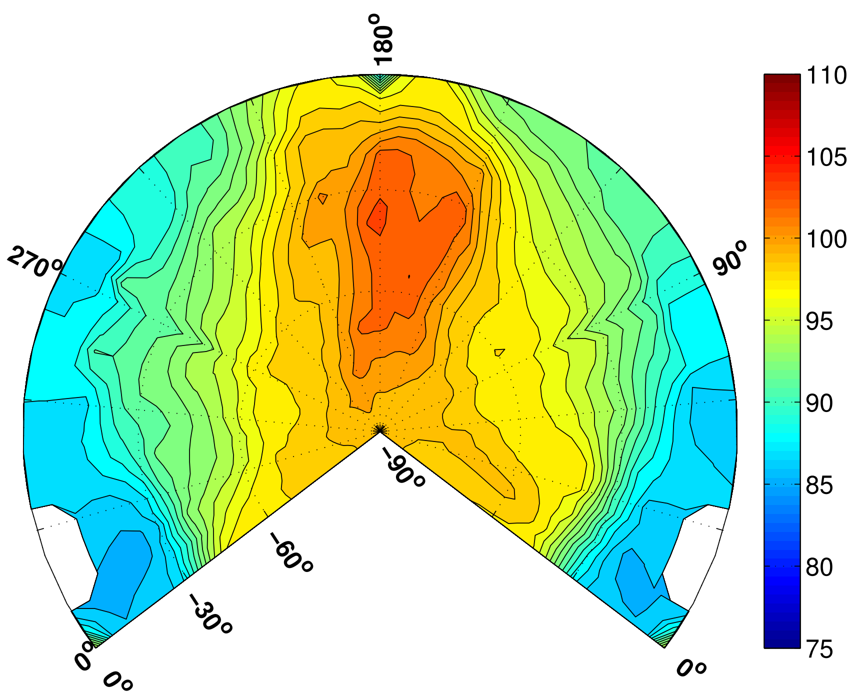

(b) BVISPL, dB

Figure 58: Descent hemi-sphere Be430159, 81.1 KTAS, -6.6°

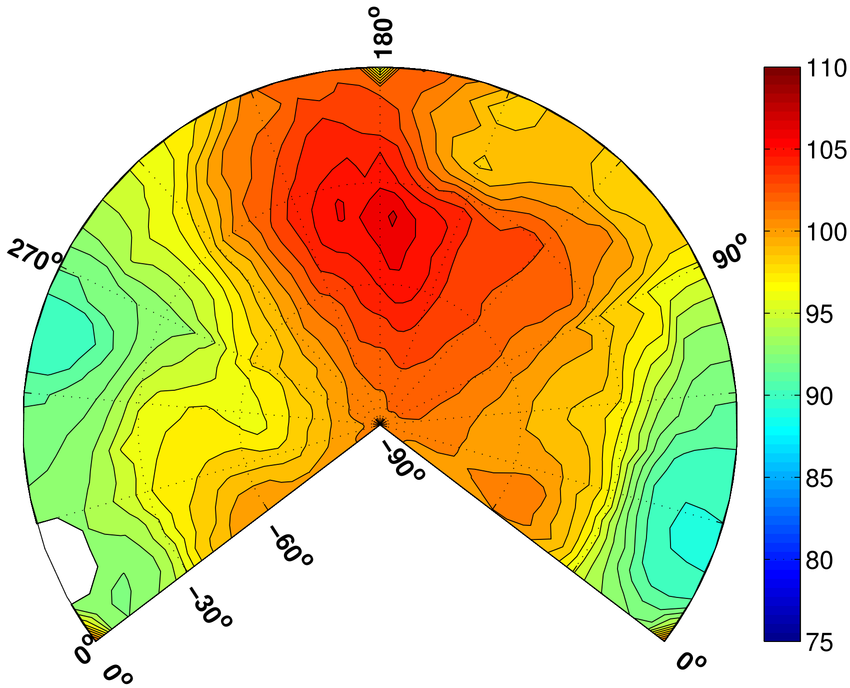

(a) OASPL, dB

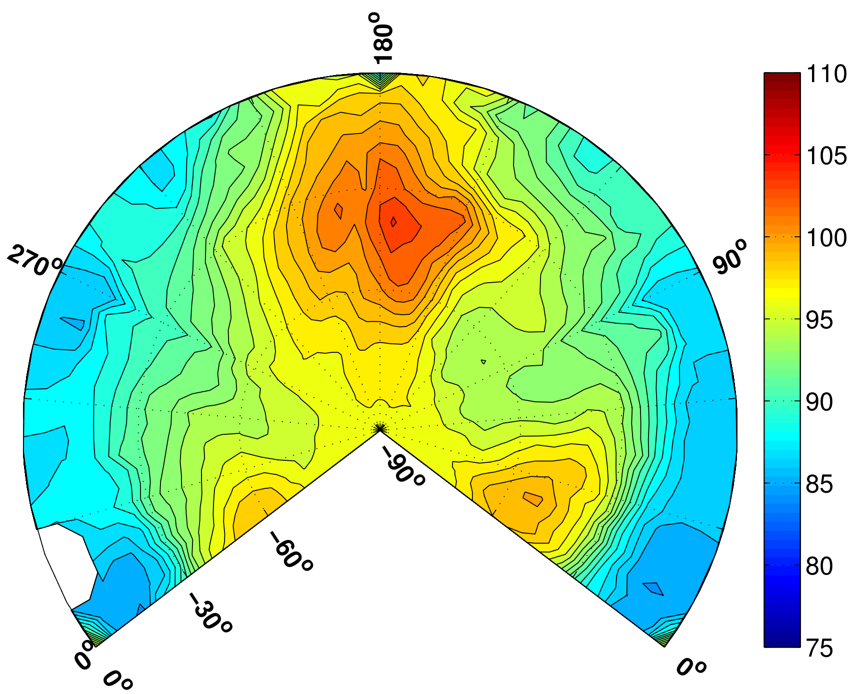

(b) BVISPL, dB

Figure 59: Descent hemi-sphere Be430177, 82.2 KTAS, -6.4°

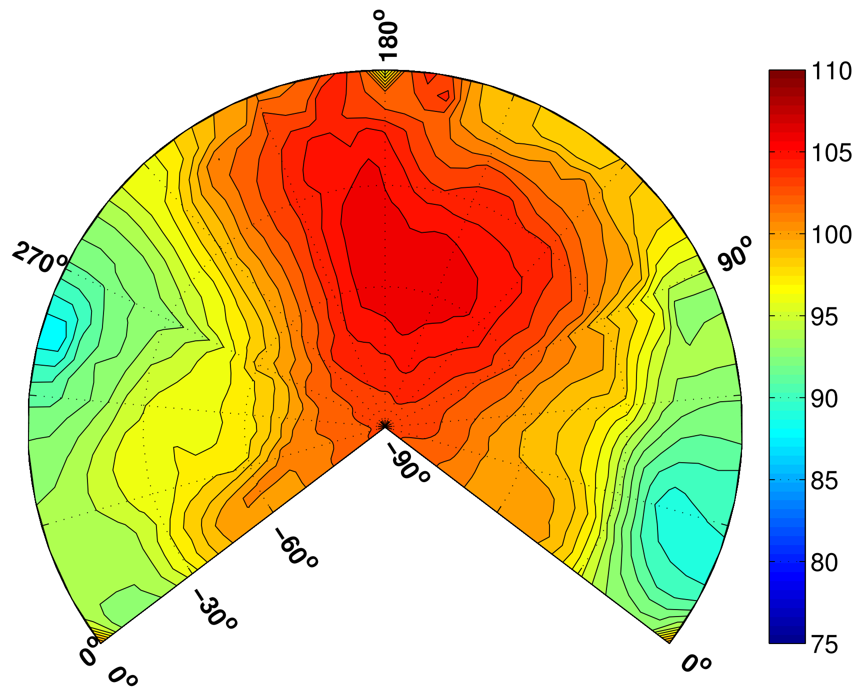

(a) OASPL, dB

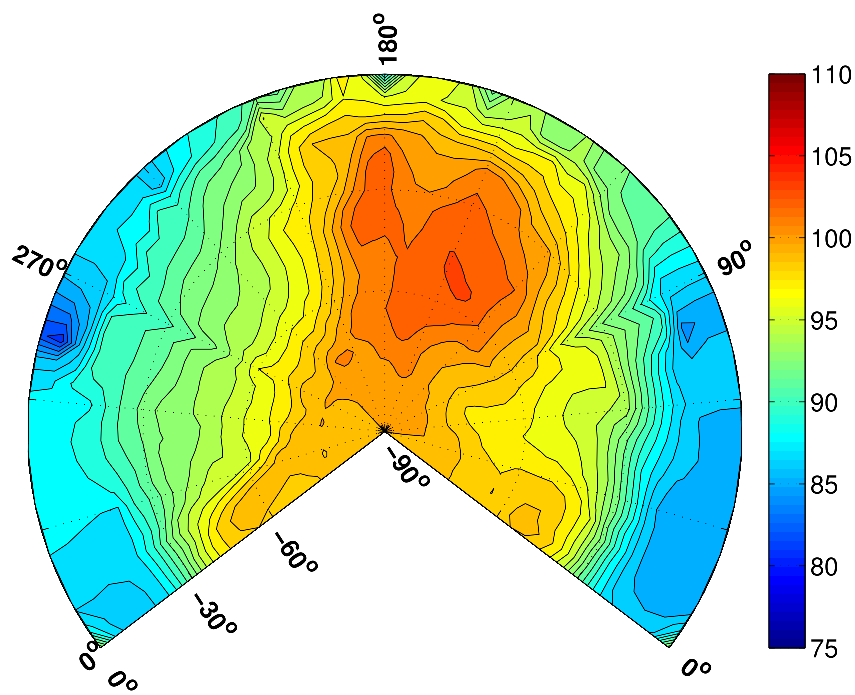

(b) BVISPL, dB

Figure 60: Descent hemi-sphere Be430178, 82.1 KTAS, -6.9°

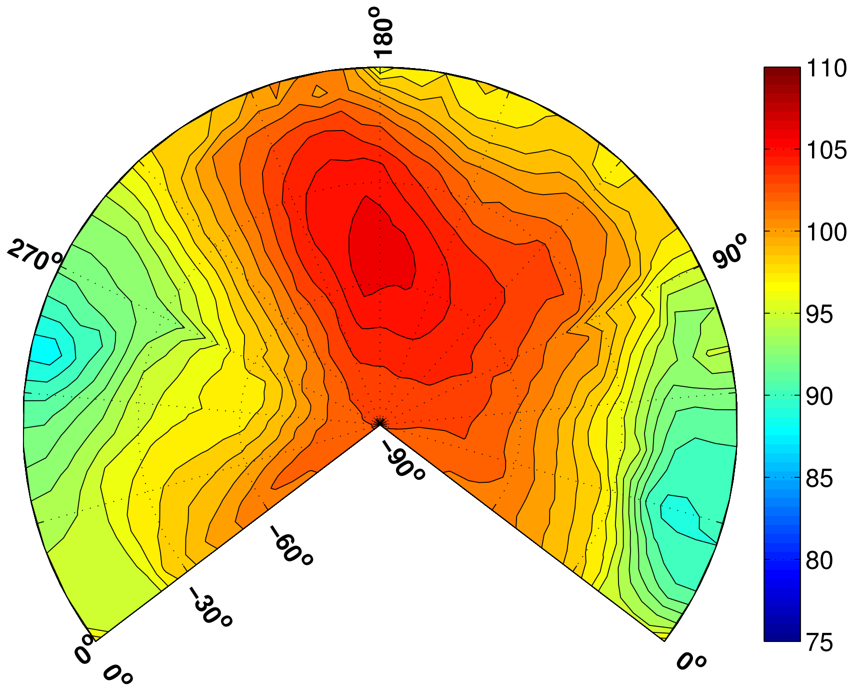

(a) OASPL, dB

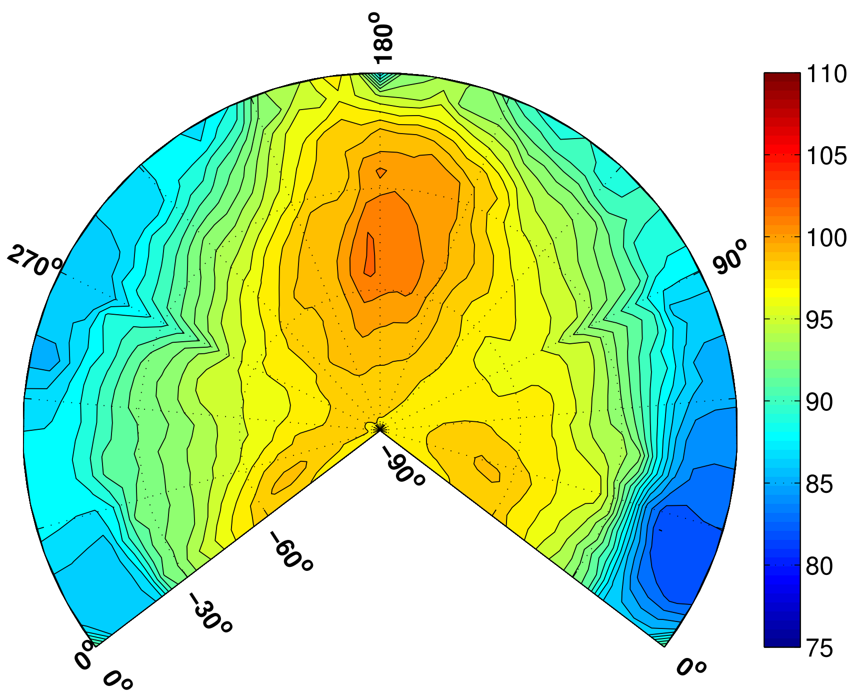

(b) BVISPL, dB

Figure 61: Descent hemi-sphere Be430182, 61.4 KTAS, -8.1°

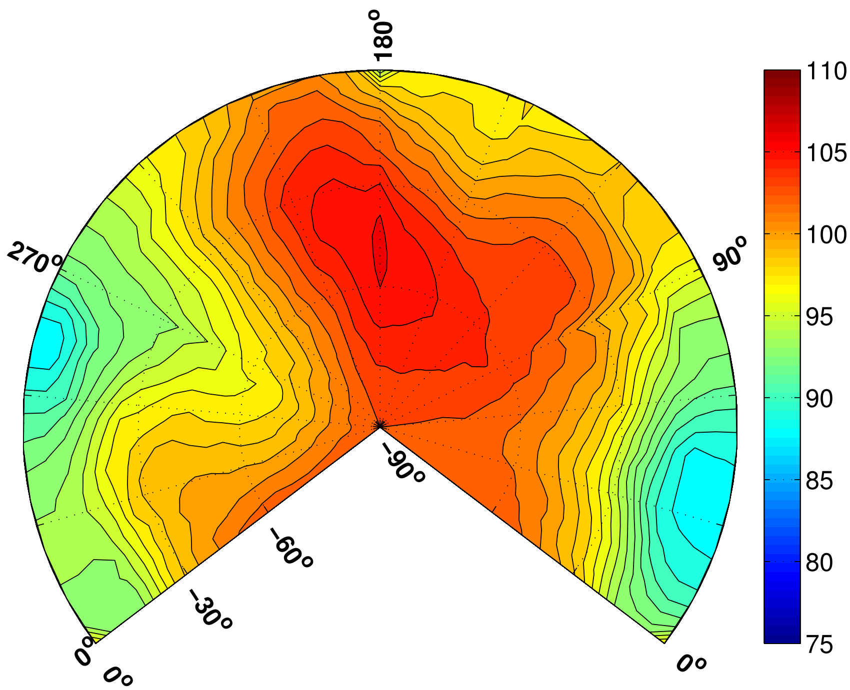

(a) OASPL, dB

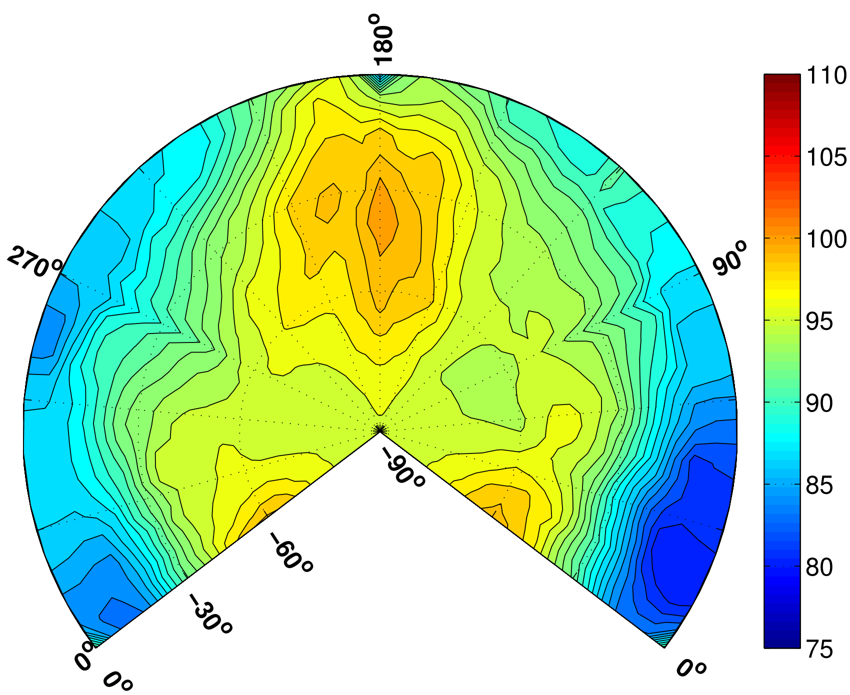

(b) BVISPL, dB

Figure 62: Descent hemi-sphere Be430183, 55.2 KTAS, -8.4°

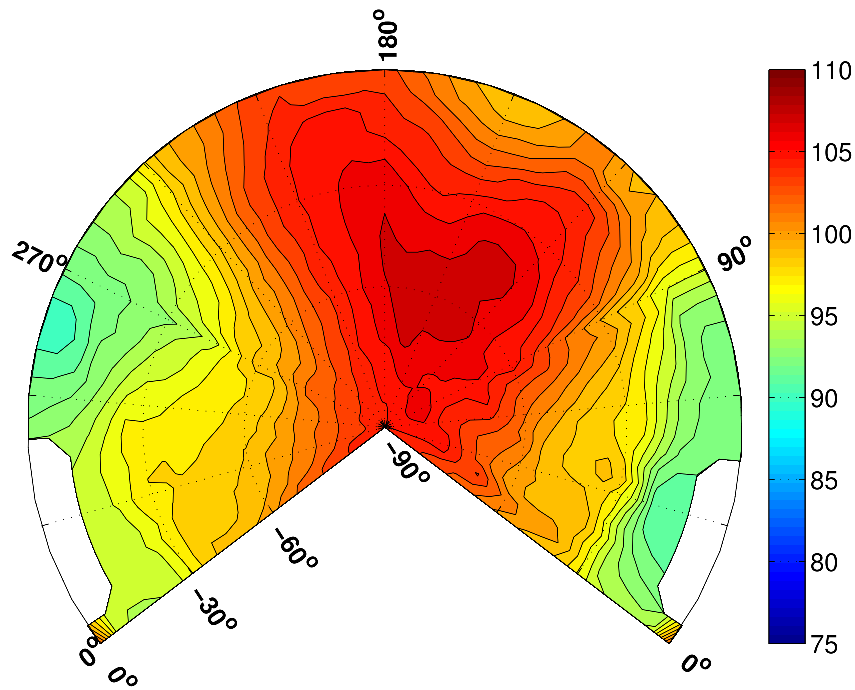

(a) OASPL, dB

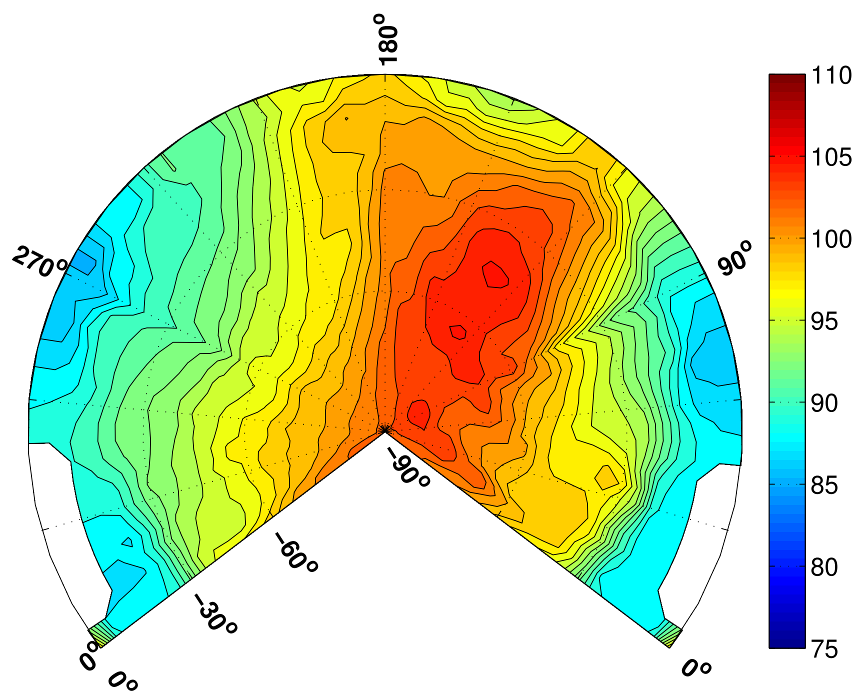

(b) BVISPL, dB

Figure 63: Descent hemi-sphere Be430184, 81.3 KTAS, -8.5°

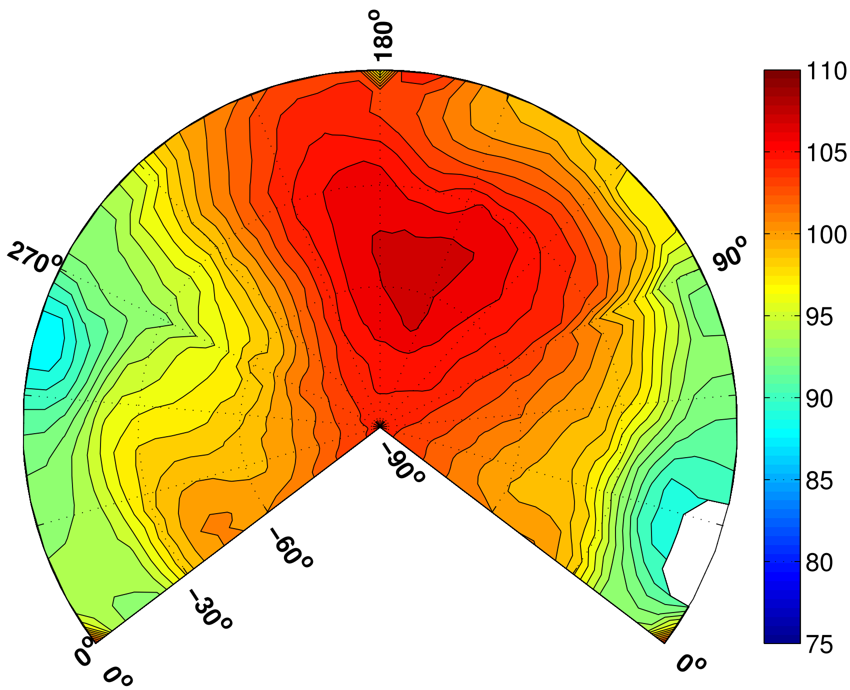

(a) OASPL, dB

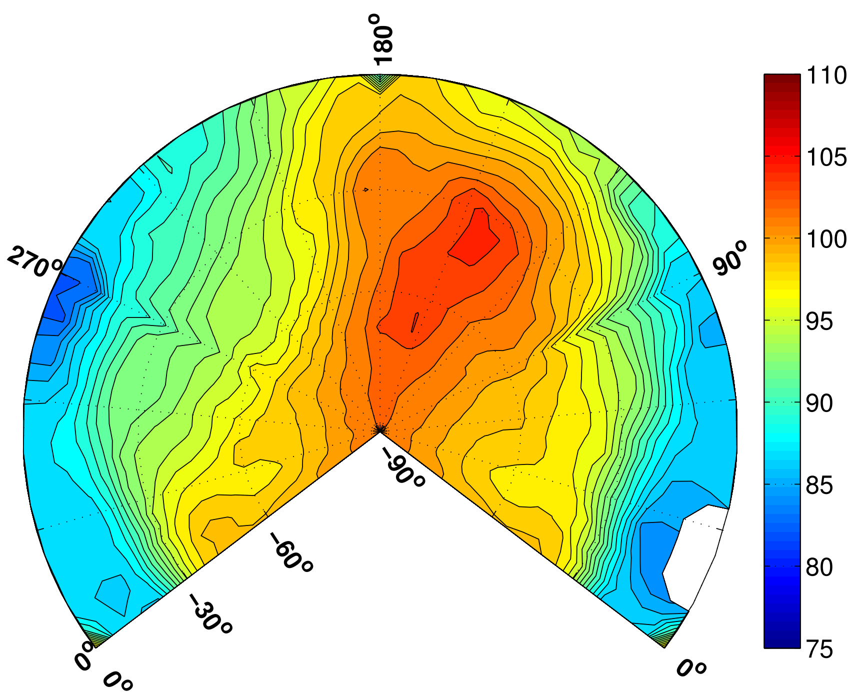

(b) BVISPL, dB

Figure 64: Descent hemi-sphere Be430185, 82.2 KTAS, -9.0°

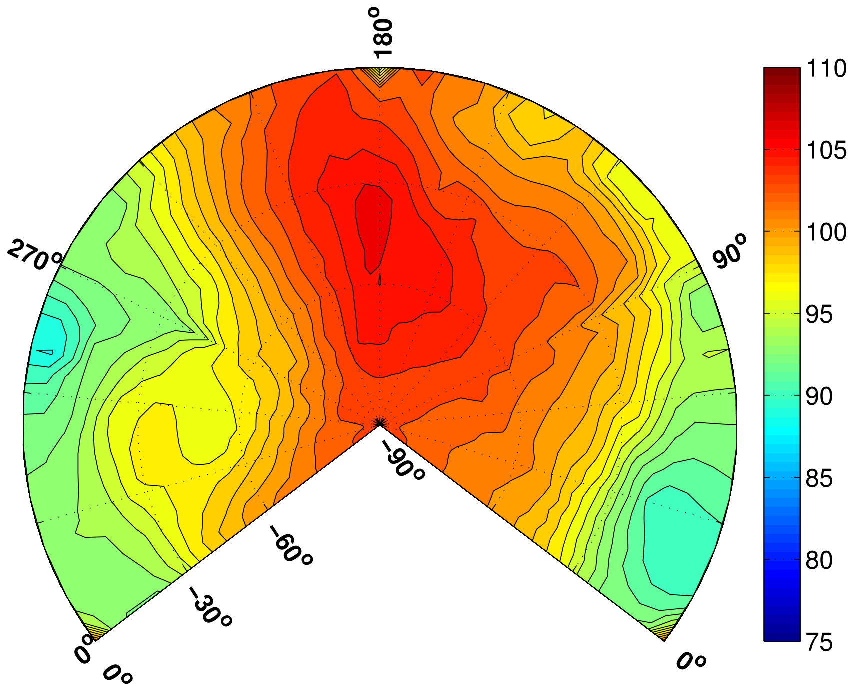

(a) OASPL, dB

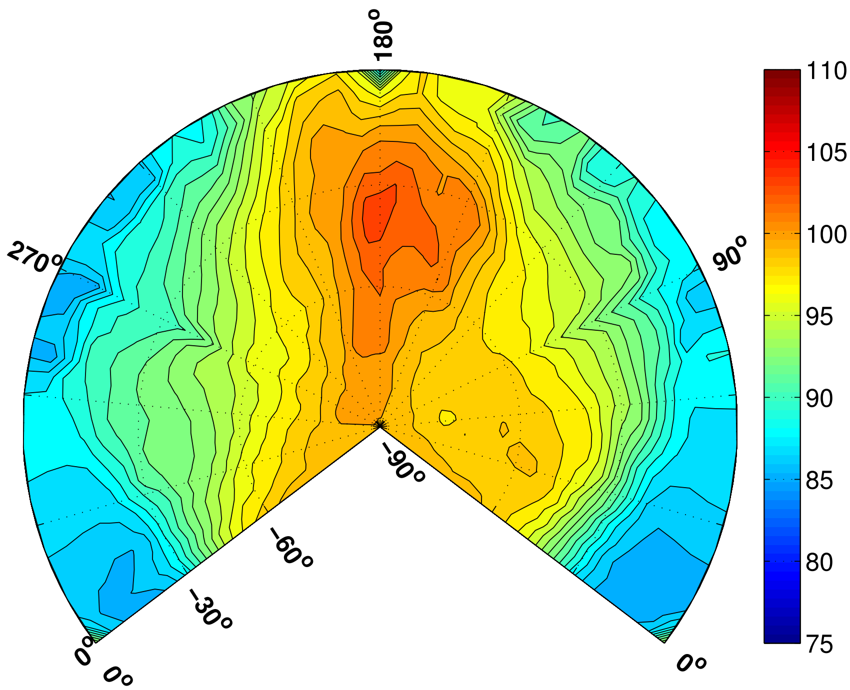

(b) BVISPL, dB

Figure 65: Descent hemi-sphere Be430187, 87.1 KTAS, -7.5°

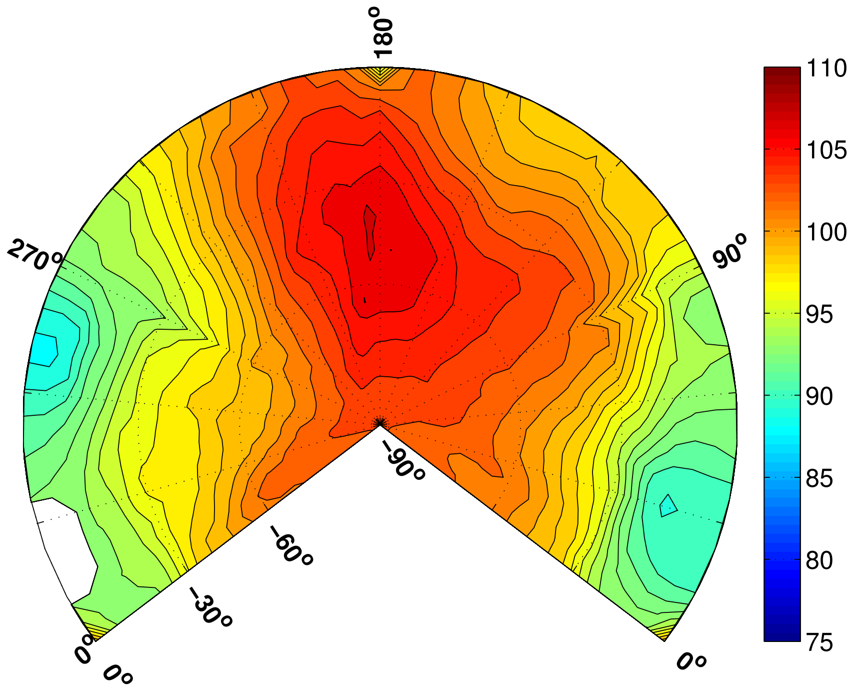

(a) OASPL, dB

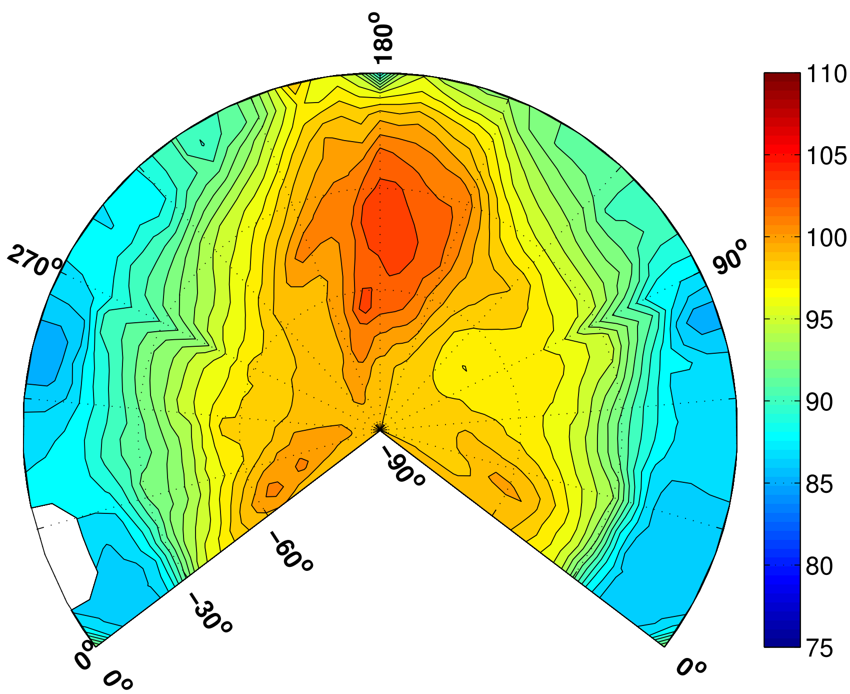

(b) BVISPL, dB

Figure 66: Descent hemi-sphere Be430188, 85.7 KTAS, -5.9°

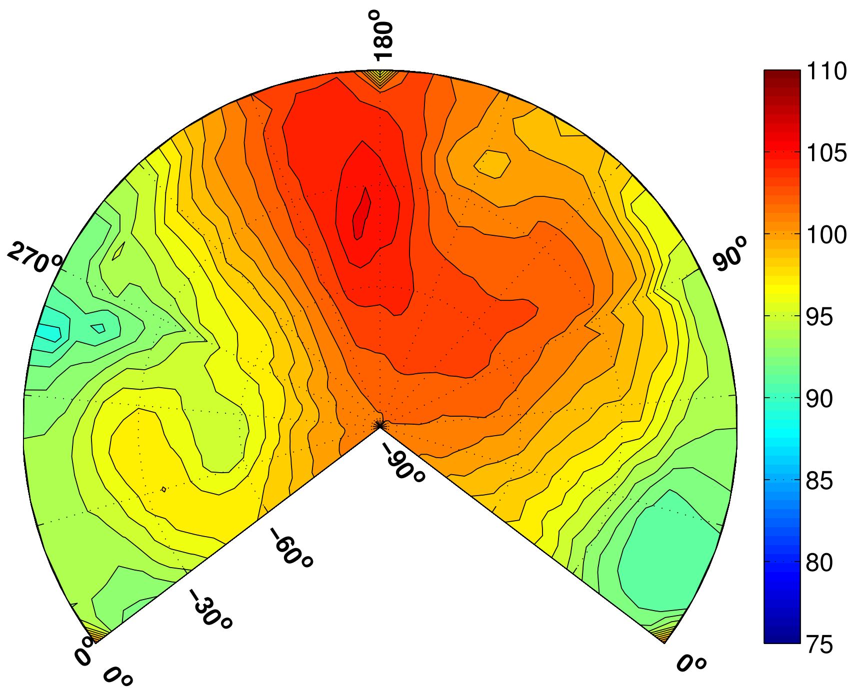

(a) OASPL, dB

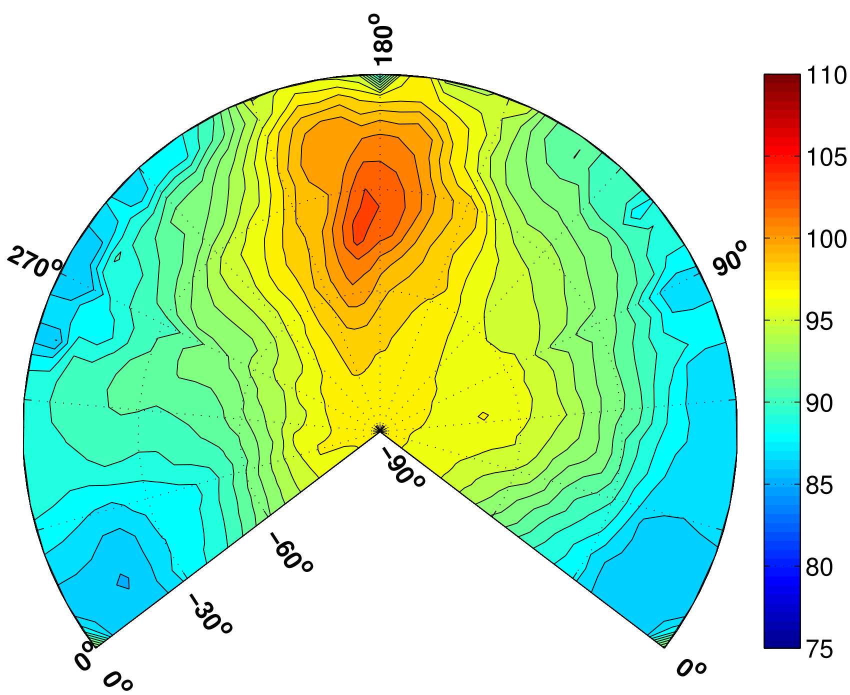

(b) BVISPL, dB

Figure 67: Descent hemi-sphere Be430189, 92.1 KTAS, -5.8°

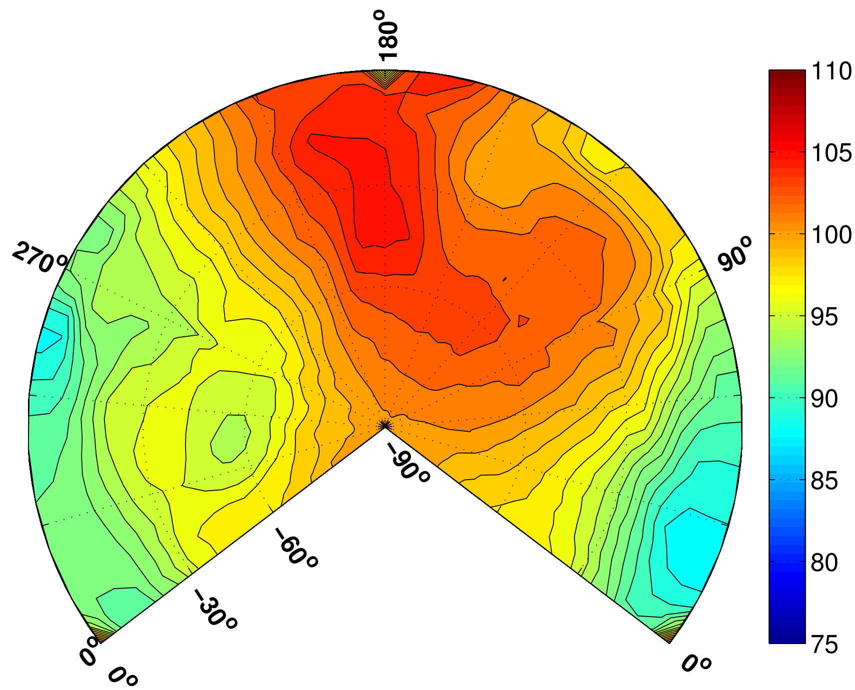

(a) OASPL, dB

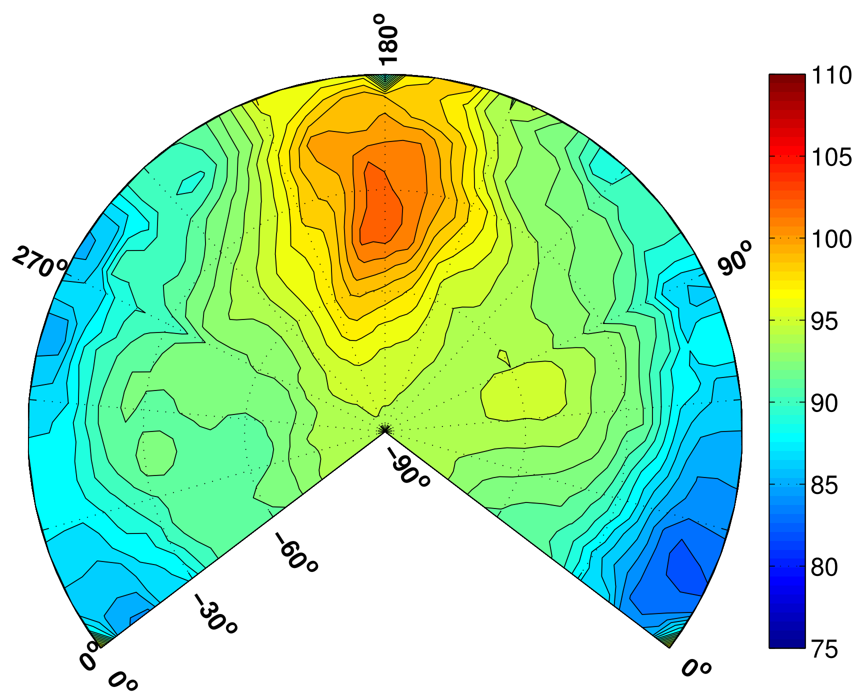

(b) BVISPL, dB

Figure 68: Descent hemi-sphere Be430190, 94.4 KTAS, -6.2°

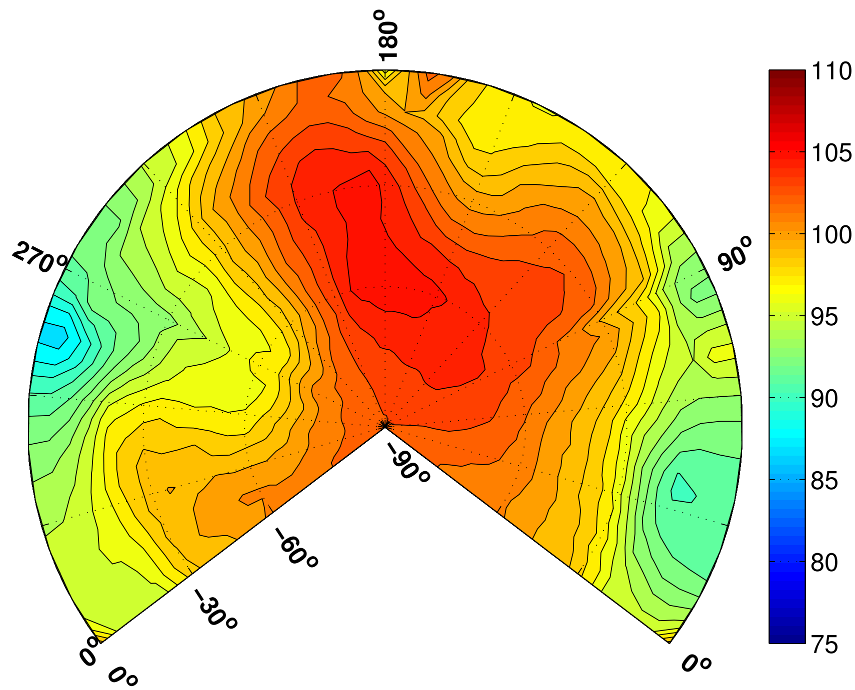

(a) OASPL, dB

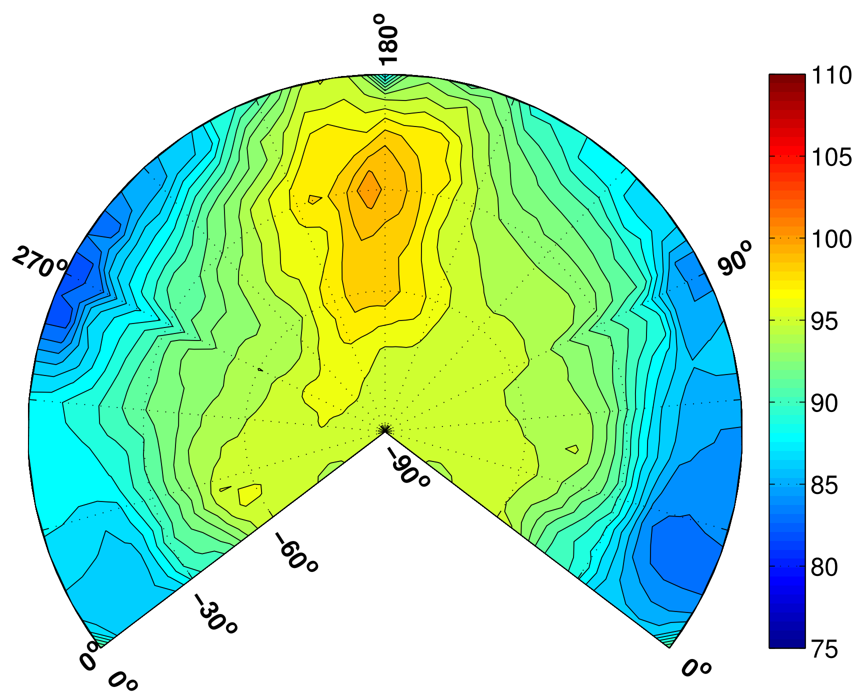

(b) BVISPL, dB

Figure 69: Descent hemi-sphere Be430191, 63.3 KTAS, -5.8°

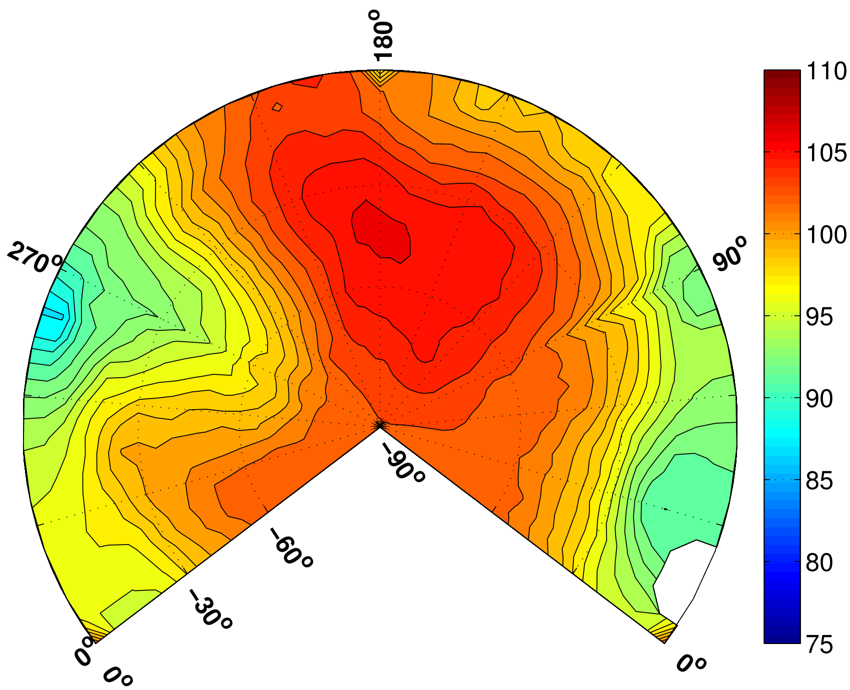

(a) OASPL, dB

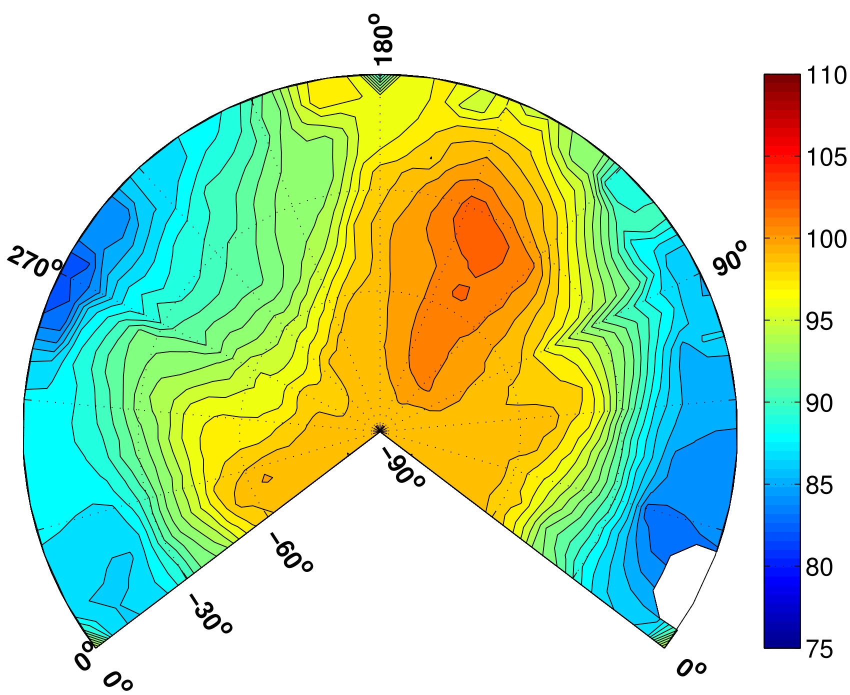

(b) BVISPL, dB

Figure 70: Descent hemi-sphere Be430192, 68.9 KTAS, -11.2°

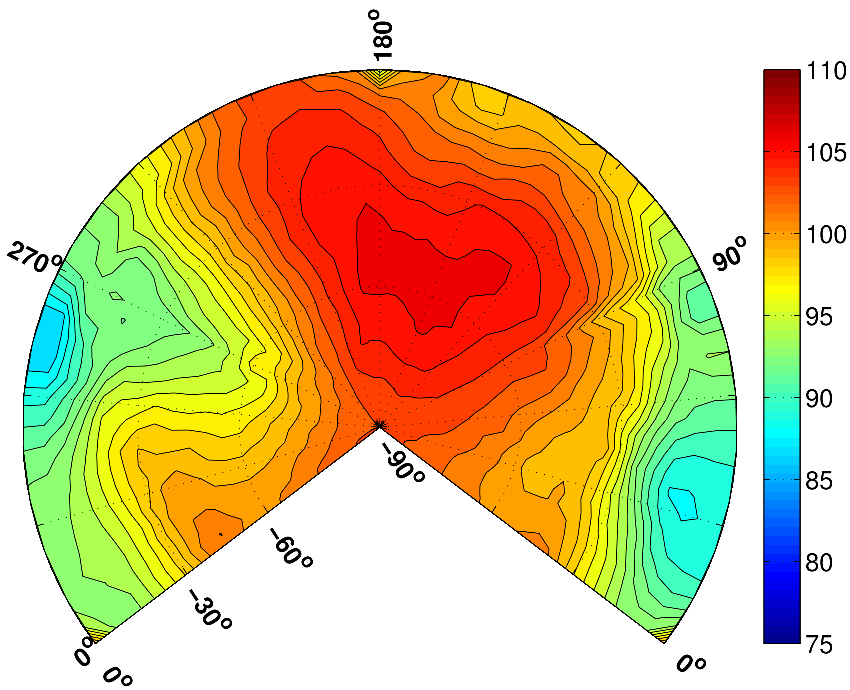

(a) OASPL, dB

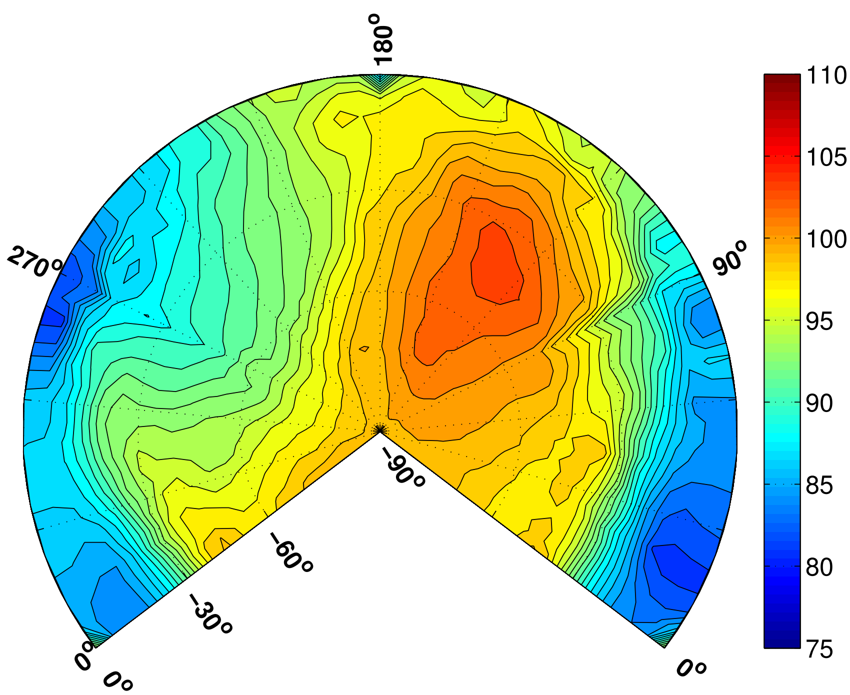

(b) BVISPL, dB

Figure 71: Descent hemi-sphere Be430193, 72.2 KTAS, -11.6°

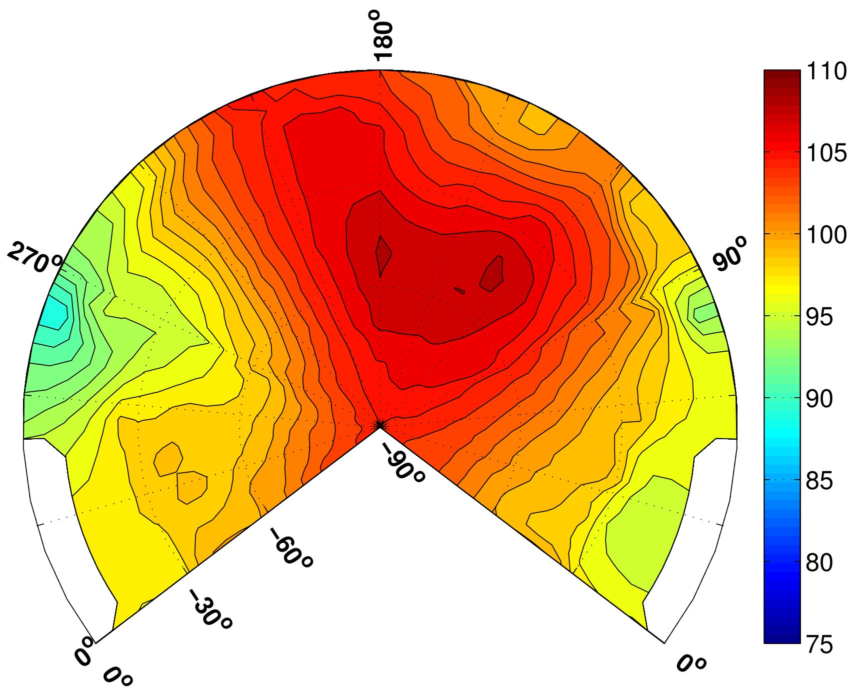

(a) OASPL, dB

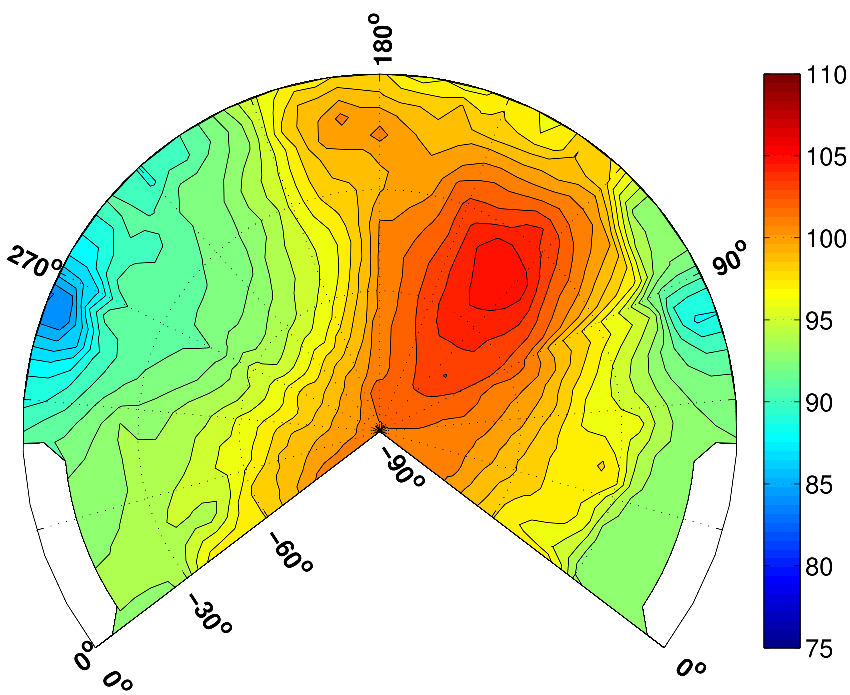

(b) BVISPL, dB

Figure 72: Descent hemi-sphere Be430194, 93.6 KTAS, -11.5°

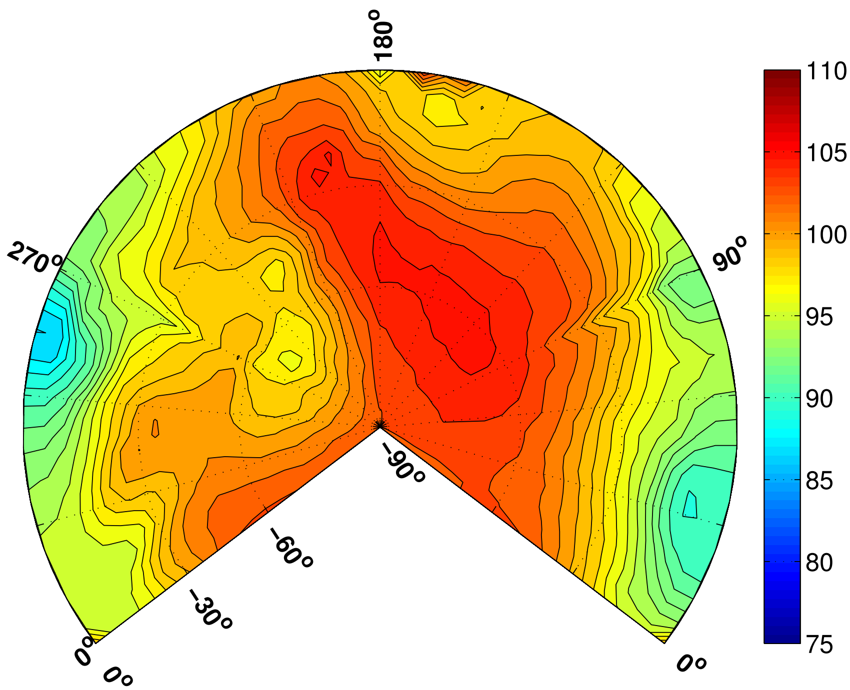

(a) OASPL, dB

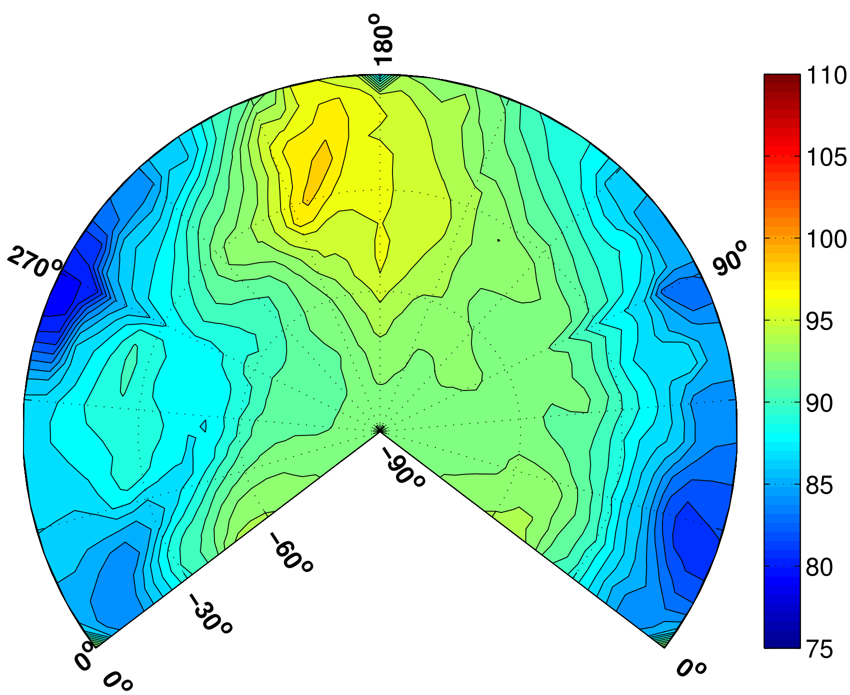

(b) BVISPL, dB

Figure 73: Descent hemi-sphere Be430195, 45.4 KTAS, -9.2°

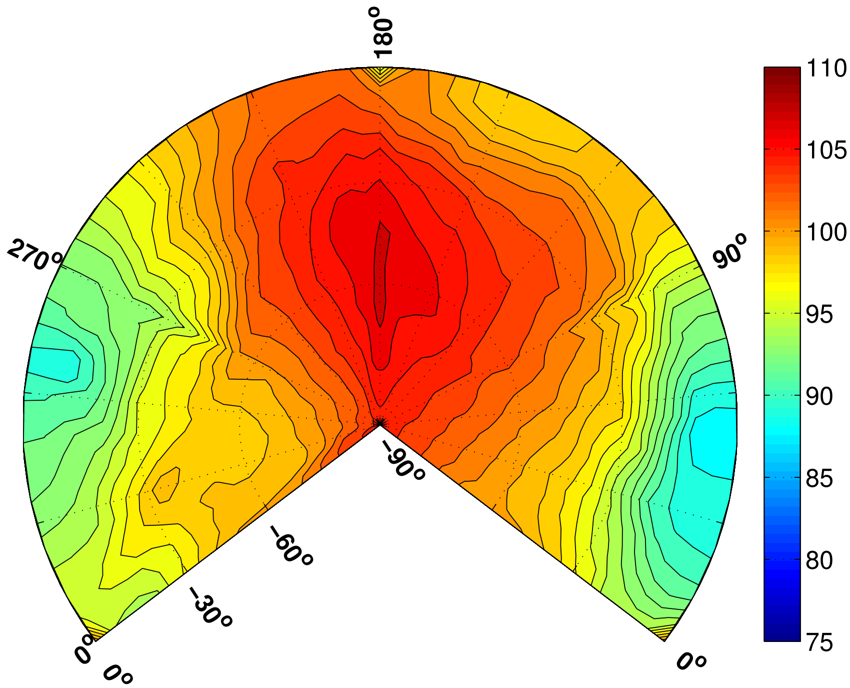

(a) OASPL, dB

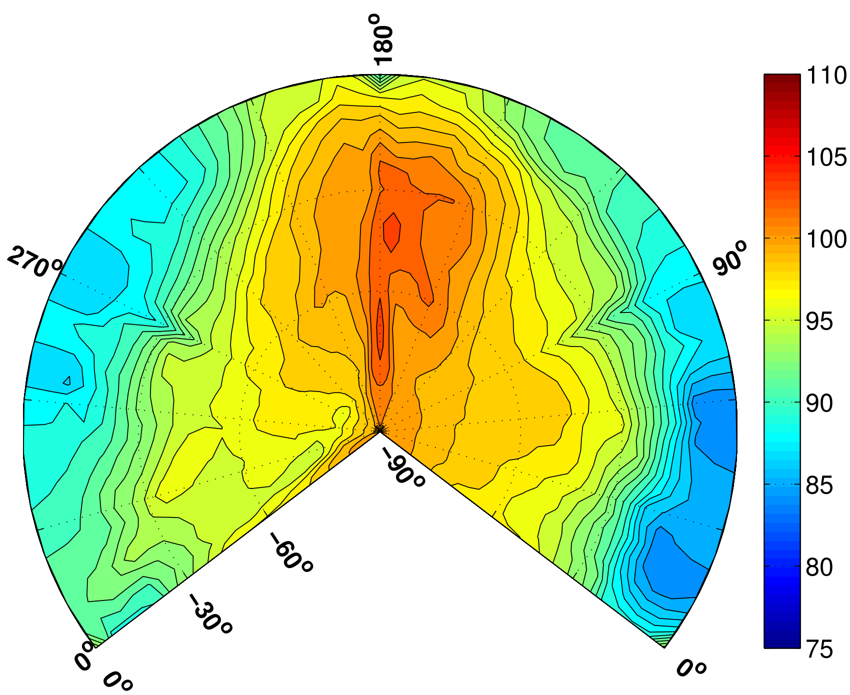

(b) BVISPL, dB

Figure 74: Descent hemi-sphere Be430196, 72.9 KTAS, -7.6°

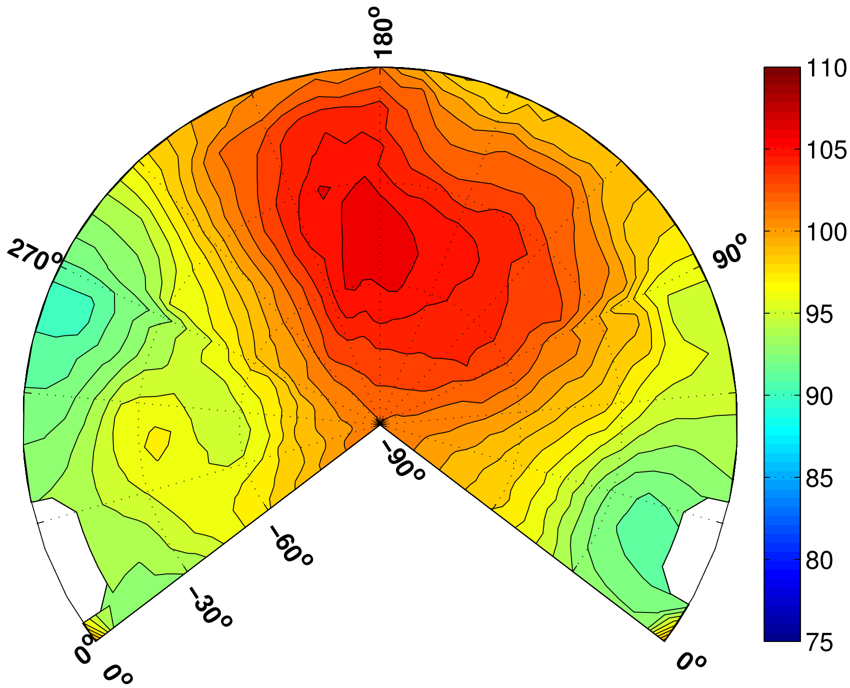

(a) OASPL, dB

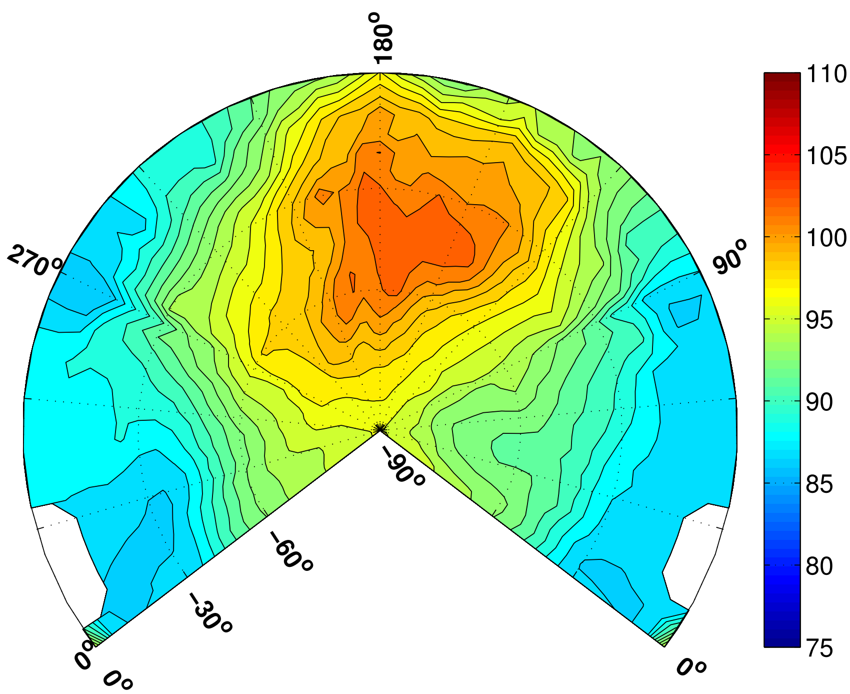

(b) BVISPL, dB

Figure 75: Descent hemi-sphere Be430197, 78.0 KTAS, -8.1°

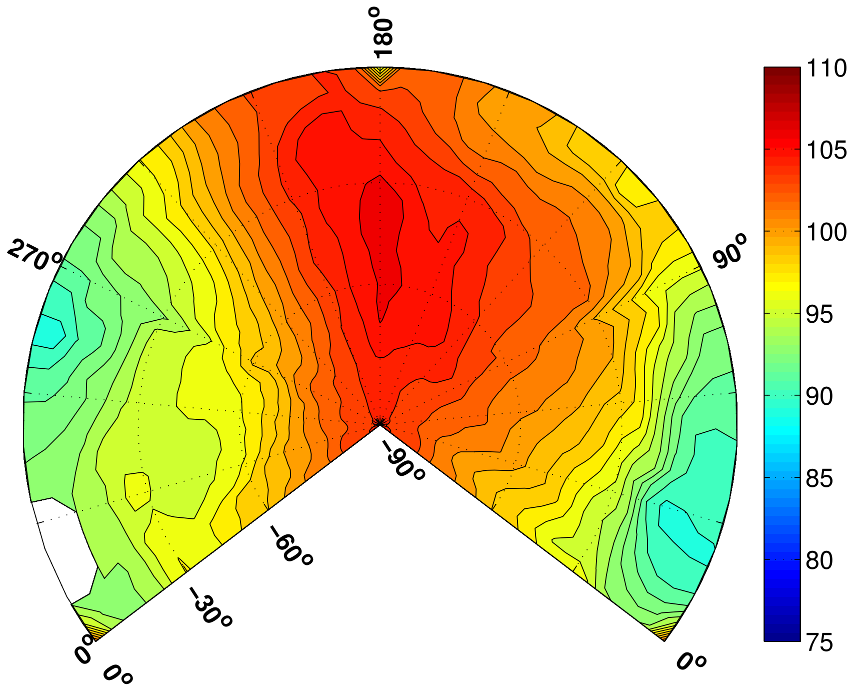

(a) OASPL, dB

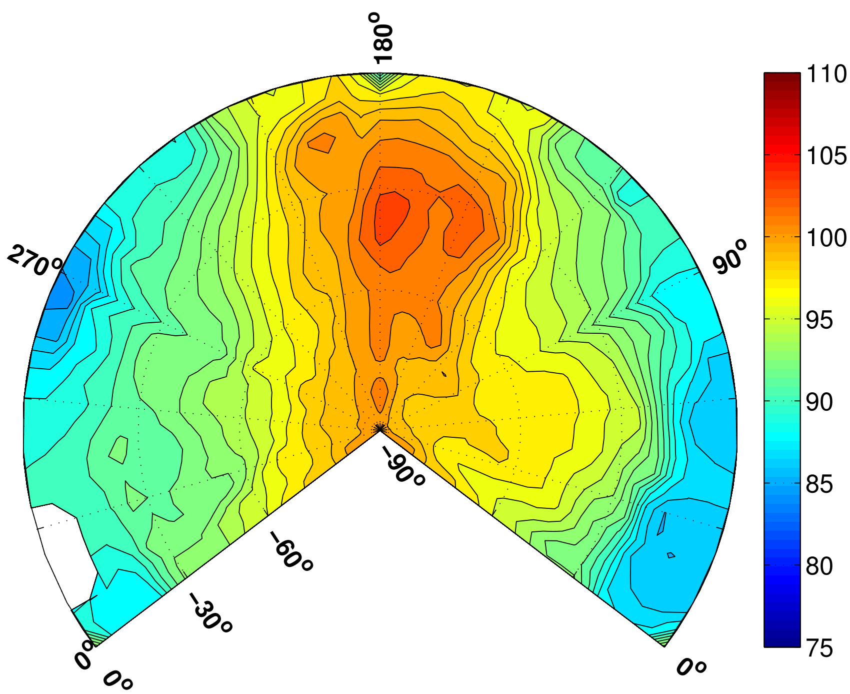

(b) BVISPL, dB

Figure 76: Descent hemi-sphere Be430198, 89.4 KTAS, -8.6°

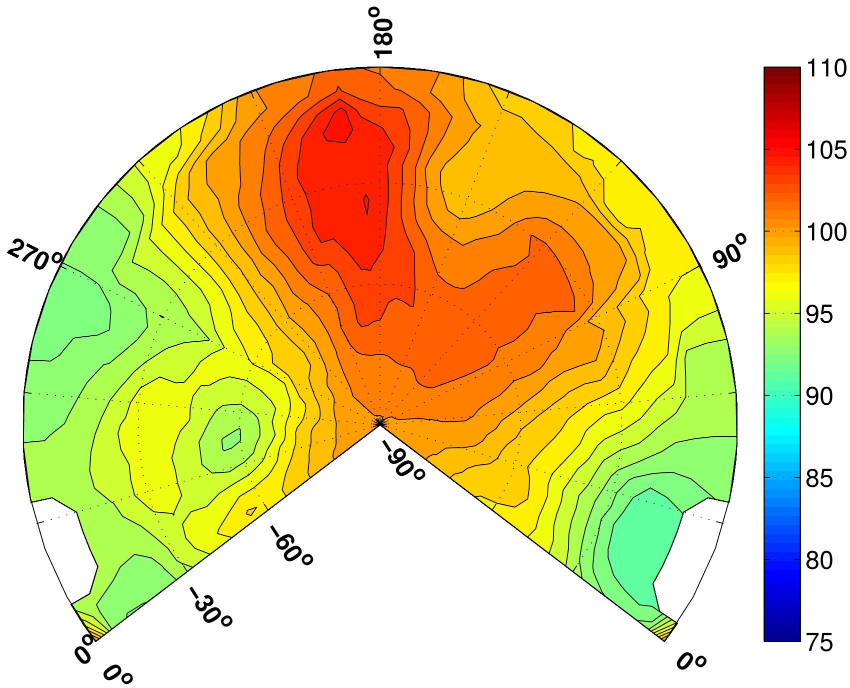

(a) OASPL, dB

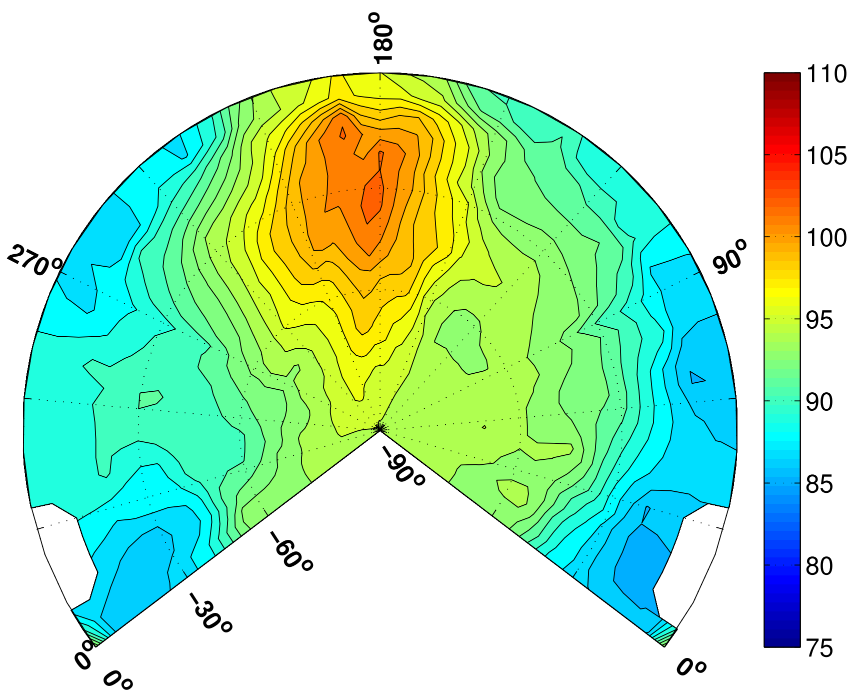

(b) BVISPL, dB

Figure 77: Descent hemi-sphere Be430199, 80.4 KTAS, -5.0°

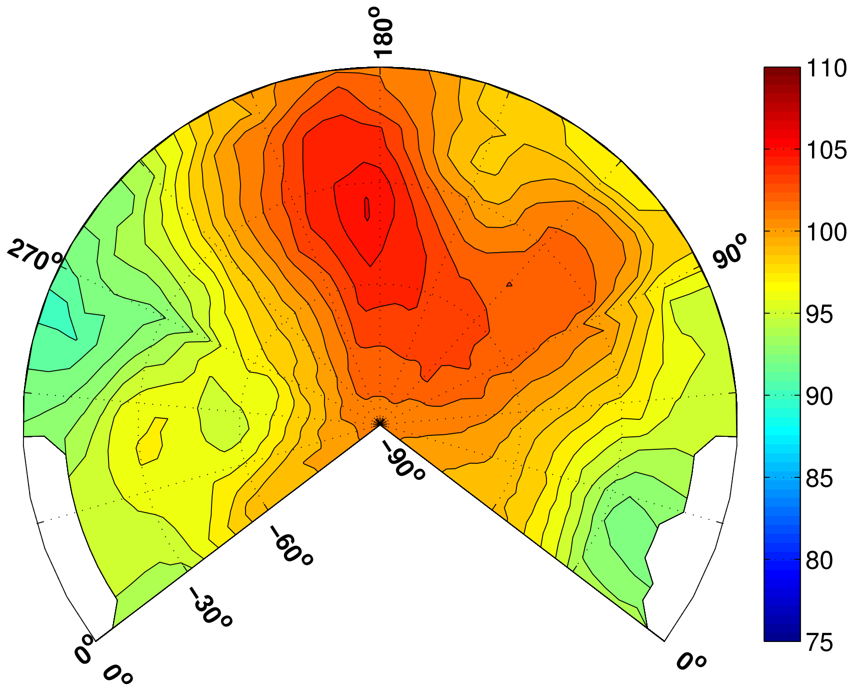

(a) OASPL, dB

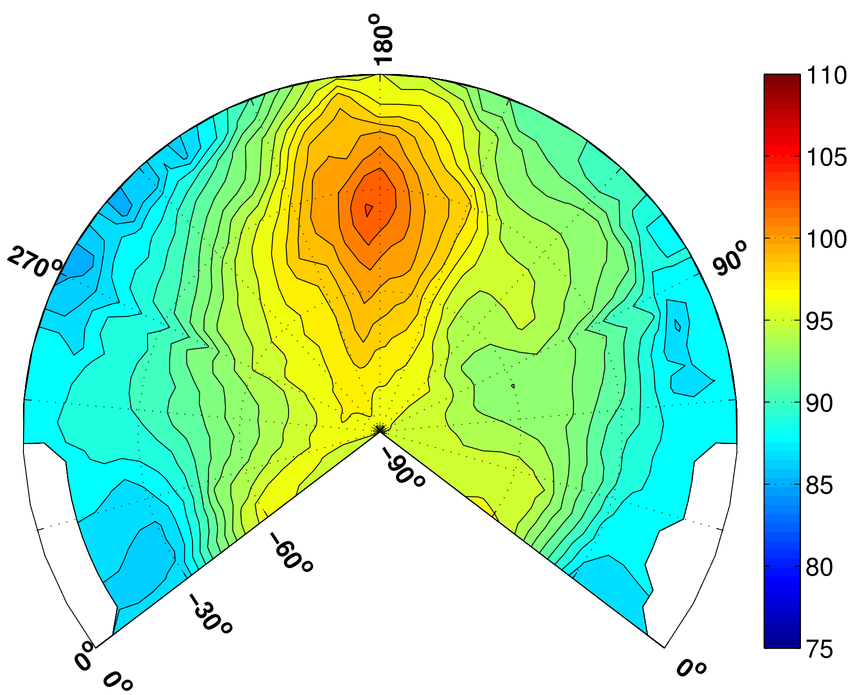

(b) BVISPL, dB

Figure 78: Descent hemi-sphere Be430200, 78.3 KTAS, -5.9°

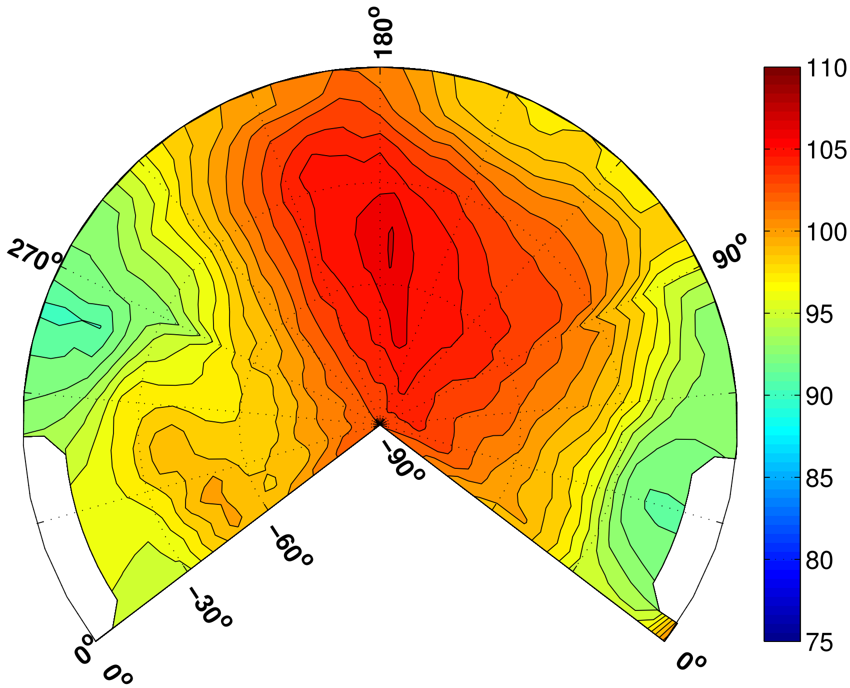

(a) OASPL, dB

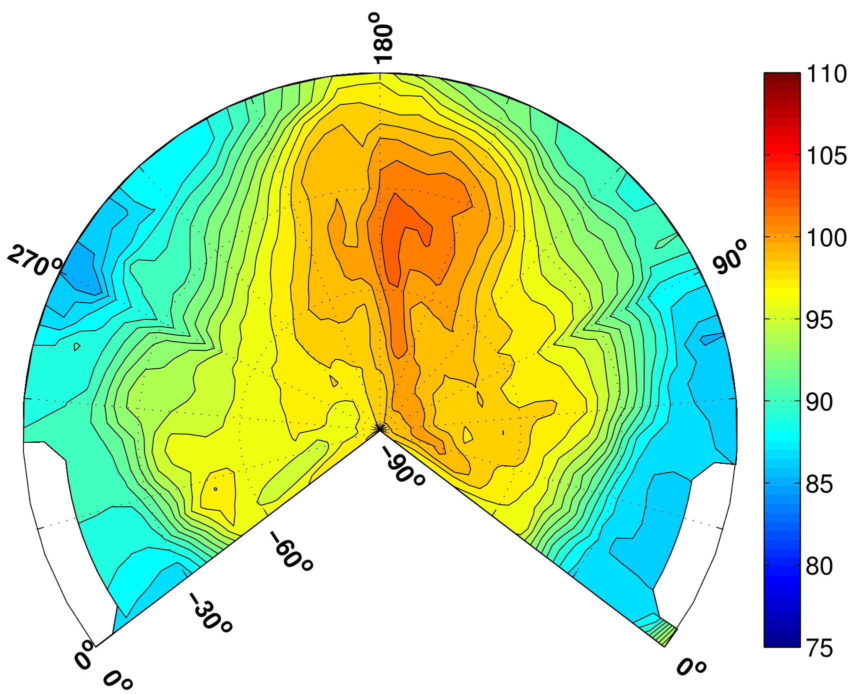

(b) BVISPL, dB

Figure 79: Descent hemi-sphere Be430201, 68.9 KTAS, -6.7°

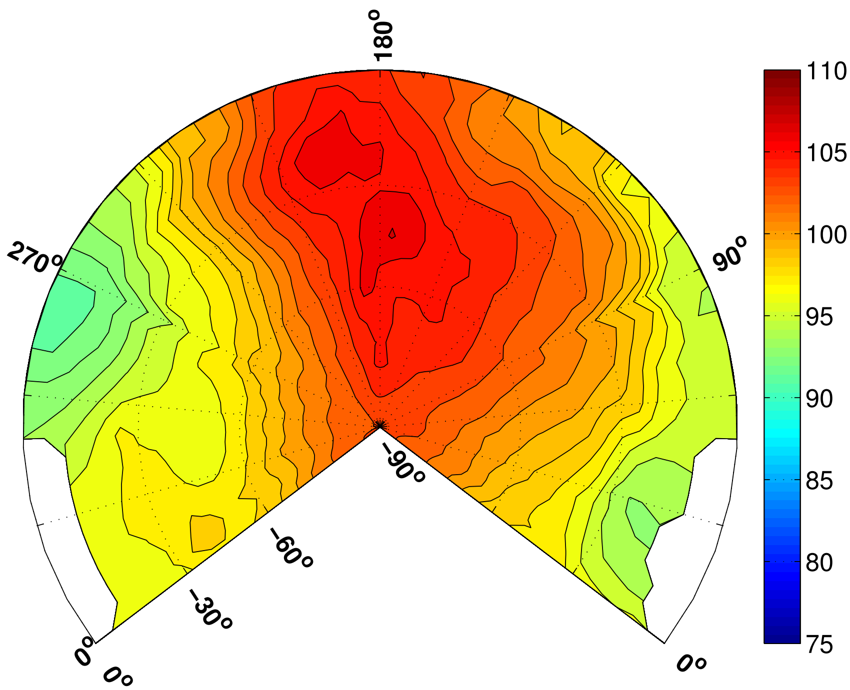

(a) OASPL, dB

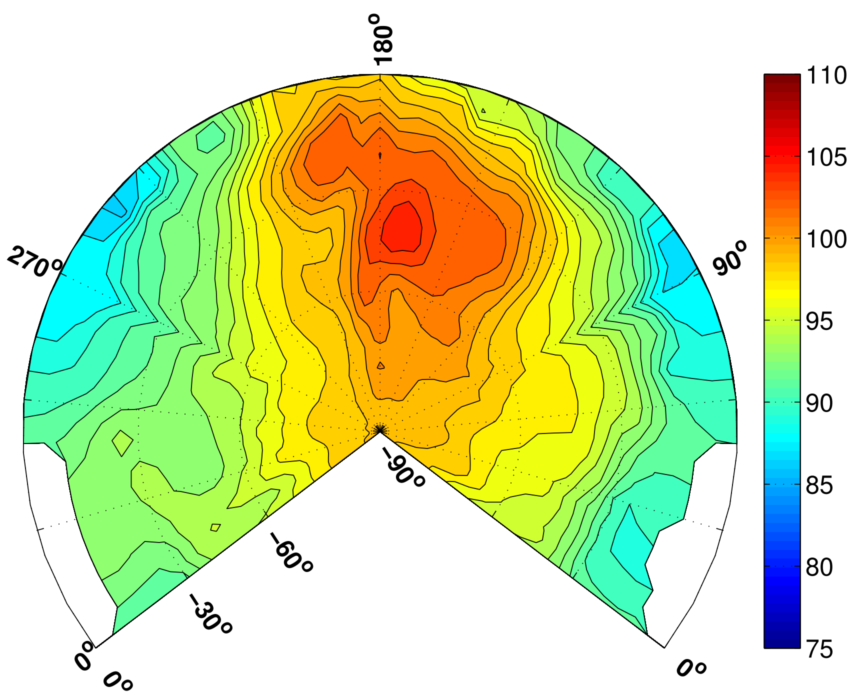

(b) BVISPL, dB

Figure 80: Descent hemi-sphere Be430202, 91.2 KTAS, -7.1°

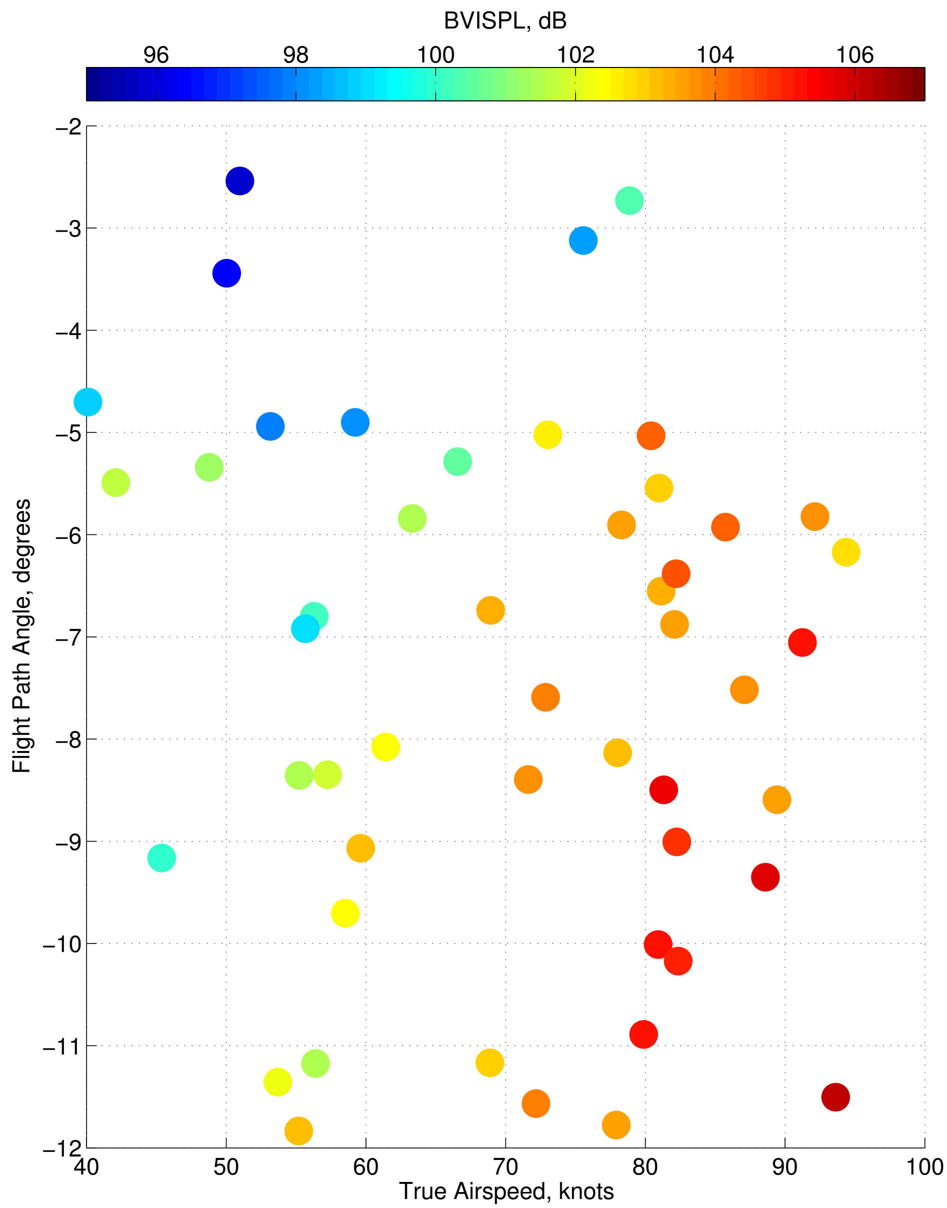

Figure 81: Source noise descent matrix maximum BVISPL.

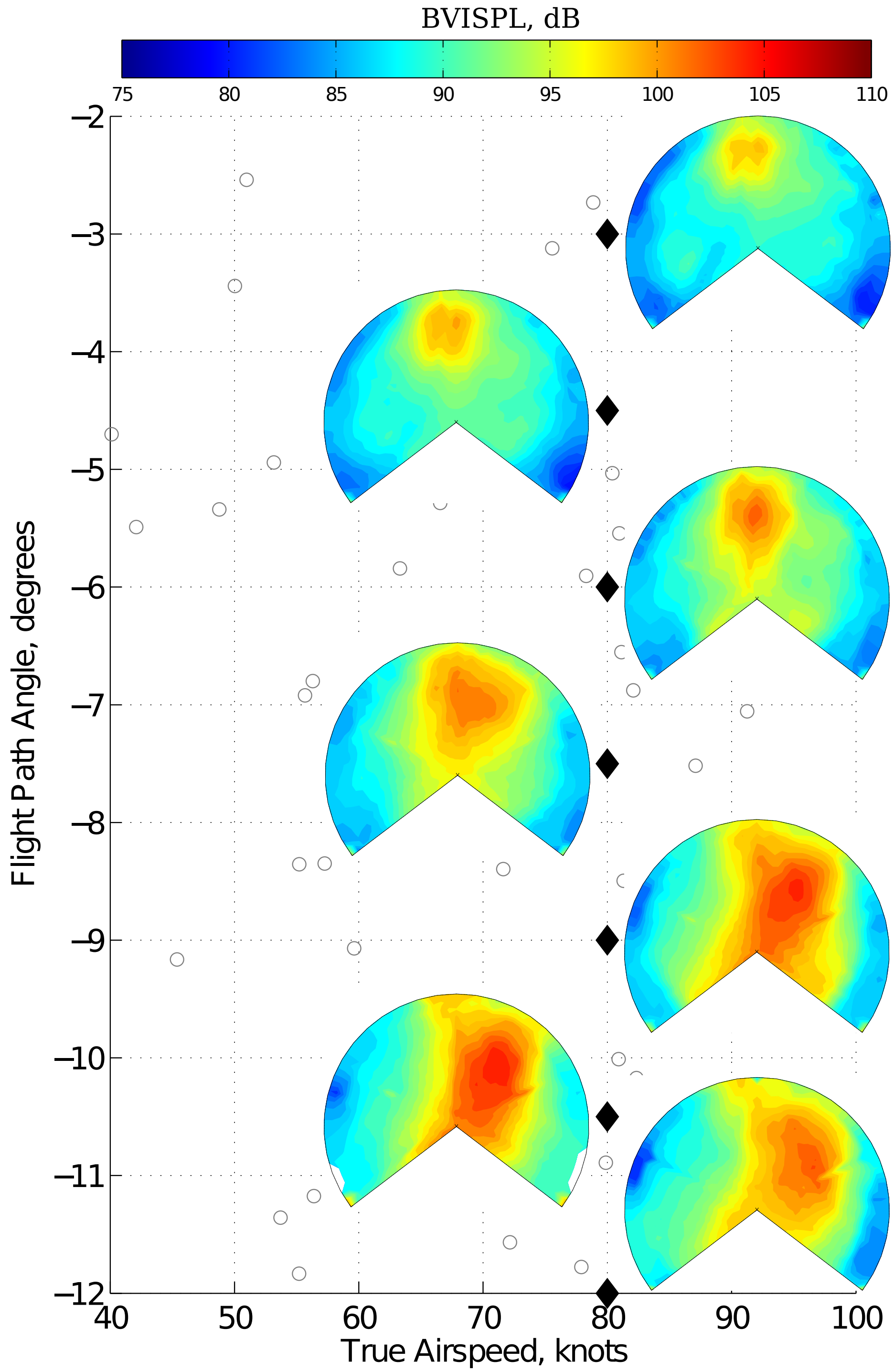

Figure 82: Flight path angle sweep at 80 knots true airspeed.

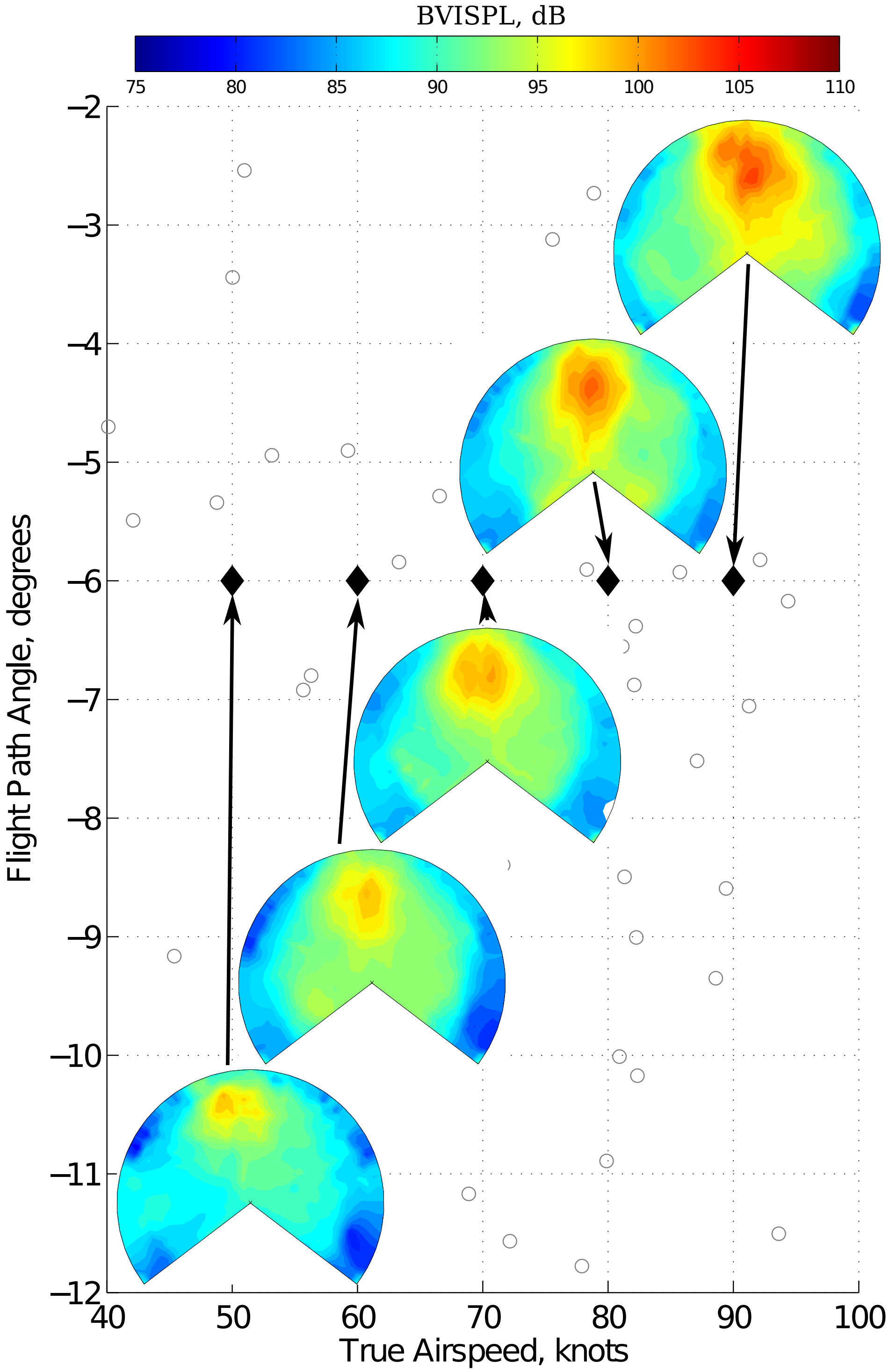

Figure 83: True airspeed sweep at -6° flight path angle.

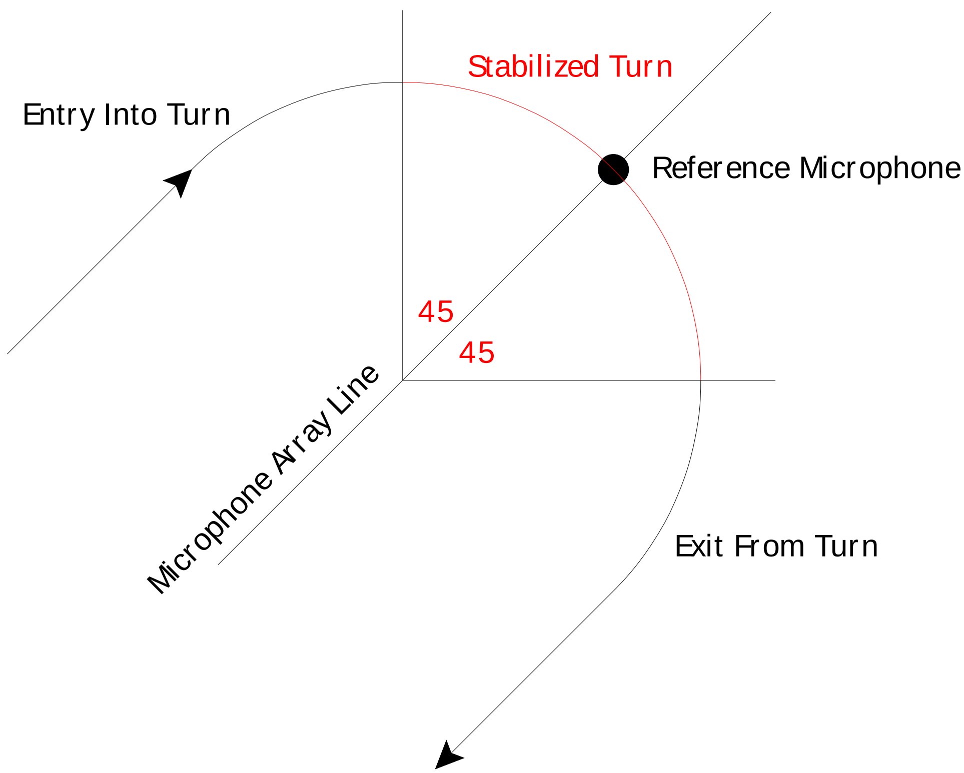

Figure 84: Steady turn procedure sketch.

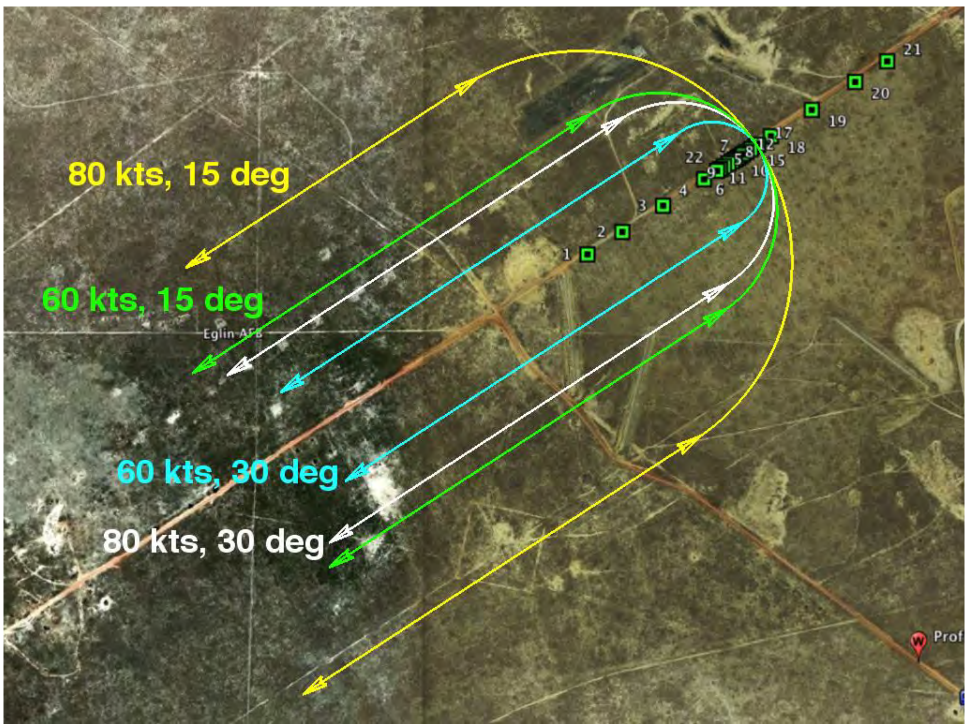

Figure 85: Steady turn flight paths (radius is to scale).

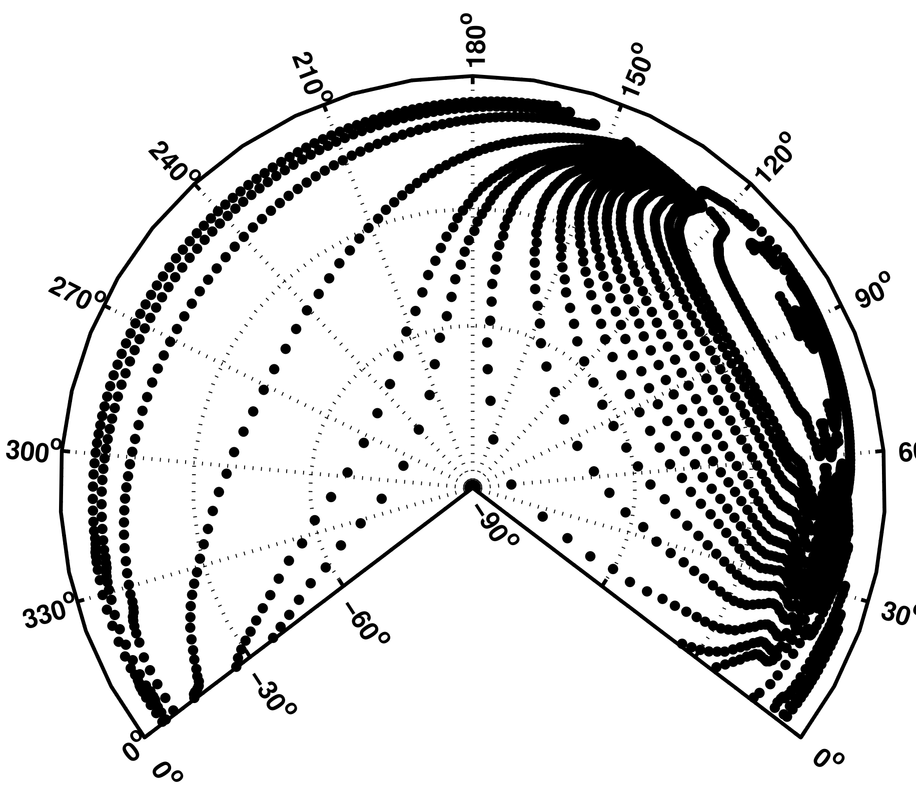

Figure 86: Steady 80 knots, 30° right turn microphone projection.

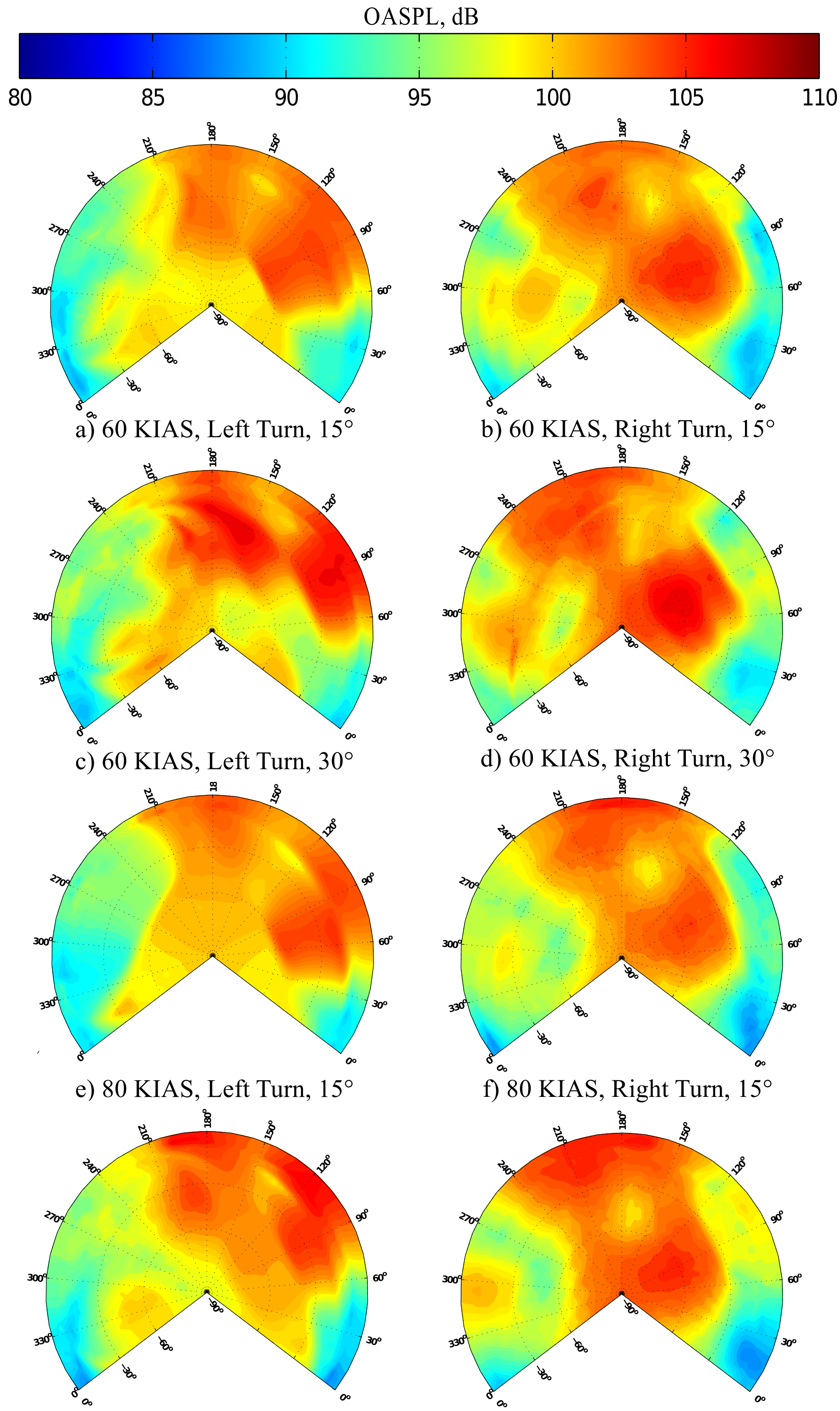

a) 60 KIAS, Left Turn, 15°
b) 60 KIAS, Right Turn, 15°
c) 60 KIAS, Left Turn, 30°
d) 60 KIAS, Right Turn, 30°
e) 80 KIAS, Left Turn, 15°
f) 80 KIAS, Right Turn, 15°
g) 80 KIAS, Left Turn, 30°
h) 80 KIAS, Right Turn, 30°

Figure 87: Steady turn OASPL semi-spheres.

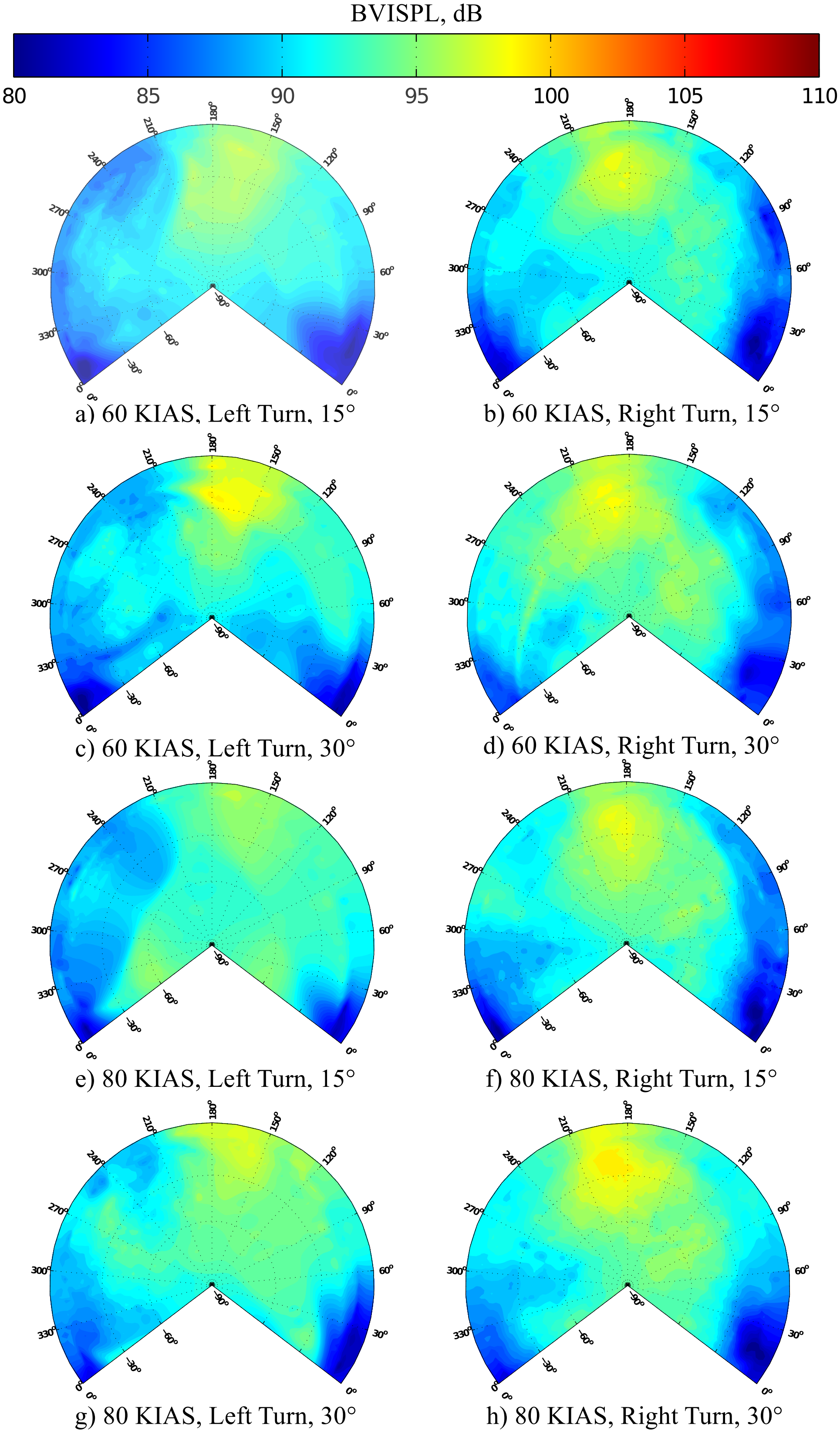

Figure 88: Steady turn BVISPL semi-spheres.

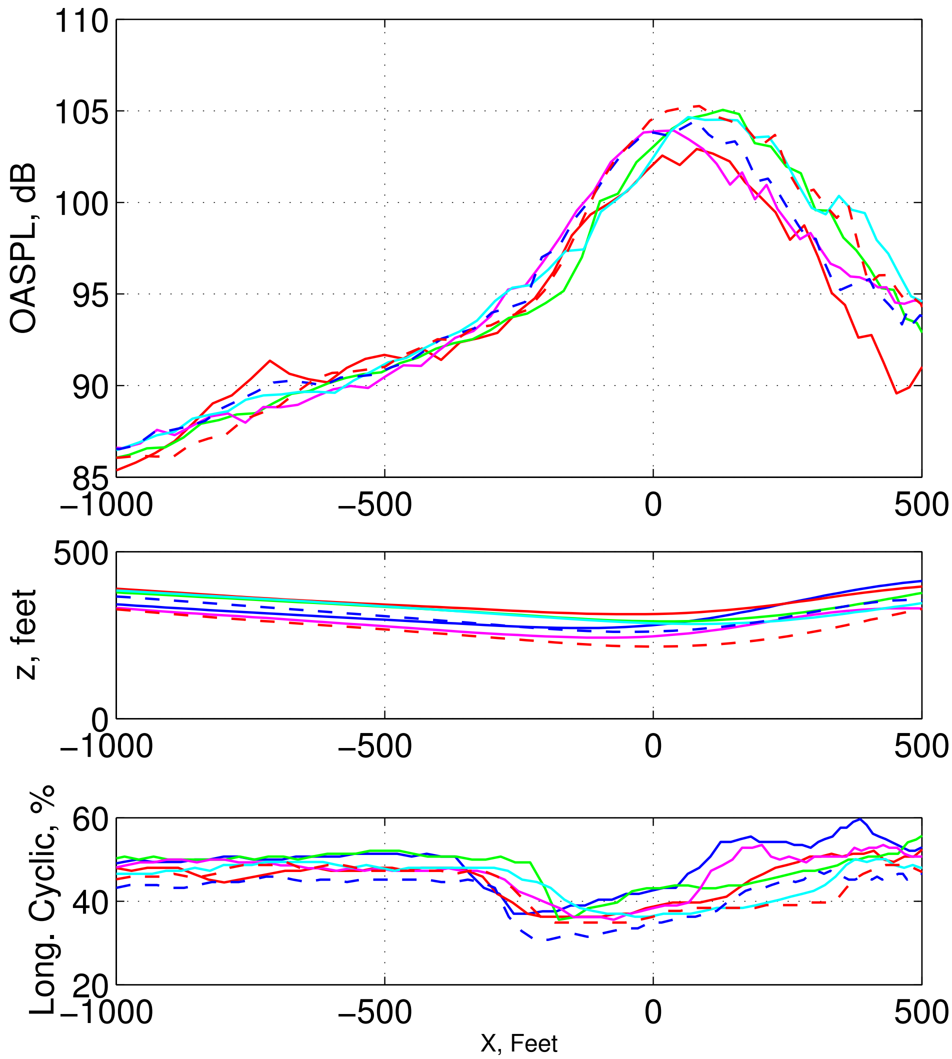

Figure 89: Cyclic pitch up from 80 knot, 6° descent housekeeping points.

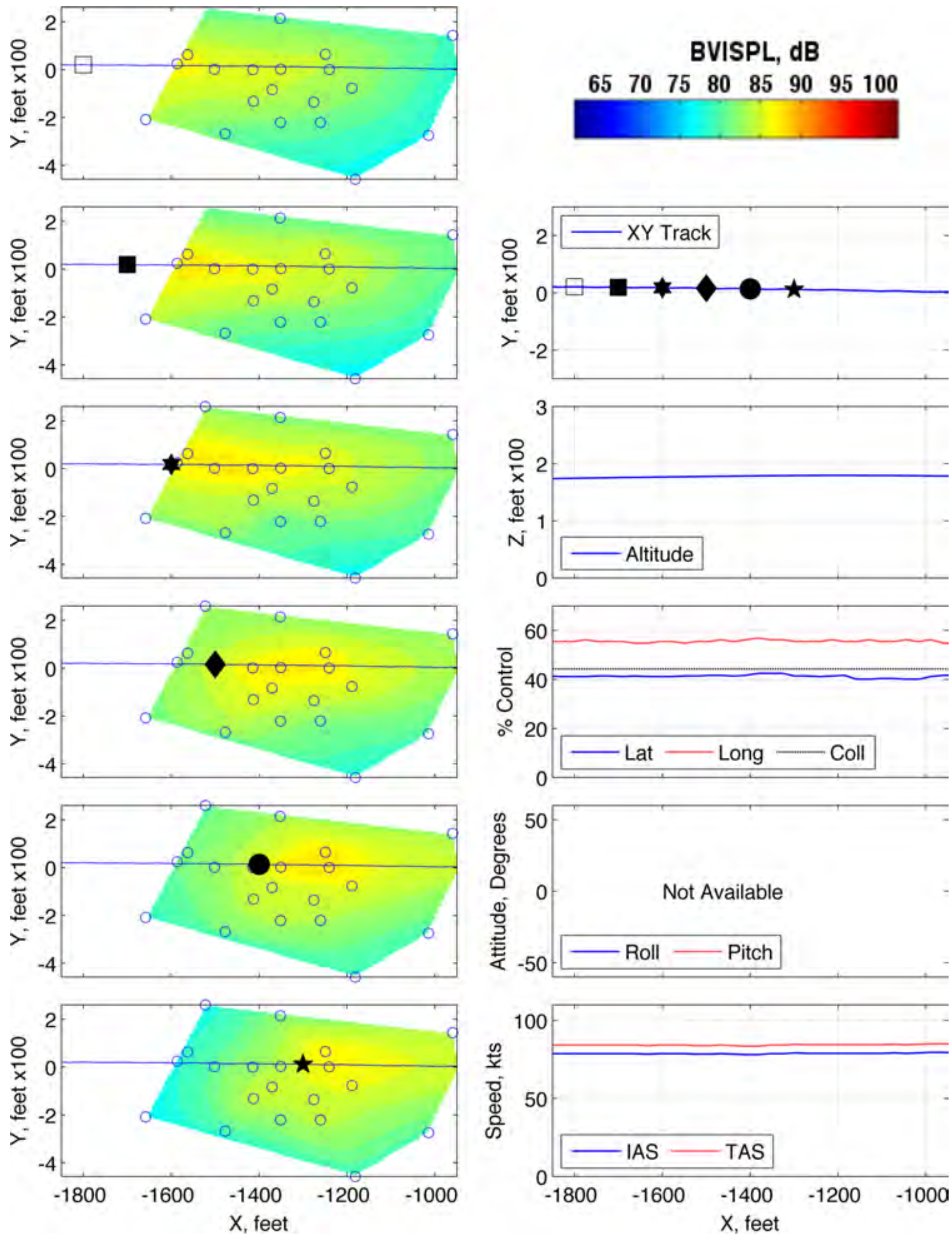

Figure 90: Maneuver condition L1, 80 KIAS, level, run number 278301

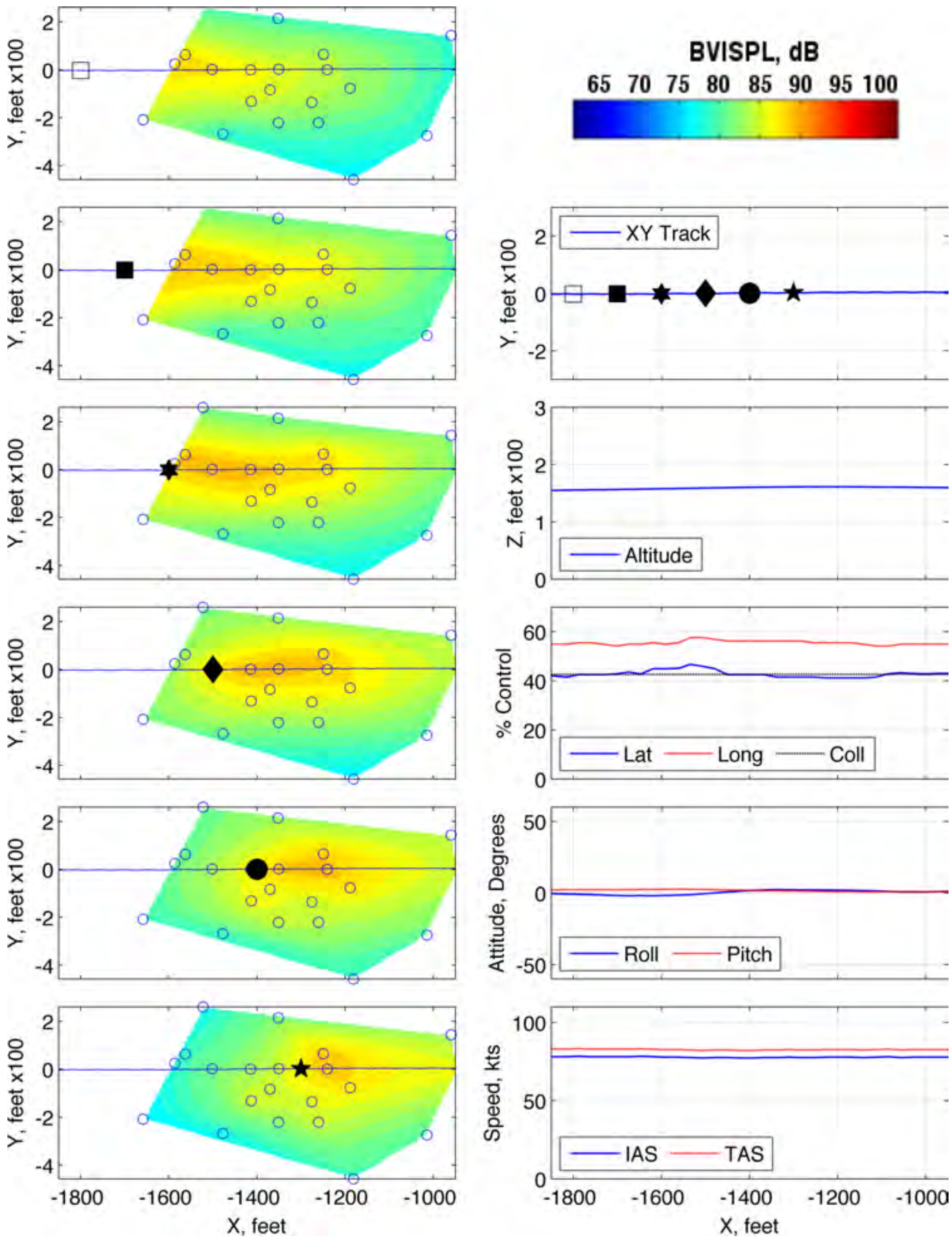

Figure 91: Maneuver condition L1, 80 KIAS, level, run number 280341

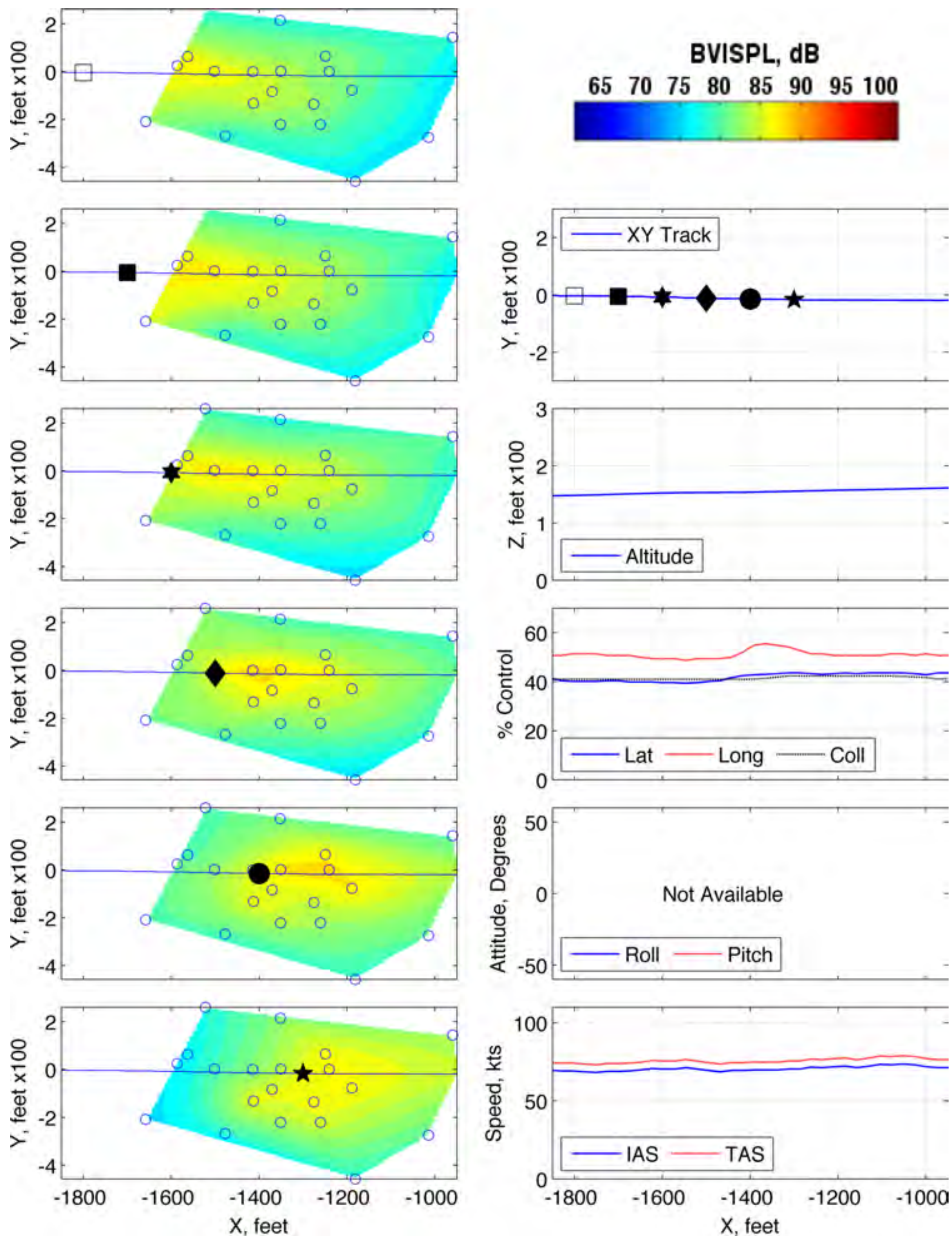

Figure 92: Maneuver condition L1,80 KIAS, level, run number 280405

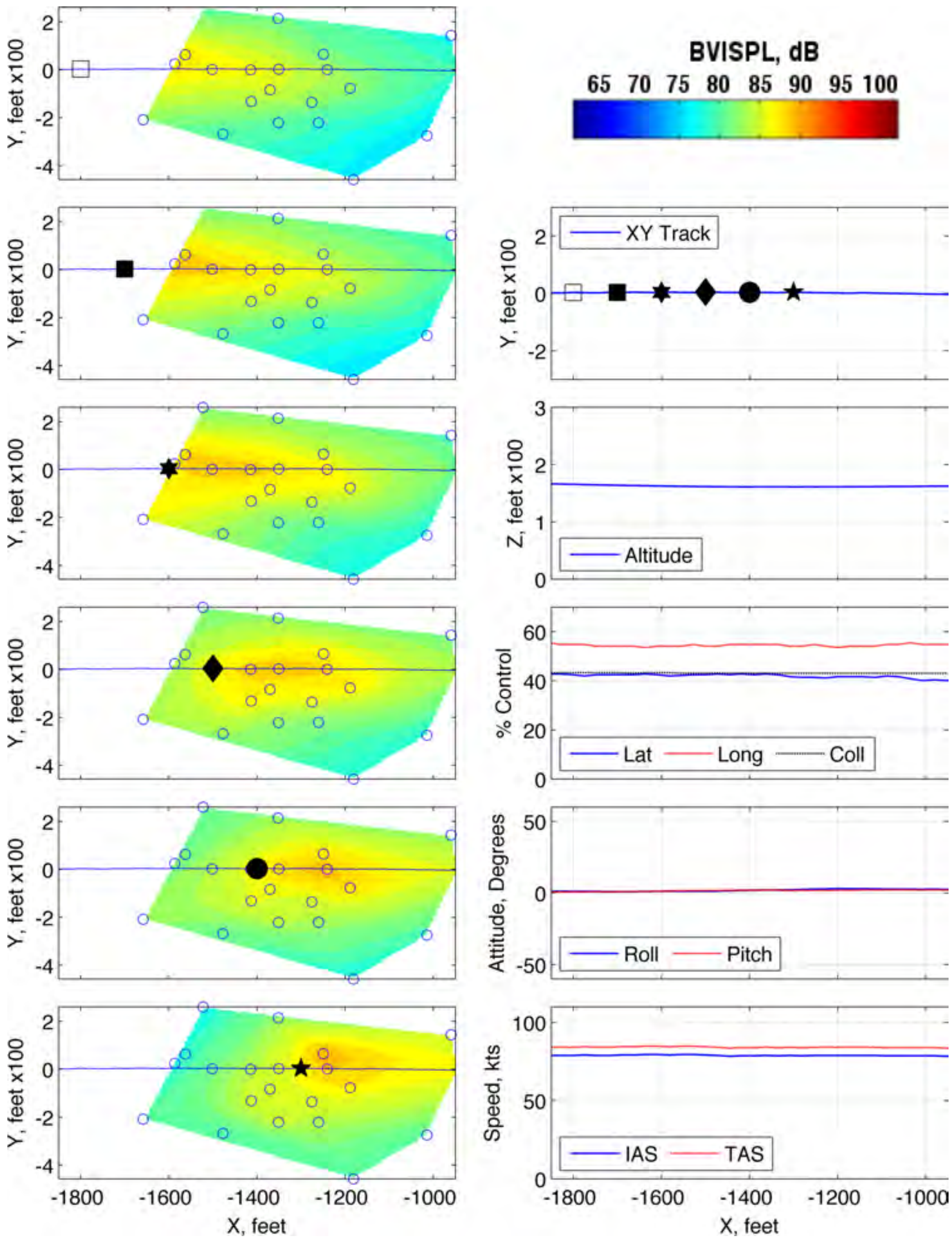

Figure 93: Maneuver condition L1, 80 KIAS, level, run number 282411

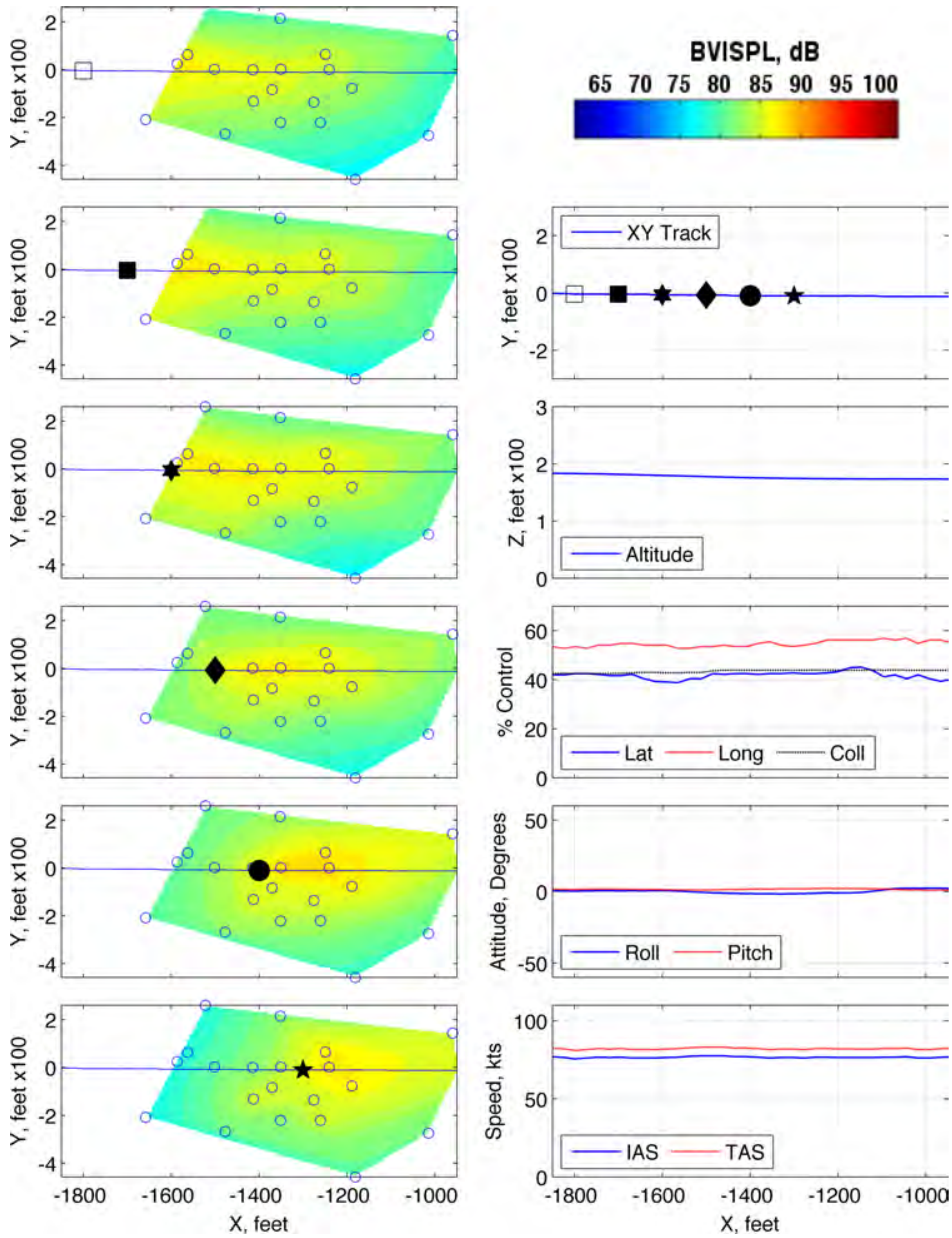

Figure 94: Maneuver condition L1, 80 KIAS, level, run number 282440

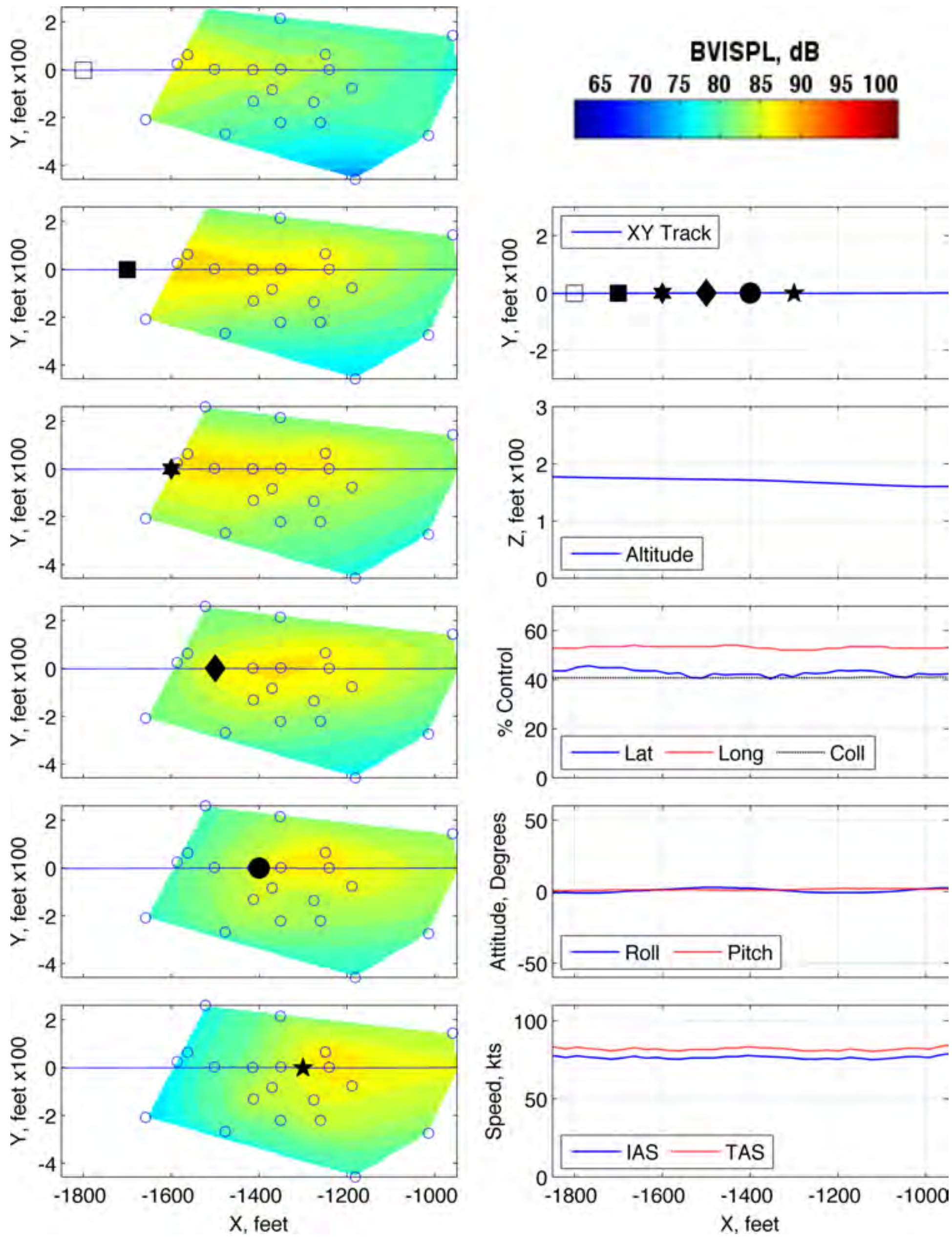

Figure 95: Maneuver condition L1, 80 KIAS, level, run number 282451

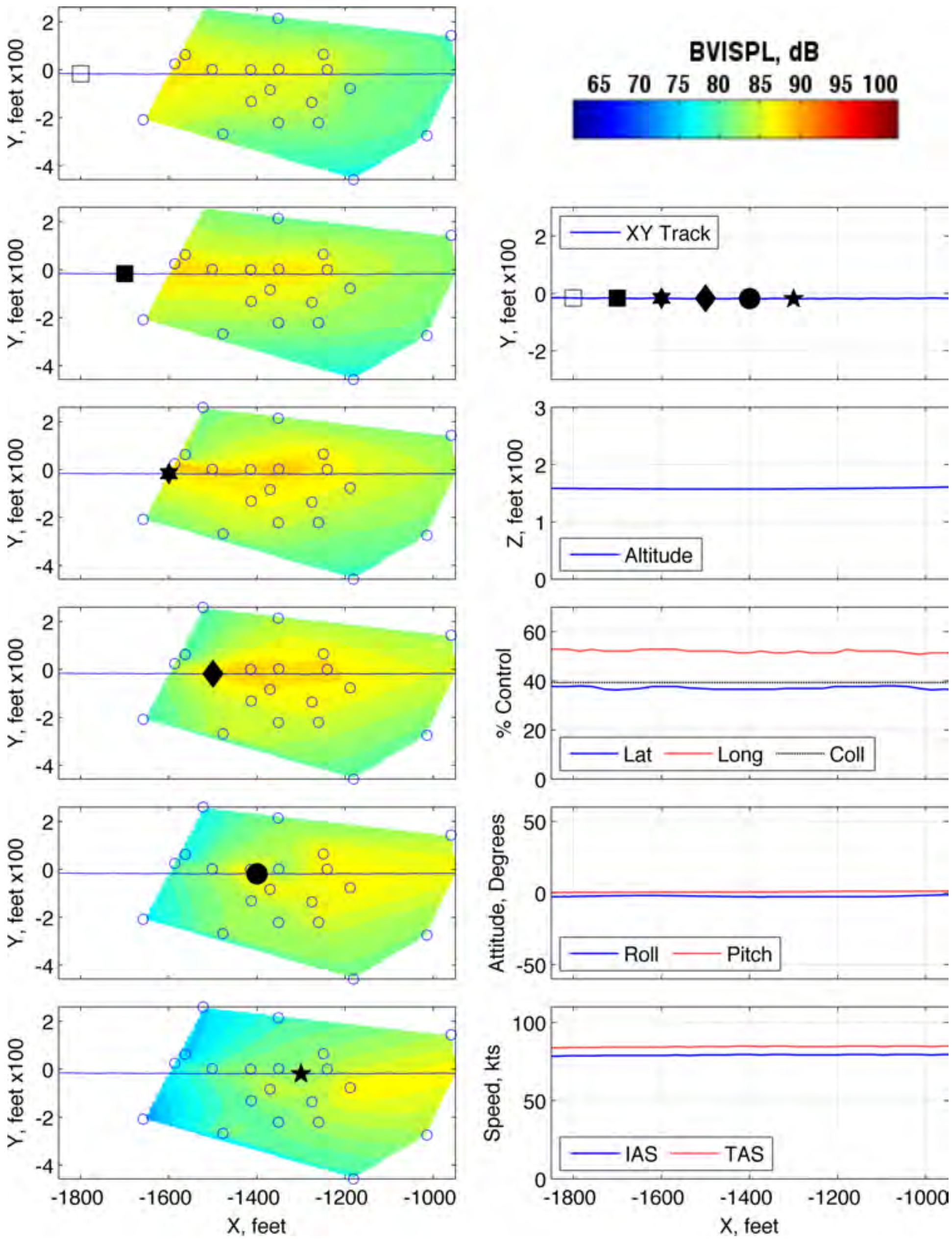

Figure 96: Maneuver condition L1, 80 KIAS, level, run number 285461

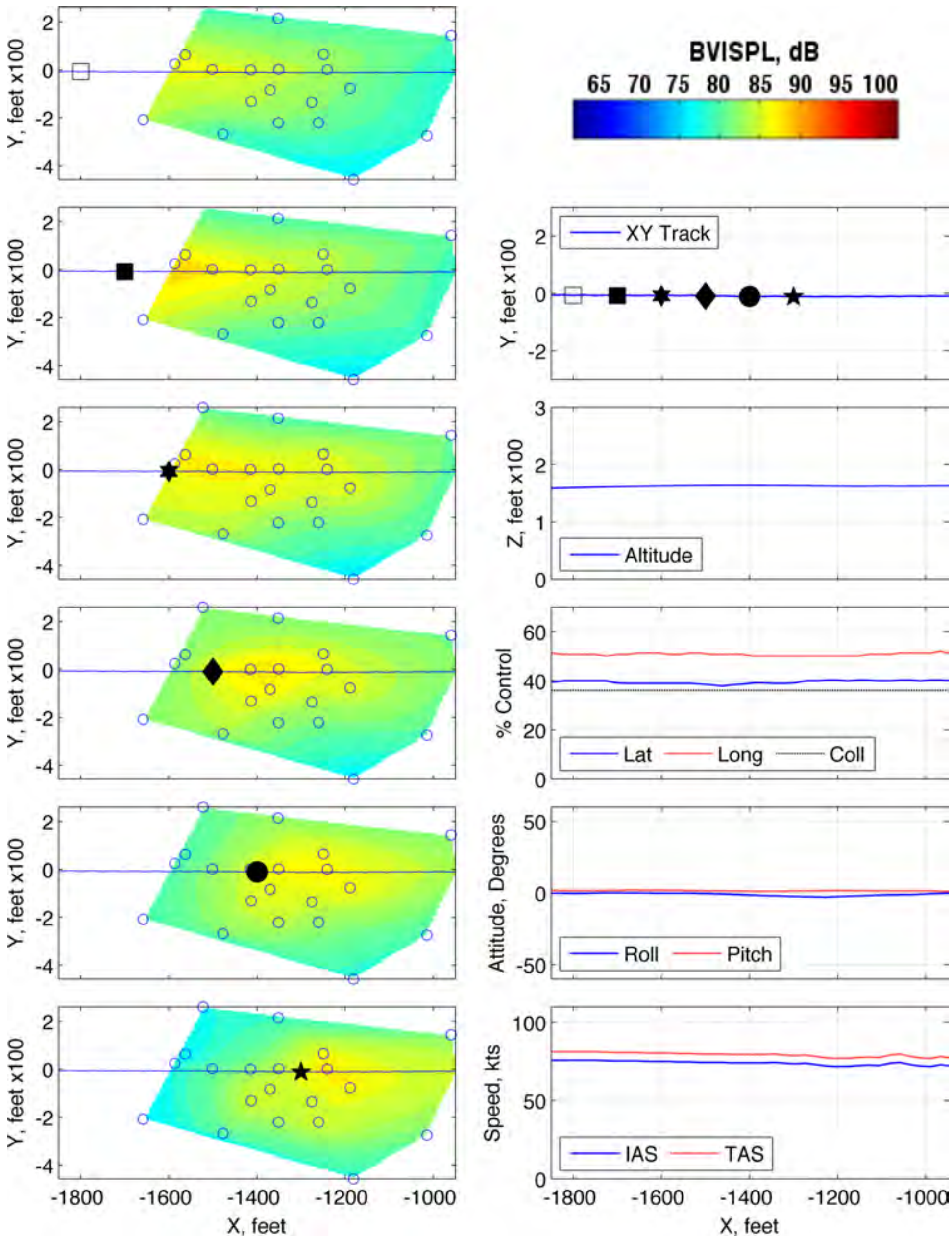

Figure 97: Maneuver condition L1, 80 KIAS, level, run number 285516

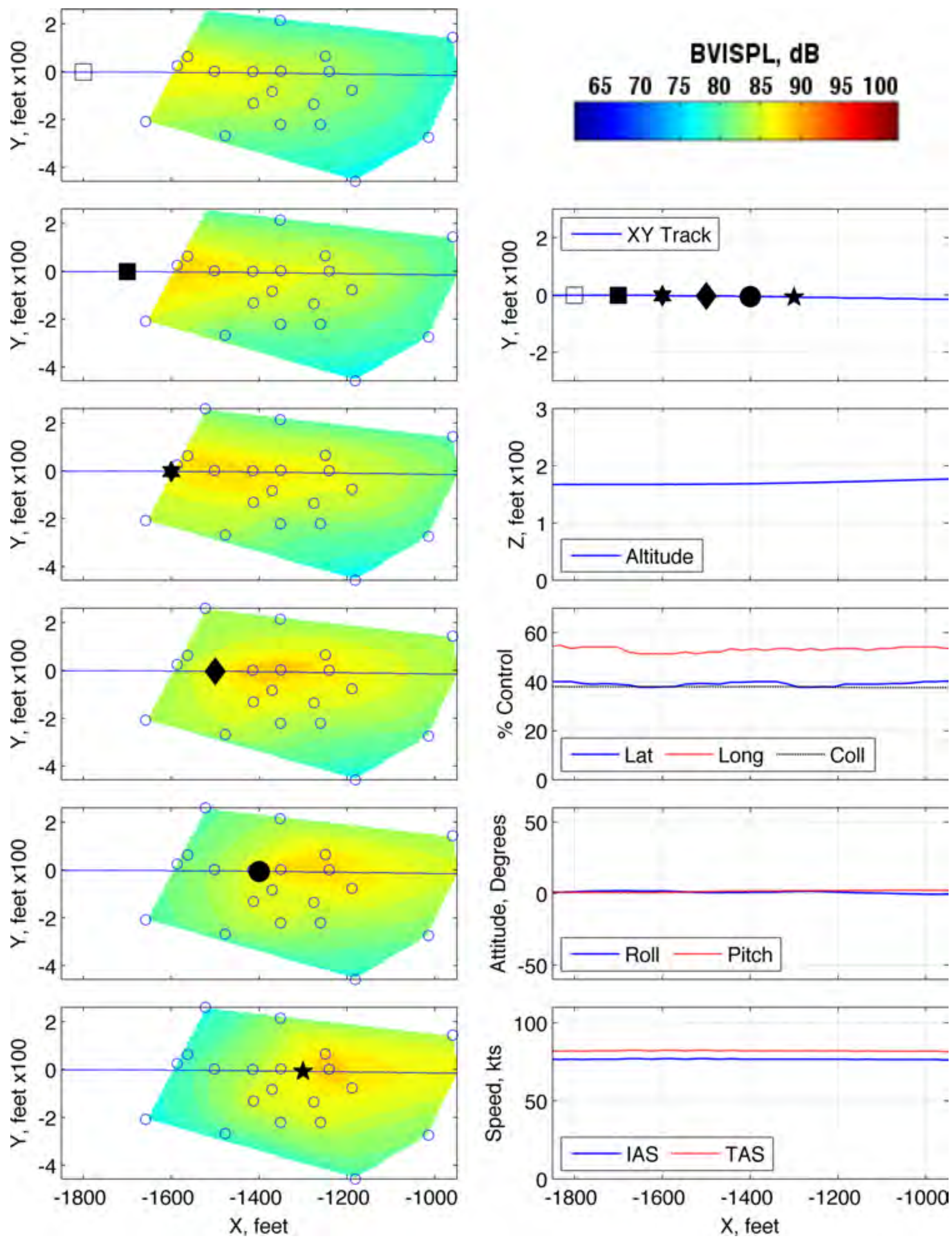

Figure 98: Maneuver condition L1, 80 KIAS, level, run number 287521

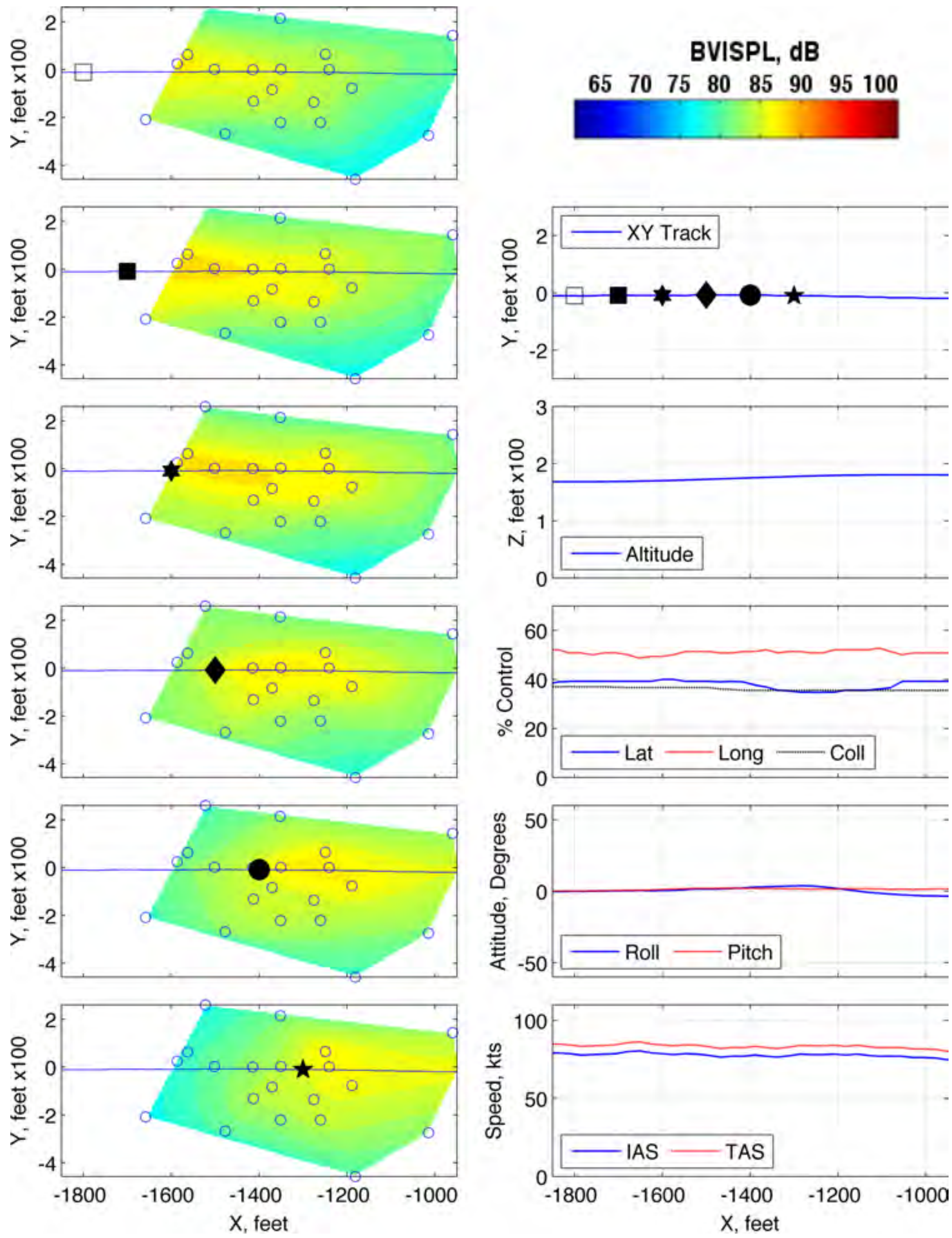

Figure 99: Maneuver condition L1, 80 KIAS, level, run number 287574

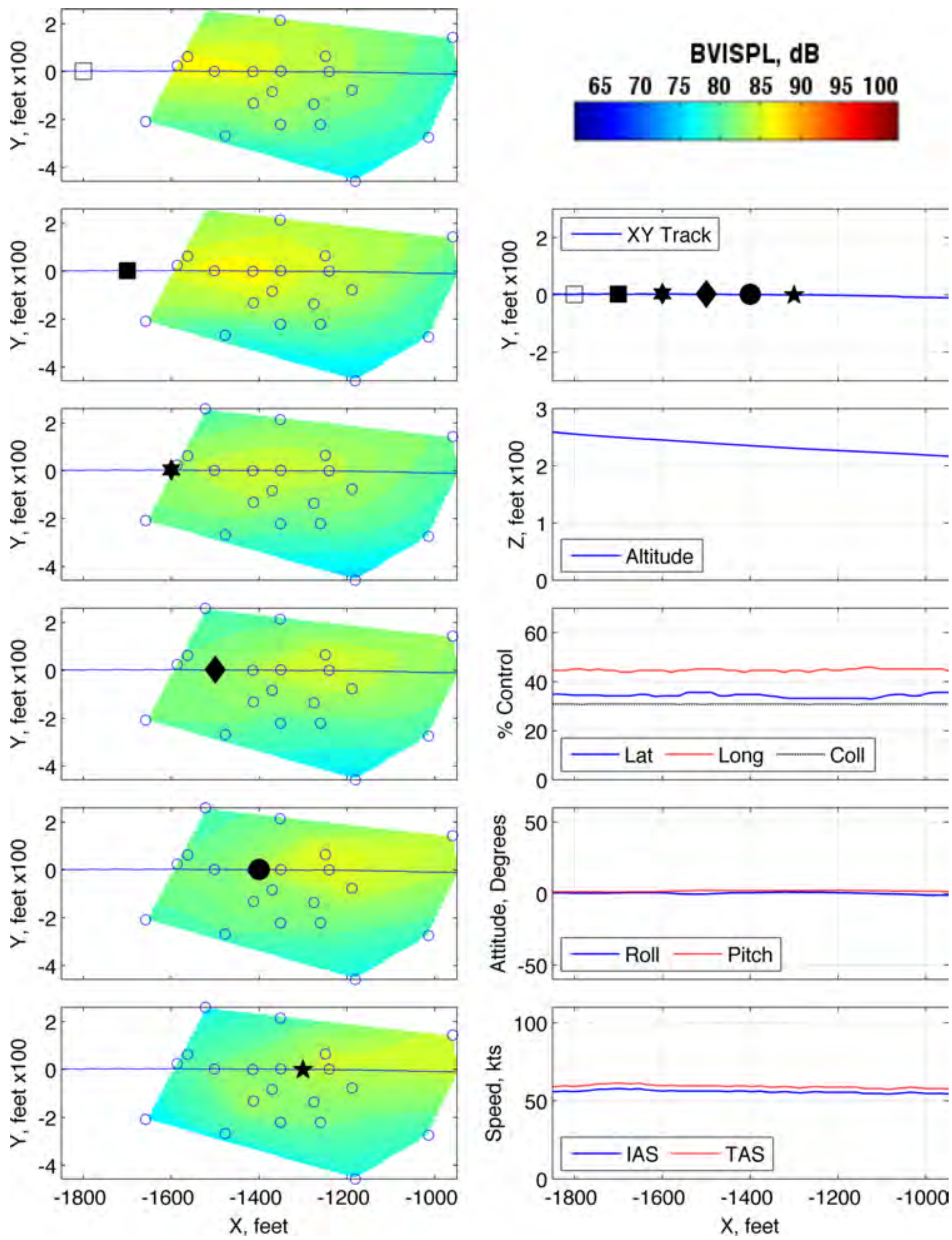

Figure 100: Maneuver condition A4, 60 KIAS, -3° , run number 285497

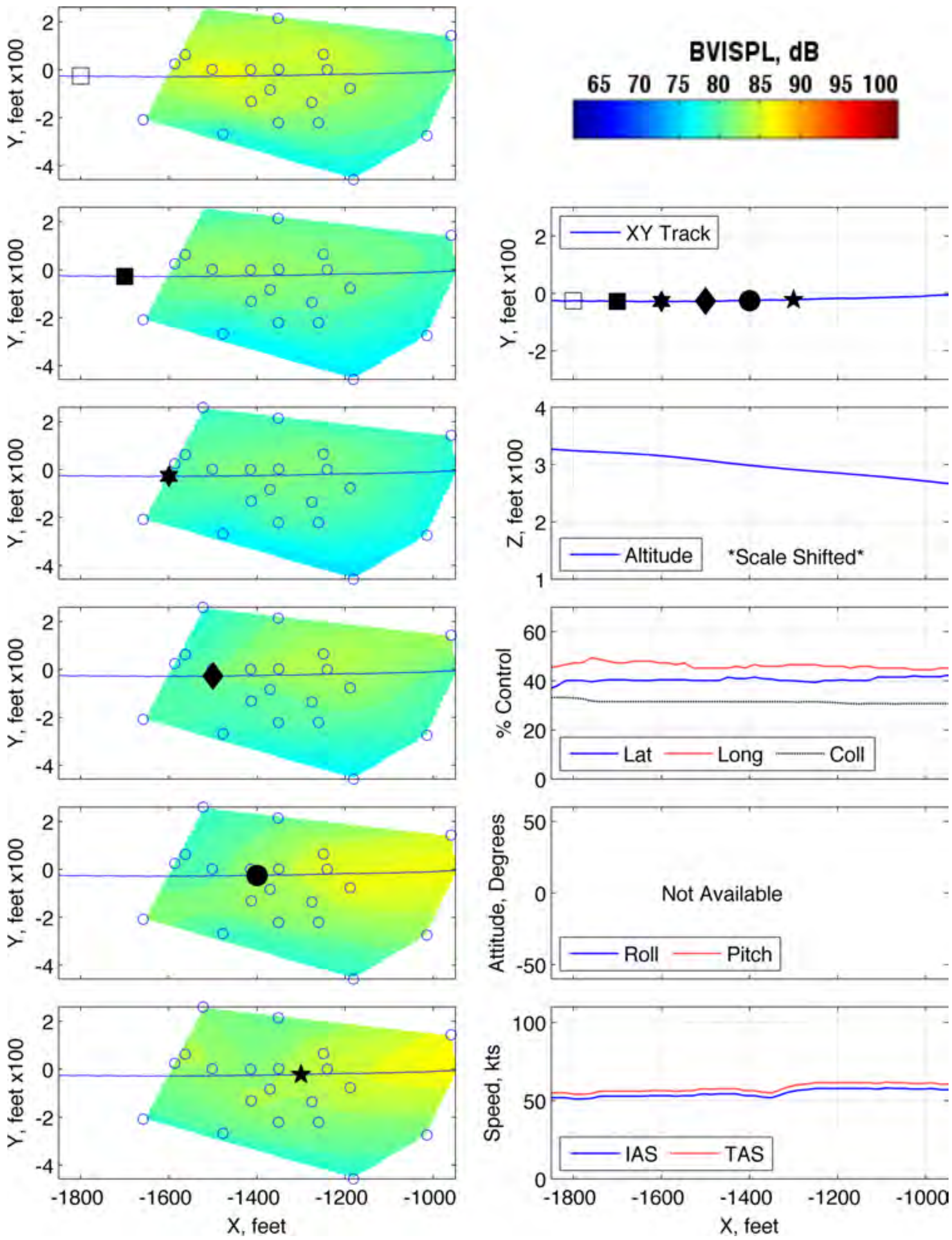

Figure 101: Maneuver condition A5, 60 KIAS, -4.5° , run number 280398

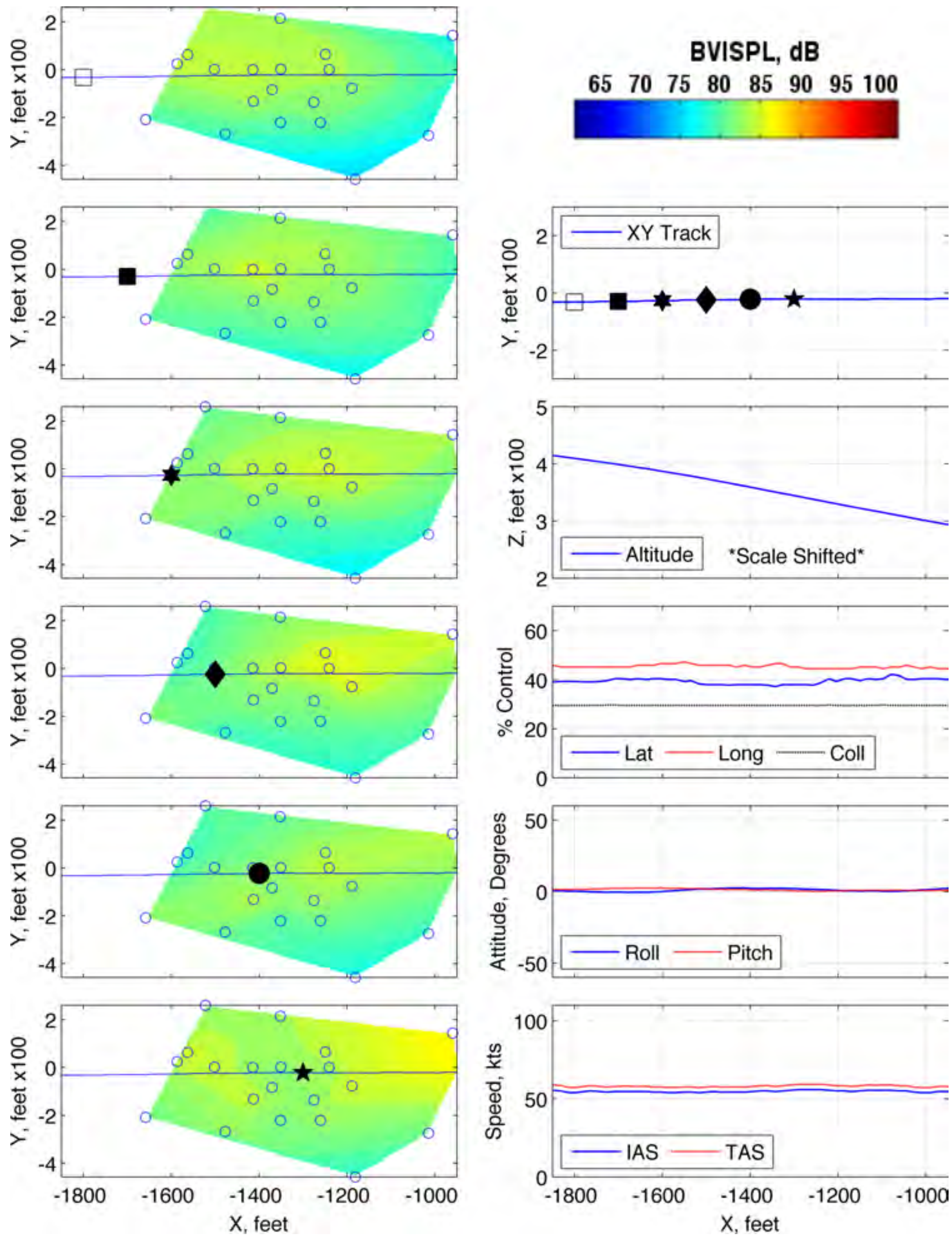

Figure 102: Maneuver condition A6, 60 KIAS, -6° , run number 282446

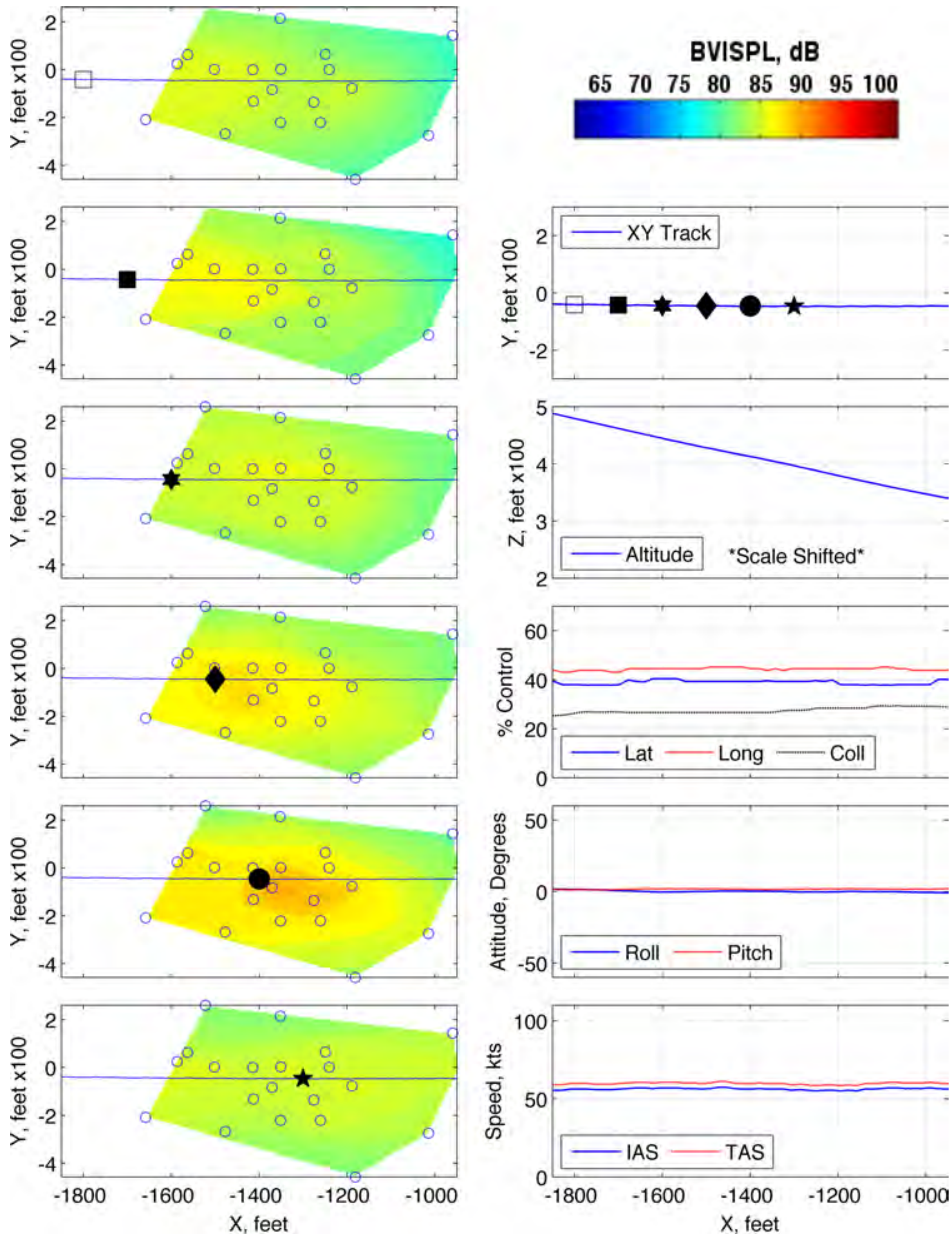

Figure 103: Maneuver condition A8, 60 KIAS, -9° , run number 282444

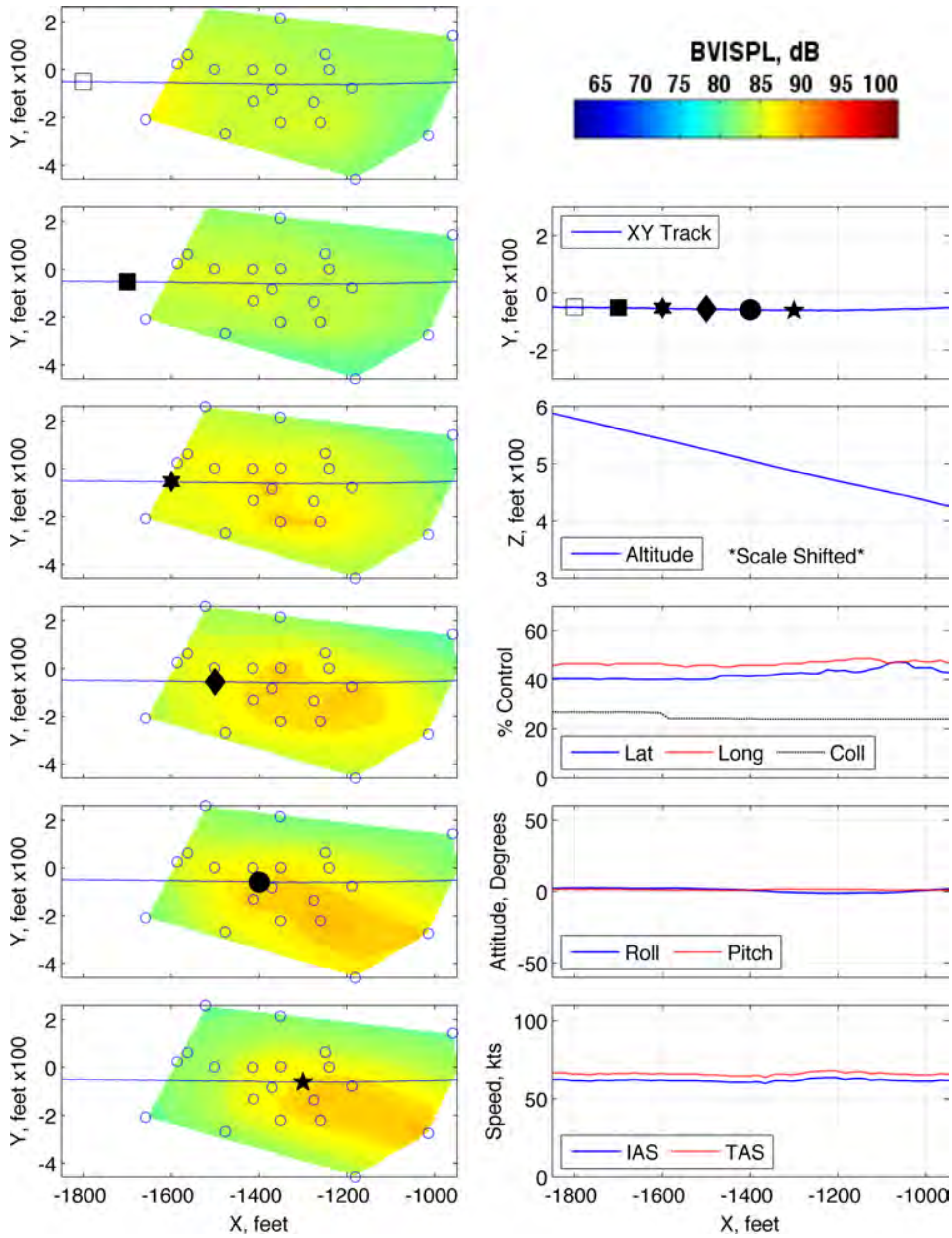

Figure 104: Maneuver condition A10, 60 KIAS, -12° , run number 282441

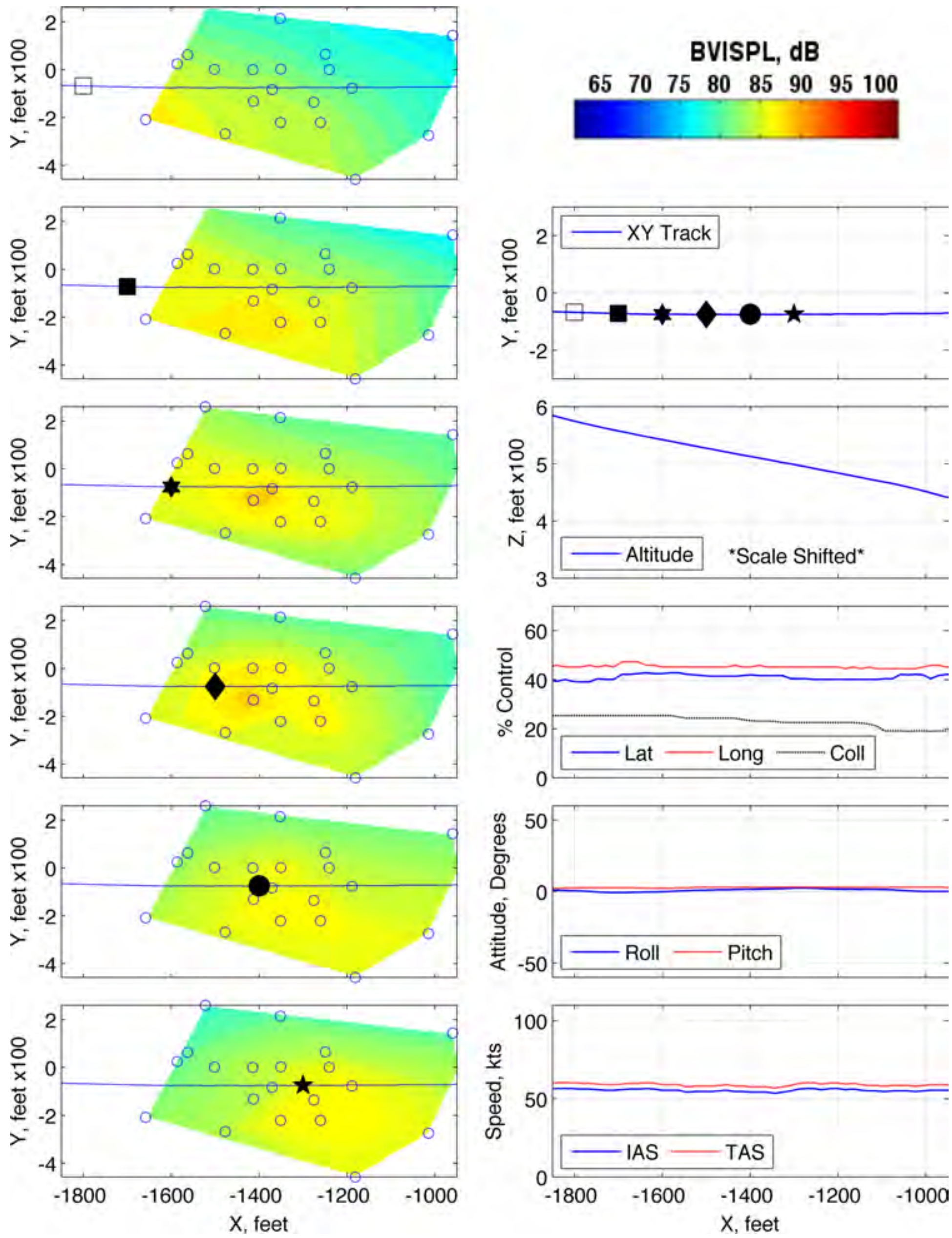

Figure 105: Maneuver condition A10, 60 KIAS, -12° , run number 282442

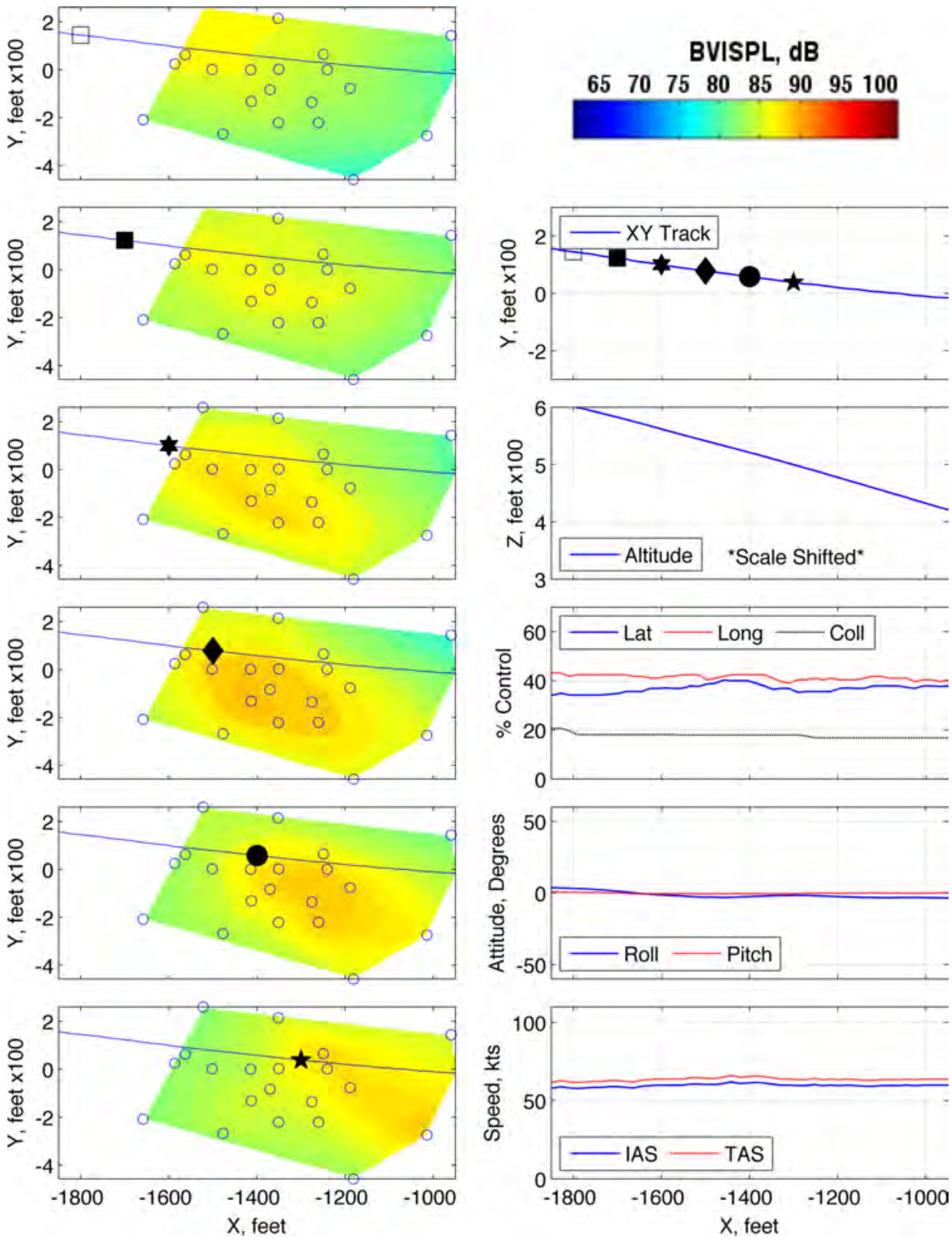

Figure 106: Maneuver condition A10, 60 KIAS, -12° , run number 285494

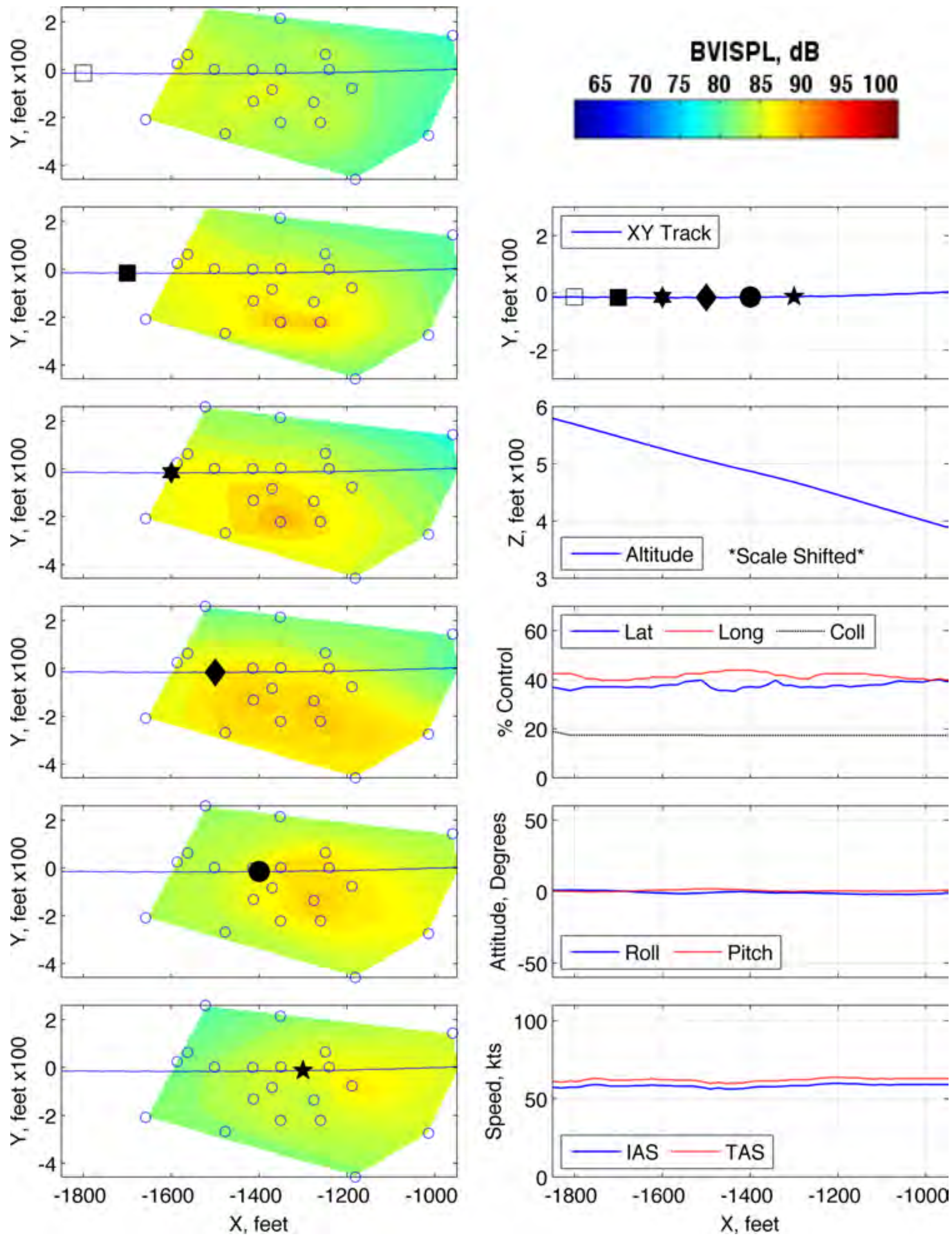

Figure 107: Maneuver condition A10, 60 KIAS, -12° , run number 285495

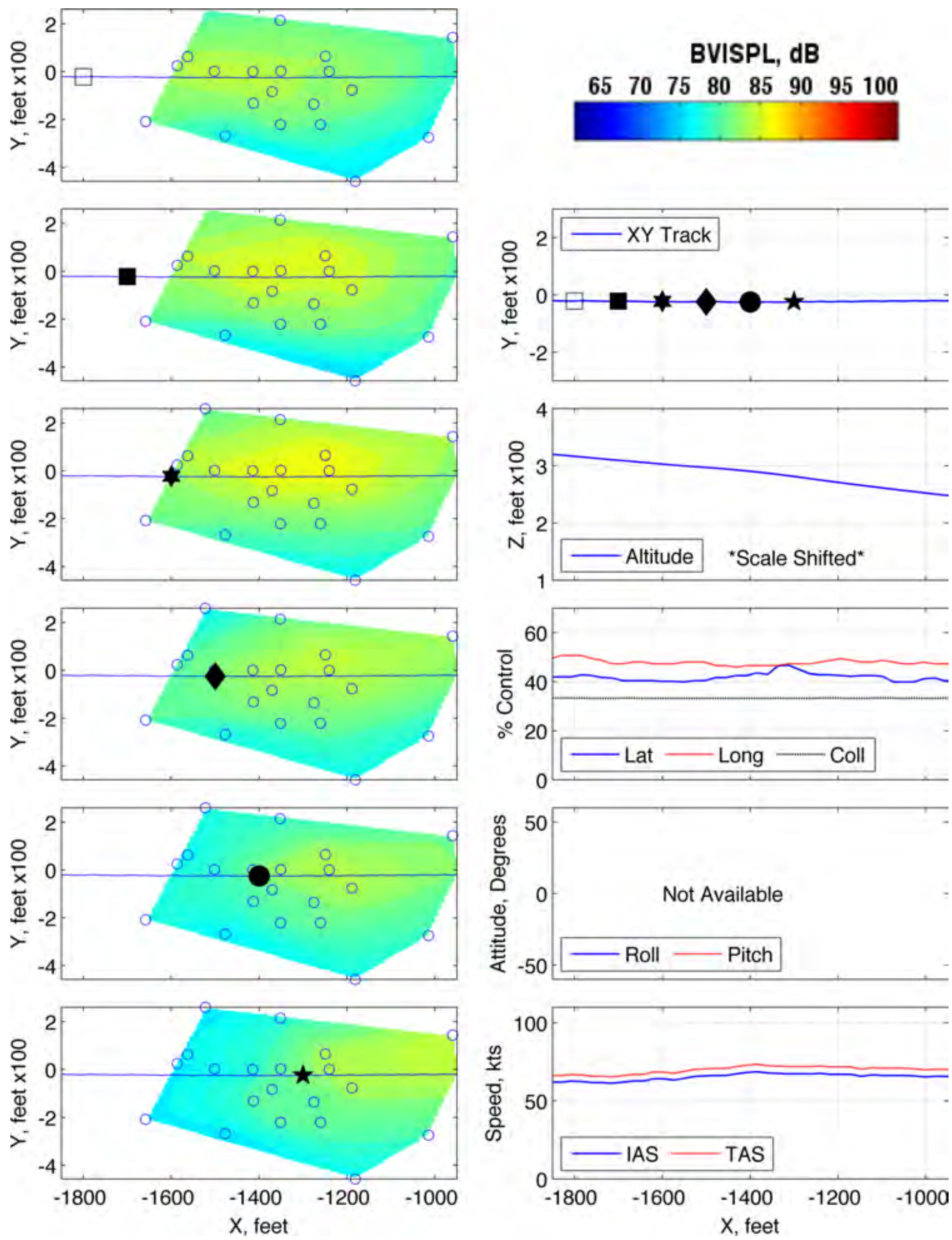

Figure 108: Maneuver condition A12, 70 KIAS, -4.5° , run number 280399

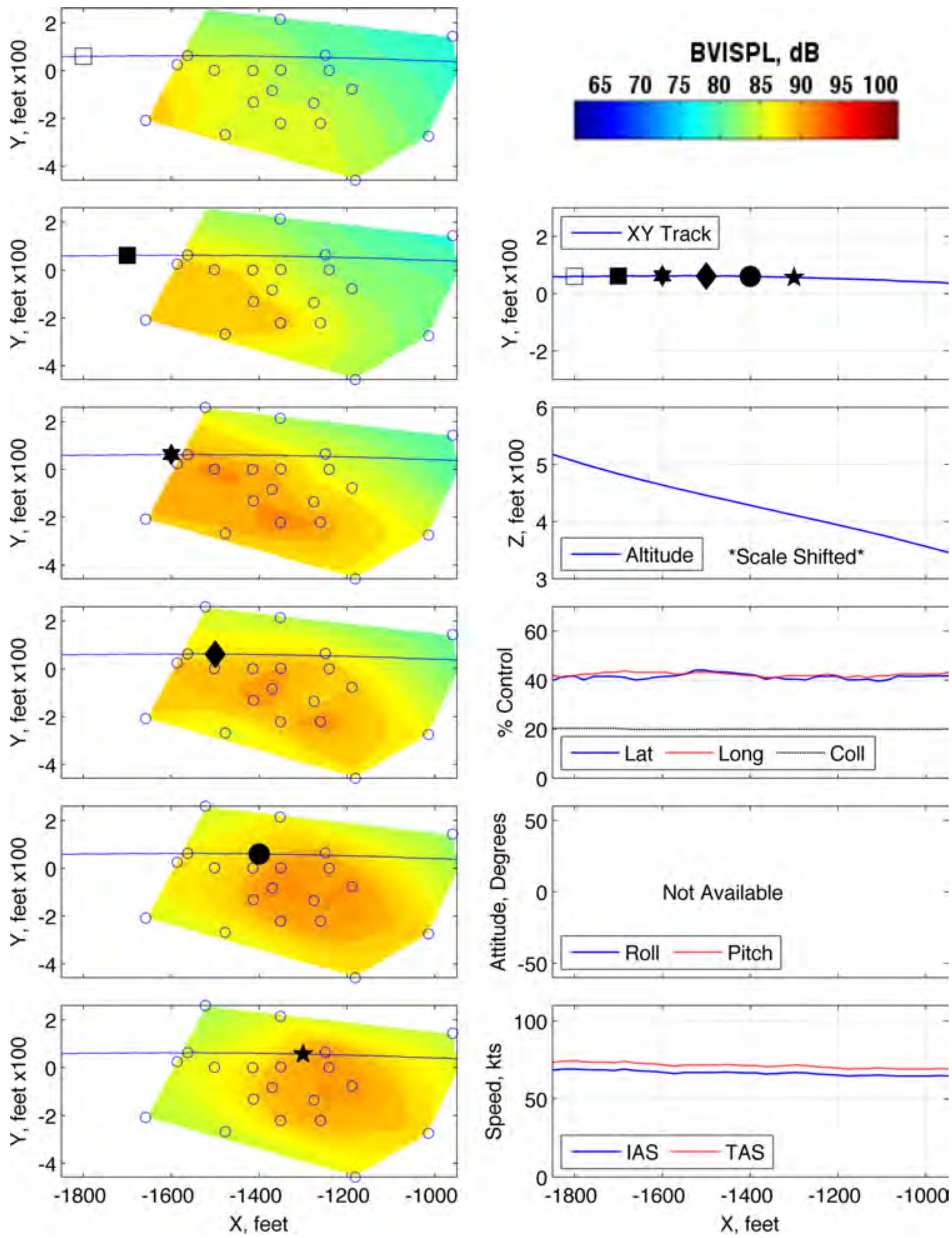

Figure 109: Maneuver condition A16, 70 KIAS, -10.5° , run number 280402

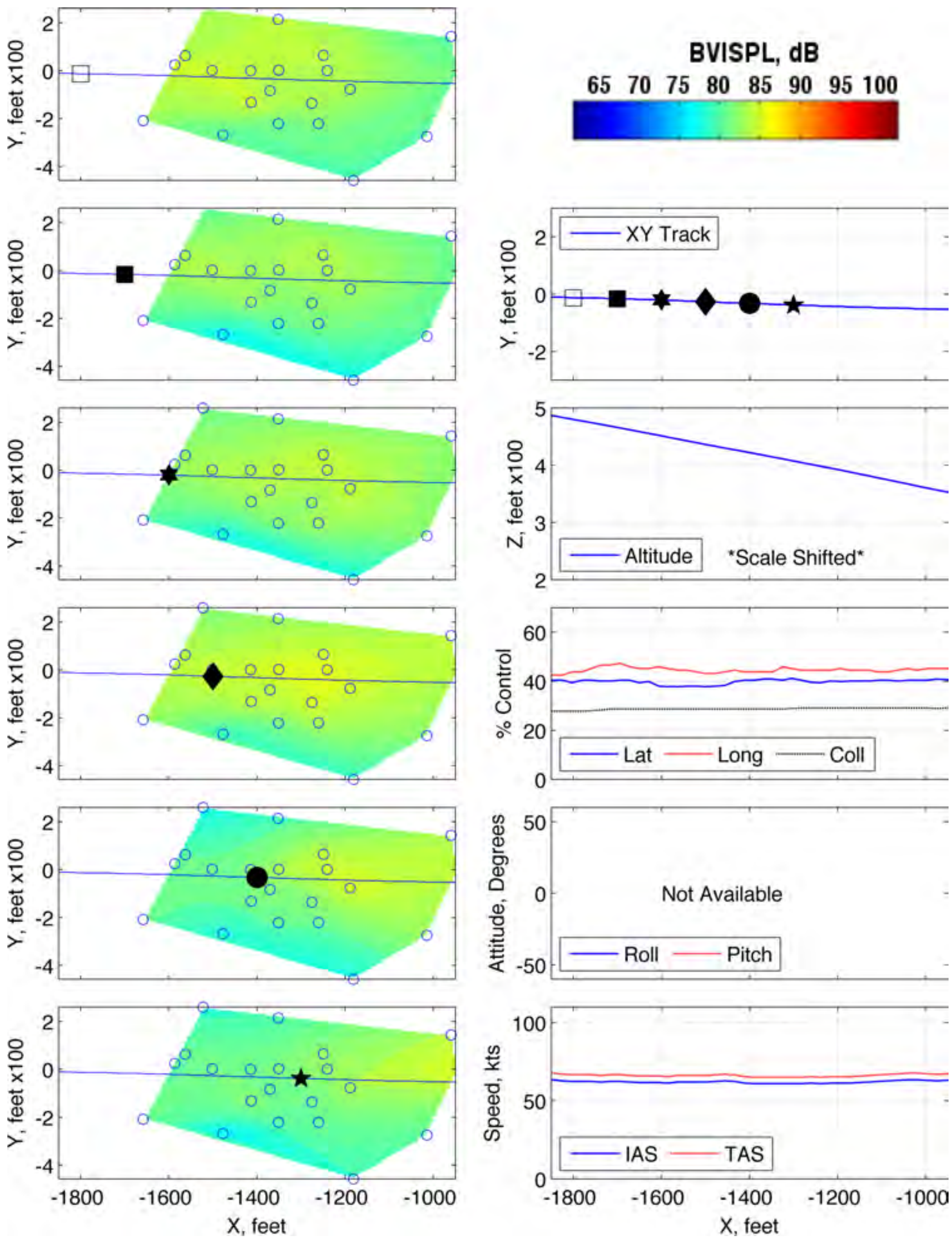

Figure 110: Maneuver condition A16, 70 KIAS, -10.5° , run number 280403

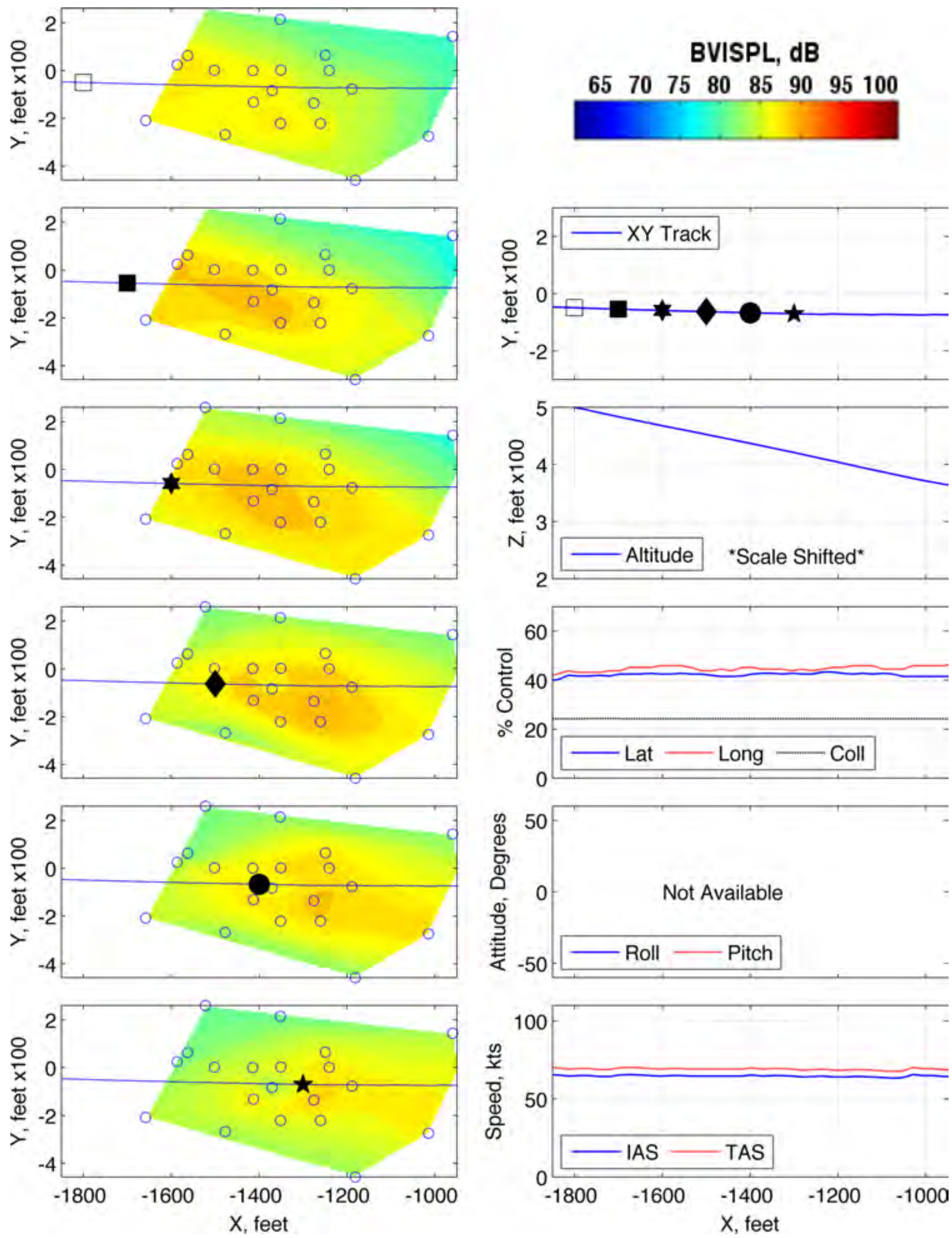

Figure 111: Maneuver condition A16, 70 KIAS, -10.5° , run number 280404

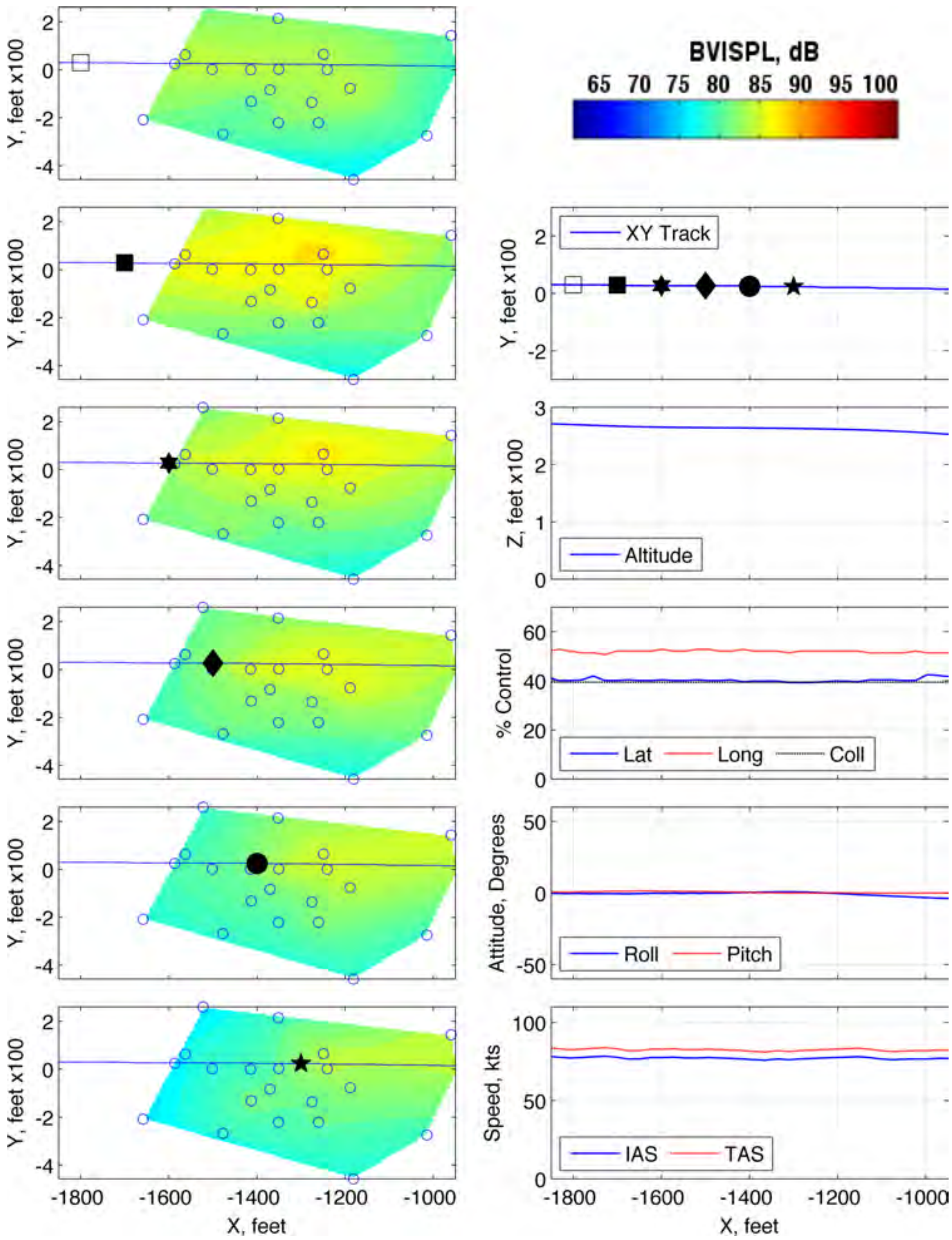

Figure 112: Maneuver condition A18, 80 KIAS, -3° , run number 282449

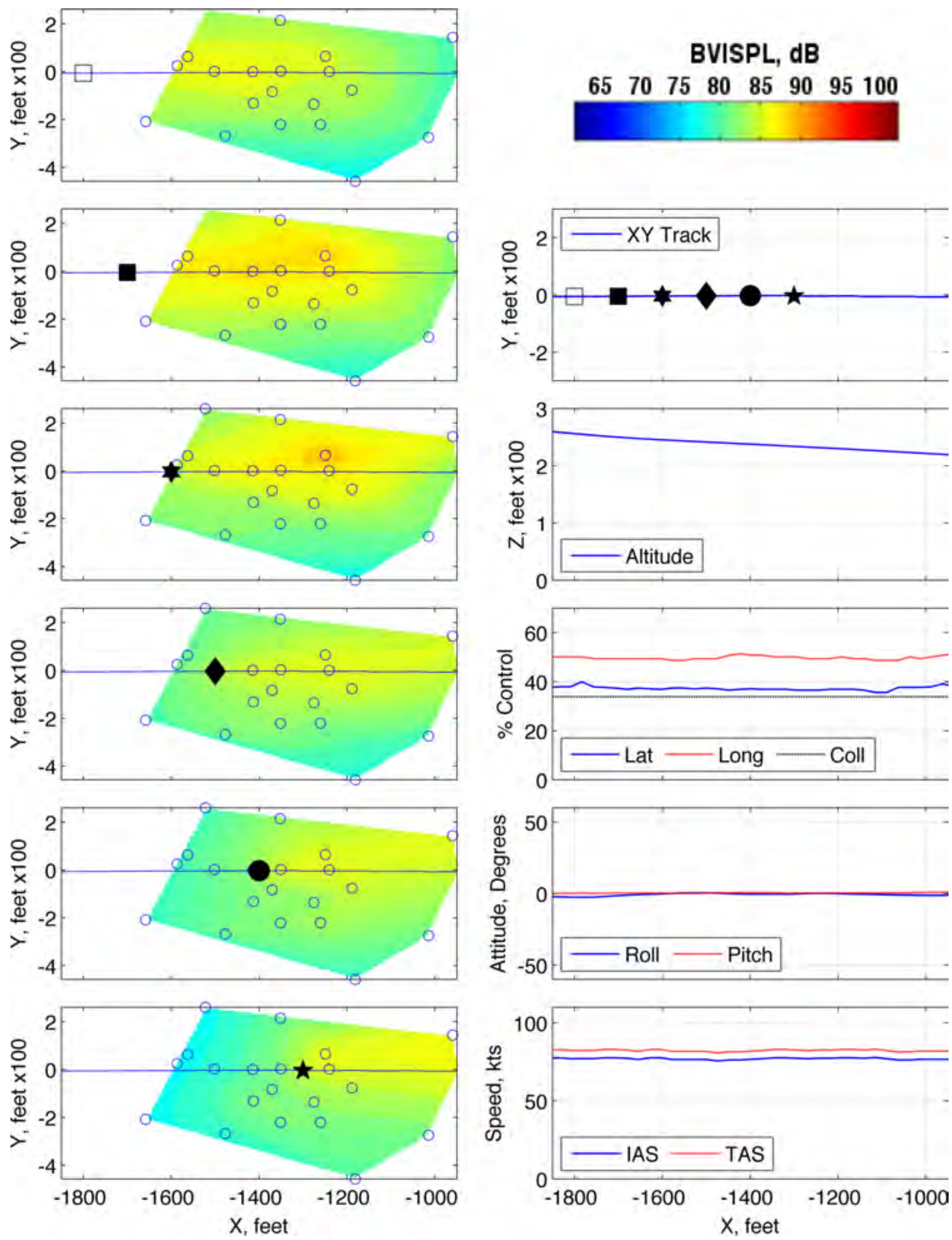

Figure 113: Maneuver condition A18, 80 KIAS, -3° , run number 285498

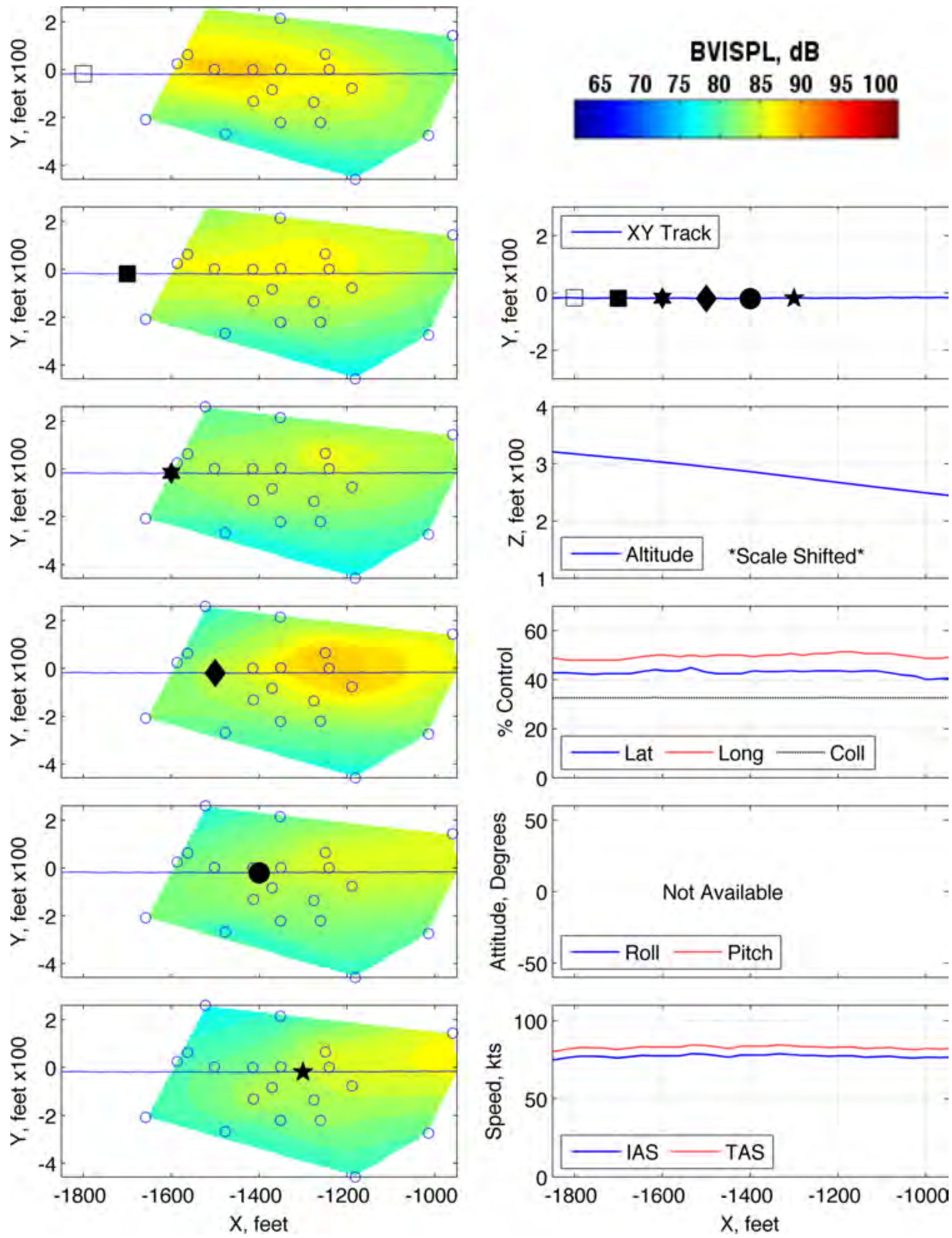

Figure 114: Maneuver condition A19, 80 KIAS, -4.5° , run number 280400

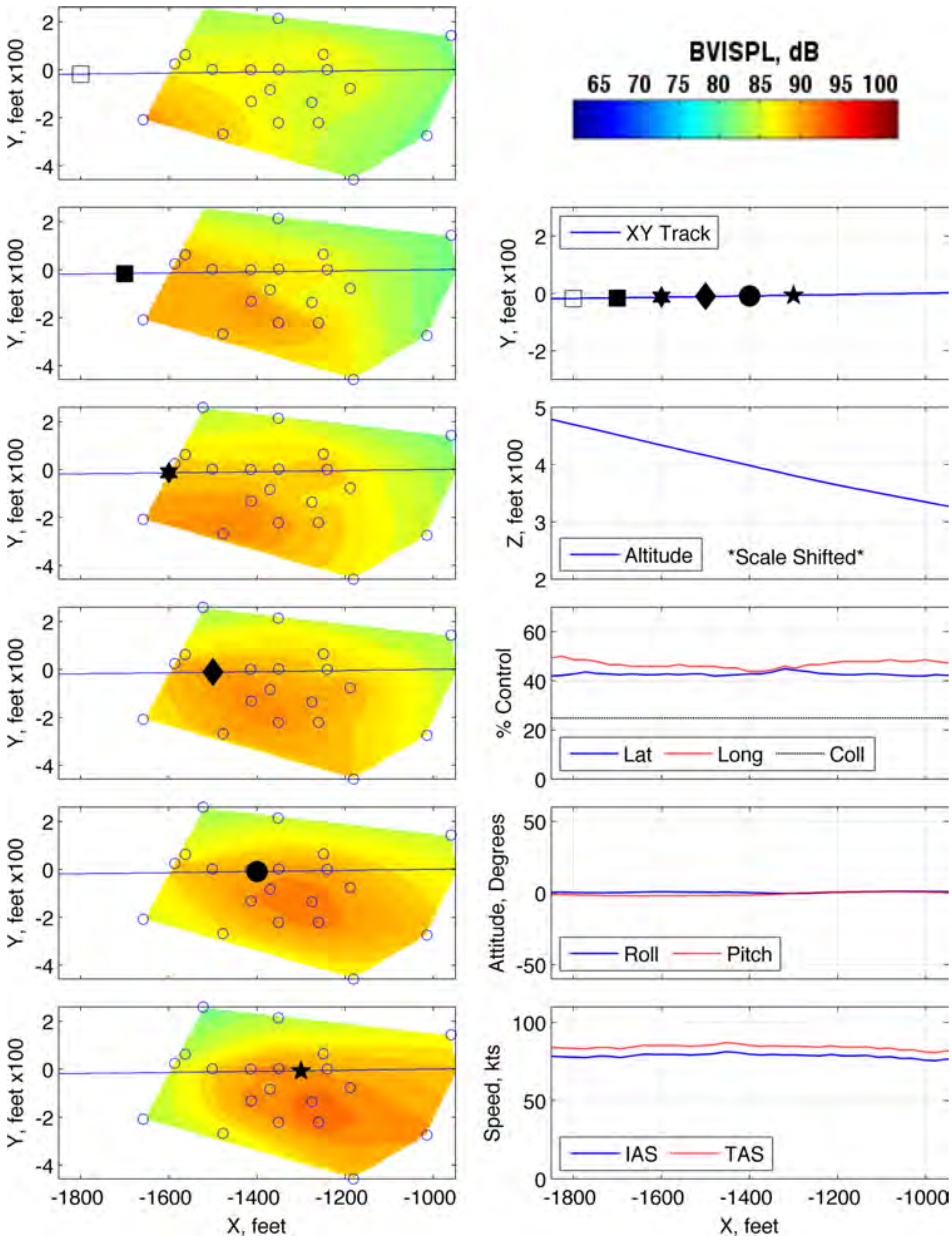

Figure 115: Maneuver condition A22, 80 KIAS, -9° , run number 282445

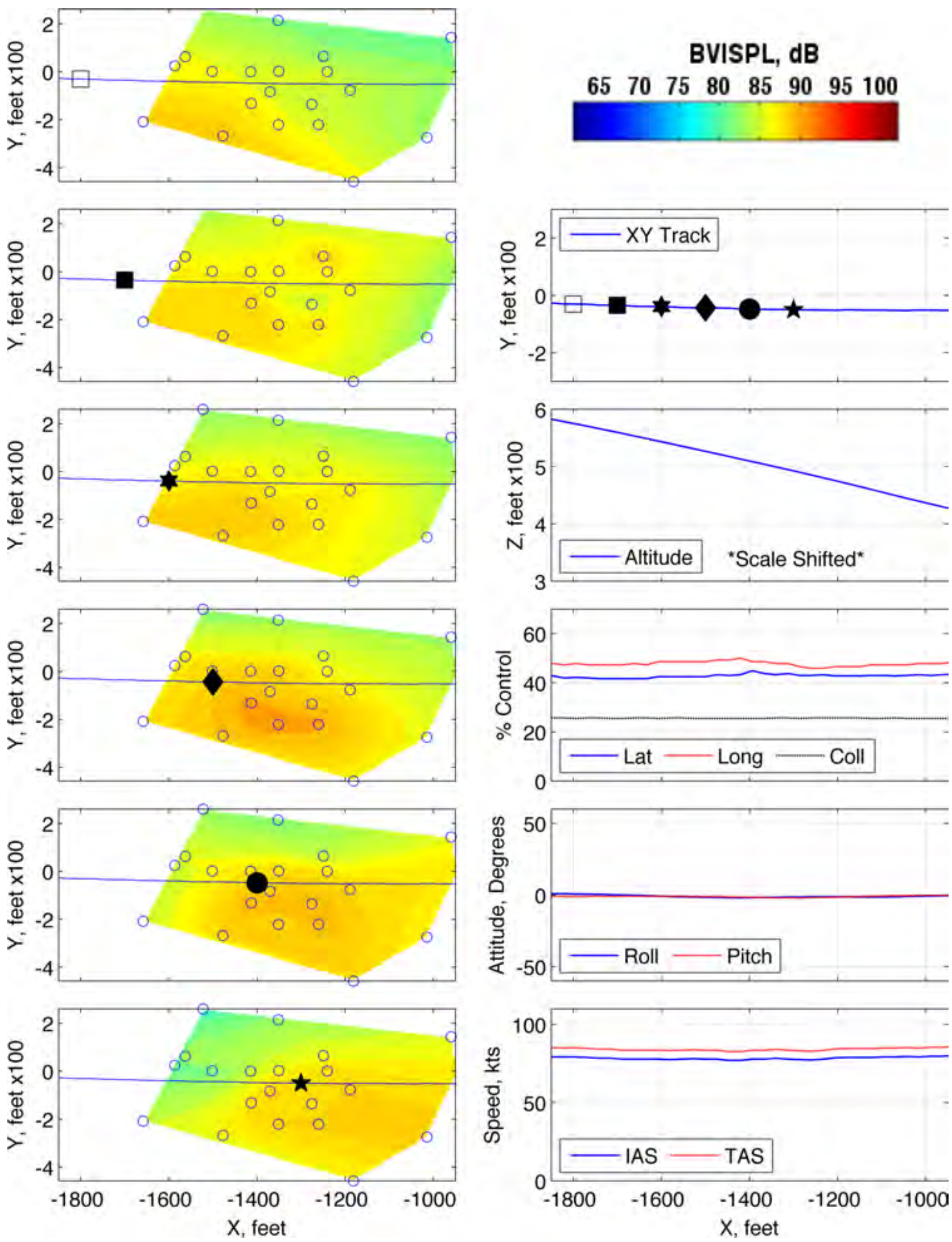

Figure 116: Maneuver condition A24, 80 KIAS, -12° , run number 282443

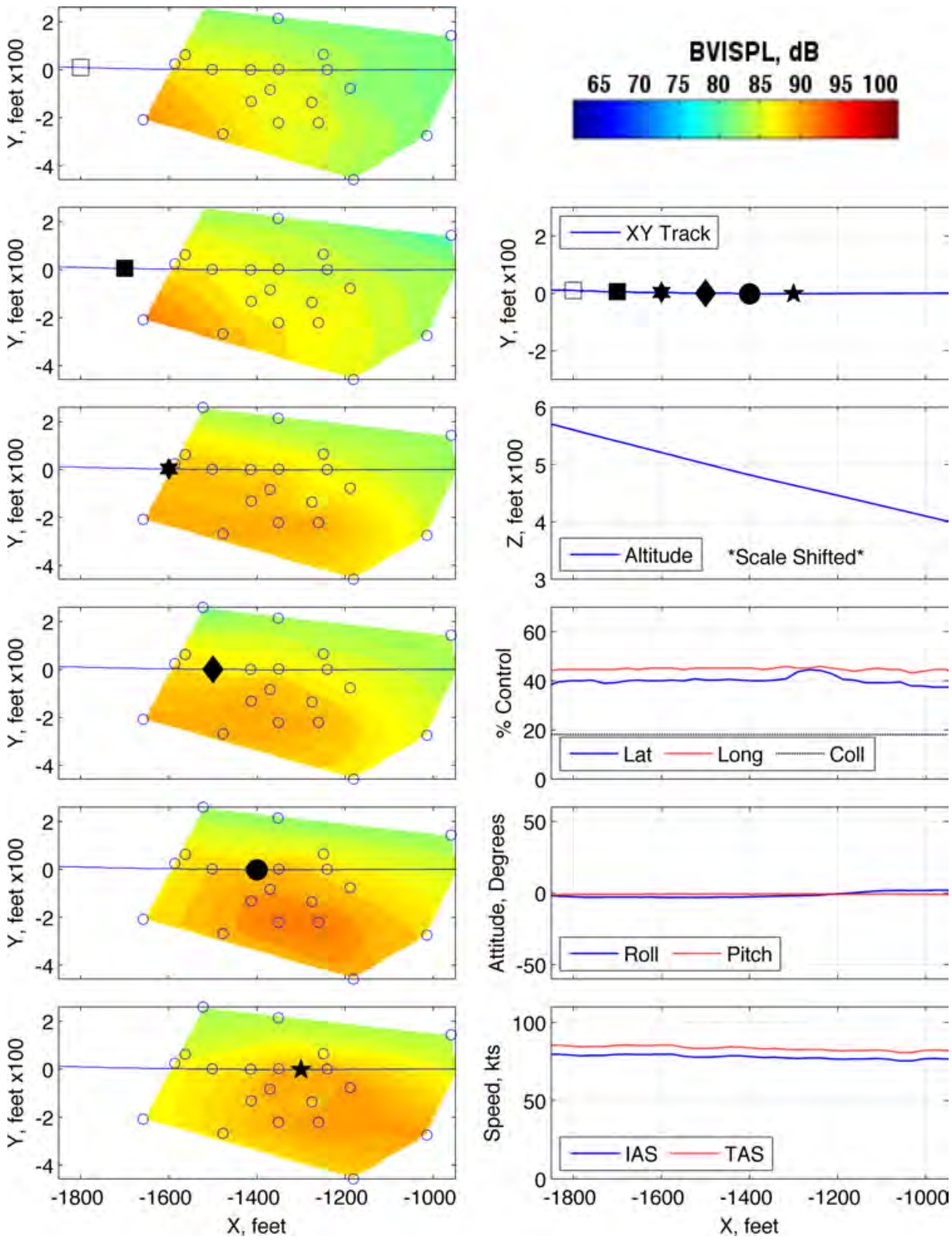

Figure 117: Maneuver condition A24, 80 KIAS, -12° , run number 285496

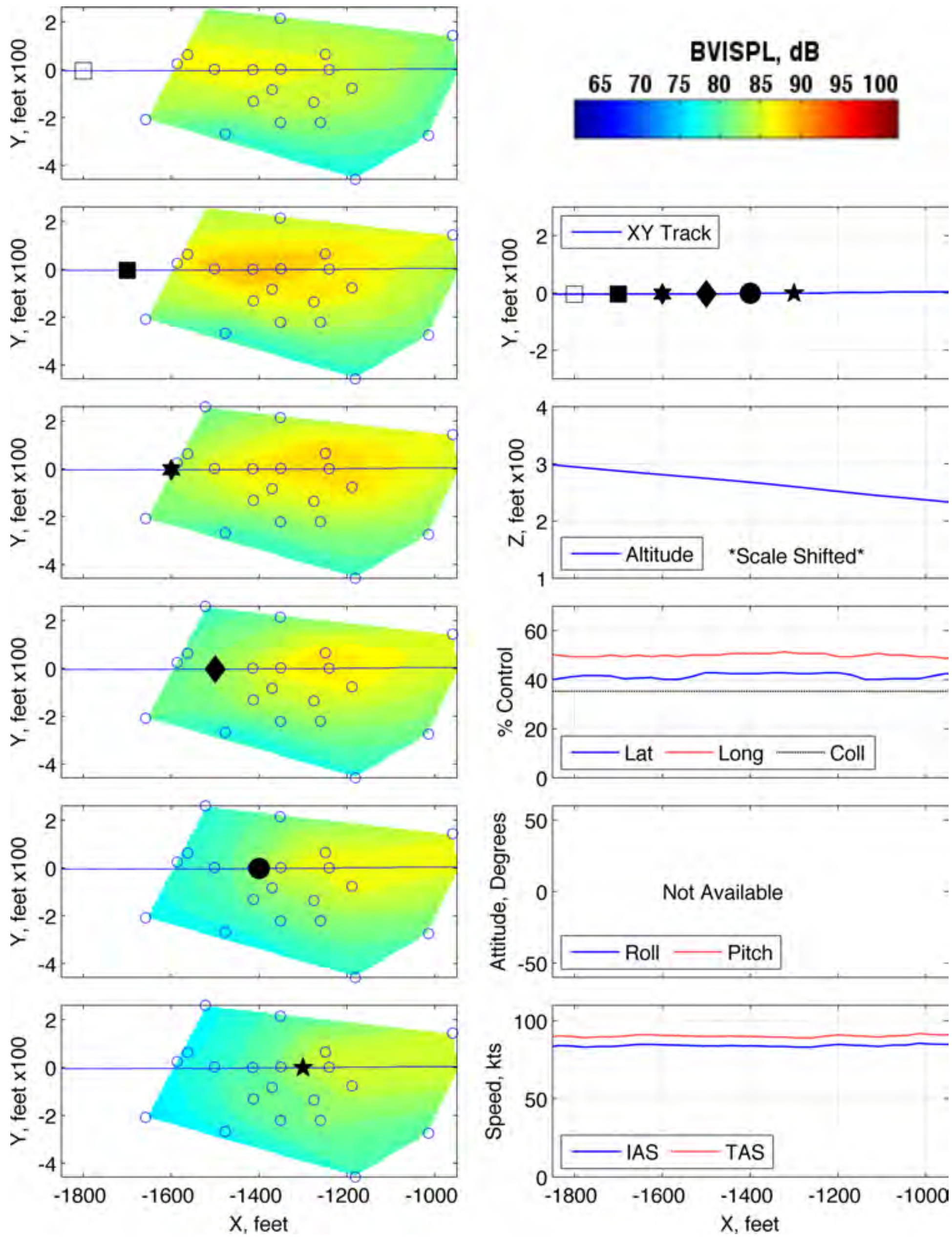

Figure 118: Maneuver condition A26, 90 KIAS, -4.5° run number 280401

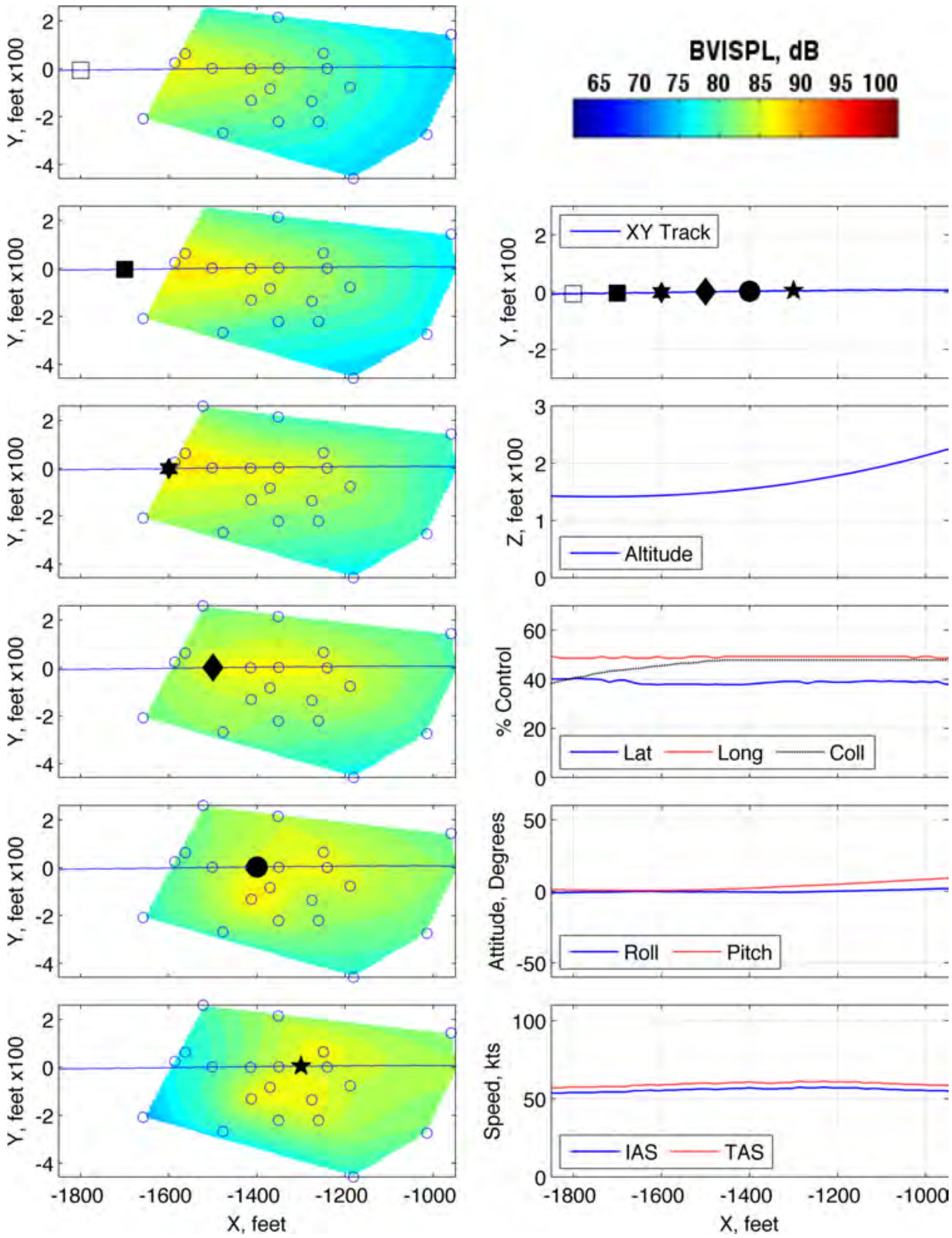

Figure 119: Maneuver condition C1, 60 KIAS, slow collective pull-up, run number 282435

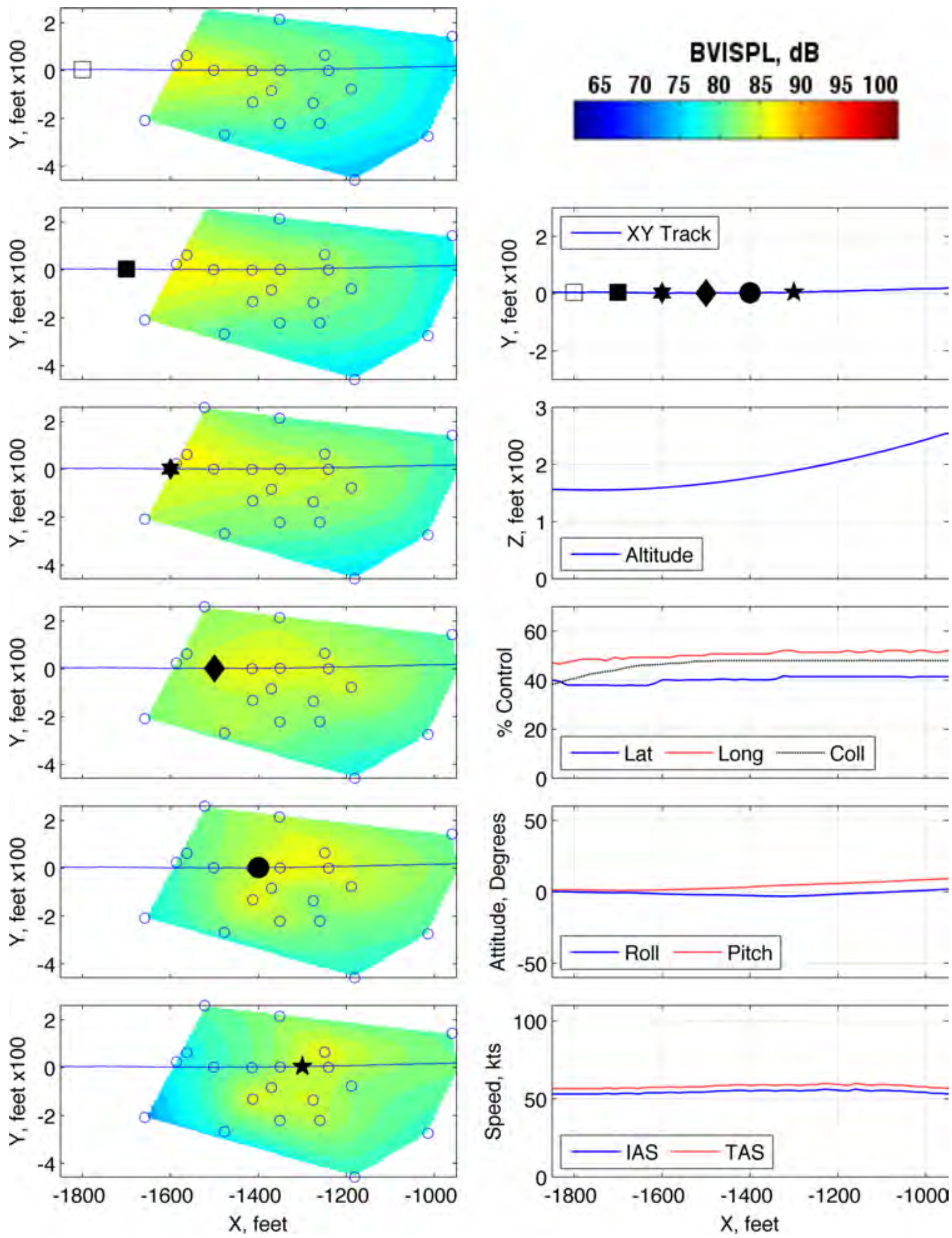

Figure 120: Maneuver condition C1, 60 KIAS, slow collective pull-up, run number 282436

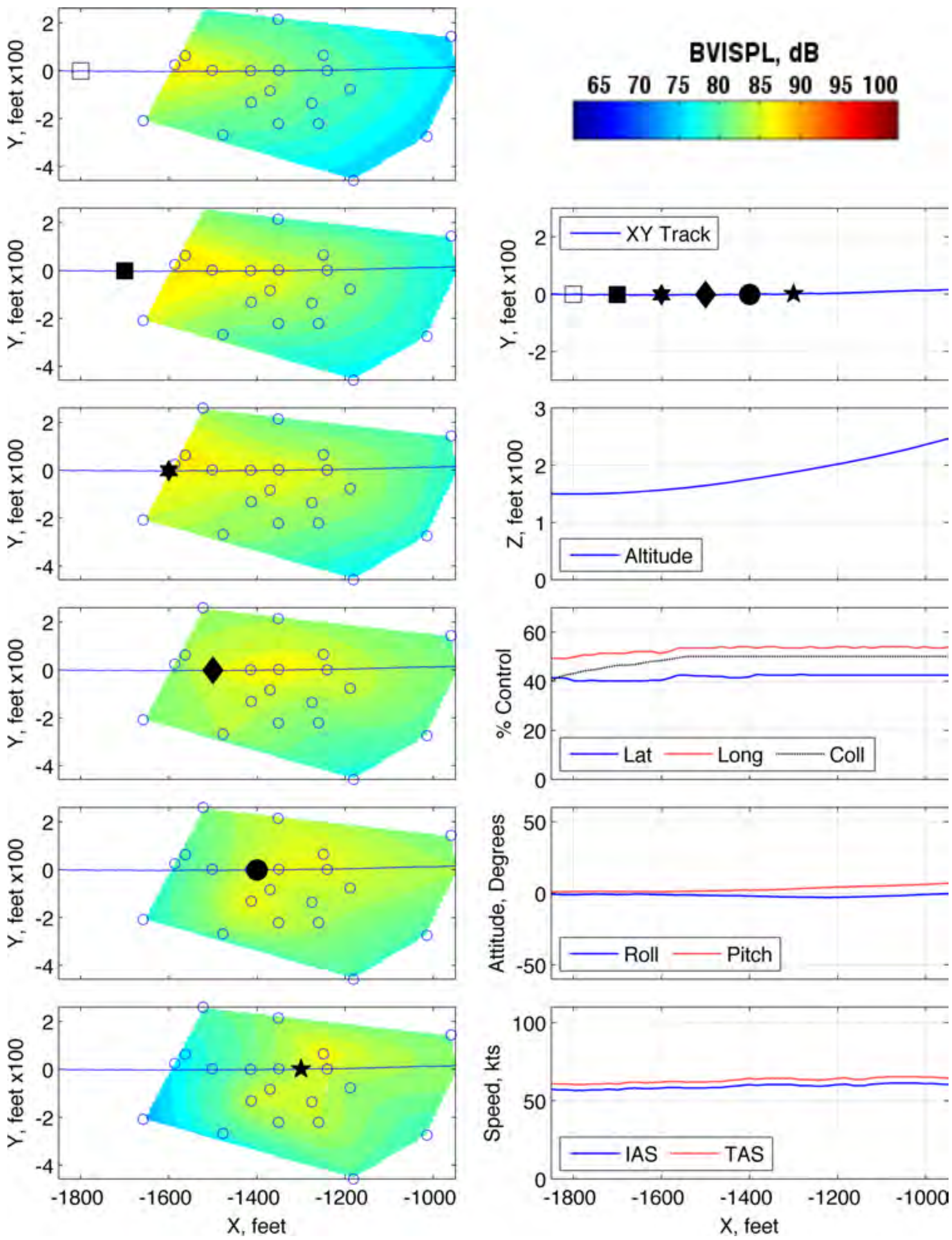

Figure 121: Maneuver condition C3, 60 KIAS, fast collective pull-up, run number 282437

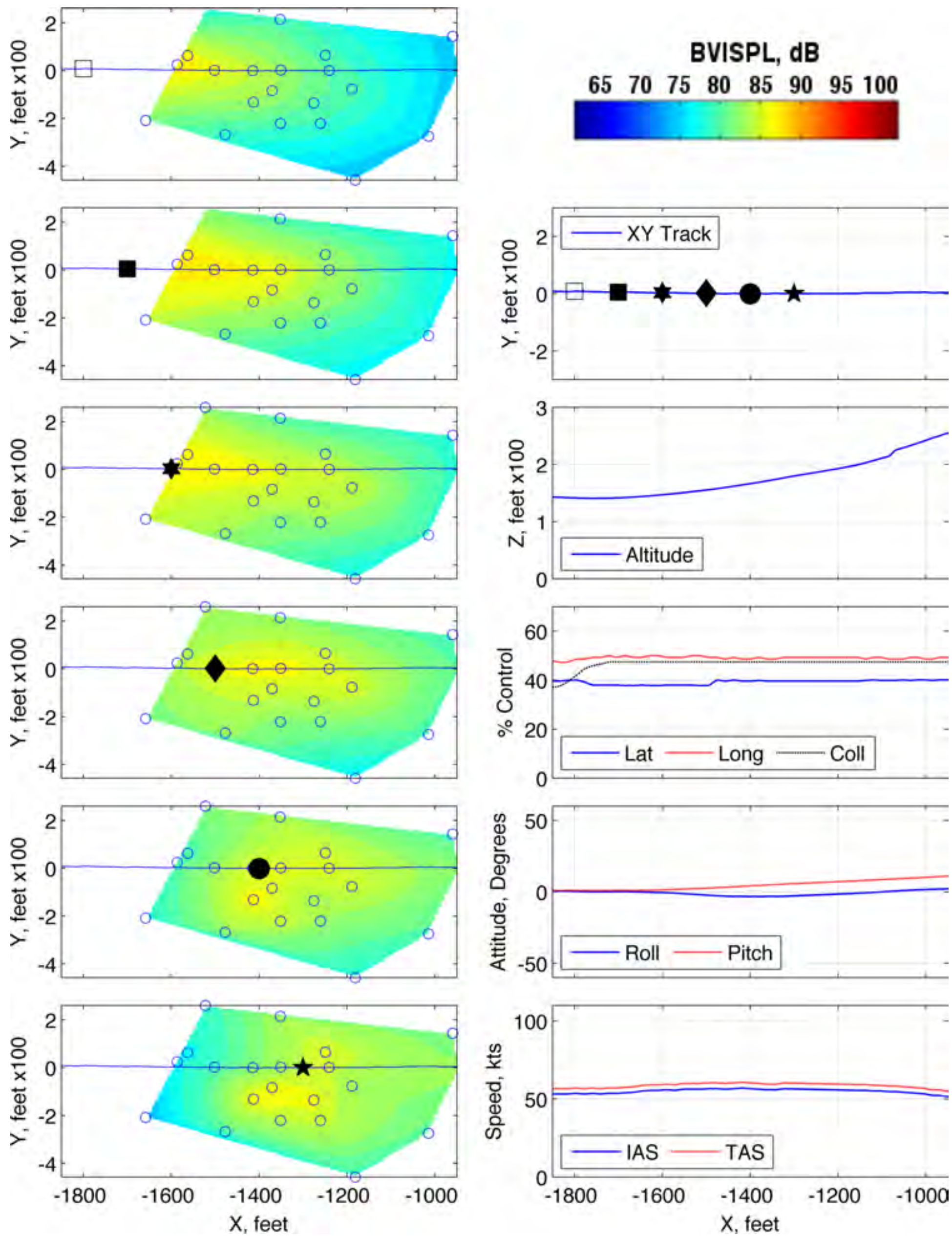

Figure 122: Maneuver condition C3, 60 KIAS, fast collective pull-up, run number 282438

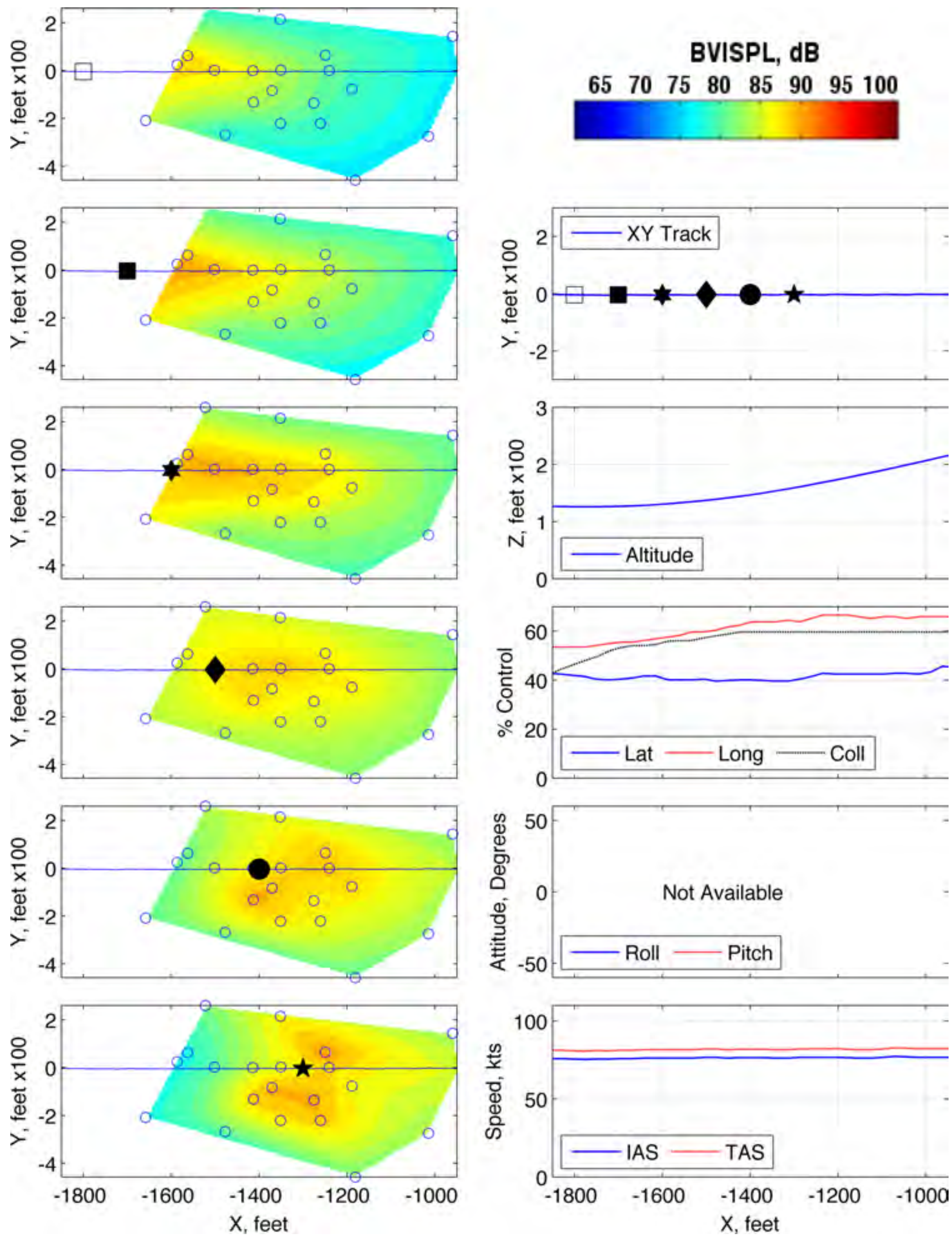

Figure 123: Maneuver condition C4, 80 KIAS, slow collective pull-up, run number 280390

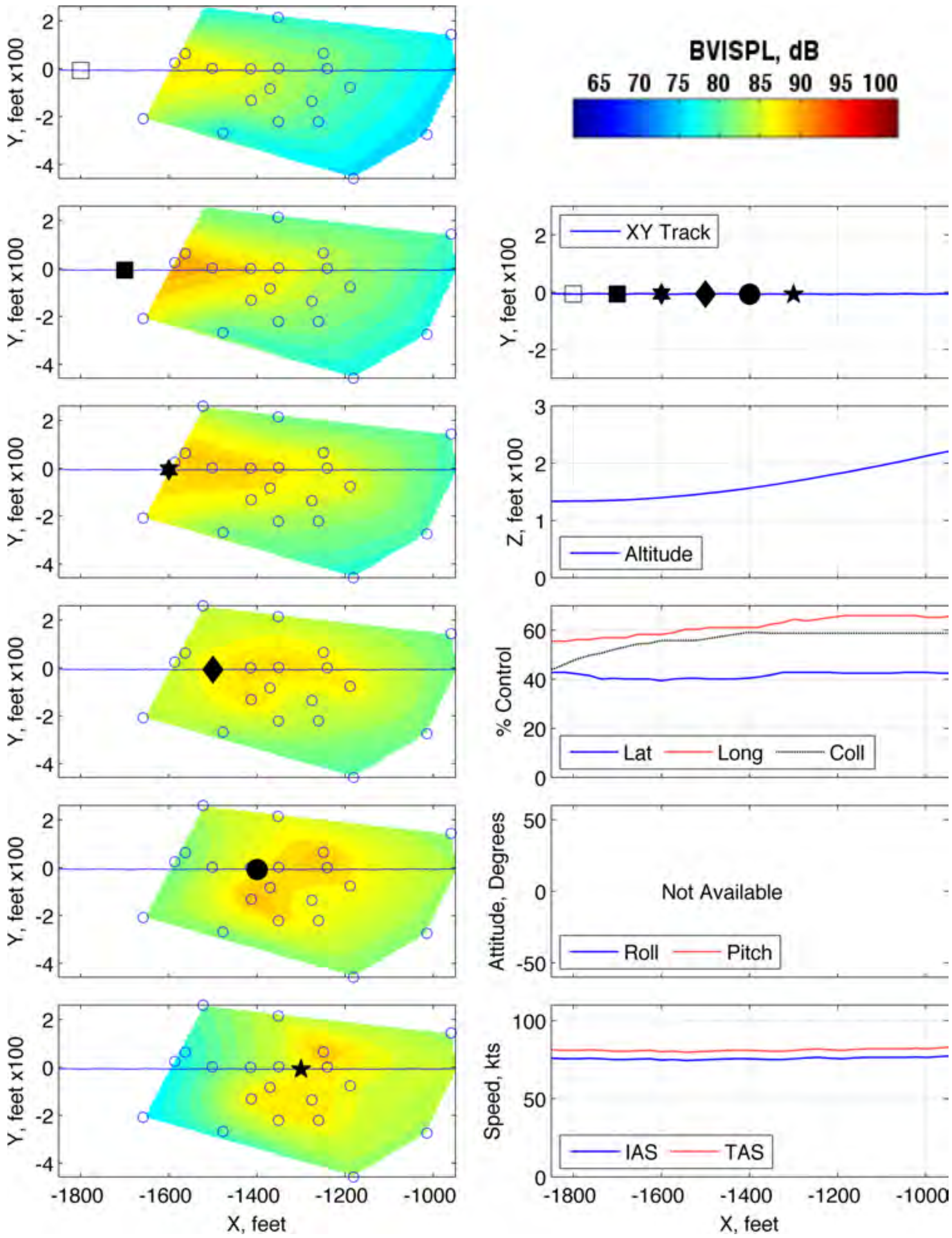

Figure 124: Maneuver condition C4, 80 KIAS, slow collective pull-up, run number 280391

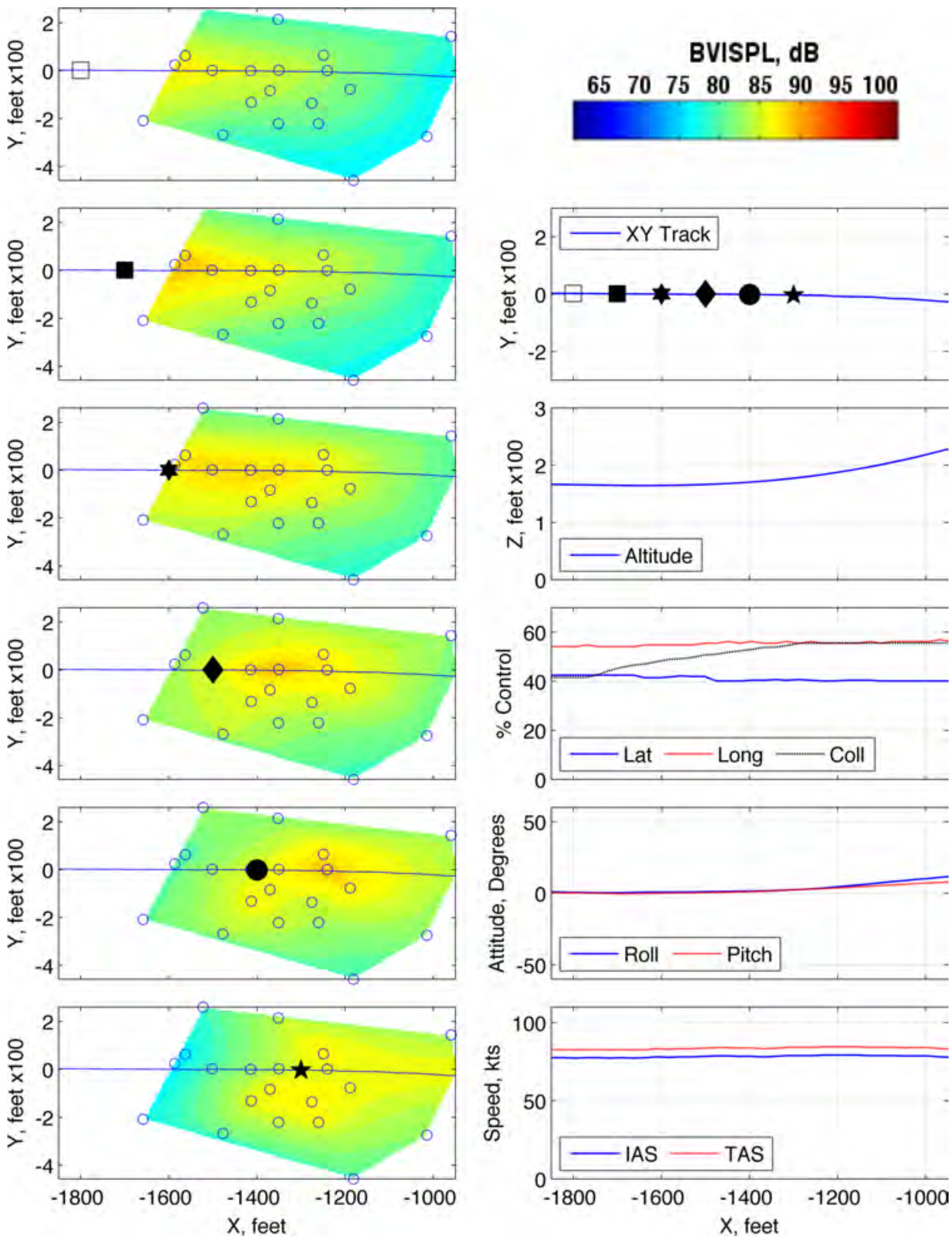

Figure 125: Maneuver condition C4, 80 KIAS, slow collective pull-up, run number 282434

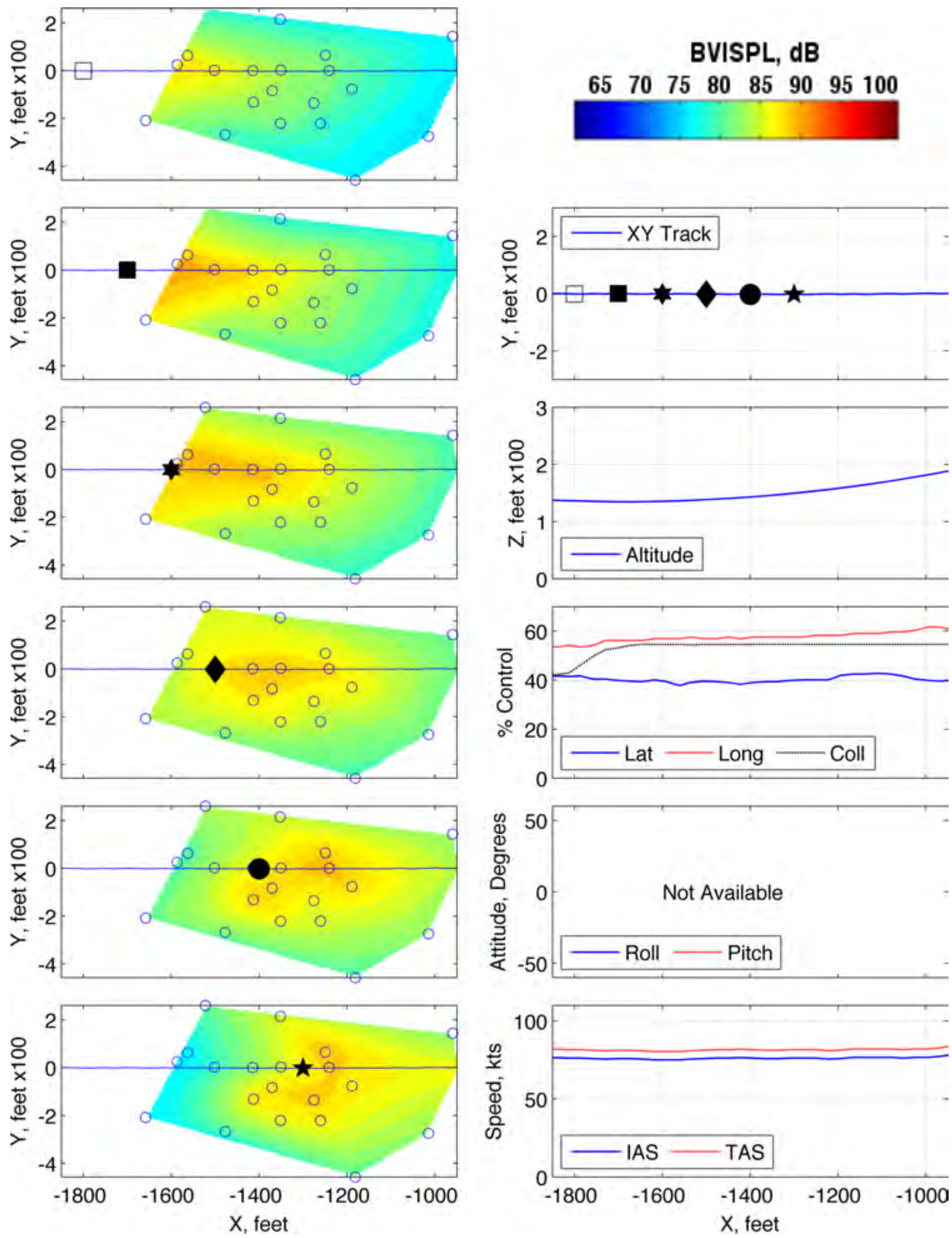

Figure 126: Maneuver condition C6, 80 KIAS, fast collective pull-up, run number 280392

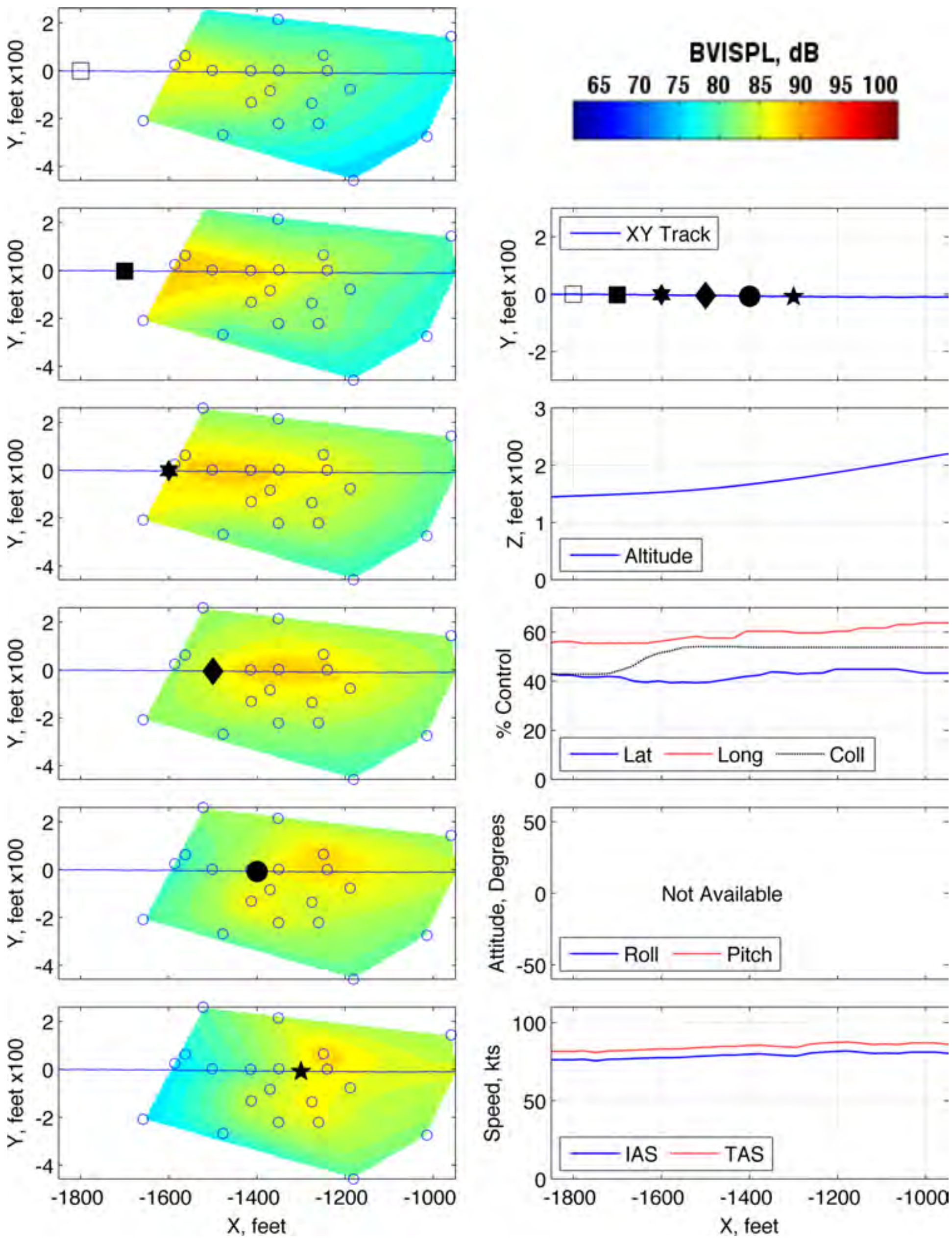

Figure 127: Maneuver condition C6, 80 KIAS, fast collective pull-up, run number 280393

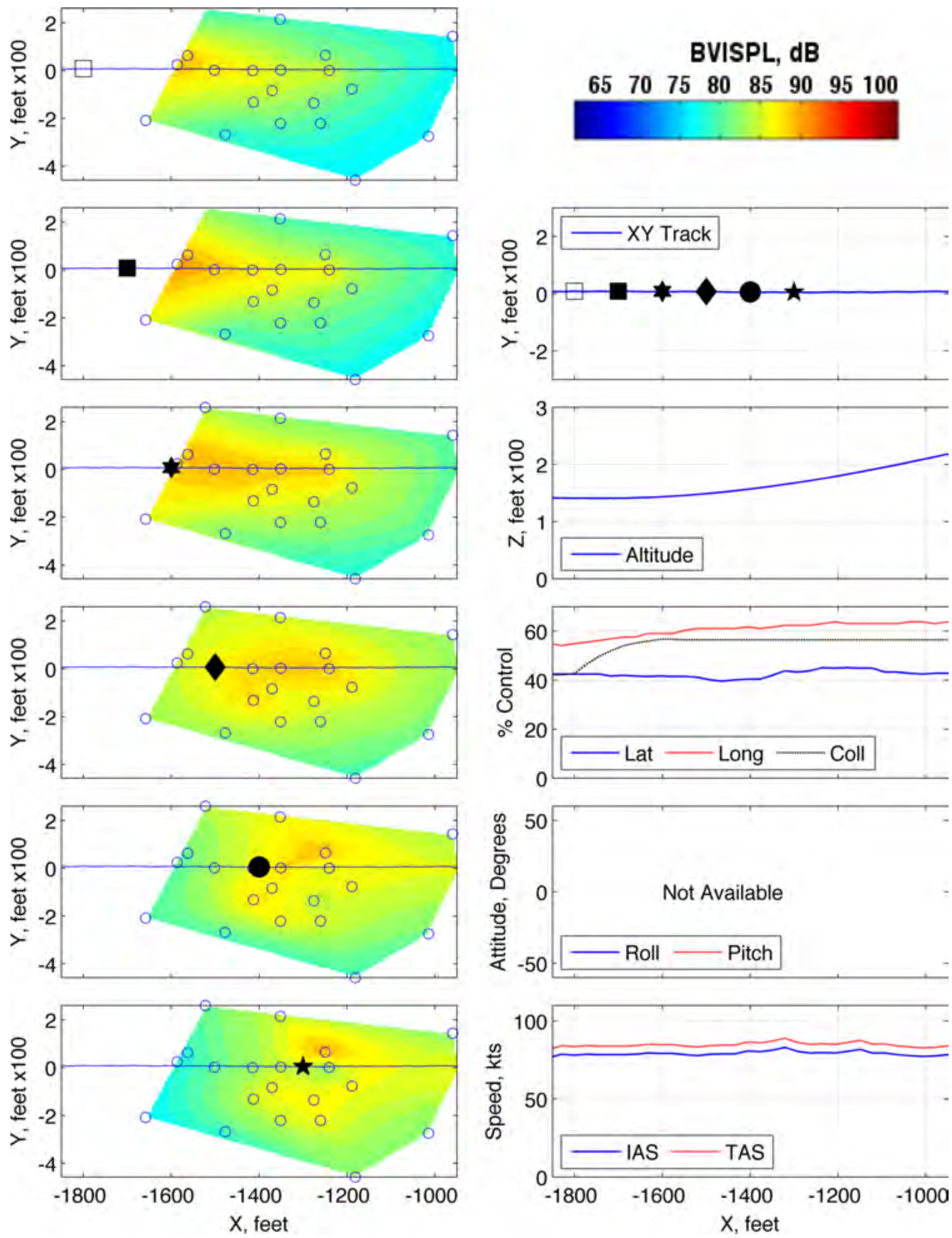

Figure 128: Maneuver condition C6, 80 KIAS, fast collective pull-up, run number 280394

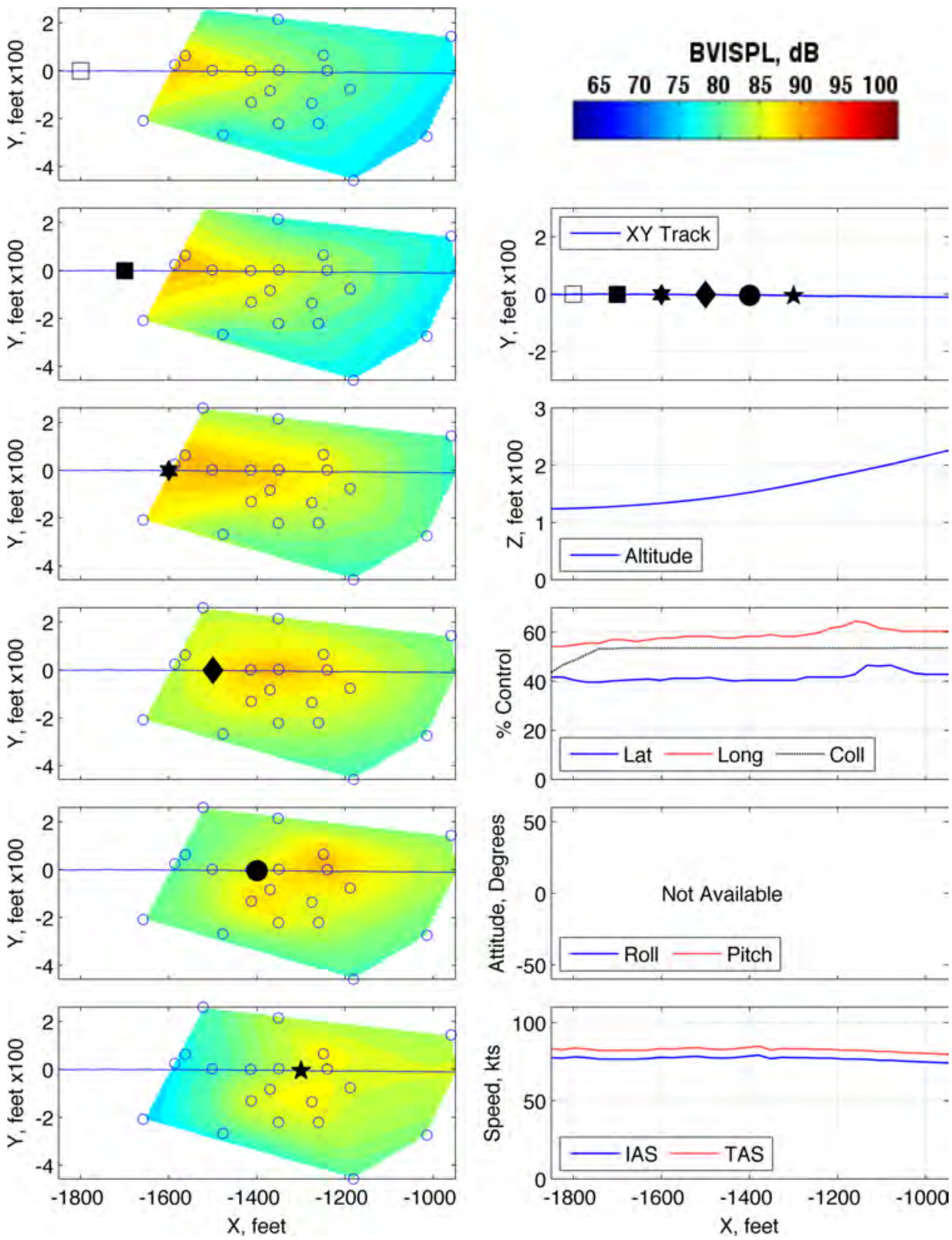

Figure 129: Maneuver condition C6, 80 KIAS, fast collective pull-up, run number 280395

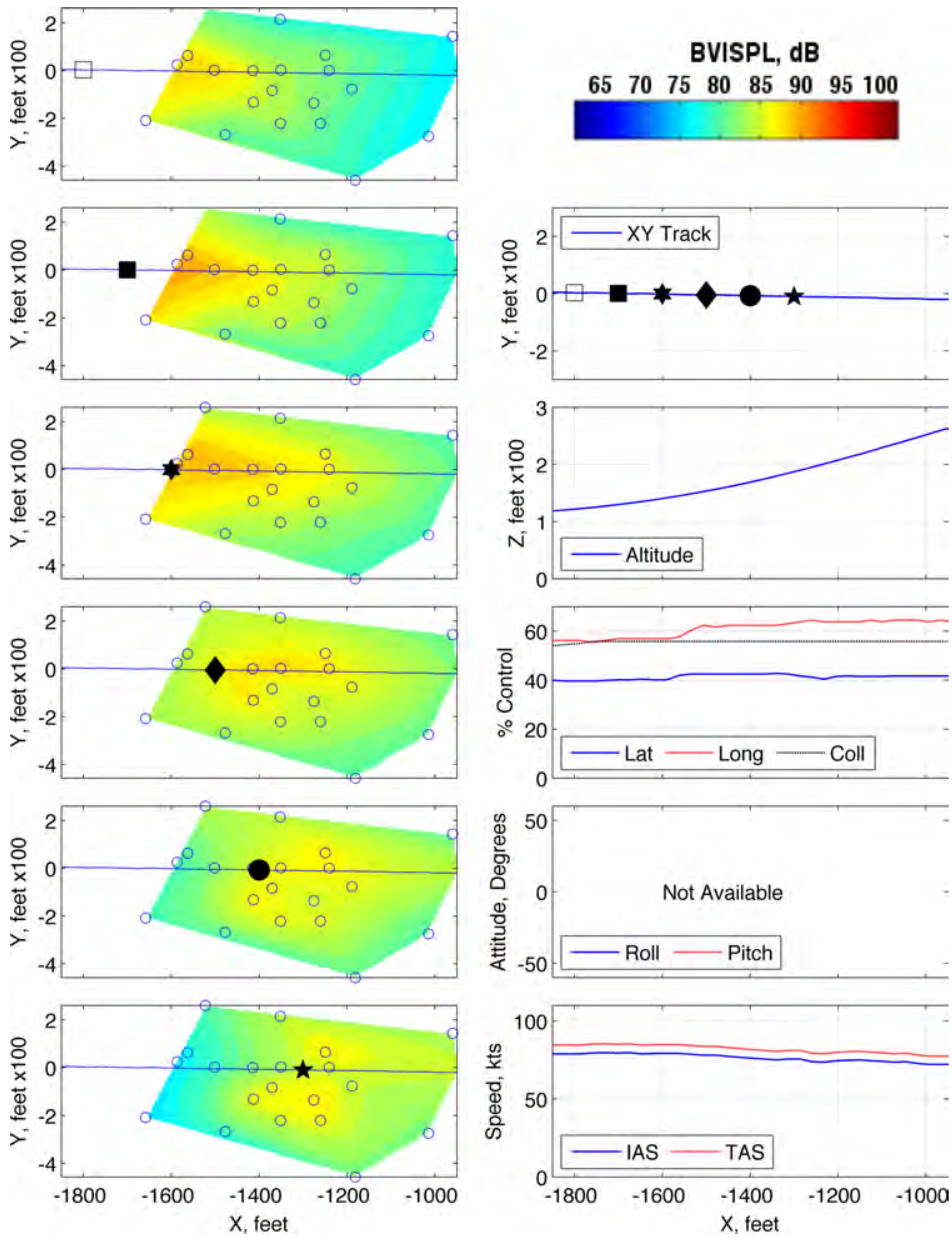

Figure 130: Maneuver condition C6, 80 KIAS, fast collective pull-up, run number 280396

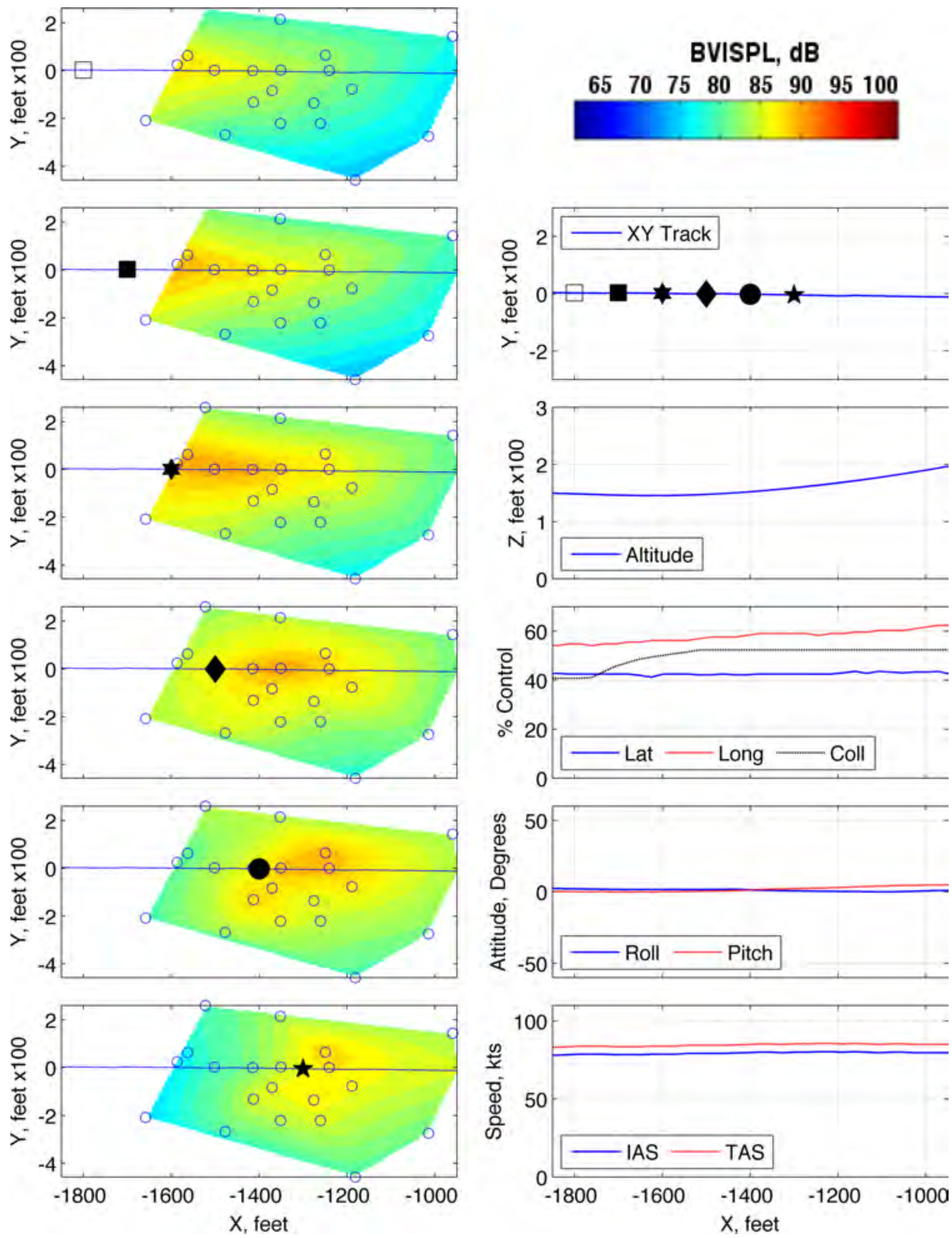

Figure 131: Maneuver condition C6, 80 KIAS, fast collective pull-up, run number 282433

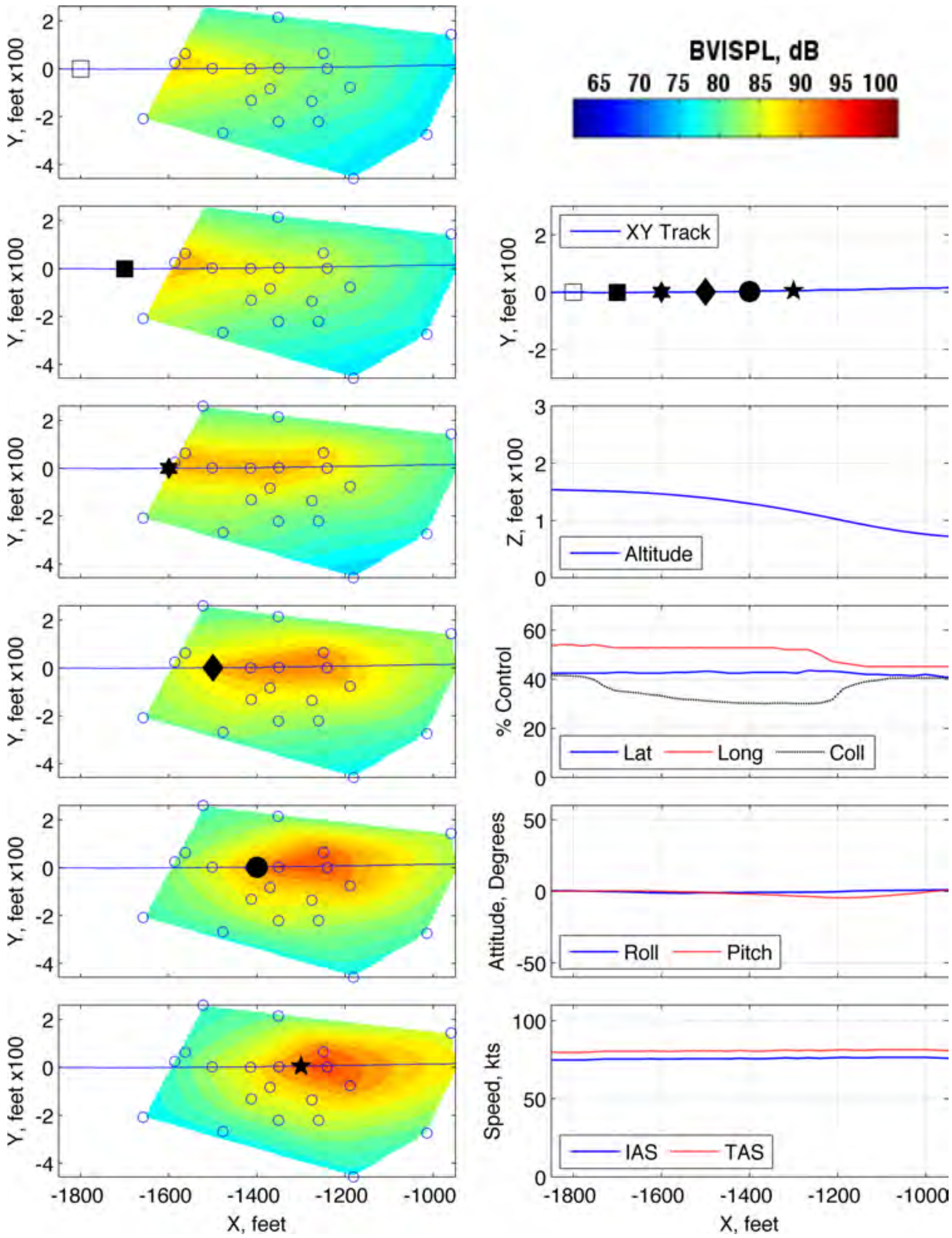

Figure 132: Maneuver condition C10, 80 KIAS, slow collective push-over, run number 282426

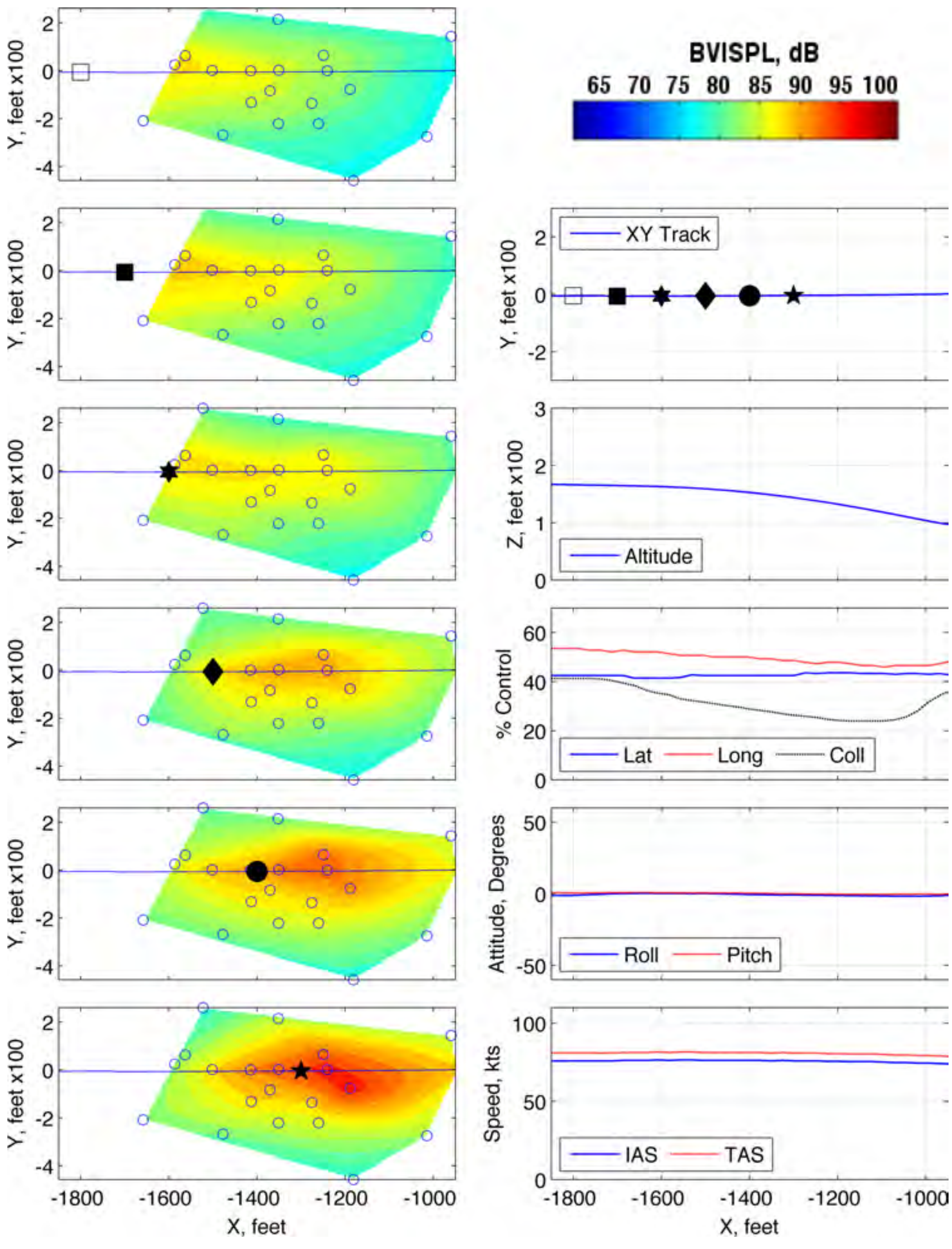

Figure 133: Maneuver condition C10, 80 KIAS, slow collective push-over, run number 282427

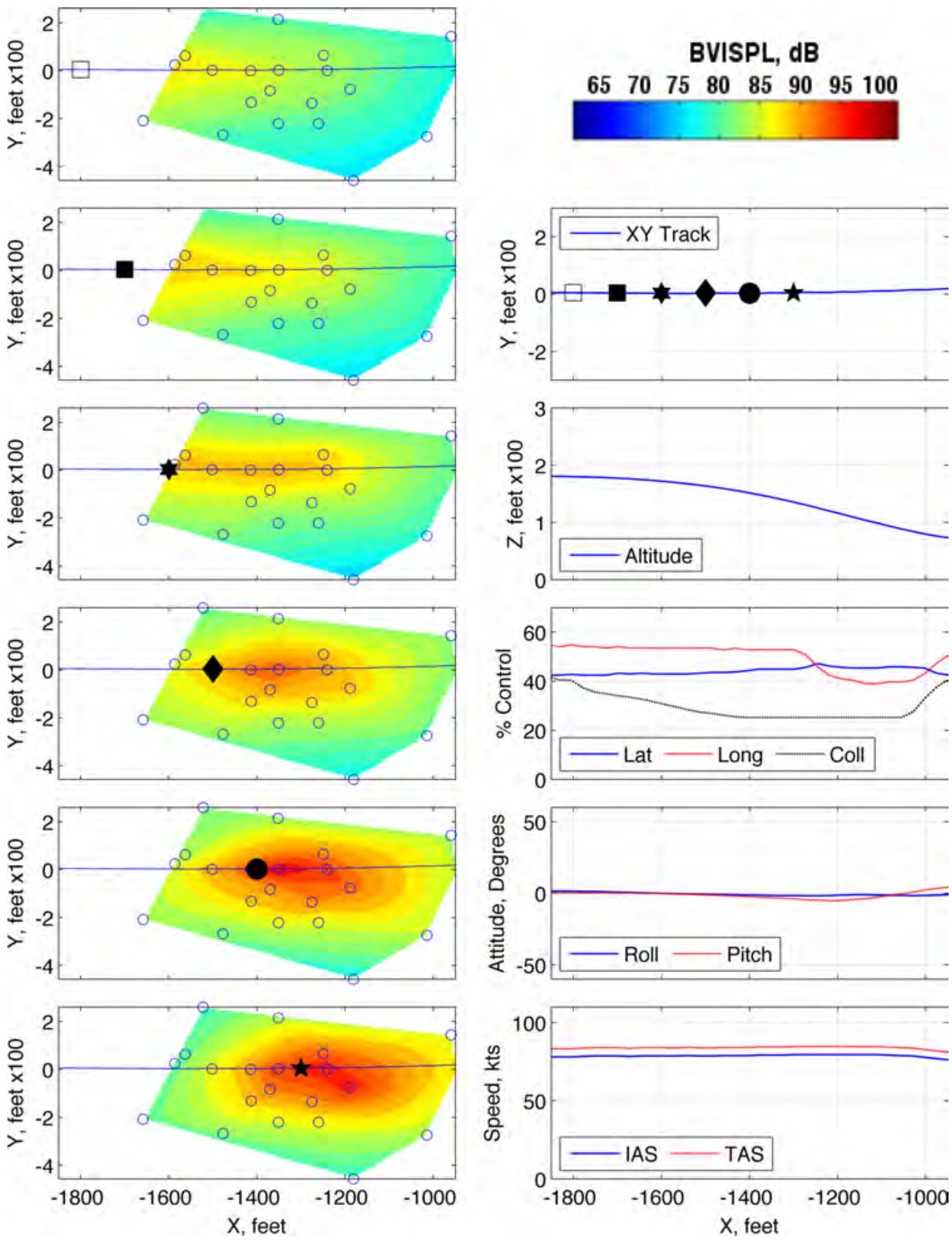

Figure 134: Maneuver condition C10, 80 KIAS, slow collective push-over, run number 282428

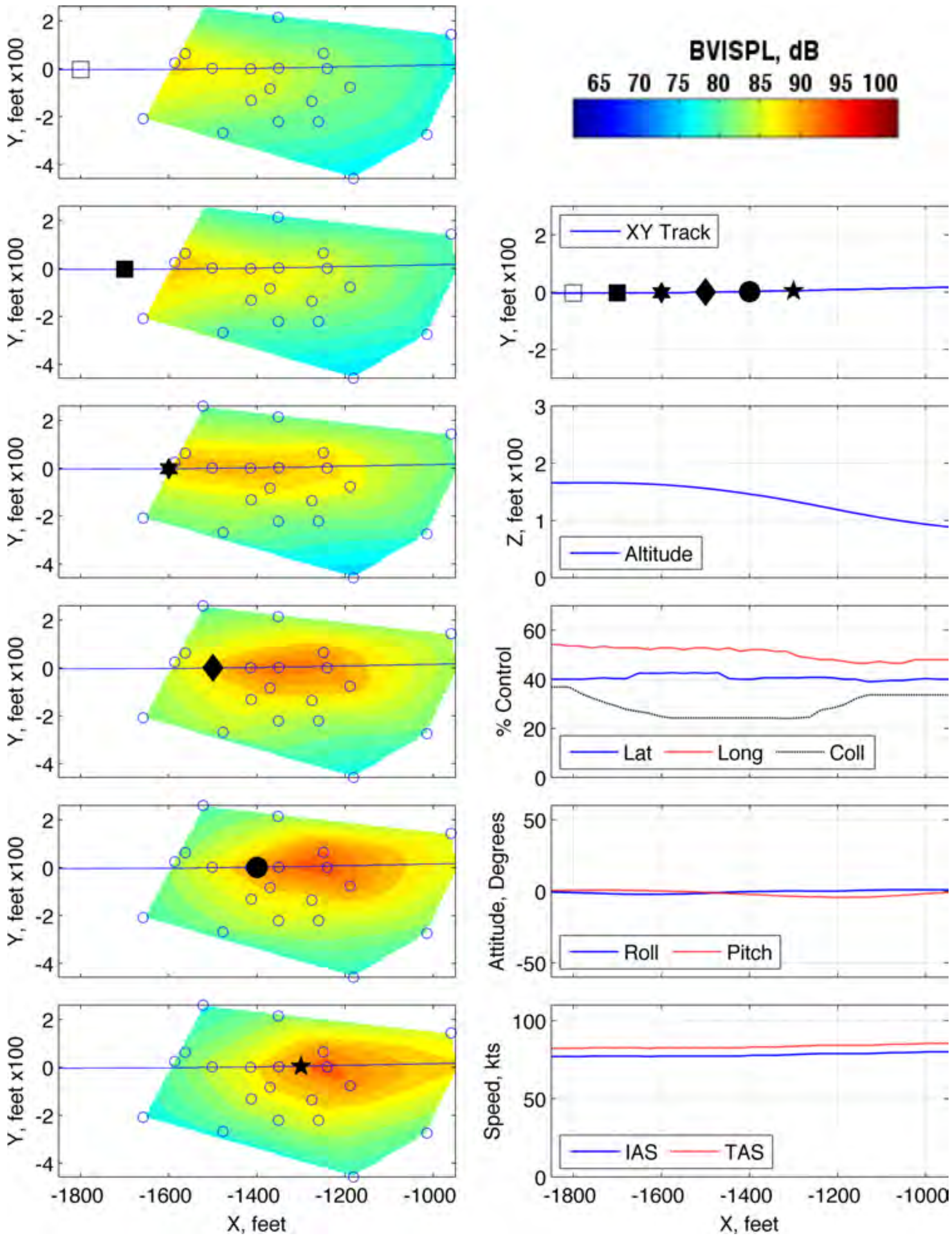

Figure 135: Maneuver condition C10, 80 KIAS, slow collective push-over, run number 287535

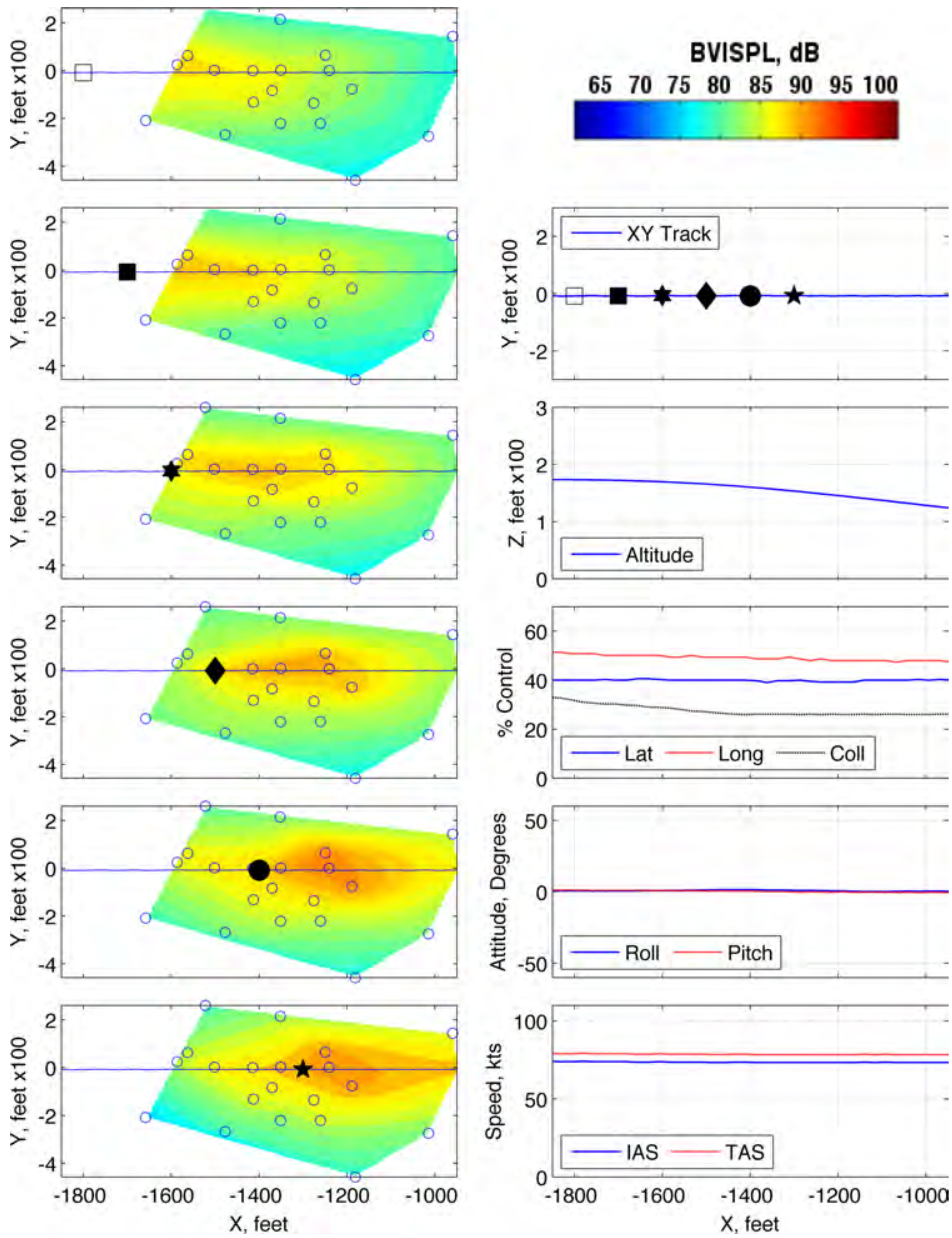

Figure 136: Maneuver condition C10, 80 KIAS, slow collective push-over, run number 287536

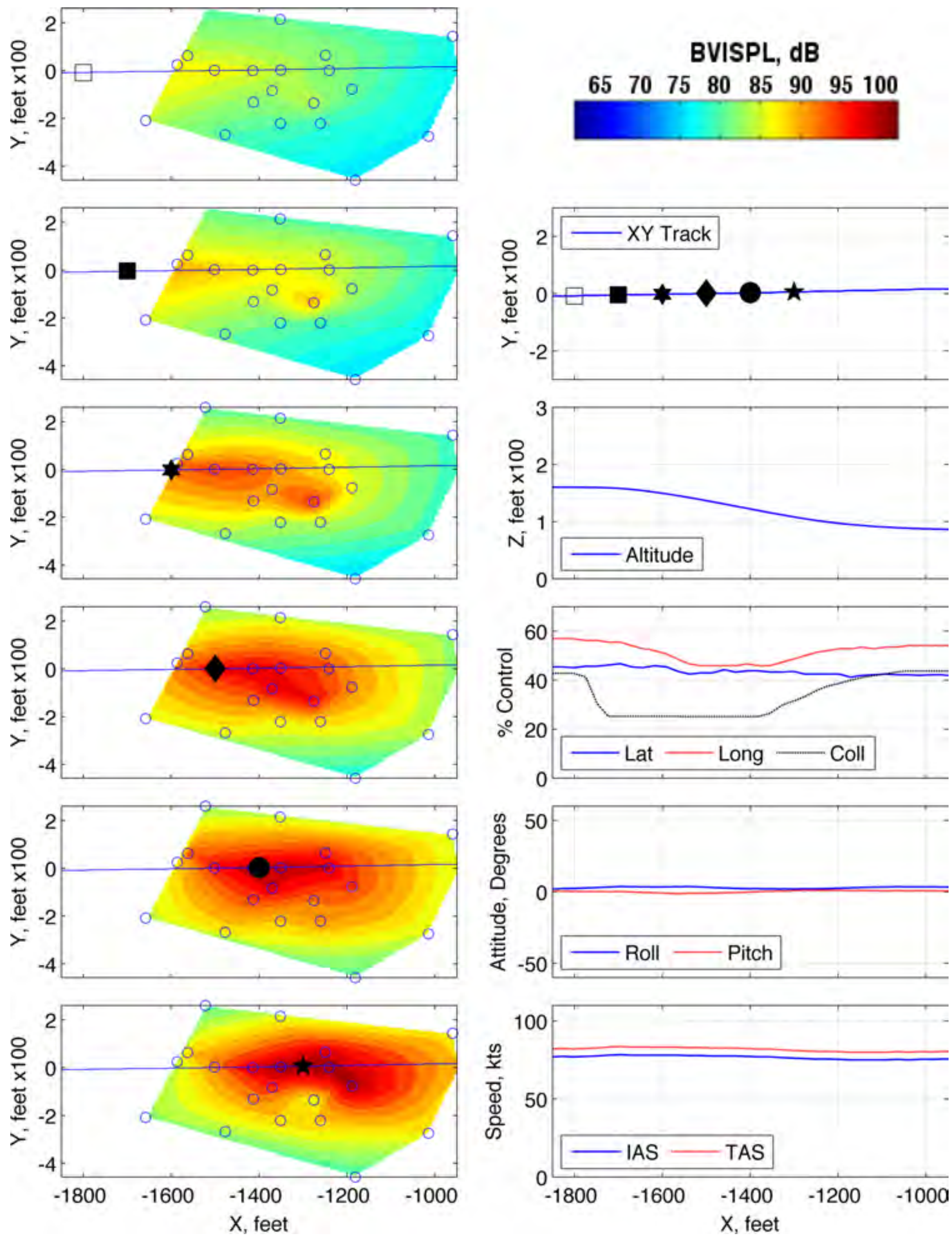

Figure 137: Maneuver condition C12, 80 KIAS, fast collective push-over, run number 282429

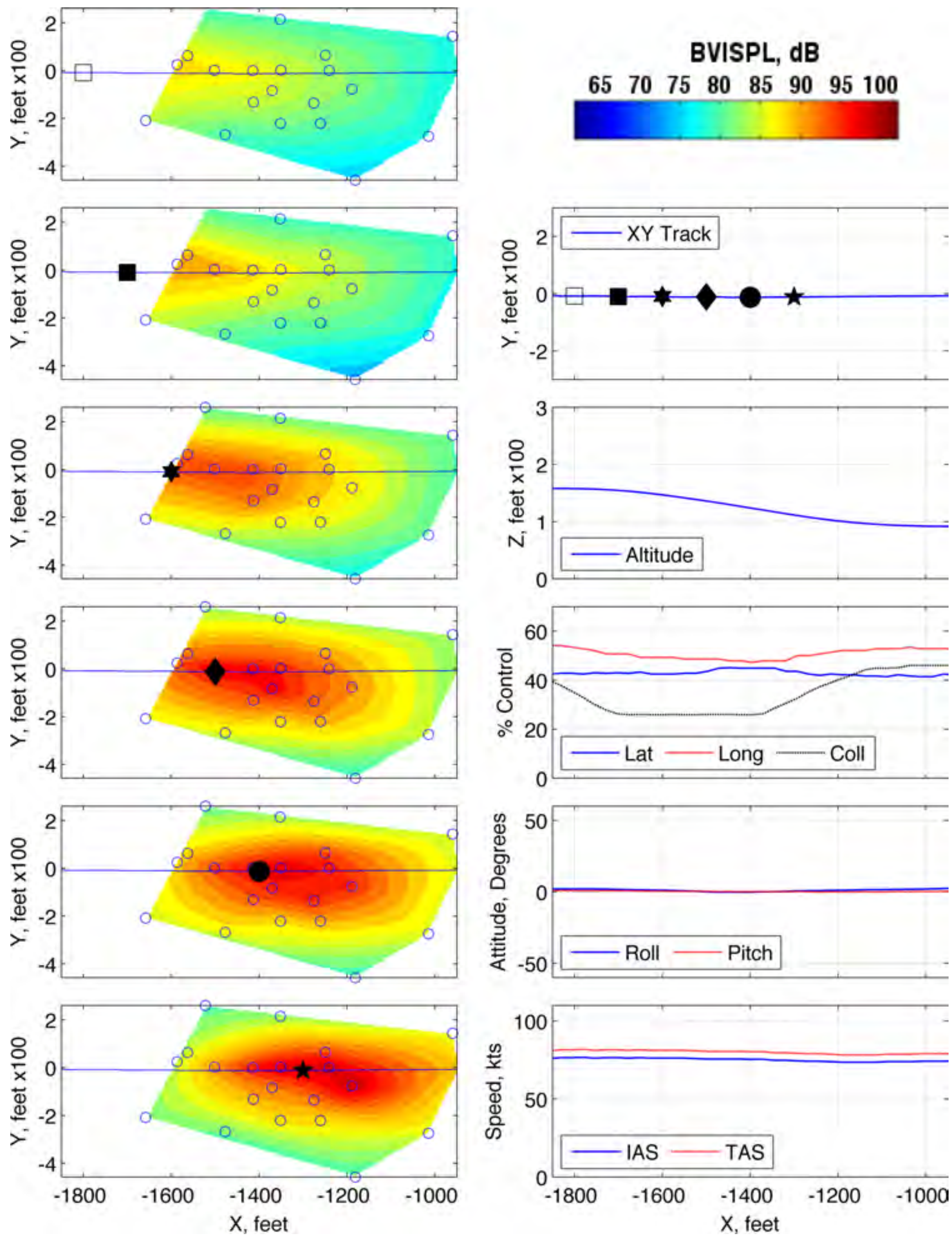

Figure 138: Maneuver condition C12, 80 KIAS, slow collective push-over, run number 282430

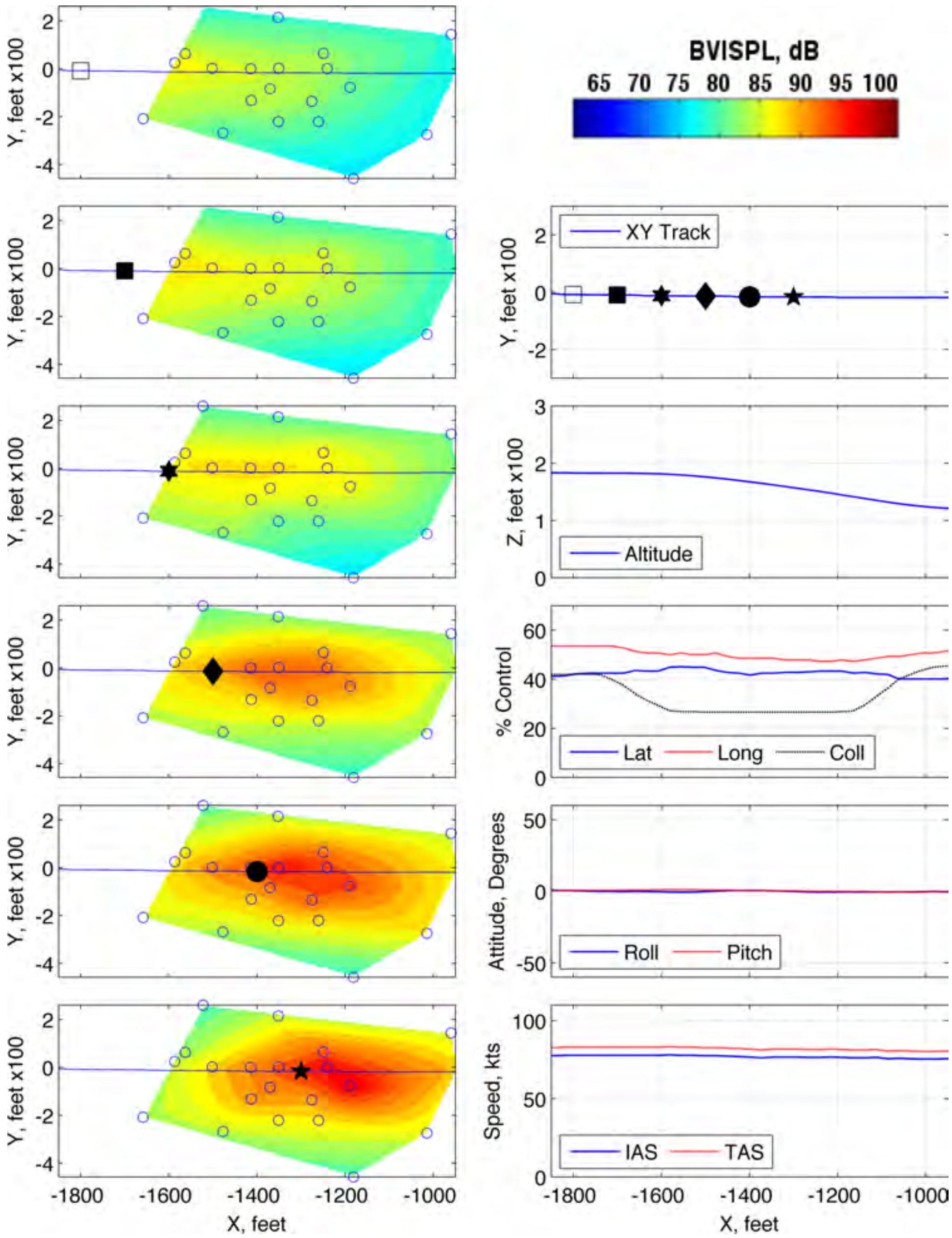

Figure 139: Maneuver condition C12, 80 KIAS, slow collective push-over, run number 282431

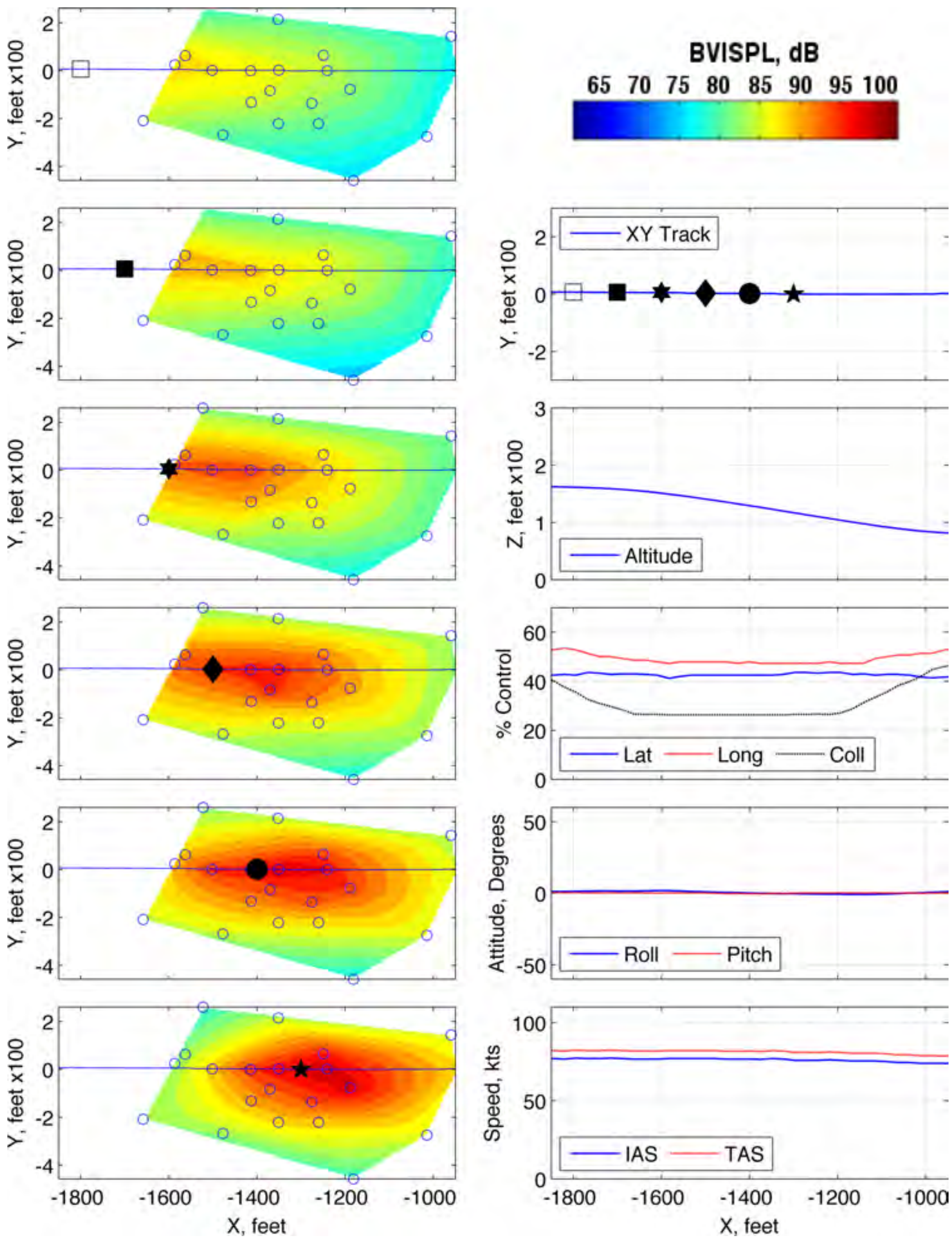

Figure 140: Maneuver condition C12, 80 KIAS, slow collective push-over, run number 282432

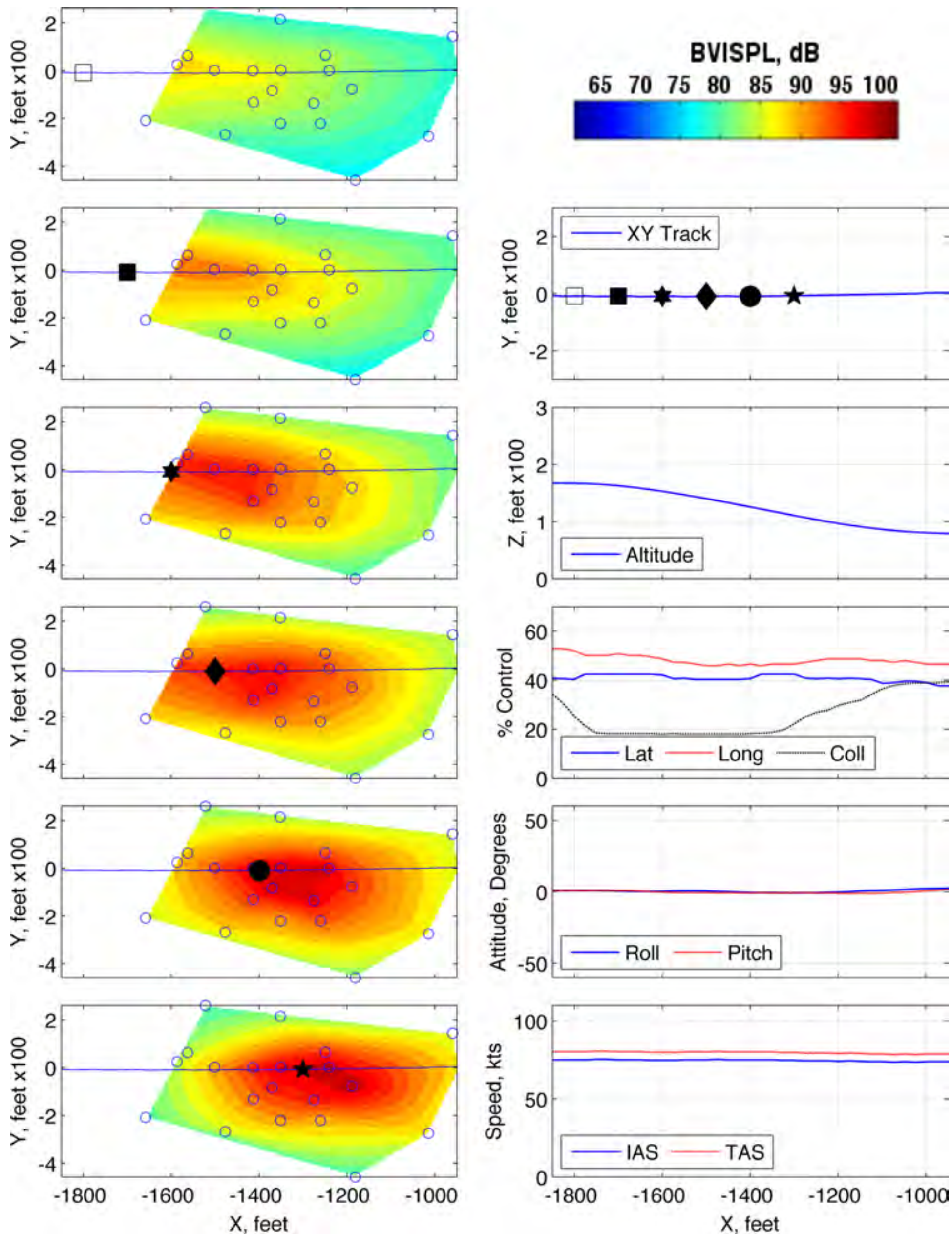

Figure 141: Maneuver condition C12, 80 KIAS, slow collective push-over, run number 287537

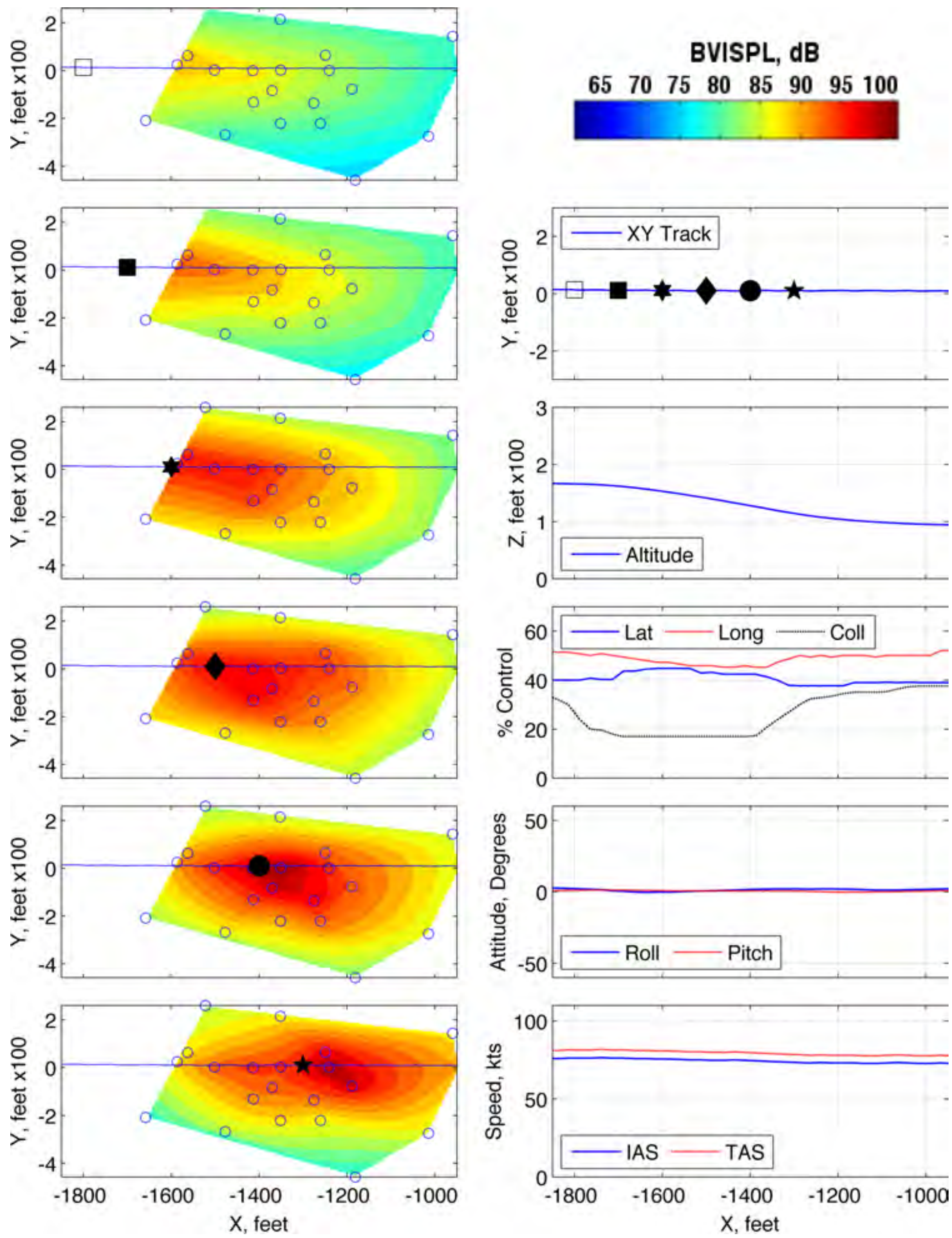

Figure 142: Maneuver condition C12, 80 KIAS, slow collective push-over, run number 287538

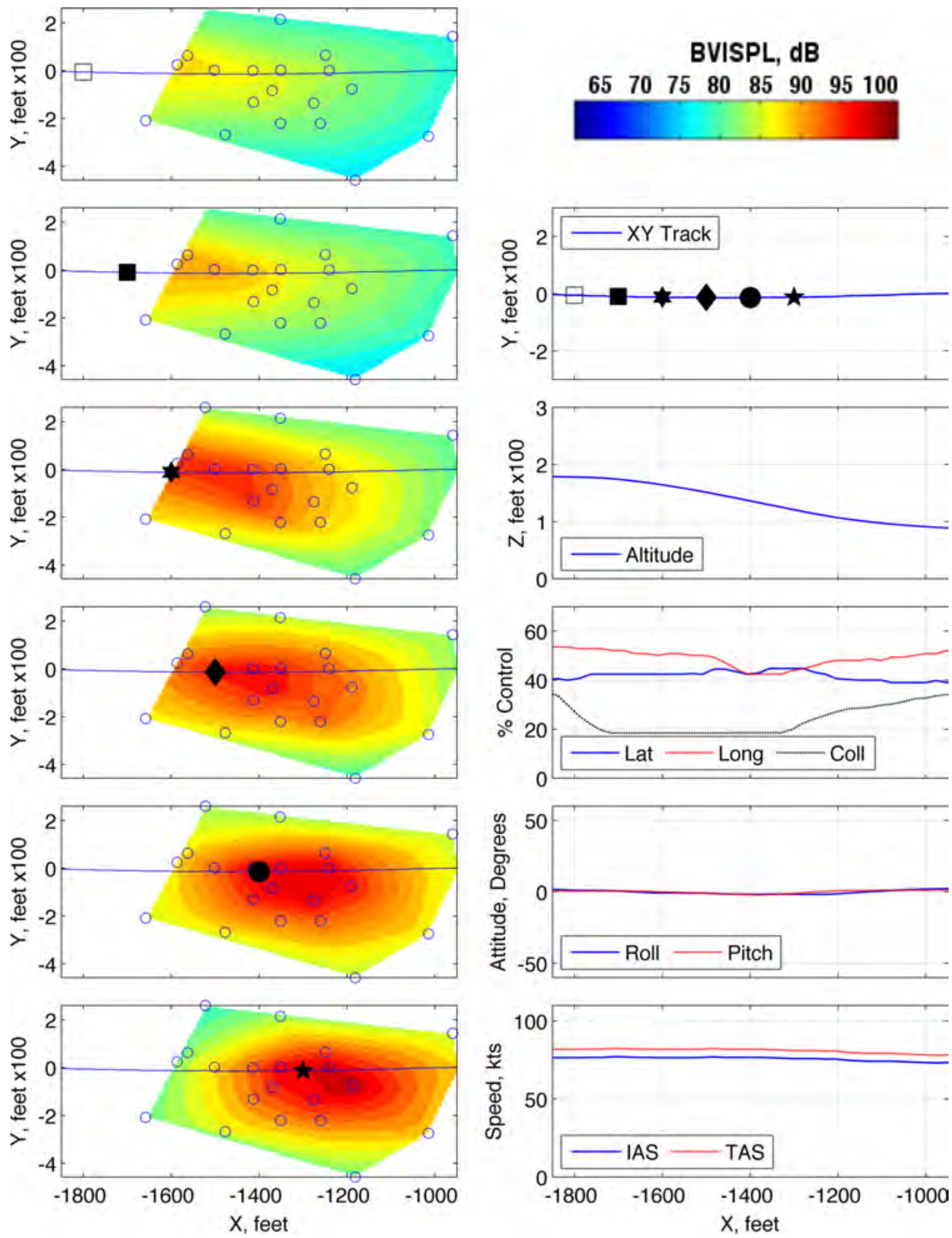

Figure 143: Maneuver condition C12, 80 KIAS, slow collective push-over, run number 287539

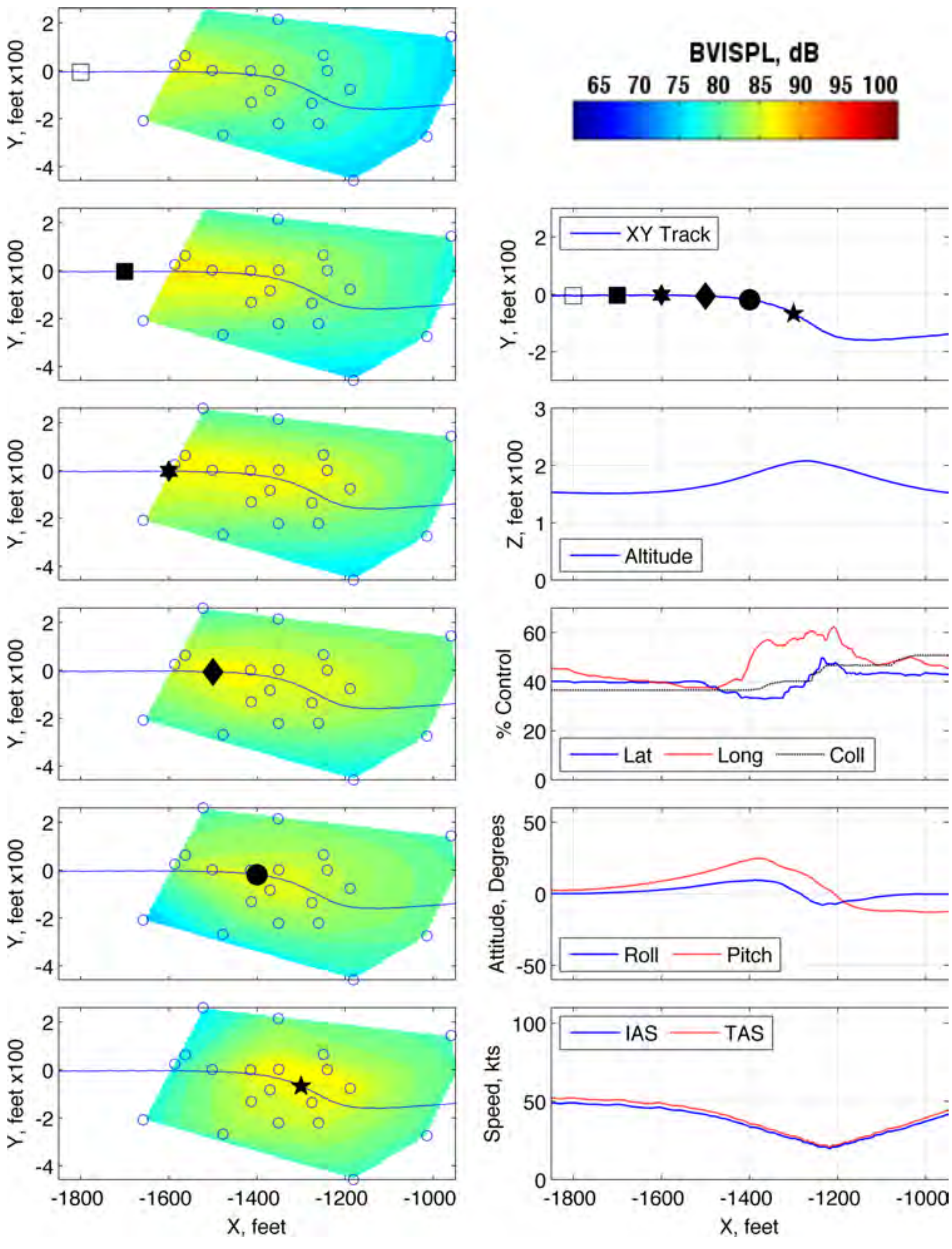

Figure 144: Maneuver condition D1, 60 KIAS, level, slow cyclic pitch up, run number 282439

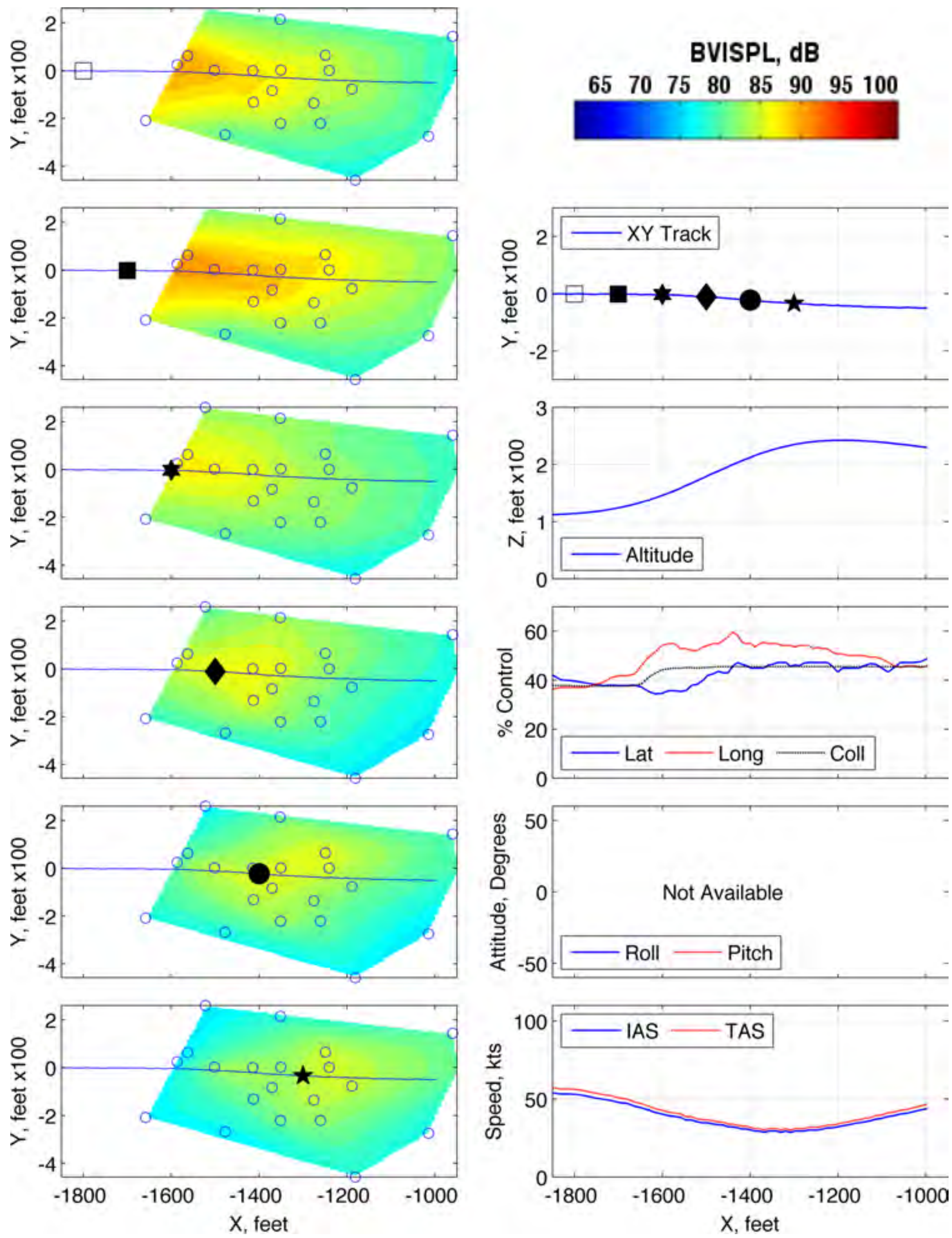

Figure 145: Maneuver condition D3, 60 KIAS, level, fast cyclic pitch up, run number 280363

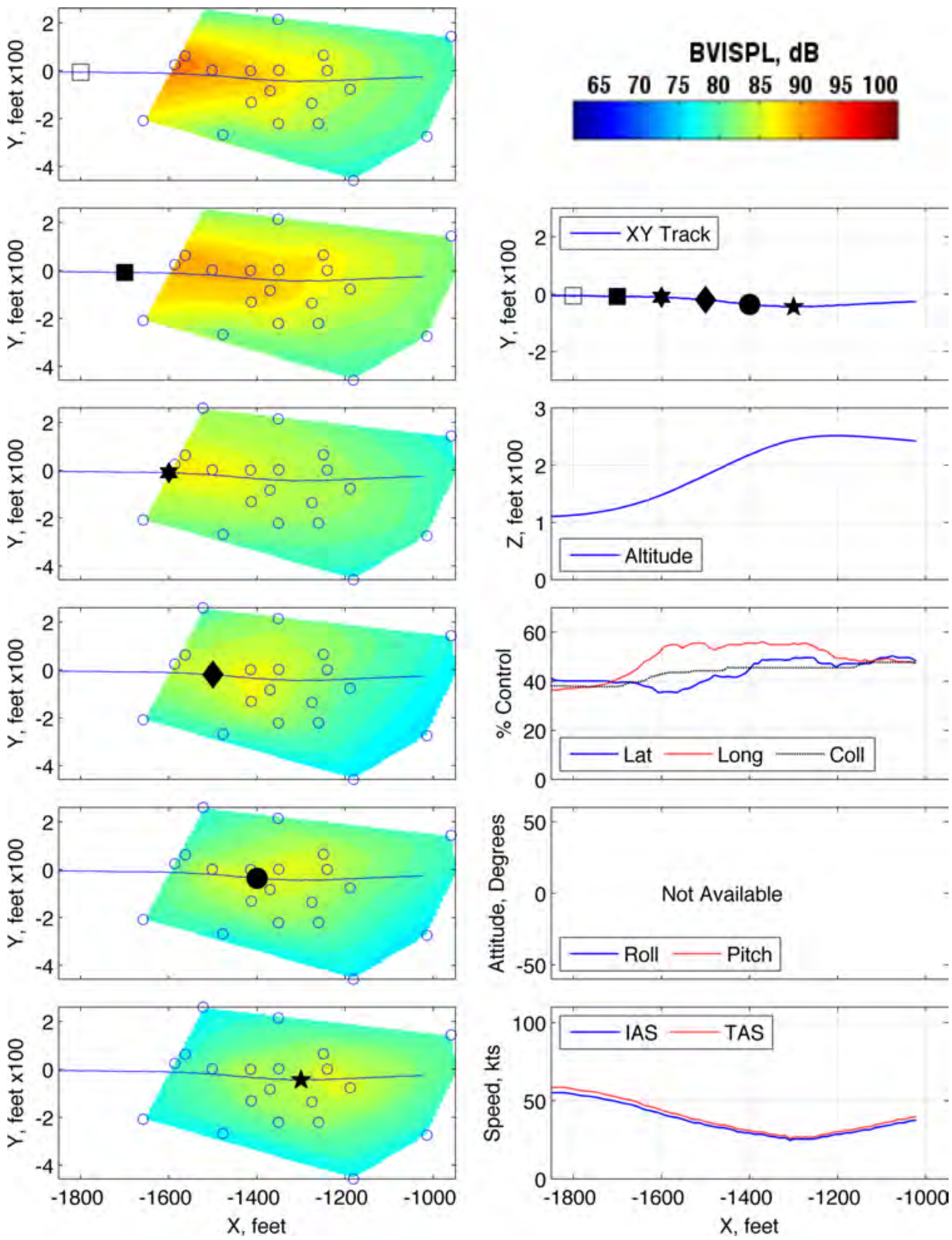

Figure 146: Maneuver condition D3, 60 KIAS, level, fast cyclic pitch up, run number 280364

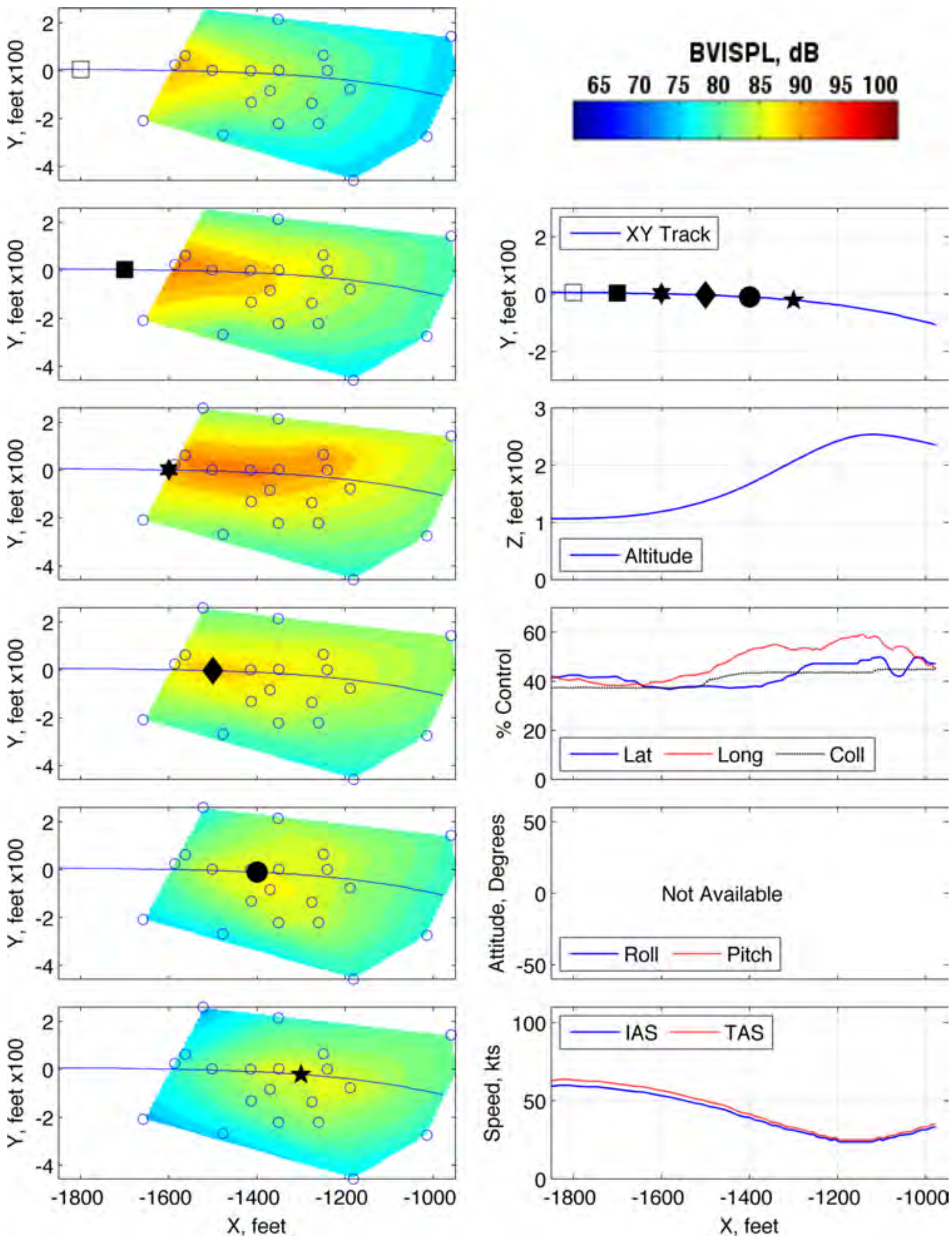

Figure 147: Maneuver condition D3, 60 KIAS, level, fast cyclic pitch up, run number 280365

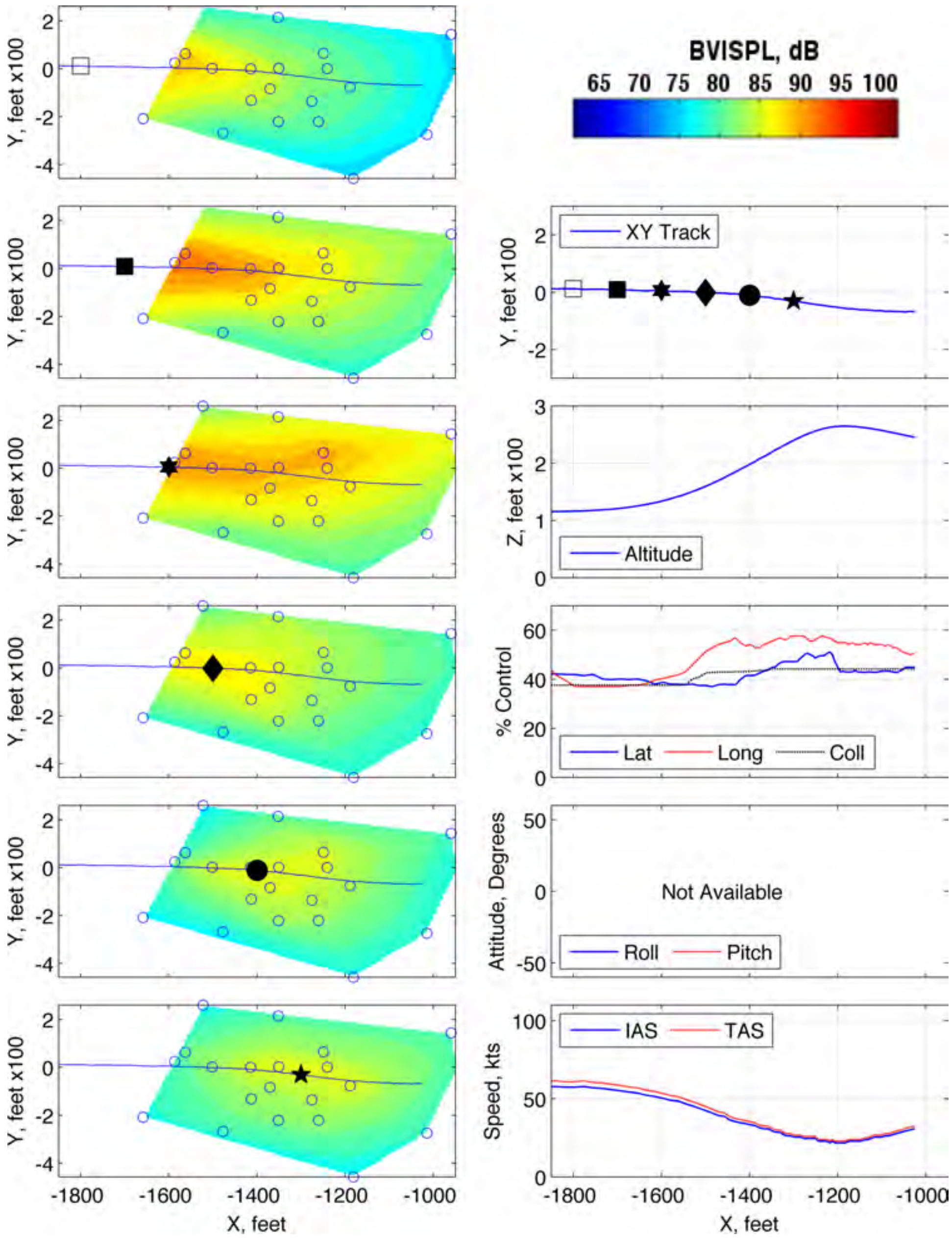

Figure 148: Maneuver condition D3, 60 KIAS, level, fast cyclic pitch up, run number 280366

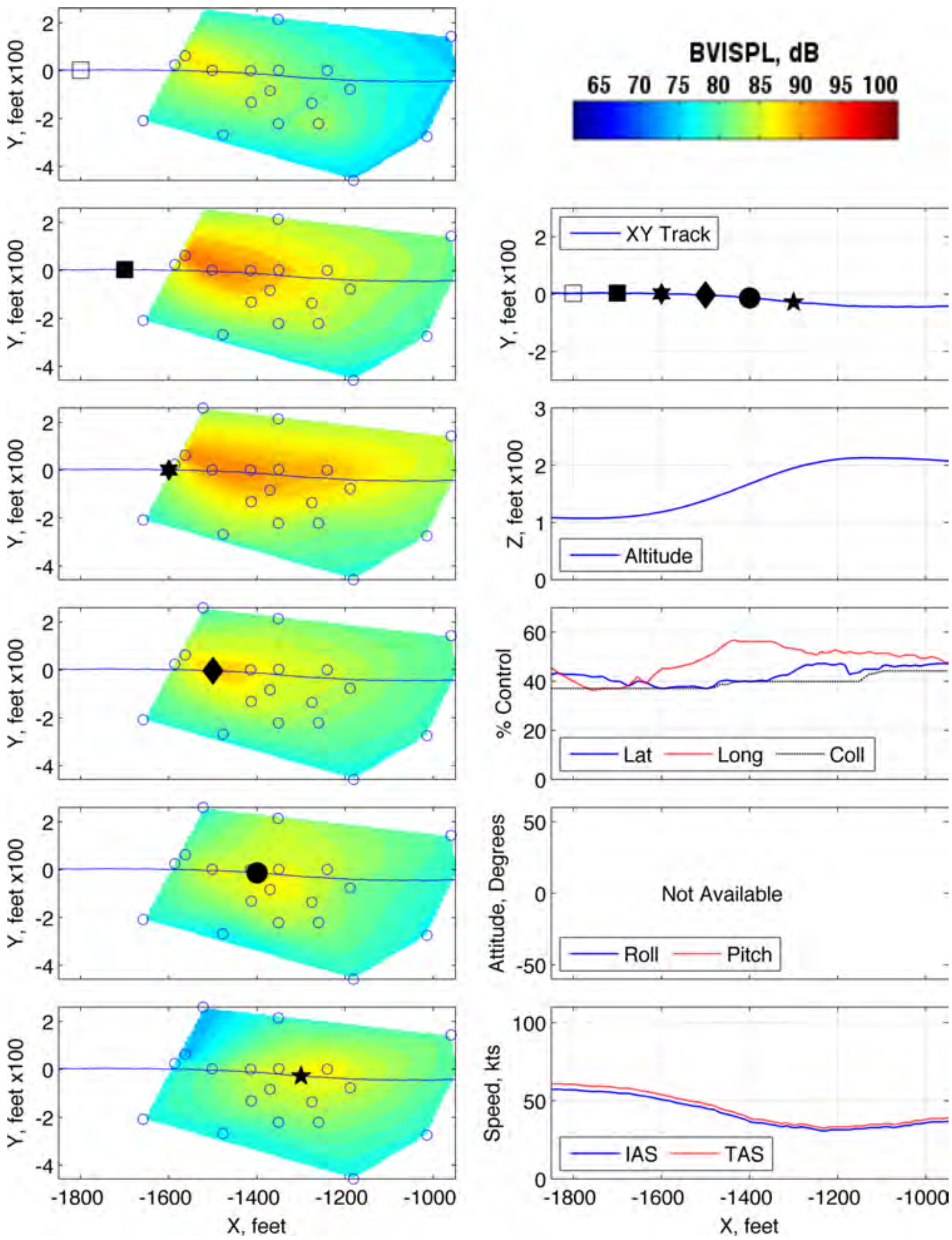

Figure 149: Maneuver condition D3, 60 KIAS, level, fast cyclic pitch up, run number 280367

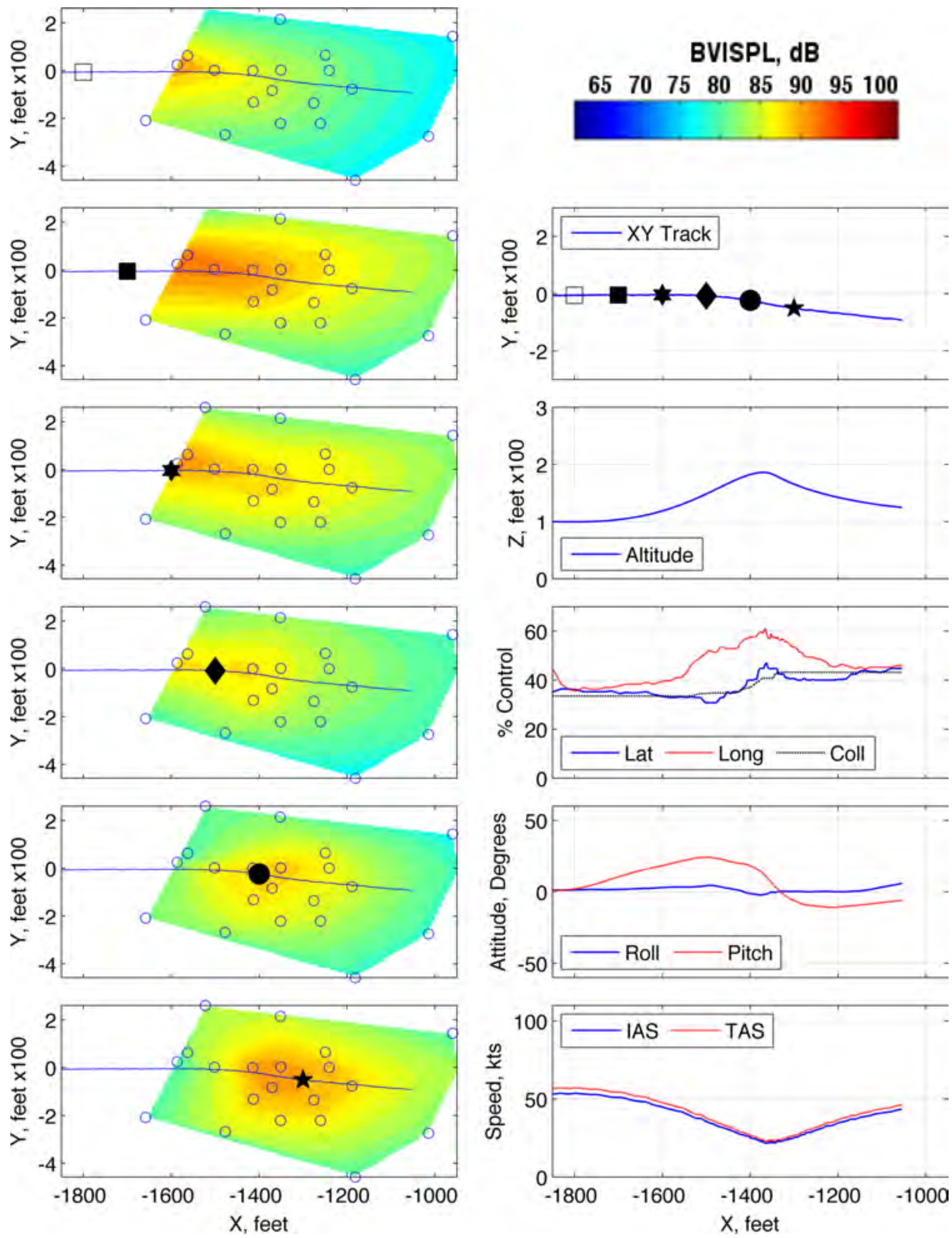

Figure 150: Maneuver condition D3, 60 KIAS, level, fast cyclic pitch up, run number 287531

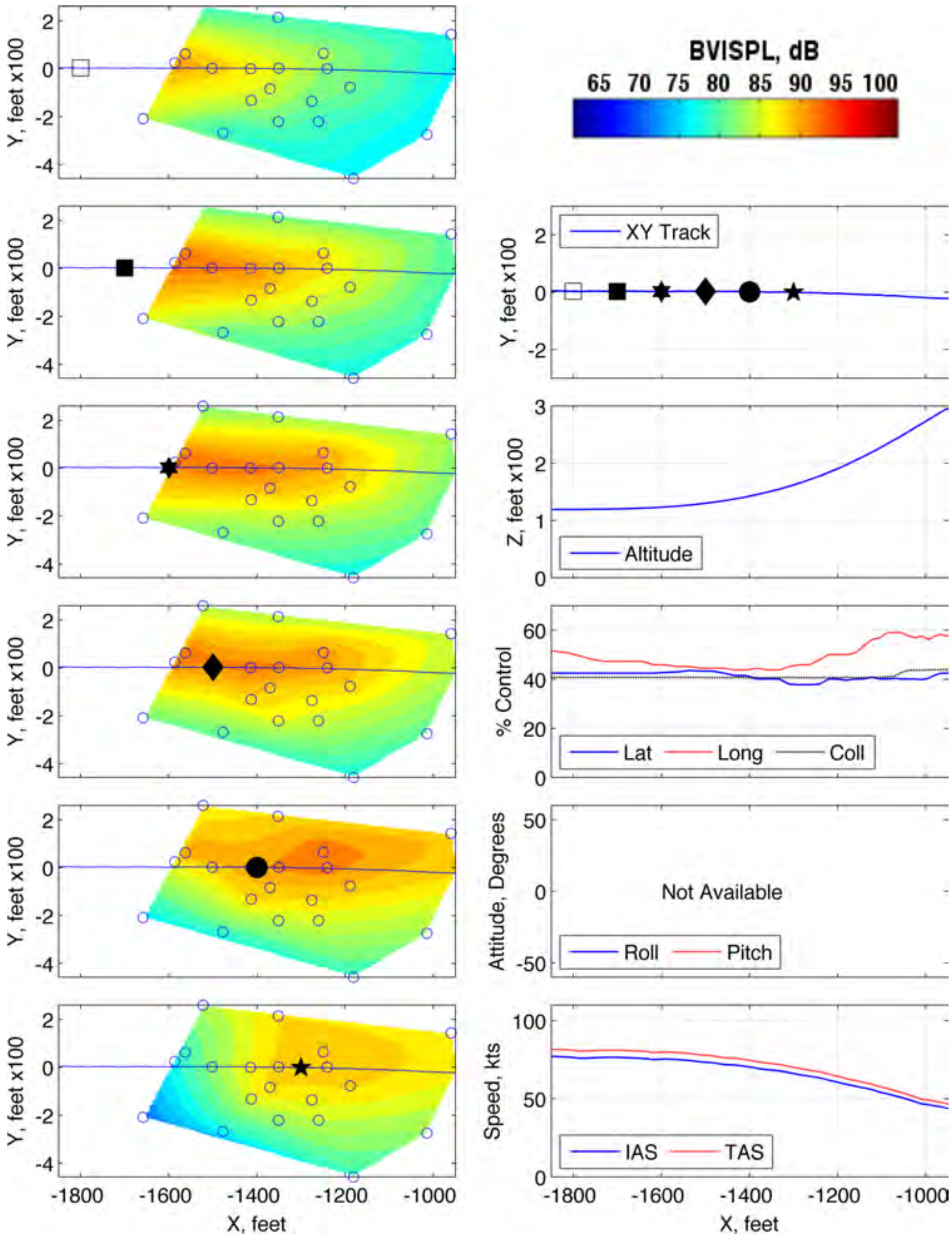

Figure 151: Maneuver condition D4, 80 KIAS, level, slow cyclic pitch up, run number 280356

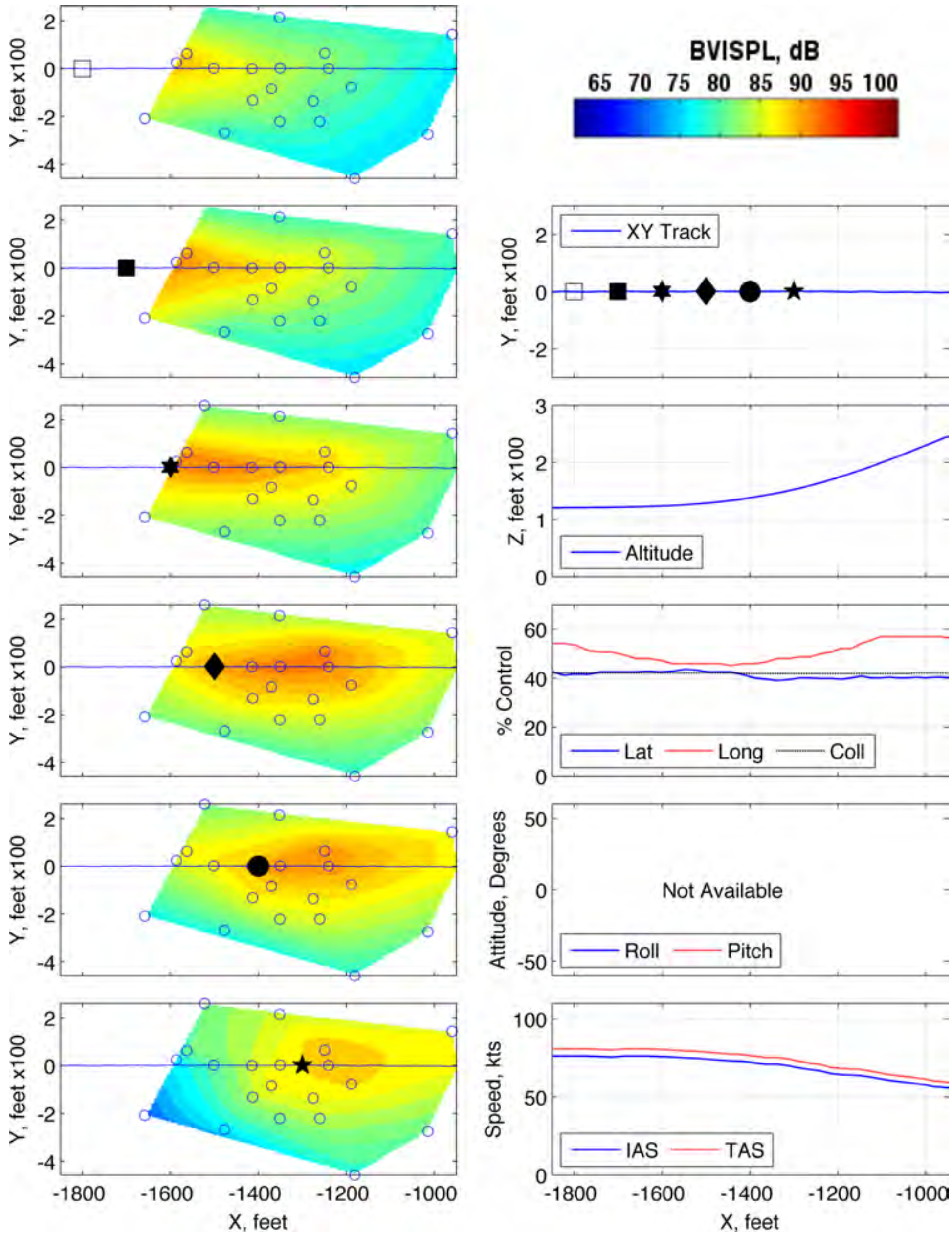

Figure 152: Maneuver condition D4, 80 KIAS, level, slow cyclic pitch up, run number 280357

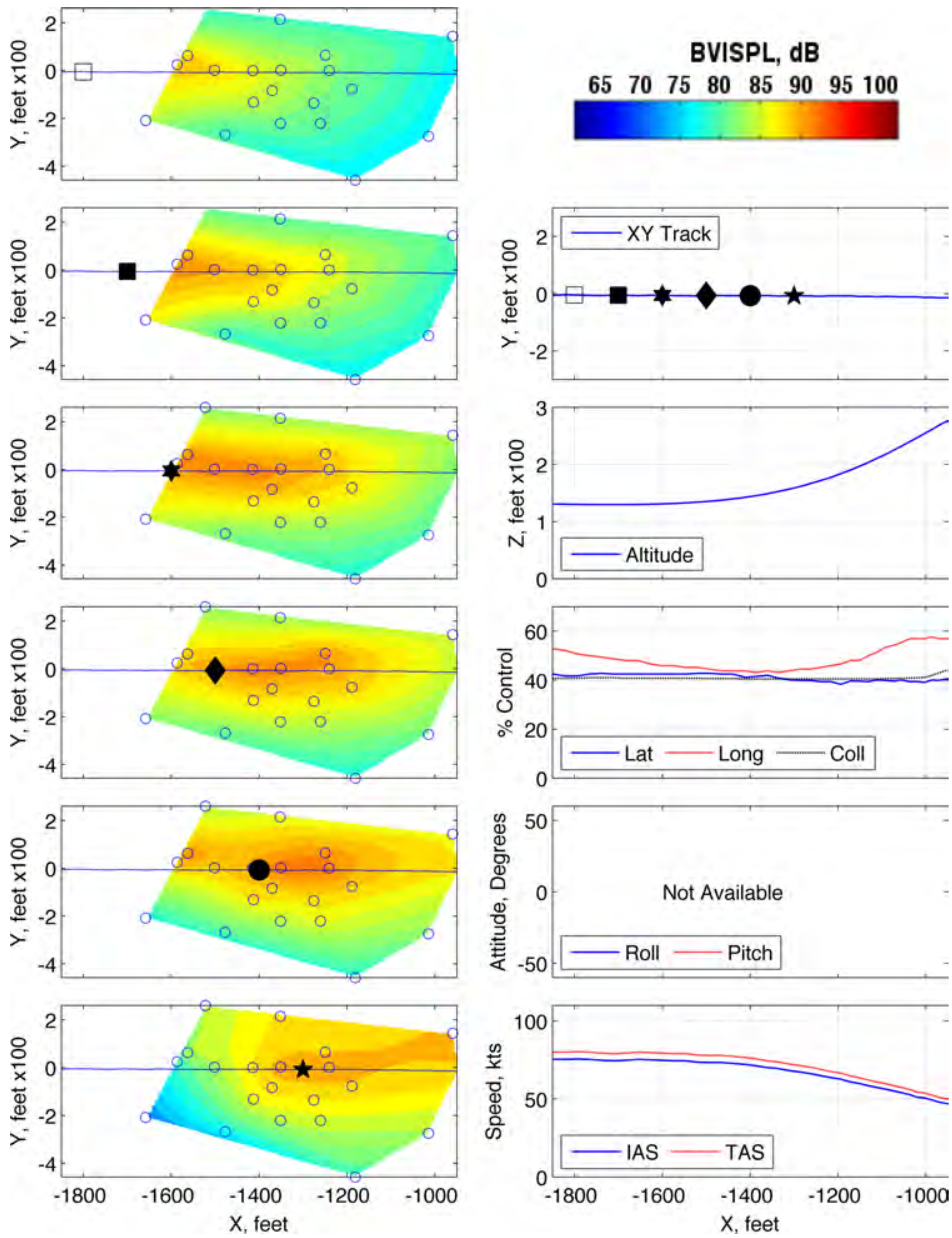

Figure 153: Maneuver condition D4, 80 KIAS, level, slow cyclic pitch up, run number 280358

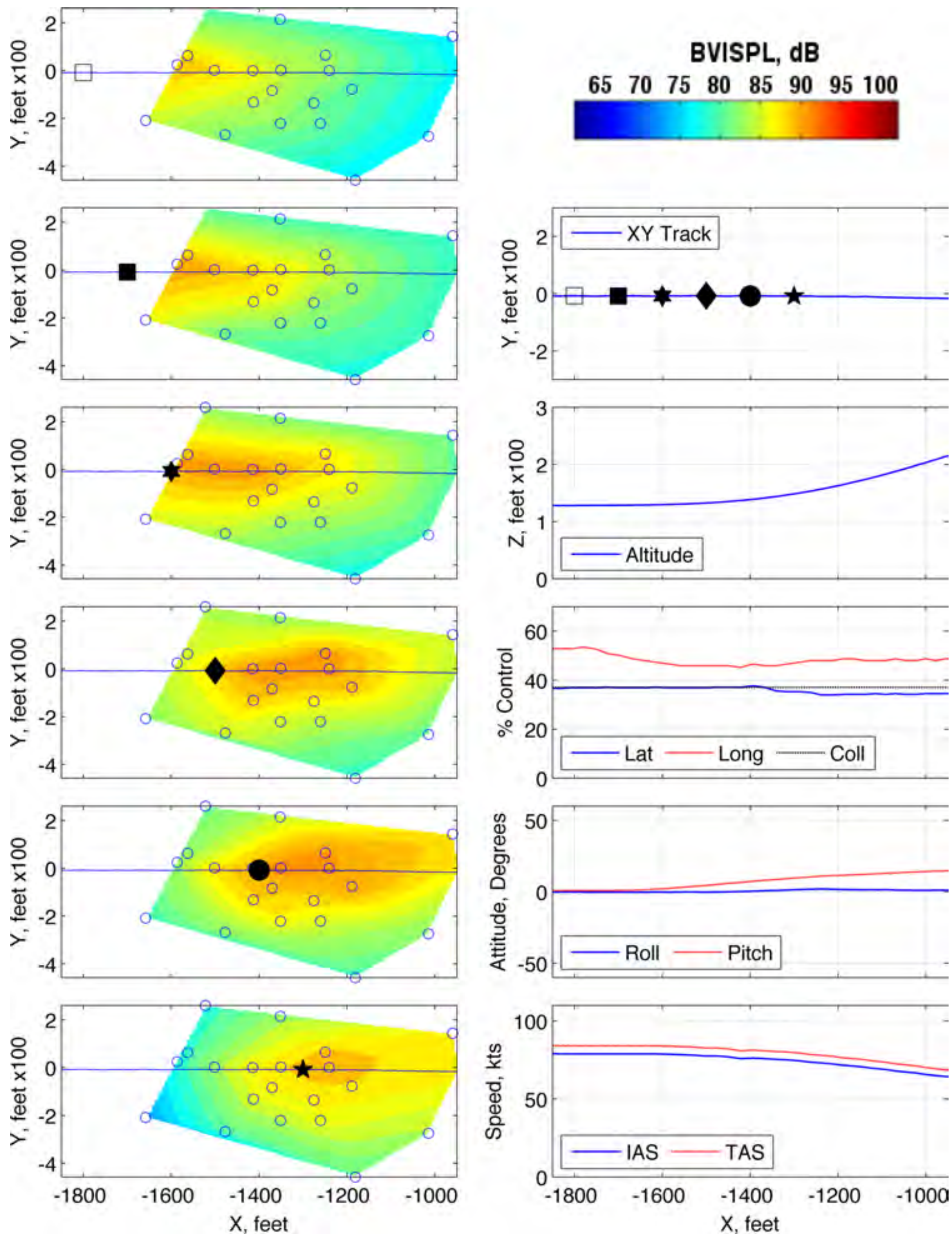

Figure 154: Maneuver condition D5, 80 KIAS, level, medium cyclic pitch up, run number 285475

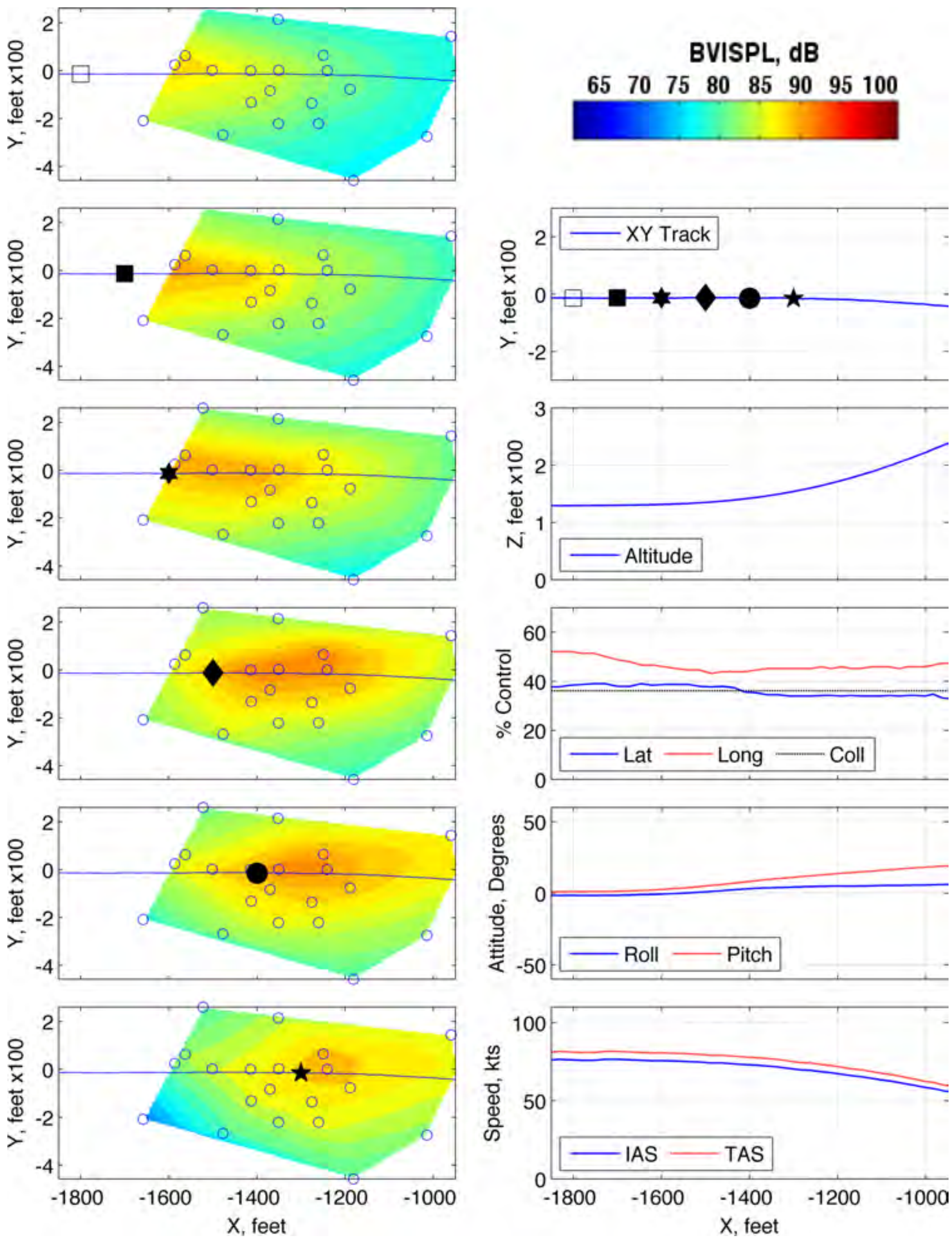

Figure 155: Maneuver condition D5, 80 KIAS, level, medium cyclic pitch up, run number 285476

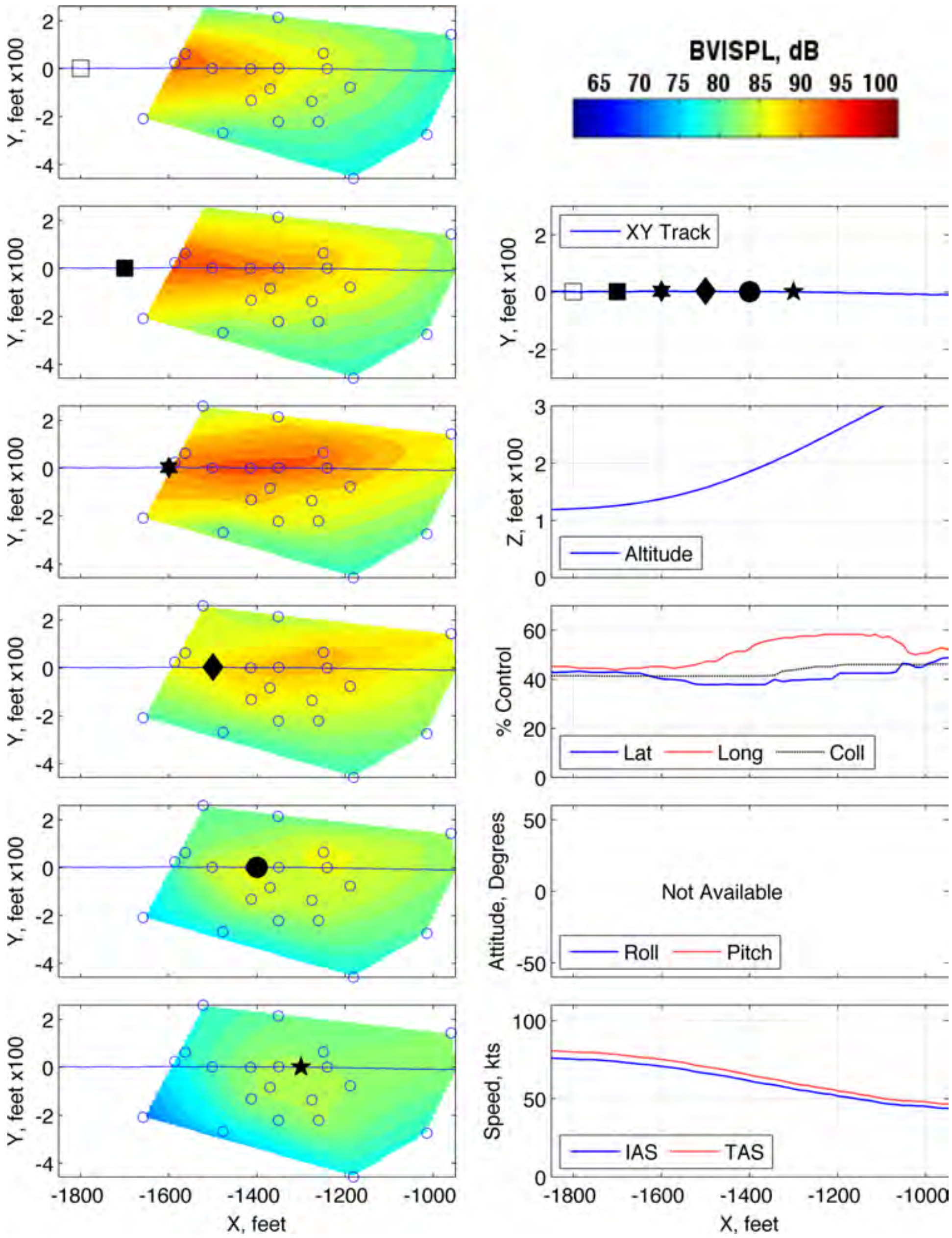

Figure 156: Maneuver condition D6, 80 KIAS, level, fast cyclic pitch up, run number 280359

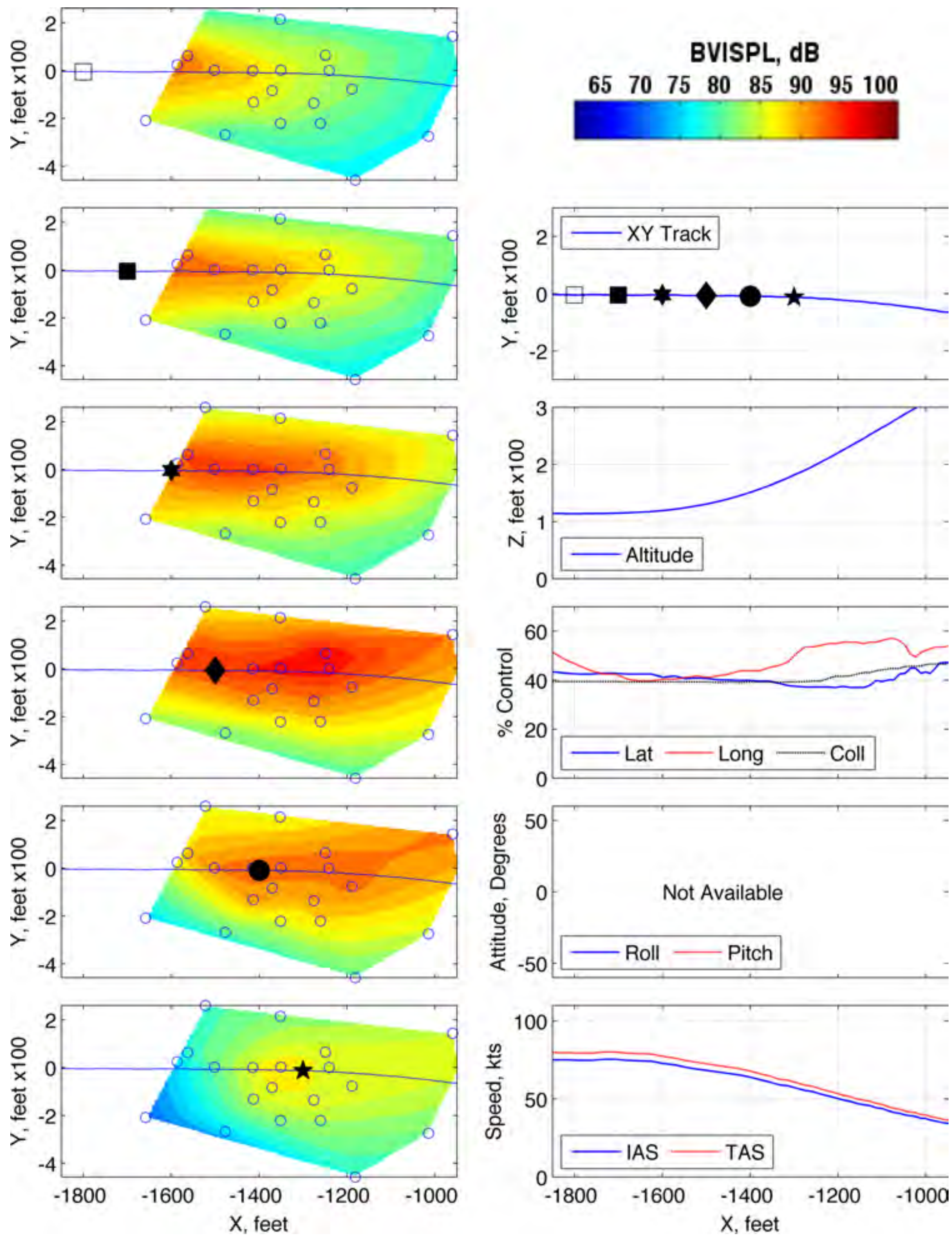

Figure 157: Maneuver condition D6, 80 KIAS, level, fast cyclic pitch up, run number 280360

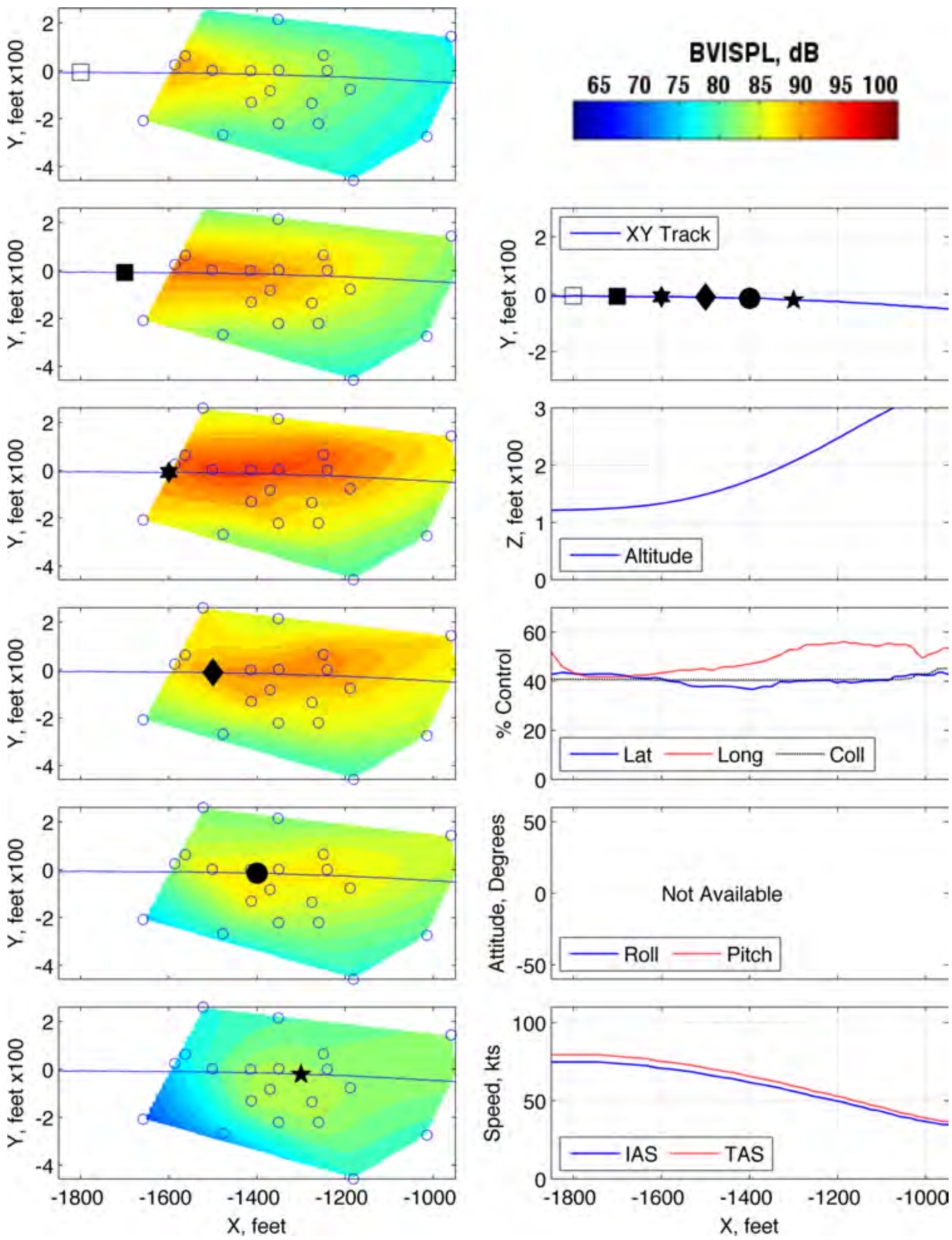

Figure 158: Maneuver condition D6, 80 KIAS, level, fast cyclic pitch up, run number 280361

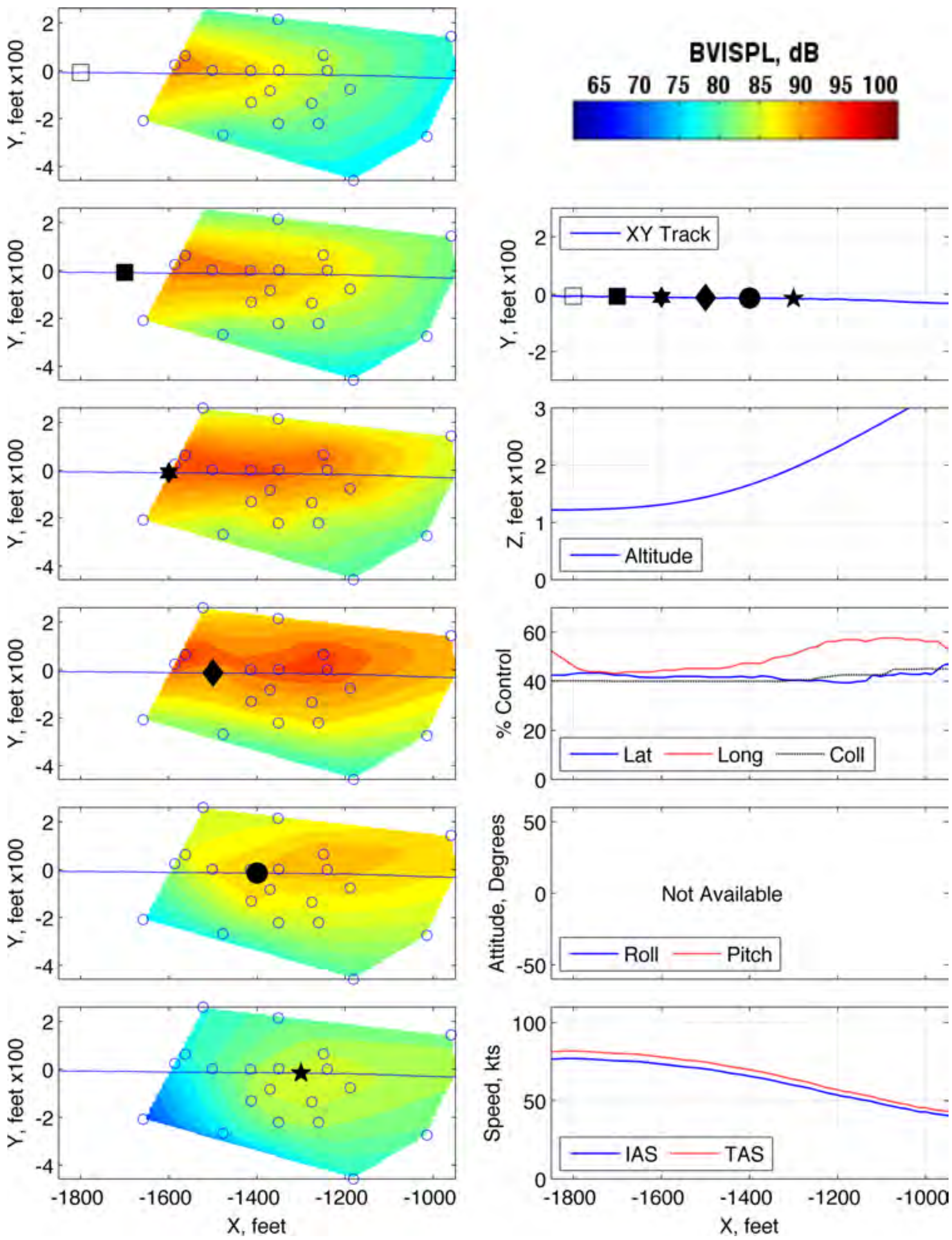

Figure 159: Maneuver condition D6, 80 KIAS, level, fast cyclic pitch up, run number 280362

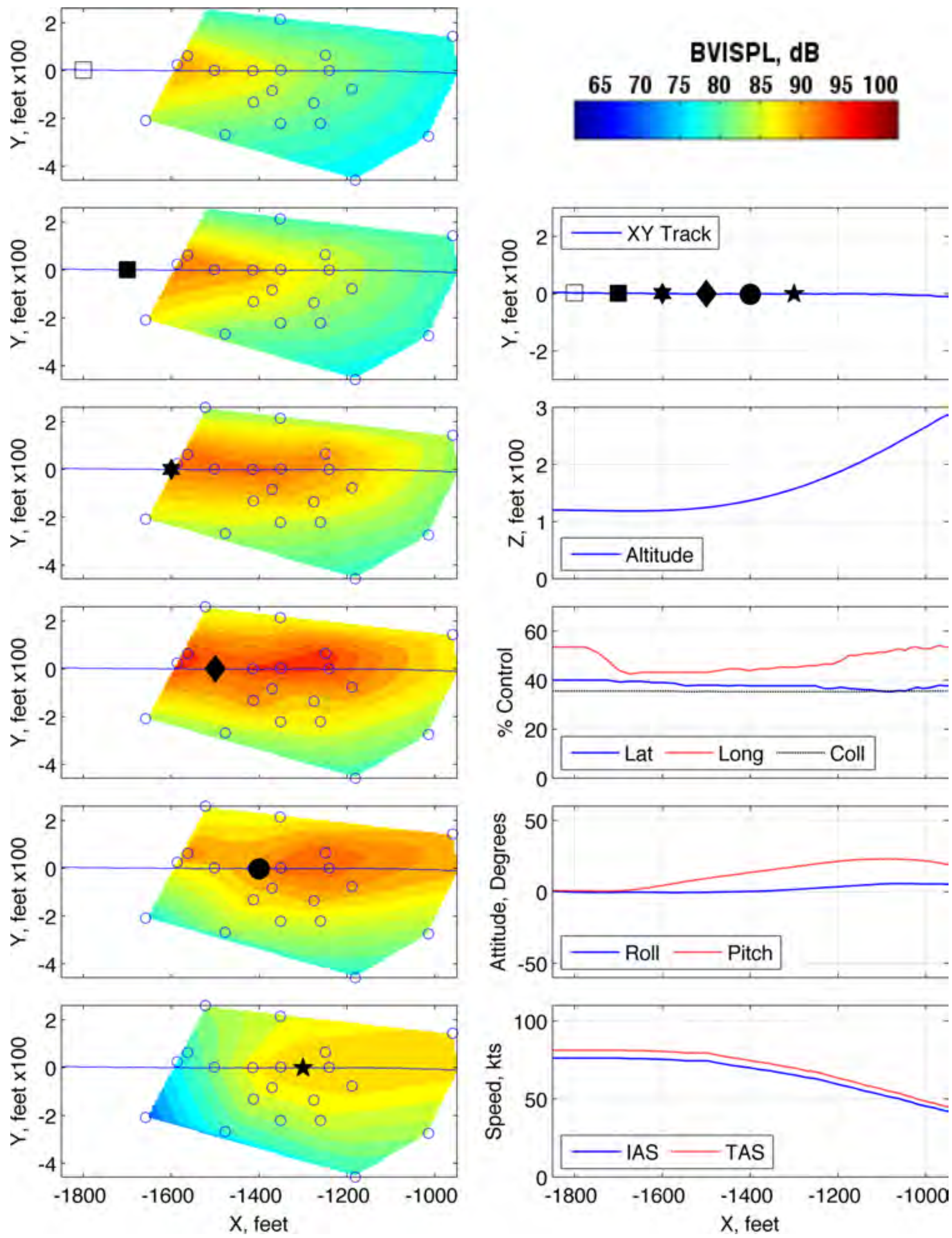

Figure 160: Maneuver condition D6, 80 KIAS, level, fast cyclic pitch up, run number 287530

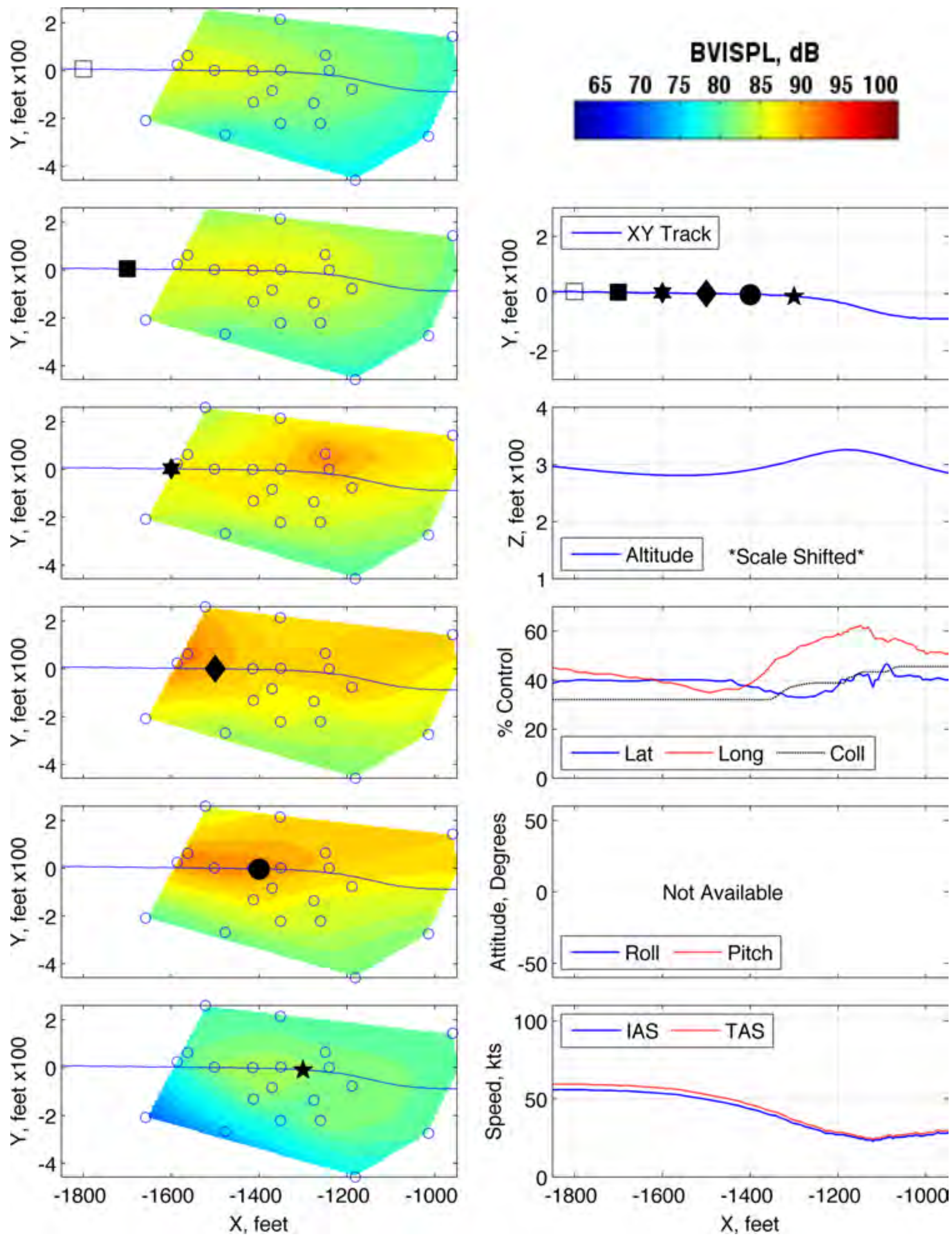

Figure 161: Maneuver condition D7, 60 KIAS, -6° , slow cyclic pitch up, run number 280350

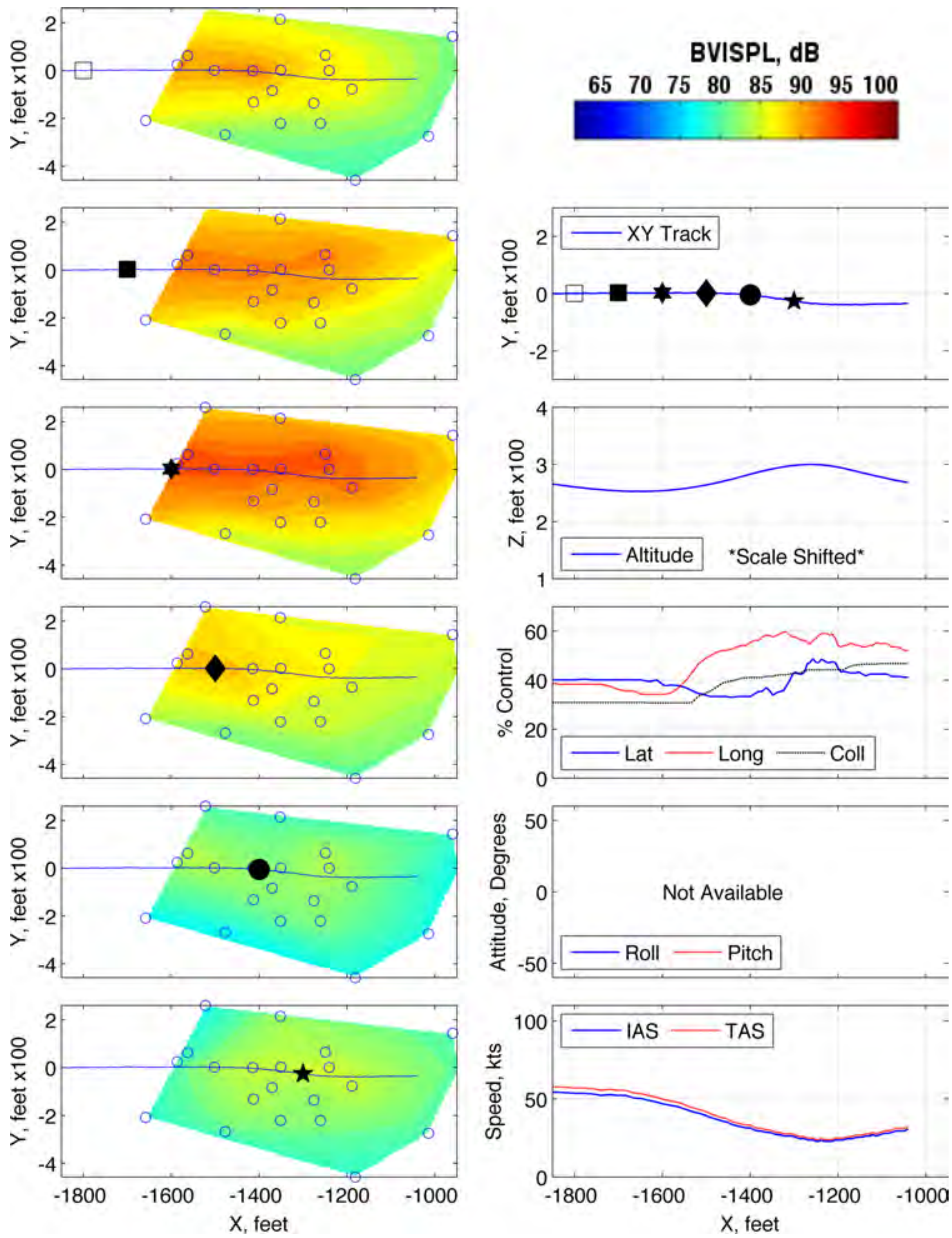

Figure 162: Maneuver condition D7, 60 KIAS, -6° , slow cyclic pitch up, run number 280351

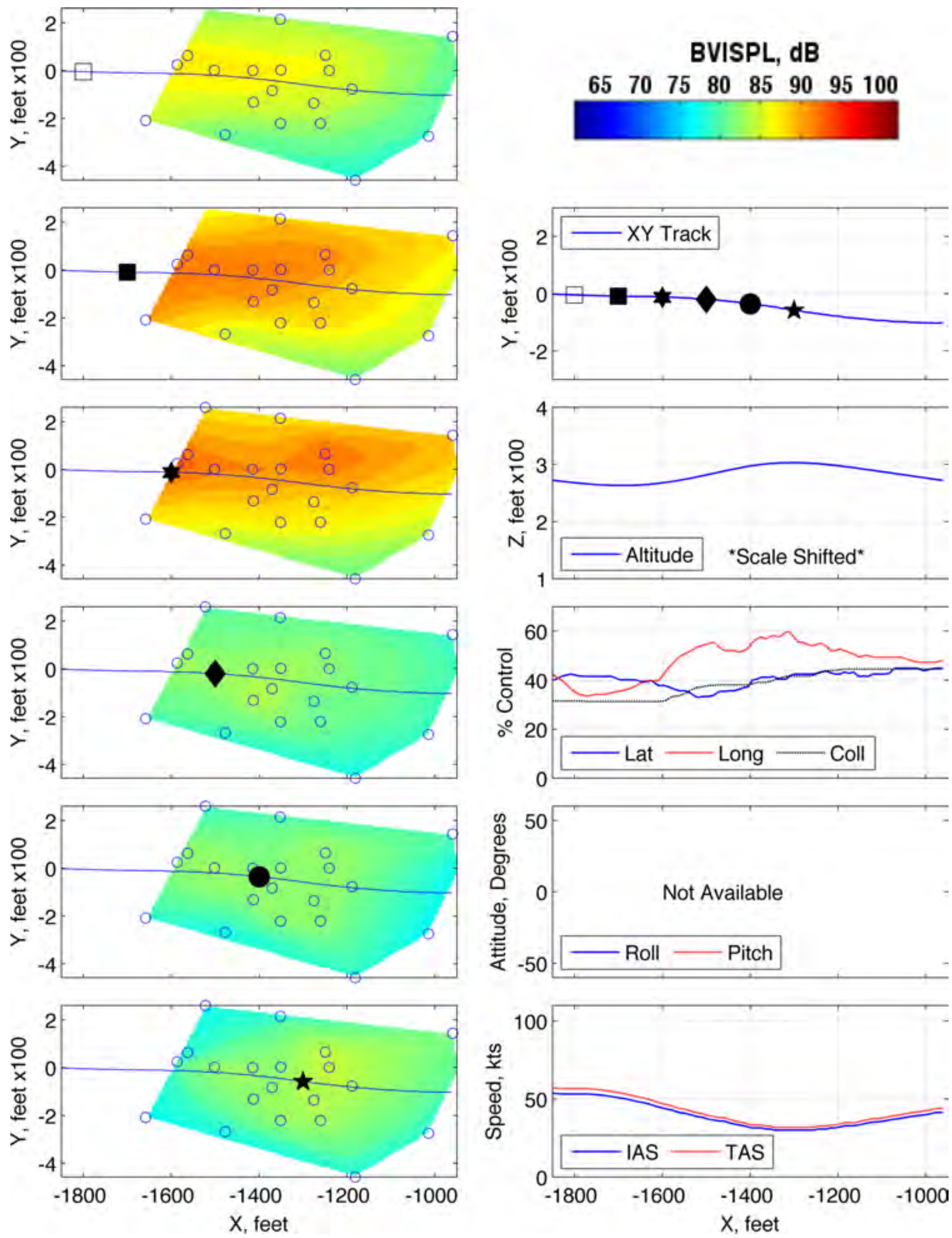

Figure 163: Maneuver condition D9, 60 KIAS, -6° , fast cyclic pitch up, run number 280352

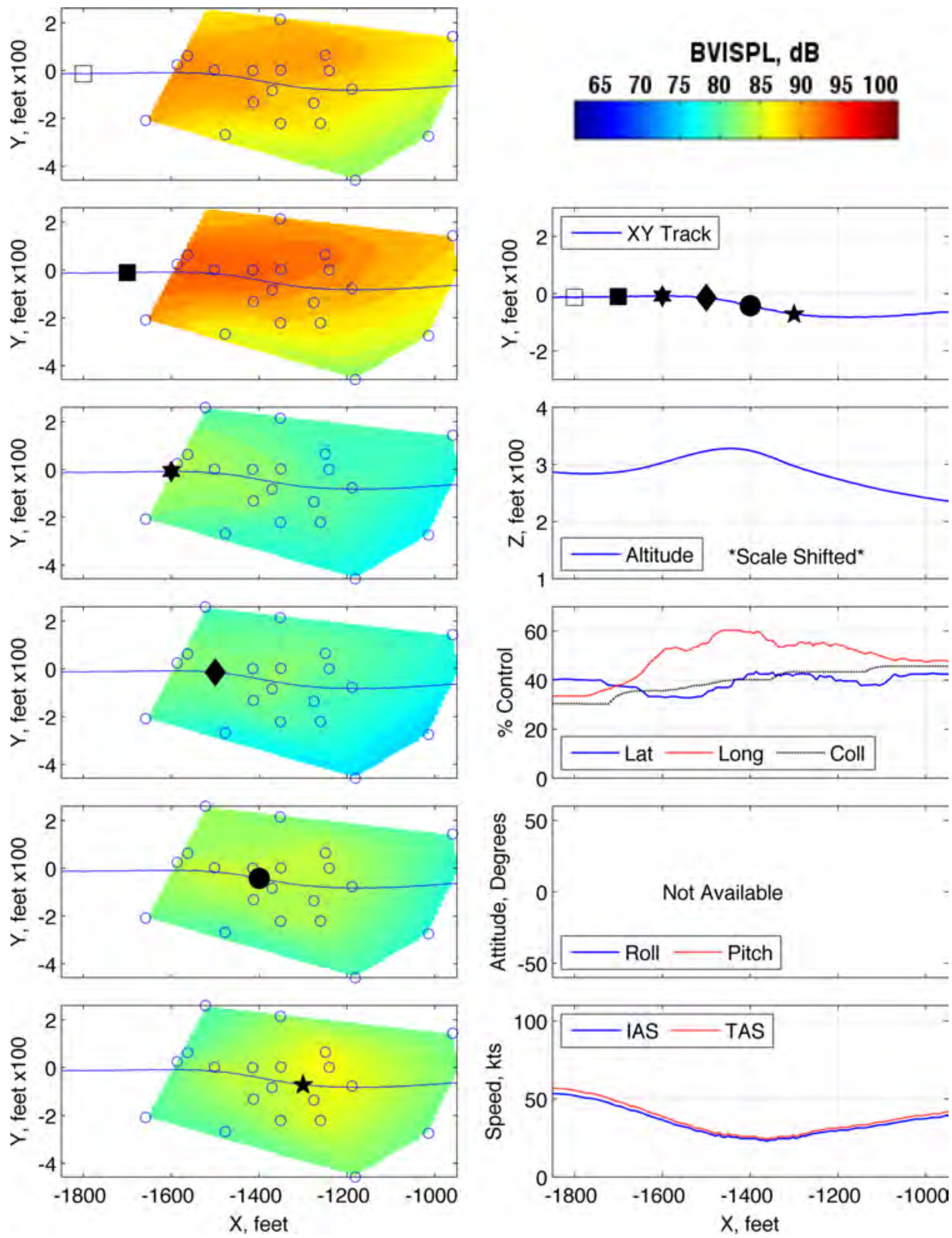

Figure 164: Maneuver condition D9, 60 KIAS, -6° , fast cyclic pitch up, run number 280353

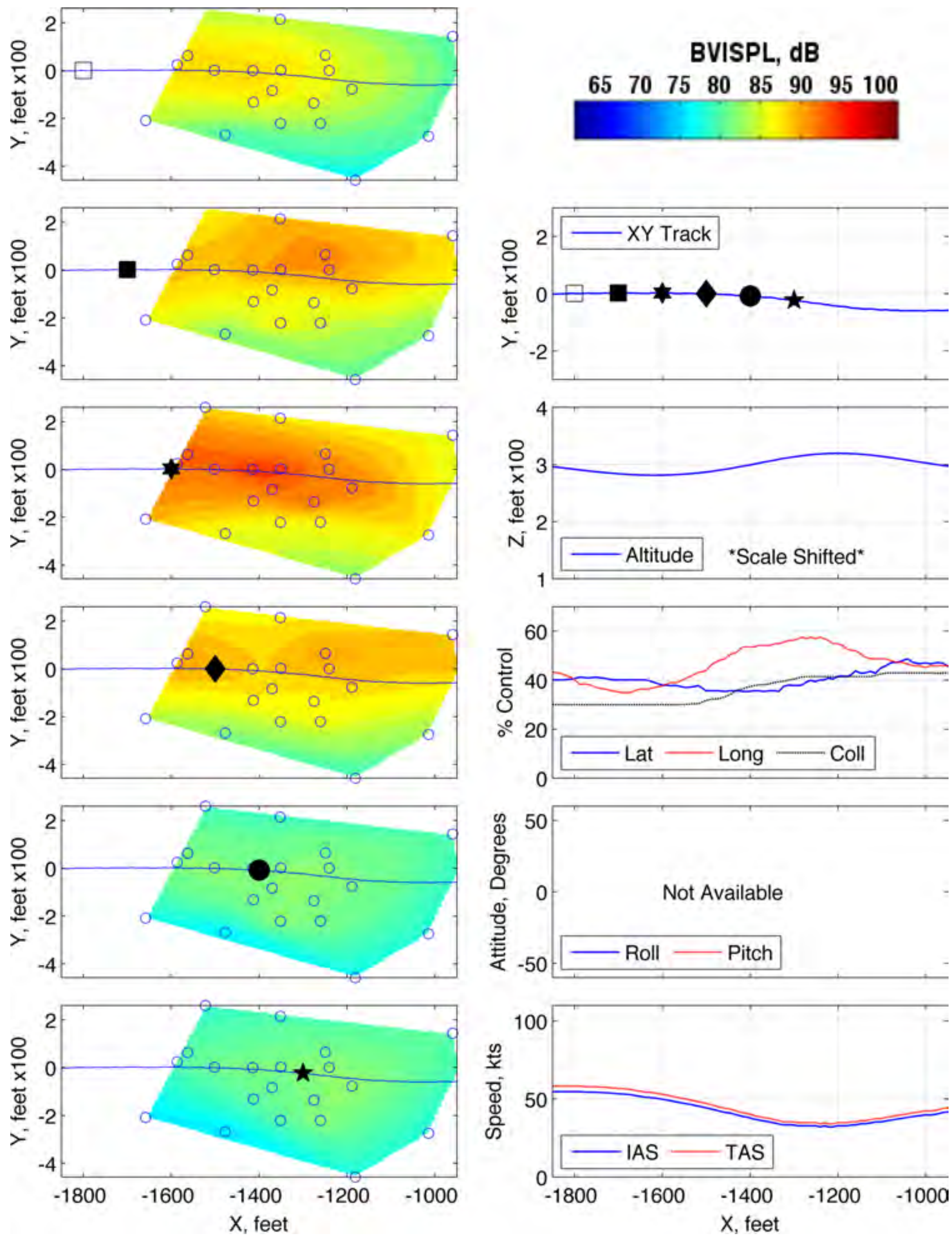

Figure 165: Maneuver condition D9, 60 KIAS, -6° , fast cyclic pitch up, run number 280354

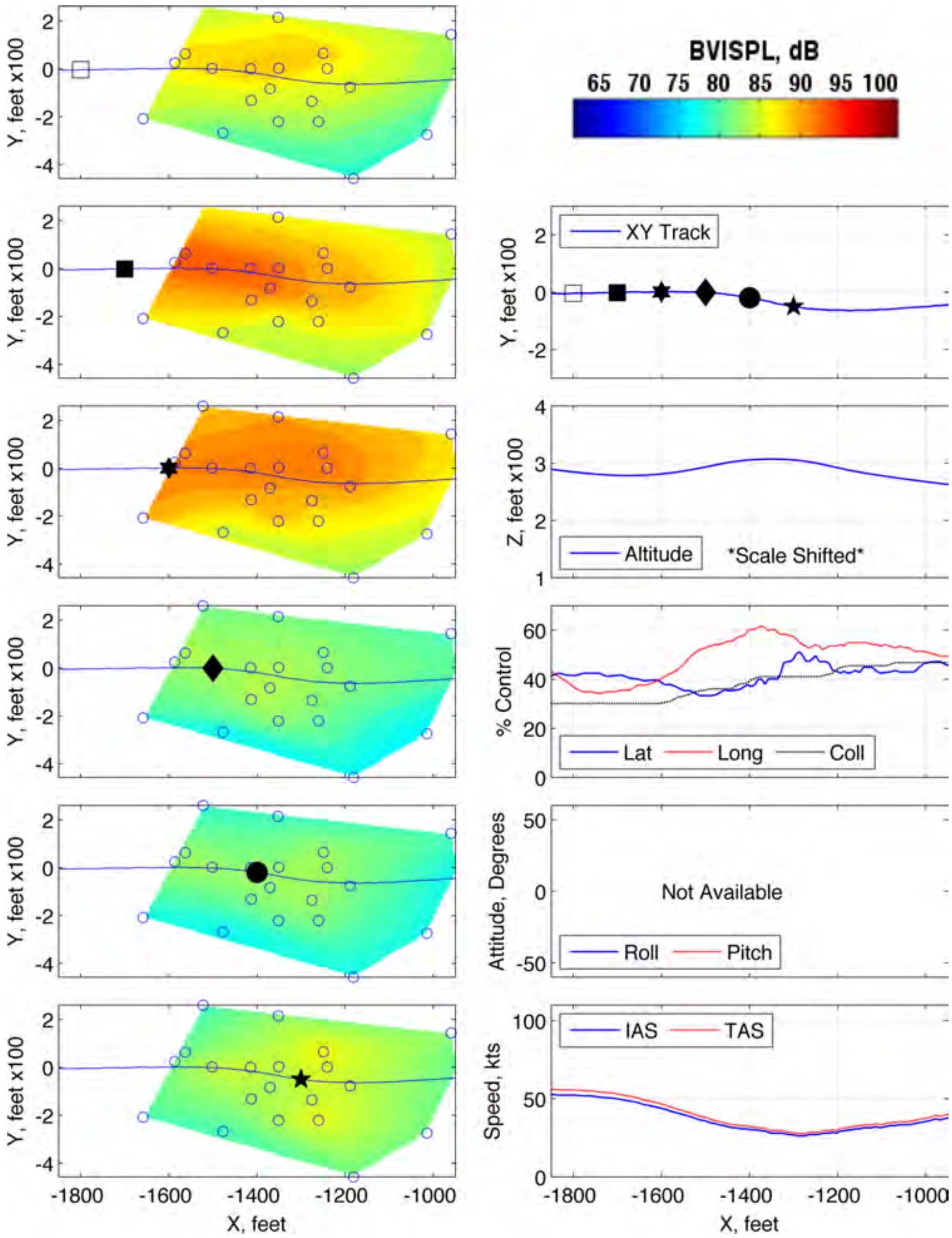

Figure 166: Maneuver condition D9, 60 KIAS, -6° , fast cyclic pitch up, run number 280355

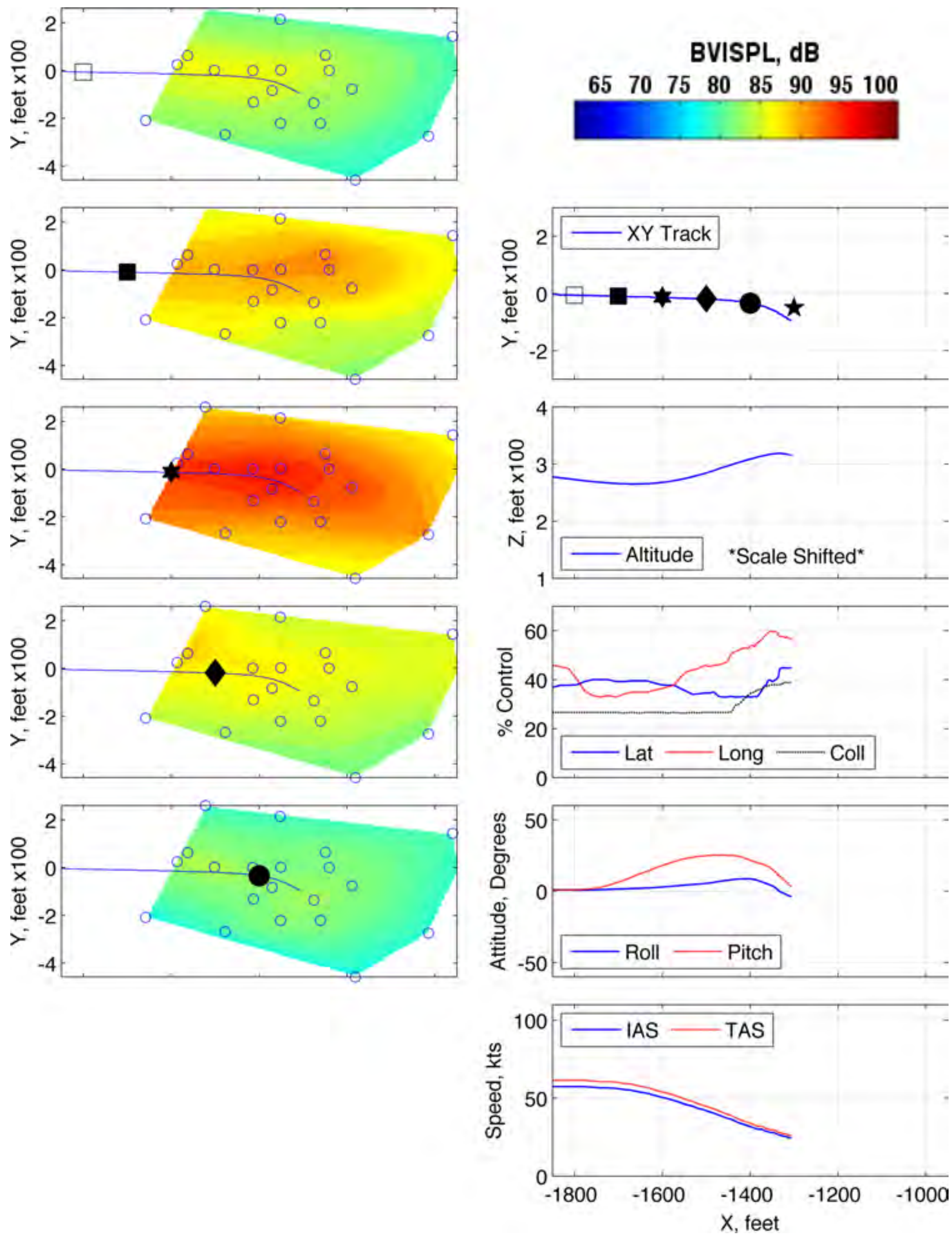

Figure 167: Maneuver condition D9, 60 KIAS, -6° , fast cyclic pitch up, run number 287533

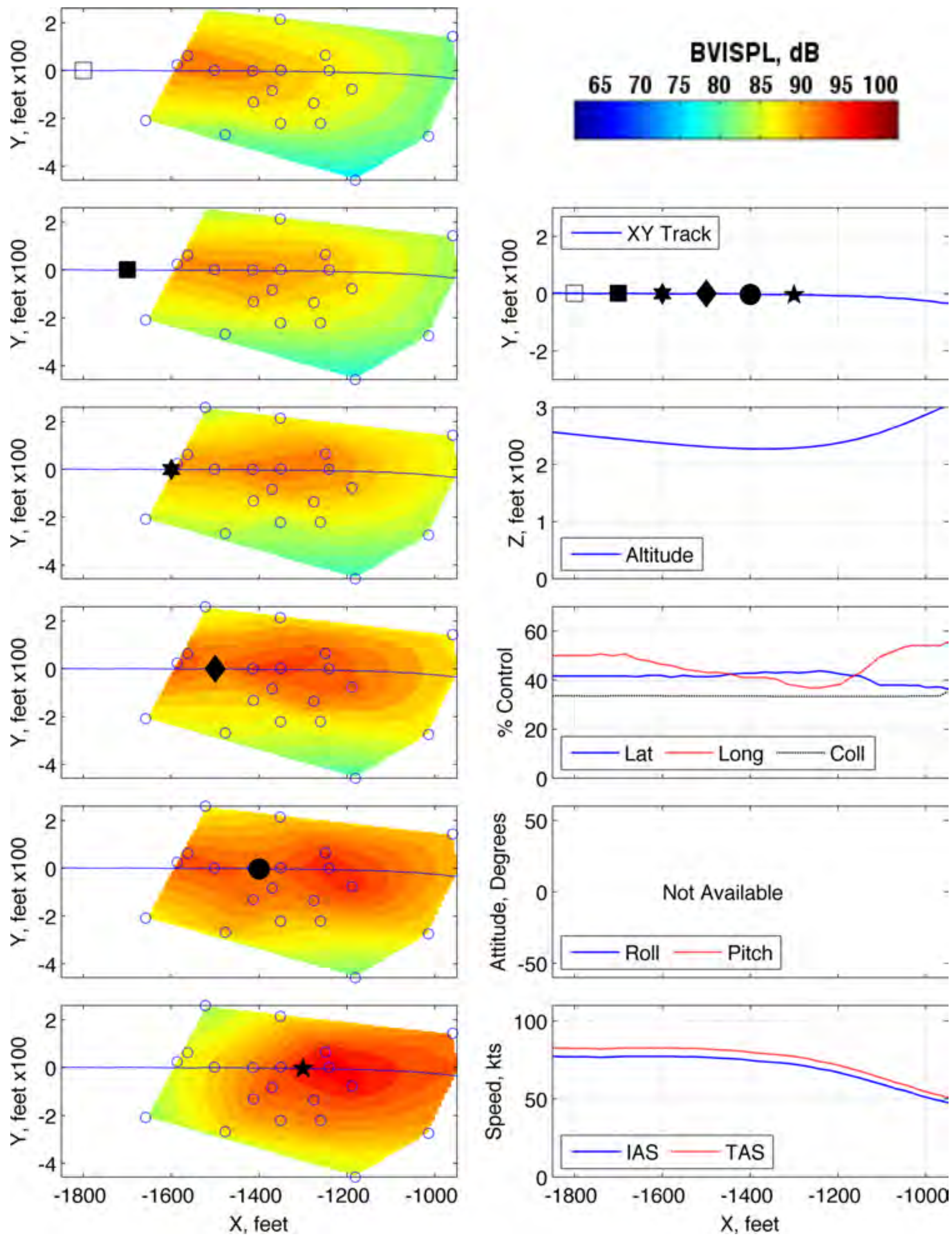

Figure 168: Maneuver condition D10, 80 KIAS, -6° , slow cyclic pitch up, run number 278303

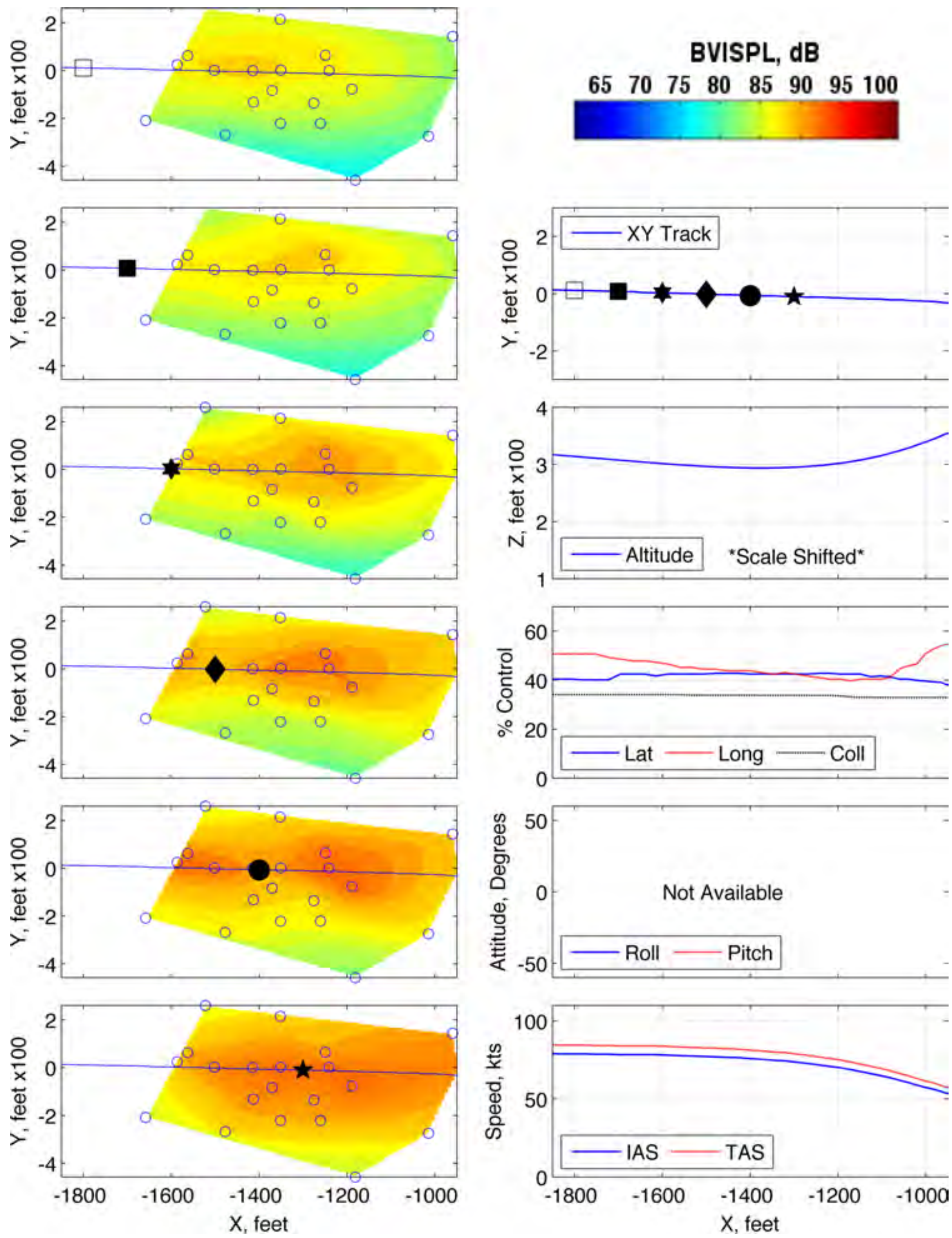

Figure 169: Maneuver condition D10, 80 KIAS, -6° , slow cyclic pitch up, run number 278304

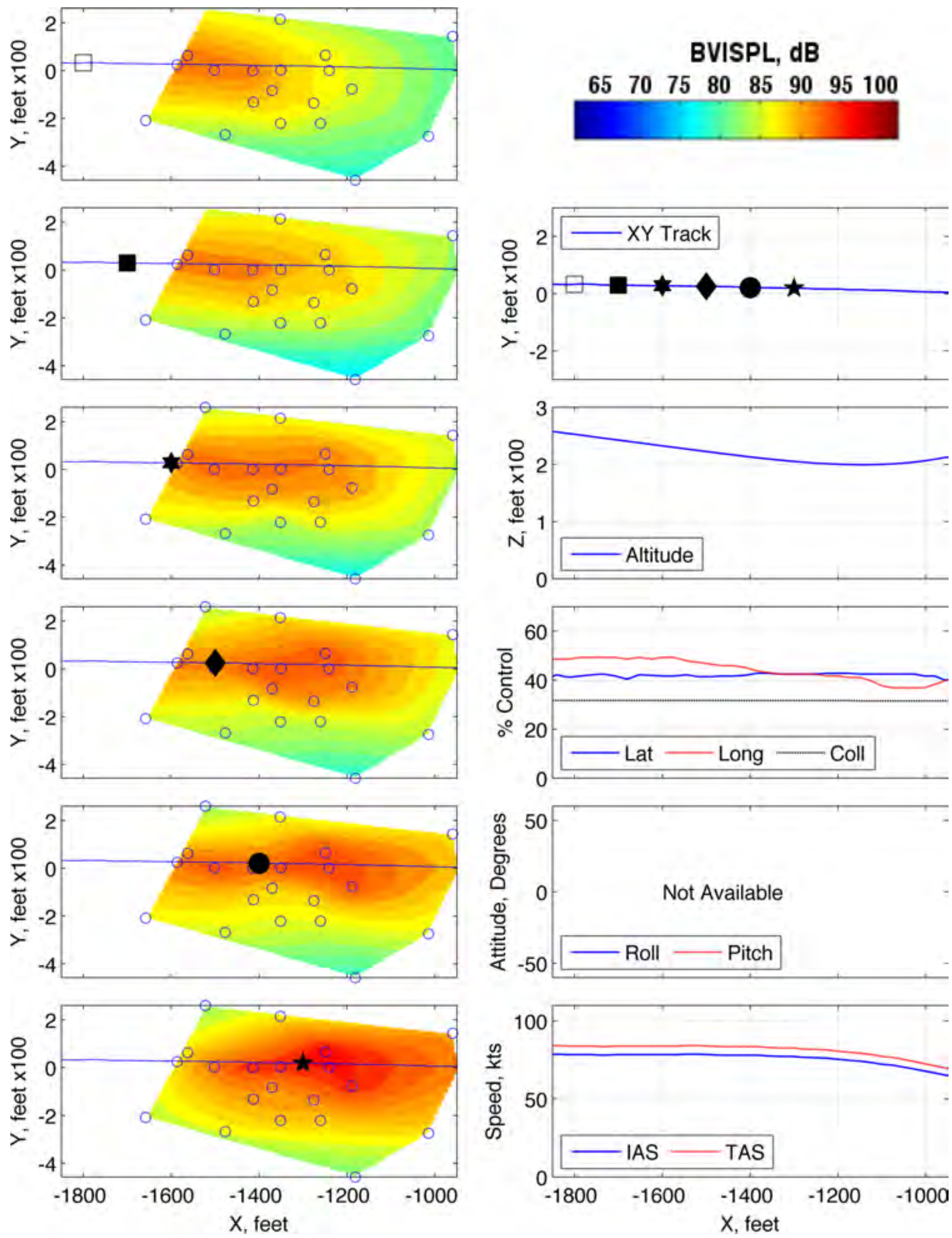

Figure 170: Maneuver condition D10, 80 KIAS, -6° , slow cyclic pitch up, run number 278305

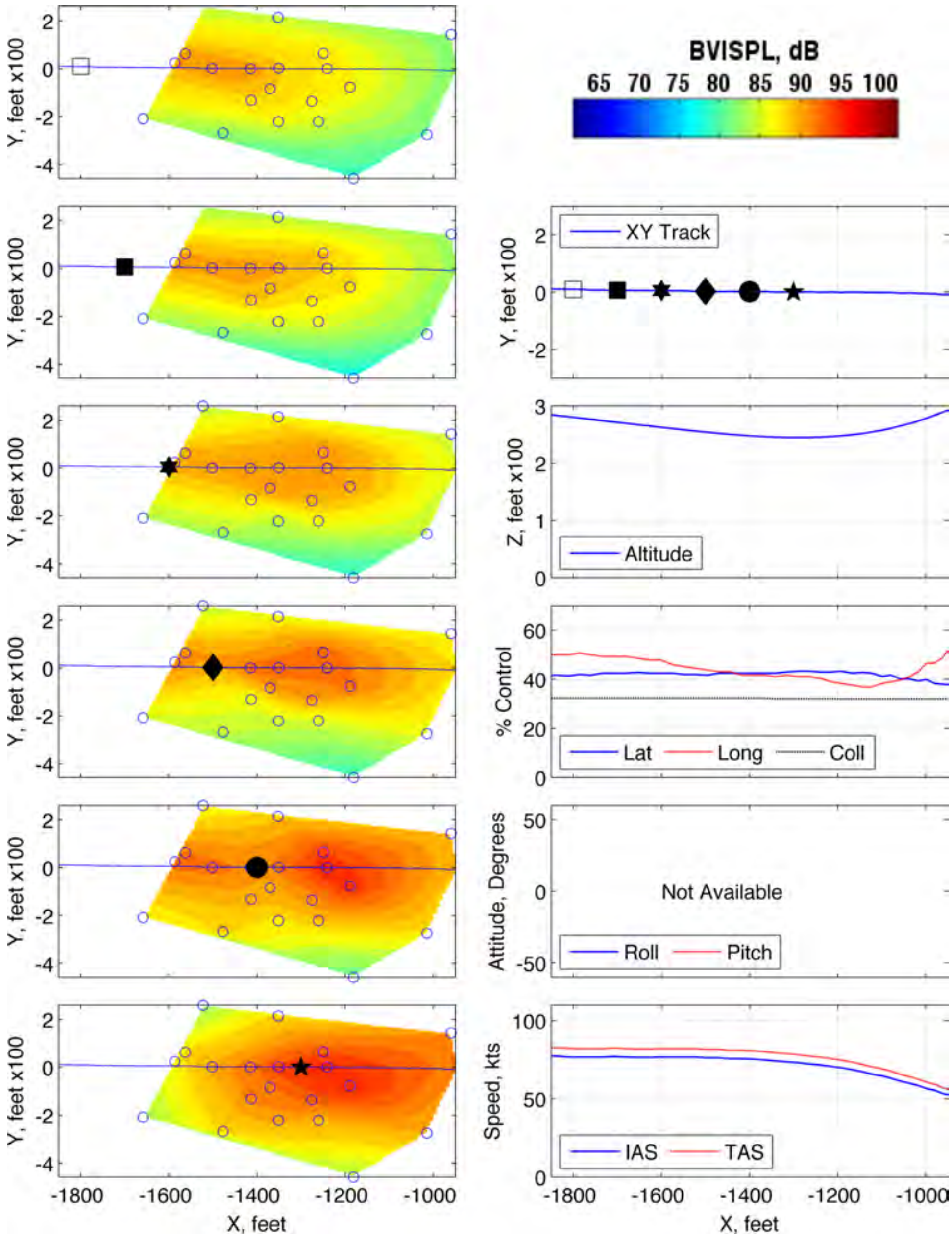

Figure 171: Maneuver condition D10, 80 KIAS, -6° , slow cyclic pitch up, run number 278306

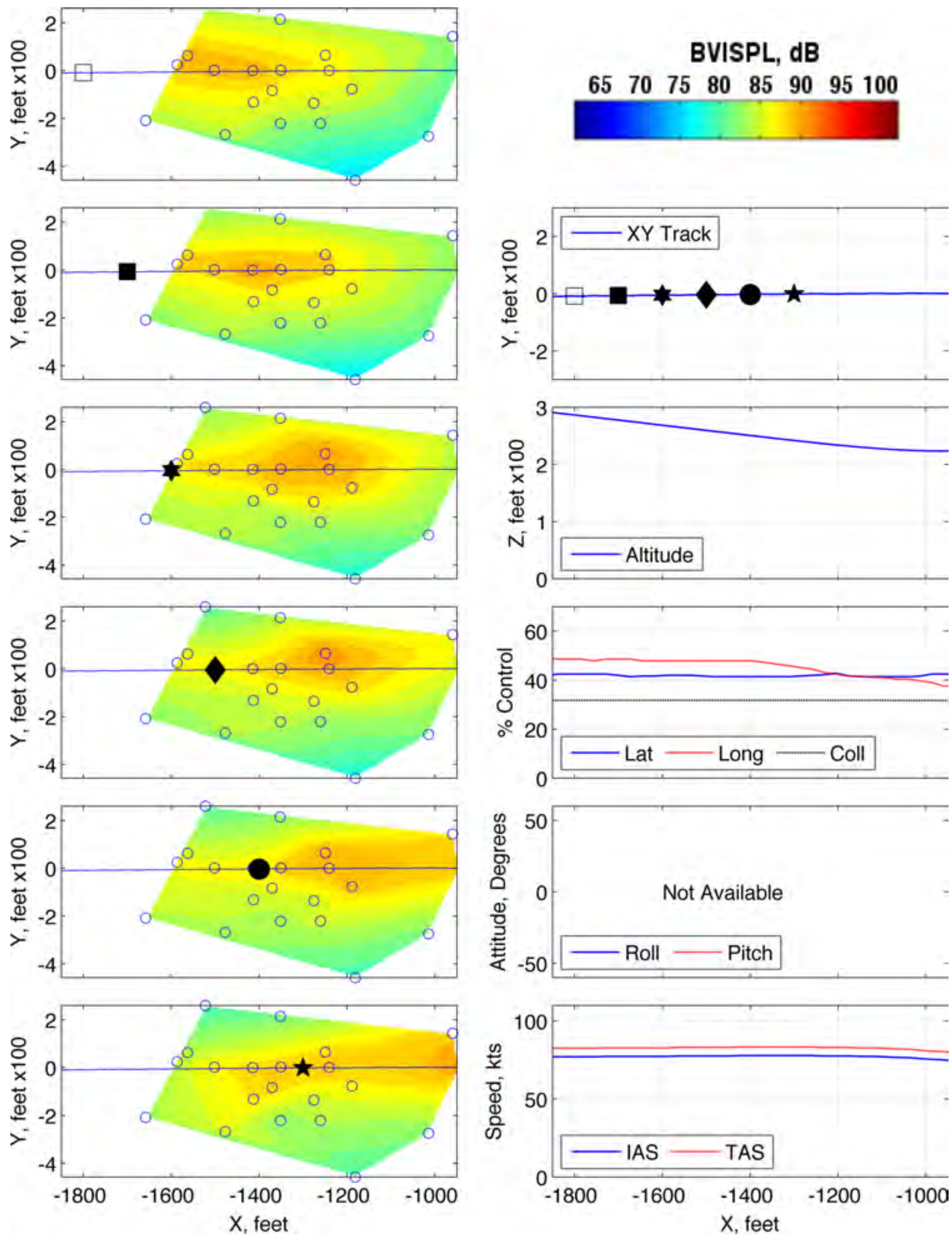

Figure 172: Maneuver condition D10, 80 KIAS, -6° , slow cyclic pitch up, run number 278330

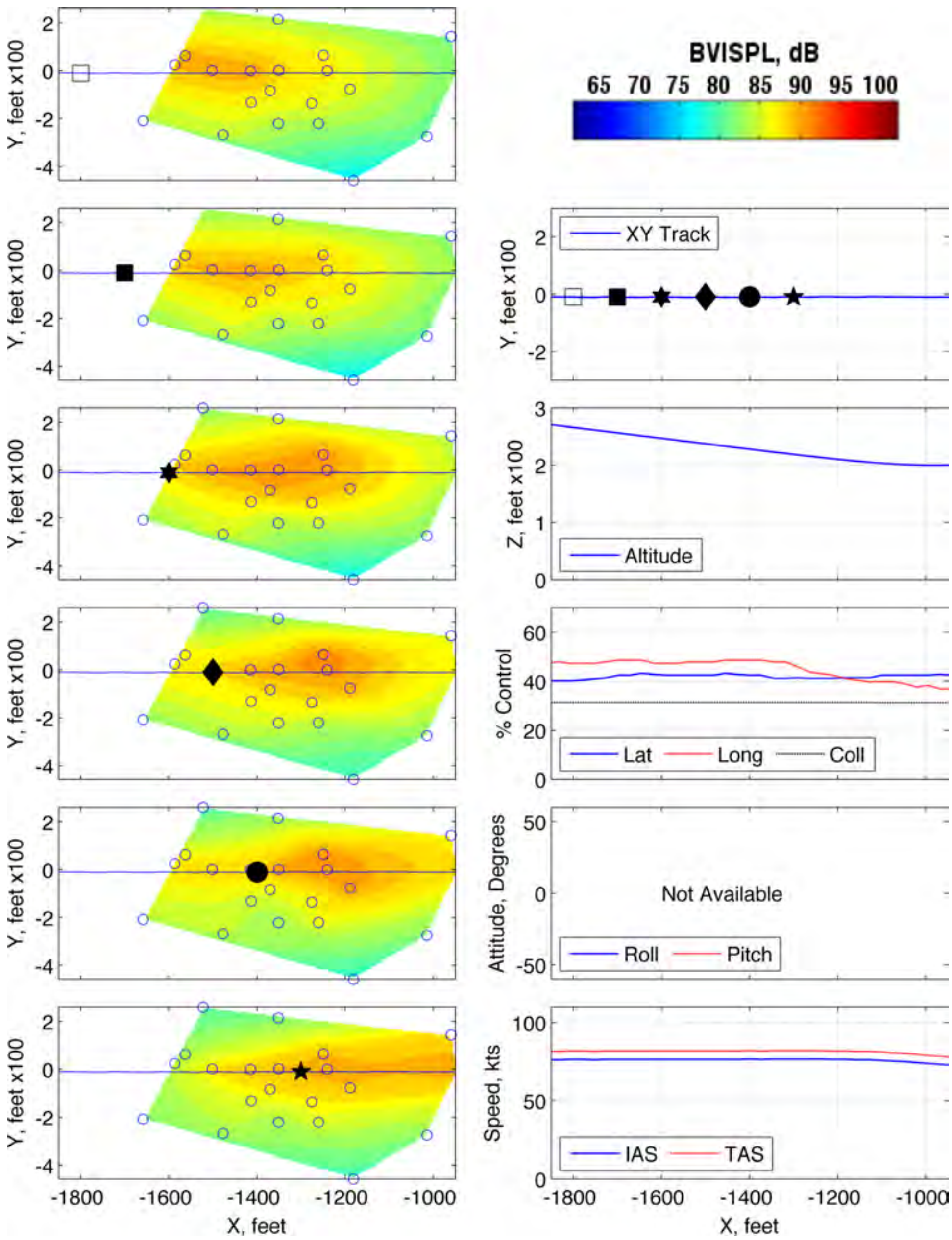

Figure 173: Maneuver condition D10, 80 KIAS, -6° , slow cyclic pitch up, run number 278331

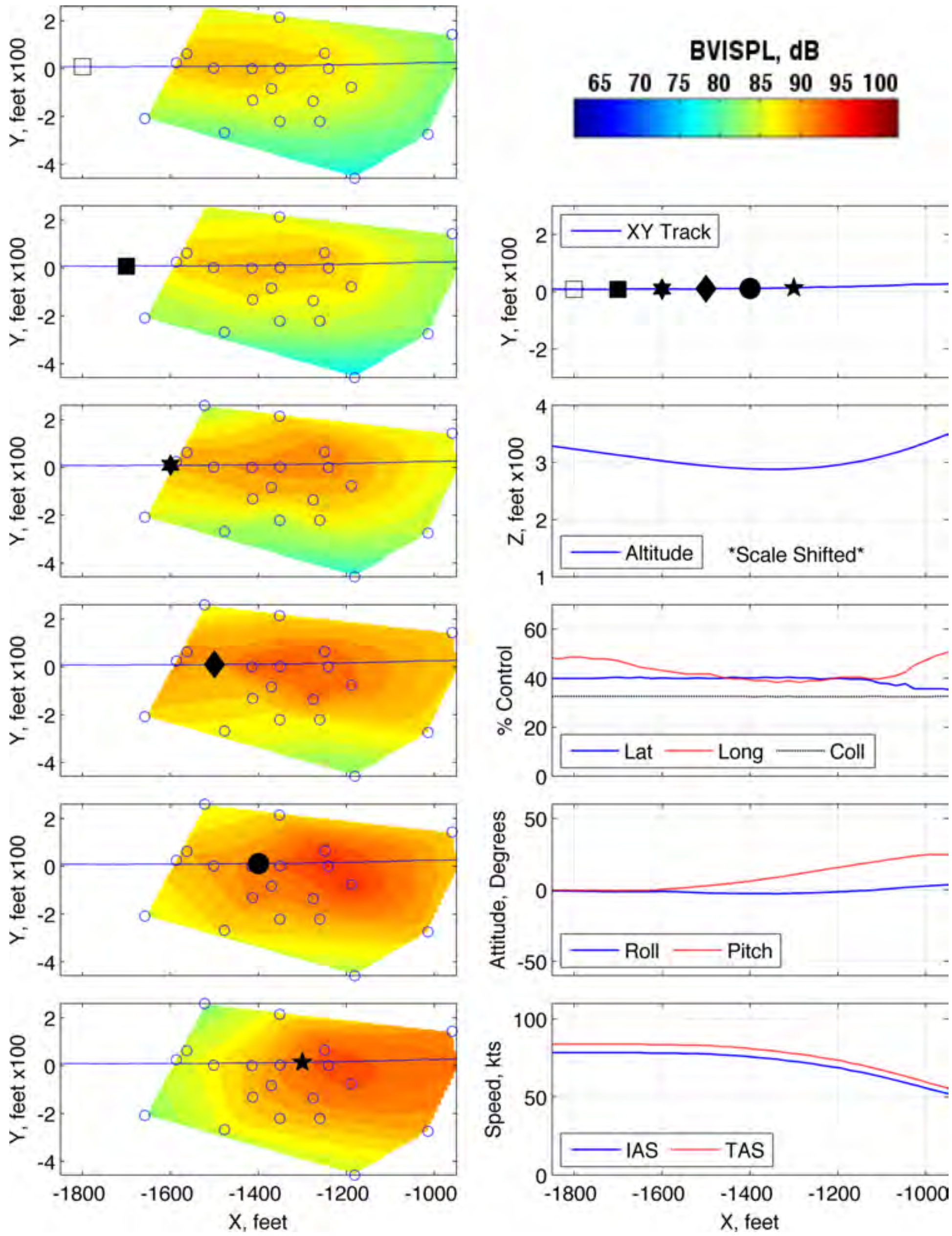

Figure 174: Maneuver condition D10, 80 KIAS, -6° , slow cyclic pitch up, run number 282413

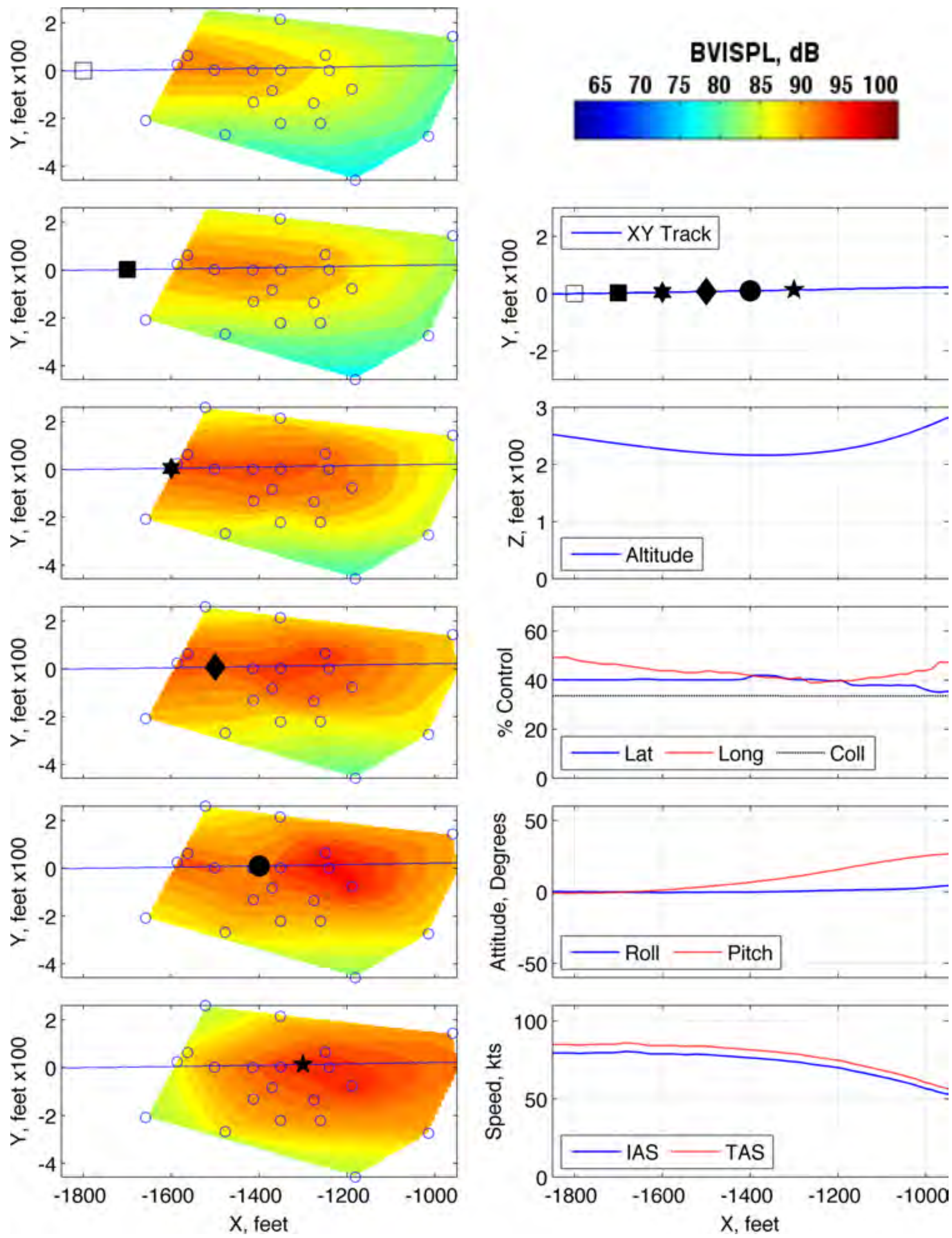

Figure 175: Maneuver condition D10, 80 KIAS, -6° , slow cyclic pitch up, run number 282414

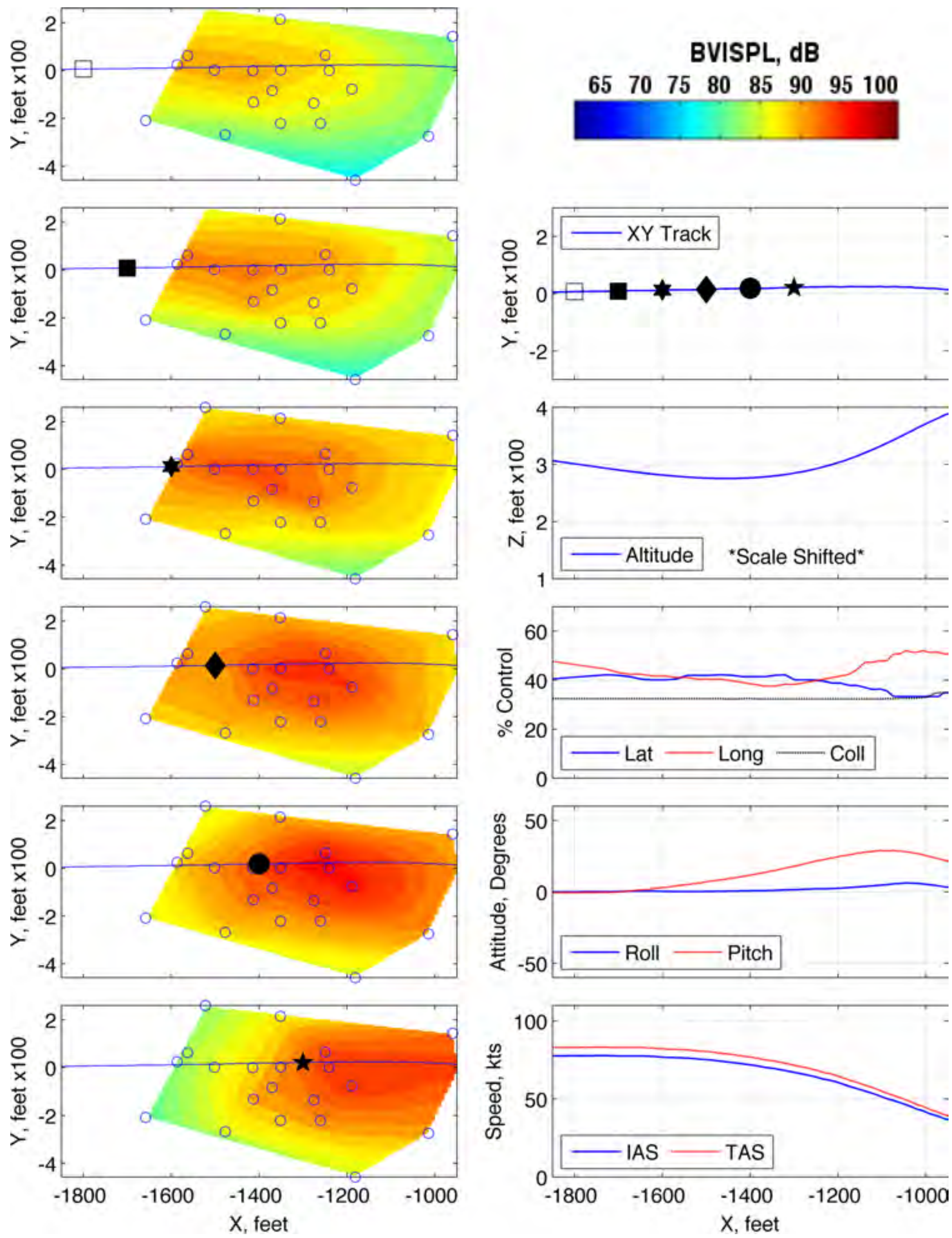

Figure 176: Maneuver condition D10, 80 KIAS, -6° , slow cyclic pitch up, run number 282415

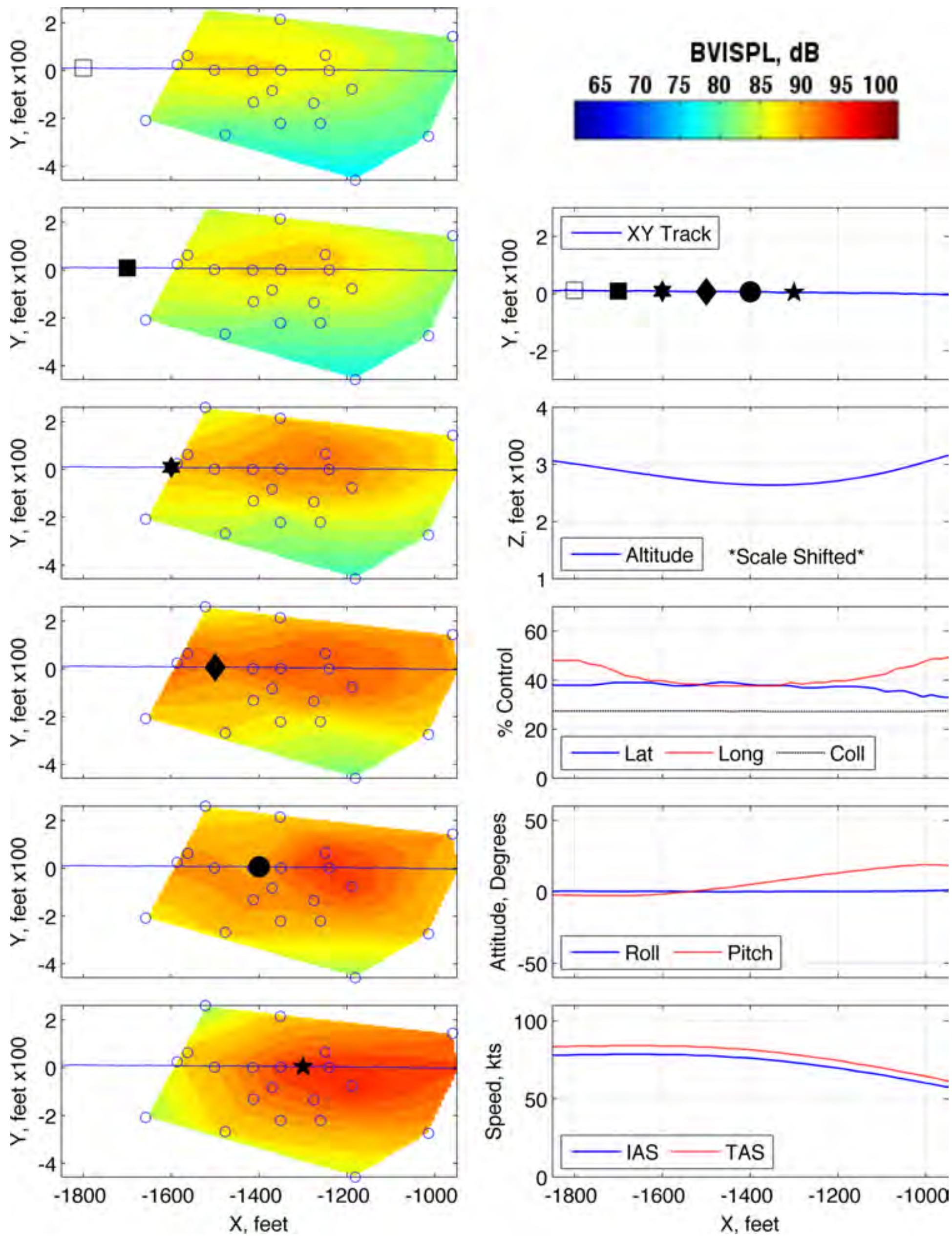

Figure 177: Maneuver condition D11, 80 KIAS, -6° , medium cyclic pitch up, run number 285478

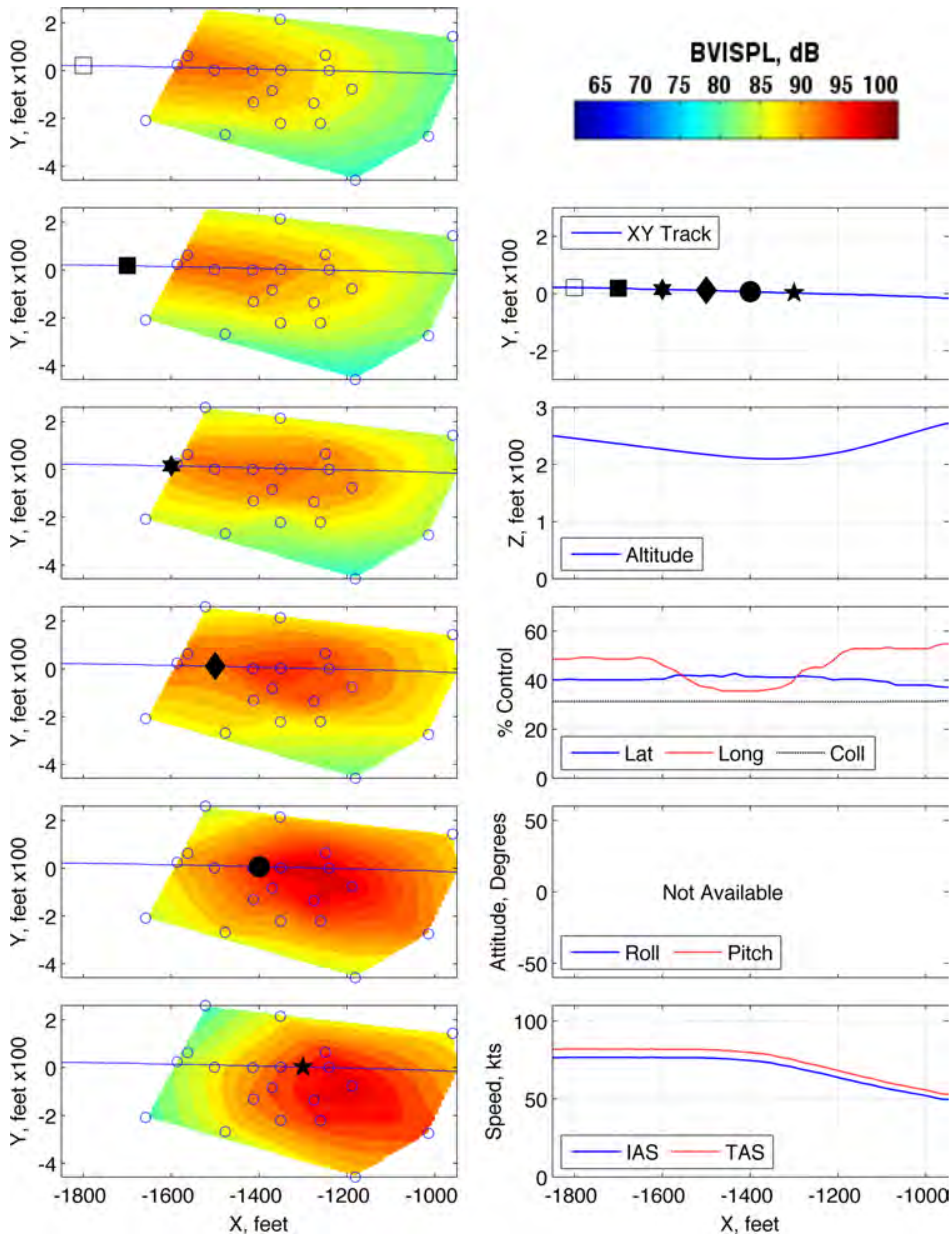

Figure 178: Maneuver condition D12, 80 KIAS, -6° , fast cyclic pitch up, run number 278302

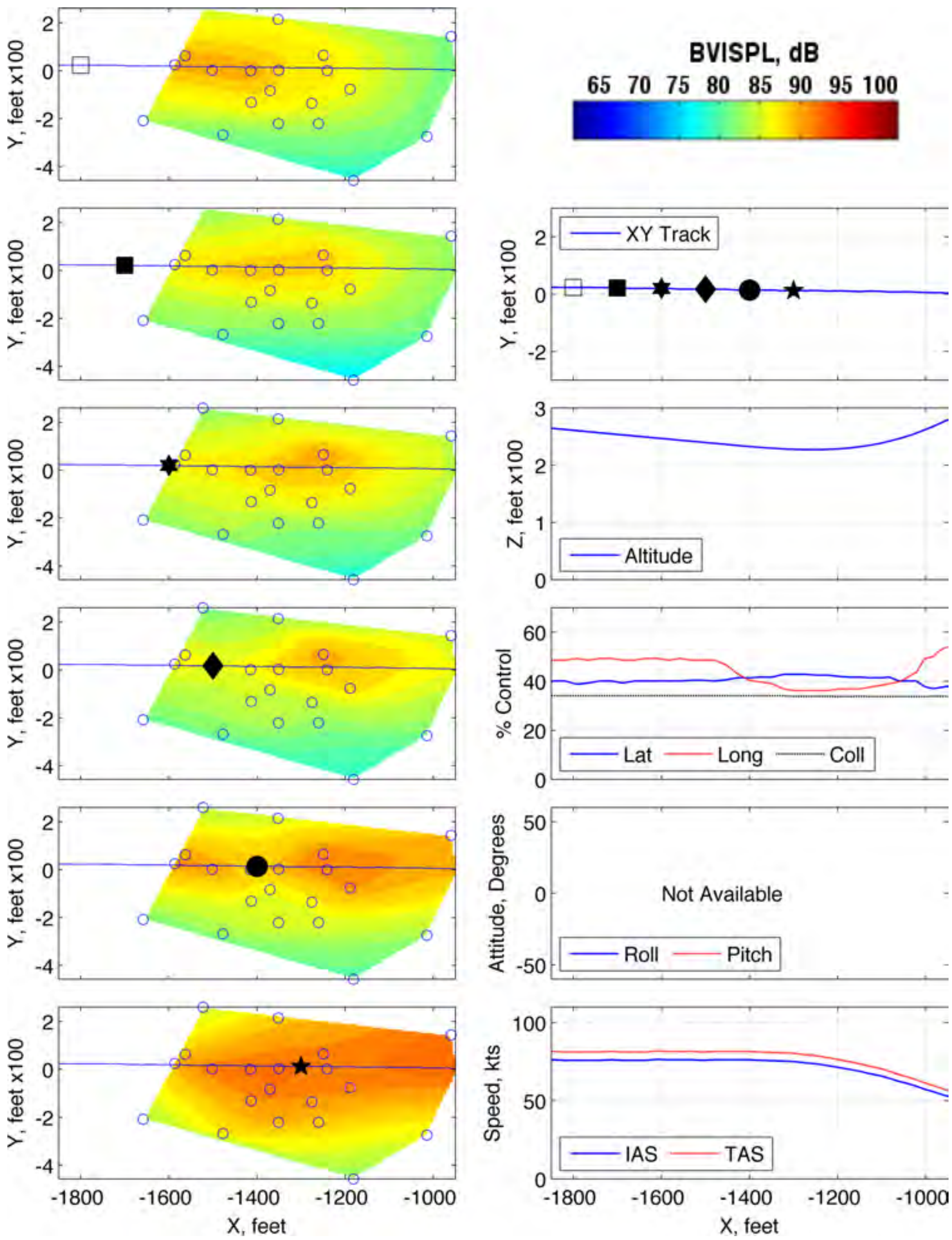

Figure 179: Maneuver condition D12, 80 KIAS, -6° , fast cyclic pitch up, run number 278307

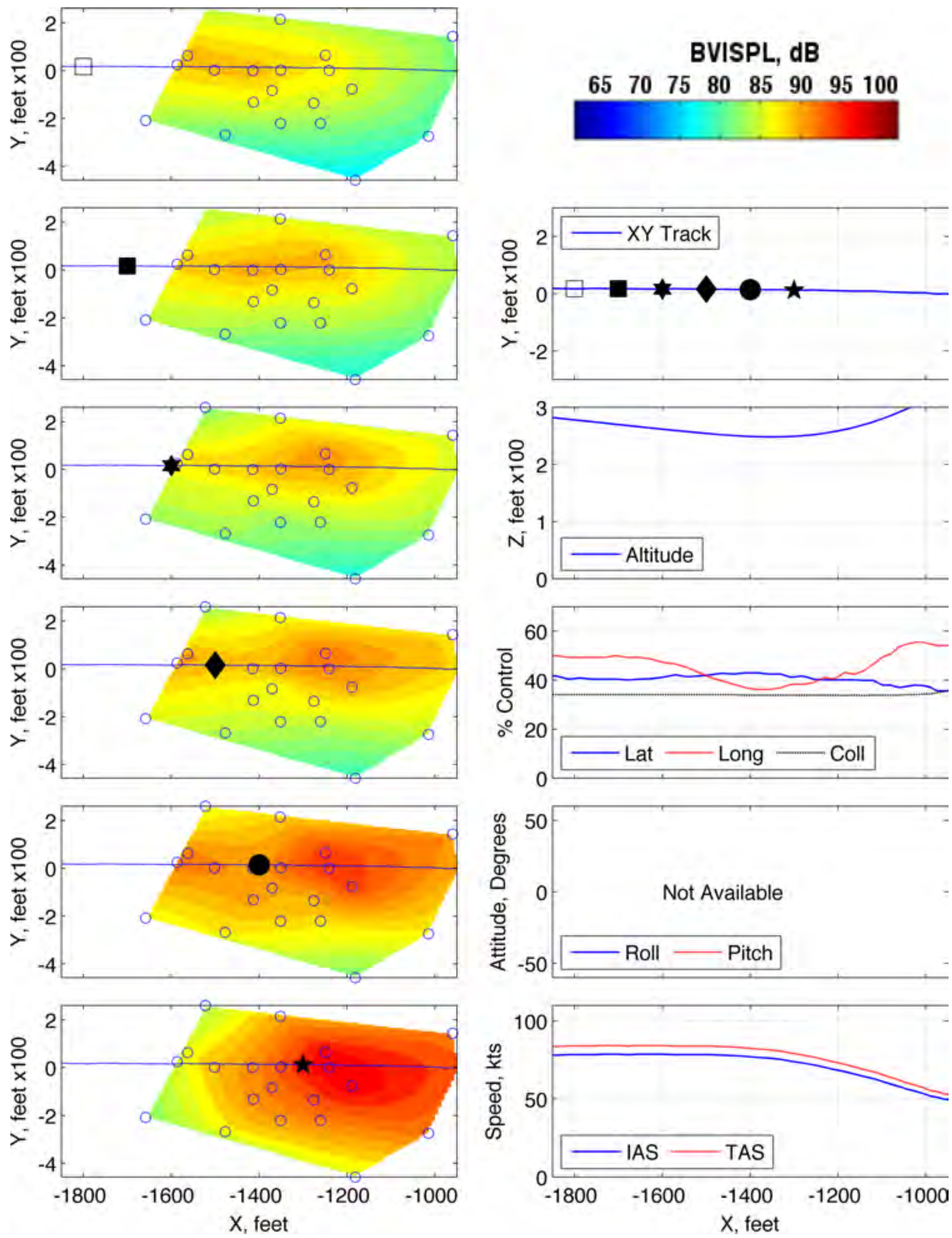

Figure 180: Maneuver condition D12, 80 KIAS, -6° , fast cyclic pitch up, run number 278308

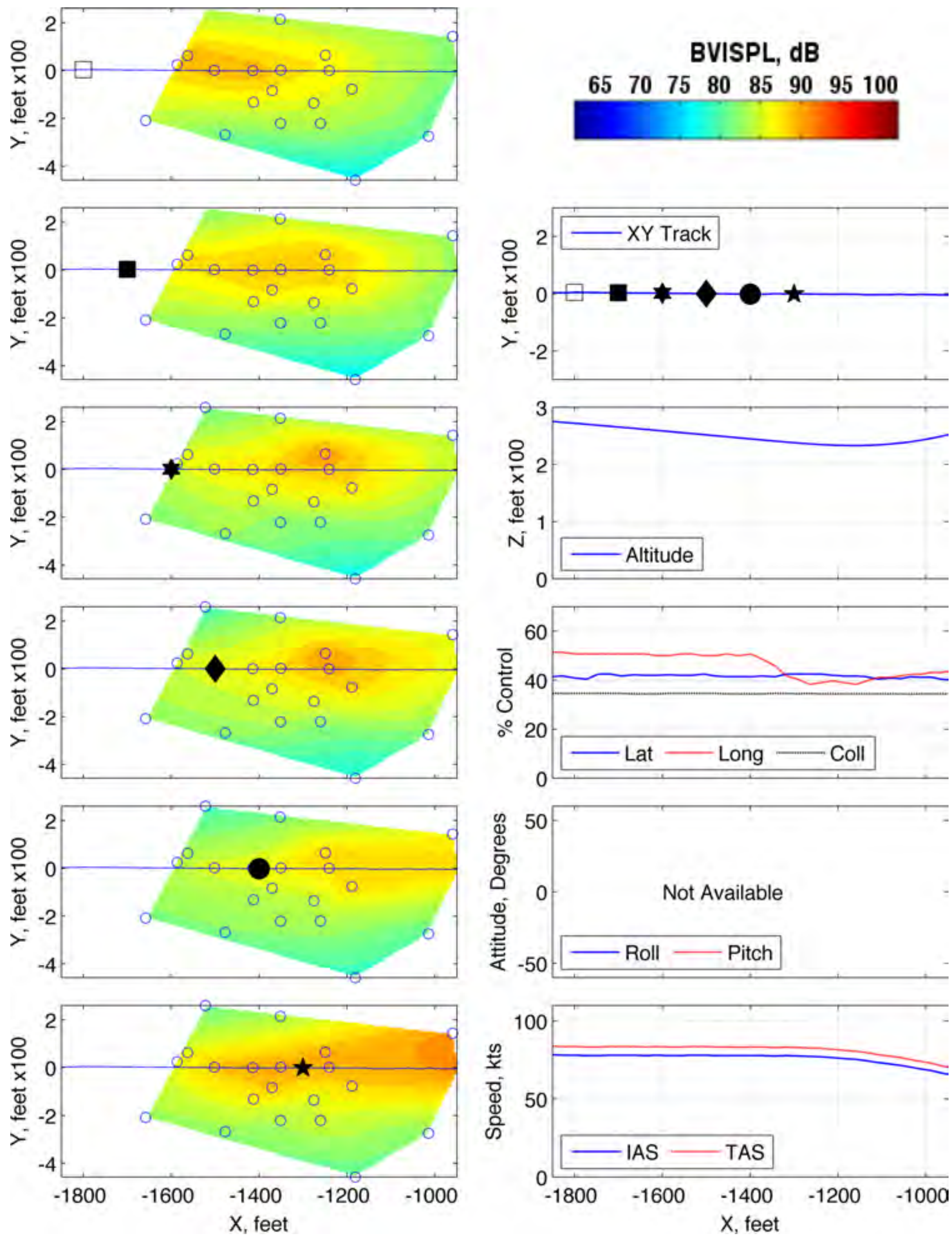

Figure 181: Maneuver condition D12, 80 KIAS, -6° , fast cyclic pitch up, run number 278309

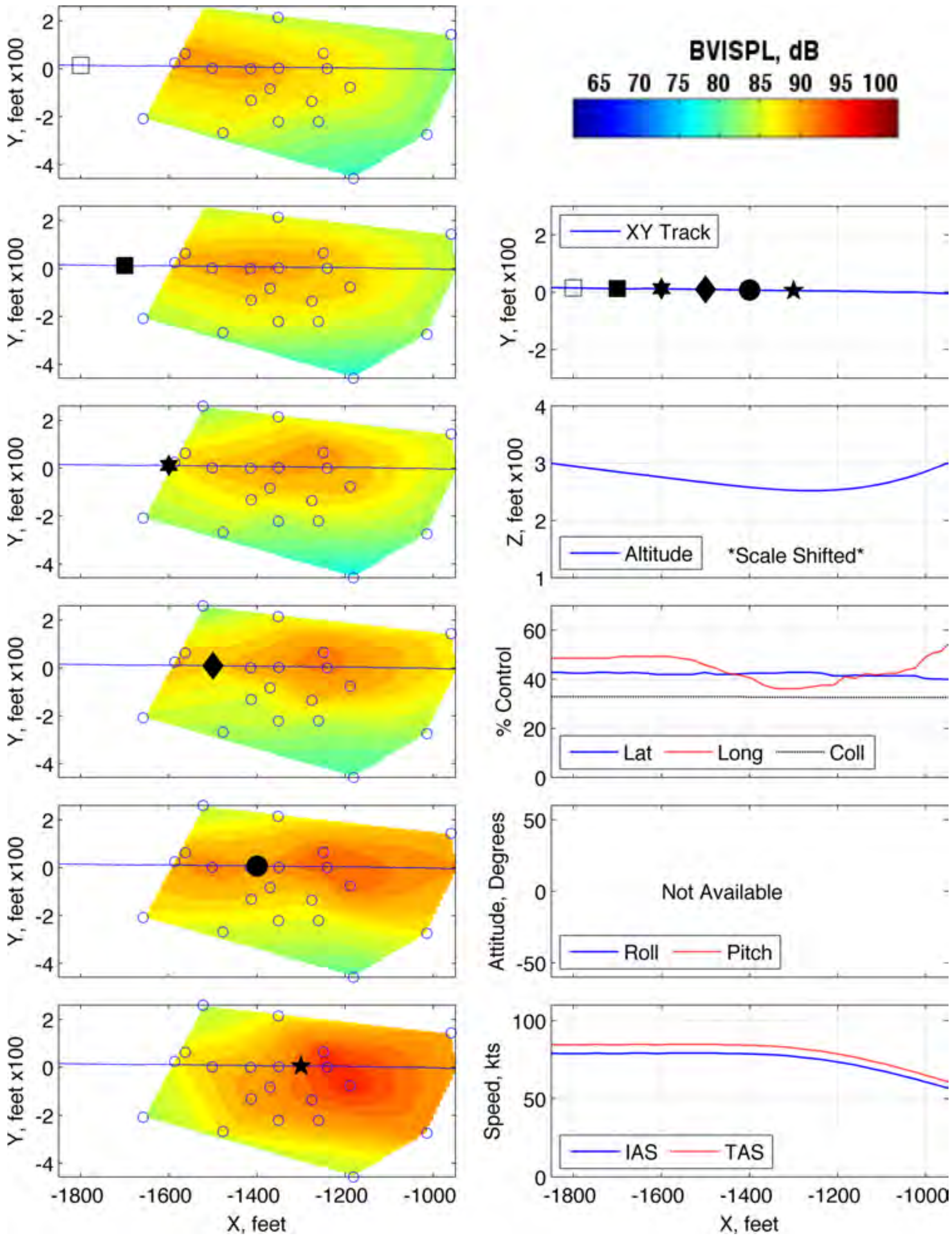

Figure 182: Maneuver condition D12, 80 KIAS, -6° , fast cyclic pitch up, run number 278310

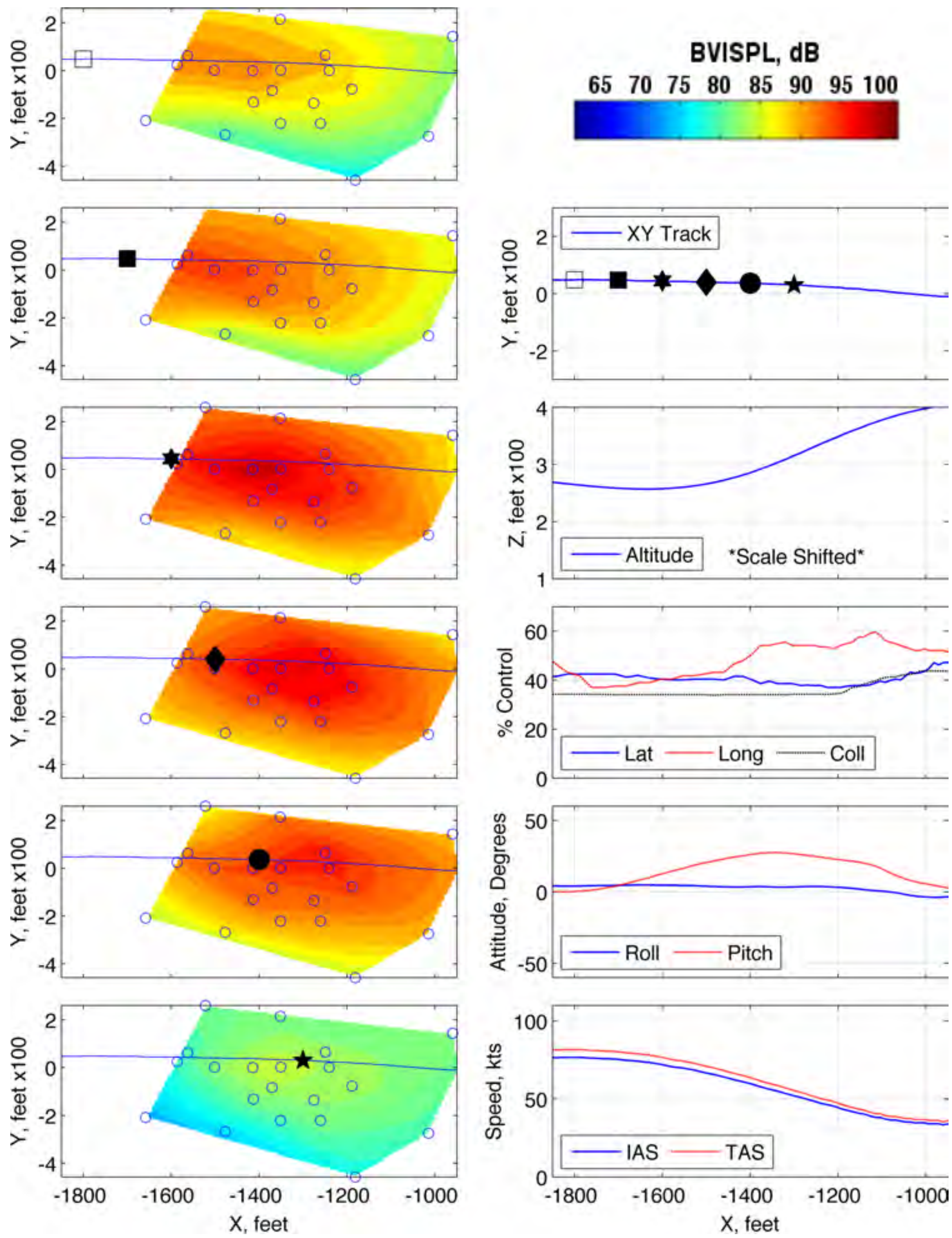

Figure 183: Maneuver condition D12, 80 KIAS, -6° , fast cyclic pitch up, run number 280342

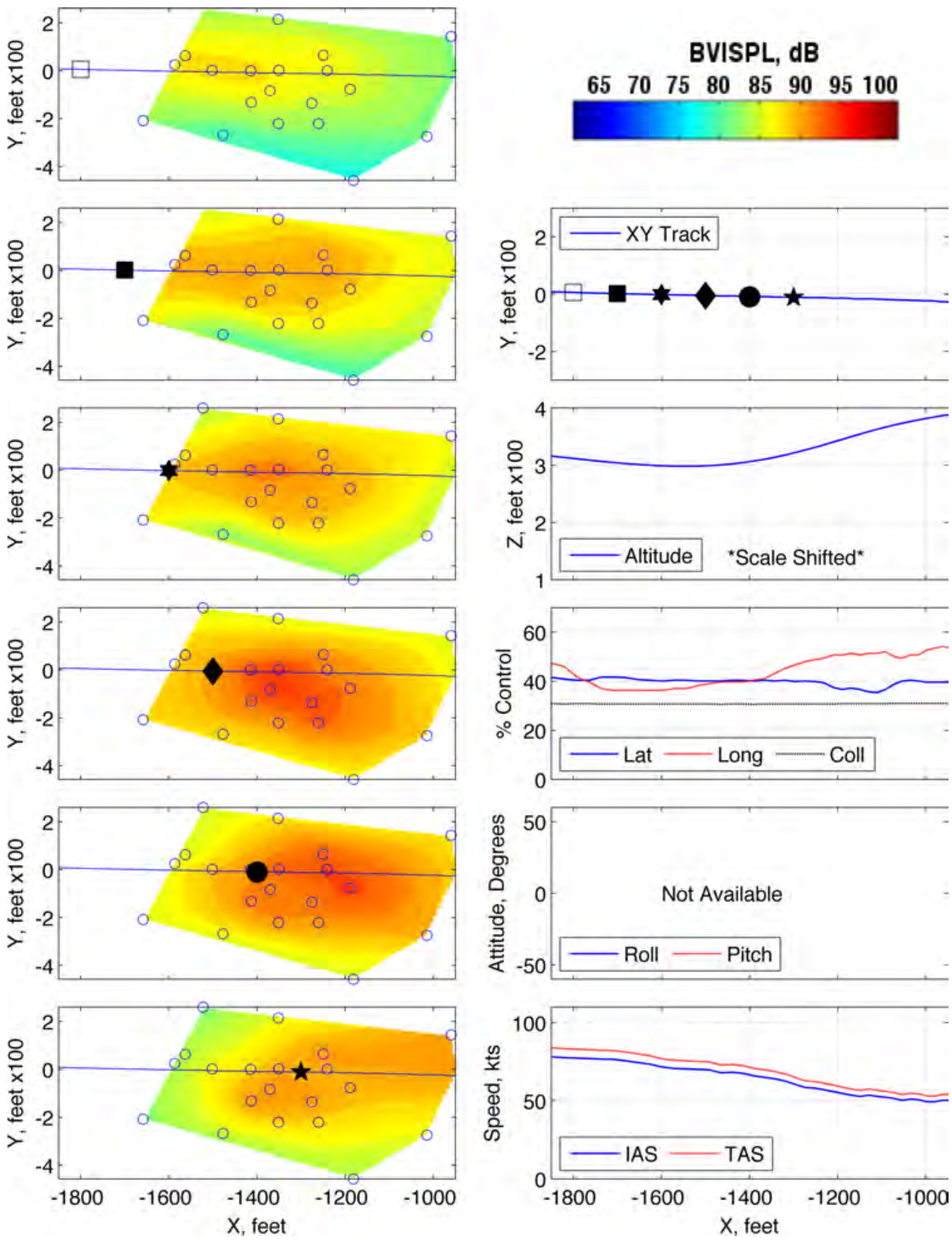

Figure 184: Maneuver condition D12, 80 KIAS, -6° , fast cyclic pitch up, run number 280406

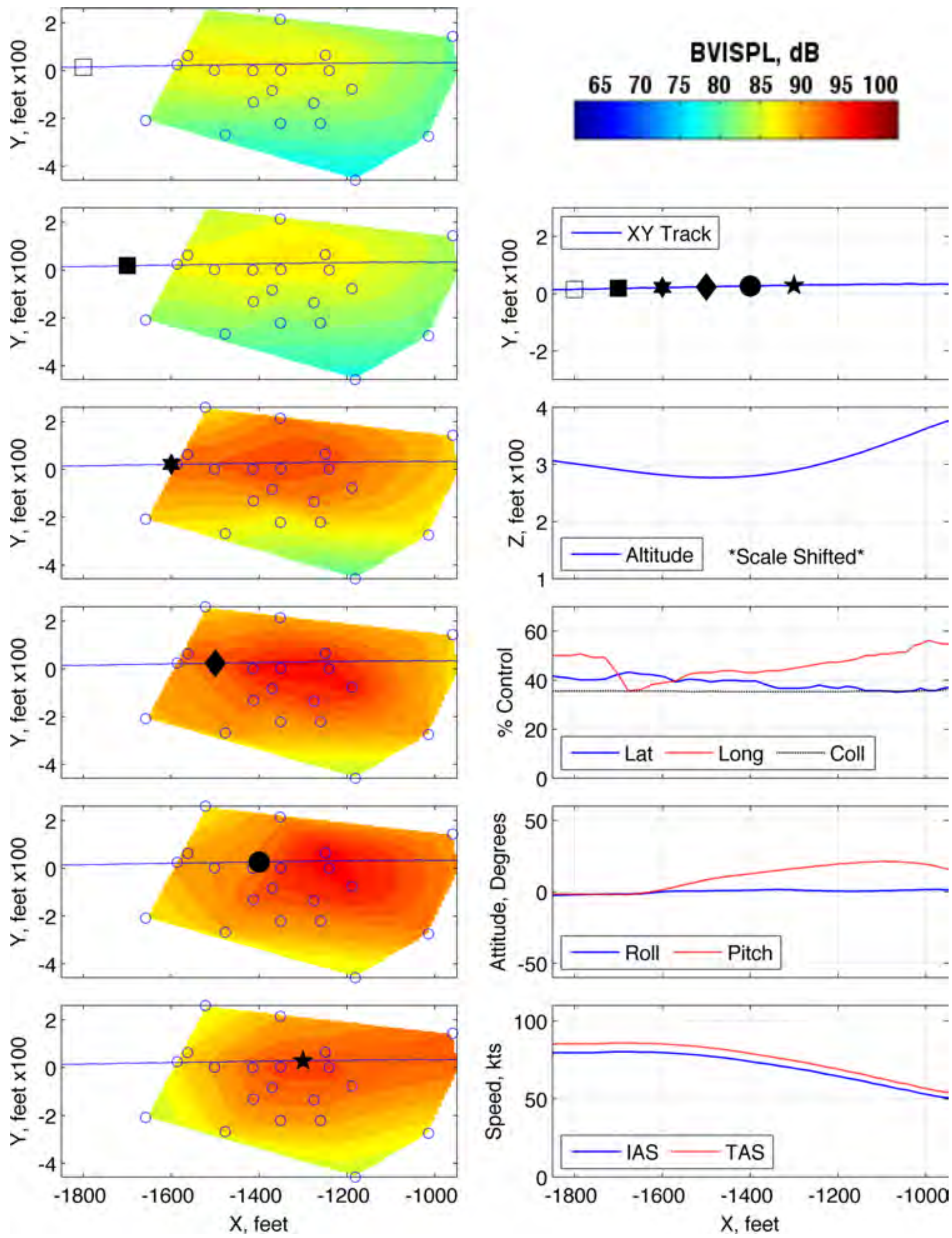

Figure 185: Maneuver condition D12, 80 KIAS, -6° , fast cyclic pitch up, run number 282412

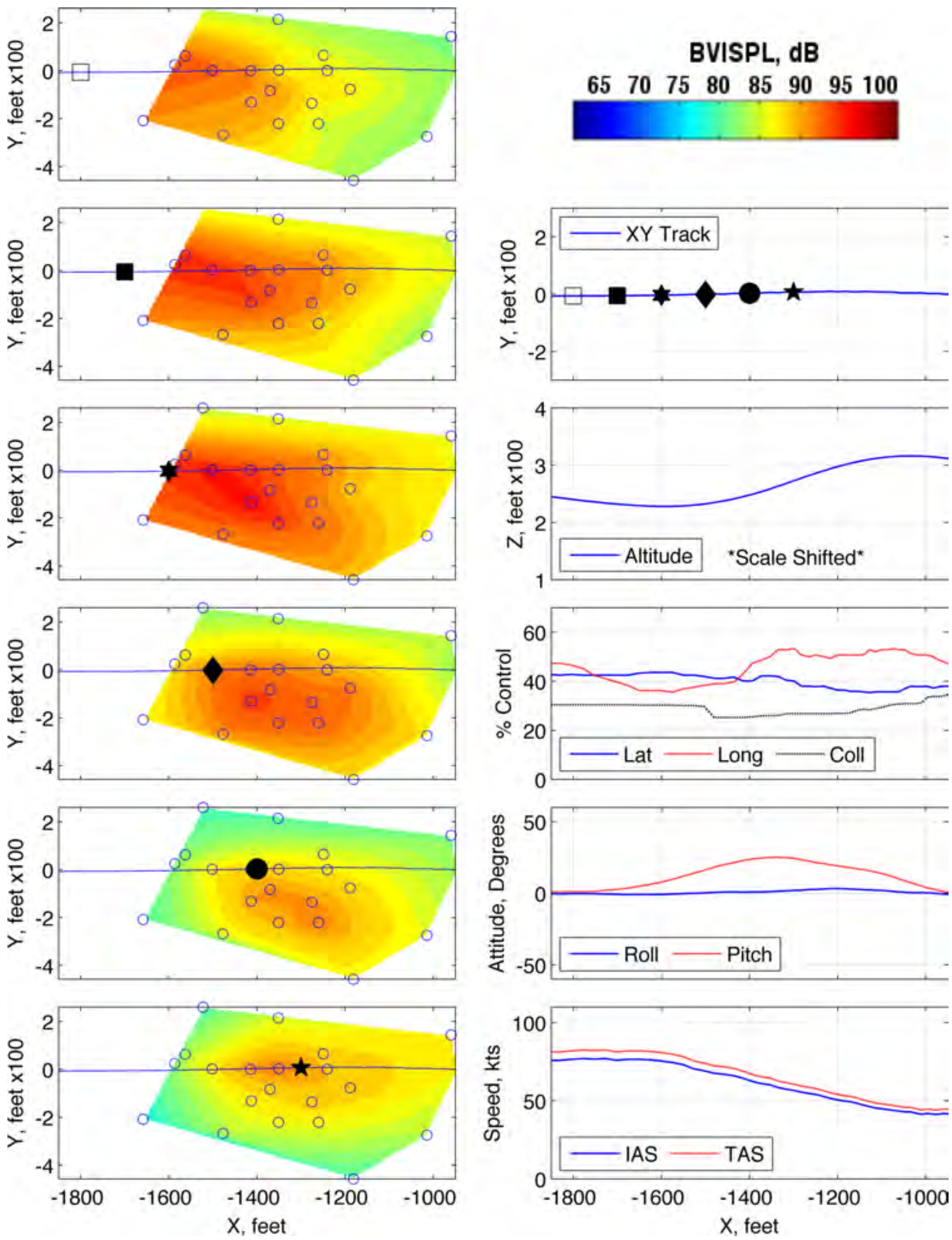

Figure 186: Maneuver condition D12, 80 KIAS, -6° , fast cyclic pitch up, run number 282450

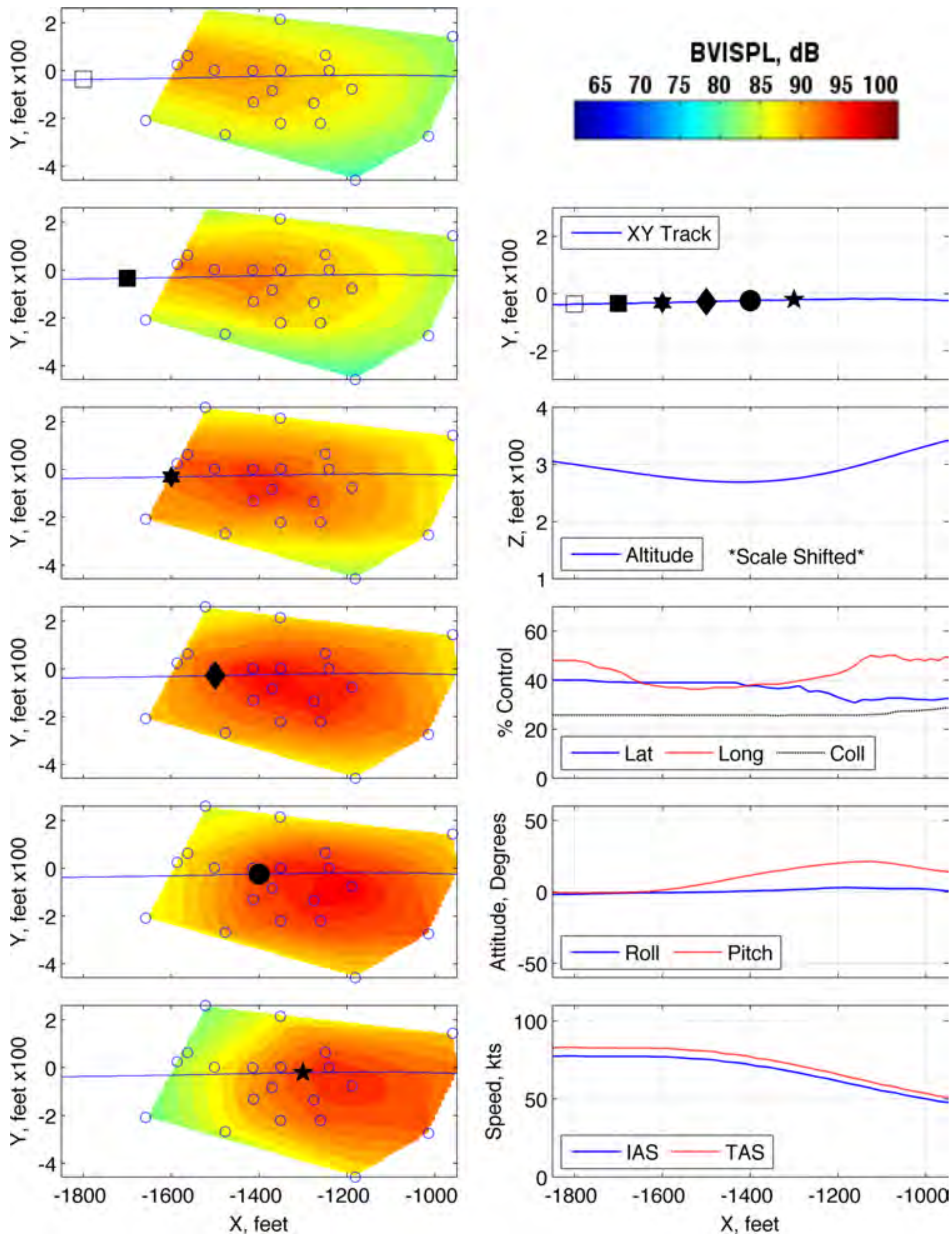

Figure 187: Maneuver condition D12, 80 KIAS, -6° , fast cyclic pitch up, run number 285462

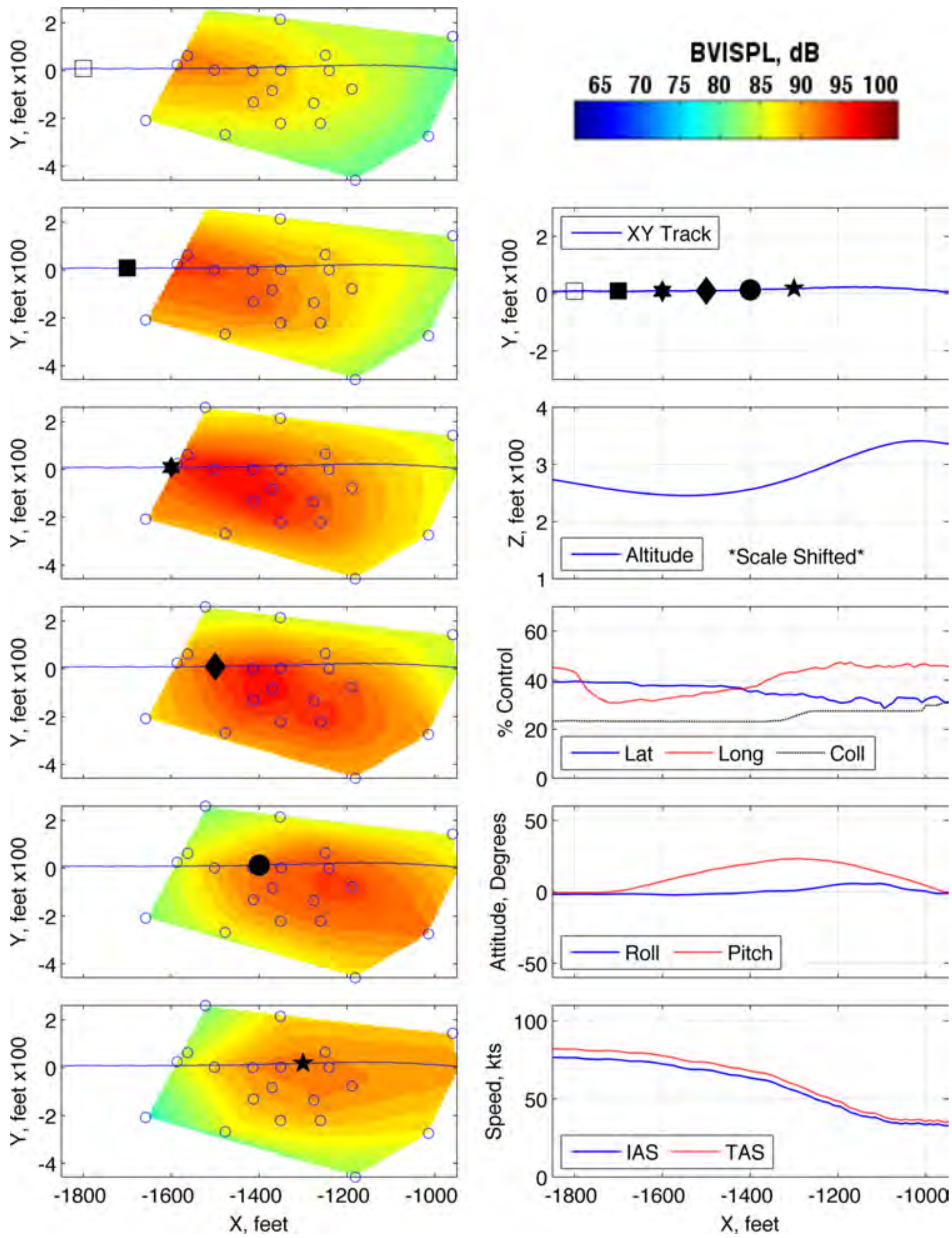

Figure 188: Maneuver condition D12, 80 KIAS, -6° , fast cyclic pitch up, run number 285517

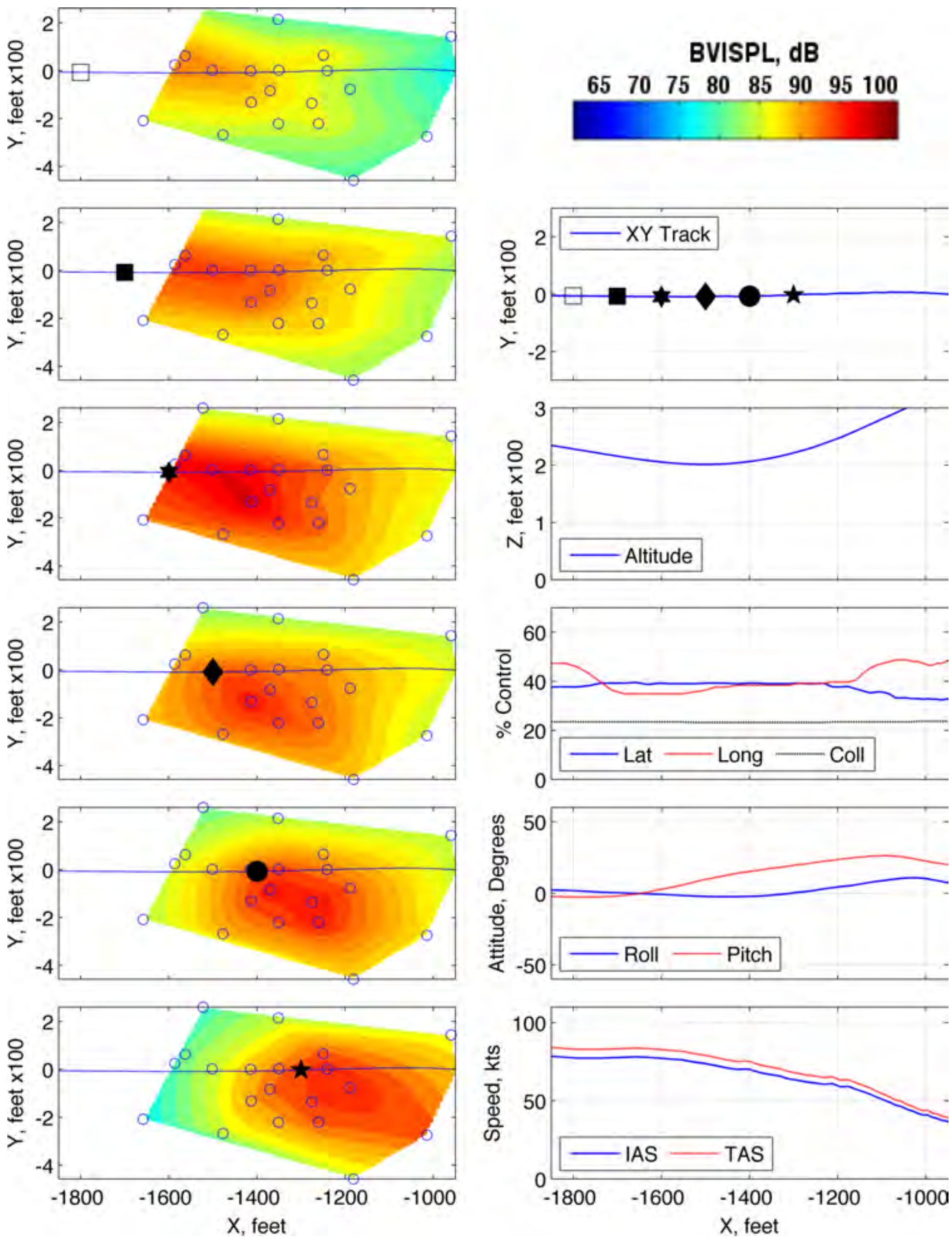

Figure 189: Maneuver condition D12, 80 KIAS, -6° , fast cyclic pitch up, run number 287575

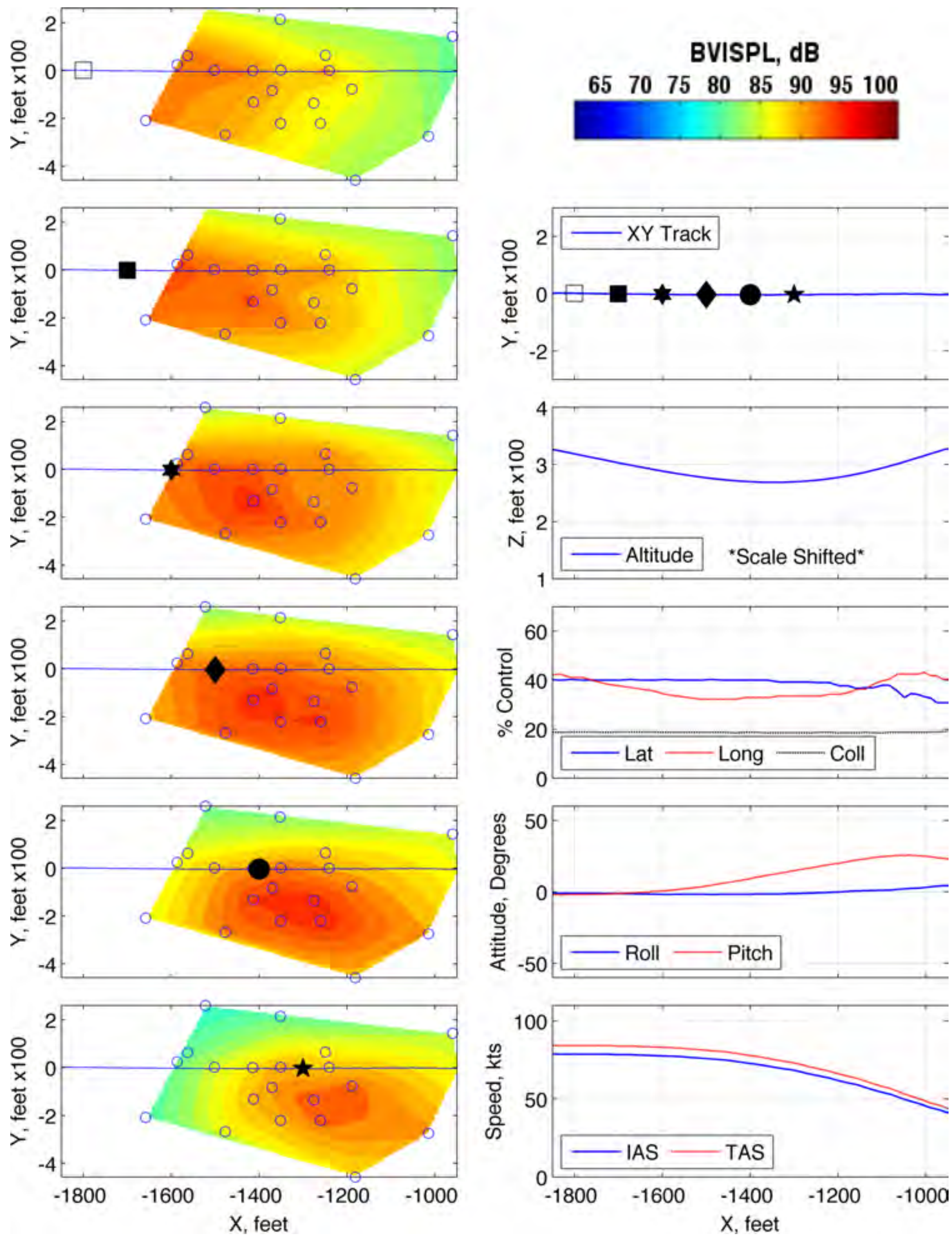

Figure 190: Maneuver condition D19, 80 KIAS, -9° , slow cyclic pitch up, run number 285490

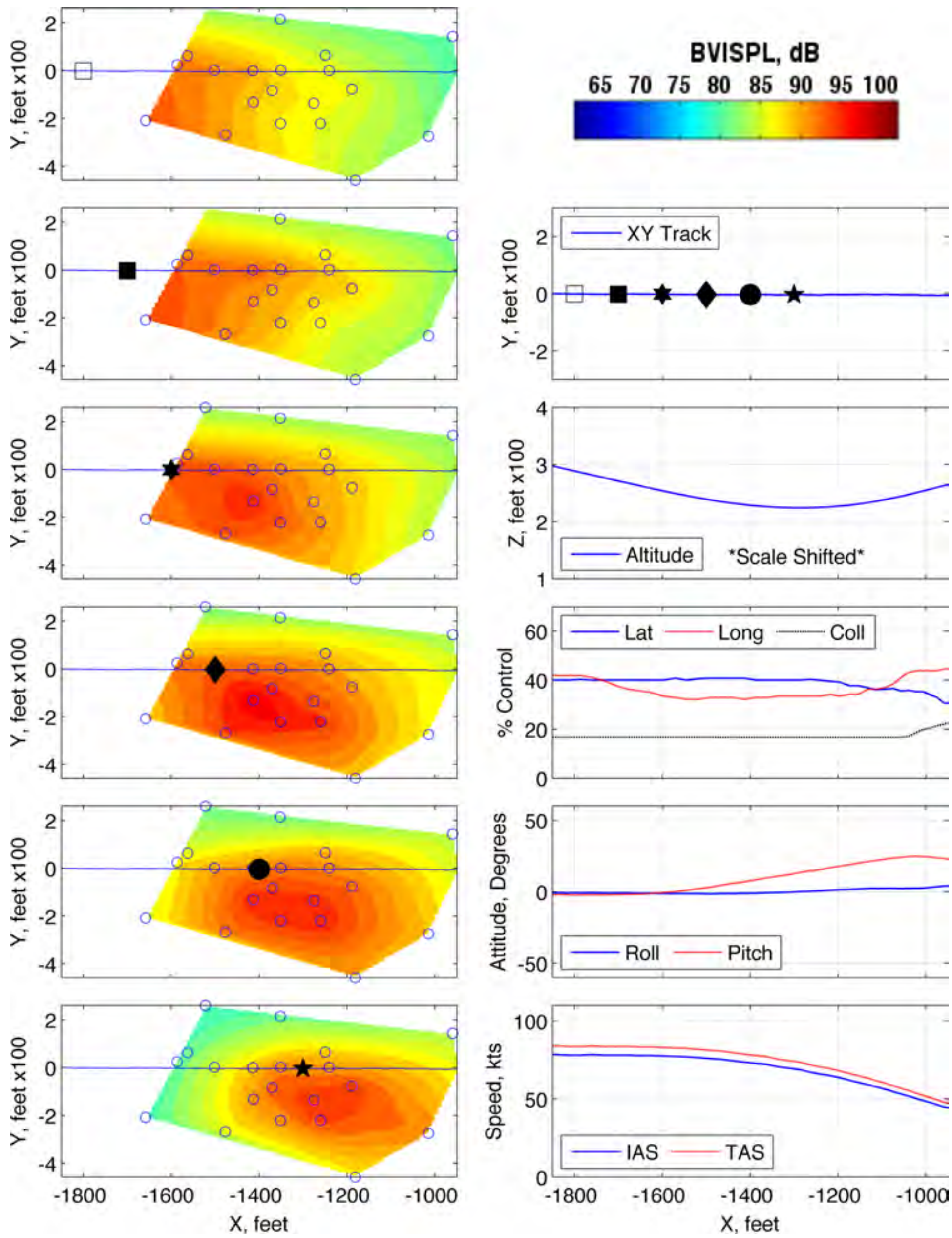

Figure 191: Maneuver condition D19, 80 KIAS, -9° , slow cyclic pitch up, run number 285491

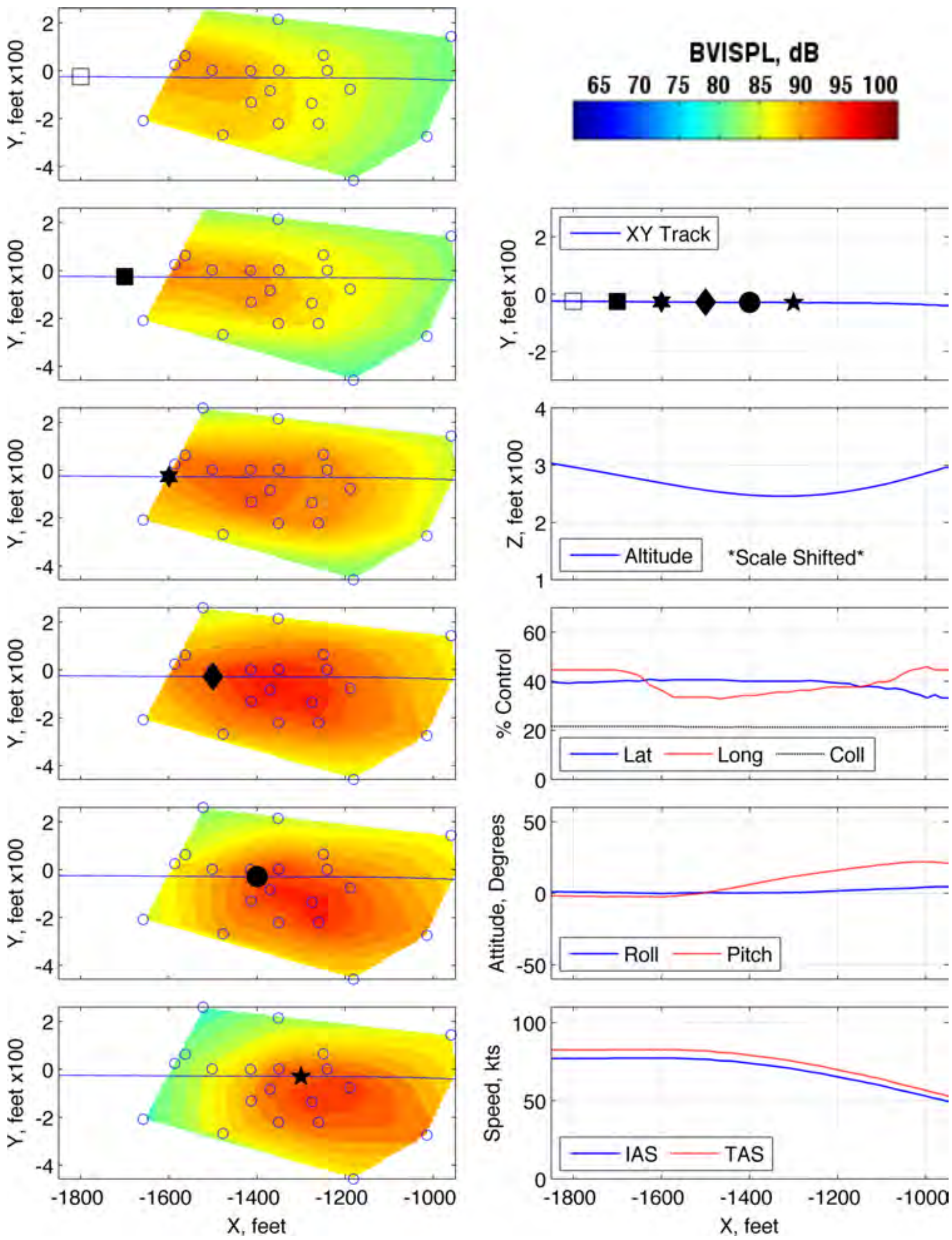

Figure 192: Maneuver condition D21, 80 KIAS, -9° , fast cyclic pitch up, run number 285492

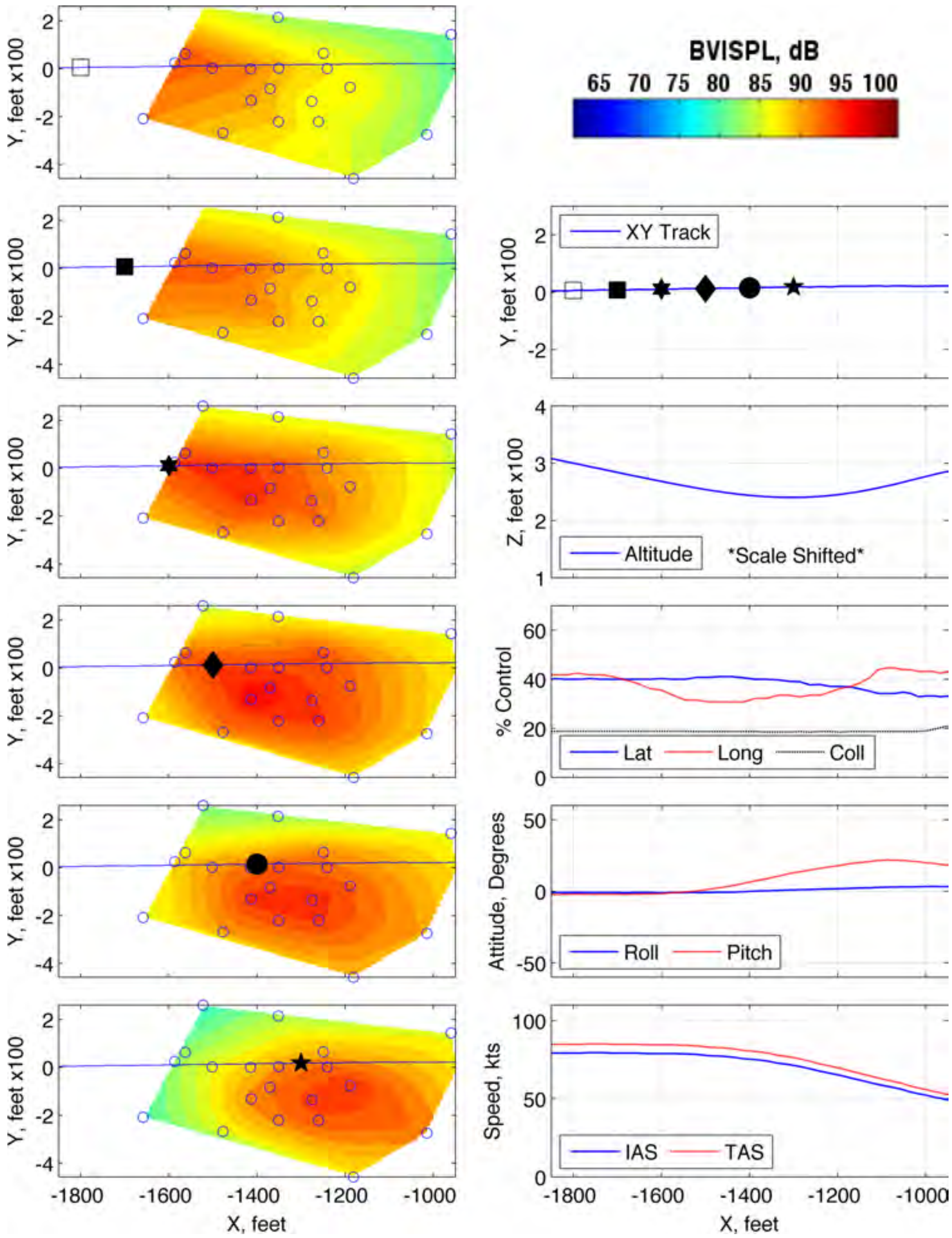

Figure 193: Maneuver condition D21, 80 KIAS, -9° , fast cyclic pitch up, run number 285493

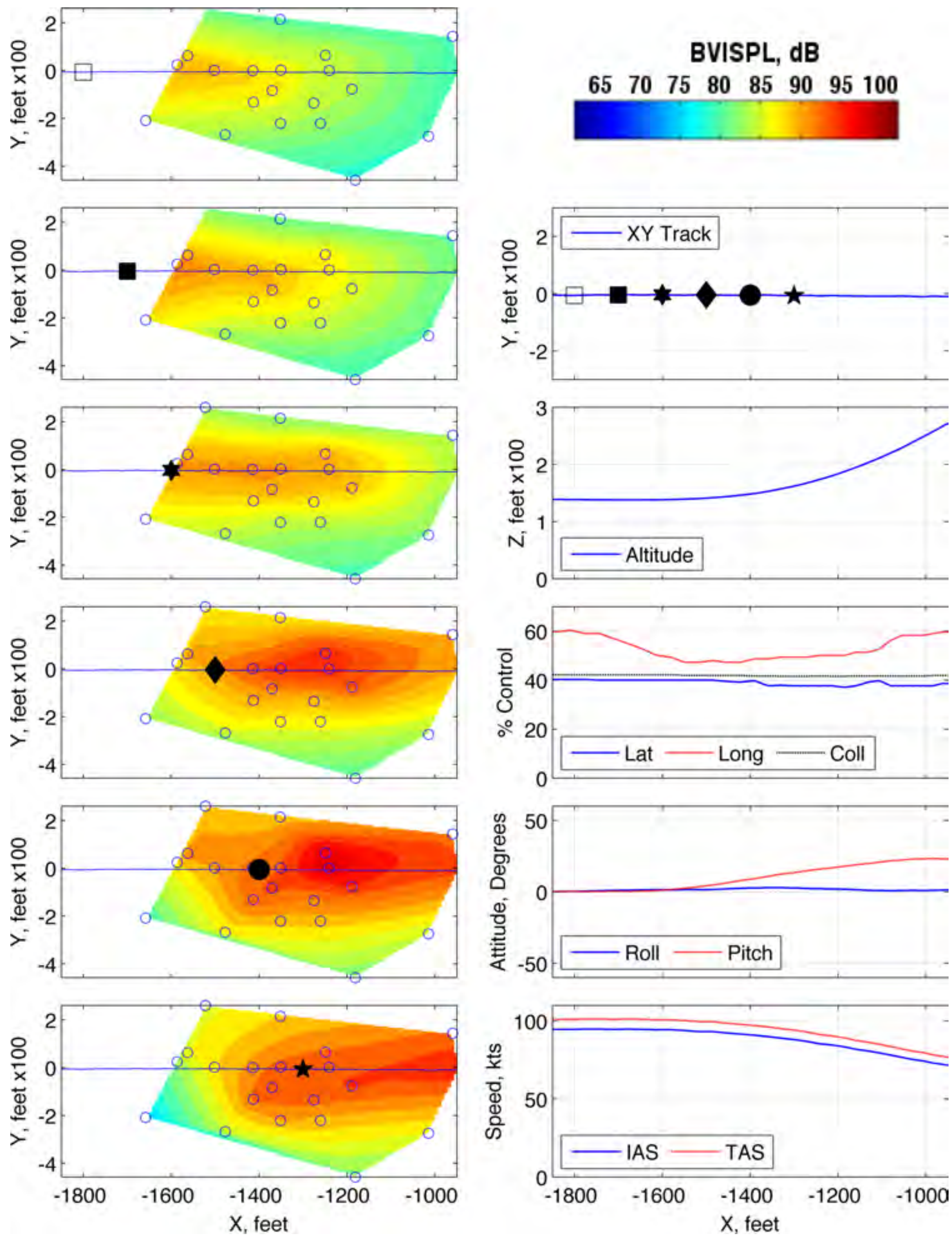

Figure 194: Maneuver condition D22, 100 KIAS, level, medium cyclic pitch up, run number 287526

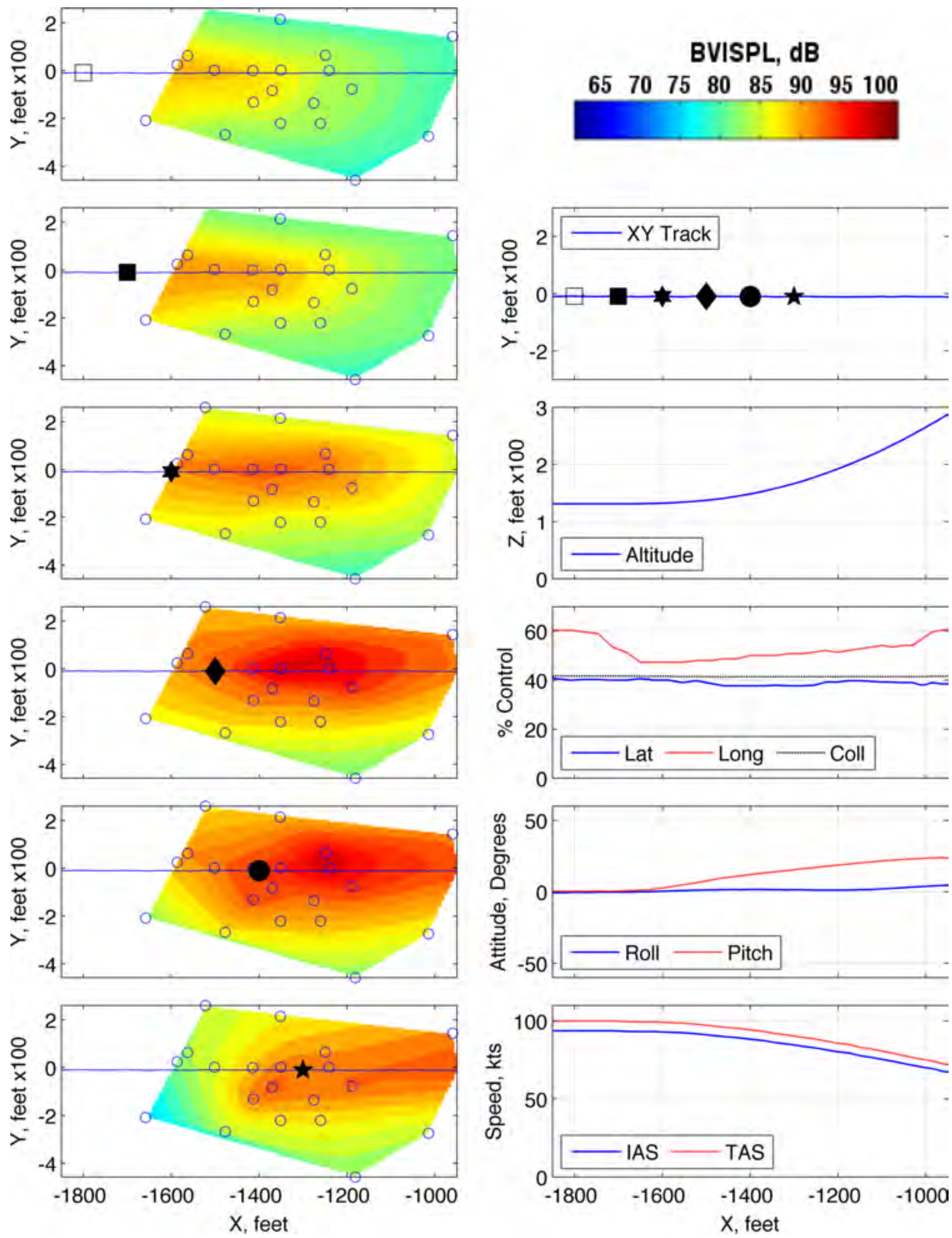

Figure 195: Maneuver condition D22, 100 KIAS, level, medium cyclic pitch up, run number 287527

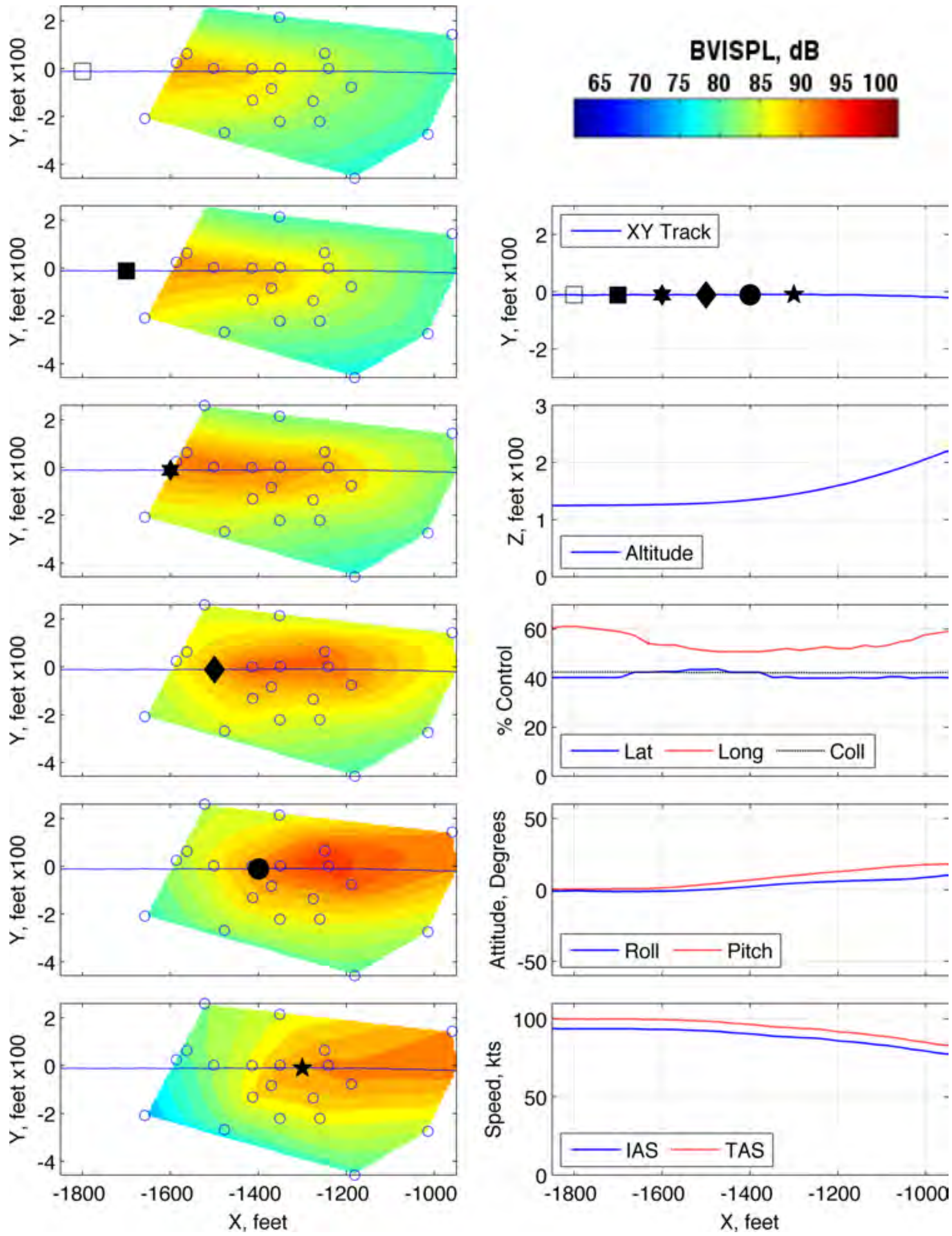

Figure 196: Maneuver condition D22, 100 KIAS, level, medium cyclic pitch up, run number 287528

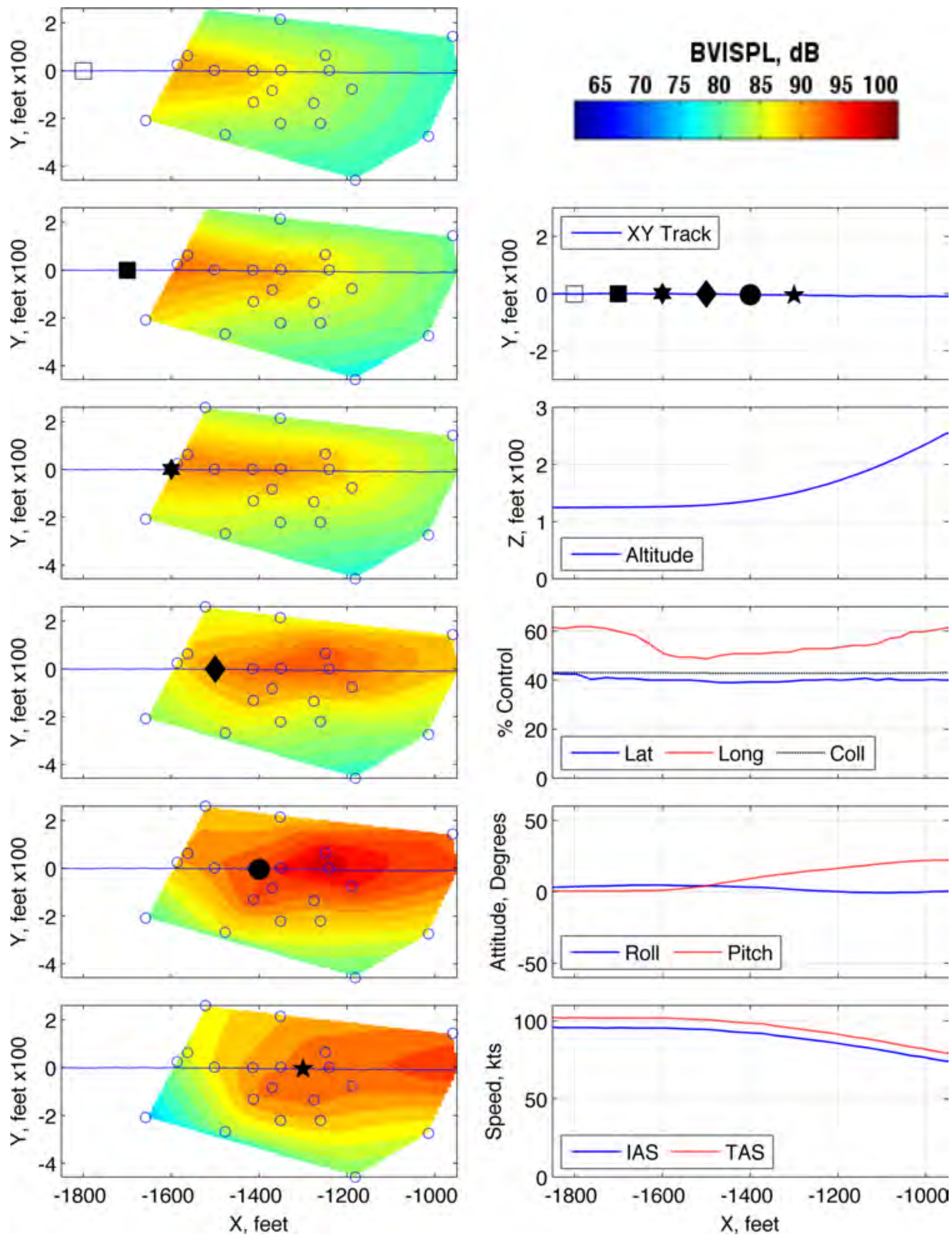

Figure 197: Maneuver condition D23, 100 KIAS, level, fast cyclic pitch up, run number 287529

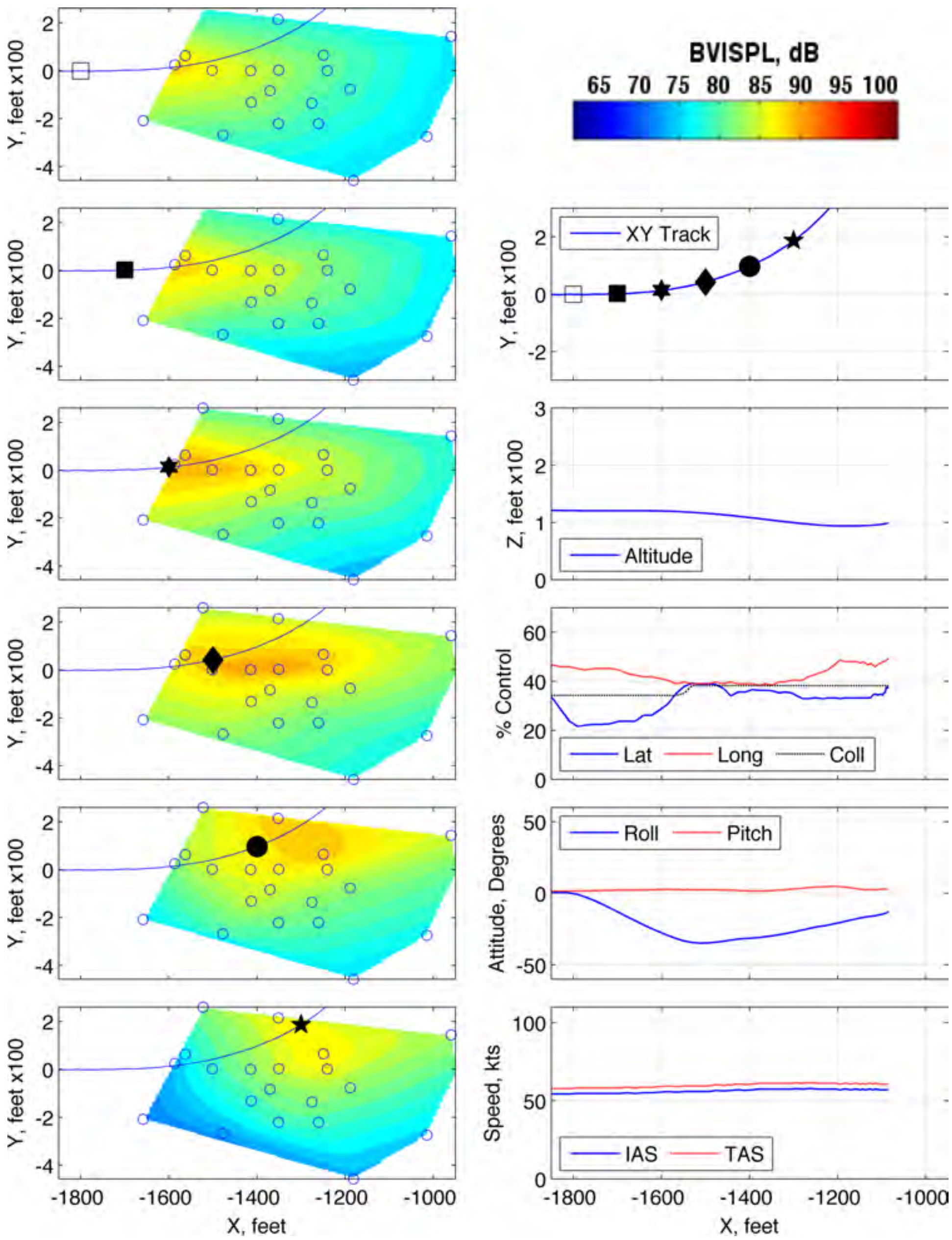

Figure 198: Maneuver condition R3, 60 KIAS, level, fast cyclic roll left, run number 285465

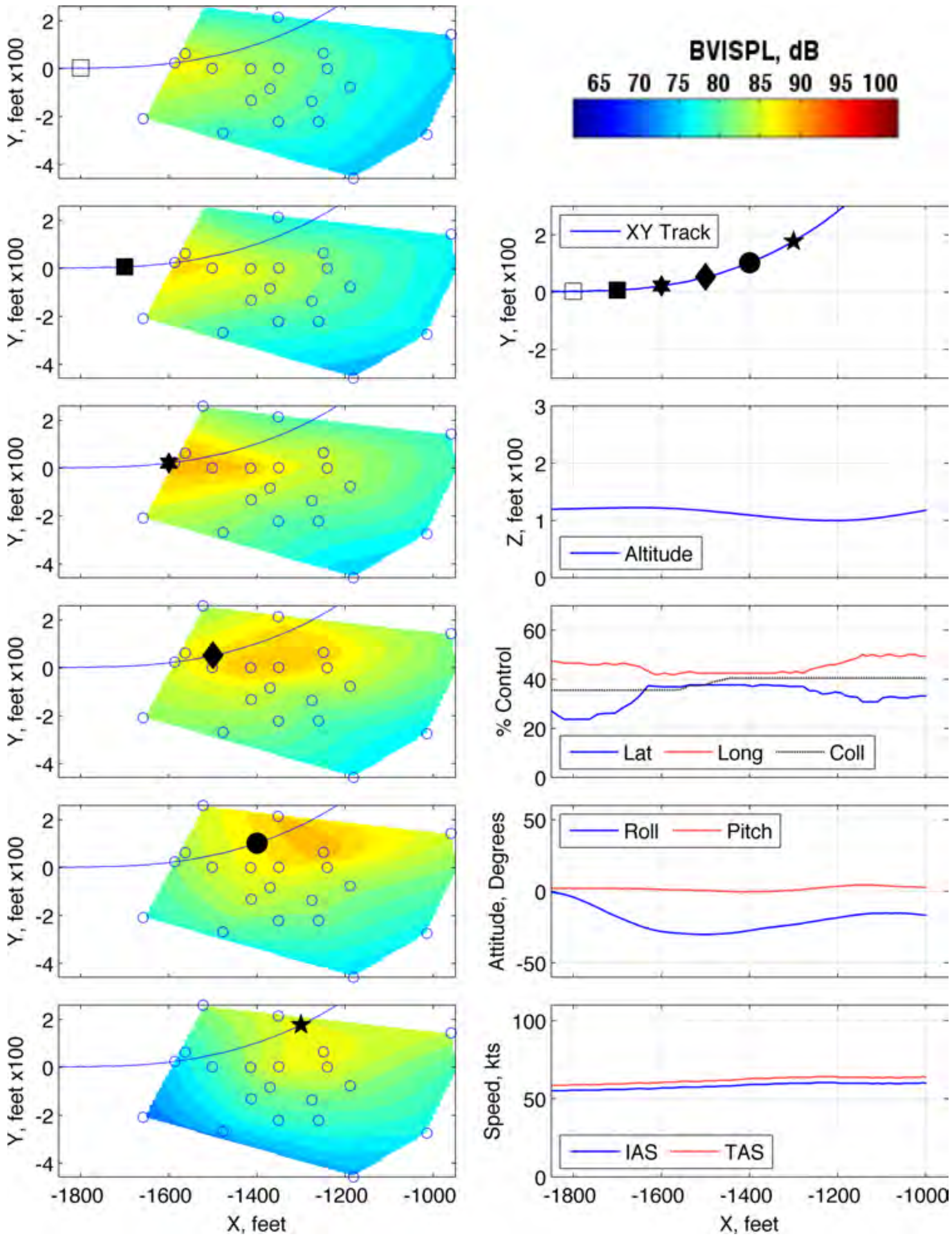

Figure 199: Maneuver condition R3, 60 KIAS, level, fast cyclic roll left, run number 285466

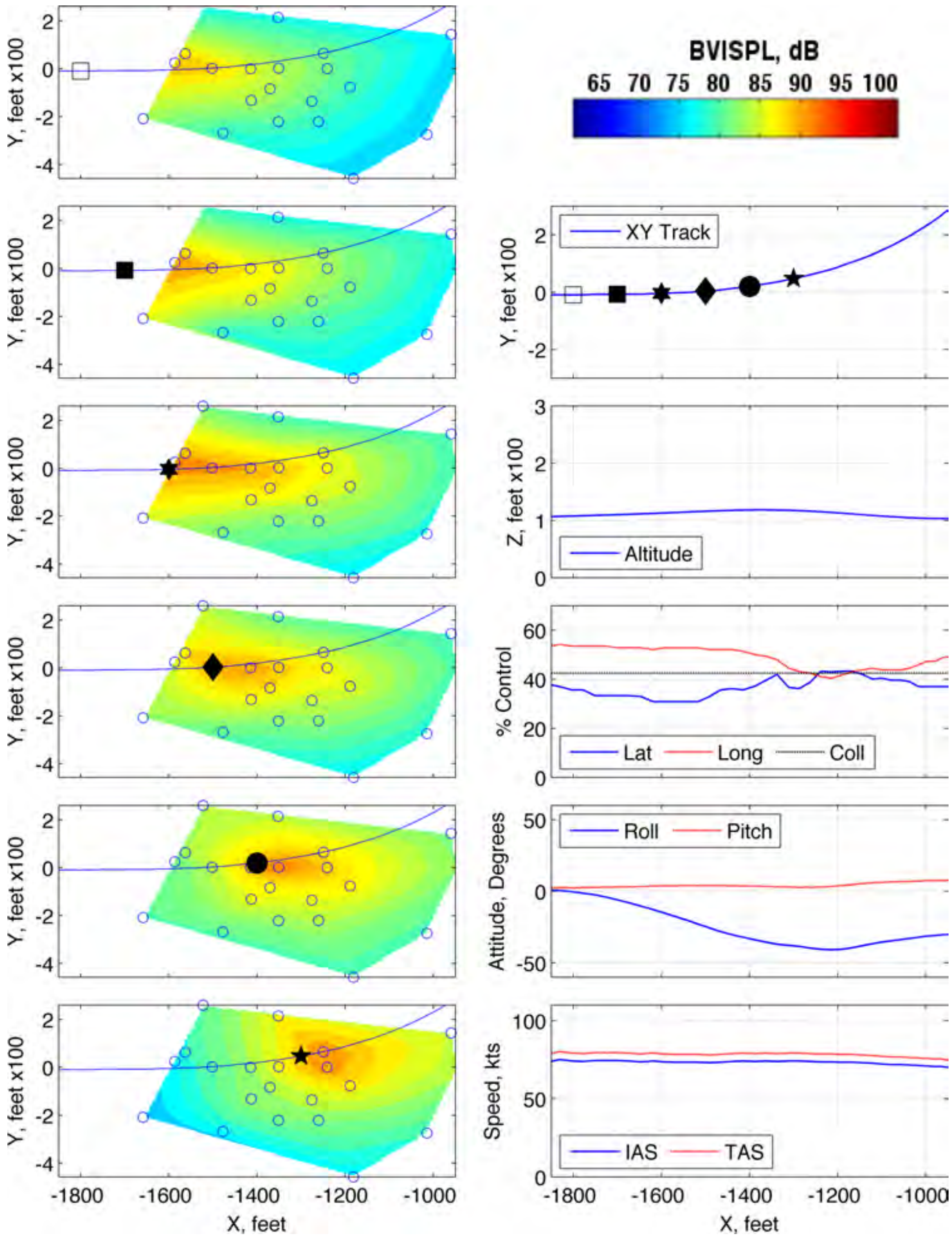

Figure 200: Maneuver condition R4, 80 KIAS, level, slow cyclic roll left, run number 280373

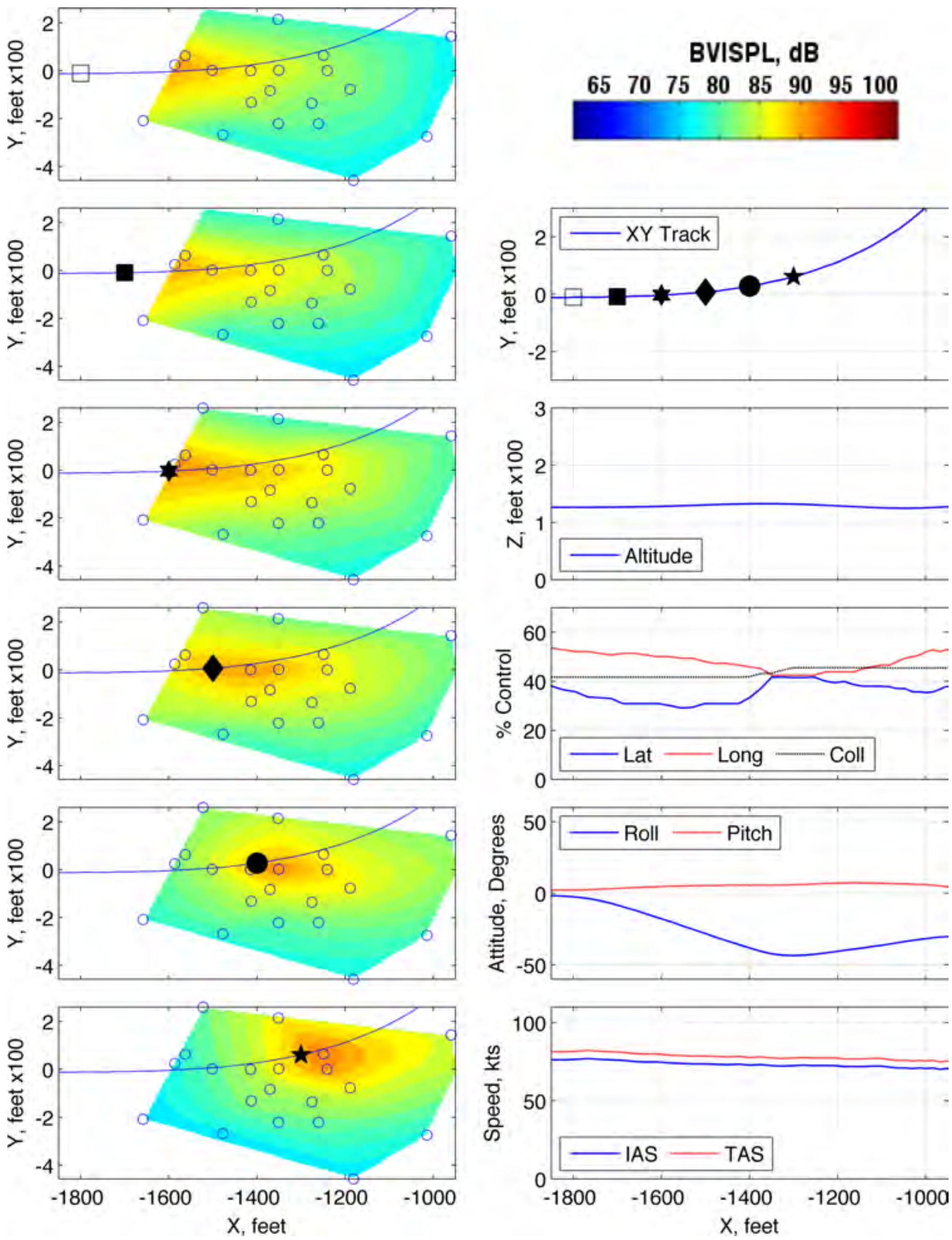

Figure 201: Maneuver condition R4, 80 KIAS, level, slow cyclic roll left, run number 280374

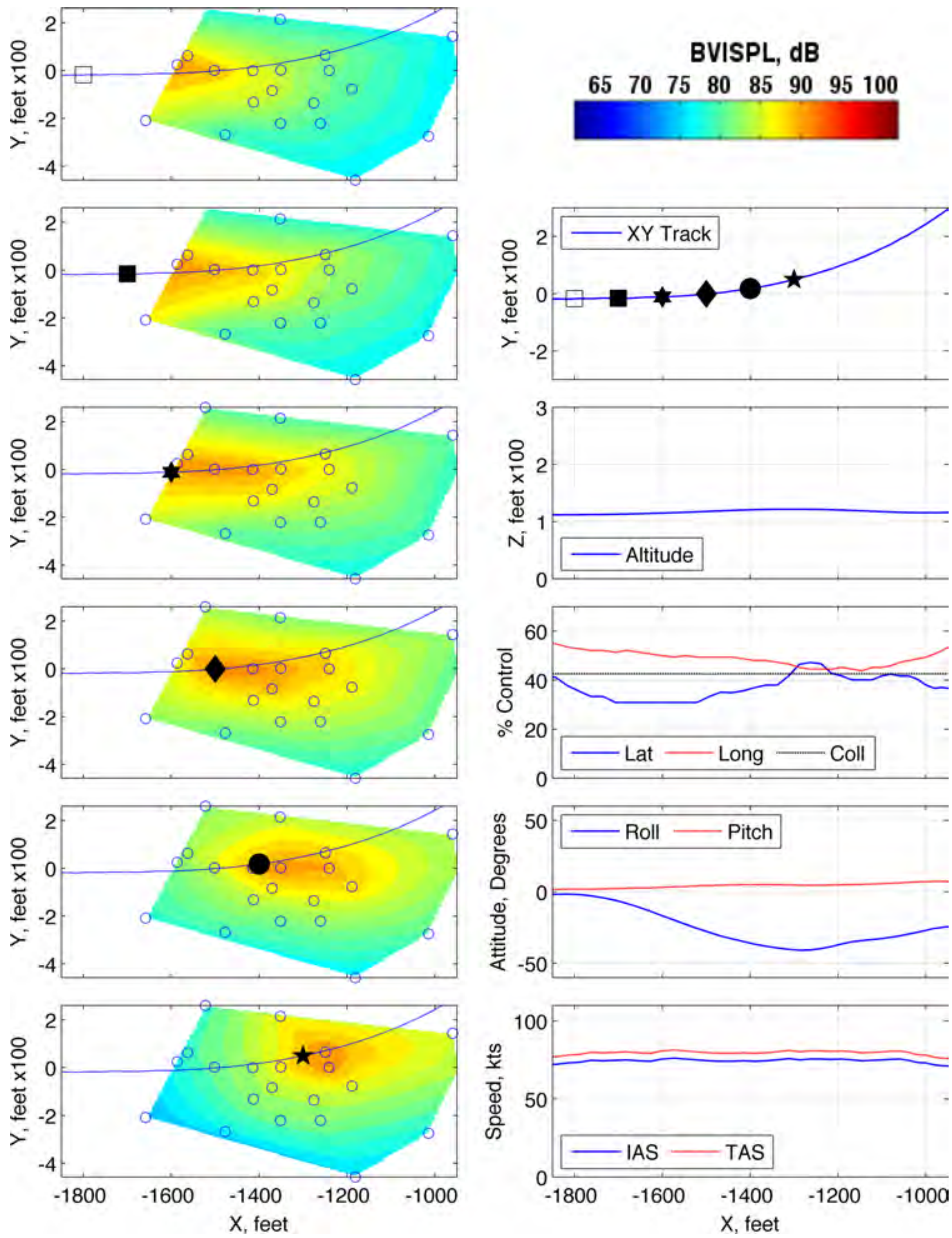

Figure 202: Maneuver condition R4, 80 KIAS, level, slow cyclic roll left, run number 280375

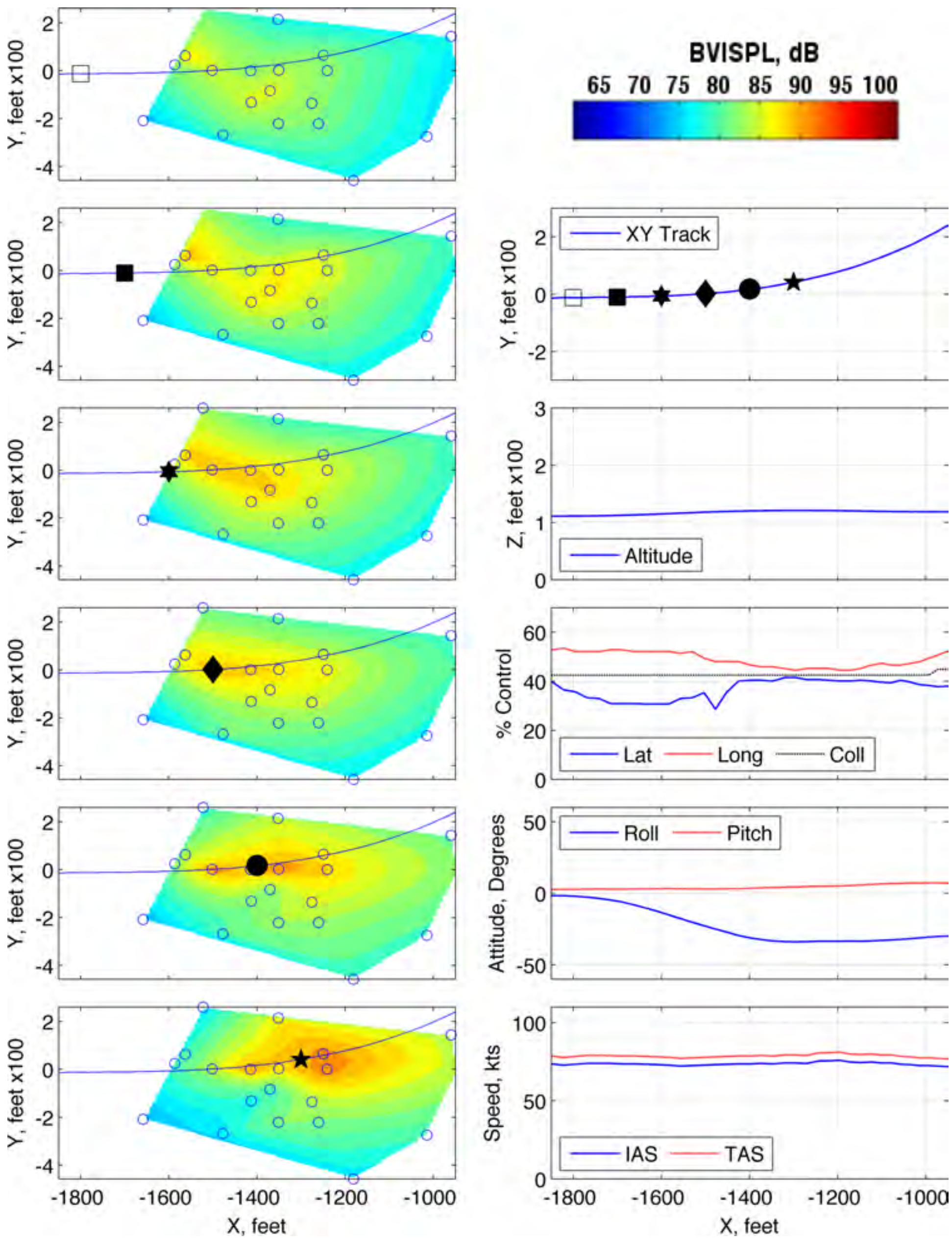

Figure 203: Maneuver condition R4, 80 KIAS, level, slow cyclic roll left, run number 280376

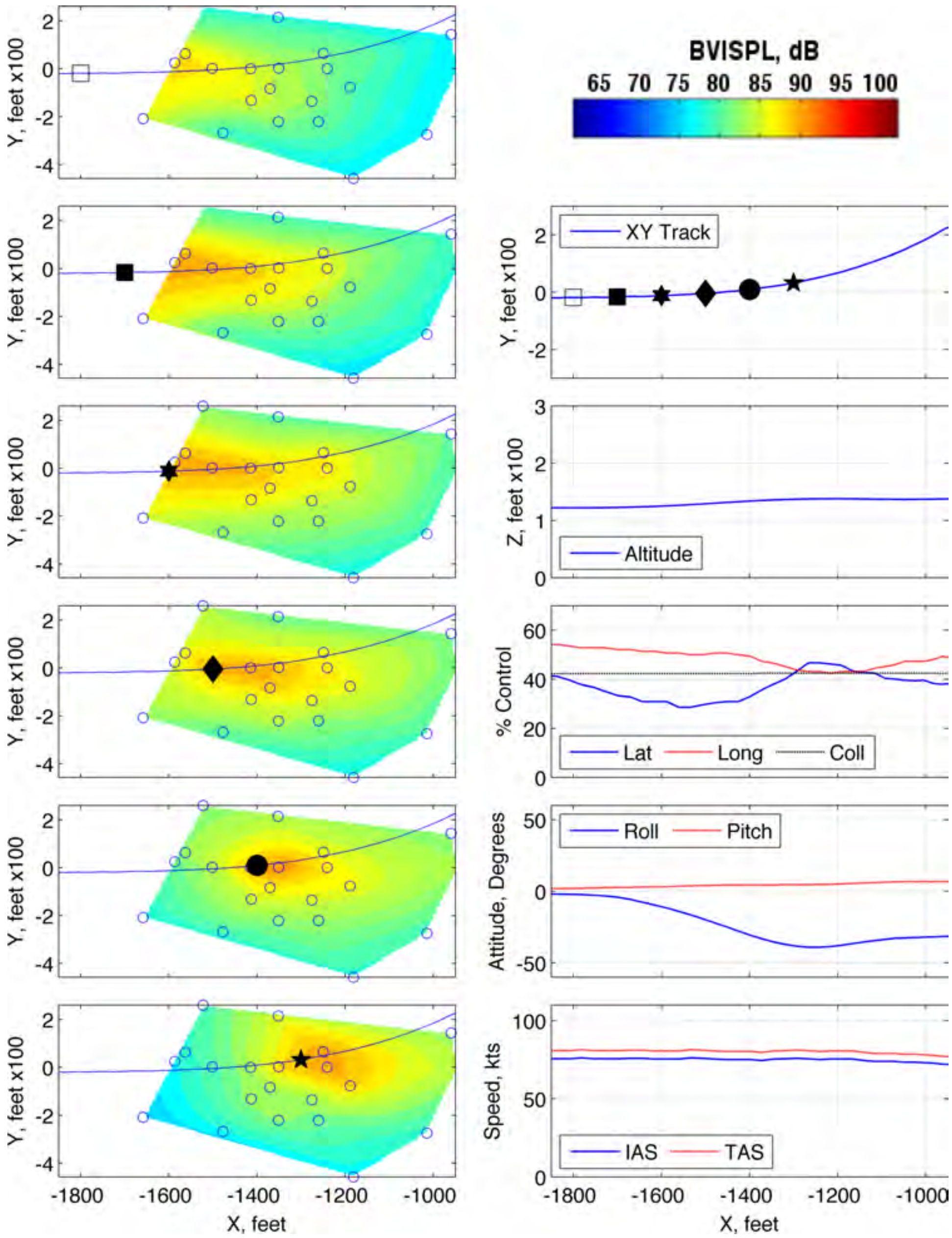

Figure 204: Maneuver condition R4, 80 KIAS, level, slow cyclic roll left, run number 280377

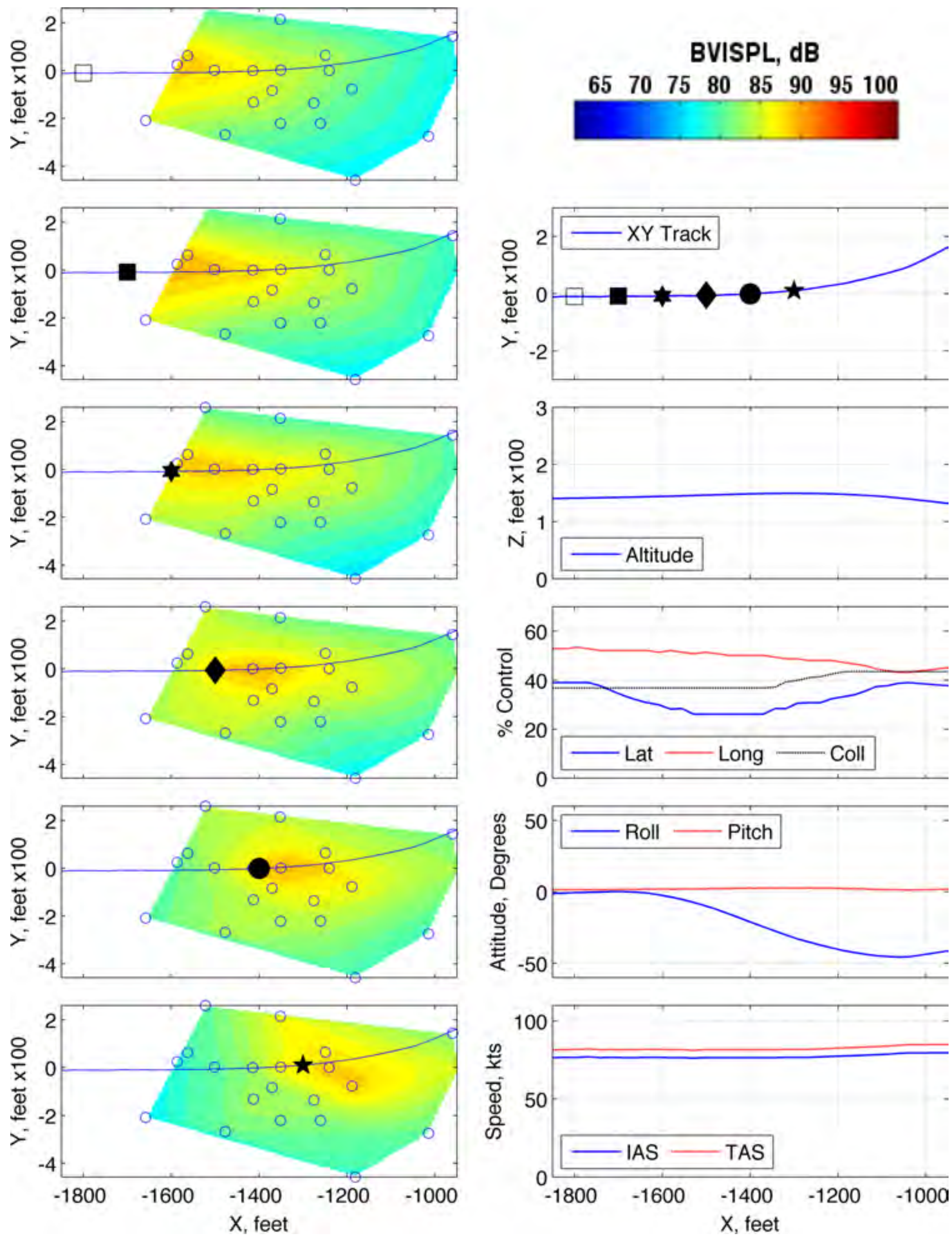

Figure 205: Maneuver condition R5, 80 KIAS, level, medium cyclic roll left, run number 285473

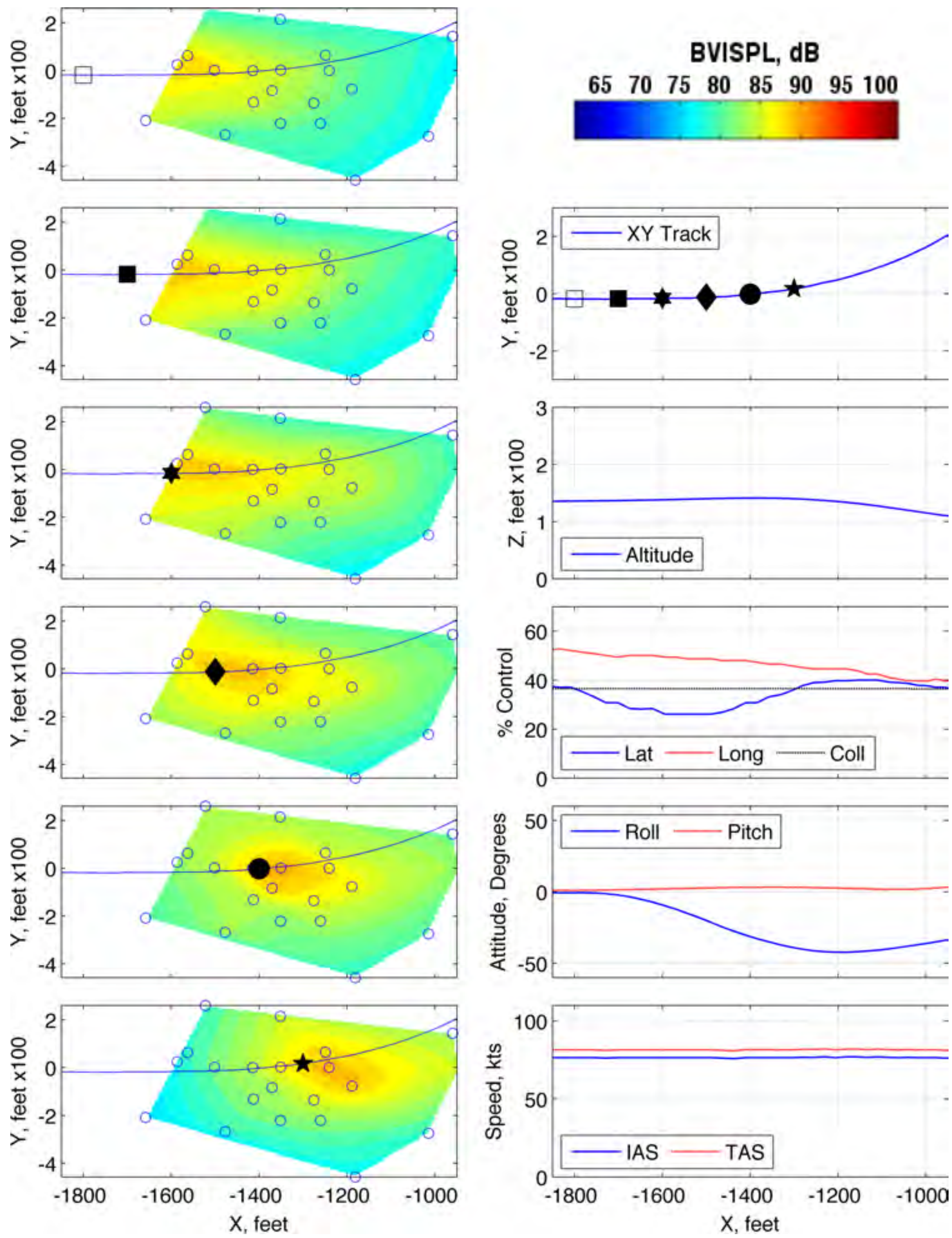

Figure 206: Maneuver condition R5, 80 KIAS, level, medium cyclic roll left, run number 285474

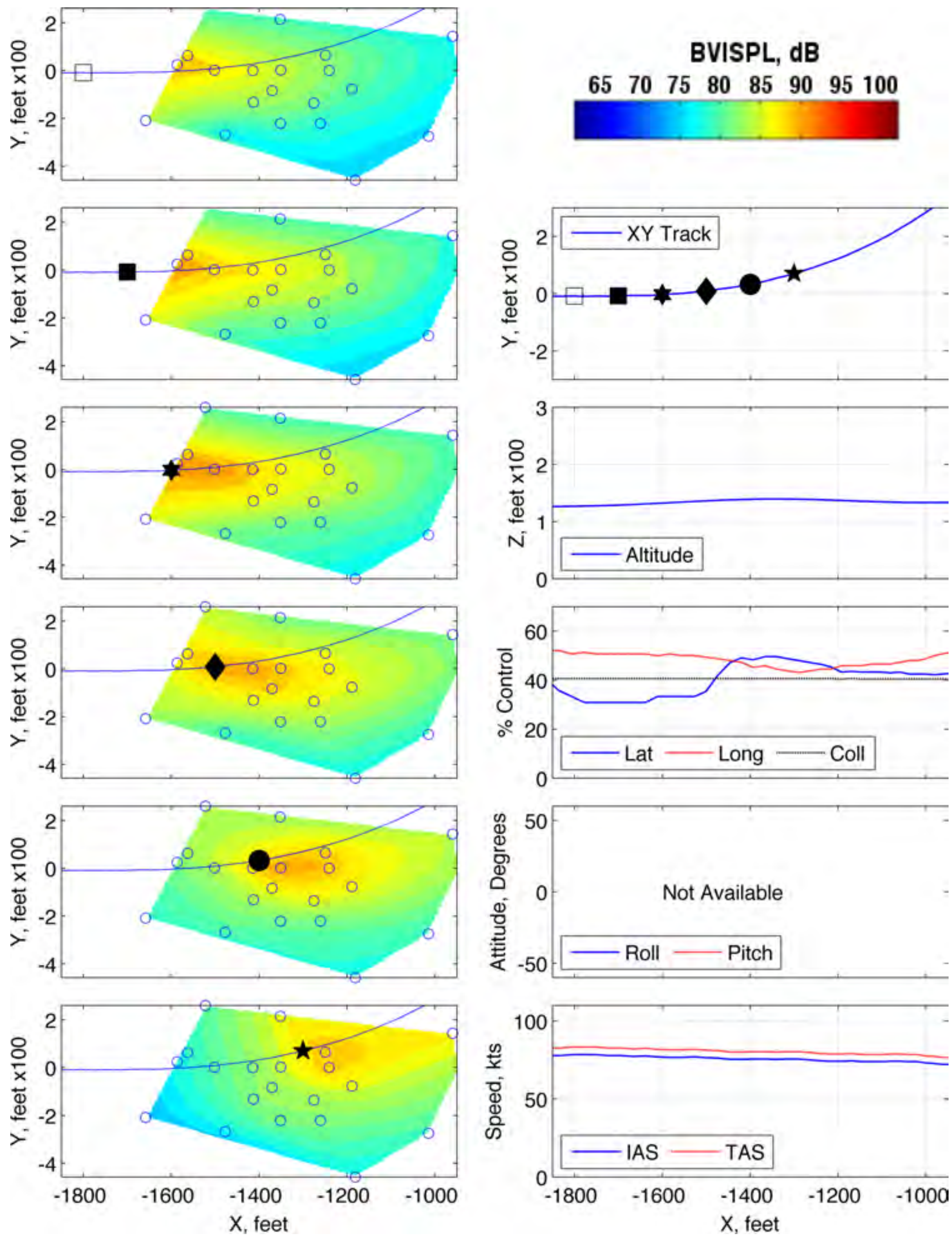

Figure 207: Maneuver condition R6, 80 KIAS, level, fast cyclic roll left, run number 280368

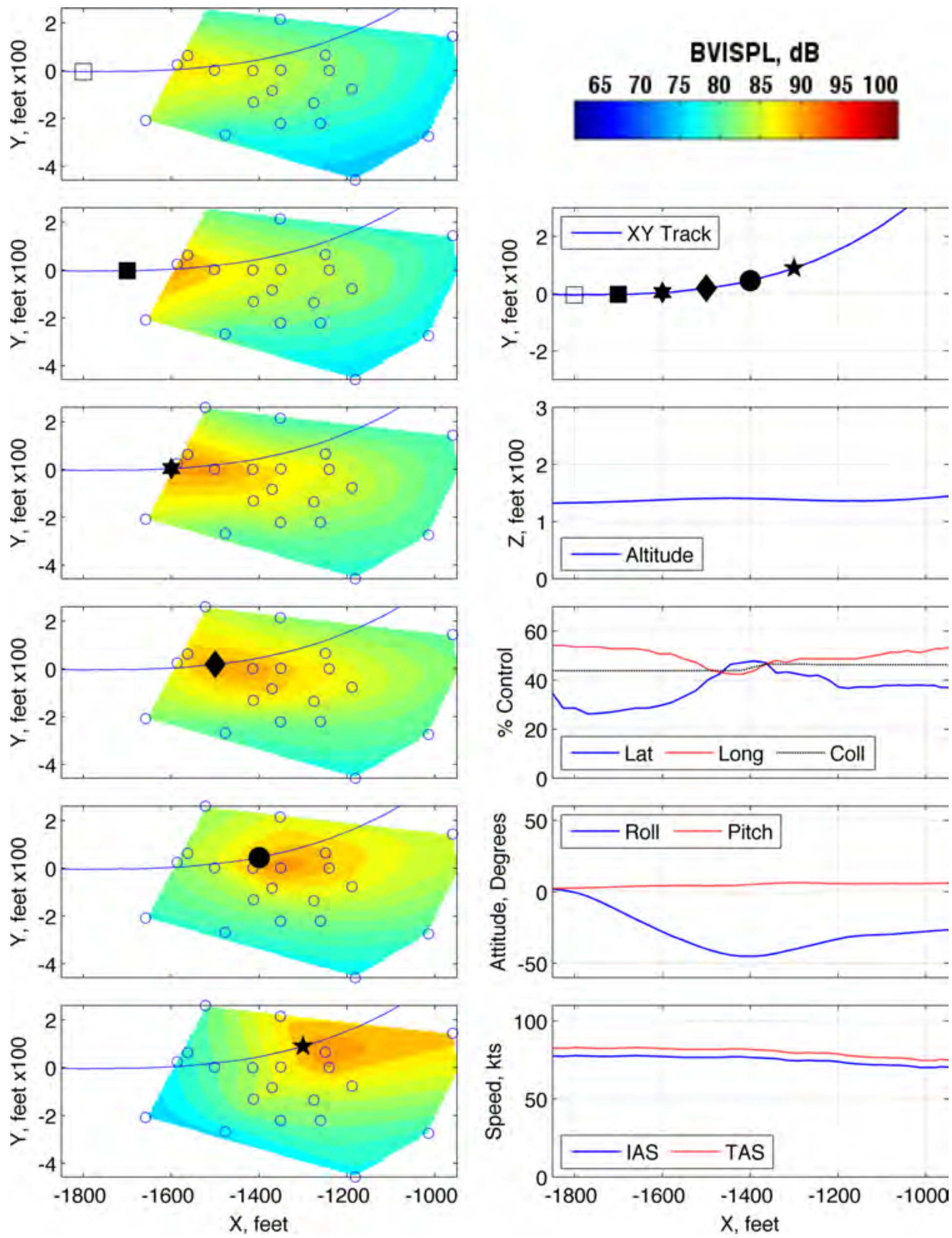

Figure 208: Maneuver condition R6, 80 KIAS, level, fast cyclic roll left, run number 280369

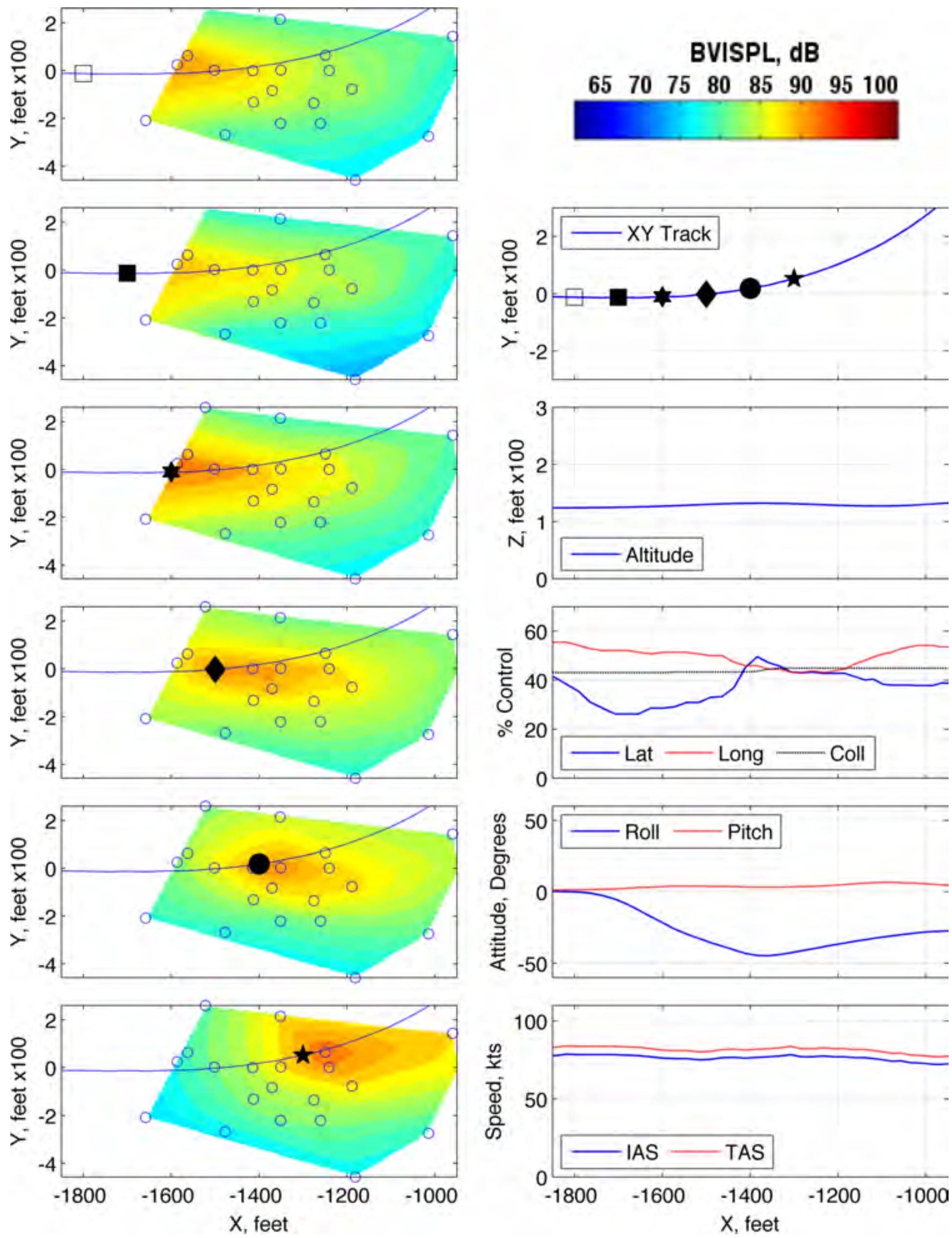

Figure 209: Maneuver condition R6, 80 KIAS, level, fast cyclic roll left, run number 280371

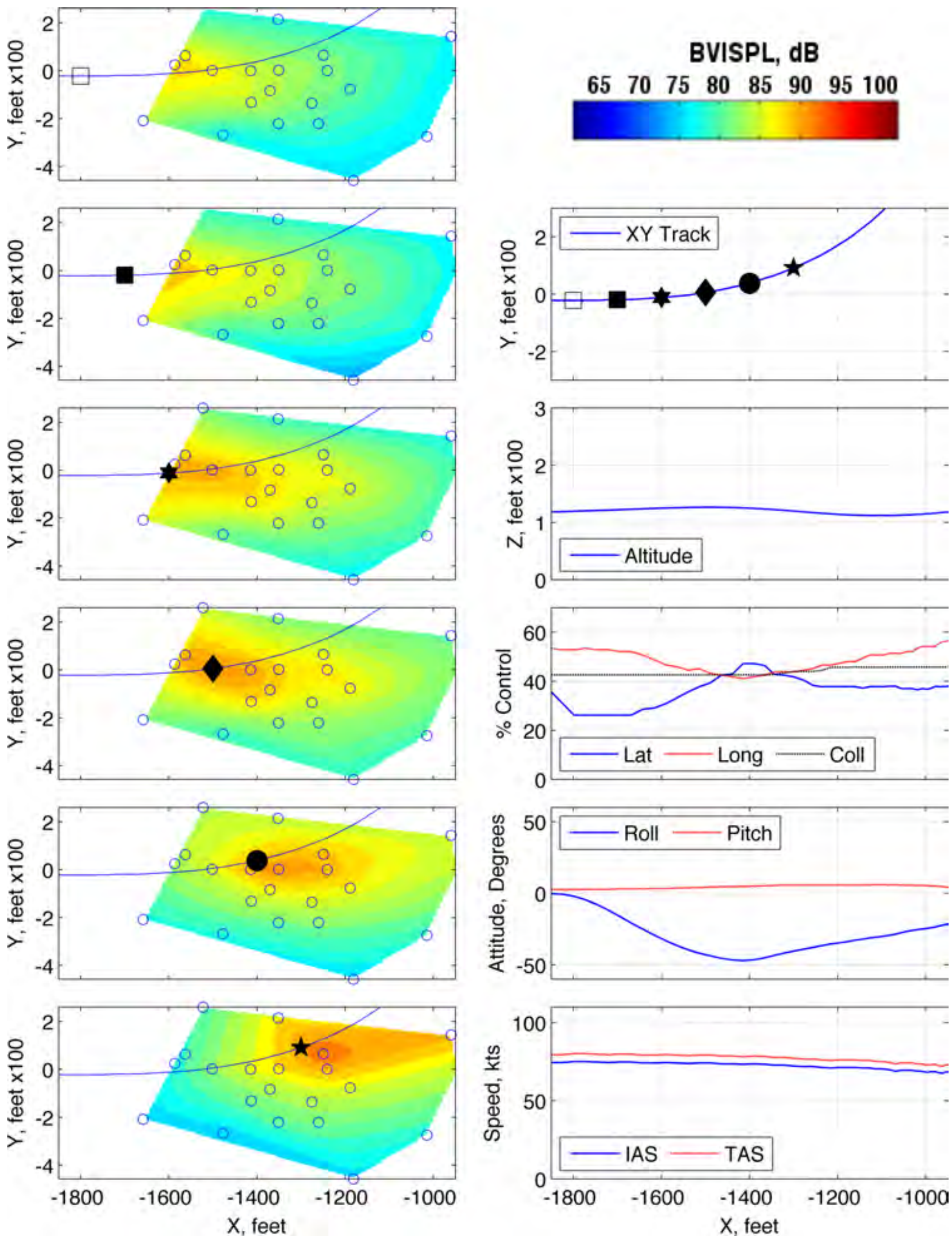

Figure 210: Maneuver condition R6, 80 KIAS, level, fast cyclic roll left, run number 280372

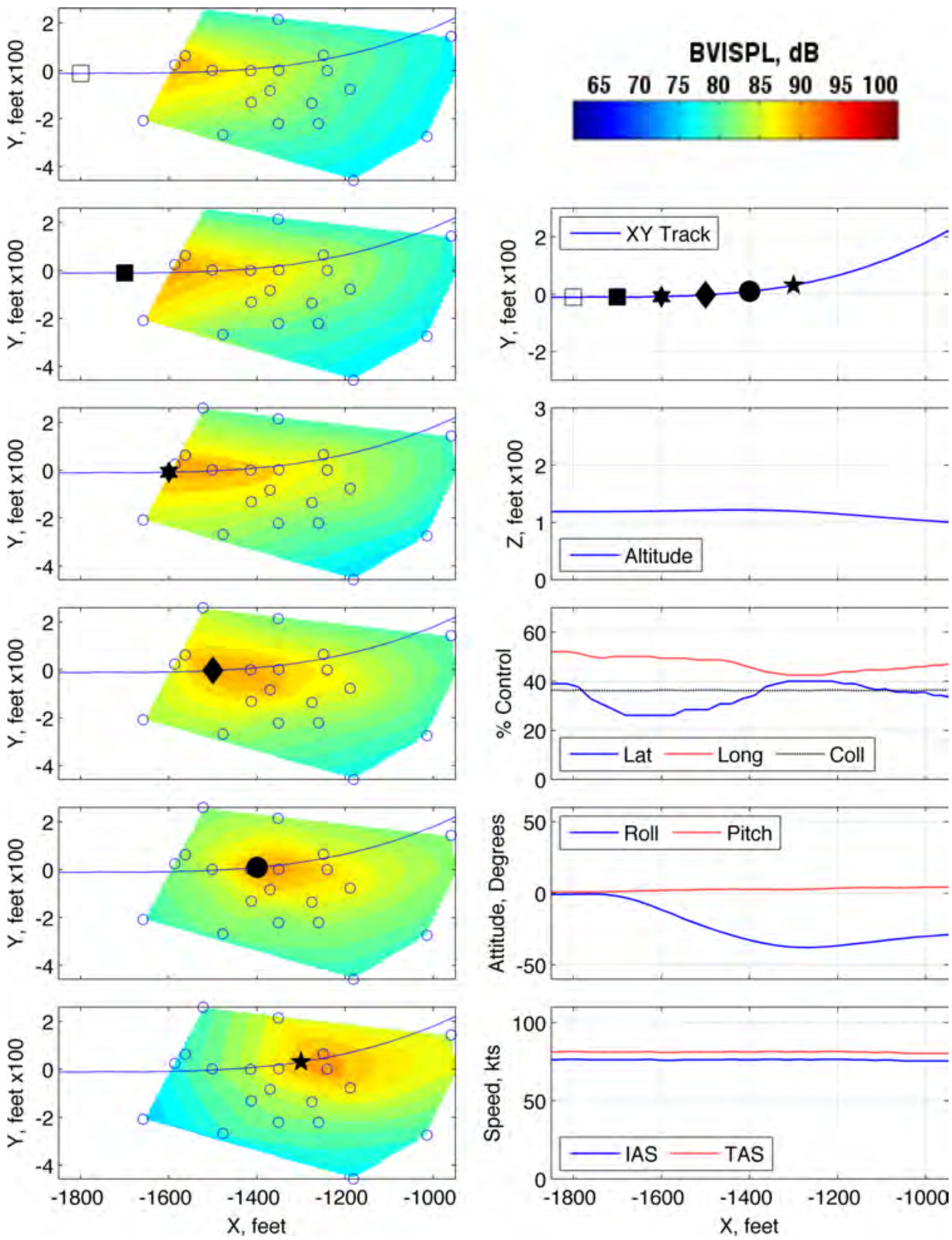

Figure 211: Maneuver condition R6, 80 KIAS, level, fast cyclic roll left, run number 285471

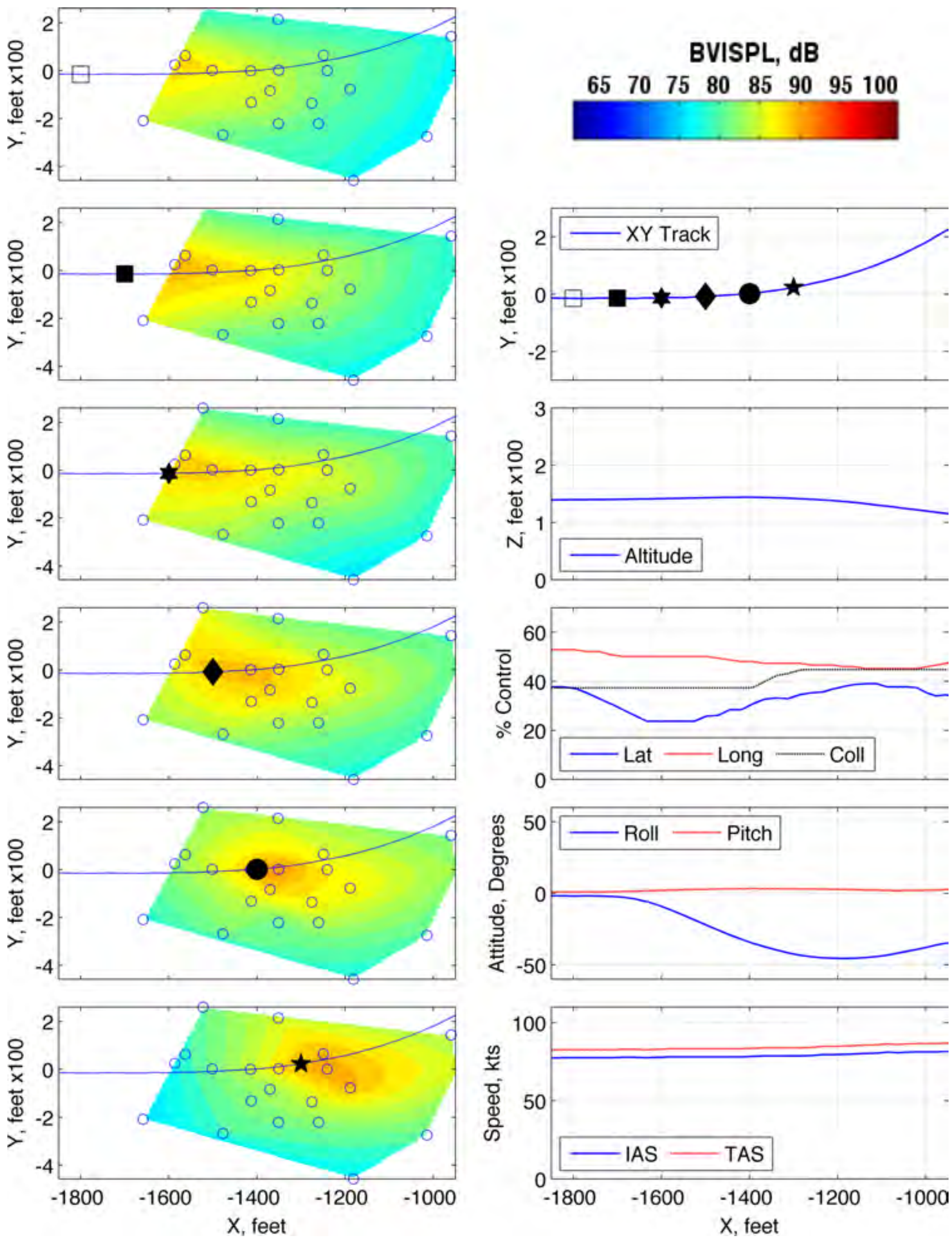

Figure 212: Maneuver condition R6, 80 KIAS, level, fast cyclic roll left, run number 285472

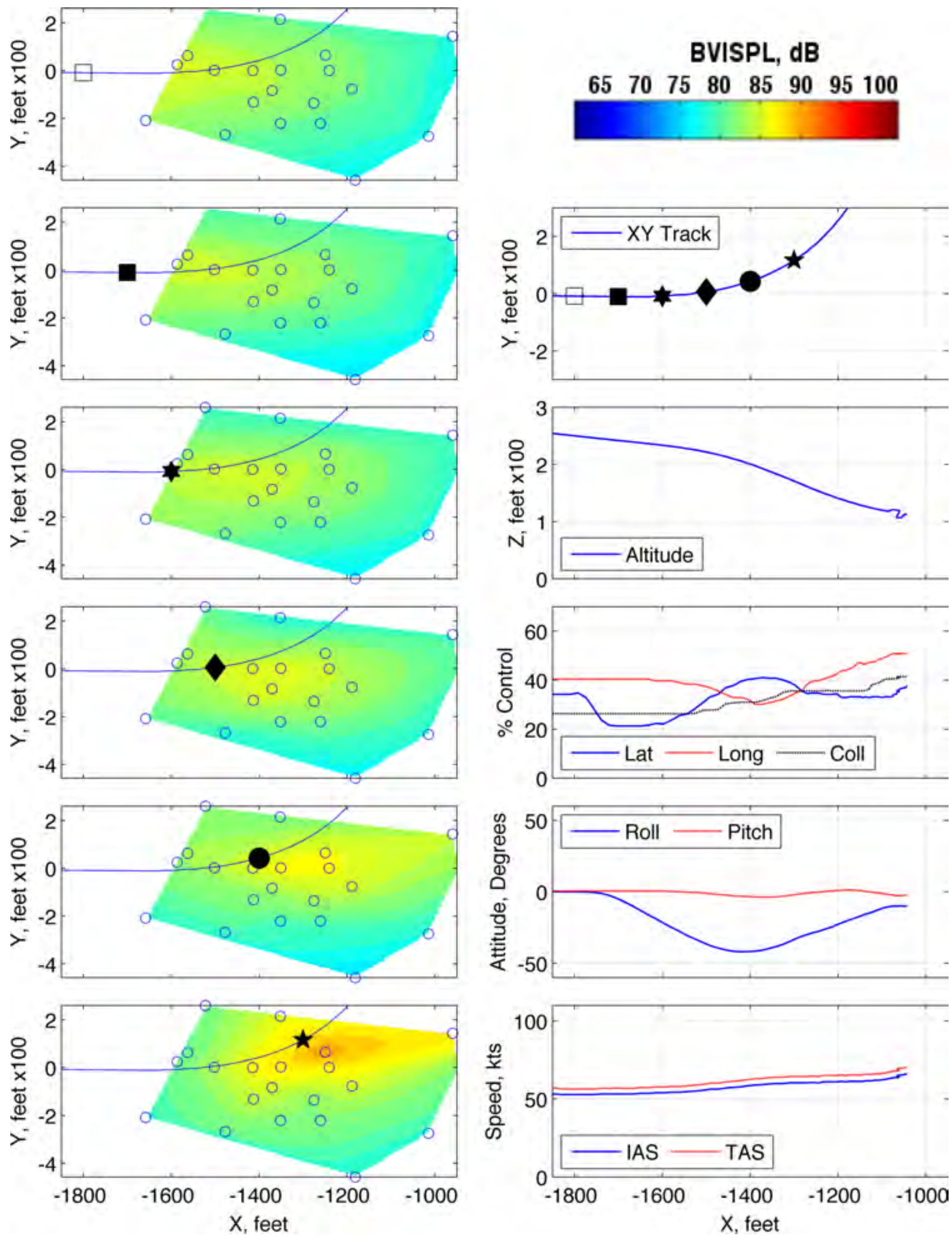

Figure 213: Maneuver condition R9, 60 KIAS, -6° , fast cyclic roll left, run number 285488

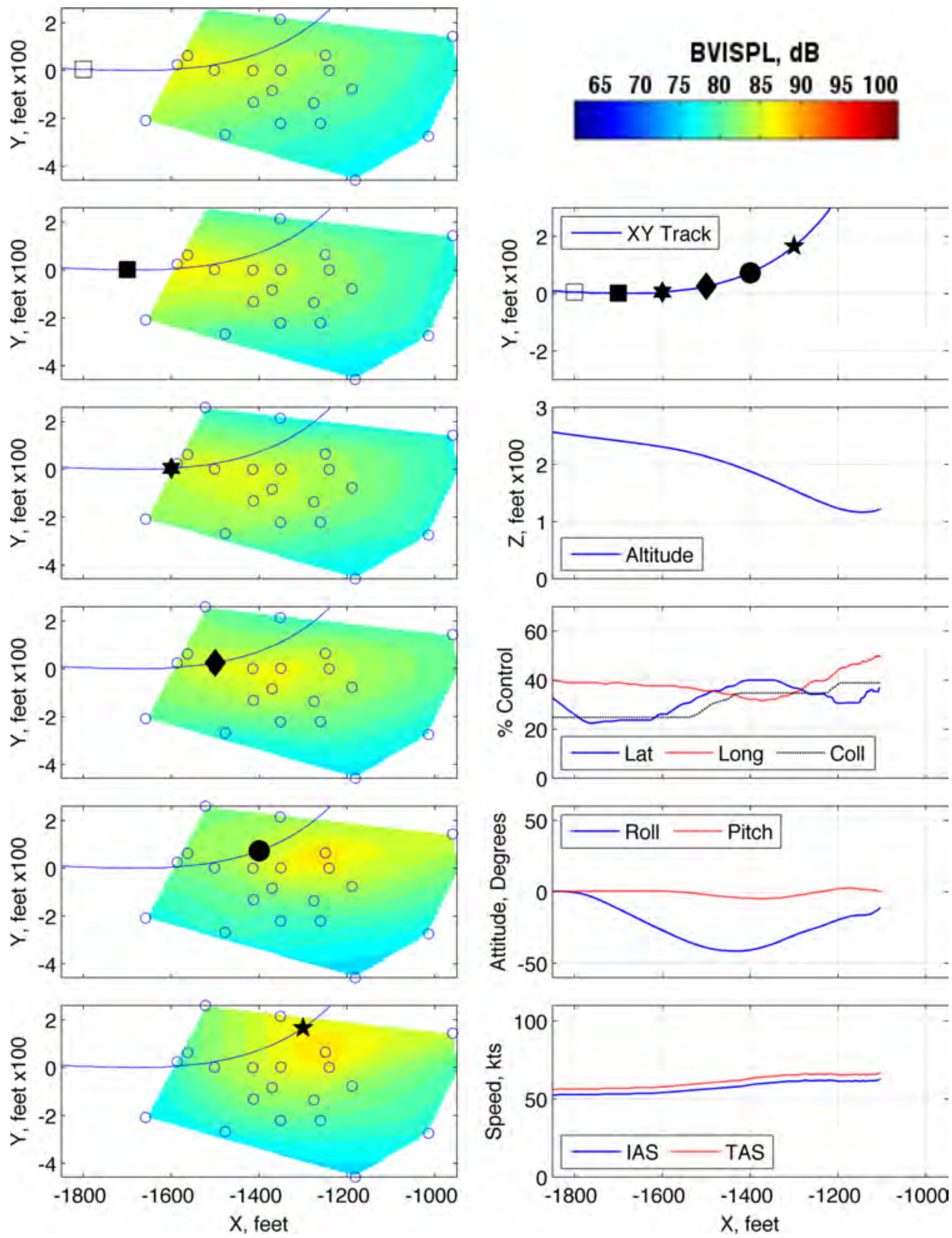

Figure 214: Maneuver condition R9, 60 KIAS, -6° , fast cyclic roll left, run number 285489

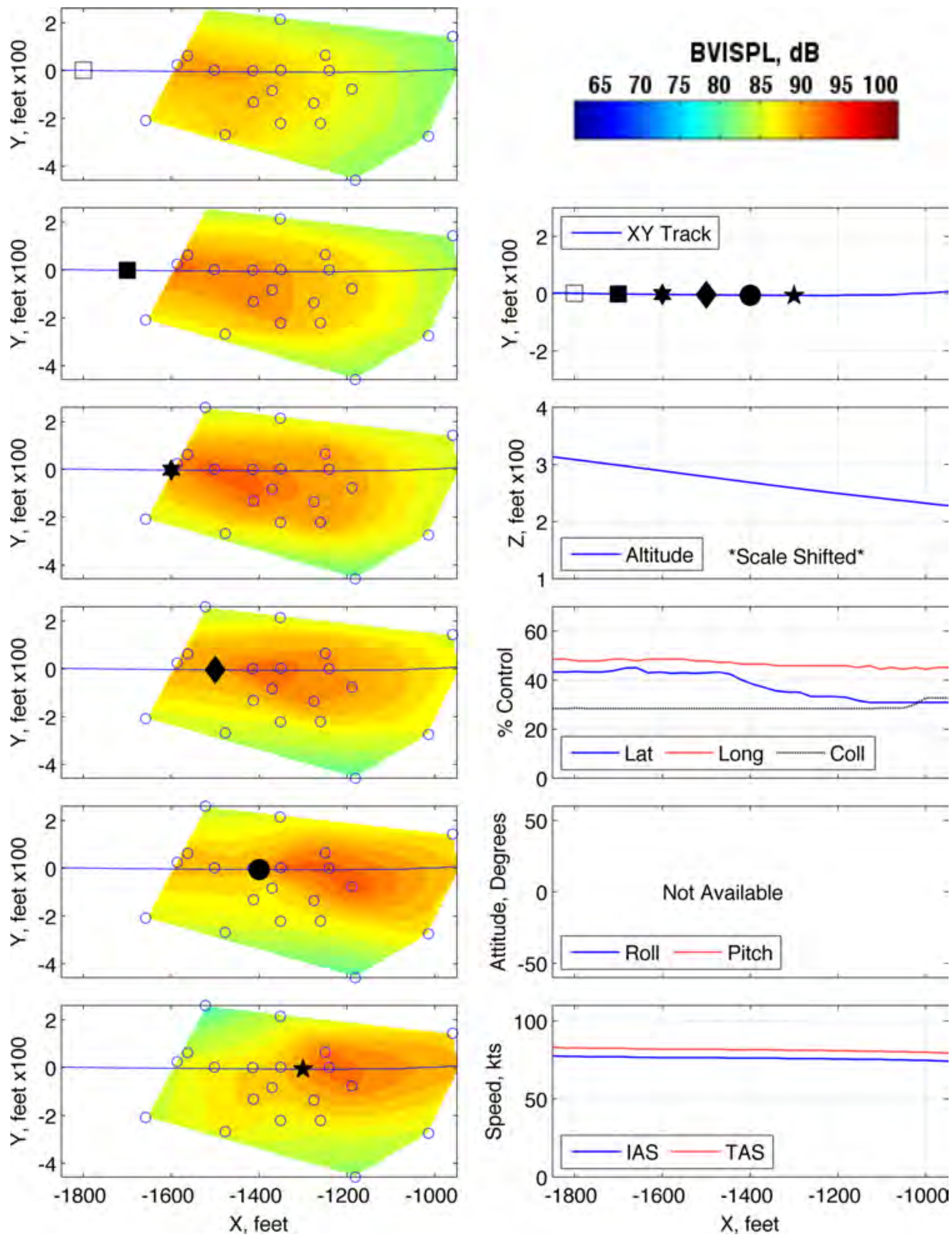

Figure 215: Maneuver condition R10, 80 KIAS, -6° , slow cyclic roll left, run number 278316

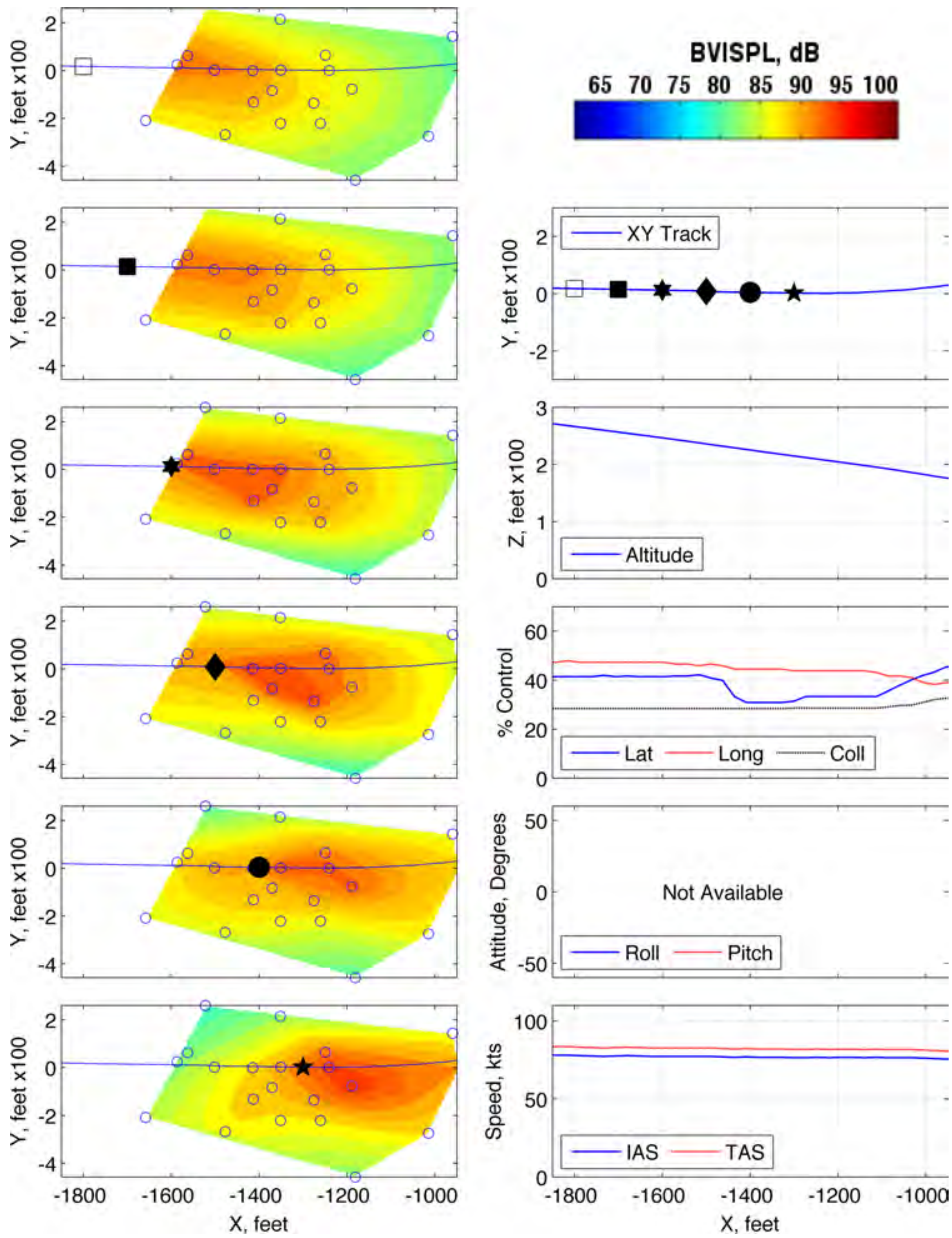

Figure 216: Maneuver condition R10, 80 KIAS, -6° , slow cyclic roll left, run number 278317

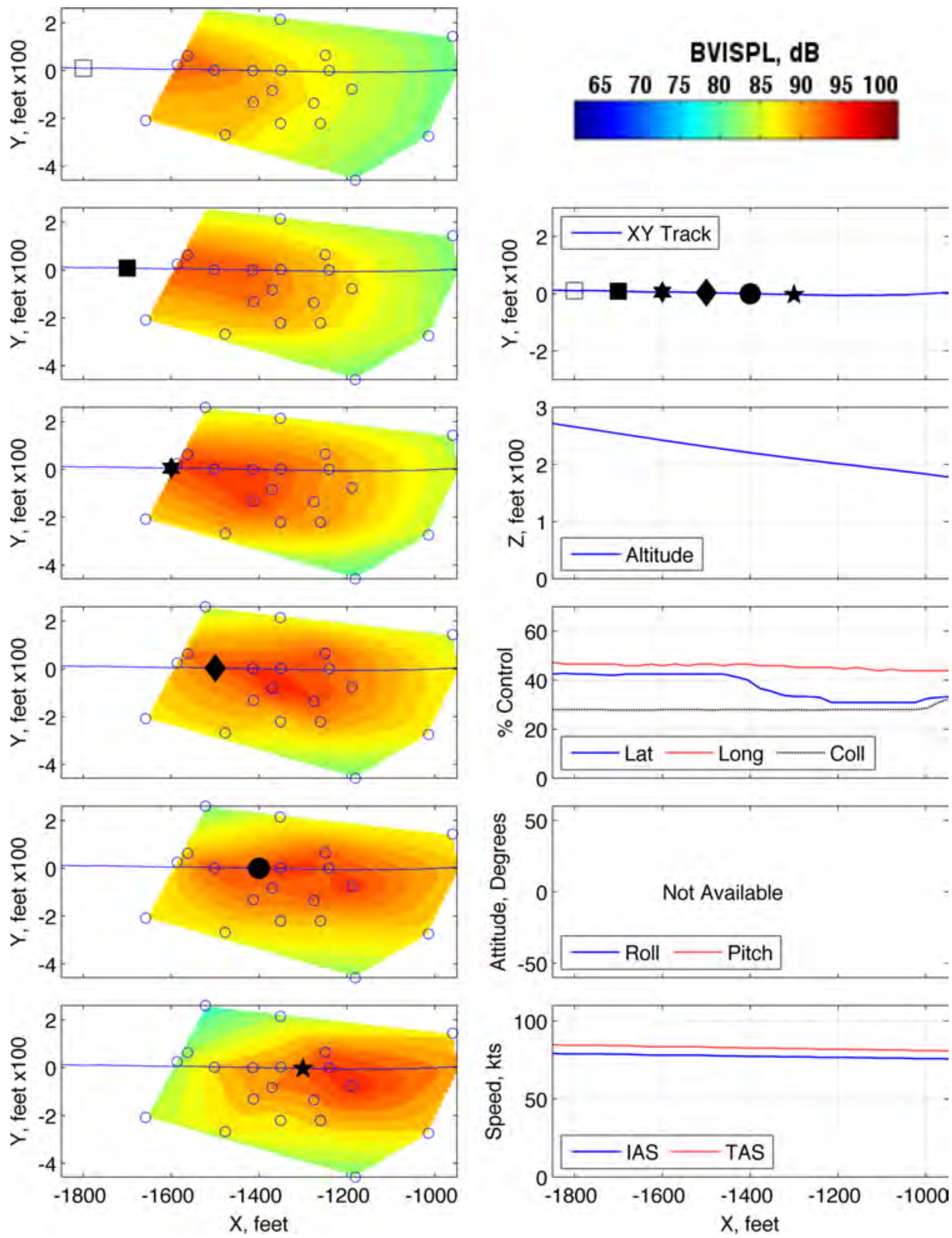

Figure 217: Maneuver condition R10, 80 KIAS, -6° , slow cyclic roll left, run number 278318

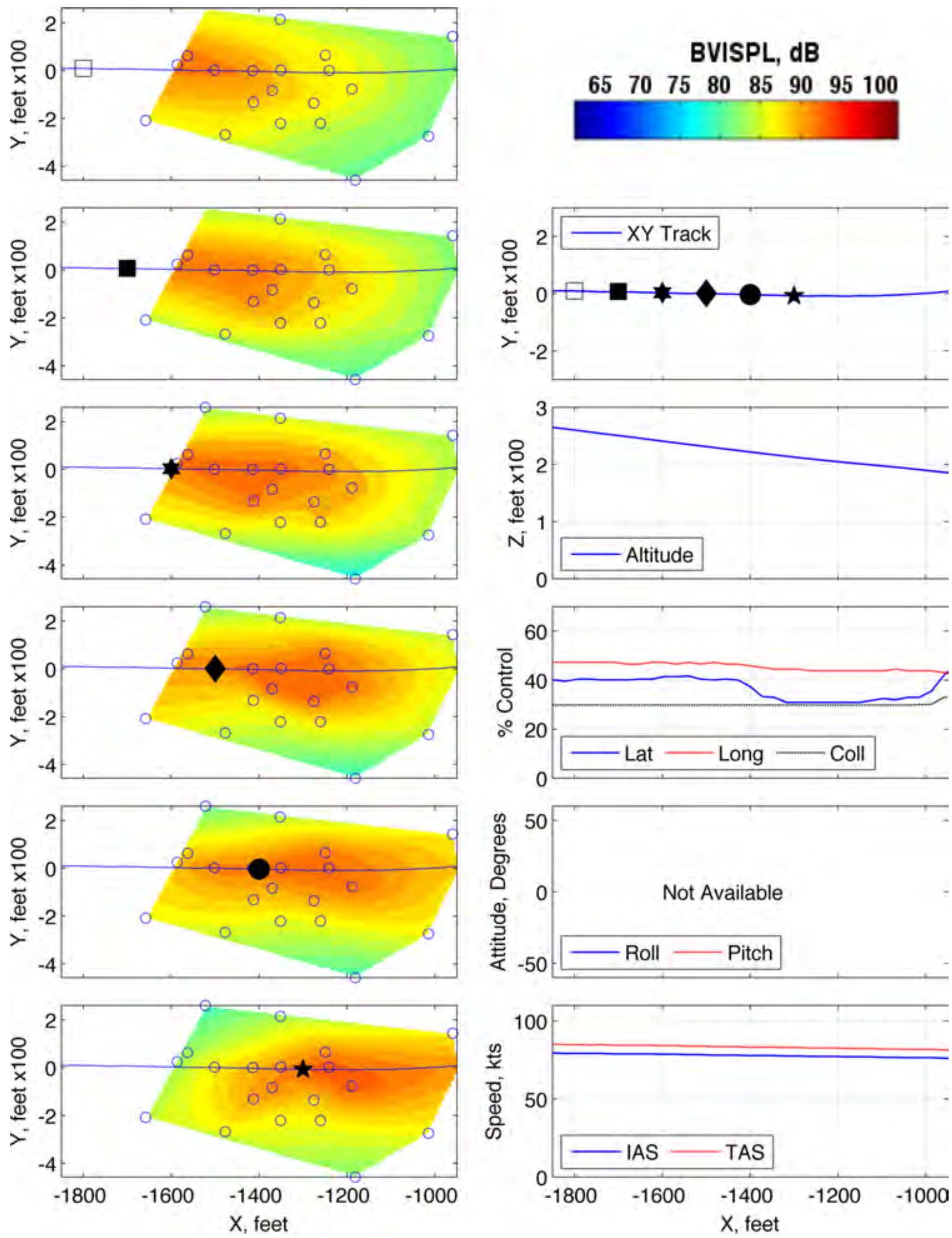

Figure 218: Maneuver condition R10, 80 KIAS, -6° , slow cyclic roll left, run number 278319

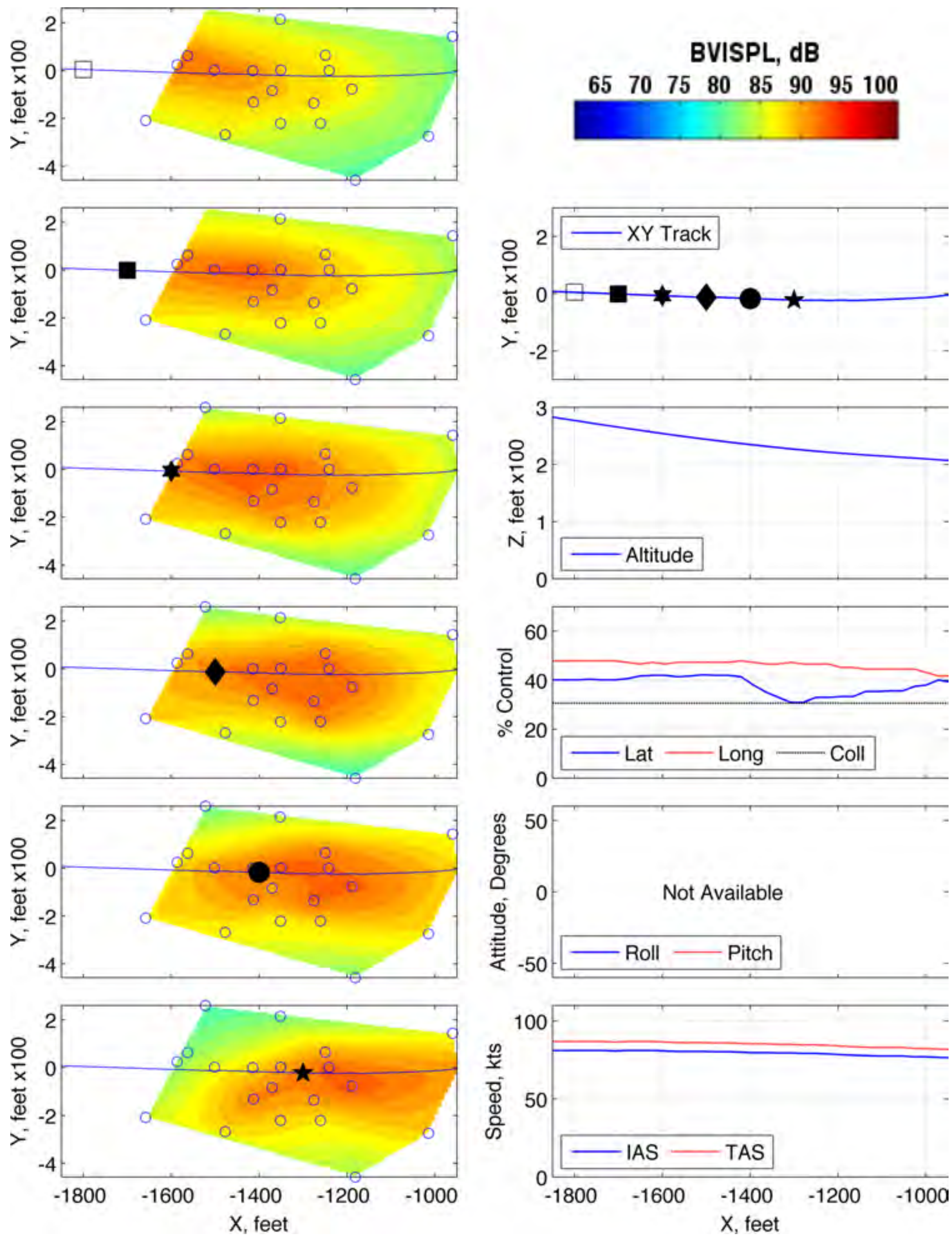

Figure 219: Maneuver condition R10, 80 KIAS, -6° , slow cyclic roll left, run number 278320

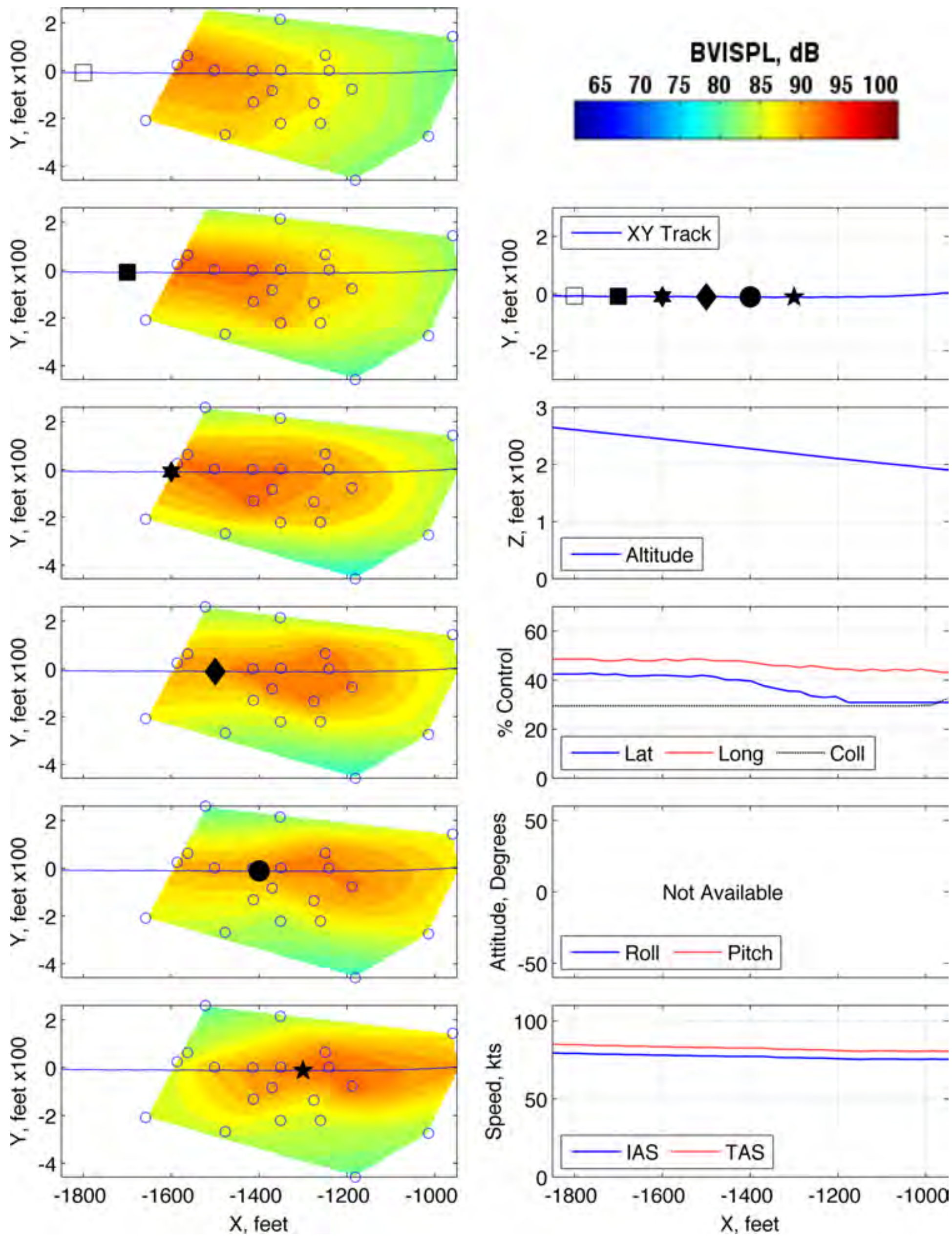

Figure 220: Maneuver condition R10, 80 KIAS, -6° , slow cyclic roll left, run number 278321

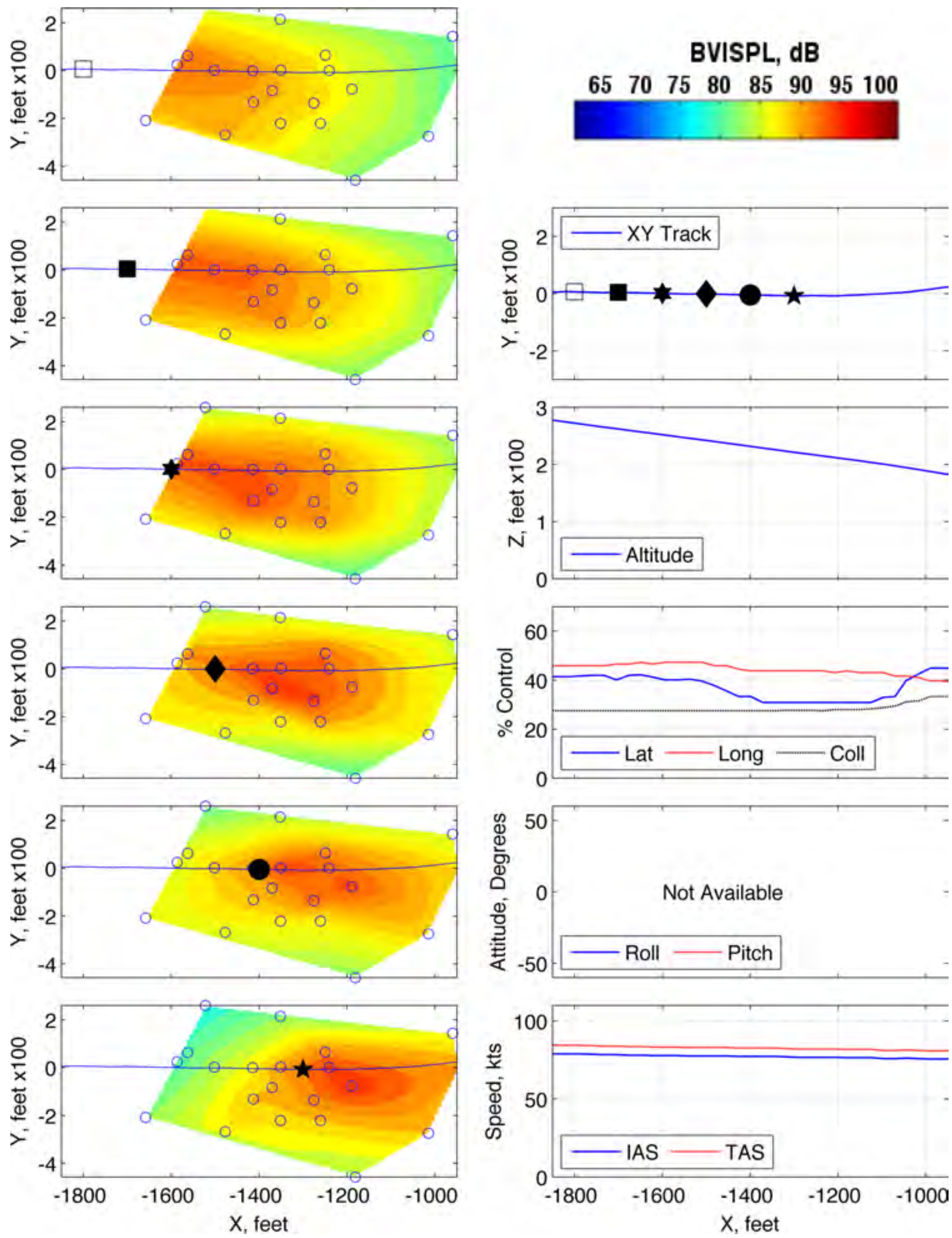

Figure 221: Maneuver condition R10, 80 KIAS, -6° , slow cyclic roll left, run number 278322

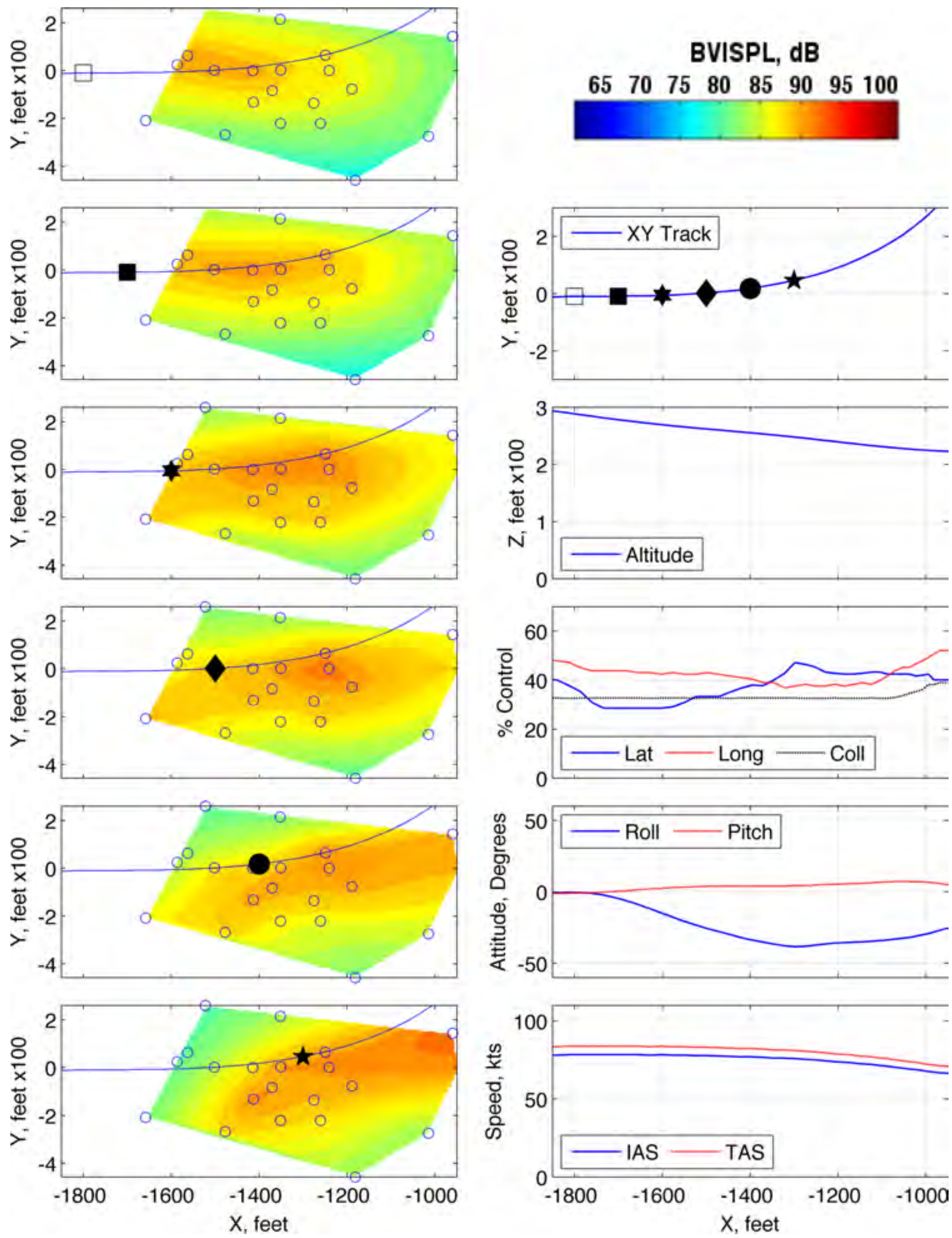

Figure 222: Maneuver condition R10, 80 KIAS, -6° , slow cyclic roll left, run number 282418

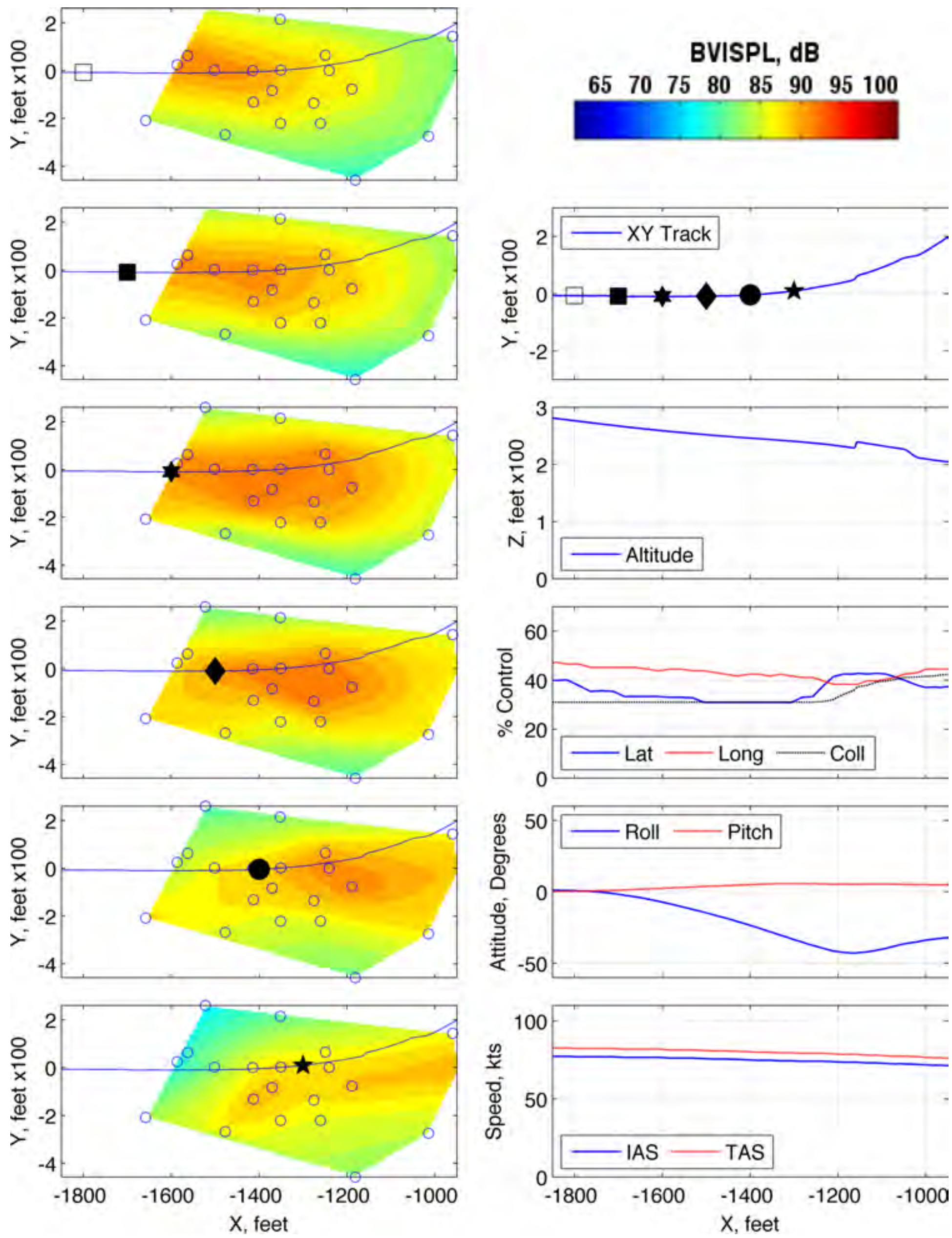

Figure 223: Maneuver condition R10, 80 KIAS, -6° , slow cyclic roll left, run number 282419

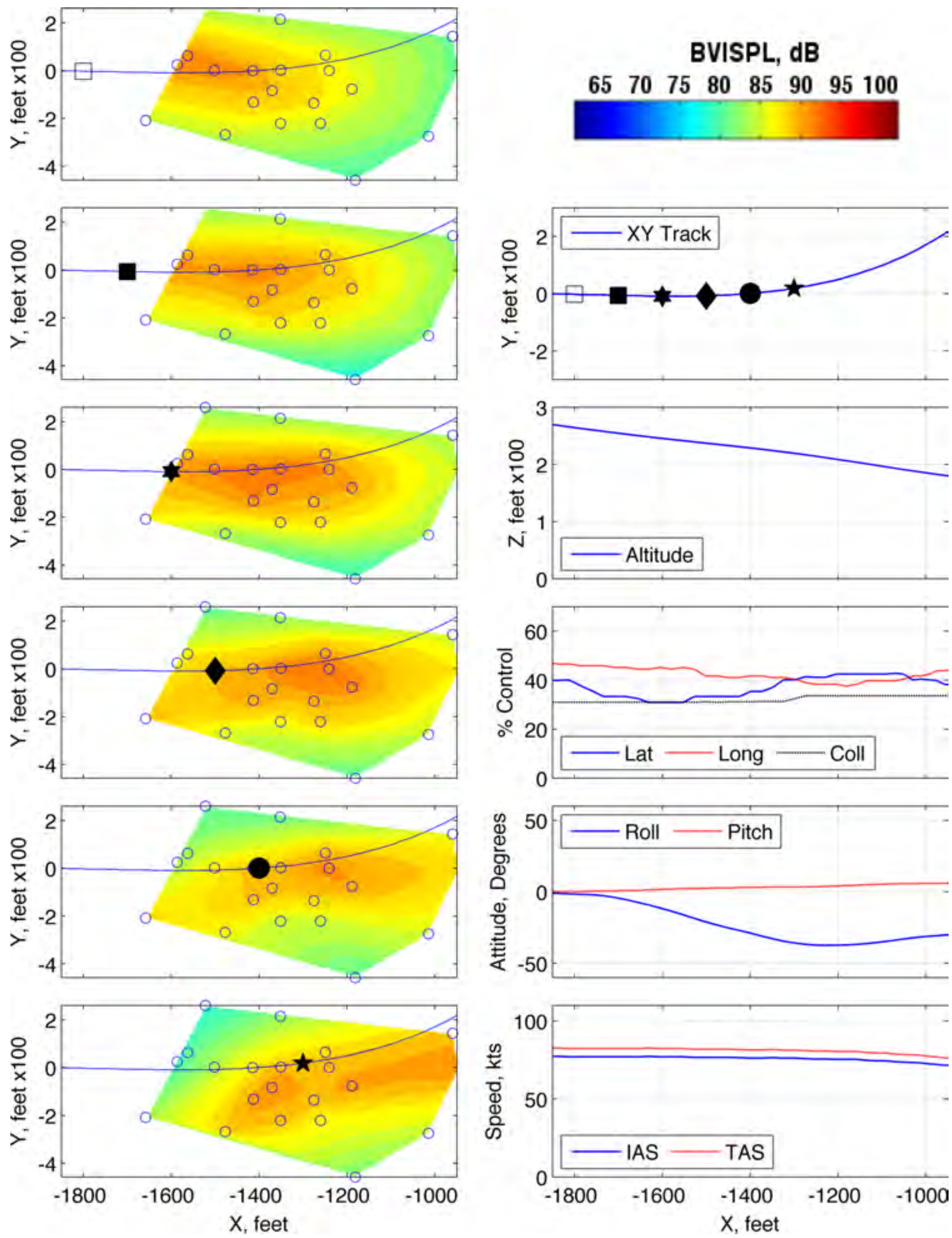

Figure 224: Maneuver condition R10, 80 KIAS, -6° , slow cyclic roll left, run number 282420

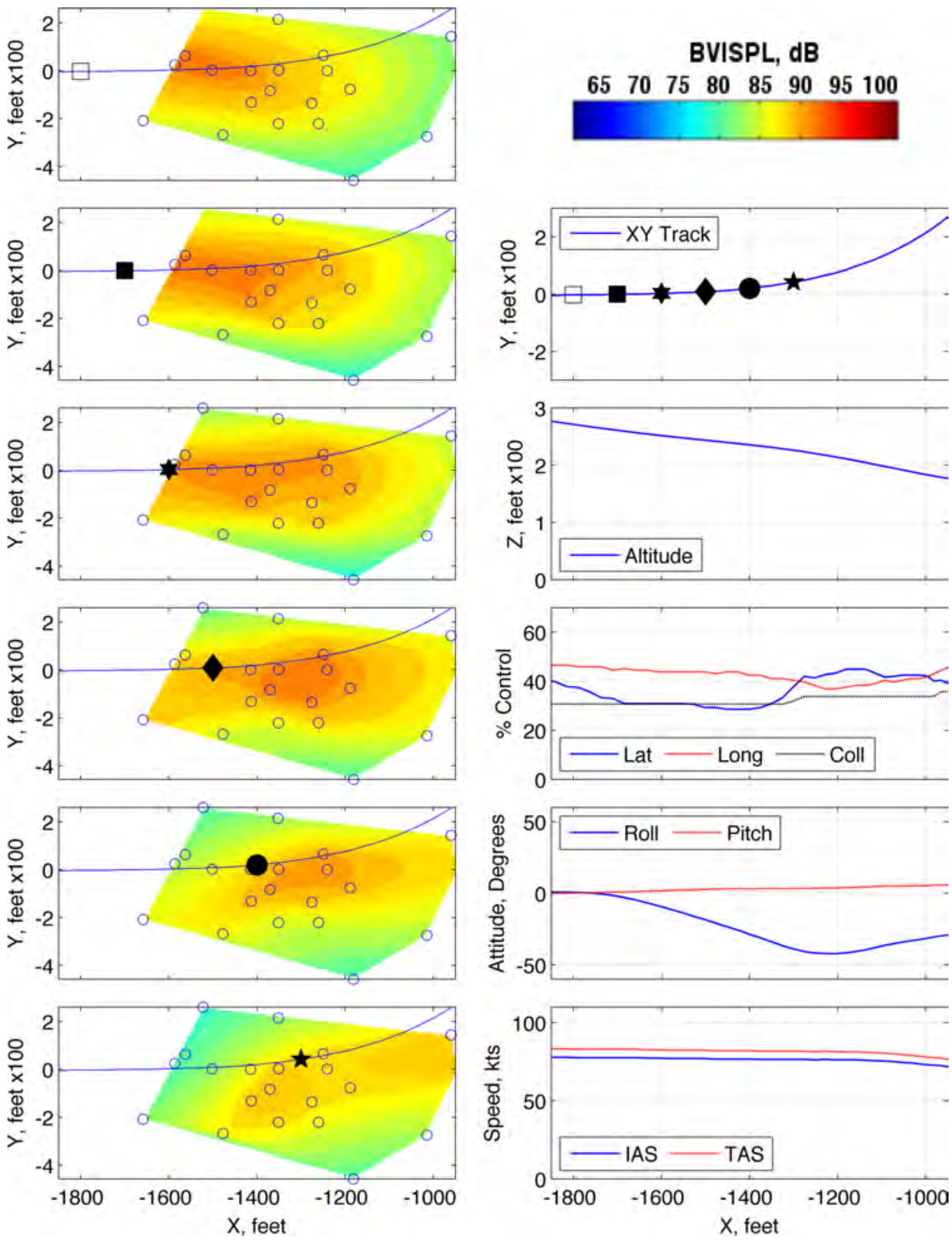

Figure 225: Maneuver condition R10, 80 KIAS, -6° , slow cyclic roll left, run number 282421

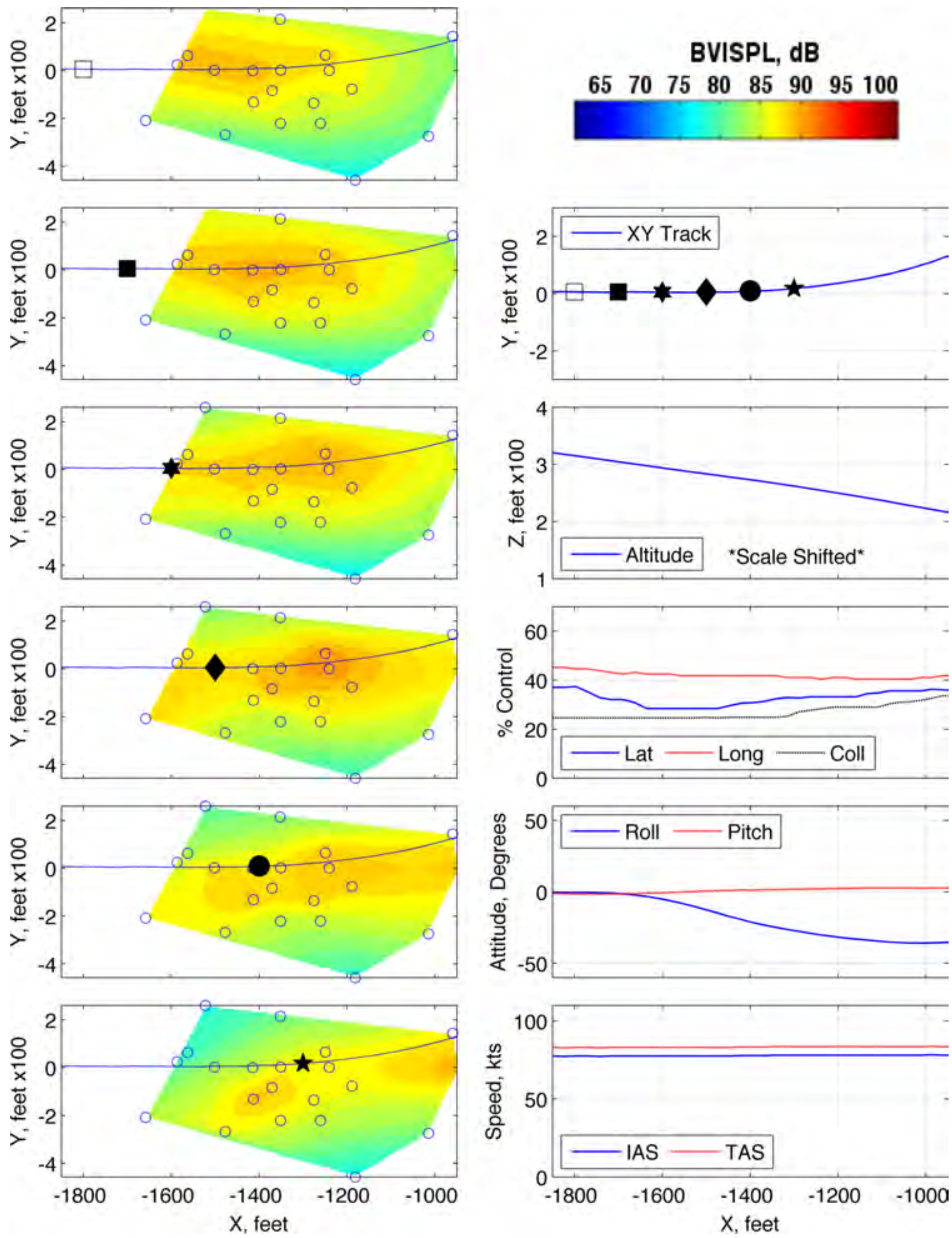

Figure 226: Maneuver condition R11, 80 KIAS, -6° , medium cyclic roll left, run number 285481

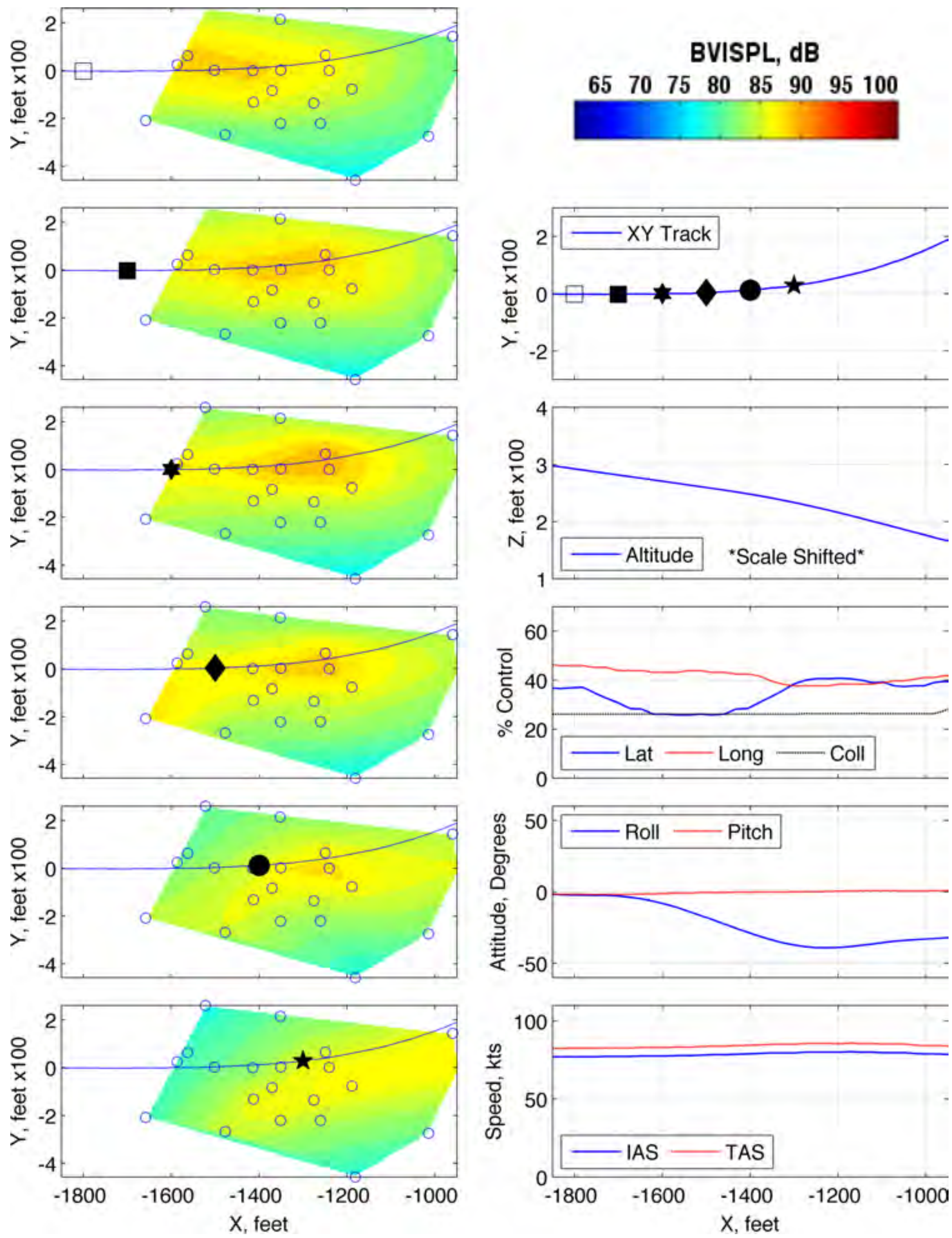

Figure 227: Maneuver condition R11, 80 KIAS, -6° , medium cyclic roll left, run number 285482

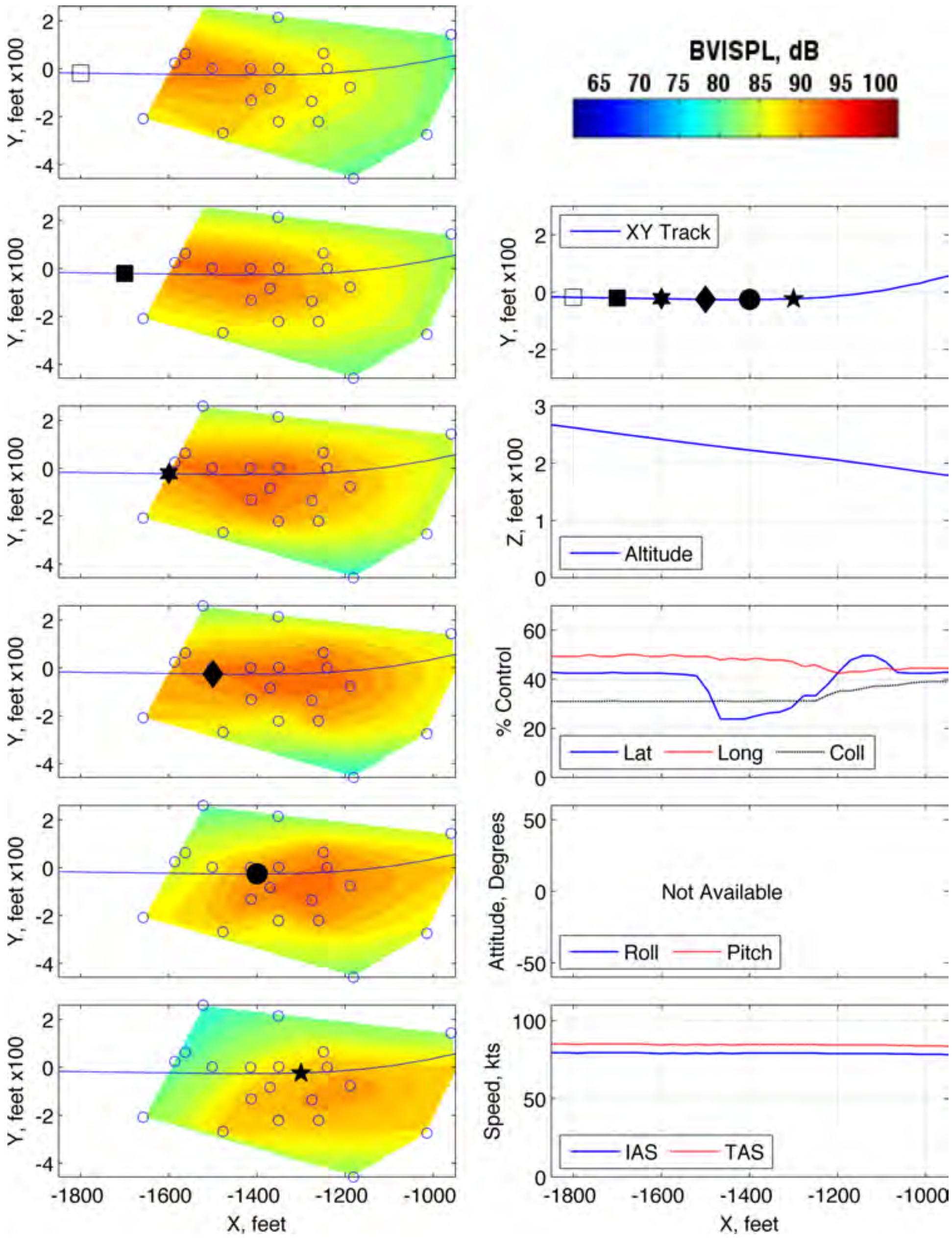

Figure 228: Maneuver condition R12, 80 KIAS, -6° , fast cyclic roll left, run number 278311

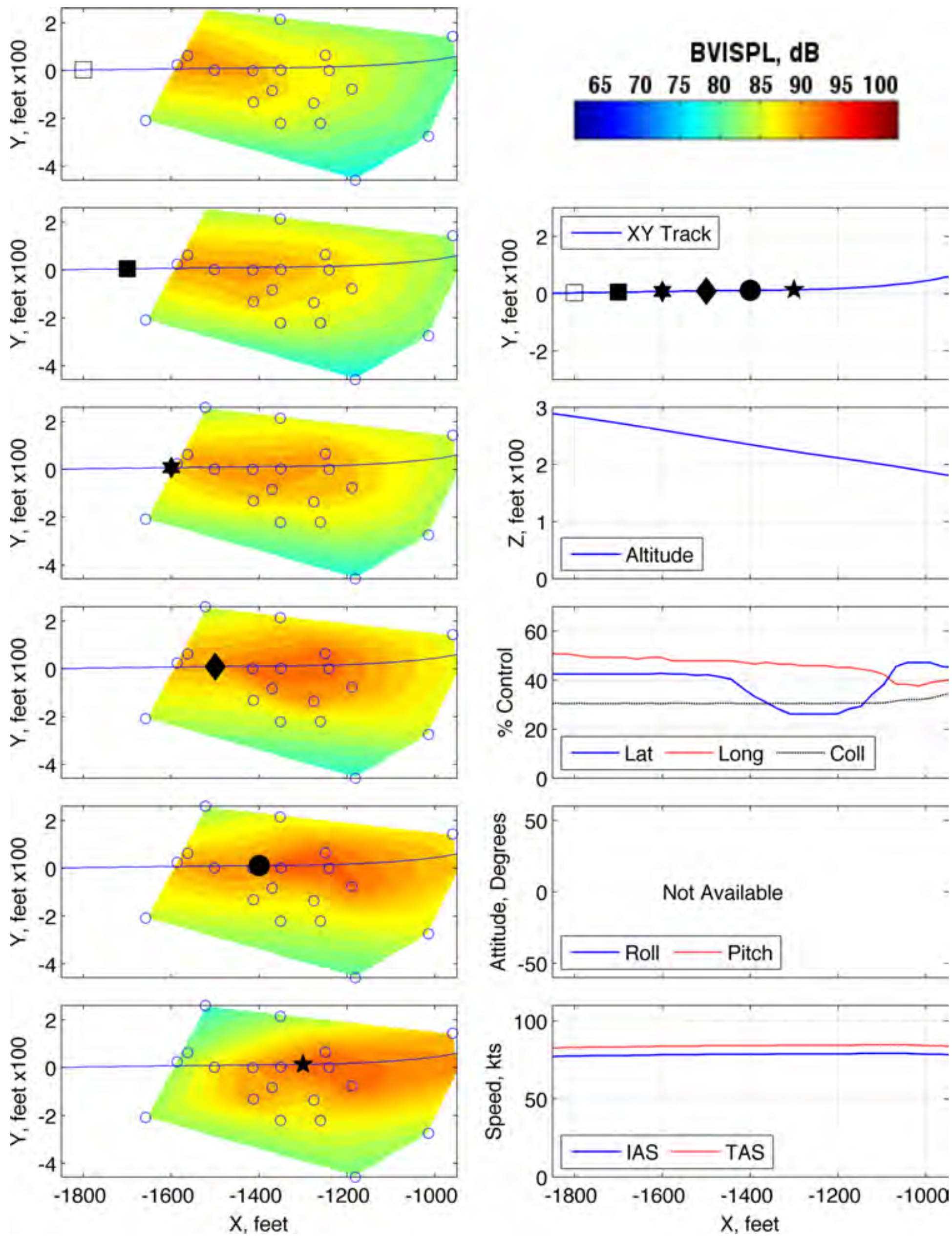

Figure 229: Maneuver condition R12, 80 KIAS, -6° , fast cyclic roll left, run number 278312

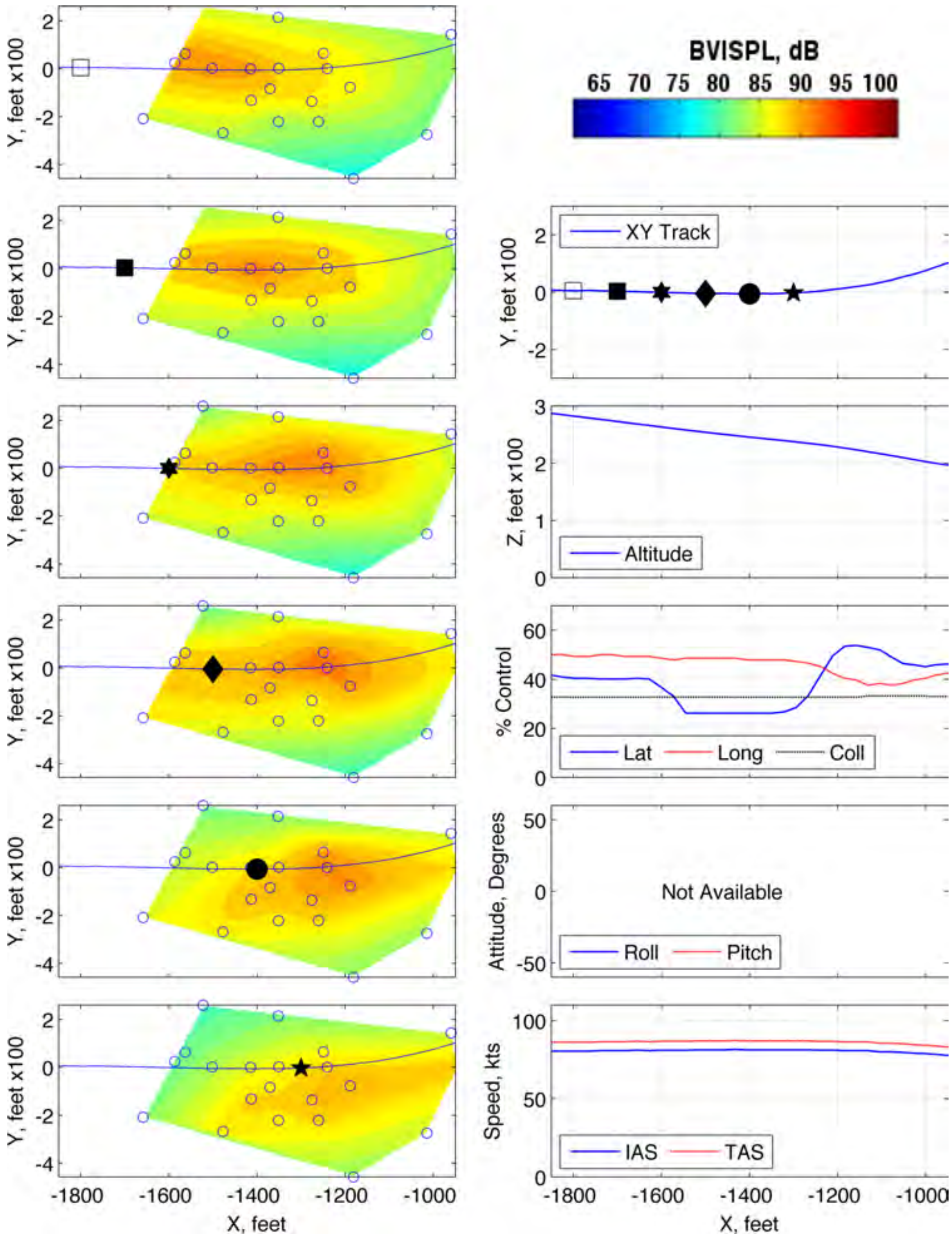

Figure 230: Maneuver condition R12, 80 KIAS, -6° , fast cyclic roll left, run number 278313

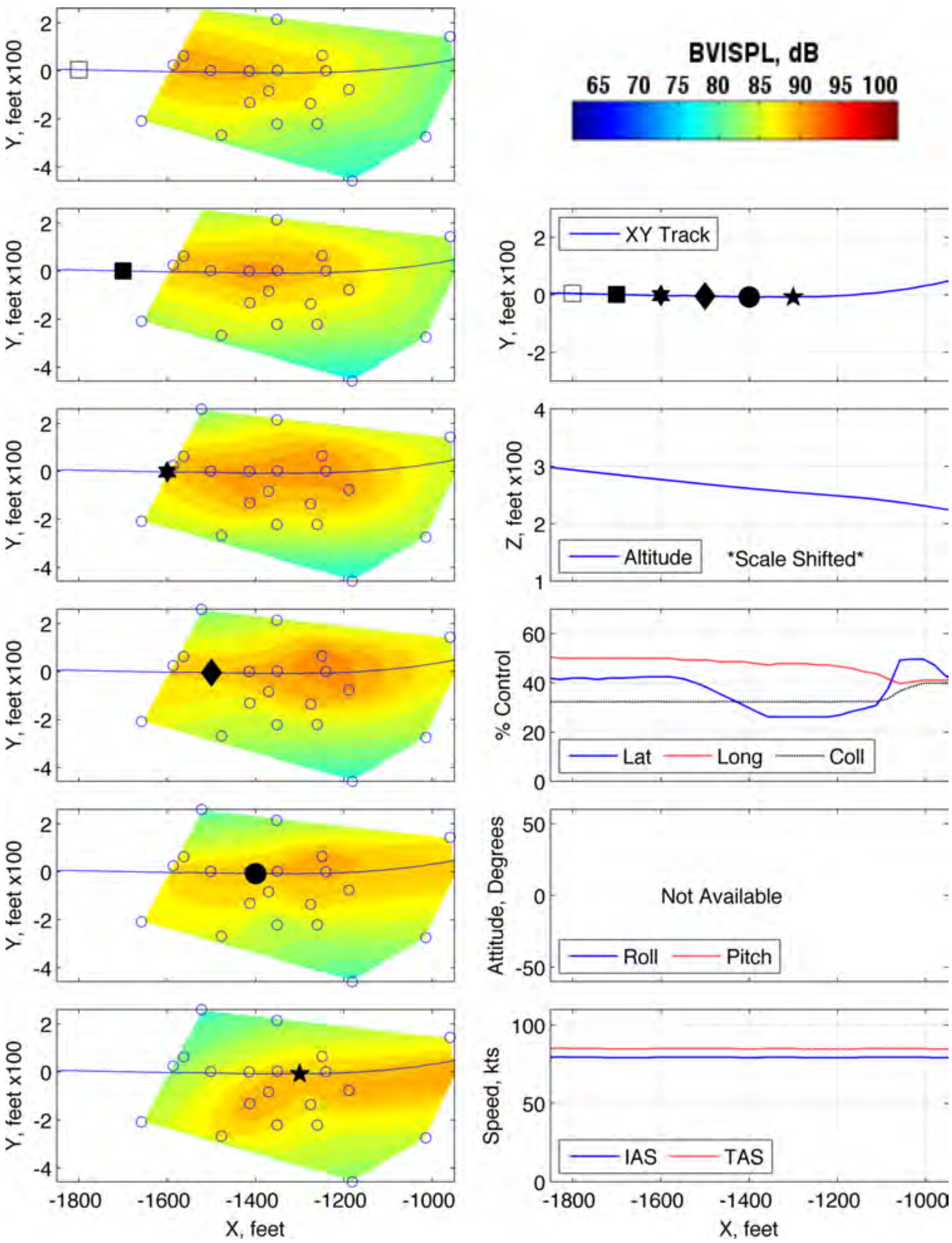

Figure 231: Maneuver condition R12, 80 KIAS, -6° , fast cyclic roll left, run number 278314

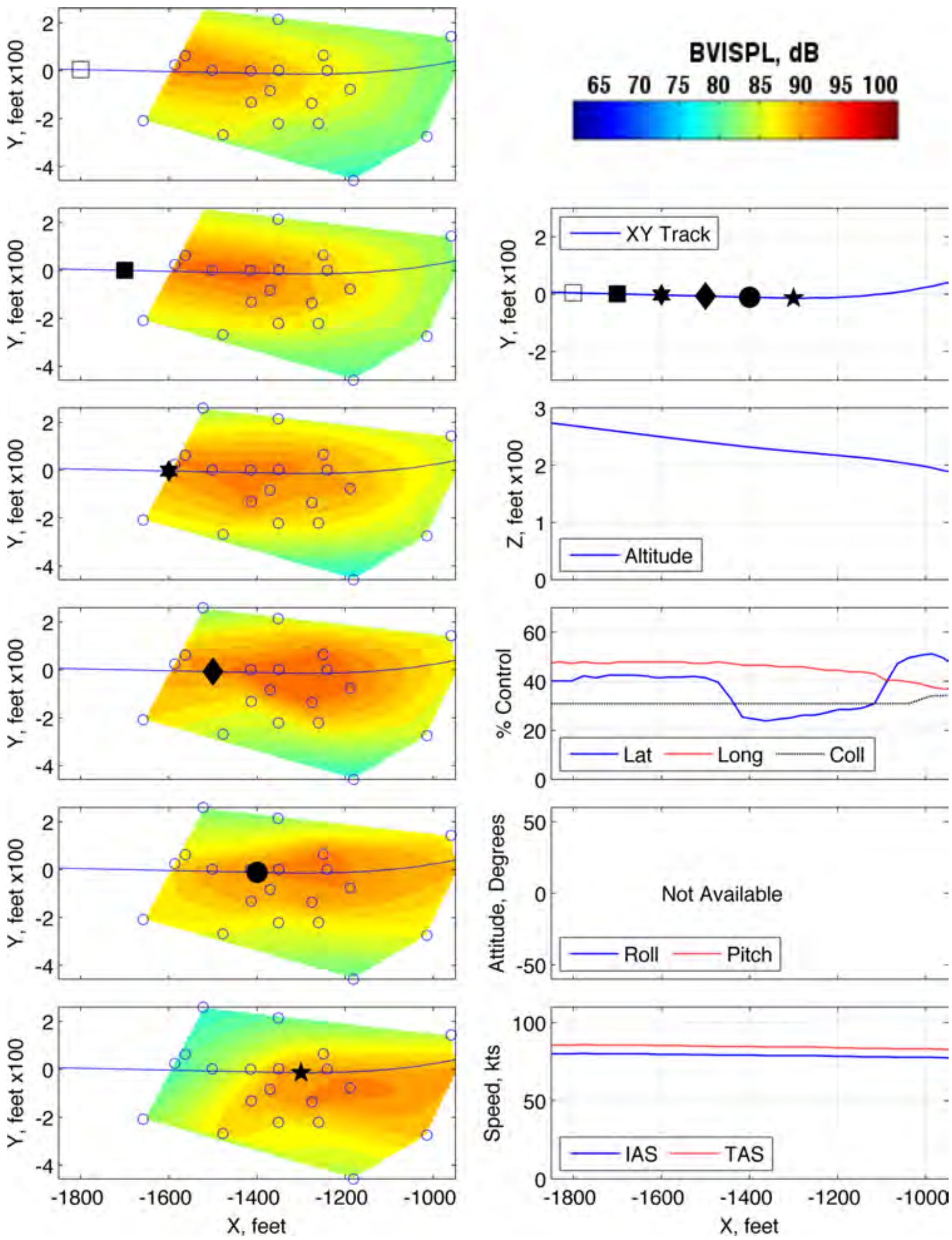

Figure 232: Maneuver condition R12, 80 KIAS, -6° , fast cyclic roll left, run number 278315

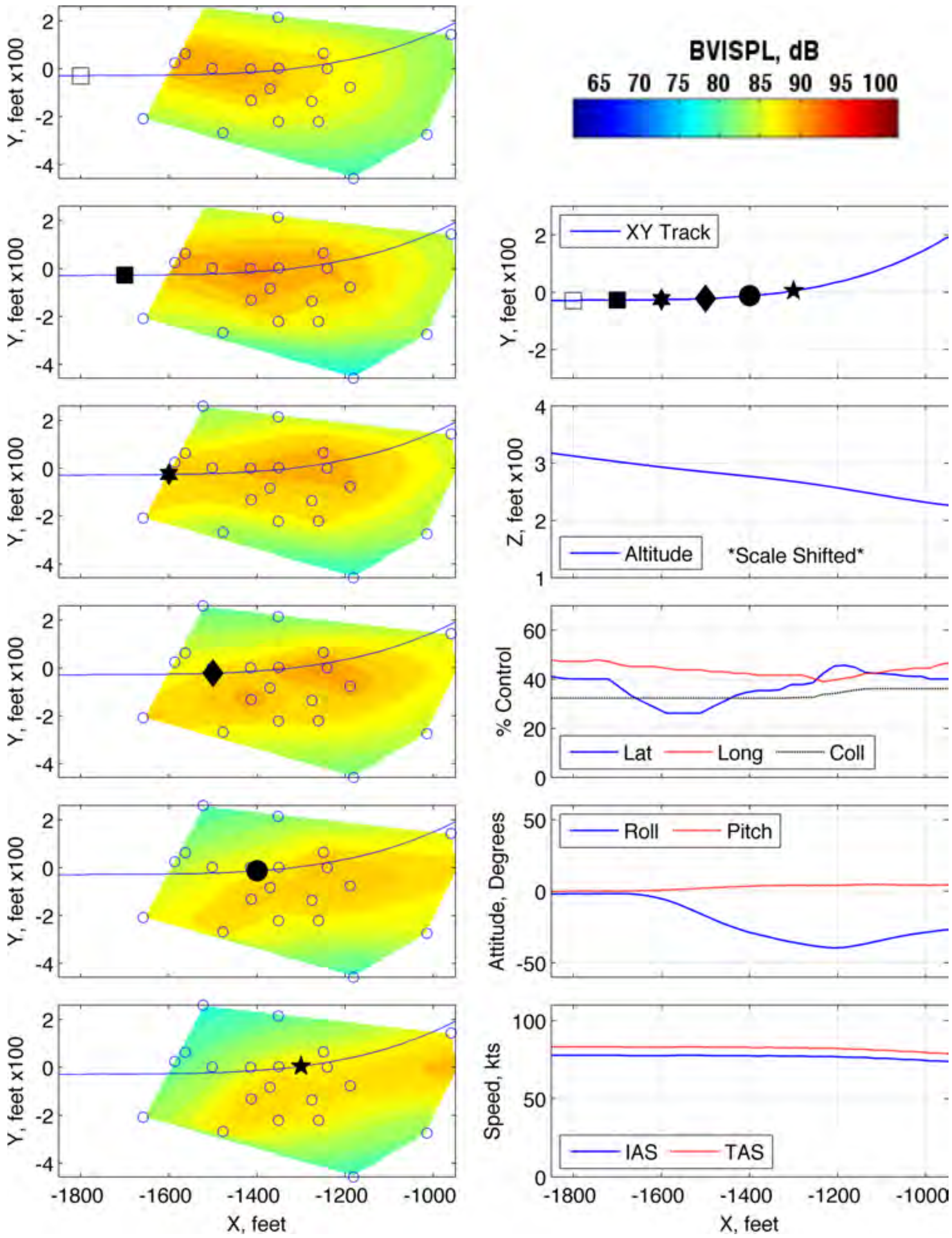

Figure 233: Maneuver condition R12, 80 KIAS, -6° , fast cyclic roll left, run number 282416

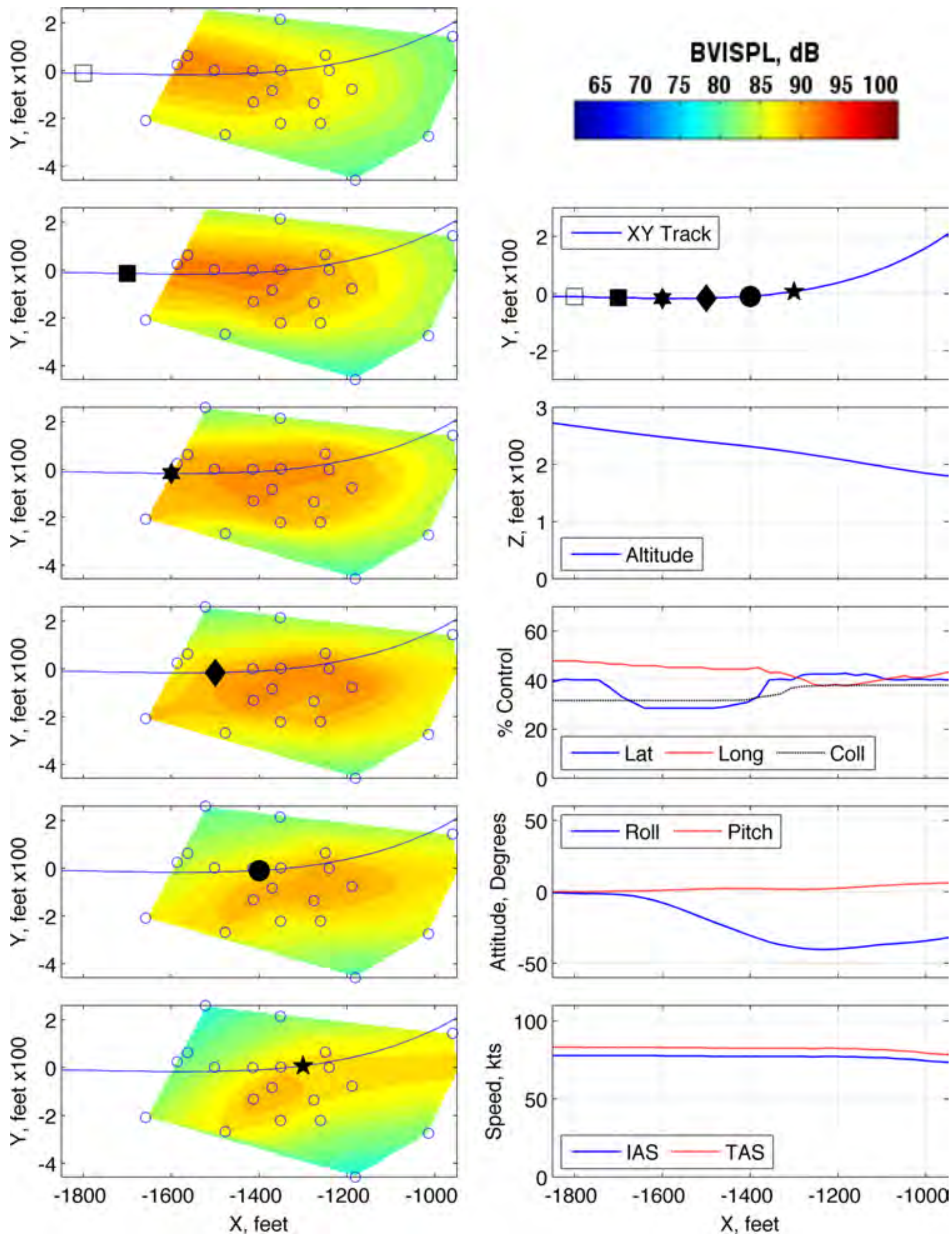

Figure 234: Maneuver condition R12, 80 KIAS, -6° , fast cyclic roll left, run number 282417

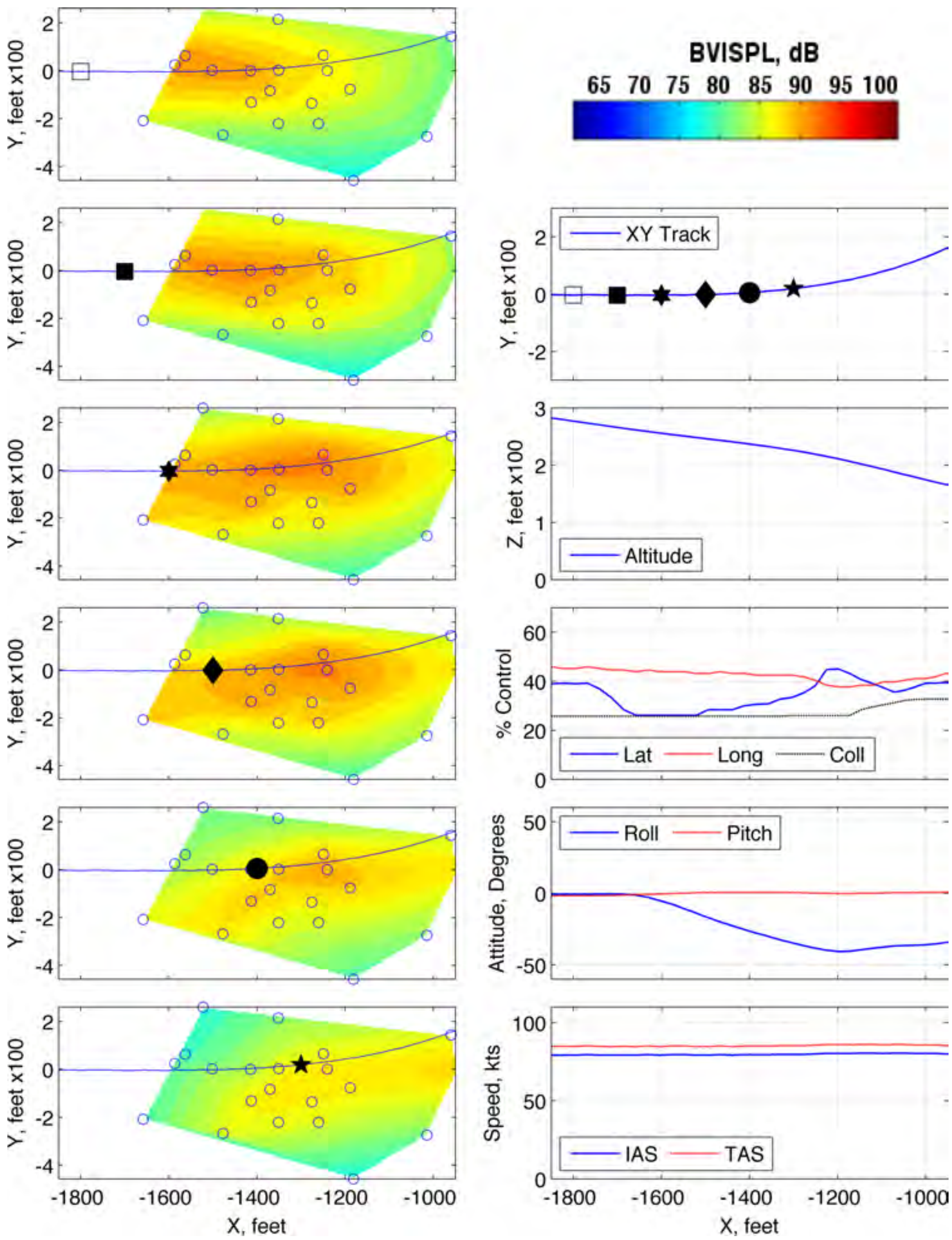

Figure 235: Maneuver condition R12, 80 KIAS, -6° , fast cyclic roll left, run number 285479

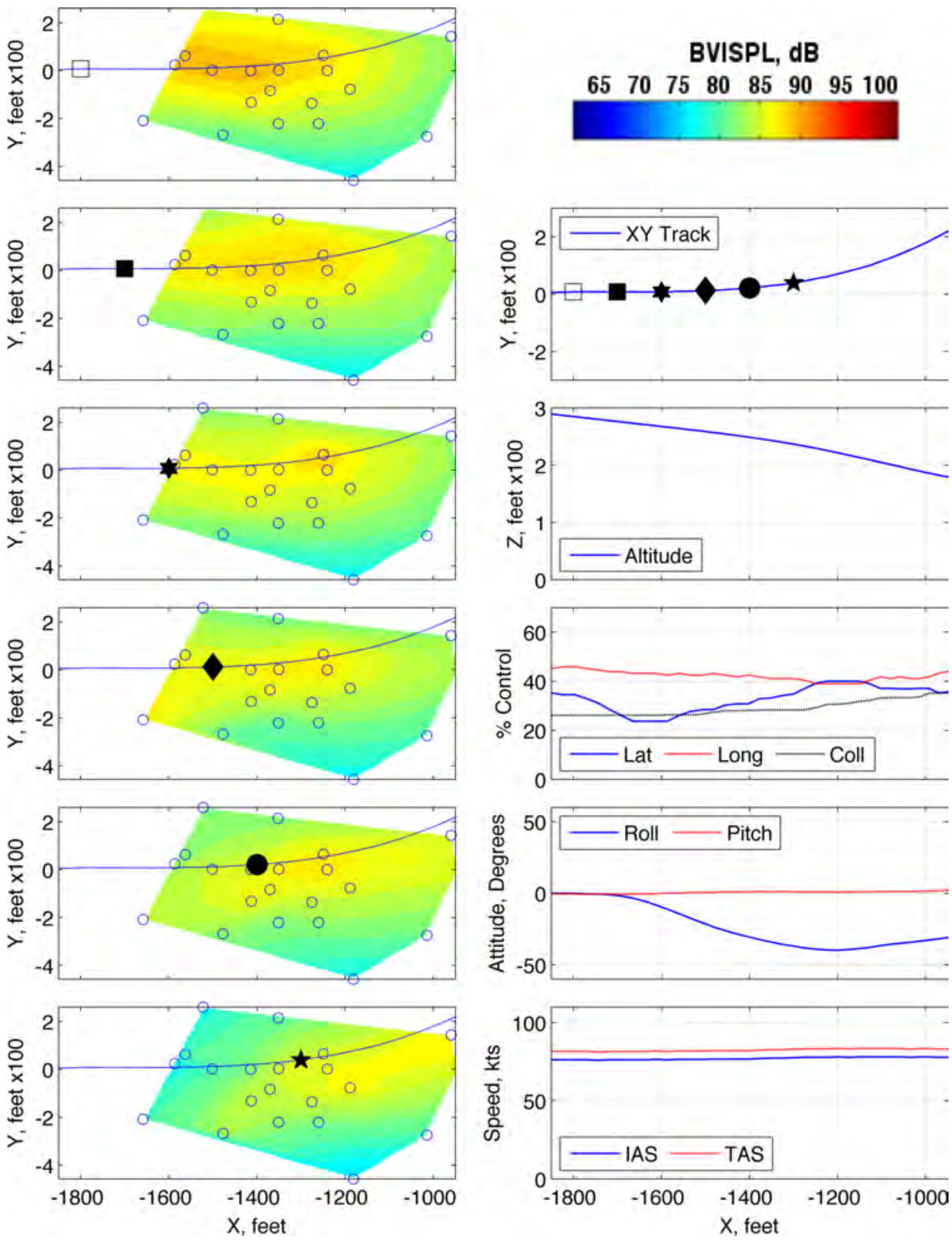

Figure 236: Maneuver condition R12, 80 KIAS, -6° , fast cyclic roll left, run number 285480

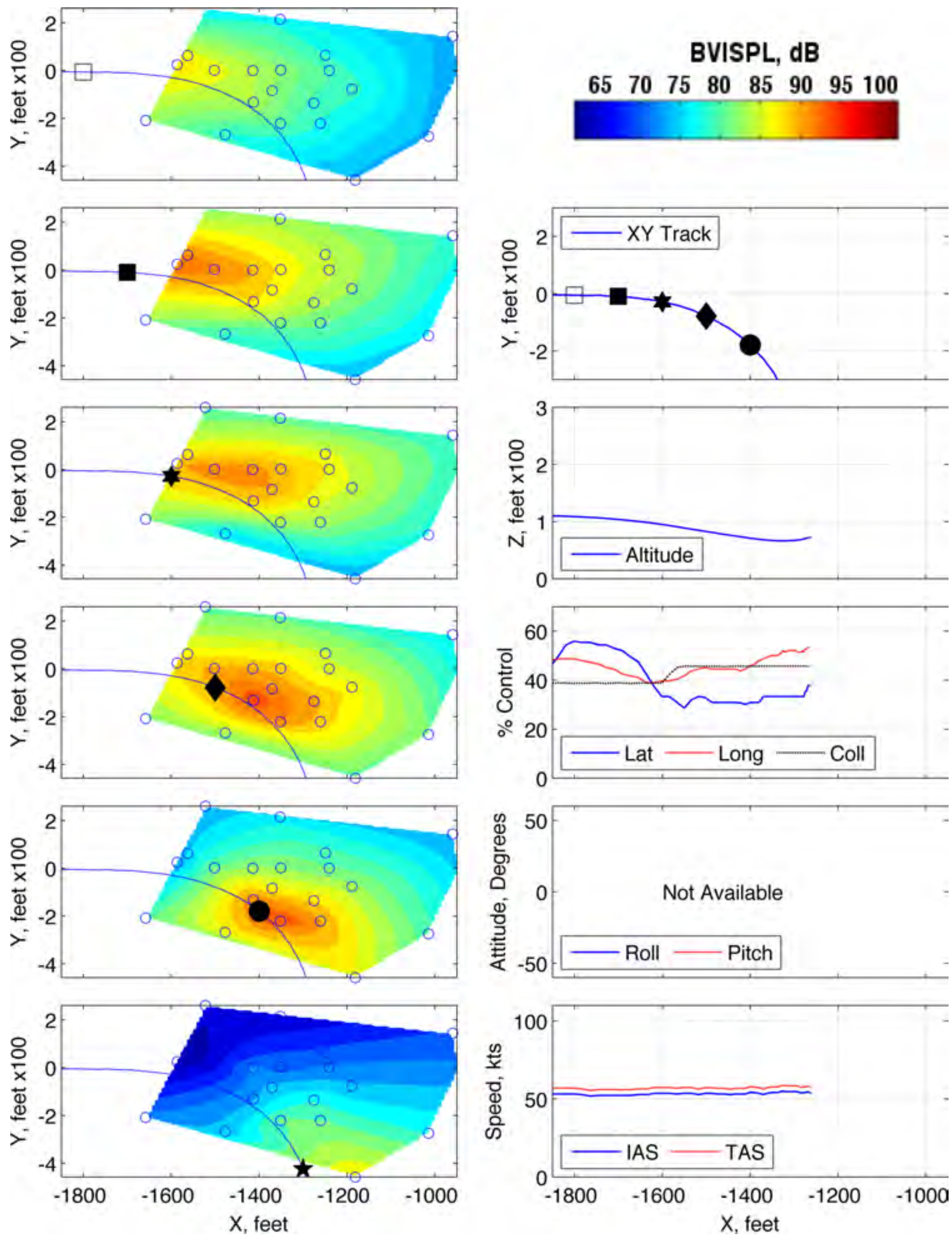

Figure 237: Maneuver condition R15, 60 KIAS, level, fast cyclic roll right, run number 280386

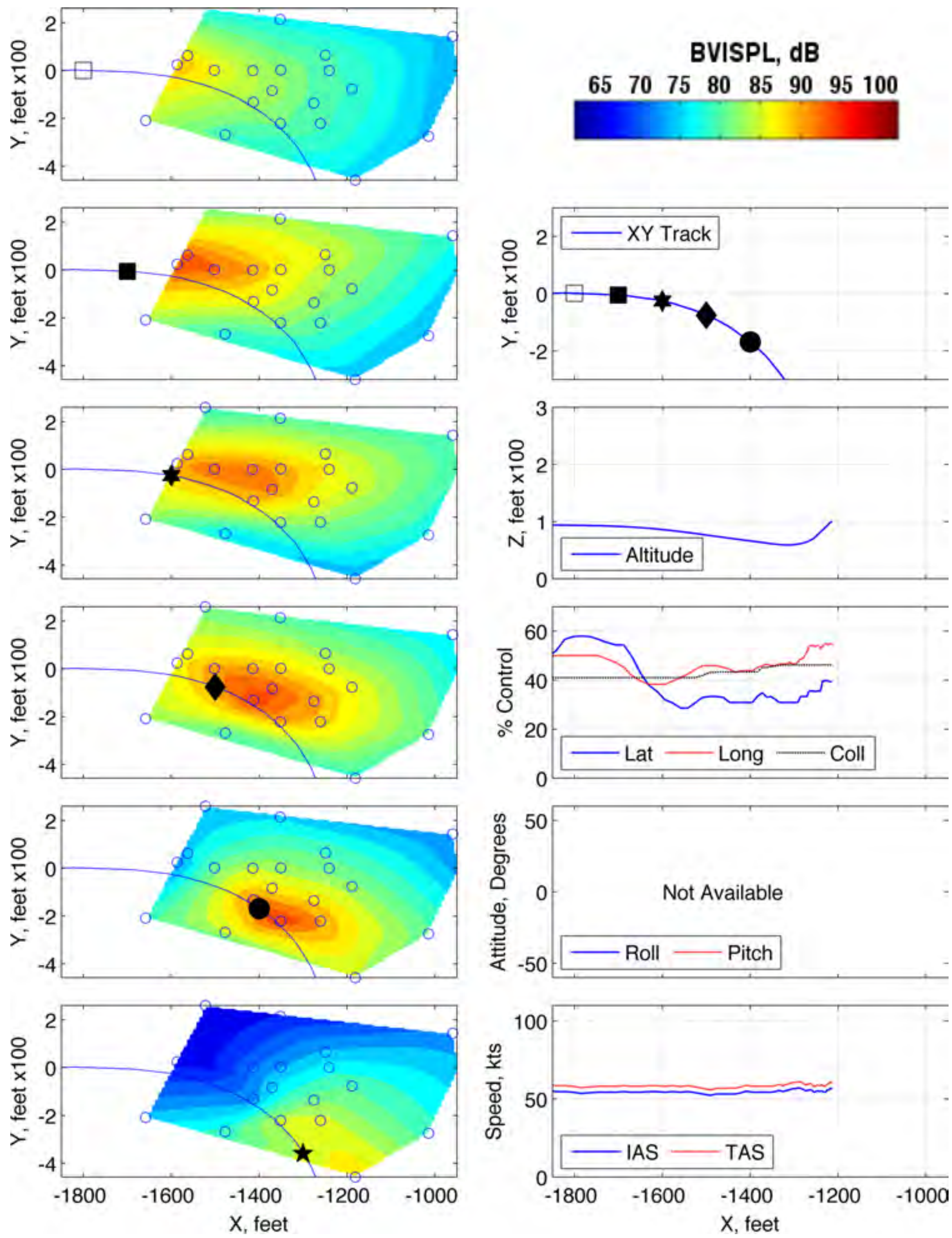

Figure 238: Maneuver condition R15, 60 KIAS, level, fast cyclic roll right, run number 280387

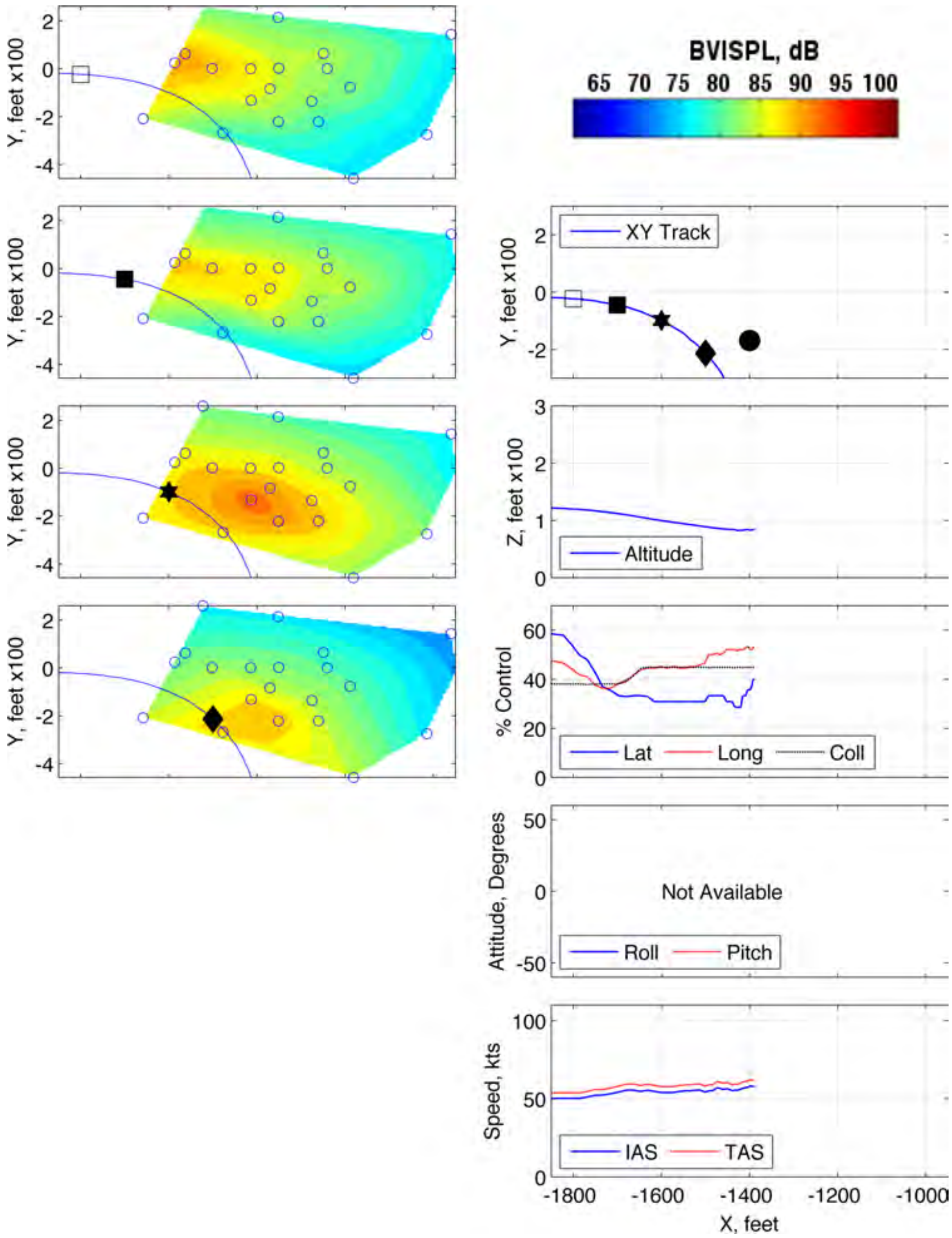

Figure 239: Maneuver condition R15, 60 KIAS, level, fast cyclic roll right, run number 280388

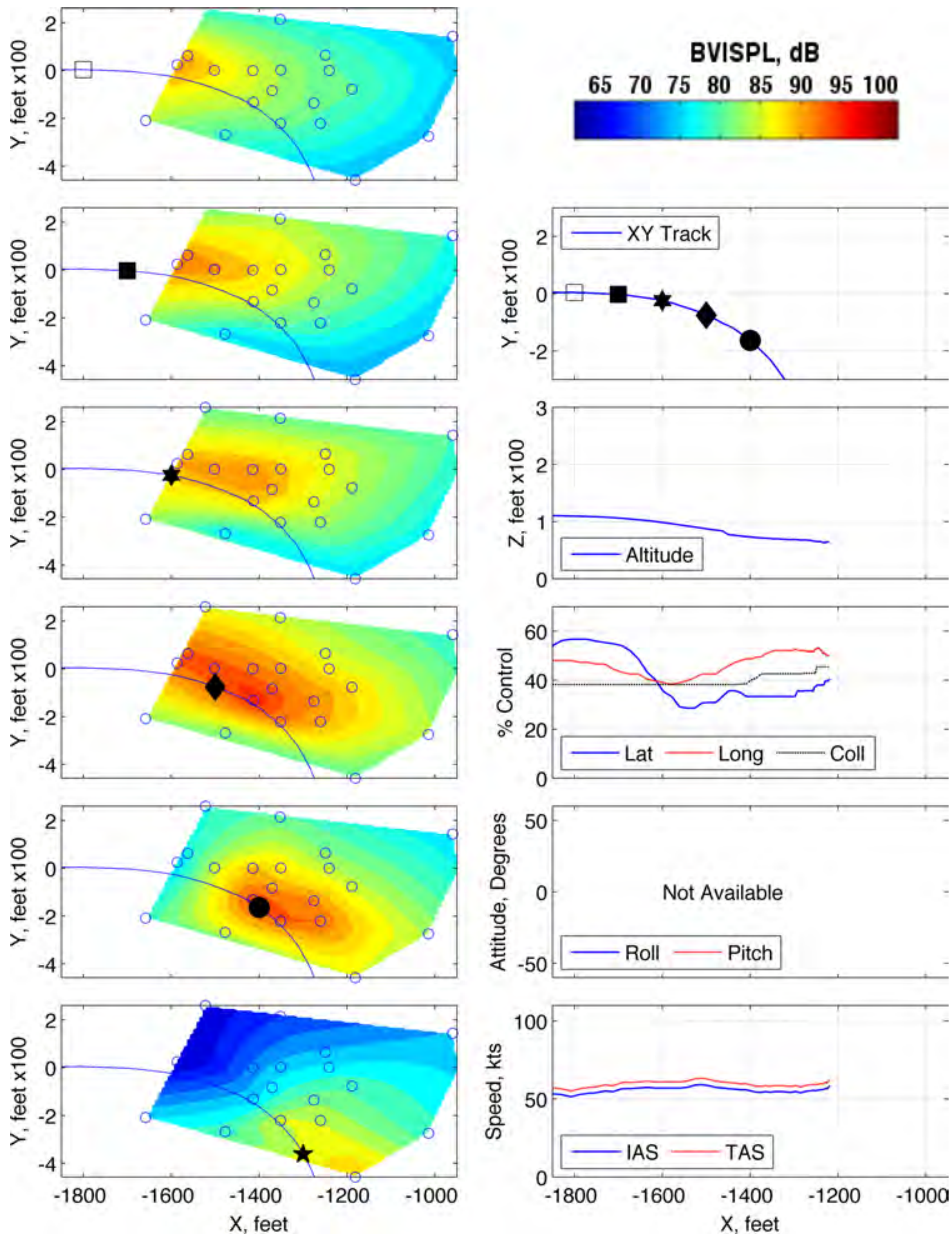

Figure 240: Maneuver condition R15, 60 KIAS, level, fast cyclic roll right, run number 280389

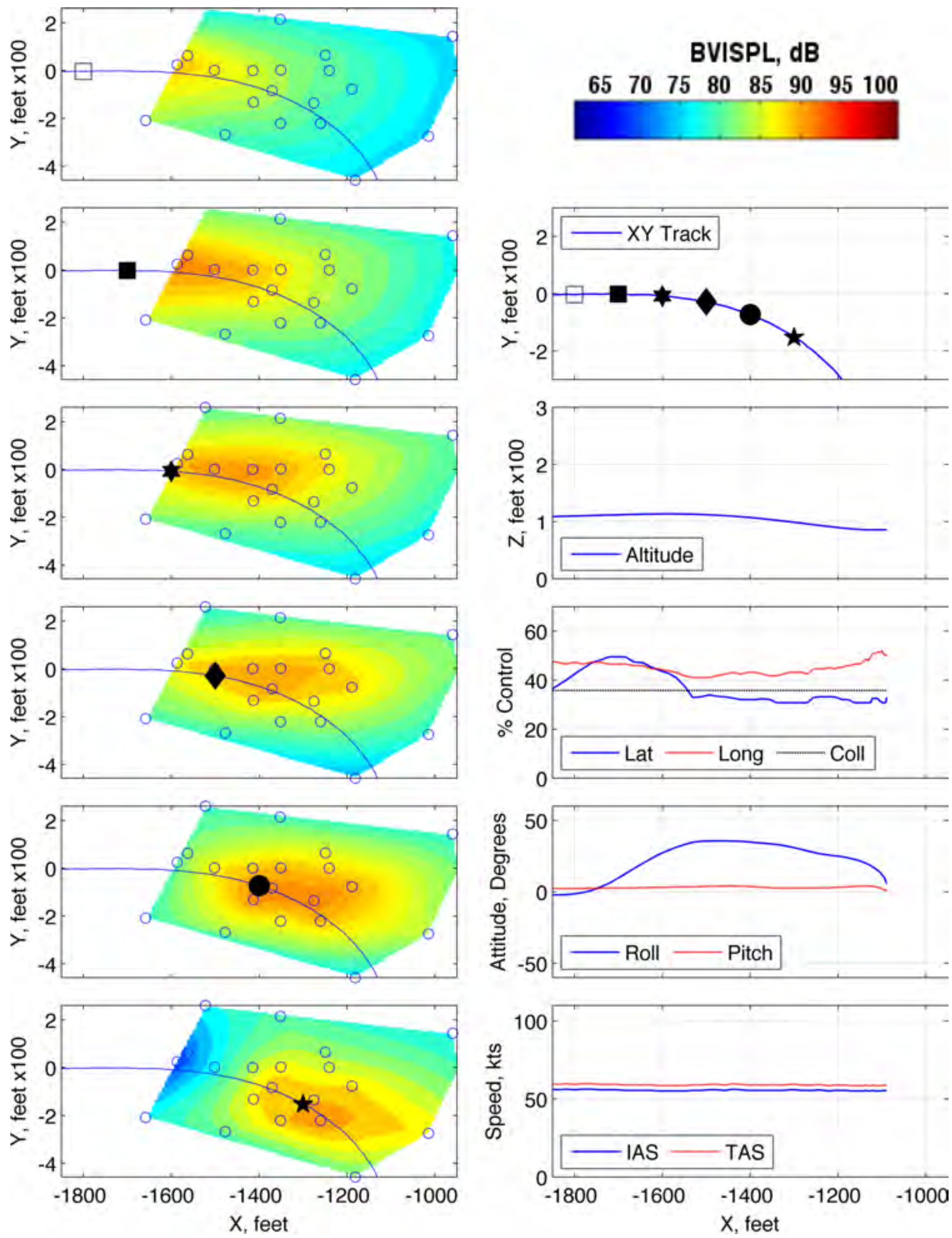

Figure 241: Maneuver condition R15, 60 KIAS, level, fast cyclic roll right, run number 285463

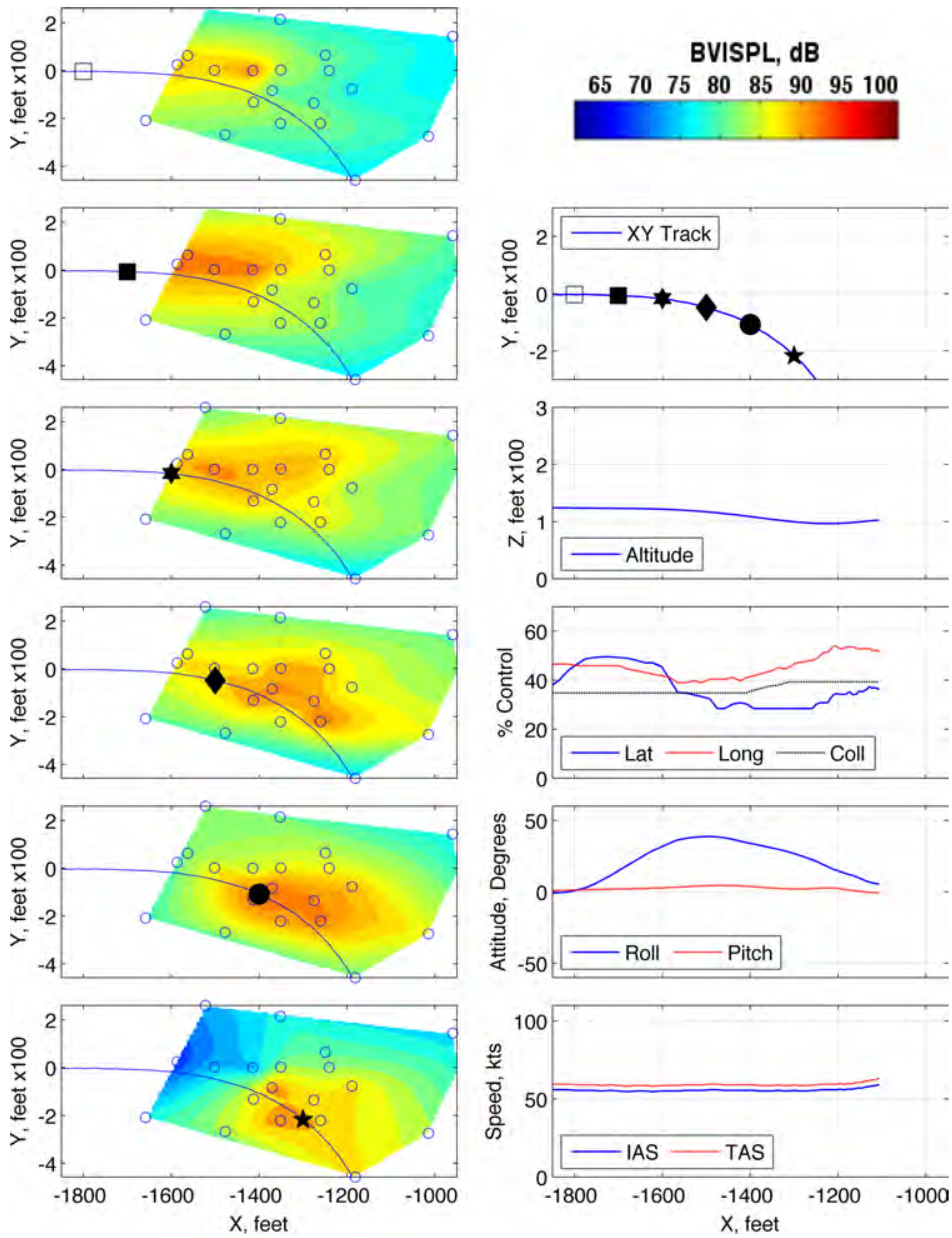

Figure 242: Maneuver condition R15, 60 KIAS, level, fast cyclic roll right, run number 285464

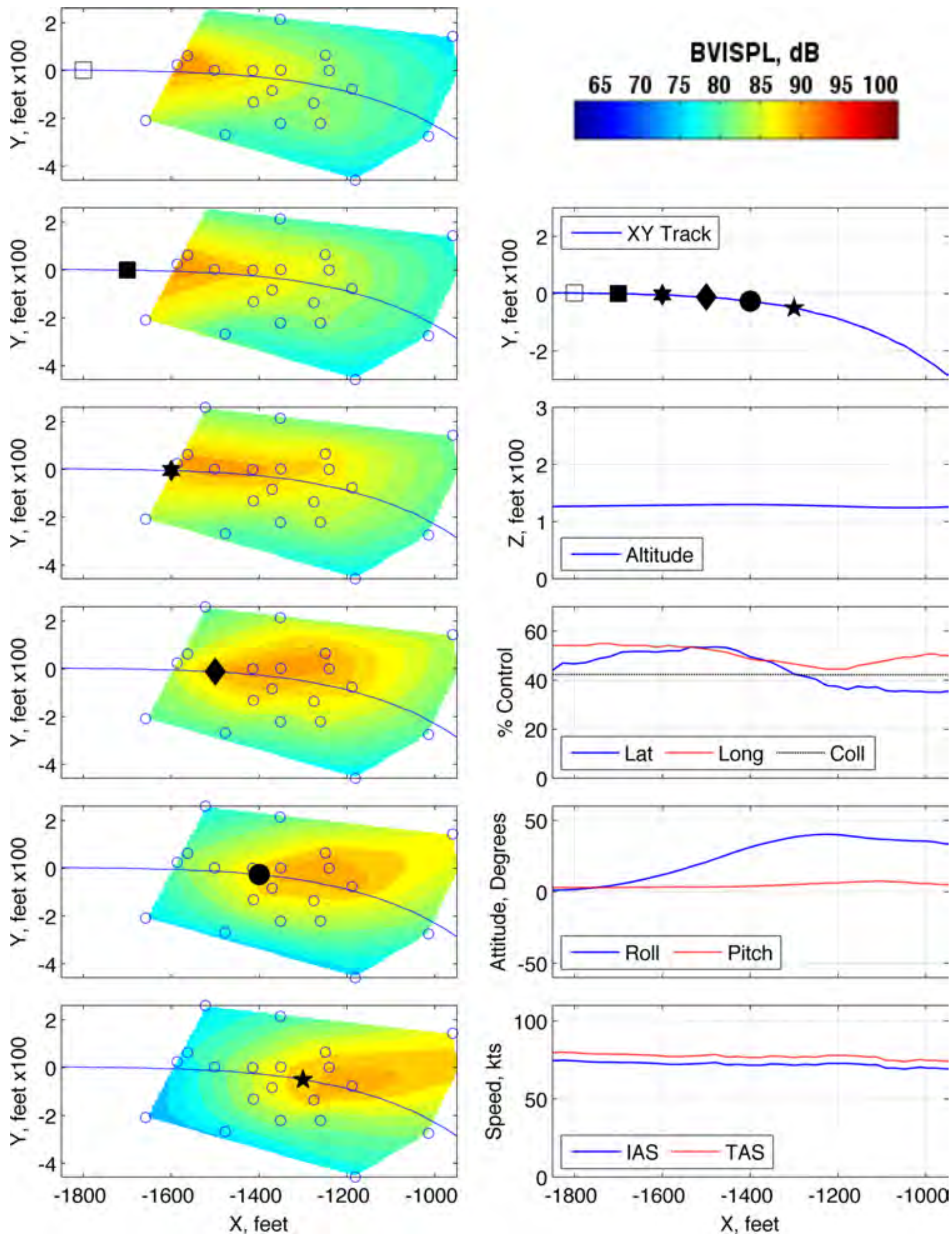

Figure 243: Maneuver condition R16, 80 KIAS, level, slow cyclic roll right, run number 280382

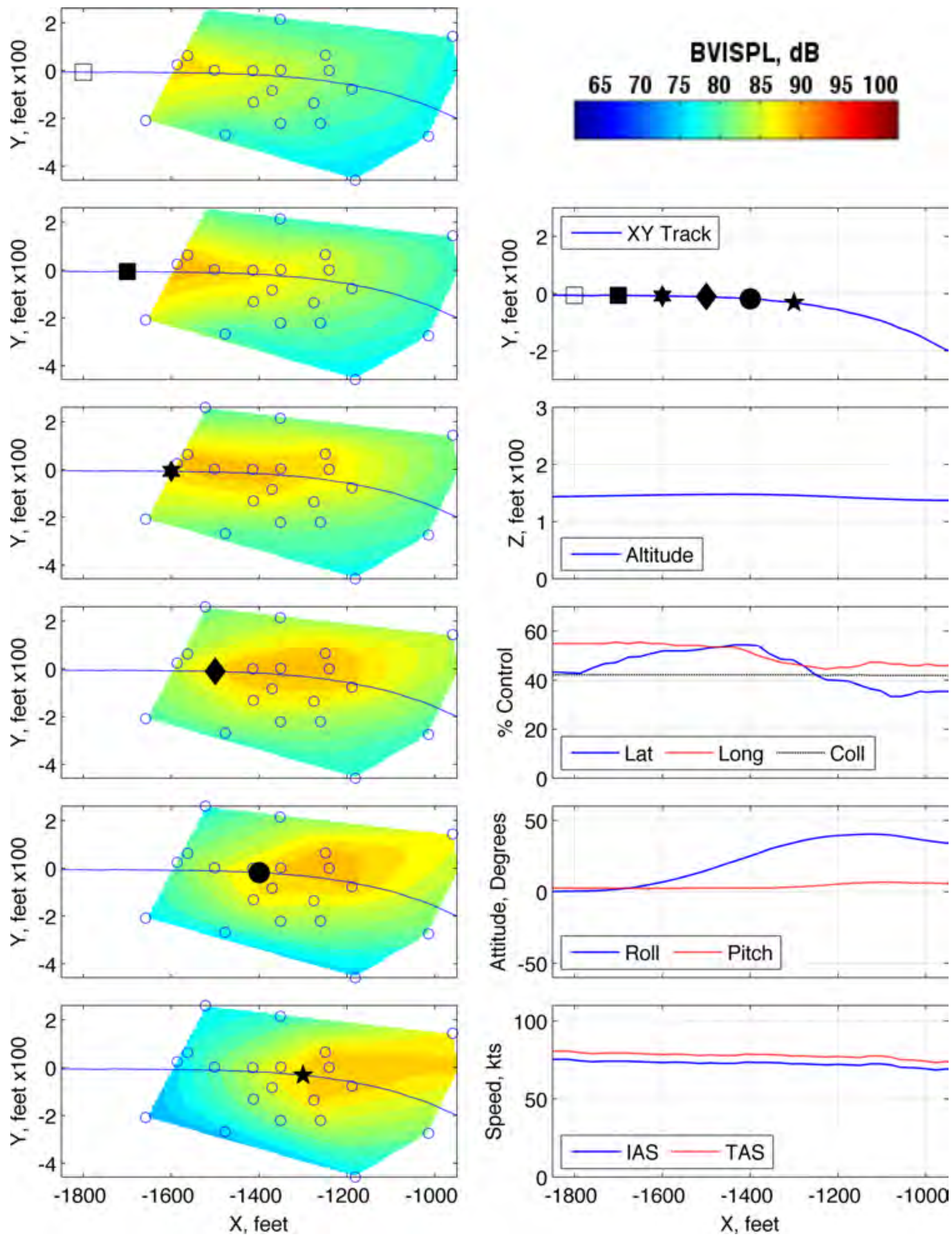

Figure 244: Maneuver condition R16, 80 KIAS, level, slow cyclic roll right, run number 280383

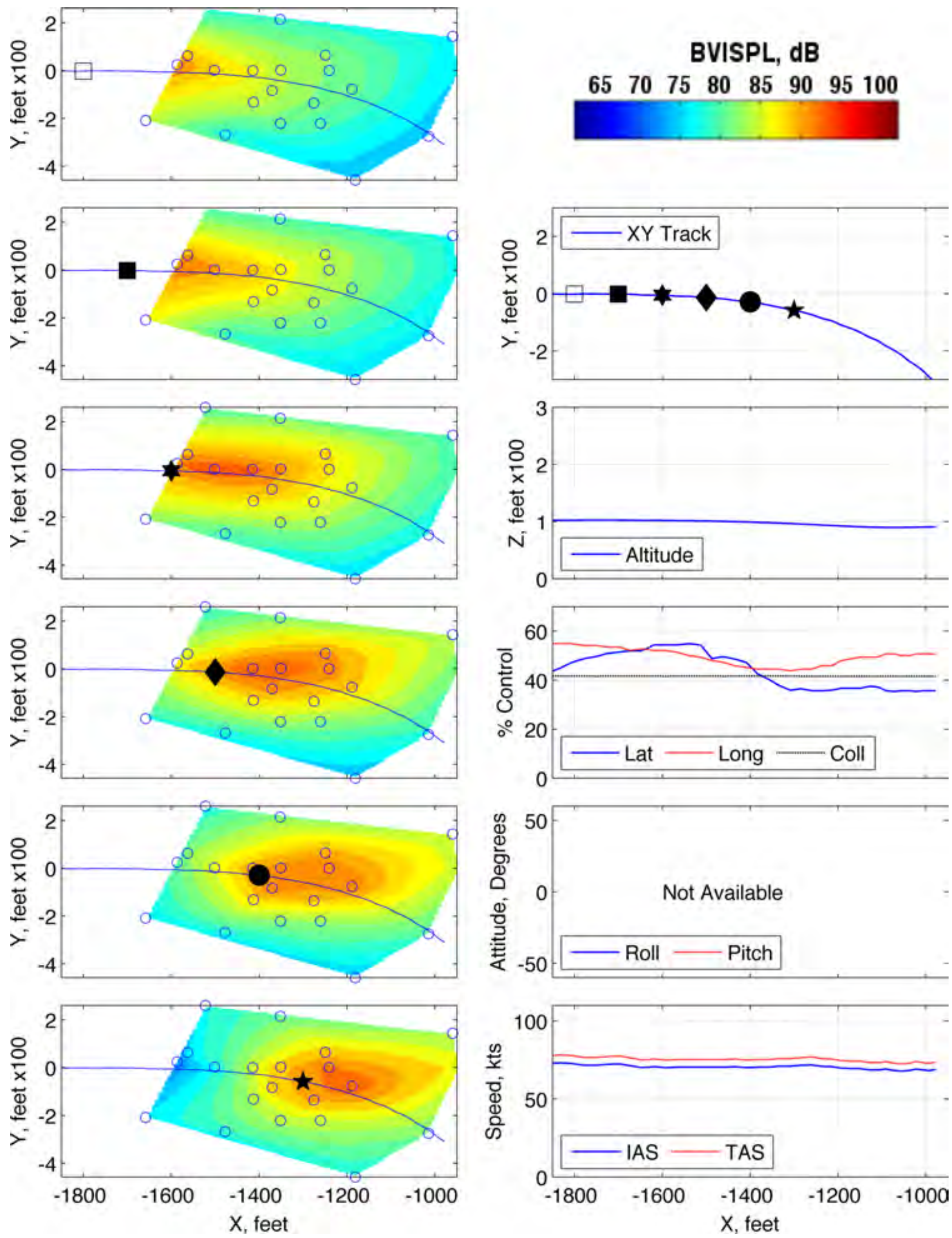

Figure 245: Maneuver condition R16, 80 KIAS, level, slow cyclic roll right, run number 280384

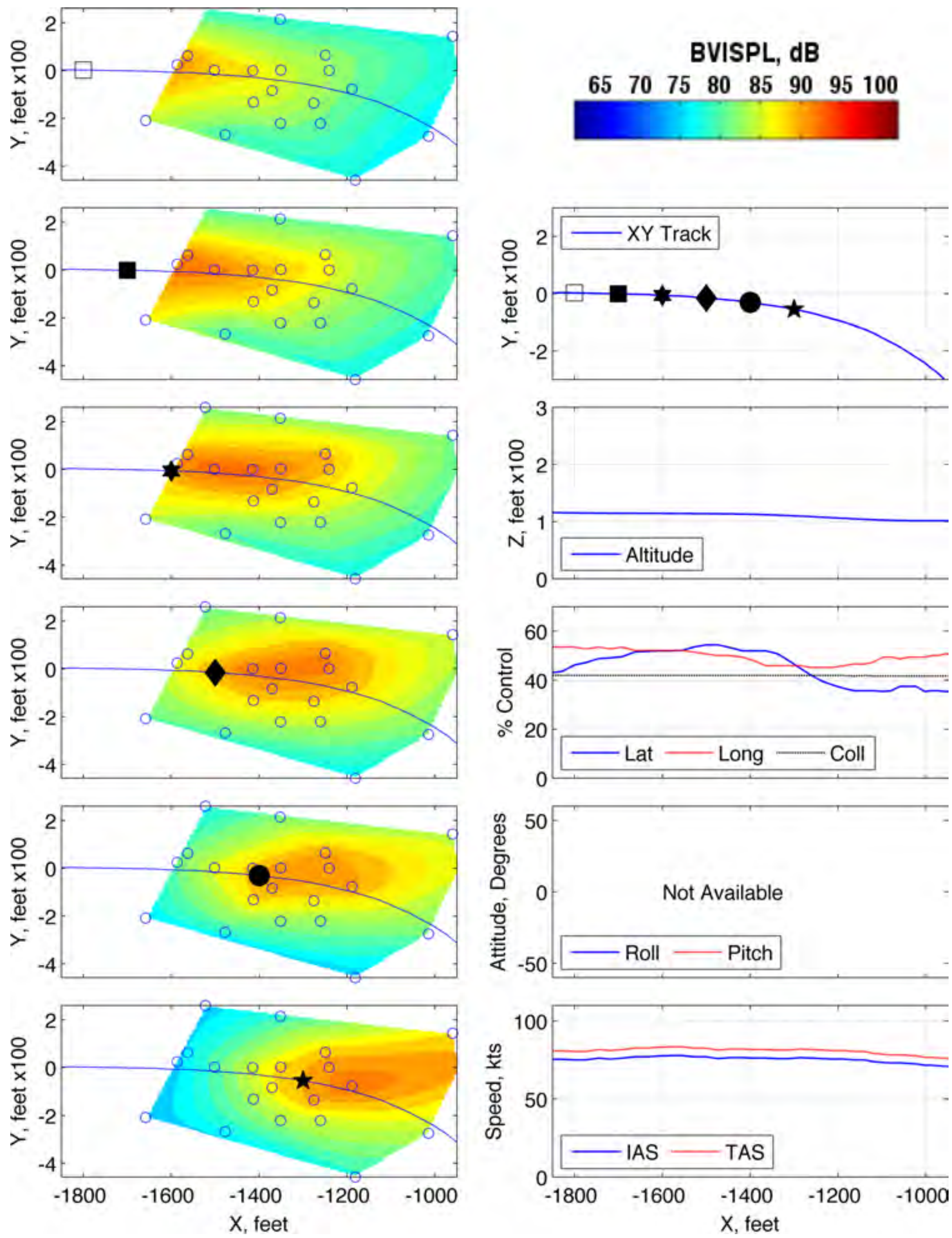

Figure 246: Maneuver condition R16, 80 KIAS, level, slow cyclic roll right, run number 280385

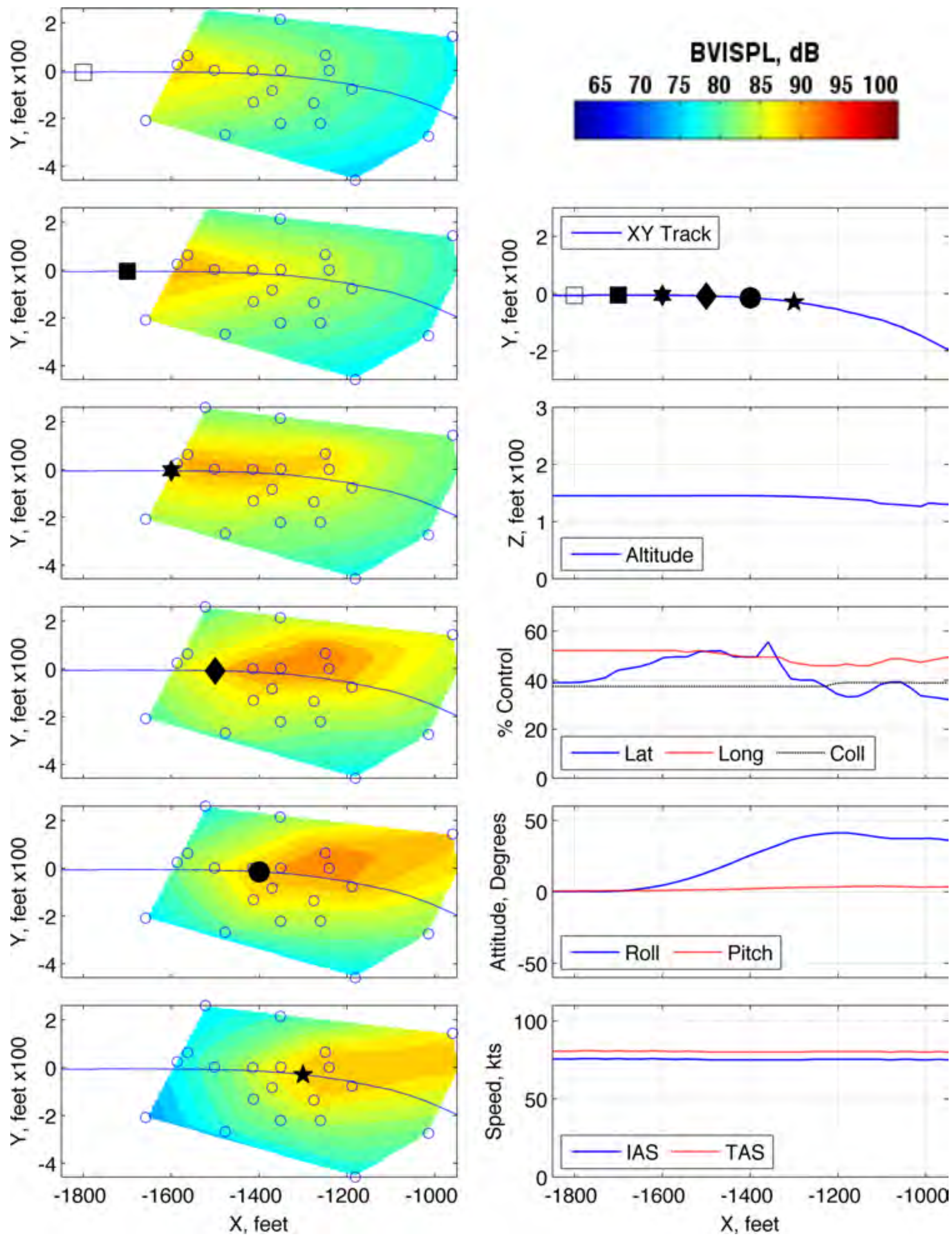

Figure 247: Maneuver condition R17, 80 KIAS, level, medium cyclic roll right, run number 285469

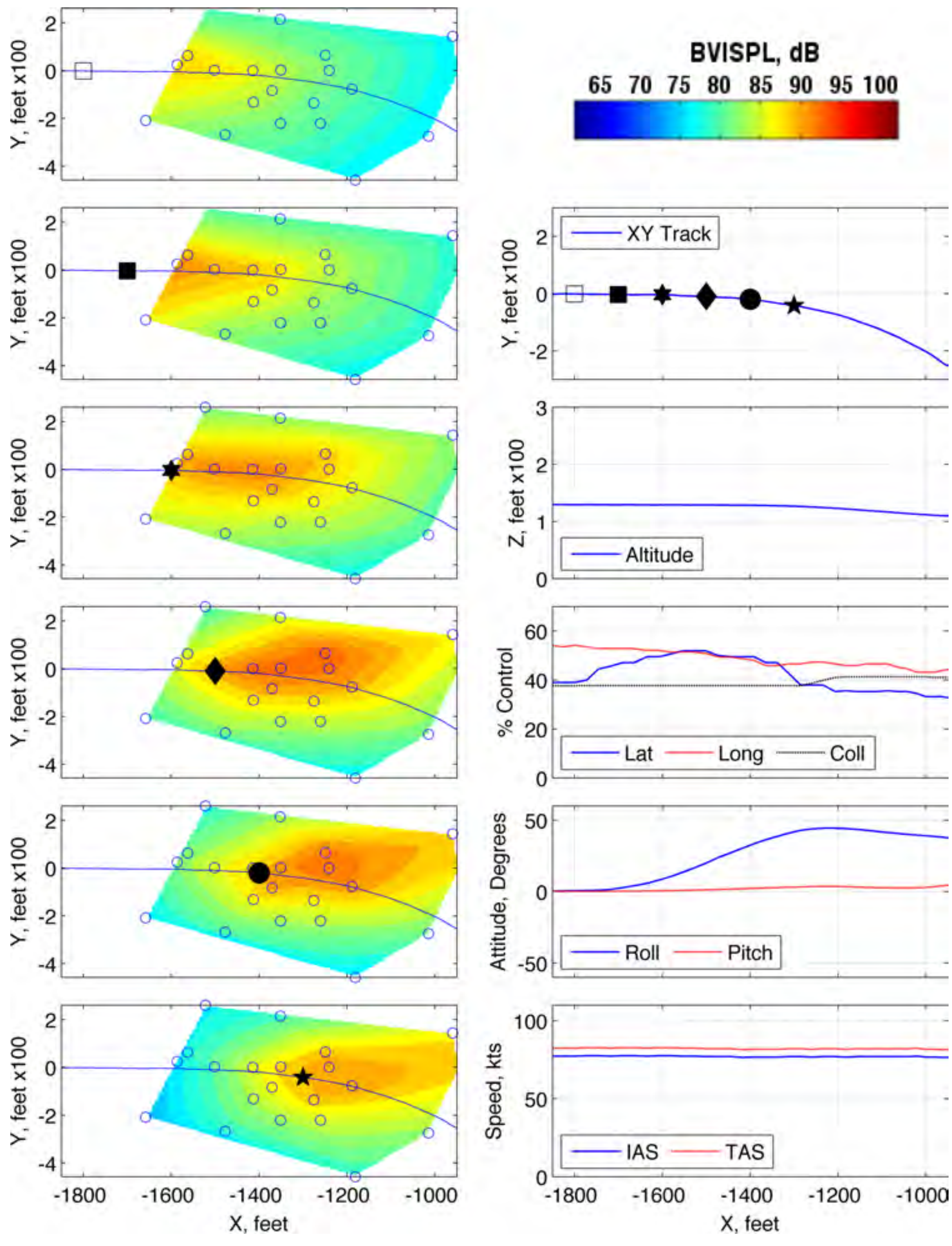

Figure 248: Maneuver condition R17, 80 KIAS, level, medium cyclic roll right, run number 285470

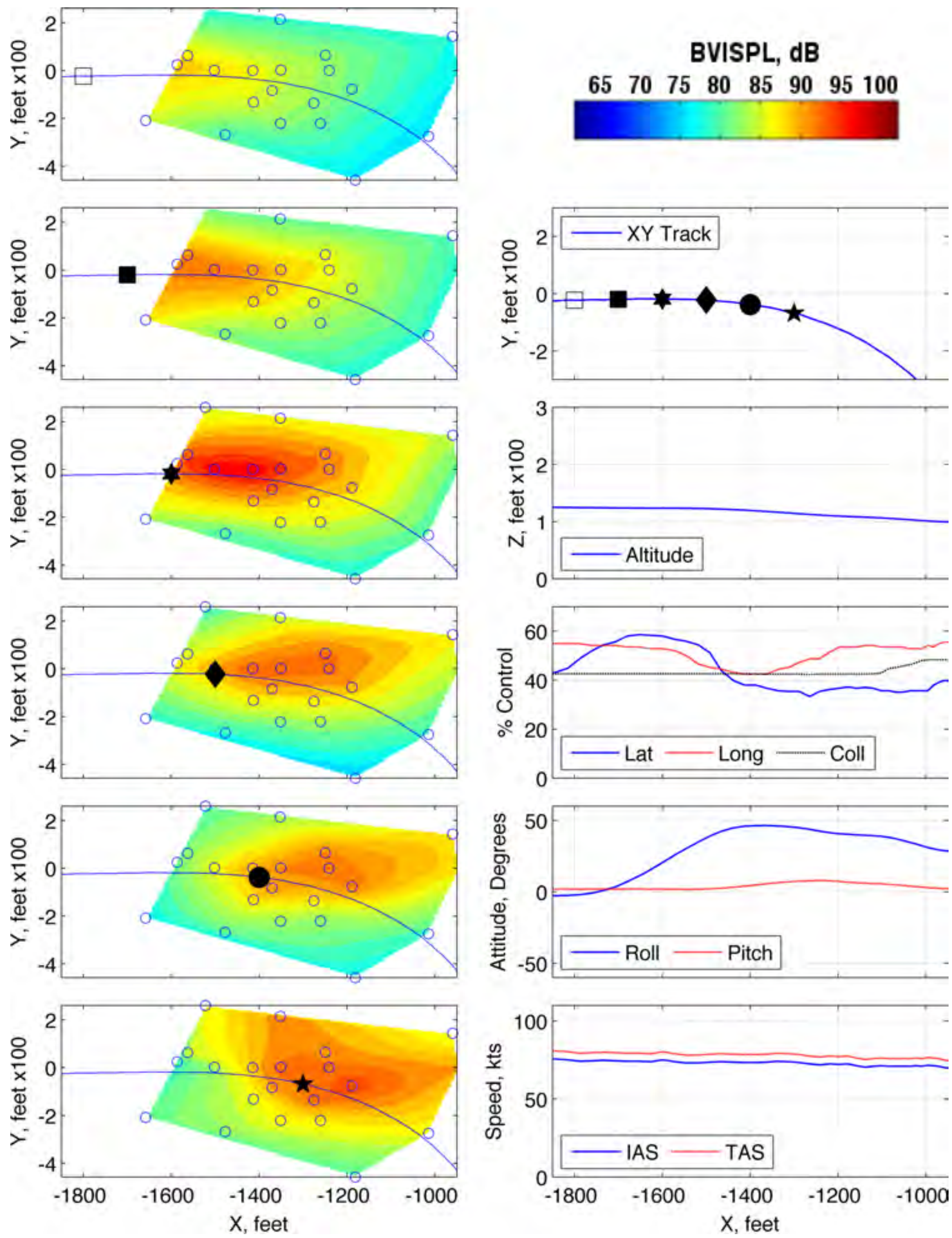

Figure 249: Maneuver condition R18, 80 KIAS, level, fast cyclic roll right, run number 280378

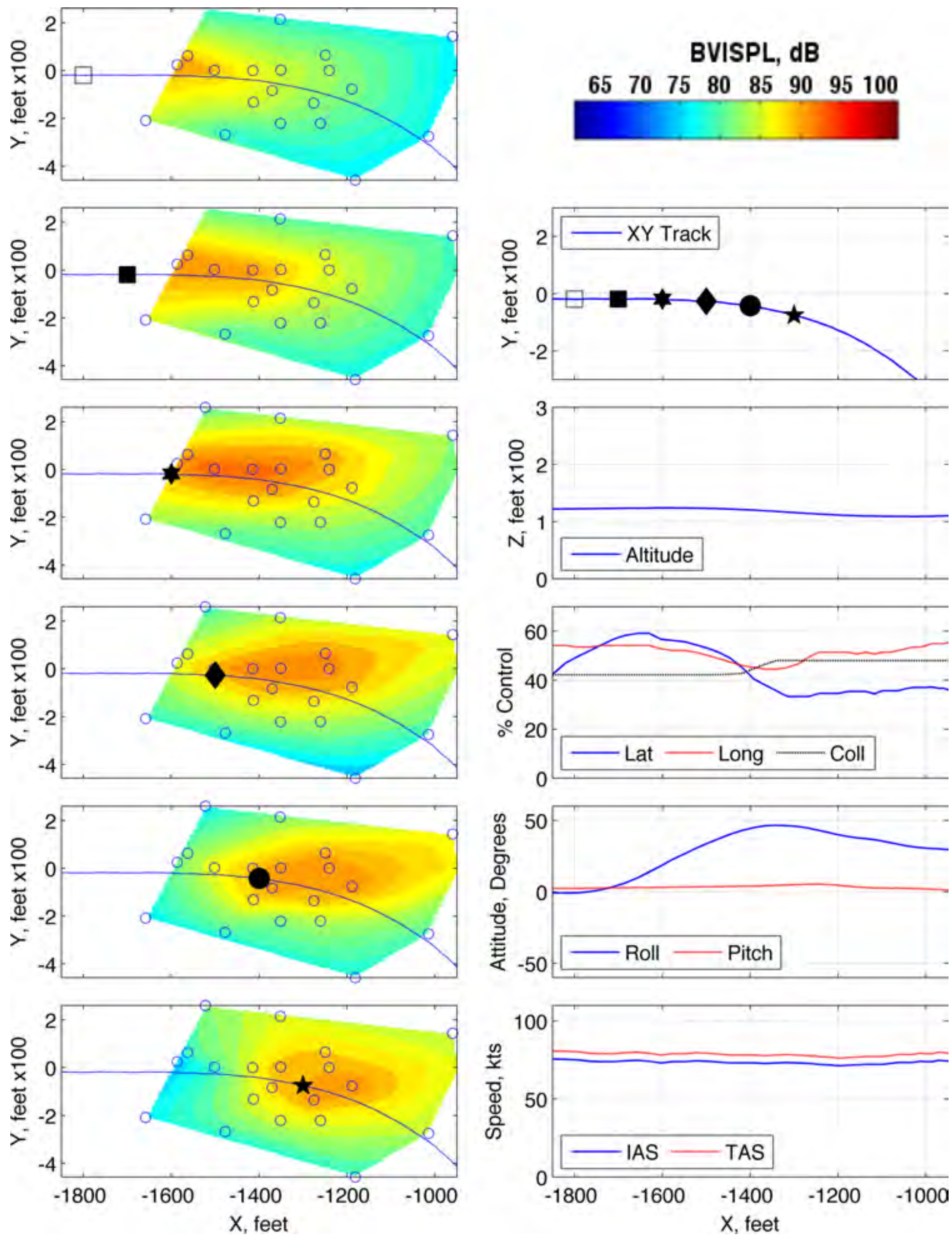

Figure 250: Maneuver condition R18, 80 KIAS, level, fast cyclic roll right, run number 280379

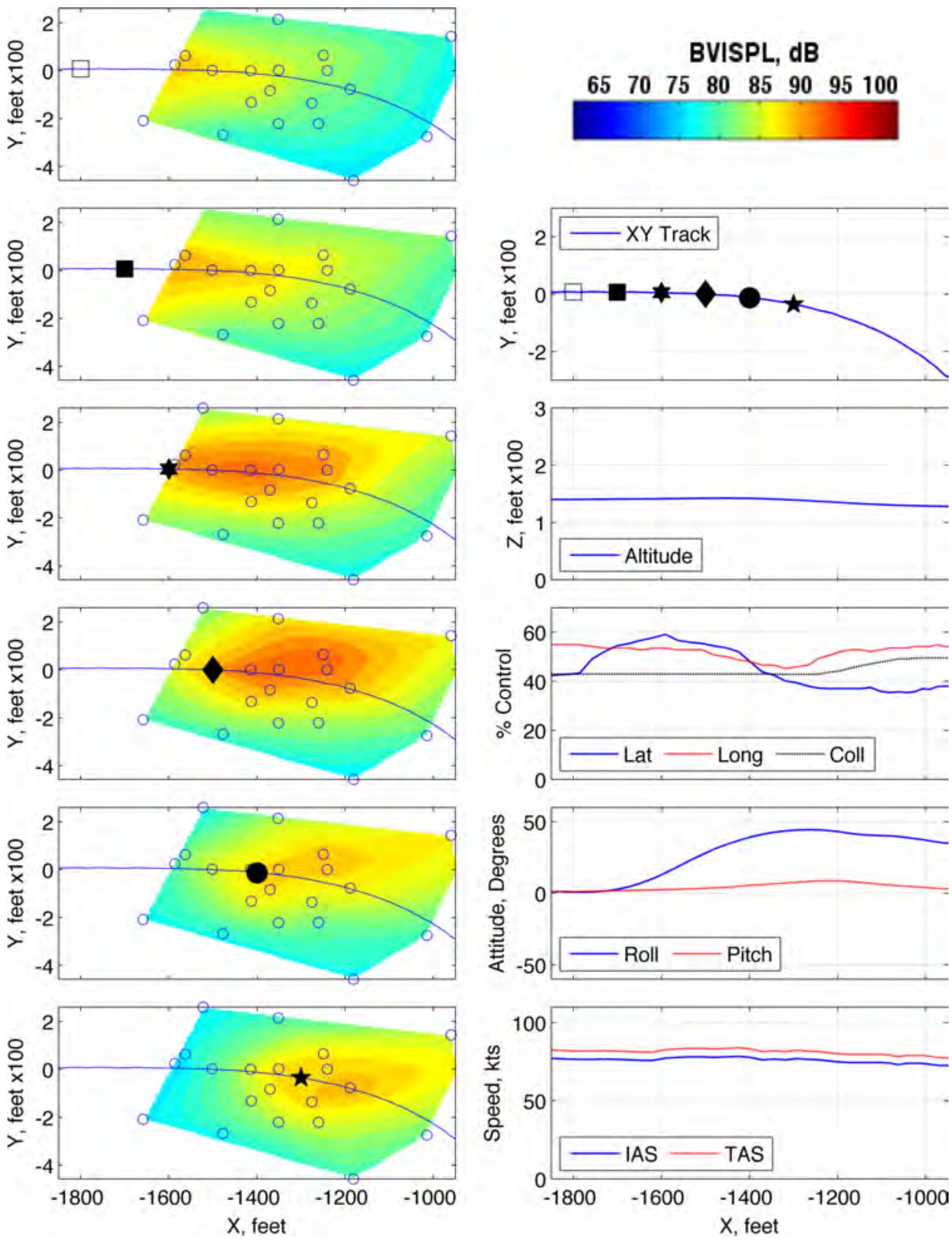

Figure 251: Maneuver condition R18, 80 KIAS, level, fast cyclic roll right, run number 280380

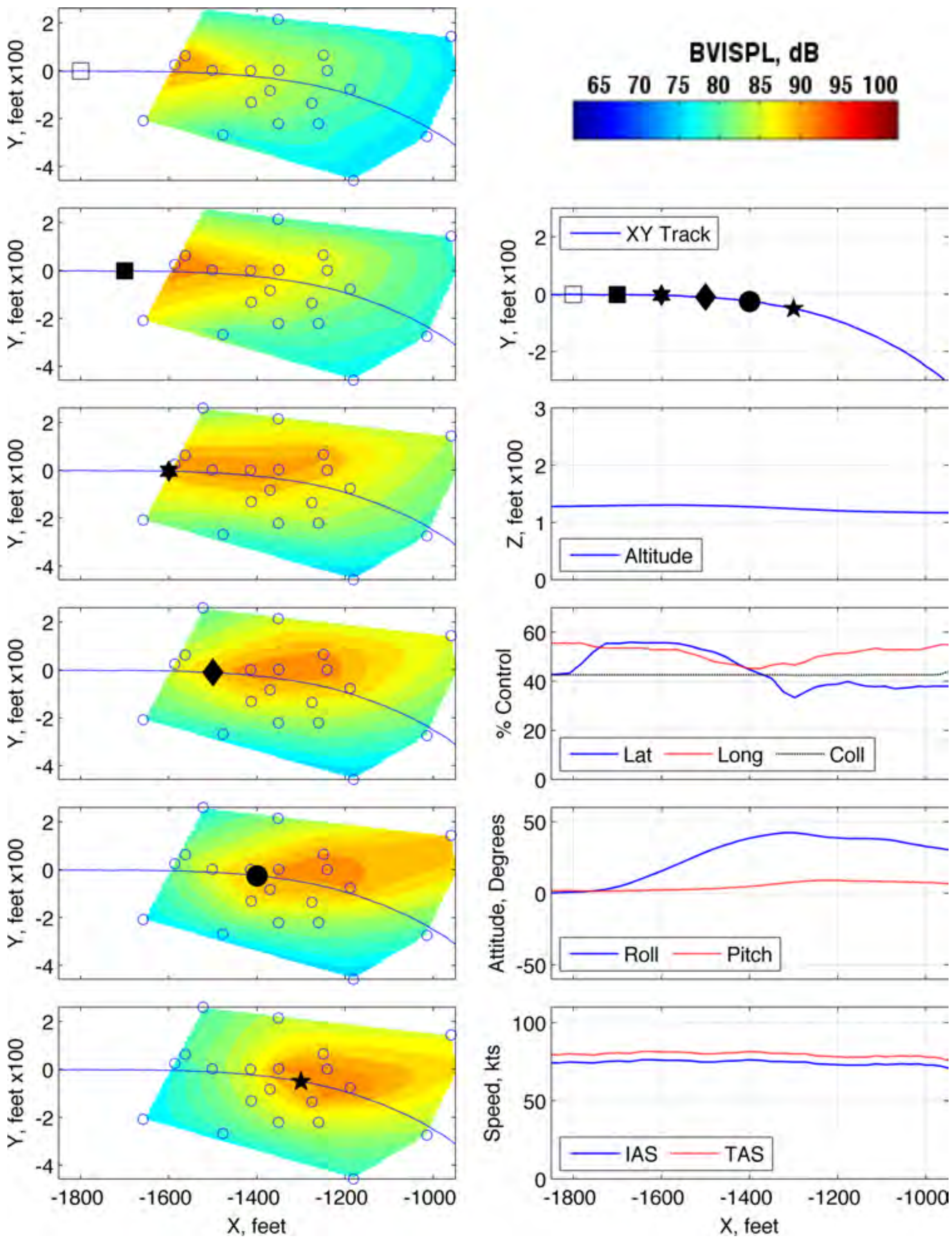

Figure 252: Maneuver condition R18, 80 KIAS, level, fast cyclic roll right, run number 280381

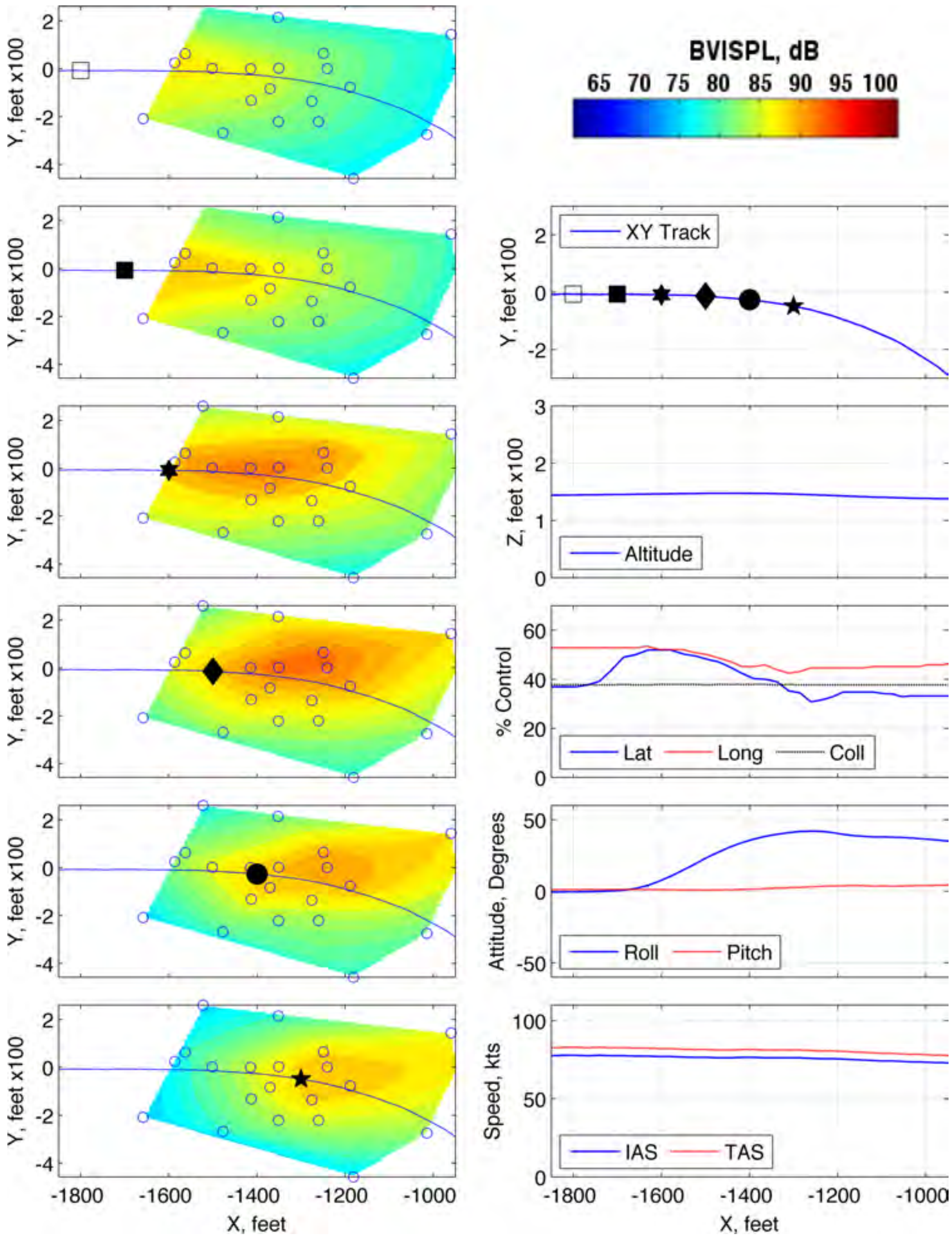

Figure 253: Maneuver condition R18, 80 KIAS, level, fast cyclic roll right, run number 285467

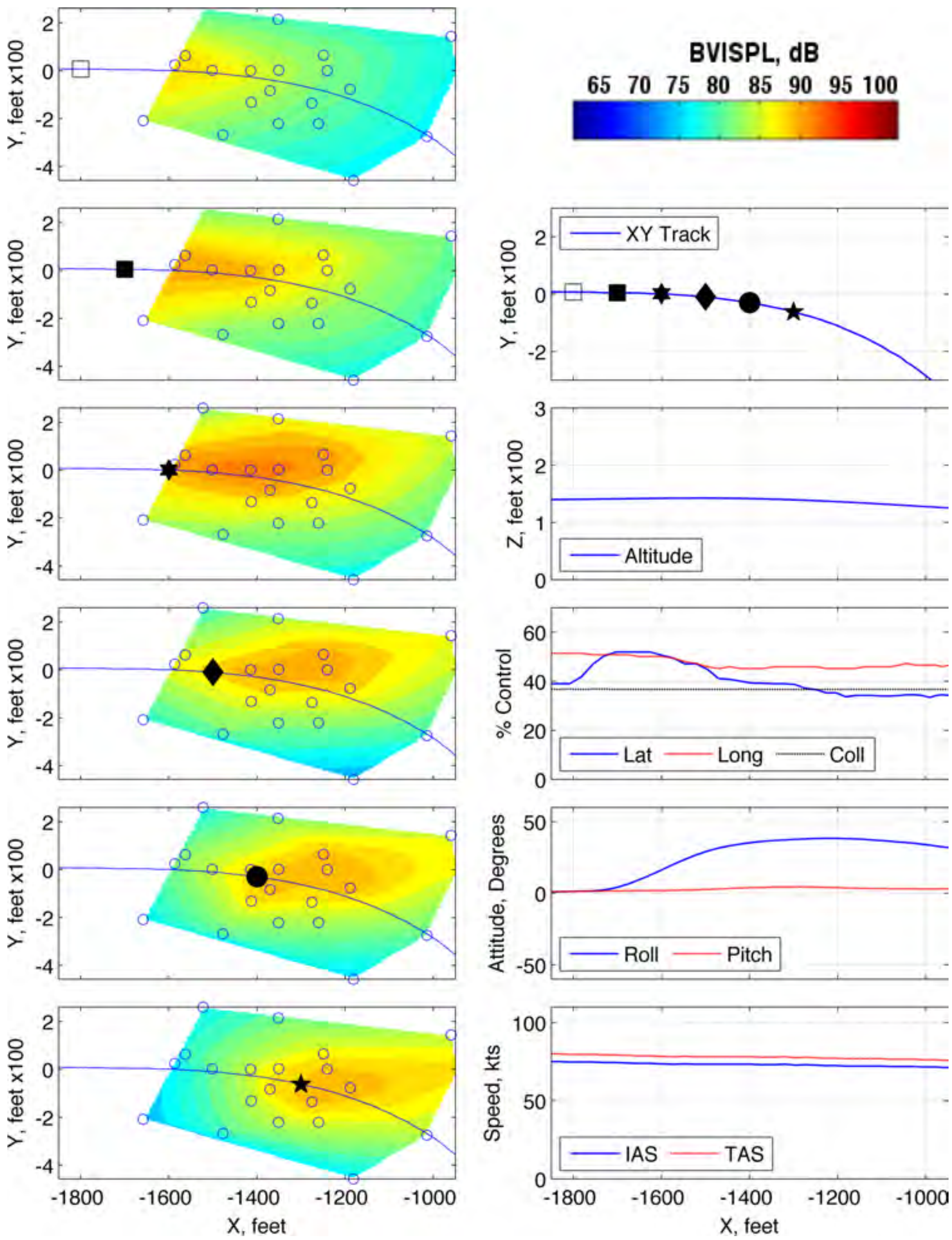

Figure 254: Maneuver condition R18, 80 KIAS, level, fast cyclic roll right, run number 285468

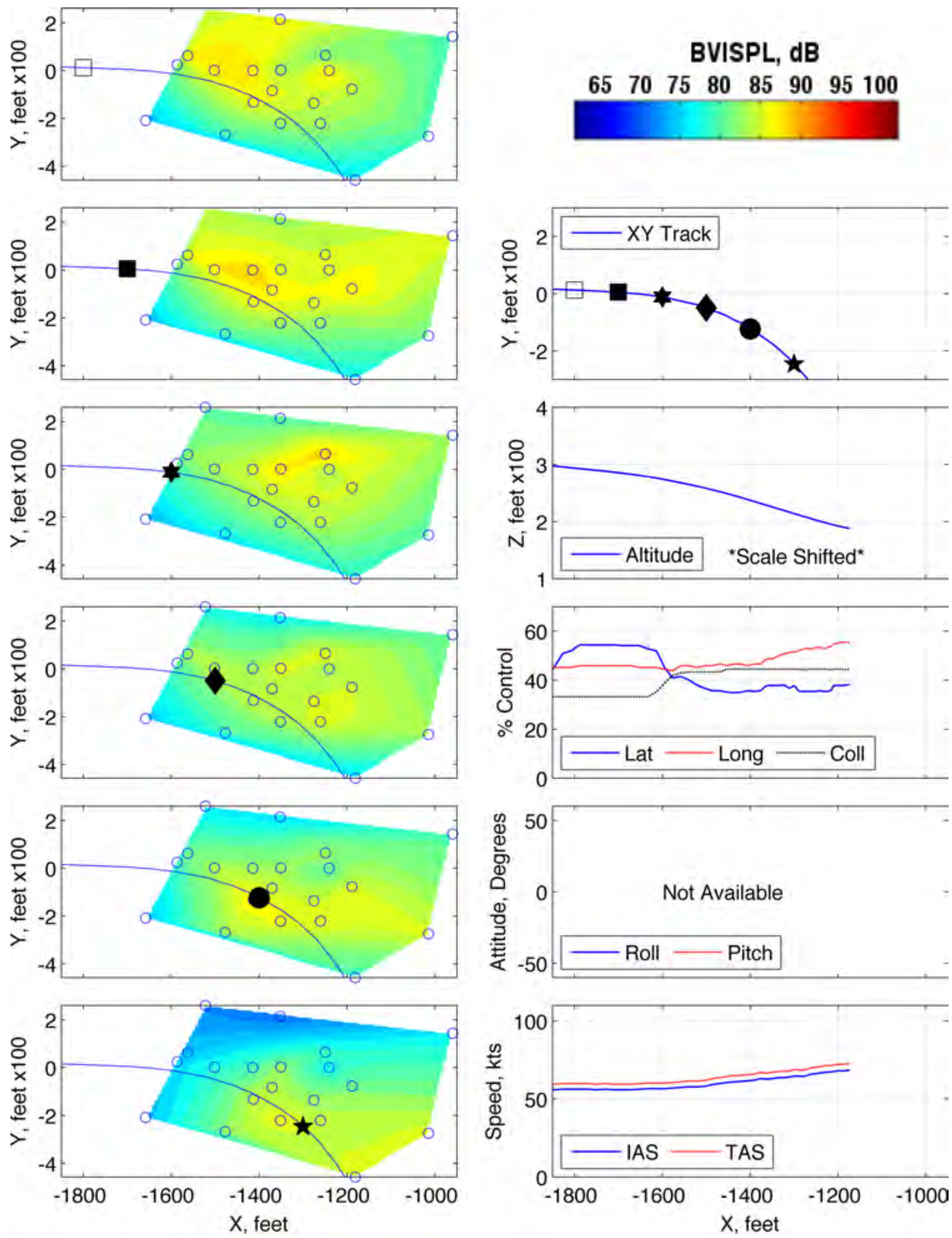

Figure 255: Maneuver condition R21, 60 KIAS, -6° , fast cyclic roll right, run number 280346

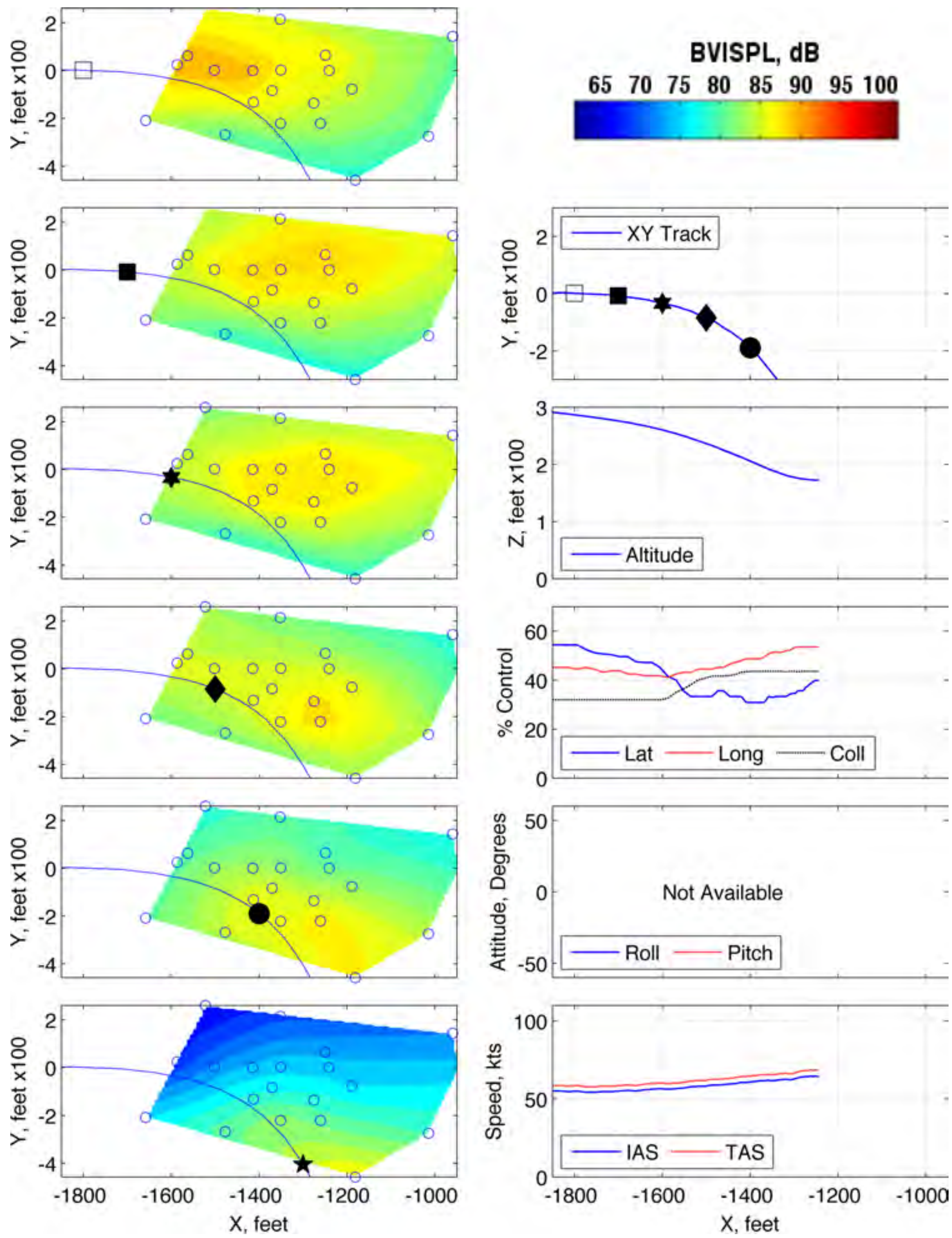

Figure 256: Maneuver condition R21, 60 KIAS, -6° , fast cyclic roll right, run number 280347

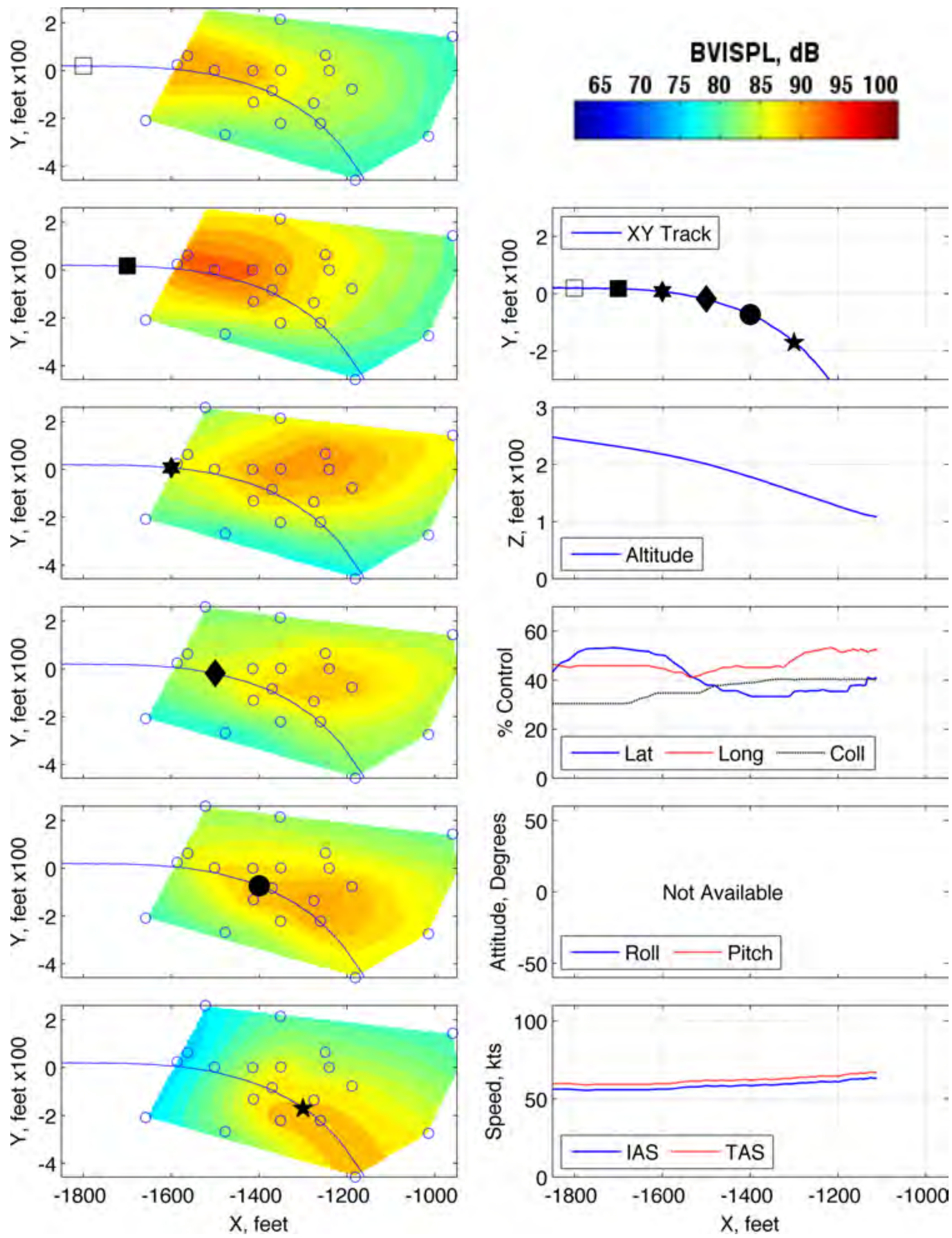

Figure 257: Maneuver condition R21, 60 KIAS, -6° , fast cyclic roll right, run number 280348

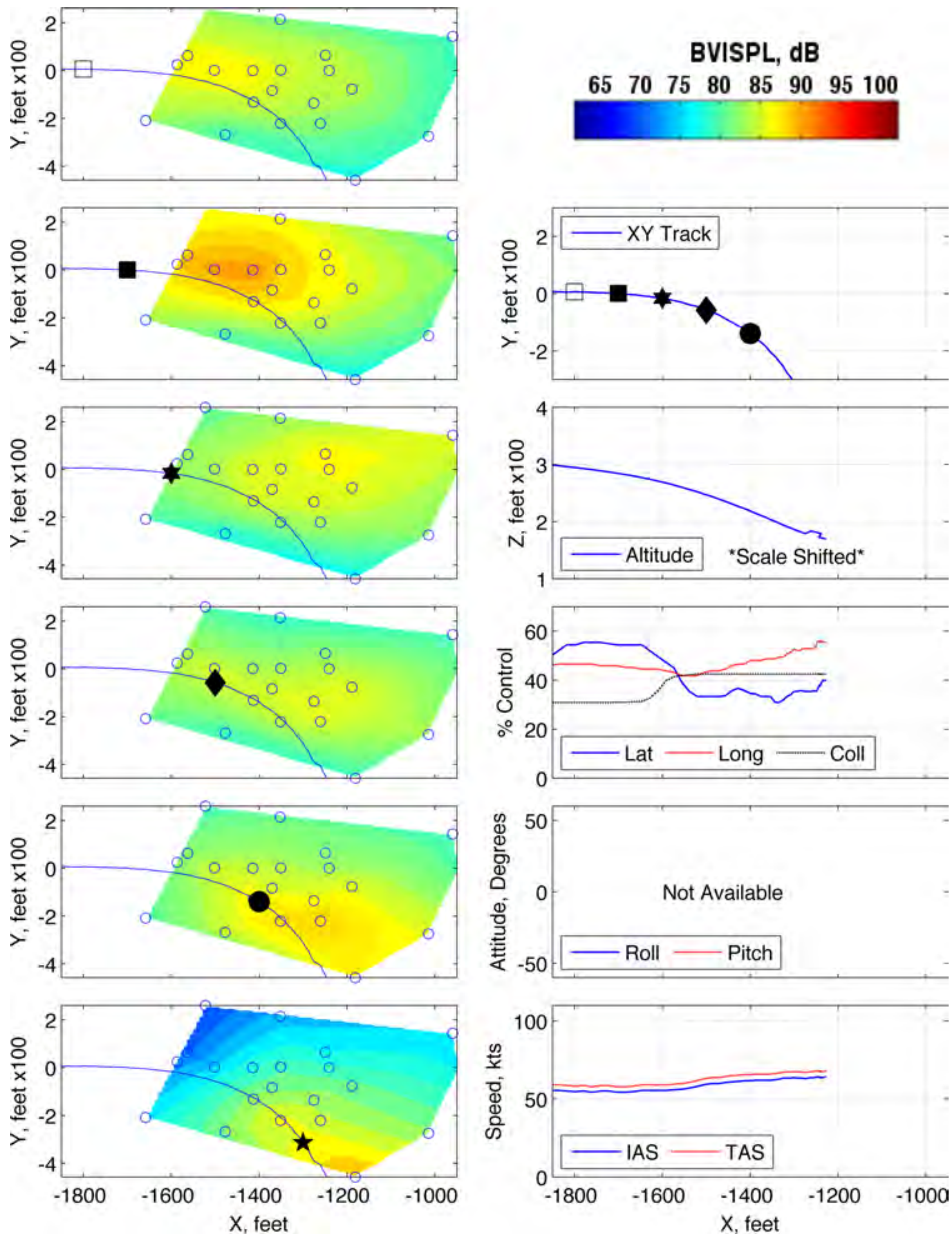

Figure 258: Maneuver condition R21, 60 KIAS, -6° , fast cyclic roll right, run number 280349

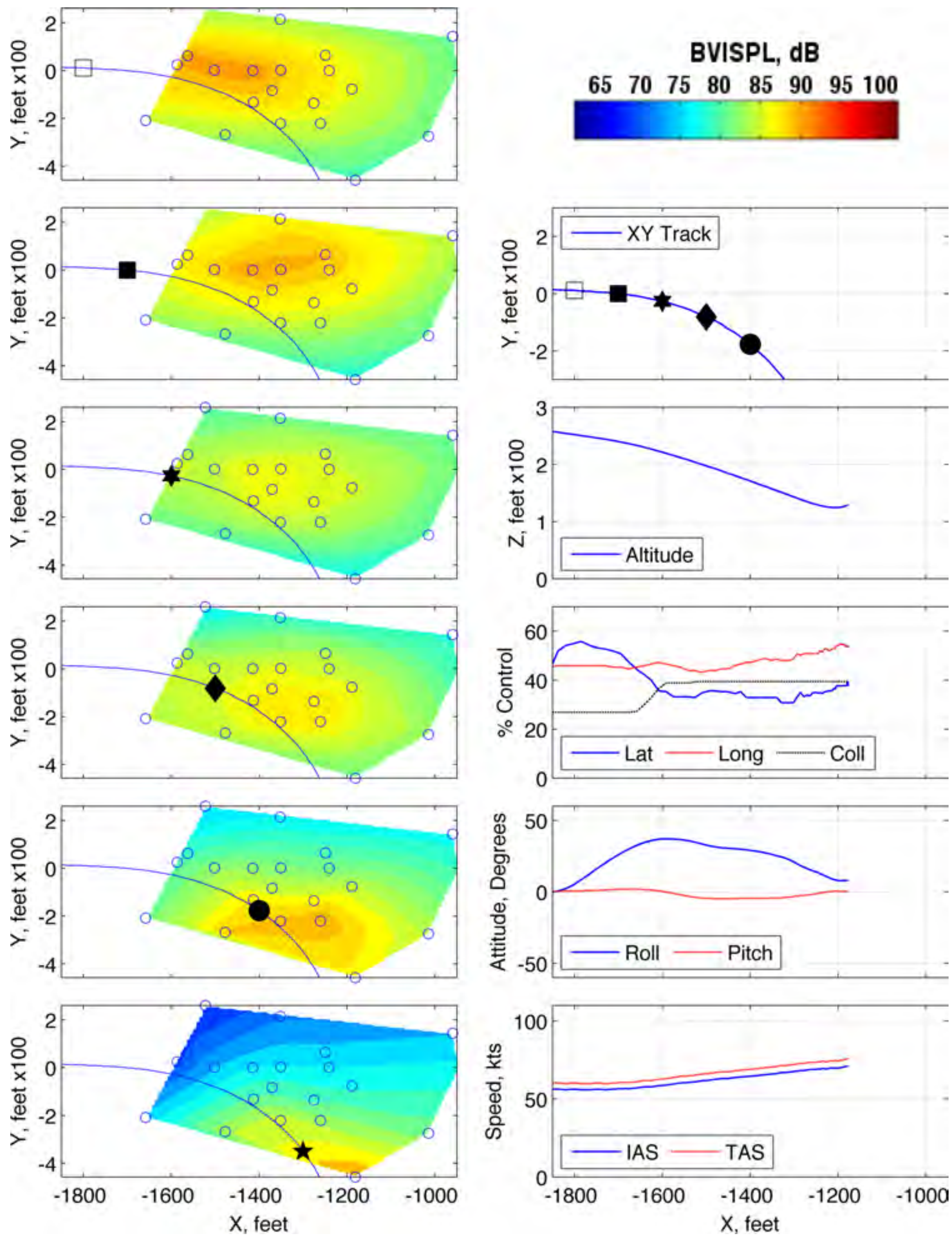

Figure 259: Maneuver condition R21, 60 KIAS, -6° , fast cyclic roll right, run number 287532

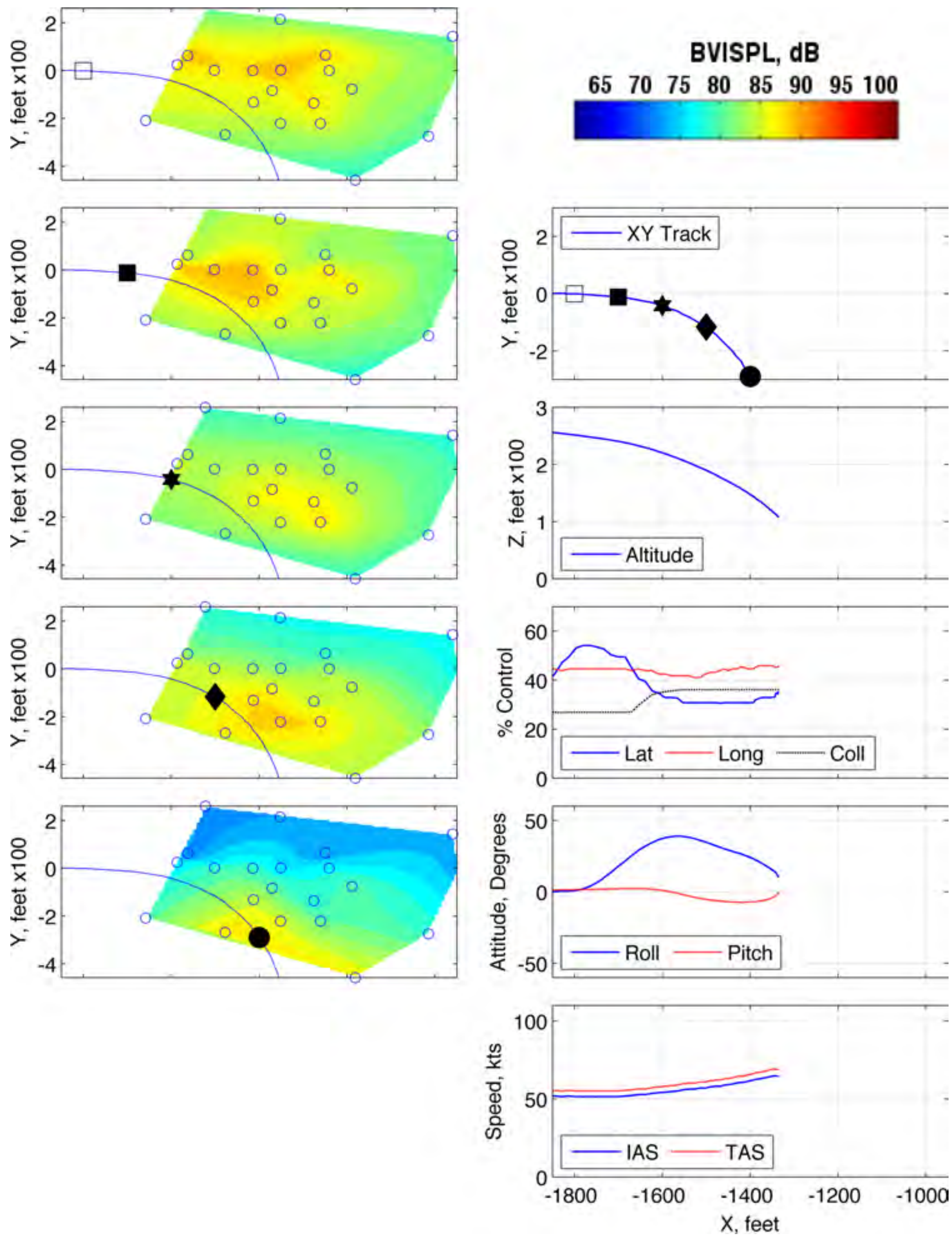

Figure 260: Maneuver condition R21, 60 KIAS, -6° , fast cyclic roll right, run number 287534

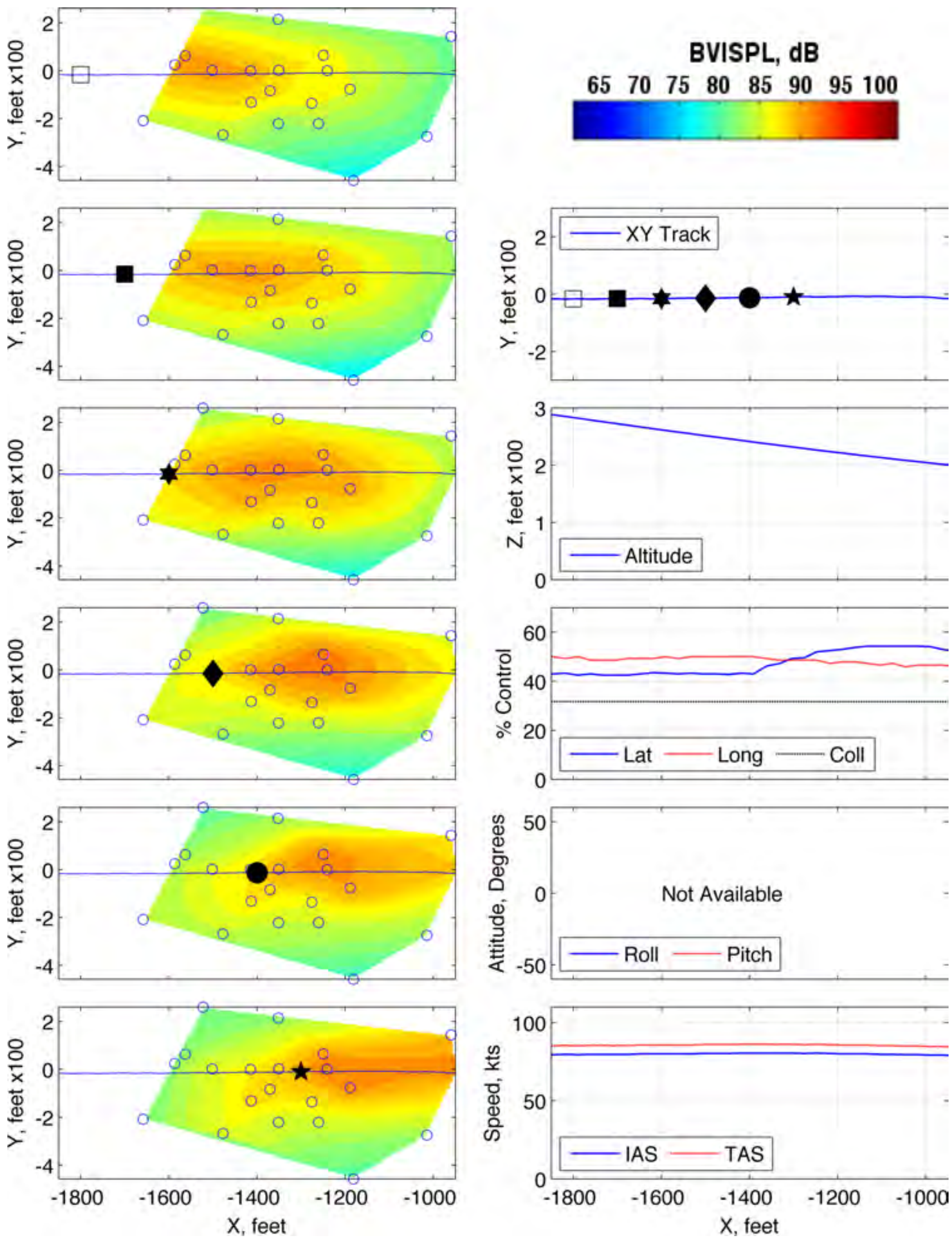

Figure 261: Maneuver condition R22, 80 KIAS, -6° , slow cyclic roll right, run number 278327

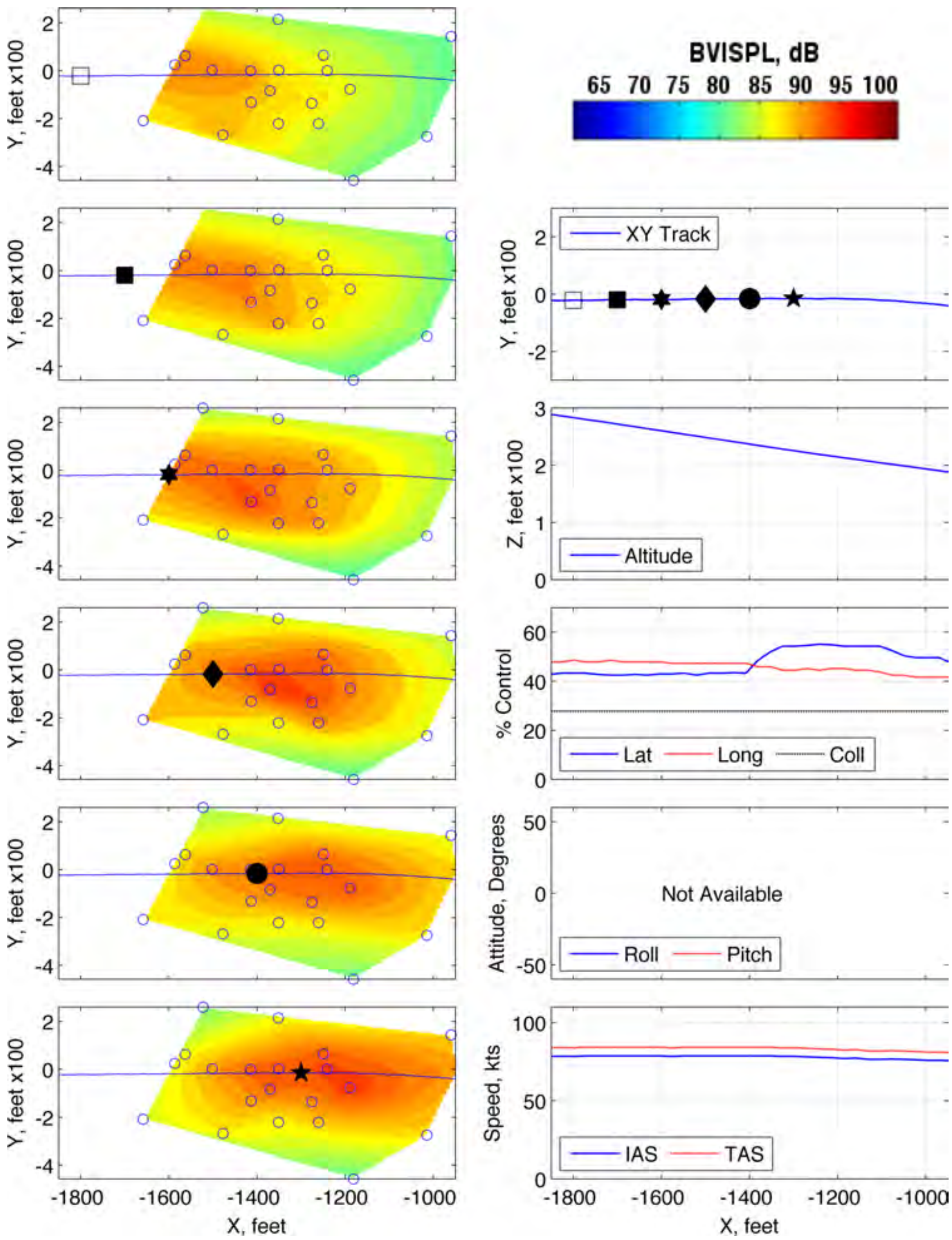

Figure 262: Maneuver condition R22, 80 KIAS, -6° , slow cyclic roll right, run number 278328

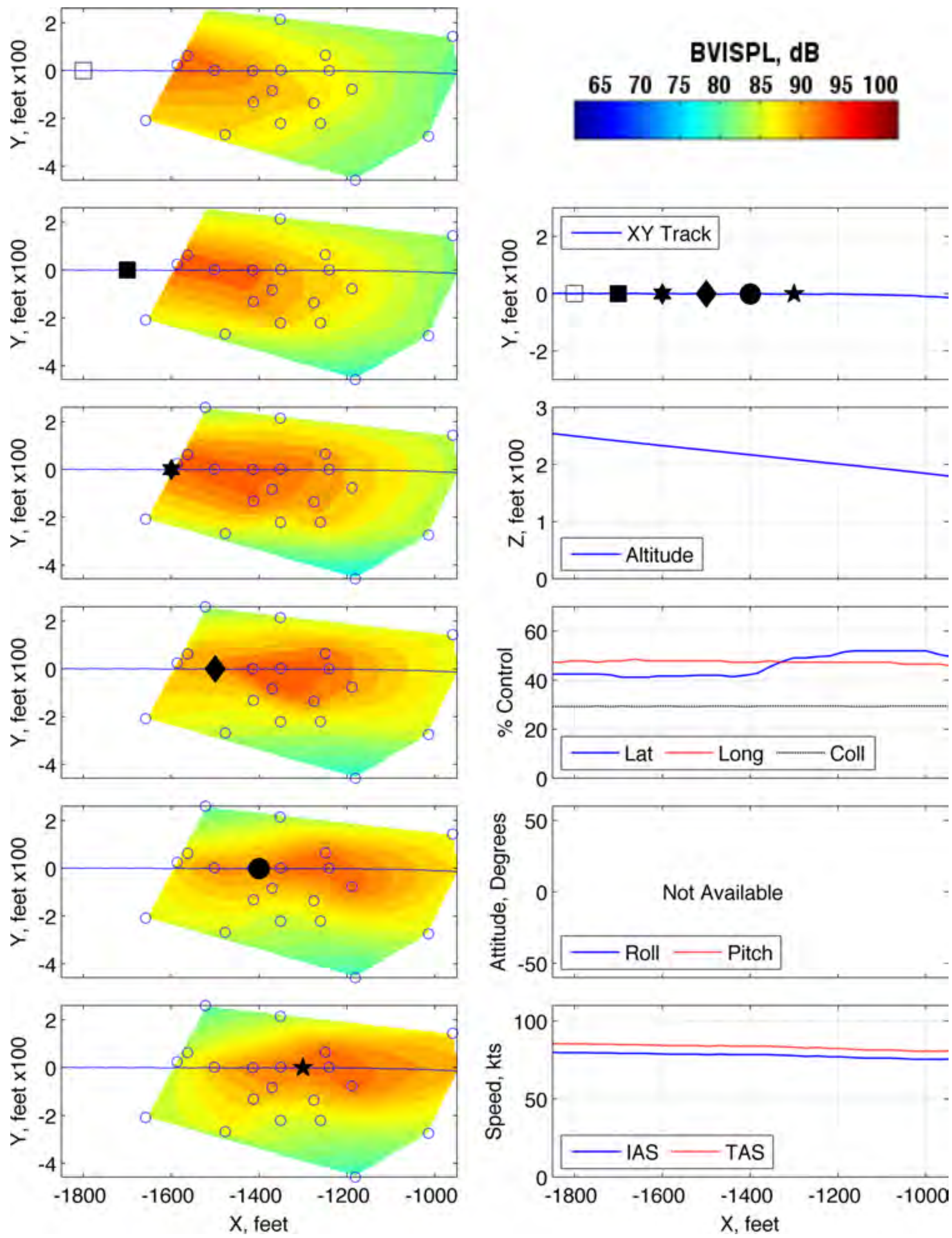

Figure 263: Maneuver condition R22, 80 KIAS, -6° , slow cyclic roll right, run number 278329

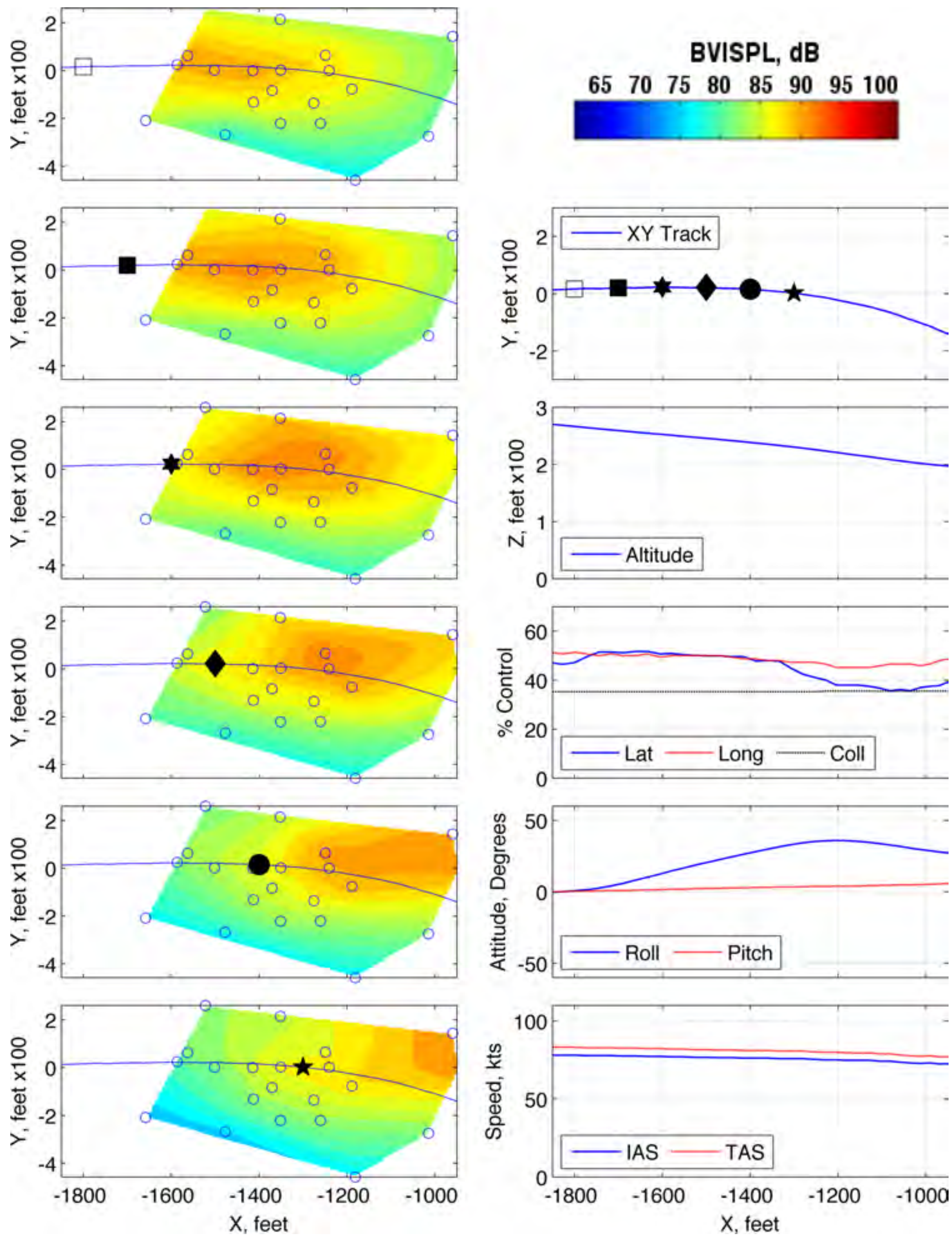

Figure 264: Maneuver condition R22, 80 KIAS, -6° , slow cyclic roll right, run number 280343

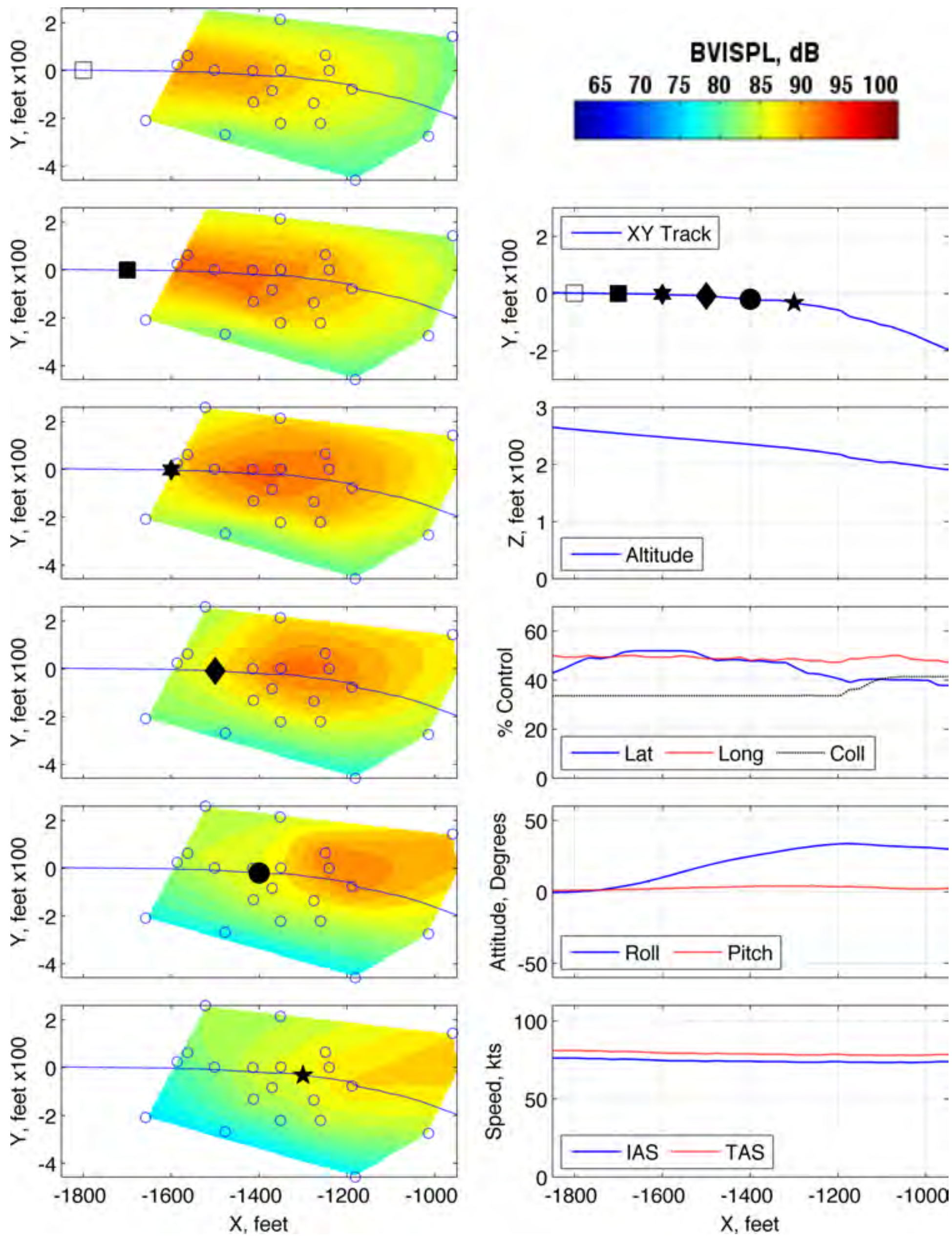

Figure 265: Maneuver condition R22, 80 KIAS, -6° , slow cyclic roll right, run number 280344

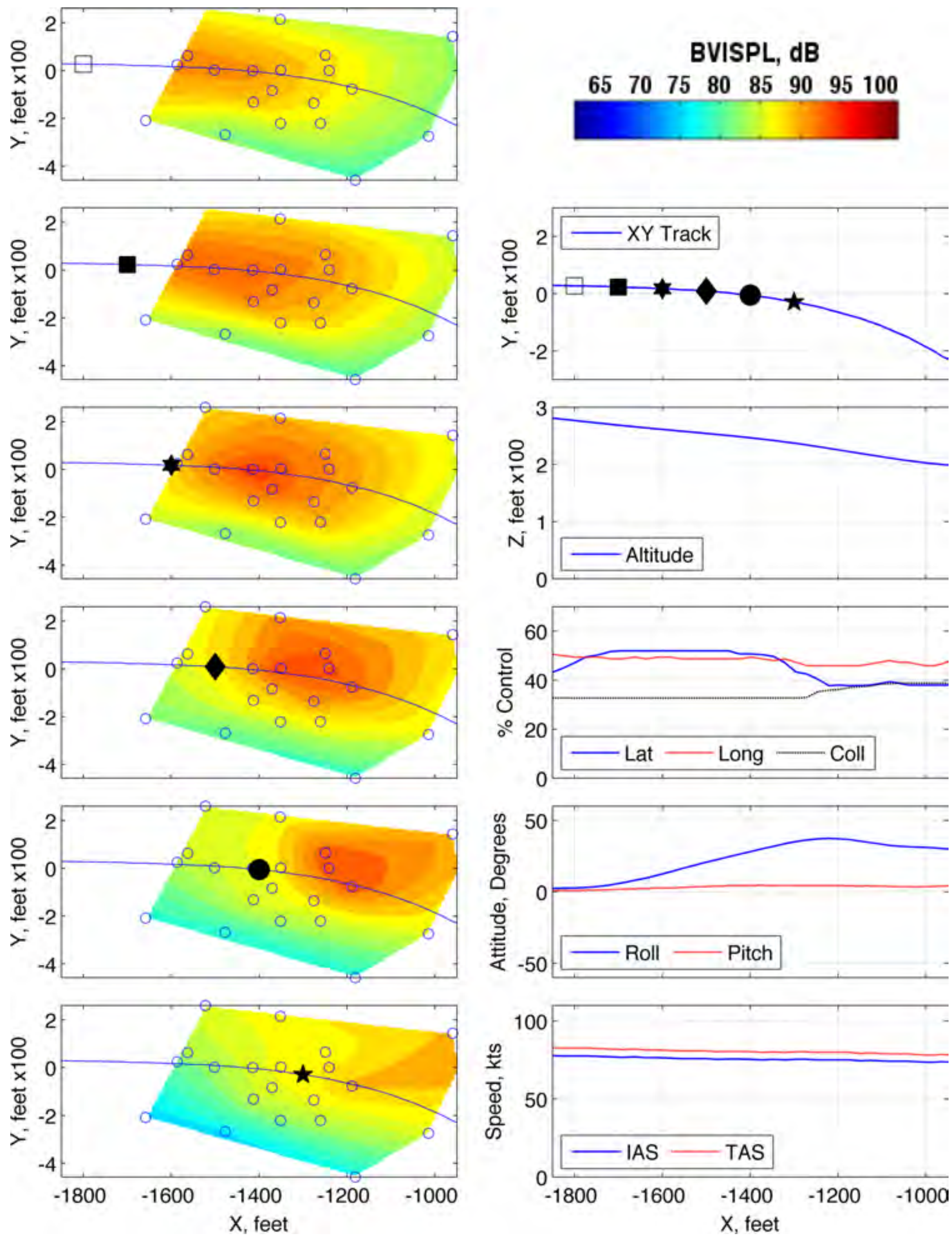

Figure 266: Maneuver condition R22, 80 KIAS, -6° , slow cyclic roll right, run number 280345

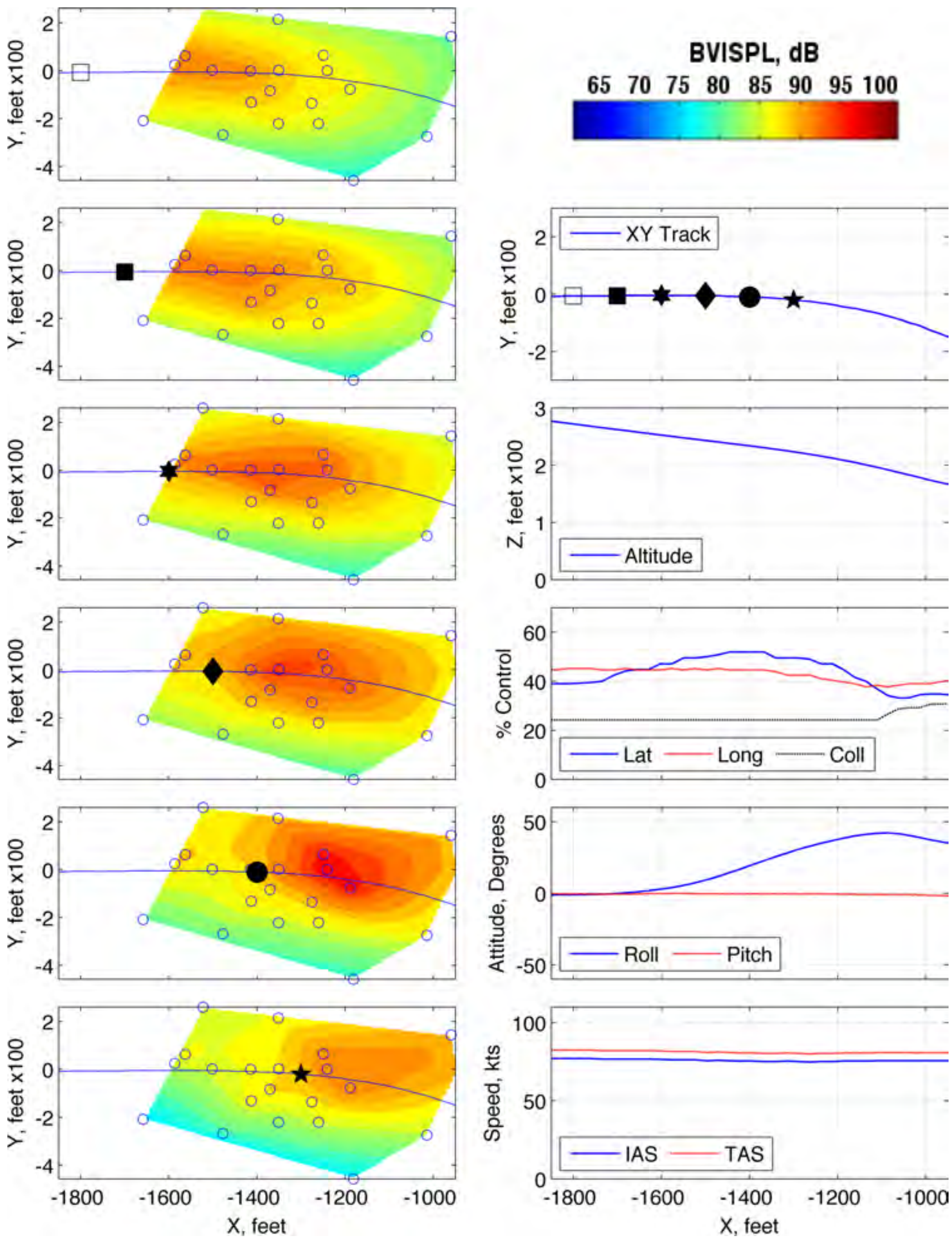

Figure 267: Maneuver condition R23, 80 KIAS, -6° , medium cyclic roll right, run number 285486

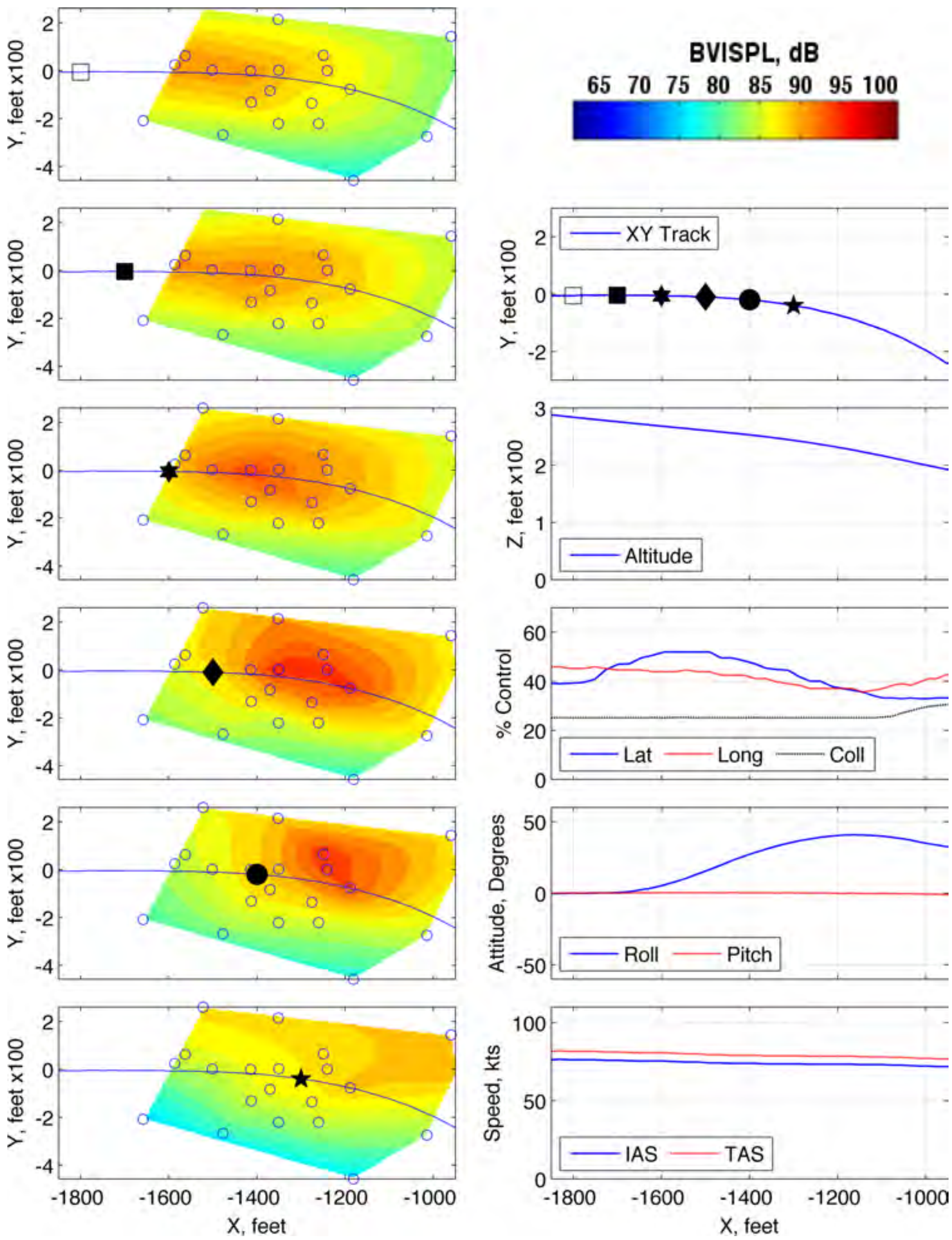

Figure 268: Maneuver condition R23, 80 KIAS, -6° , medium cyclic roll right, run number 285487

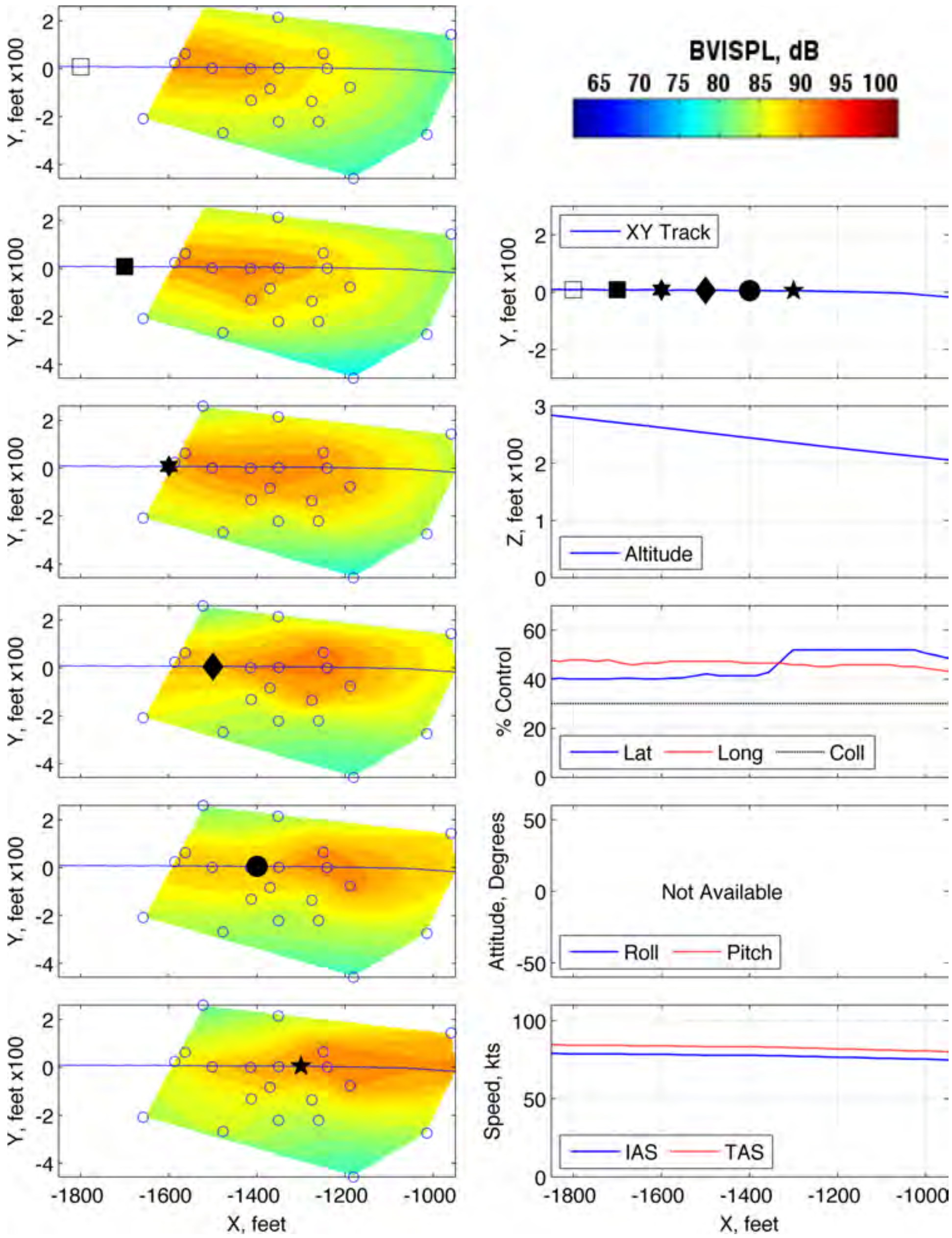

Figure 269: Maneuver condition R24, 80 KIAS, -6° , fast cyclic roll right, run number 278323

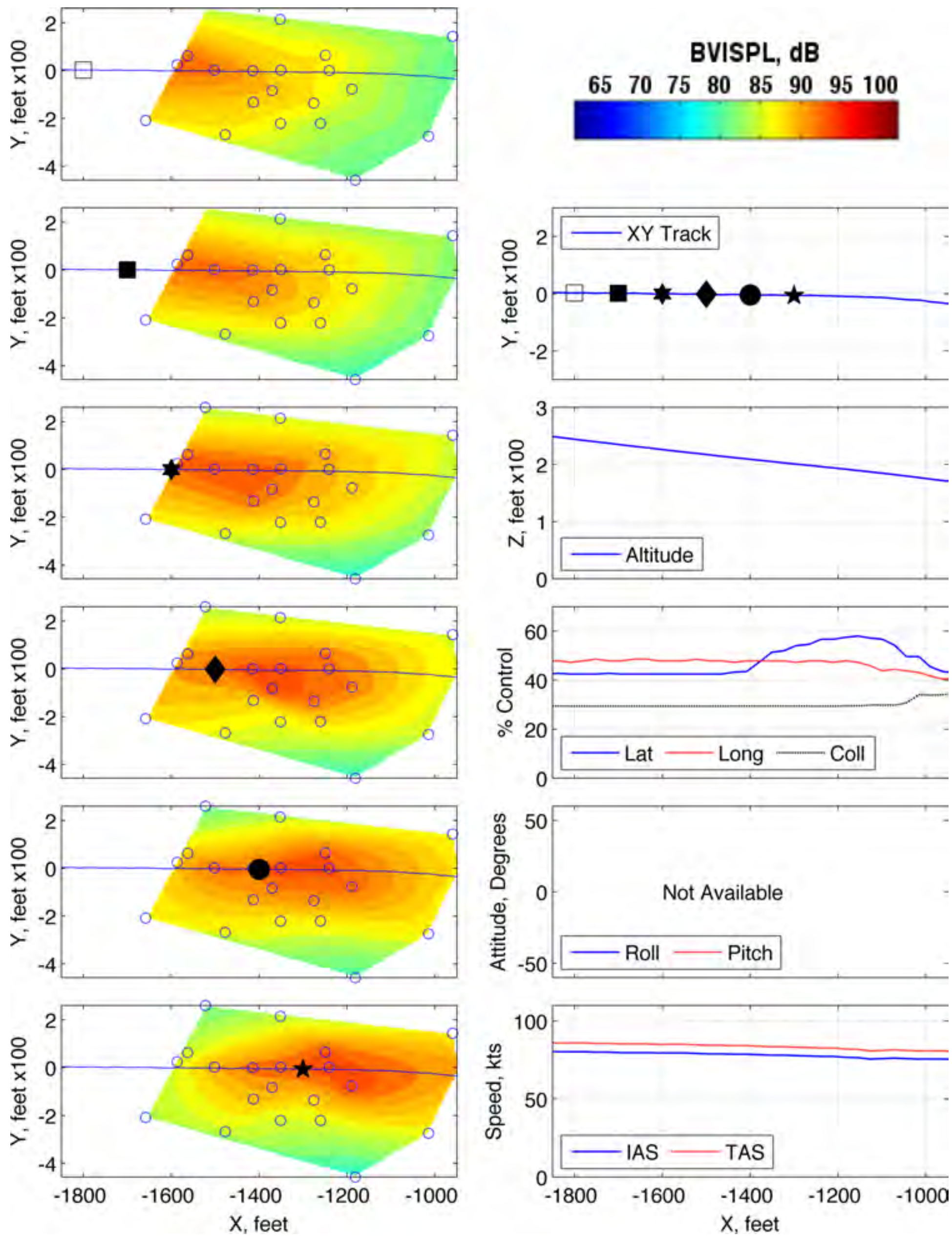

Figure 270: Maneuver condition R24, 80 KIAS, -6° , fast cyclic roll right, run number 278324

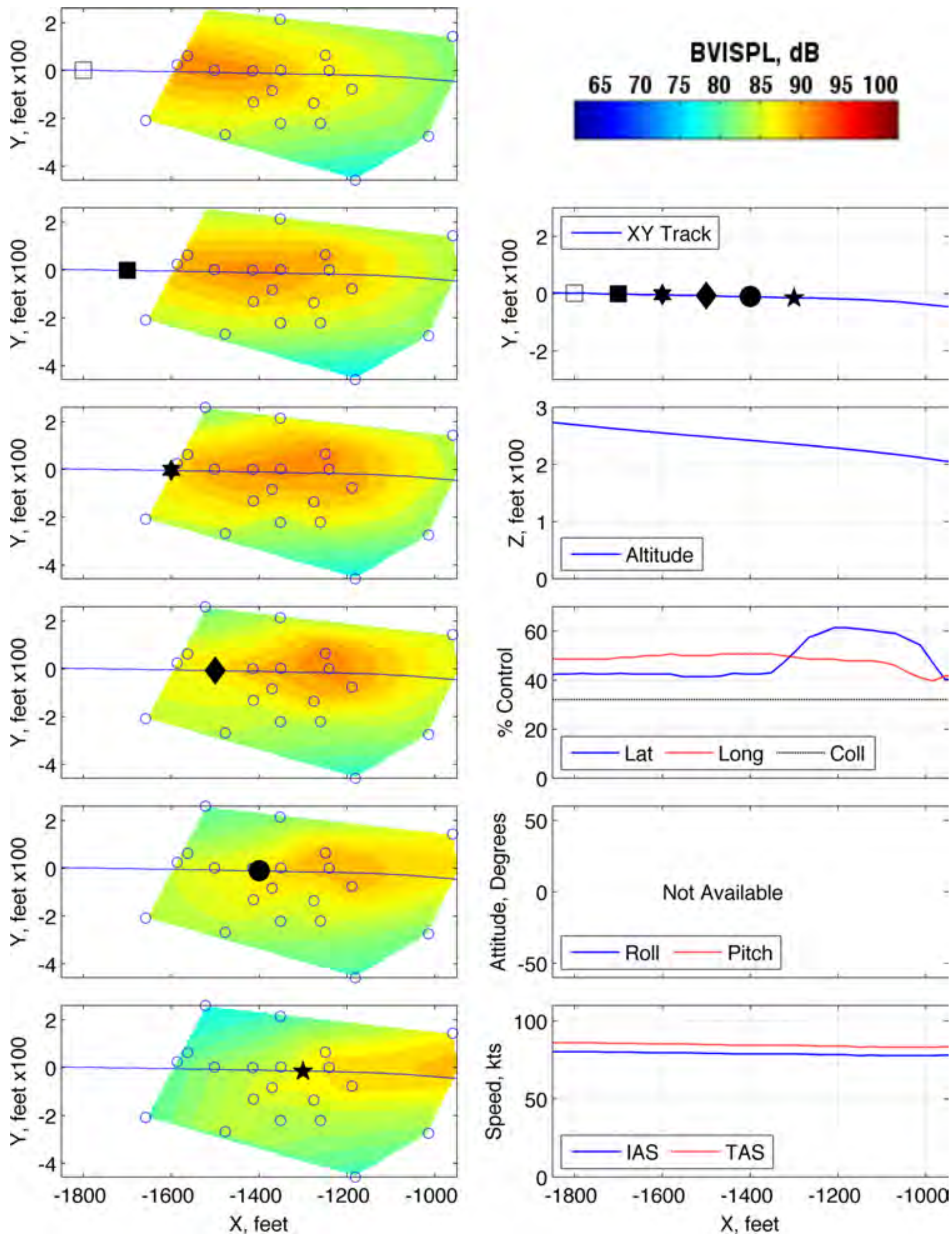

Figure 271: Maneuver condition R24, 80 KIAS, -6° , fast cyclic roll right, run number 278325

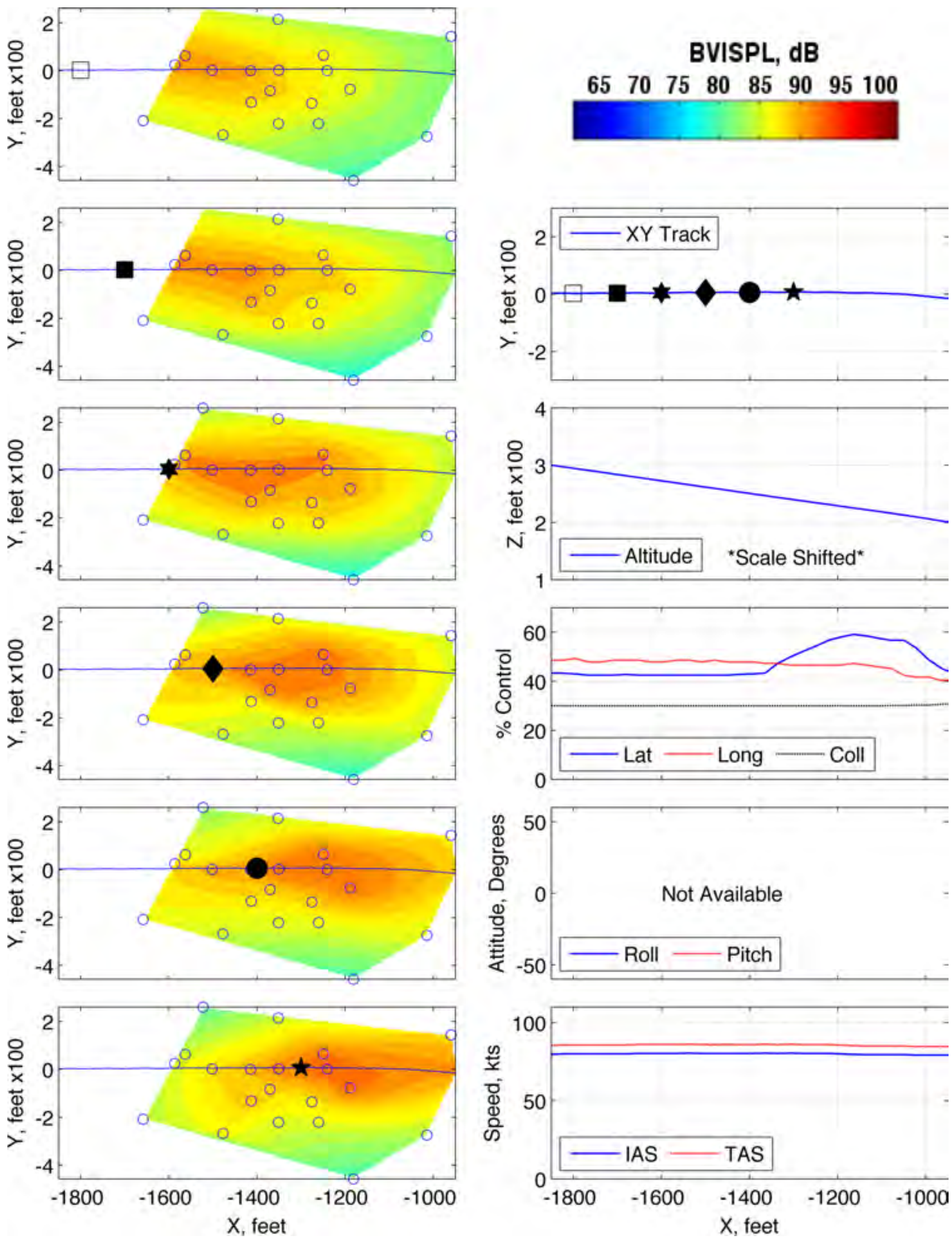

Figure 272: Maneuver condition R24, 80 KIAS, -6° , fast cyclic roll right, run number 278326

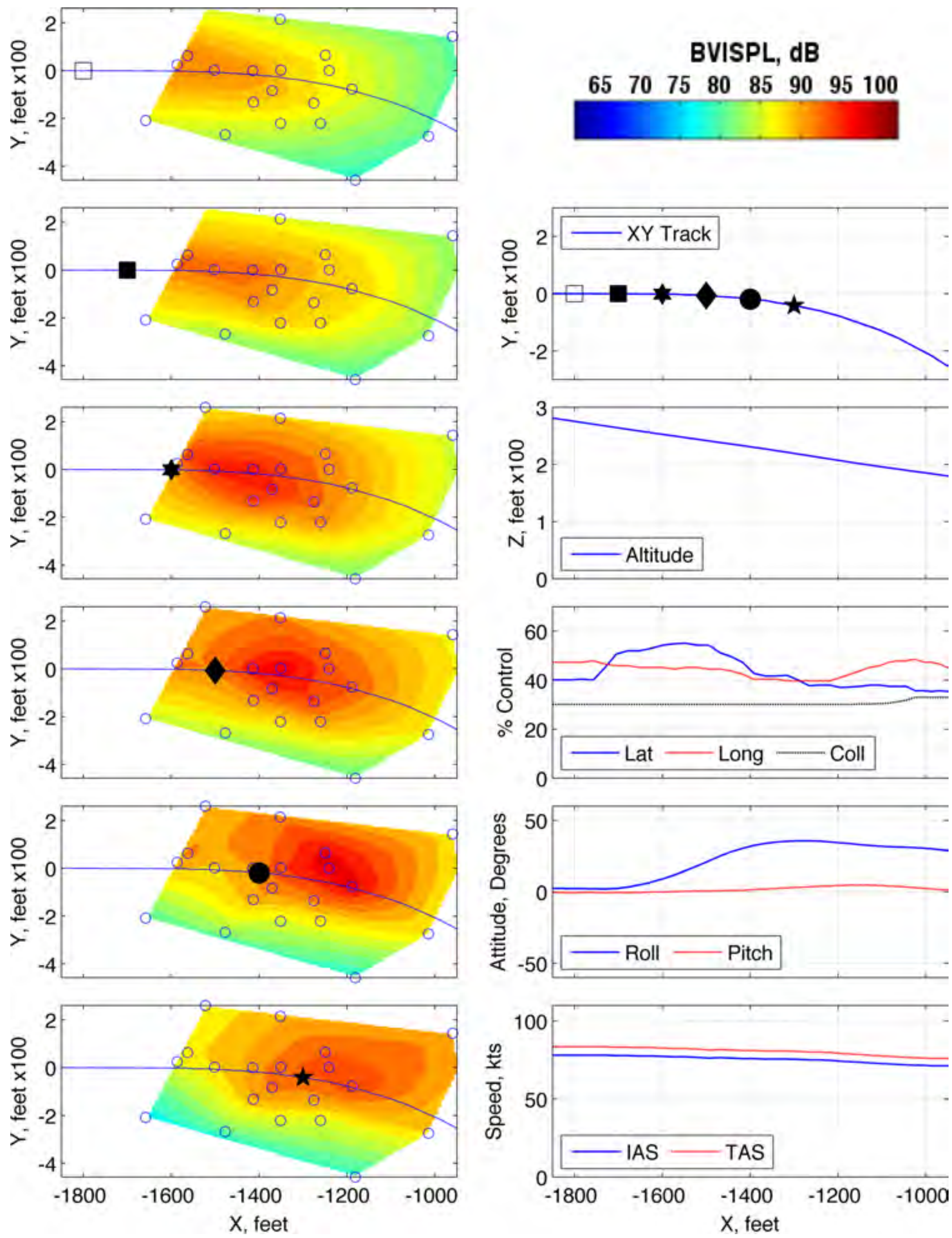

Figure 273: Maneuver condition R24, 80 KIAS, -6° , fast cyclic roll right, run number 282422

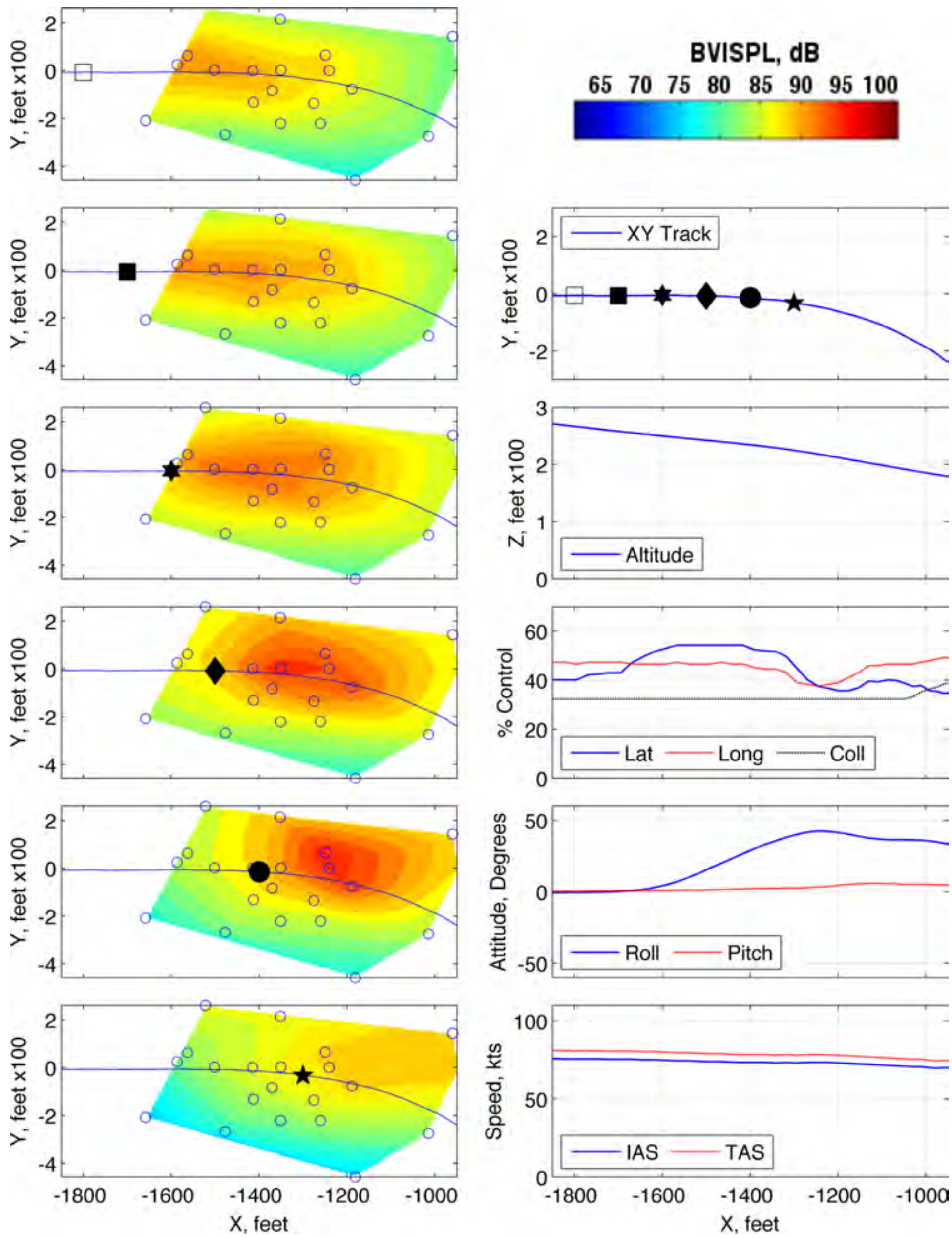

Figure 274: Maneuver condition R24, 80 KIAS, -6° , fast cyclic roll right, run number 282423

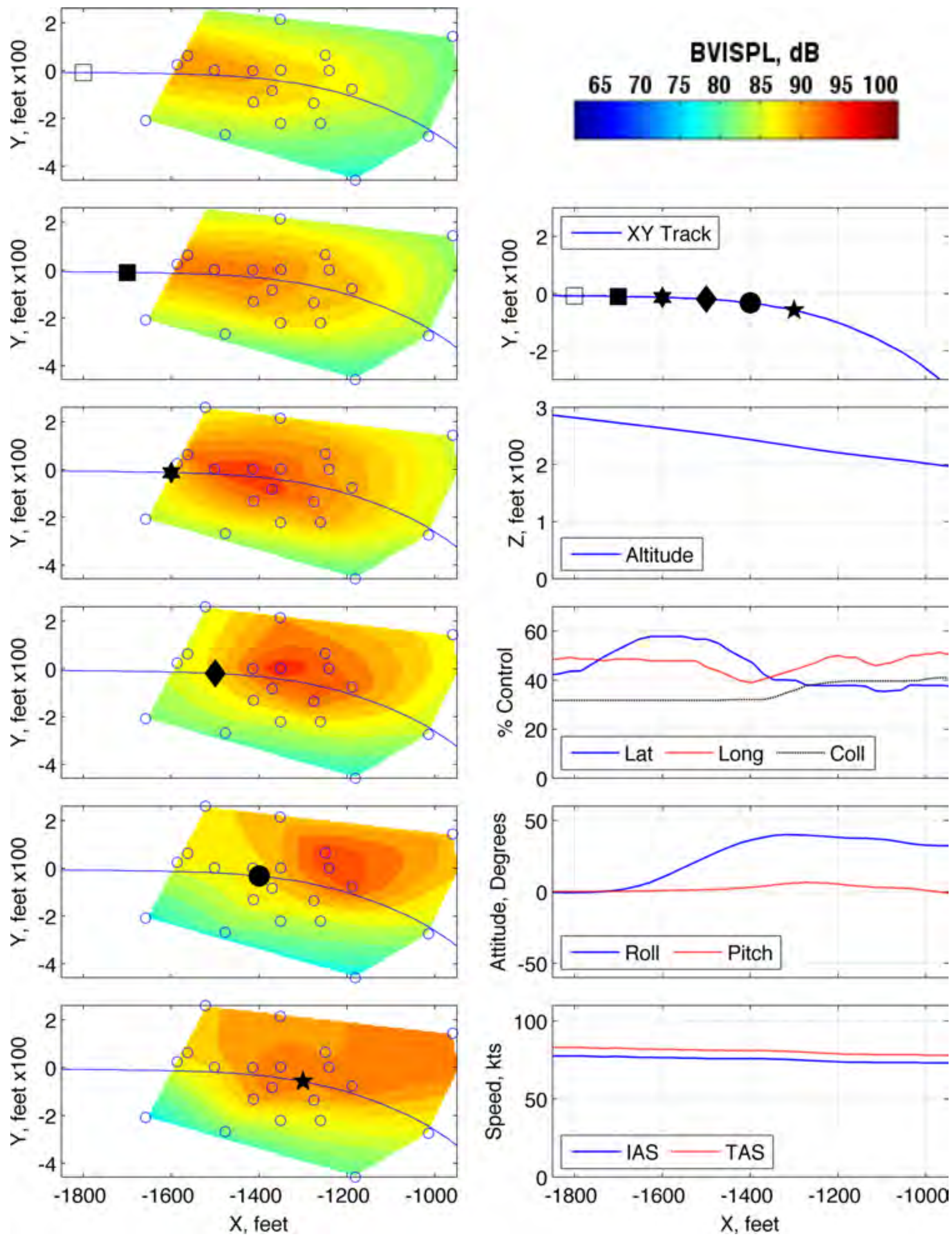

Figure 275: Maneuver condition R24, 80 KIAS, -6° , fast cyclic roll right, run number 282424

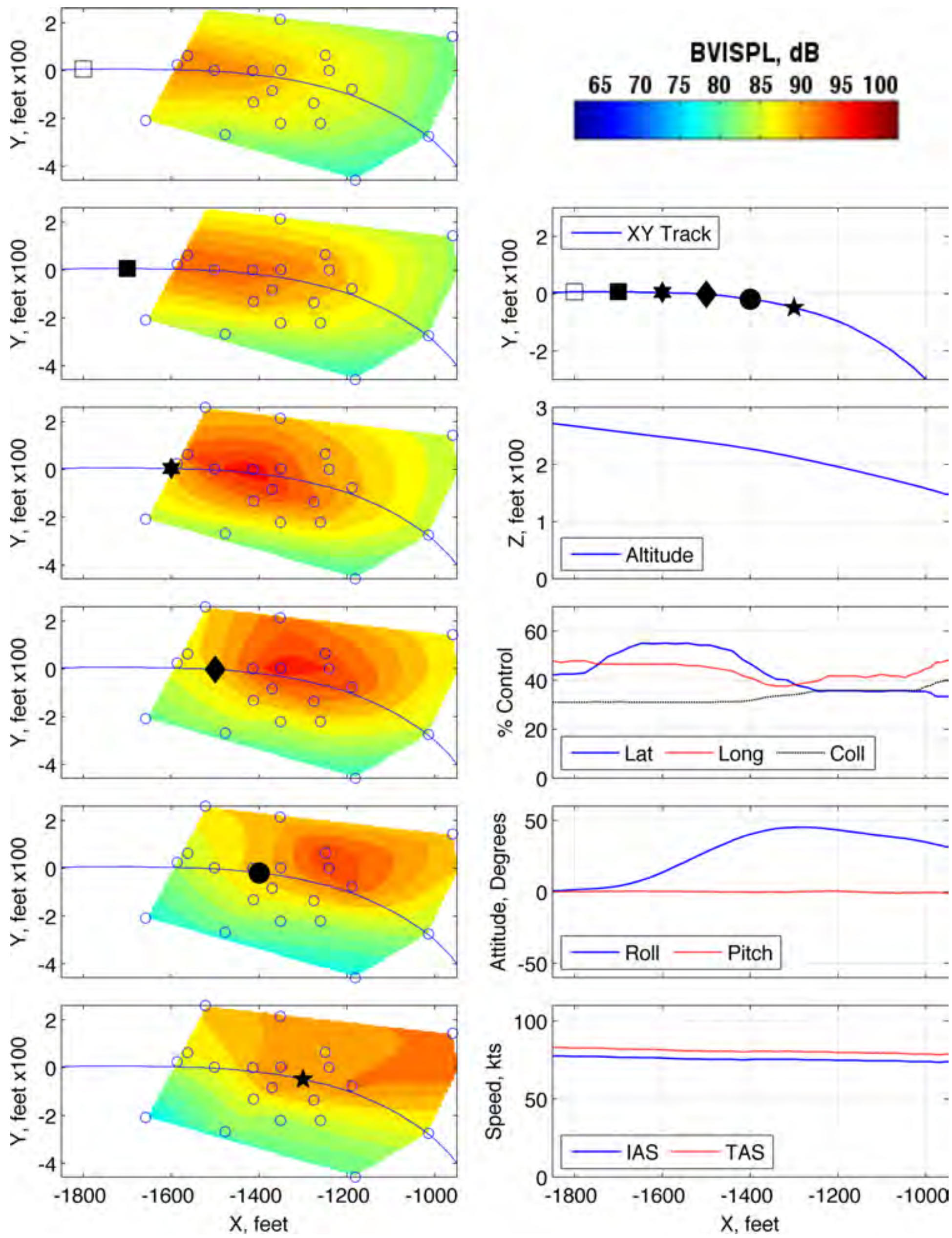

Figure 276: Maneuver condition R24, 80 KIAS, -6° , fast cyclic roll right, run number 282425

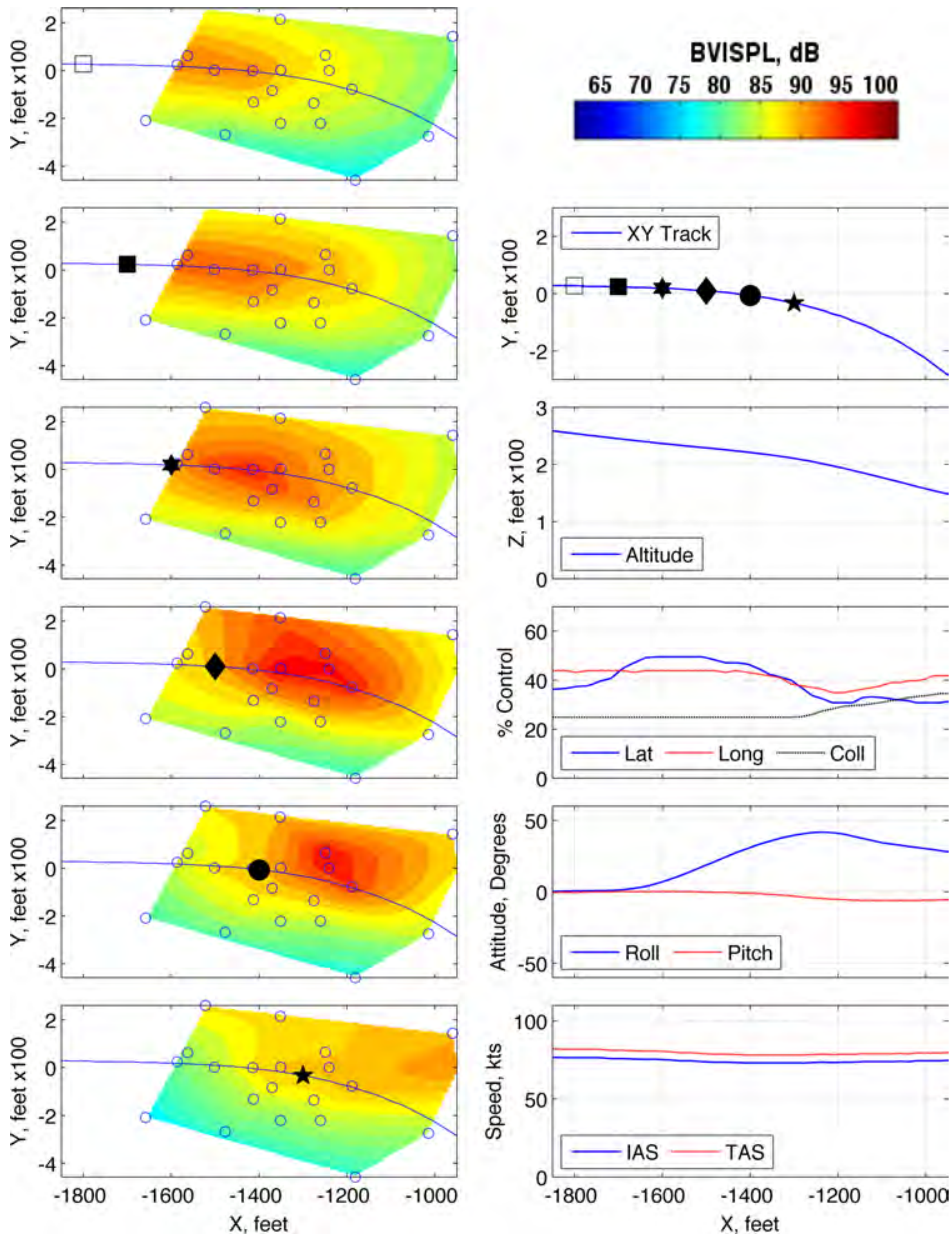

Figure 277: Maneuver condition R24, 80 KIAS, -6° , fast cyclic roll right, run number 285483

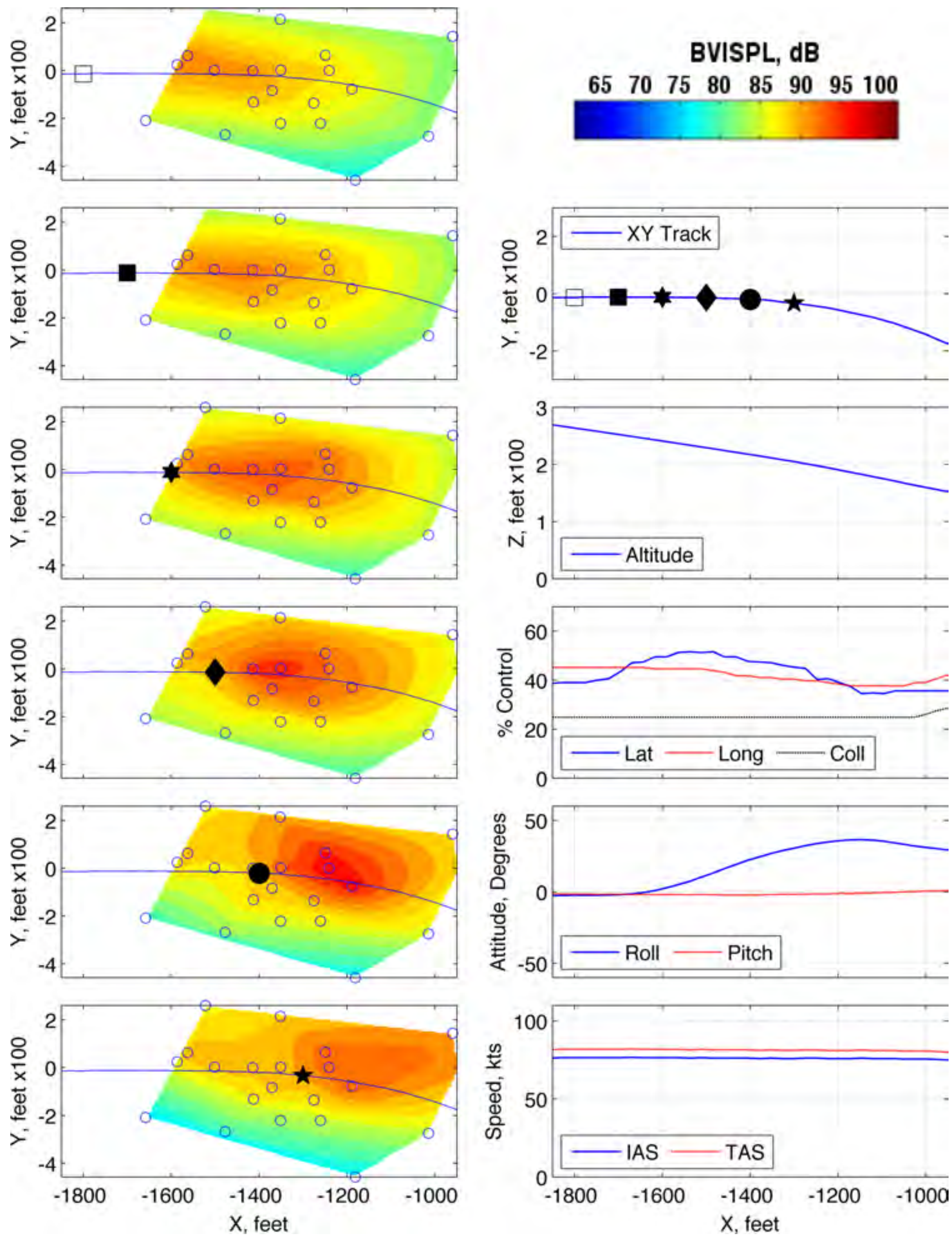

Figure 278: Maneuver condition R24, 80 KIAS, -6° , fast cyclic roll right, run number 285484

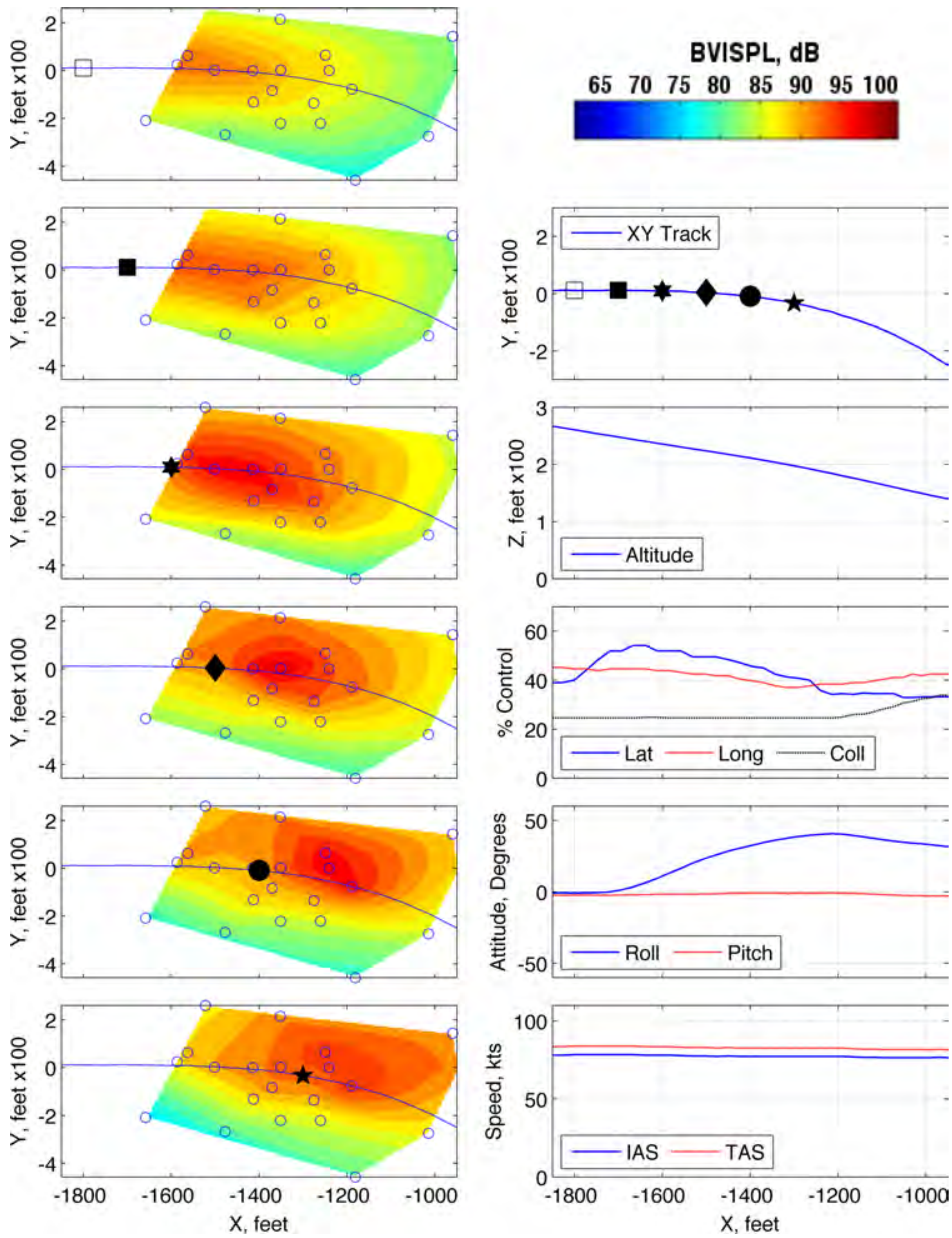

Figure 279: Maneuver condition R24, 80 KIAS, -6° , fast cyclic roll right, run number 285485

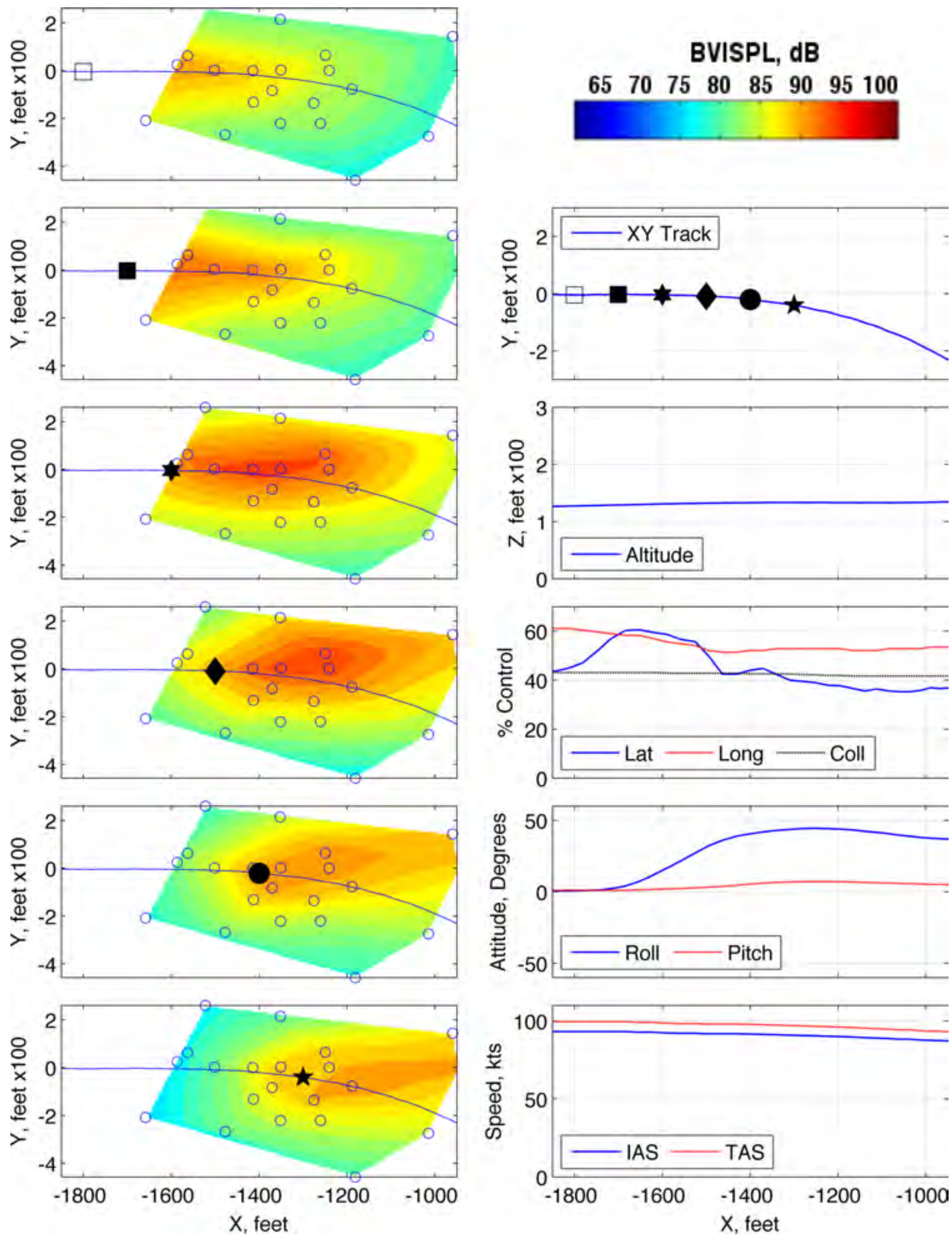

Figure 280: Maneuver condition R25, 100 KIAS, level, fast cyclic roll right, run number 287524

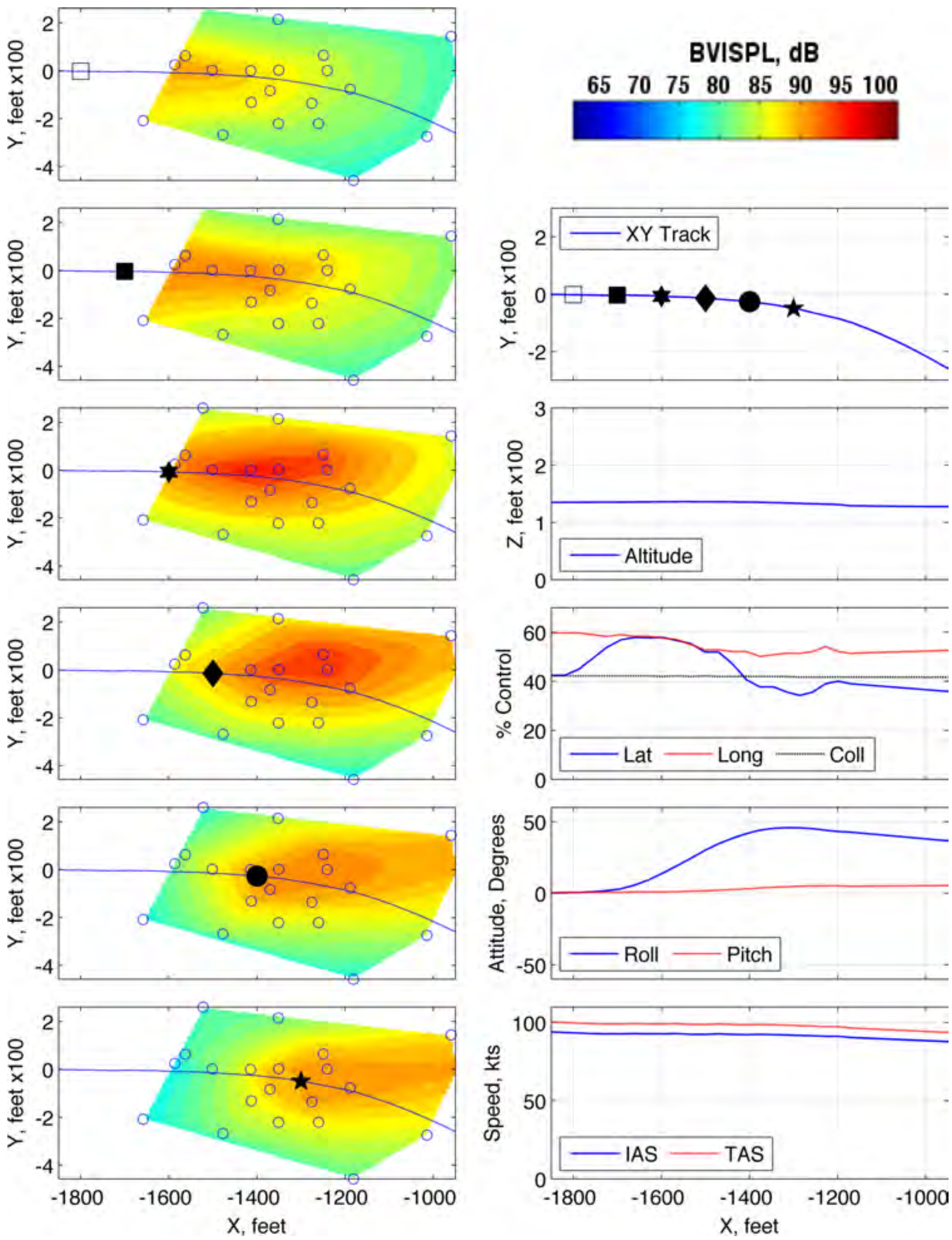

Figure 281: Maneuver condition R25, 100 KIAS, level, fast cyclic roll right, run number 287525

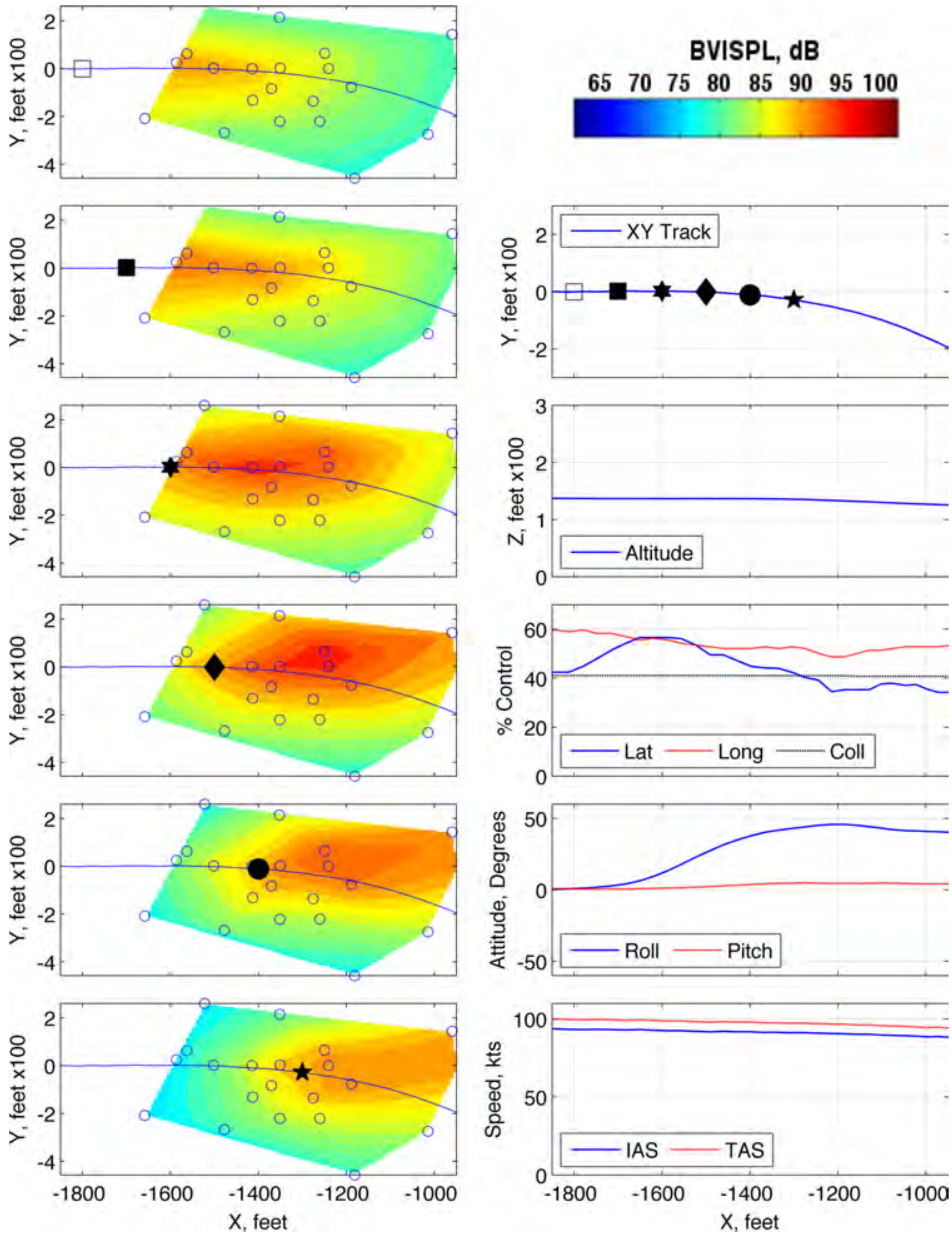

Figure 282: Maneuver condition R26, 100 KIAS, level, medium cyclic roll right, run number 287522

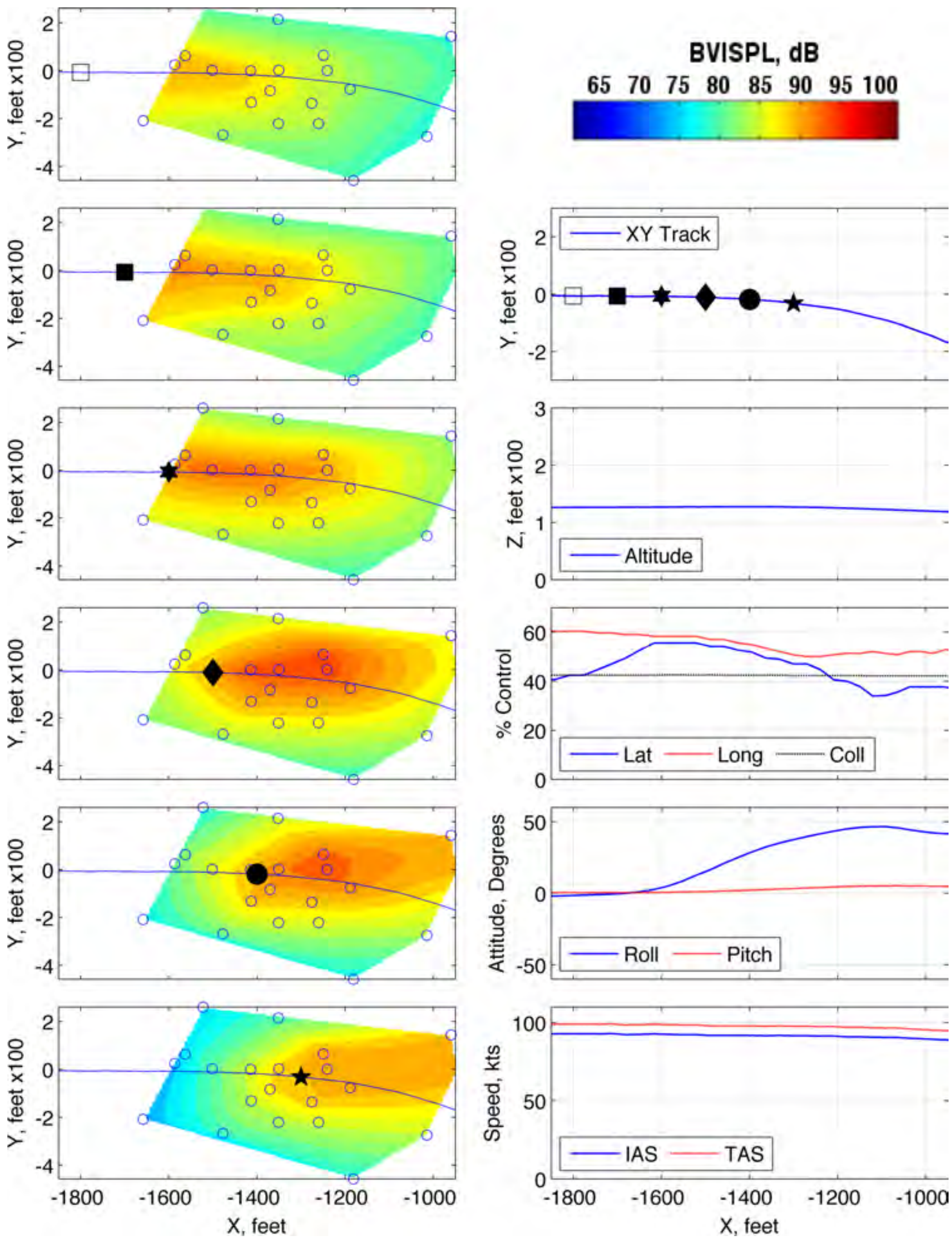

Figure 283: Maneuver condition R26, 100 KIAS, level, medium cyclic roll right, run number 287523

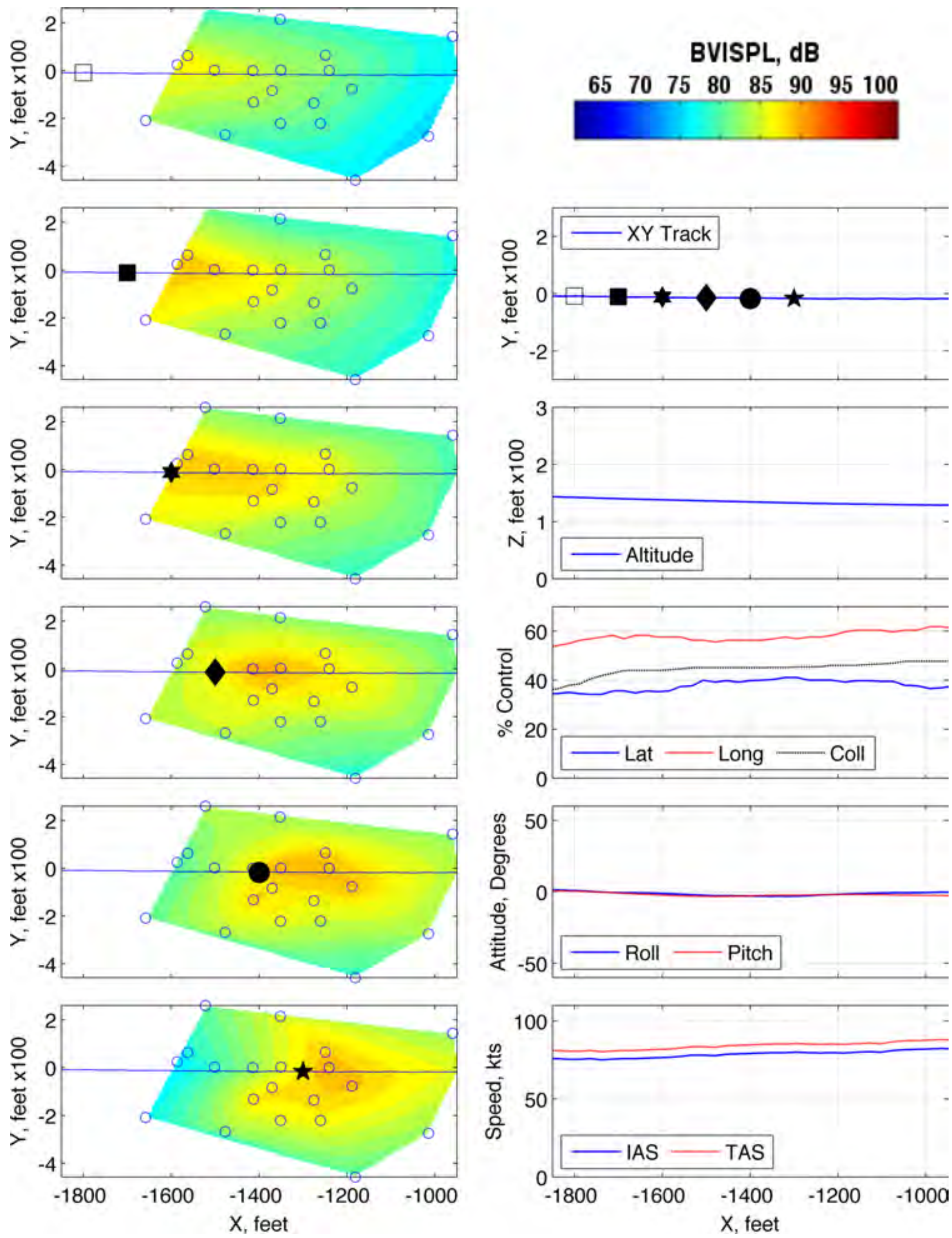

Figure 284: Maneuver condition M2, 80 to 100 KIAS, medium quick start, run number 285499

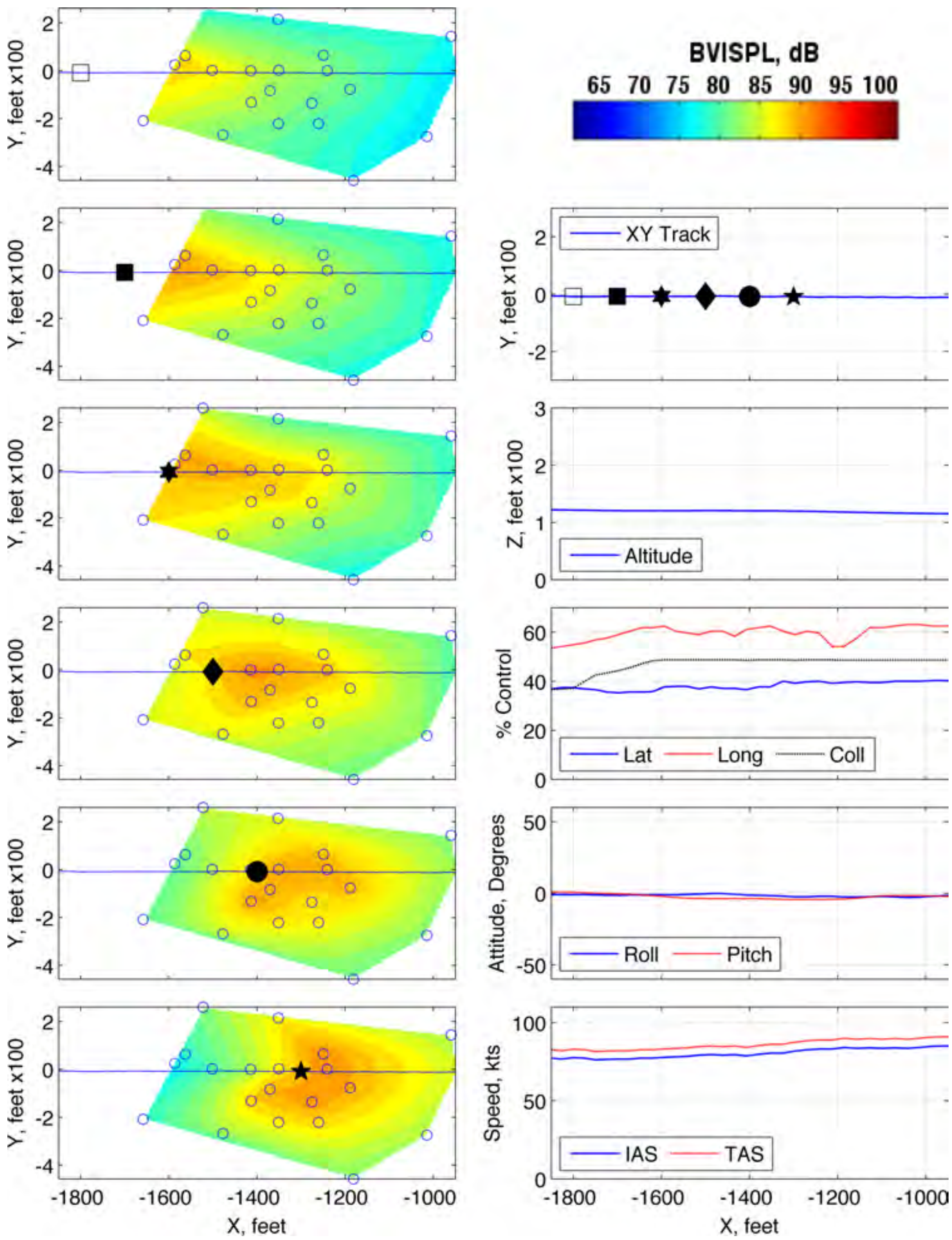

Figure 285: Maneuver condition M2, 80 to 100 KIAS, medium quick start, run number 285500

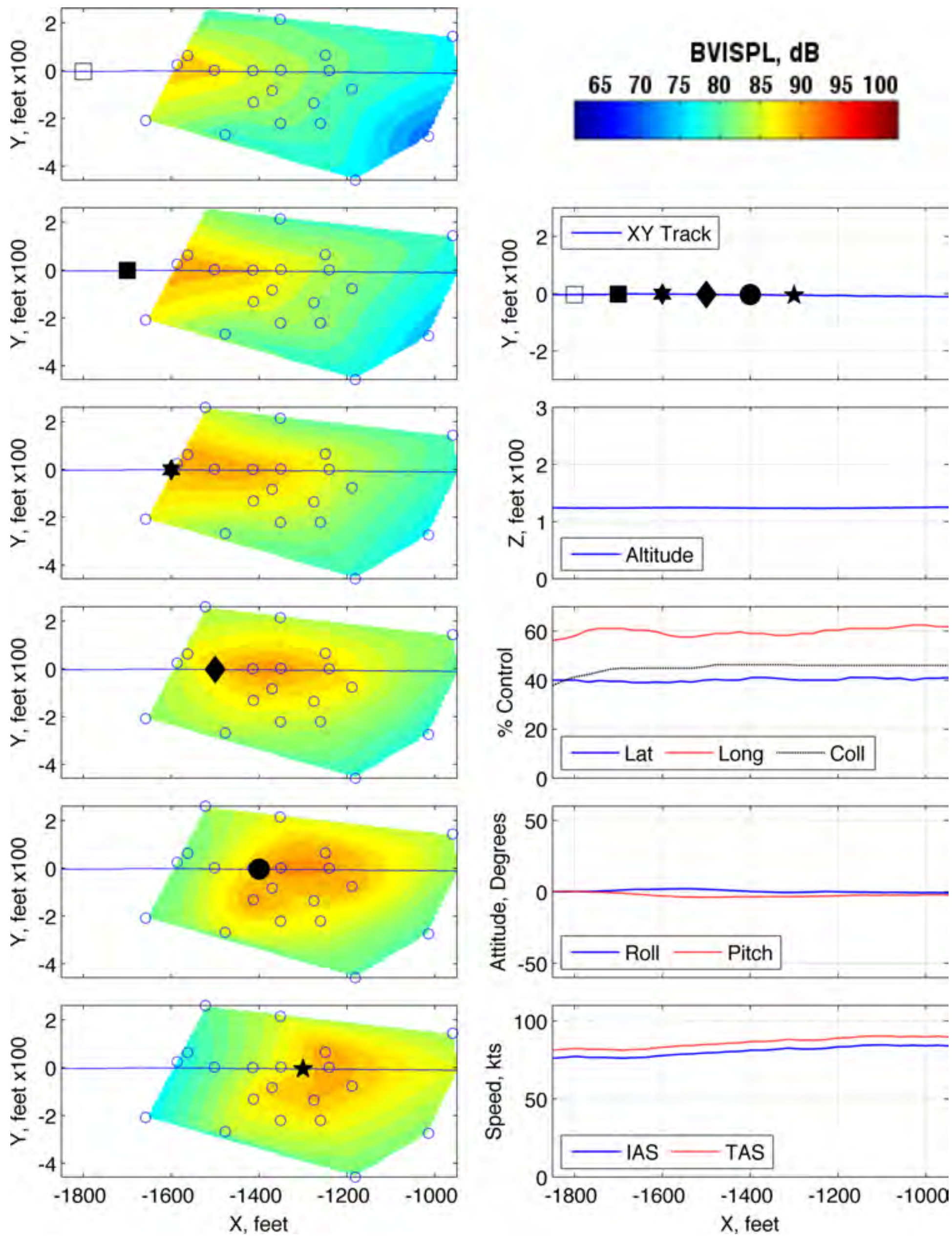

Figure 286: Maneuver condition M2, 80 to 100 KIAS, medium quick start, run number 287545

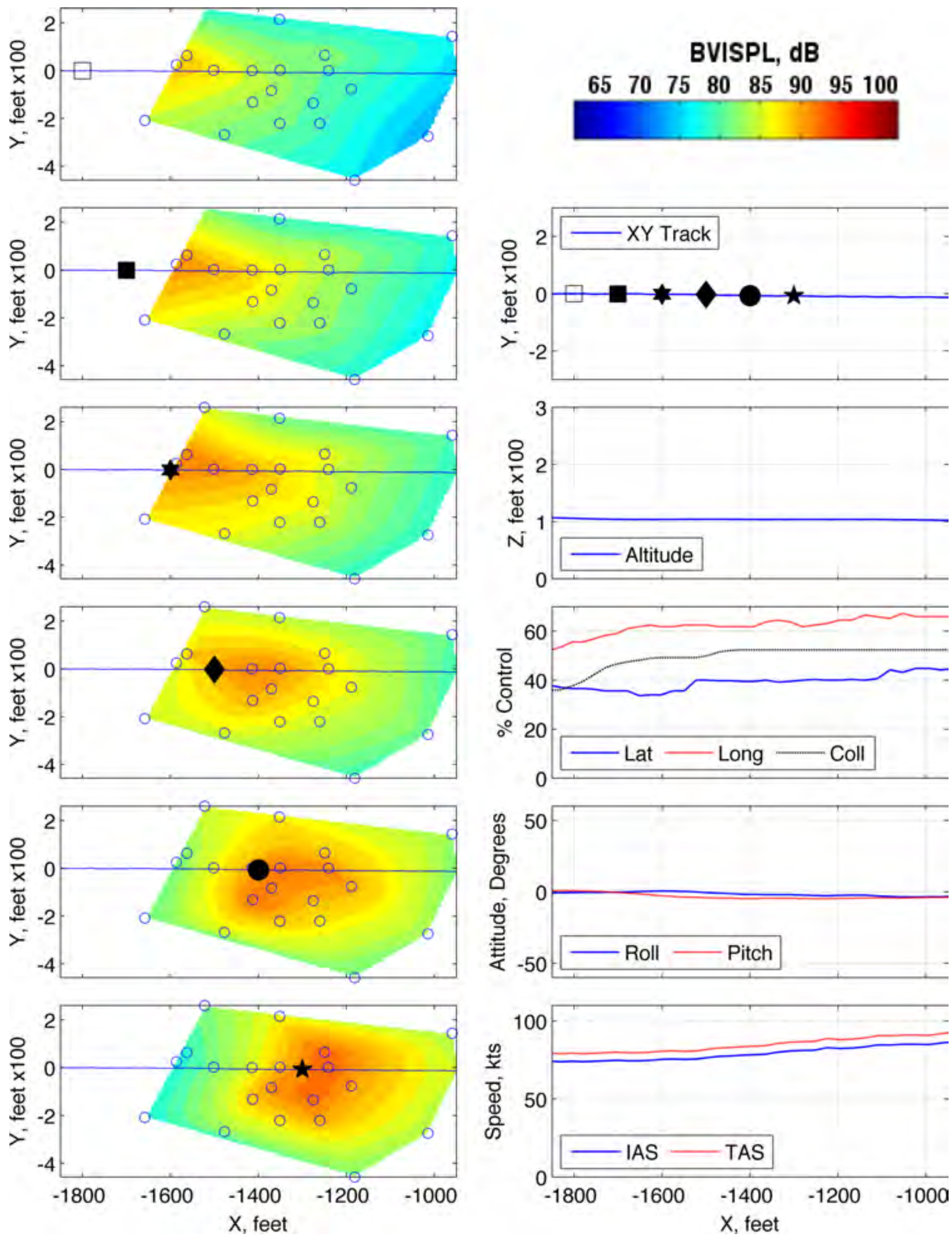

Figure 287: Maneuver condition M3, 80 to 100 KIAS, fast quick start, run number 285501

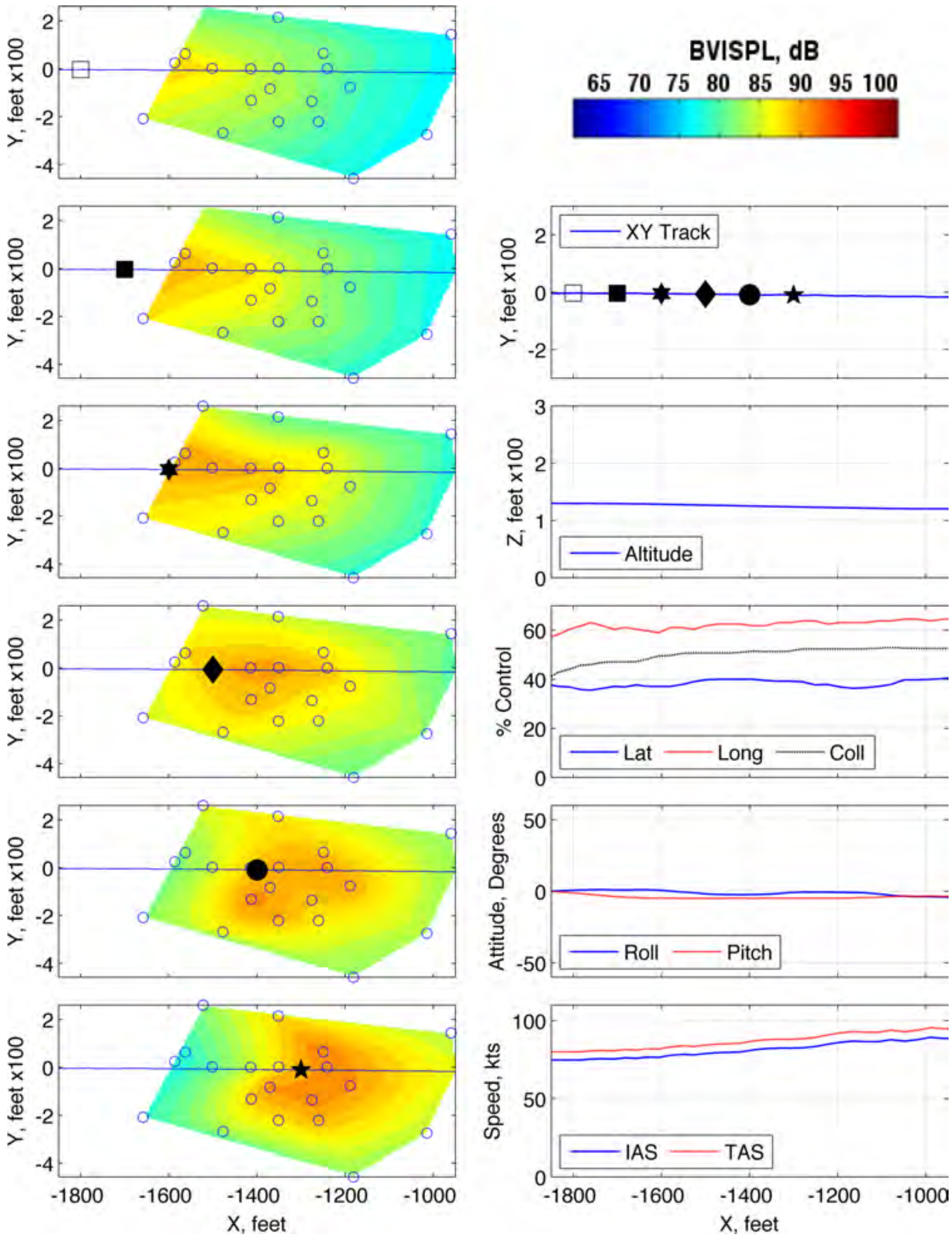

Figure 288: Maneuver condition M3, 80 to 100 KIAS, fast quick start, run number 285502

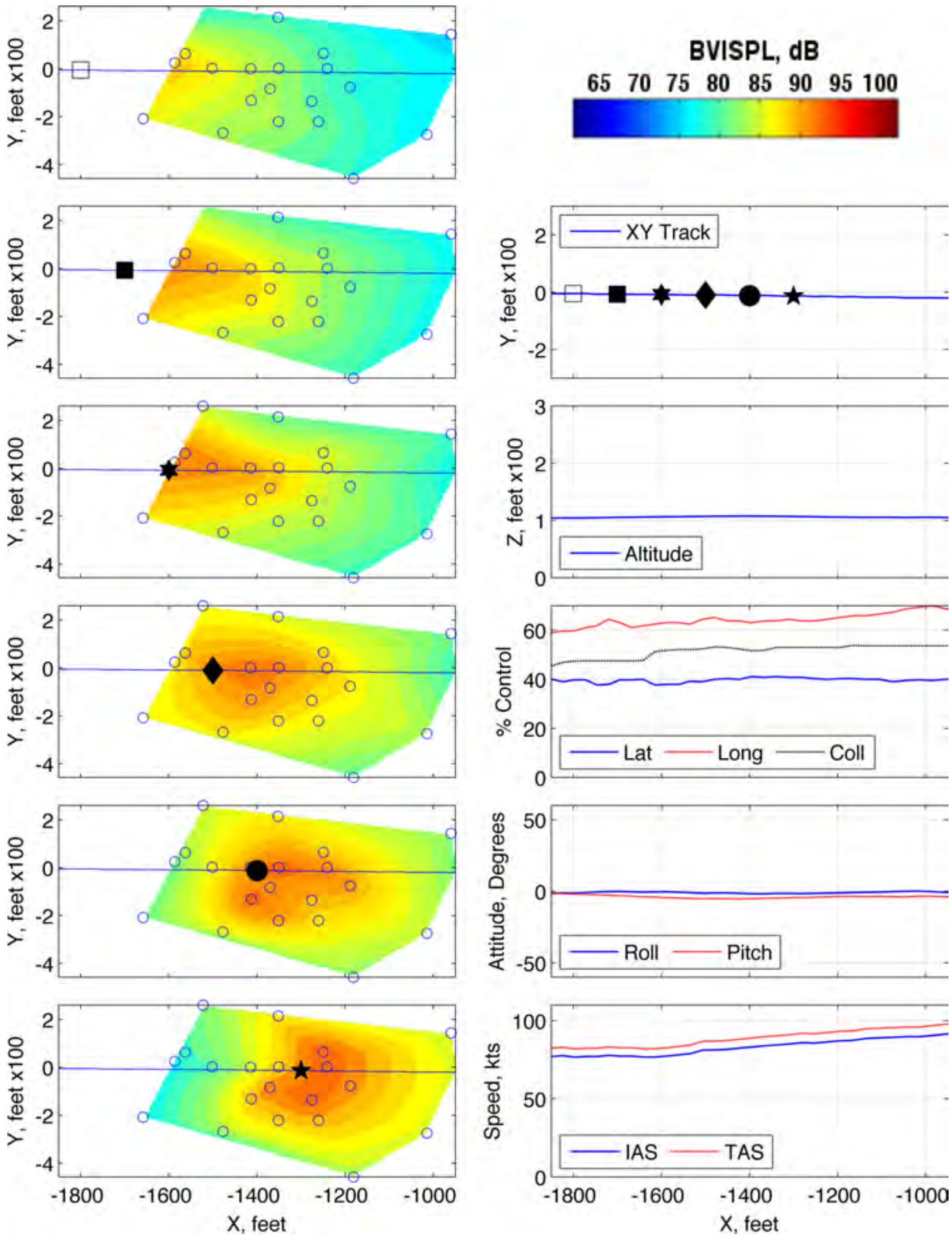

Figure 289: Maneuver condition M3, 80 to 100 KIAS, fast quick start, run number 285503

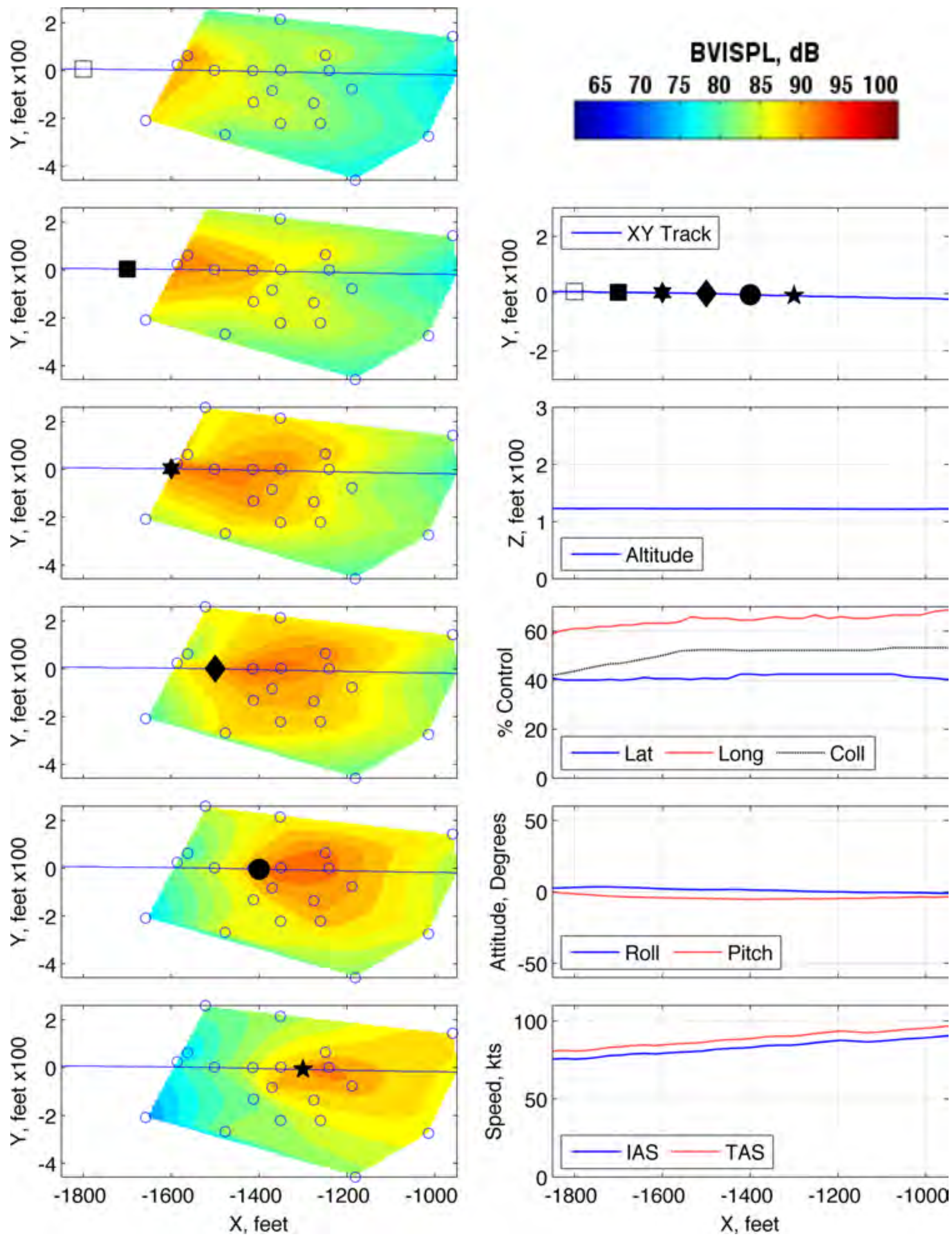

Figure 290: Maneuver condition M3, 80 to 100 KIAS, fast quick start, run number 287546

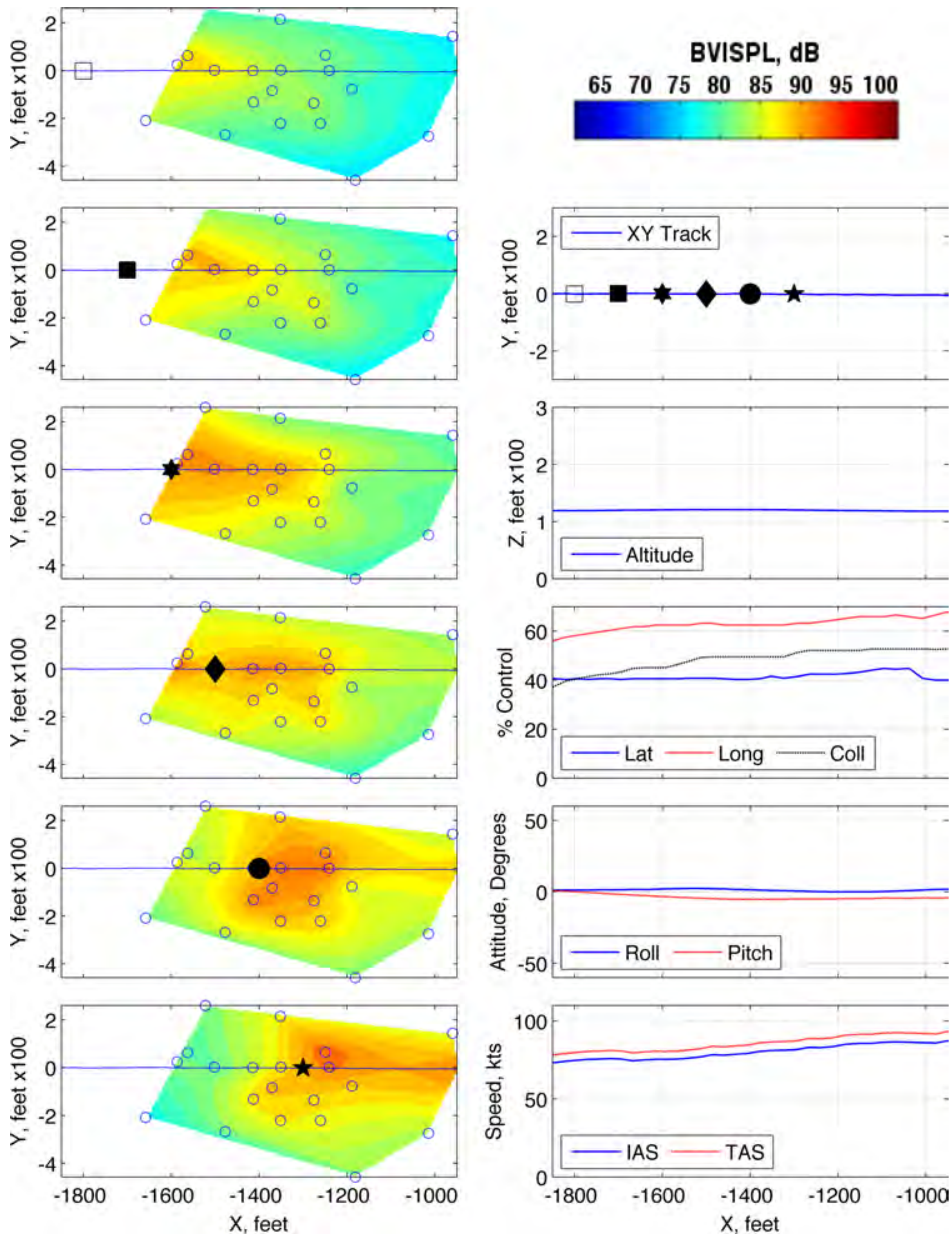

Figure 291: Maneuver condition M3, 80 to 60 KIAS, fast quick start, run number 287547

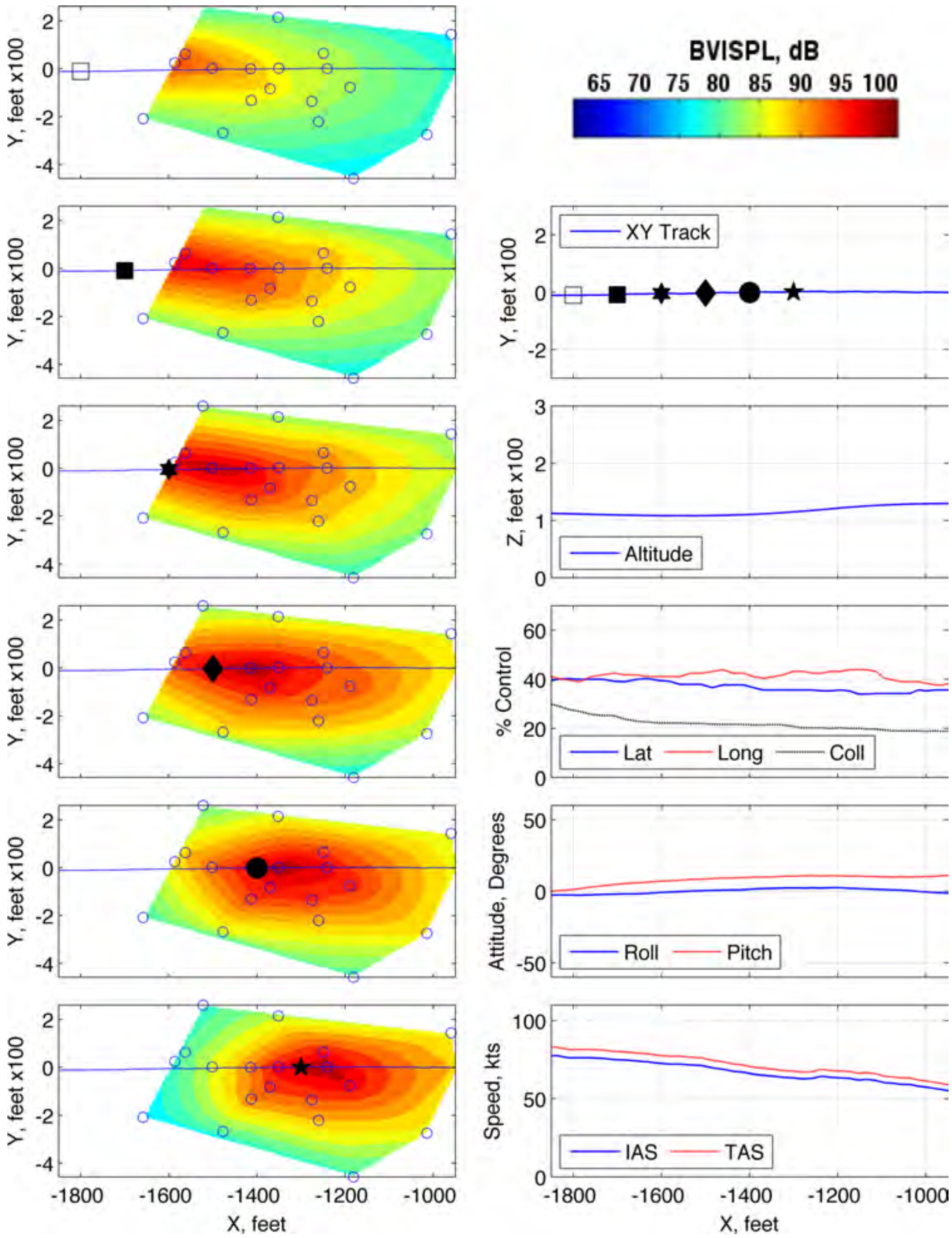

Figure 292: Maneuver condition M4, 80 to 60 KIAS, slow quick stop, run number 285504

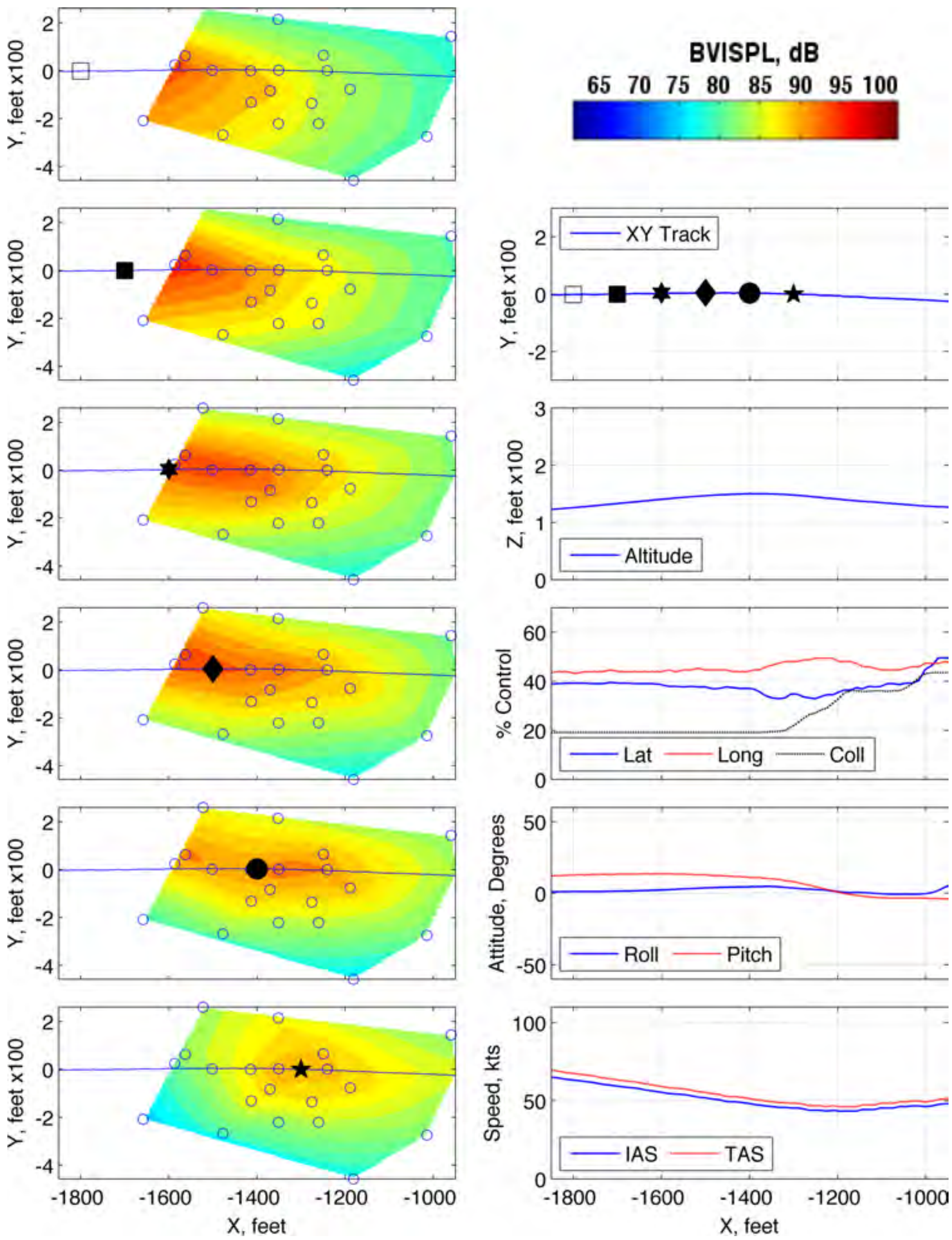

Figure 293: Maneuver condition M5, 80 to 60 KIAS, medium quick stop, run number 287540

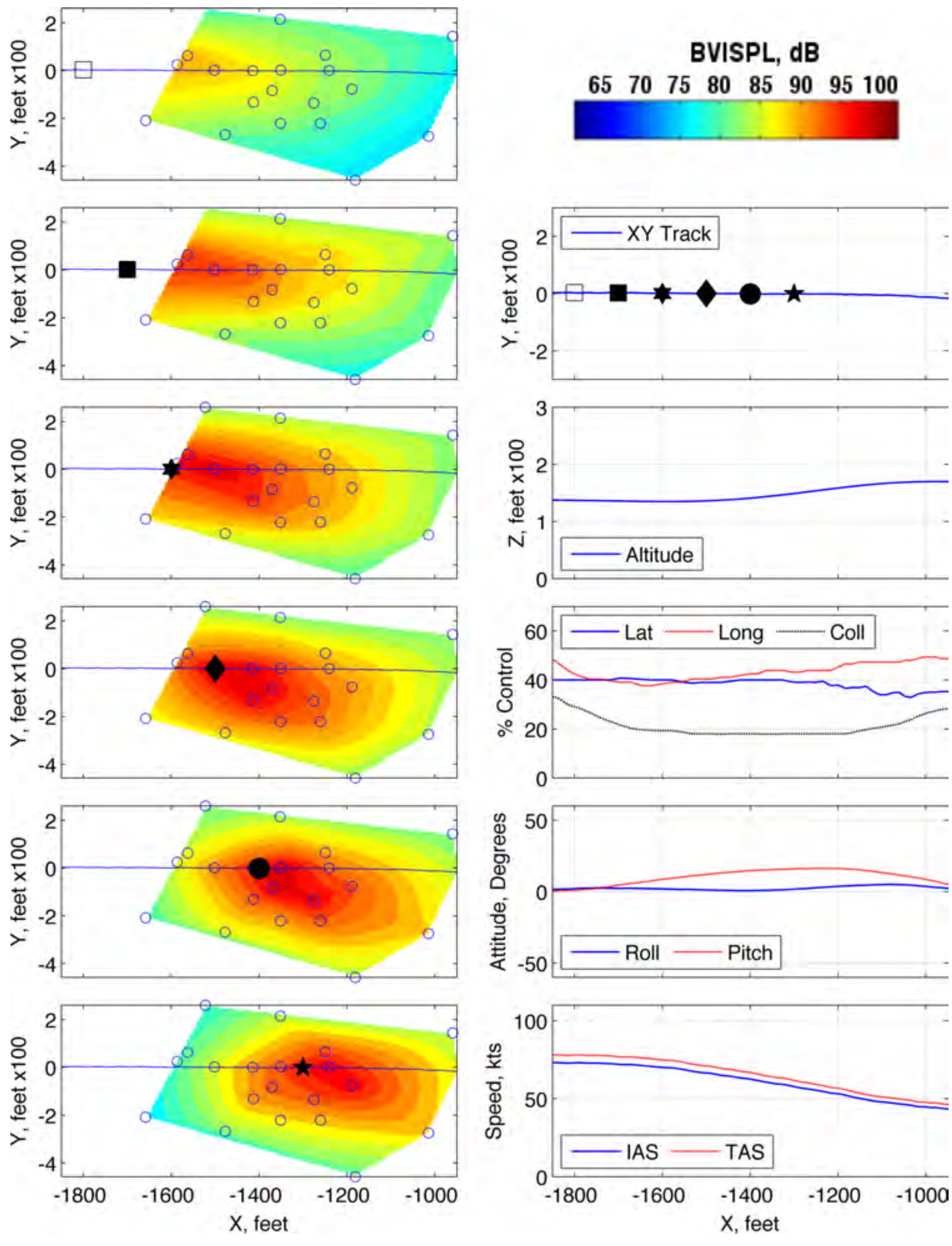

Figure 294: Maneuver condition M5, 80 to 60 KIAS, medium quick stop, run number 287541

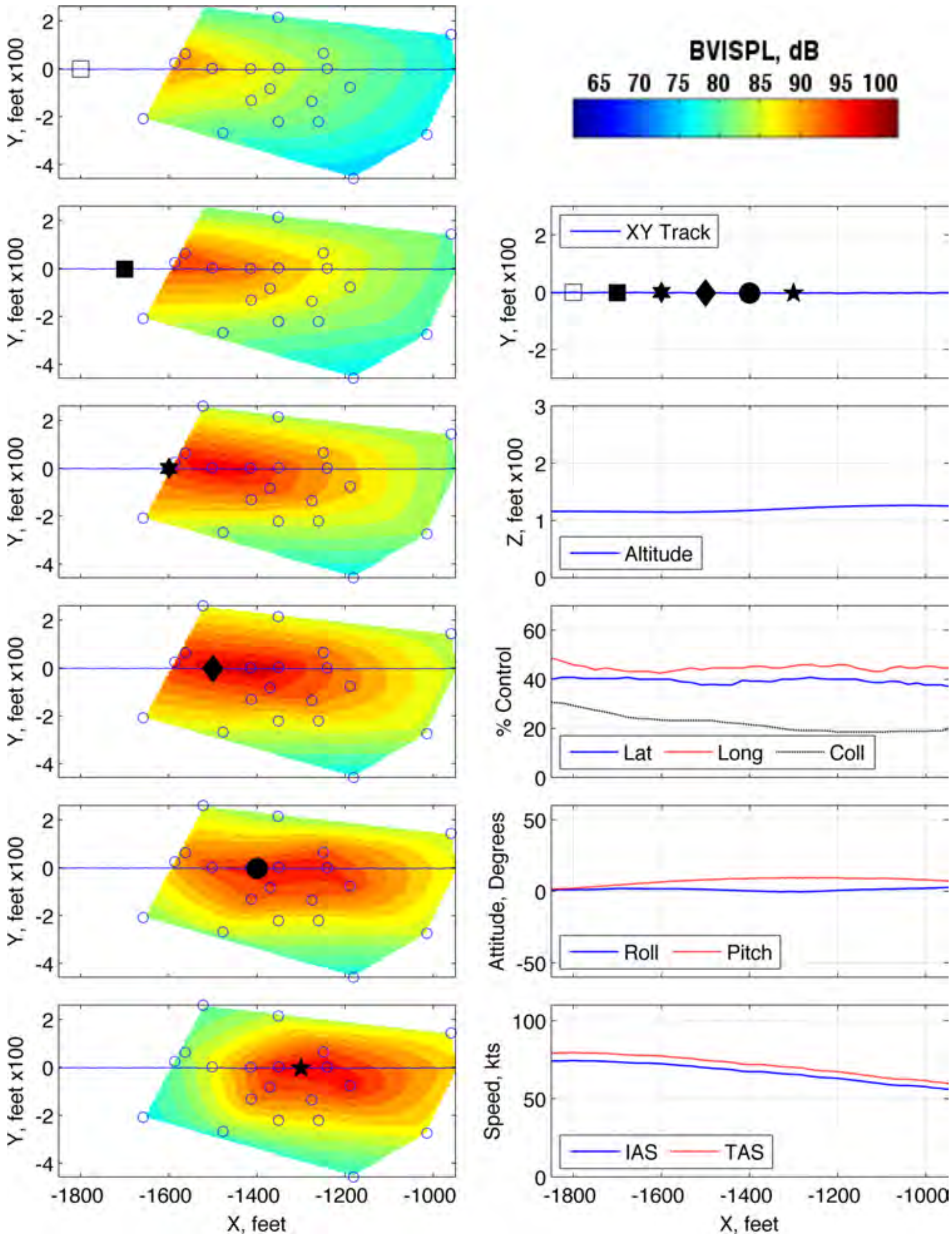

Figure 295: Maneuver condition M5, 80 to 60 KIAS, medium quick stop, run number 287542

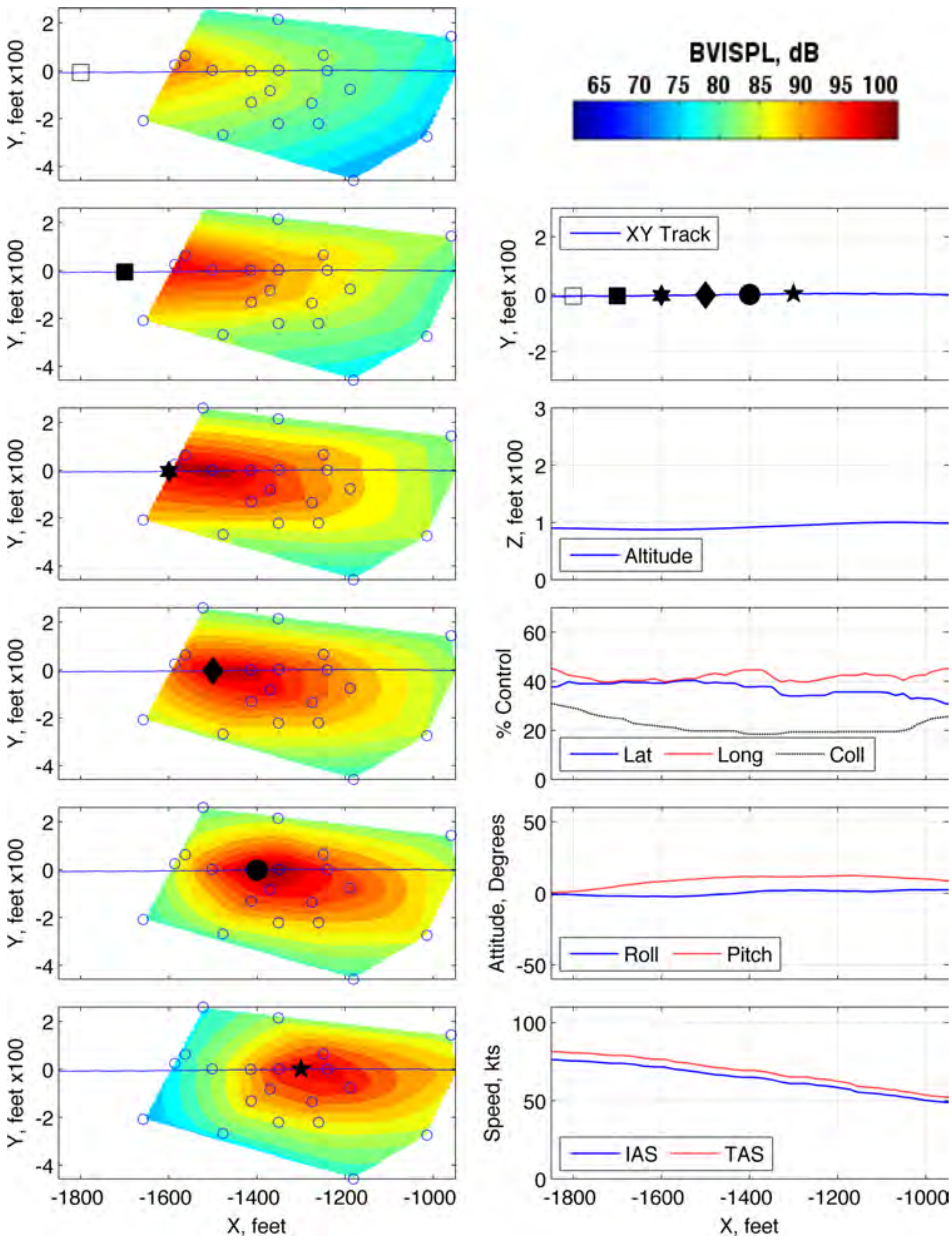

Figure 296: Maneuver condition M5, 80 to 60 KIAS, medium quick stop, run number 285505

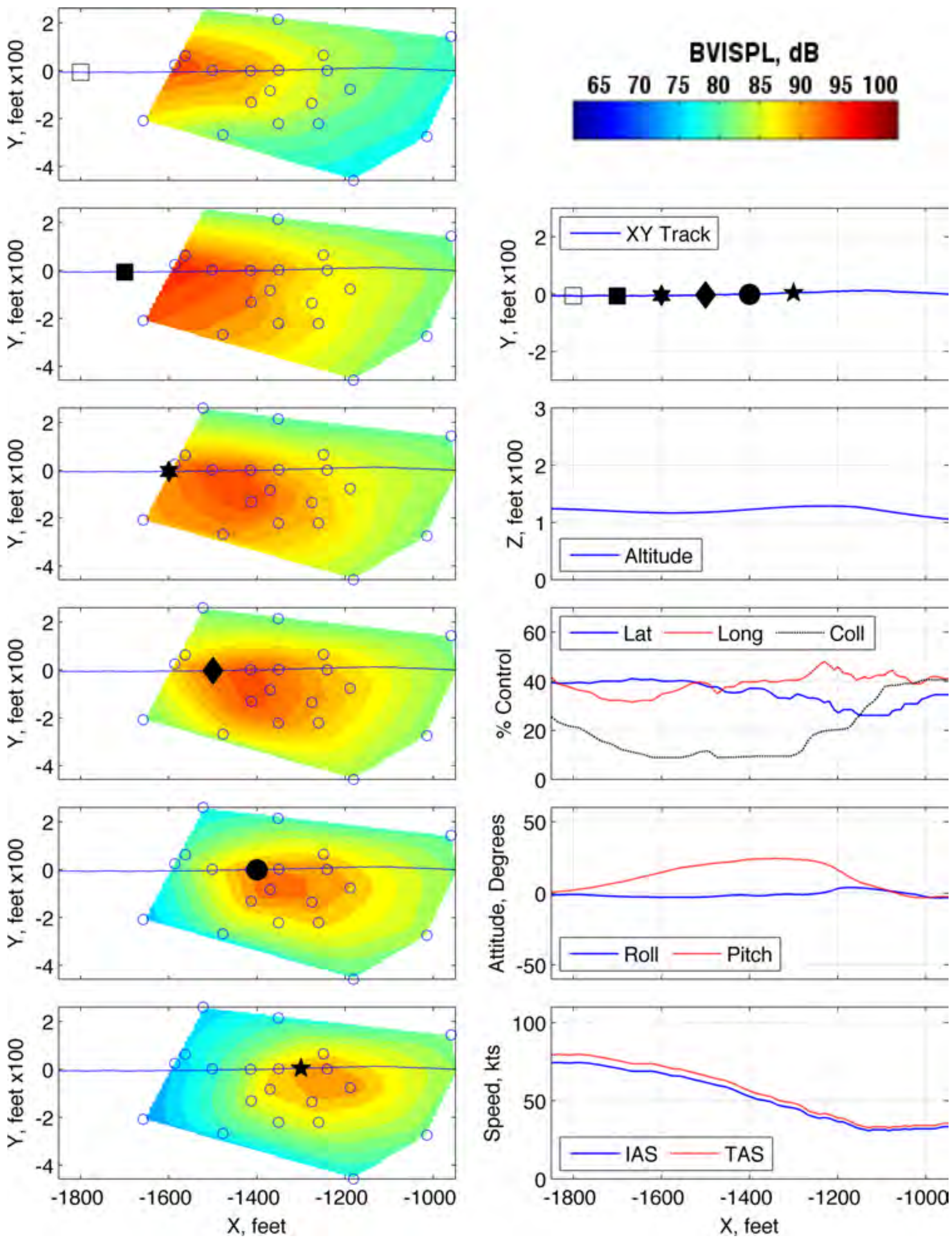

Figure 297: Maneuver condition M6, 80 to 60 KIAS, fast quick stop, run number 285506

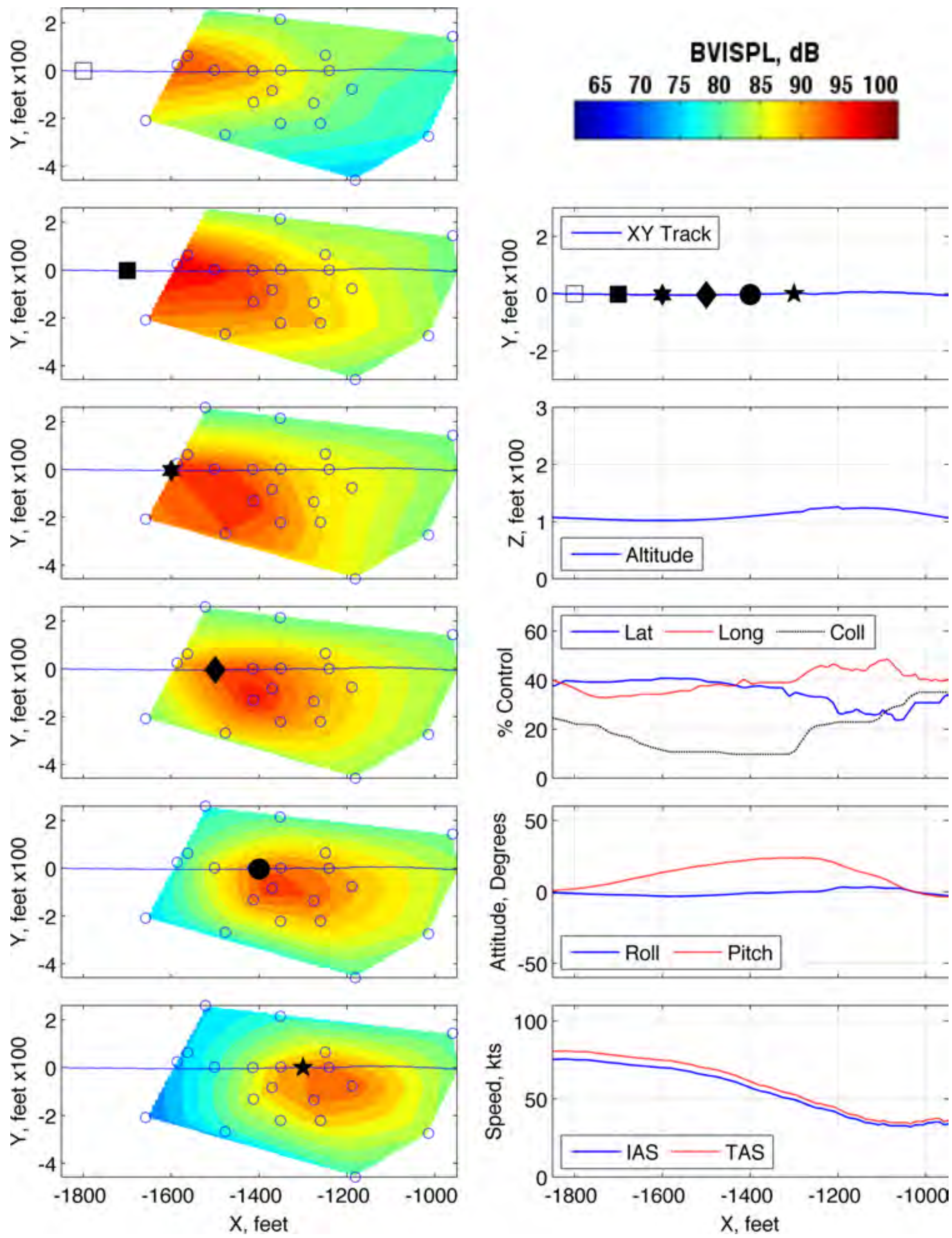

Figure 298: Maneuver condition M6, 80 to 60 KIAS, fast quick stop, run number 285507

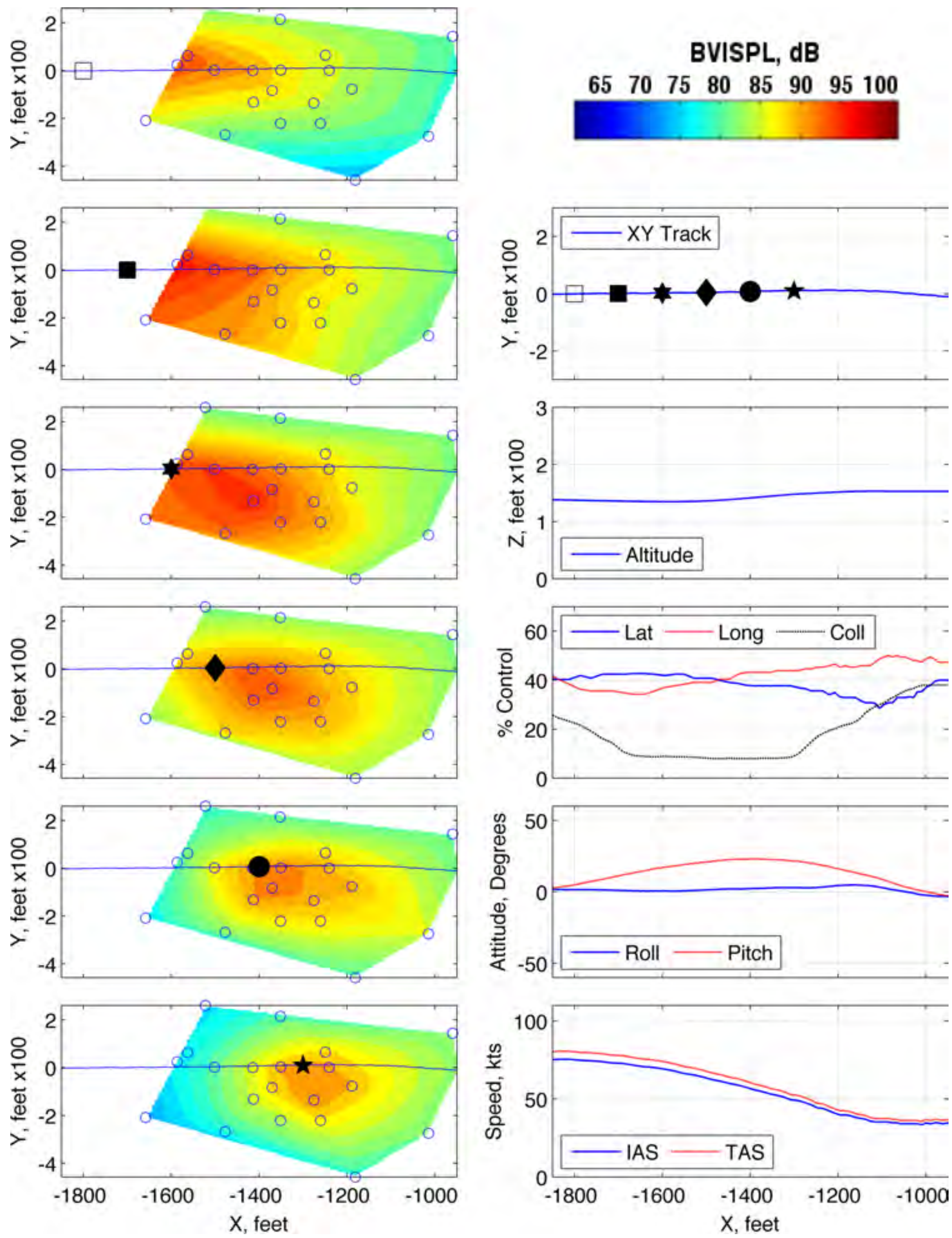

Figure 299: Maneuver condition M6, 80 to 60 KIAS, fast quick stop, run number 287543

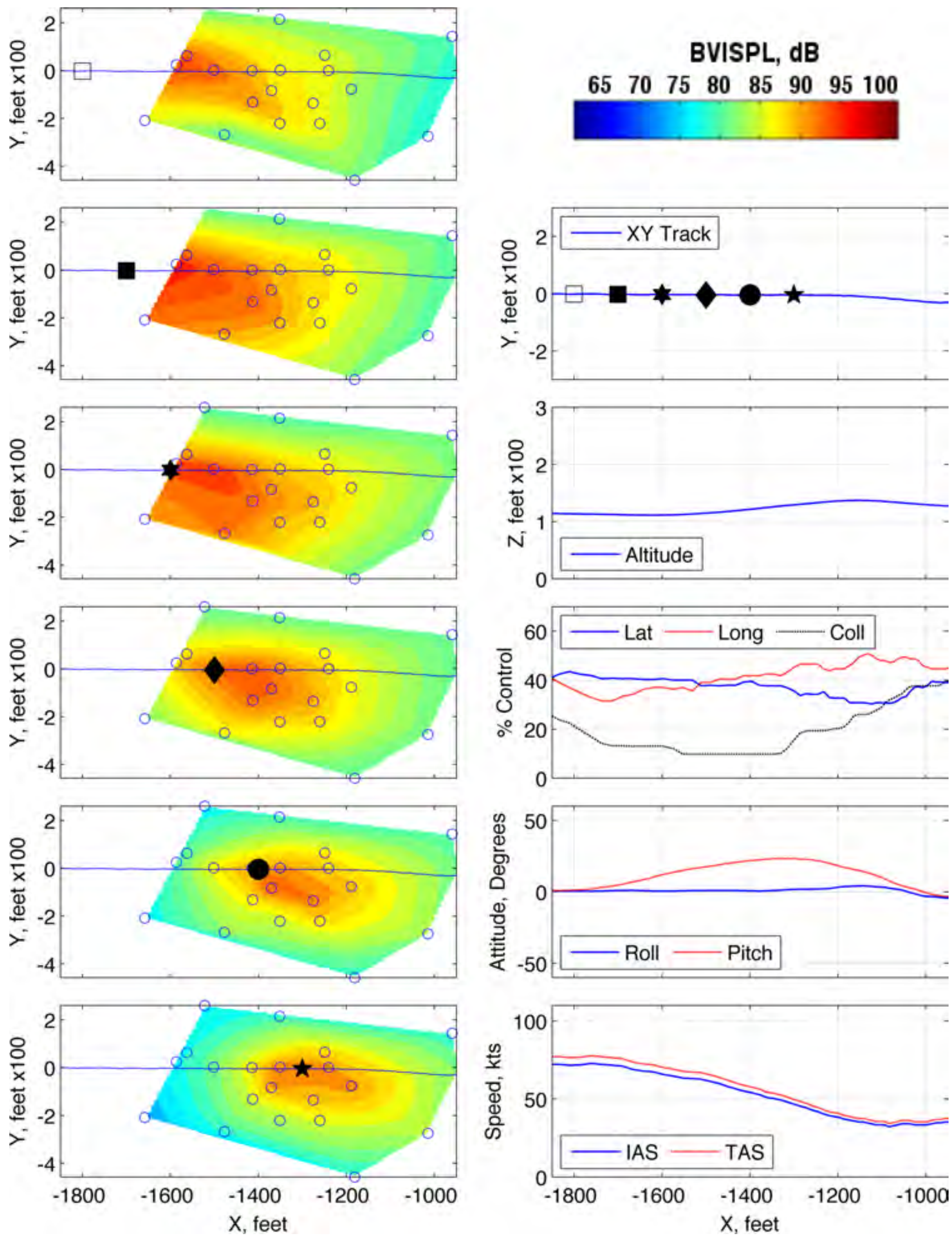

Figure 300: Maneuver condition M6, 80 to 60 KIAS, fast quick stop, run number 287544

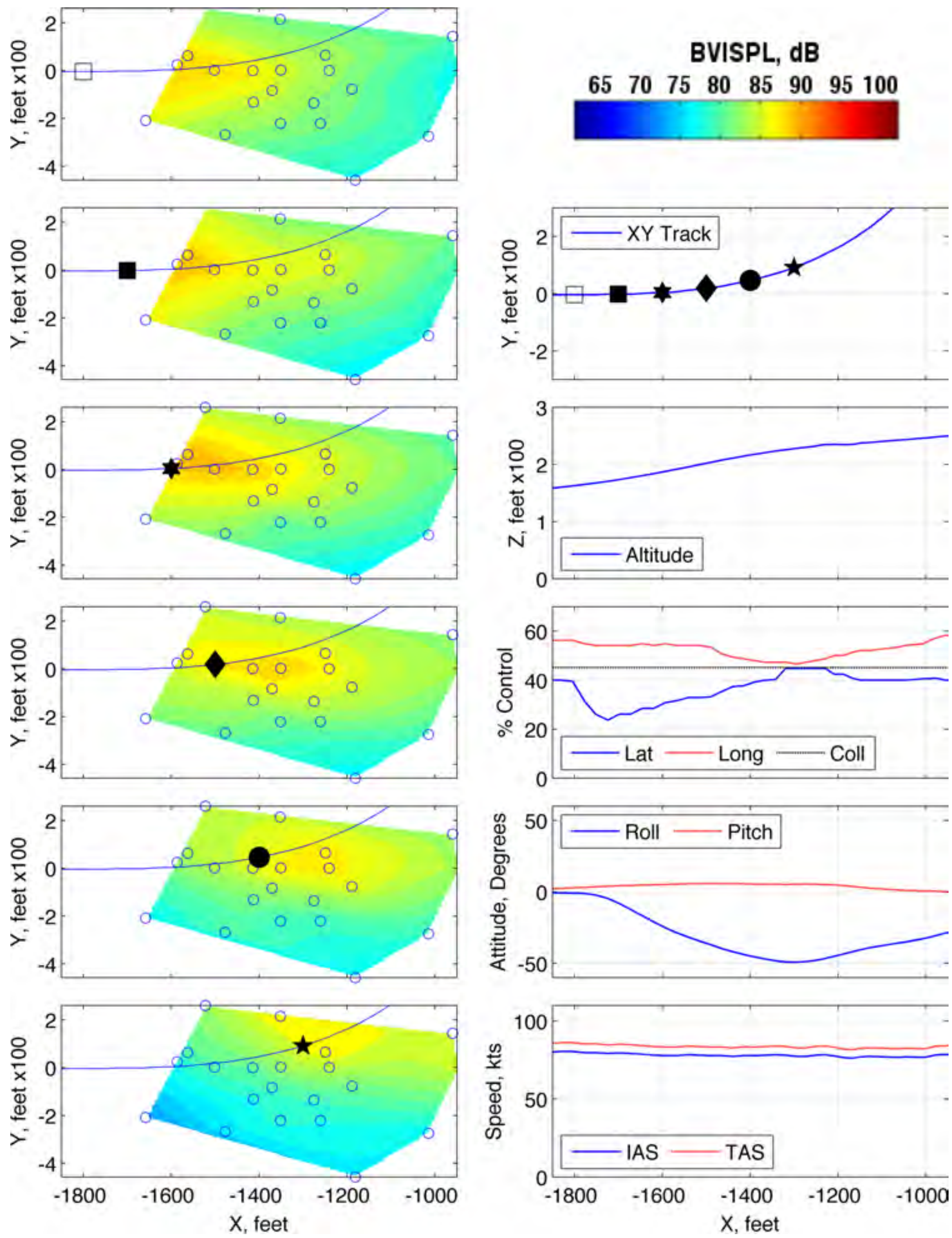

Figure 301: Maneuver condition Z6, 80 KIAS, 0° to 6° , roll left, run number 287550

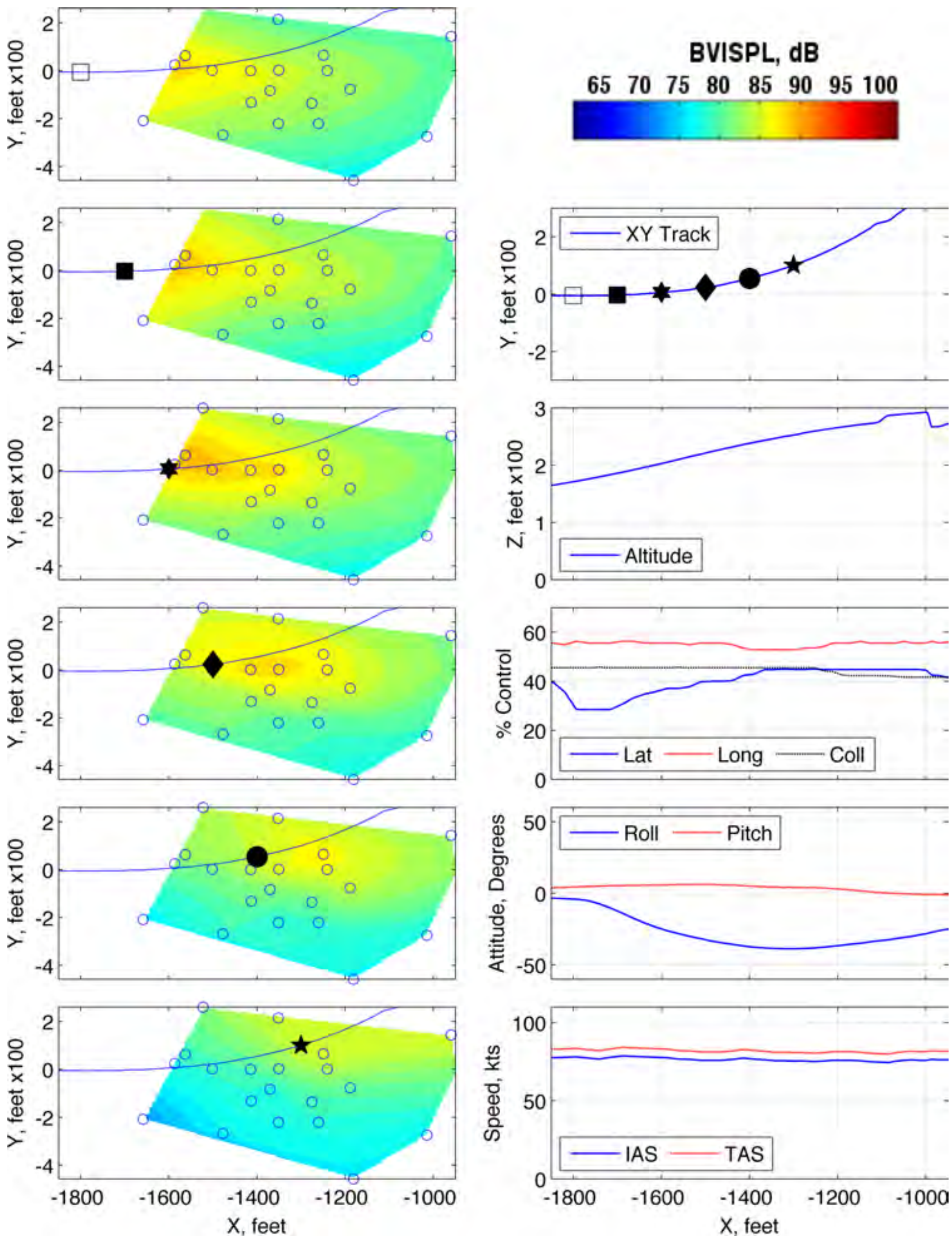

Figure 302: Maneuver condition Z6, 80 KIAS, 0° to 6° , roll left, run number 287551

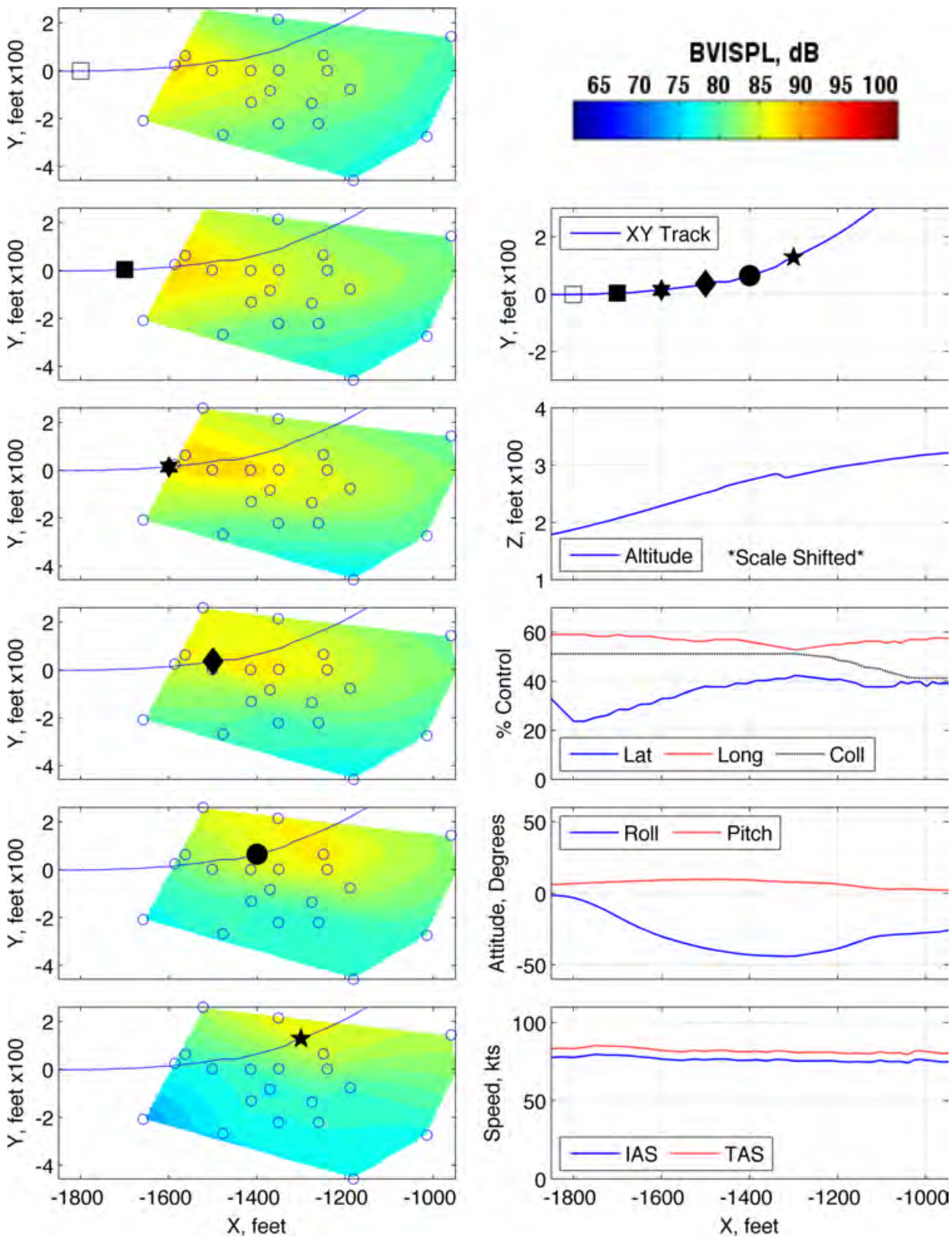

Figure 303: Maneuver condition Z9, 80 KIAS, 0° to 9° , roll left, run number 287555

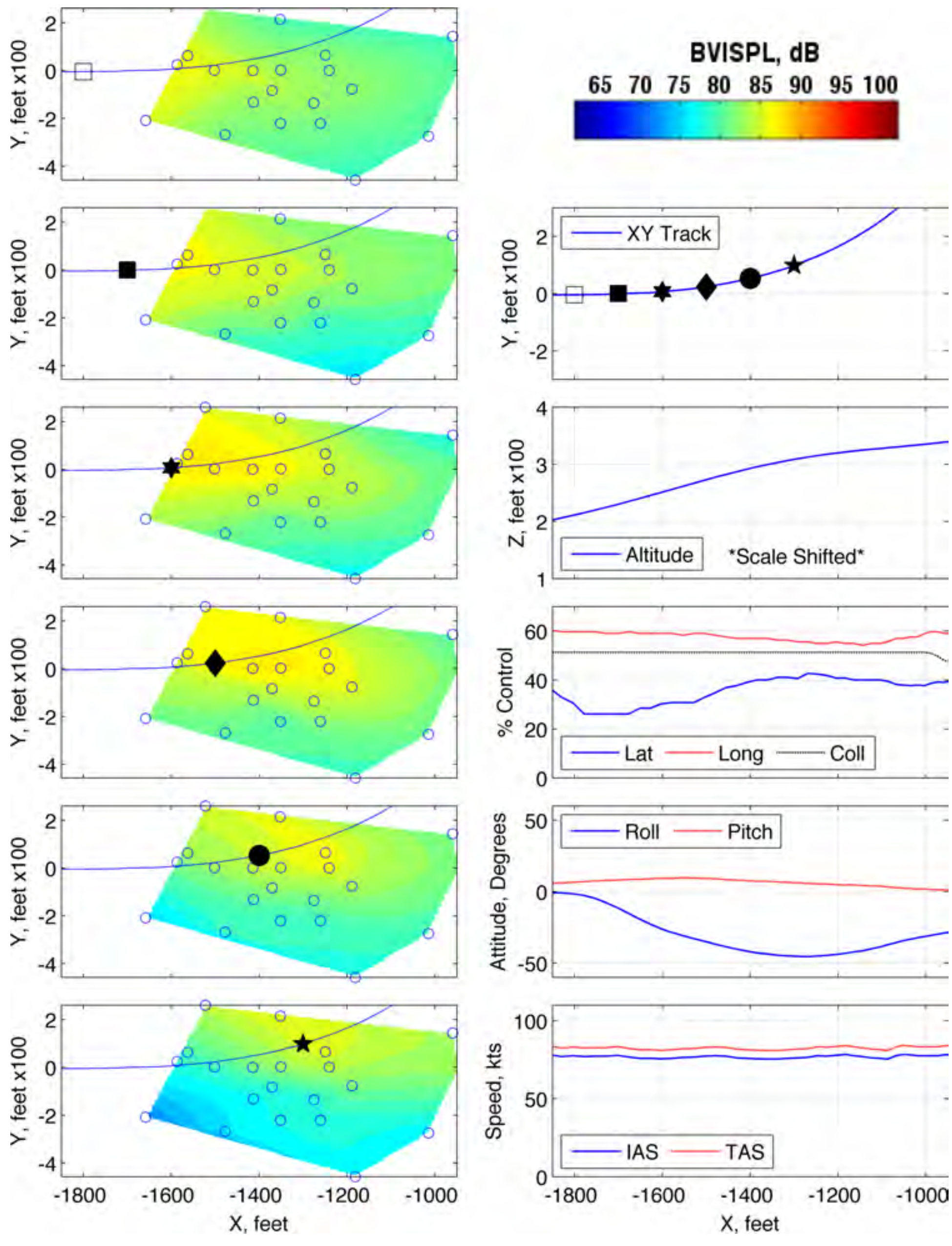

Figure 304: Maneuver condition Z9, 80 KIAS, 0° to 9° , roll left, run number 287556

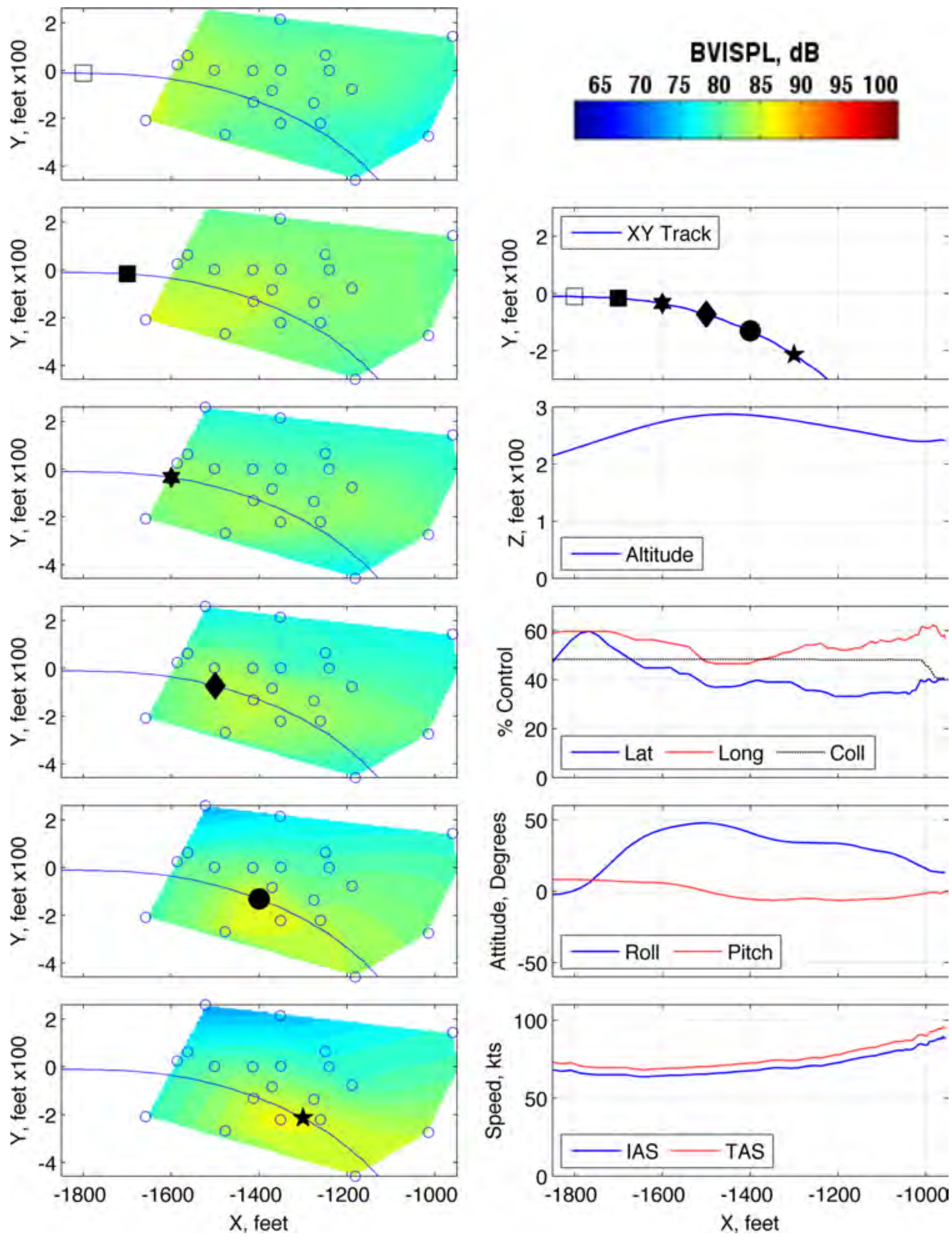

Figure 305: Maneuver condition Z15, 80 KIAS, 0° to 6° , roll right, run number 285513

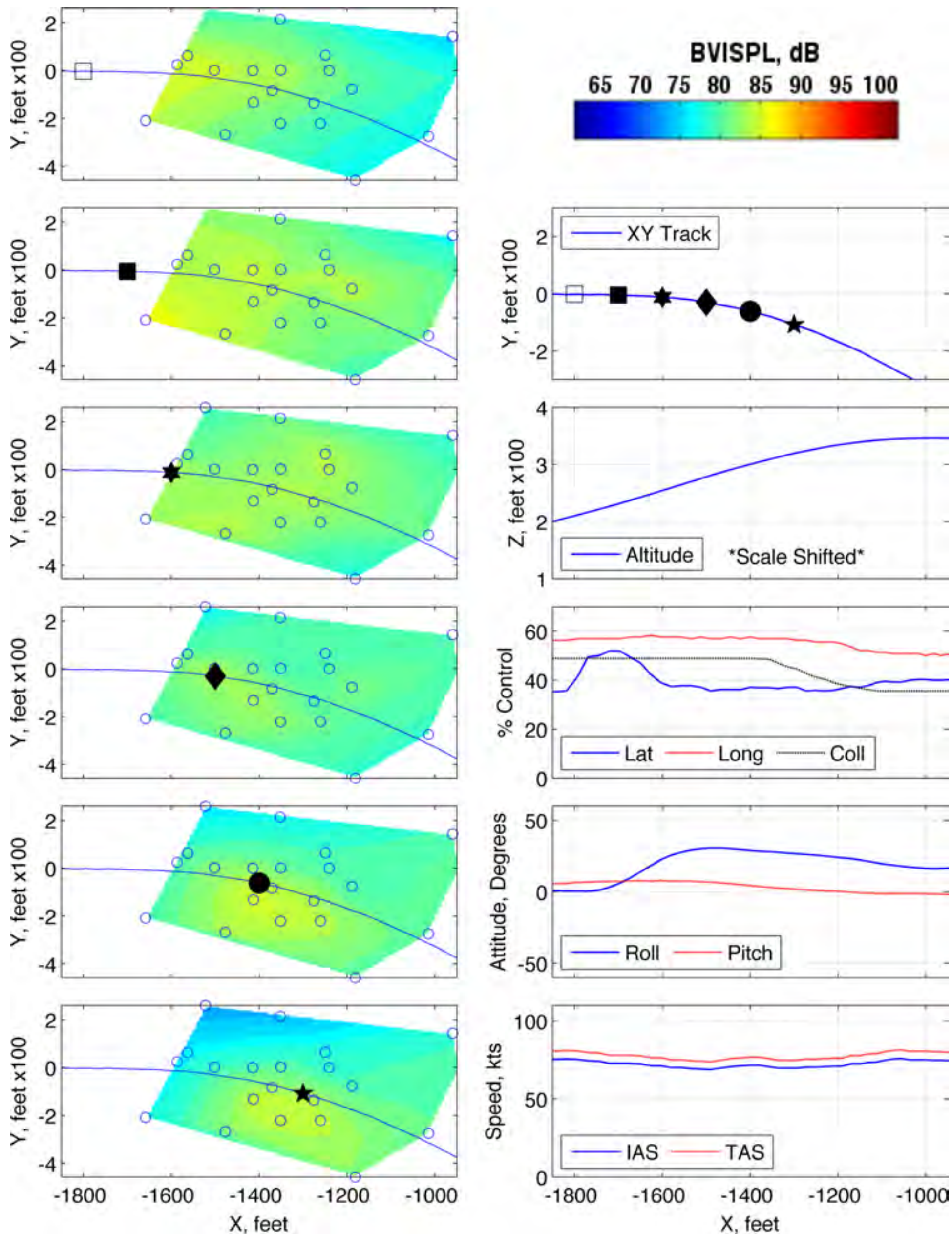

Figure 306: Maneuver condition Z15, 80 KIAS, 0° to 6° , roll right, run number 285514

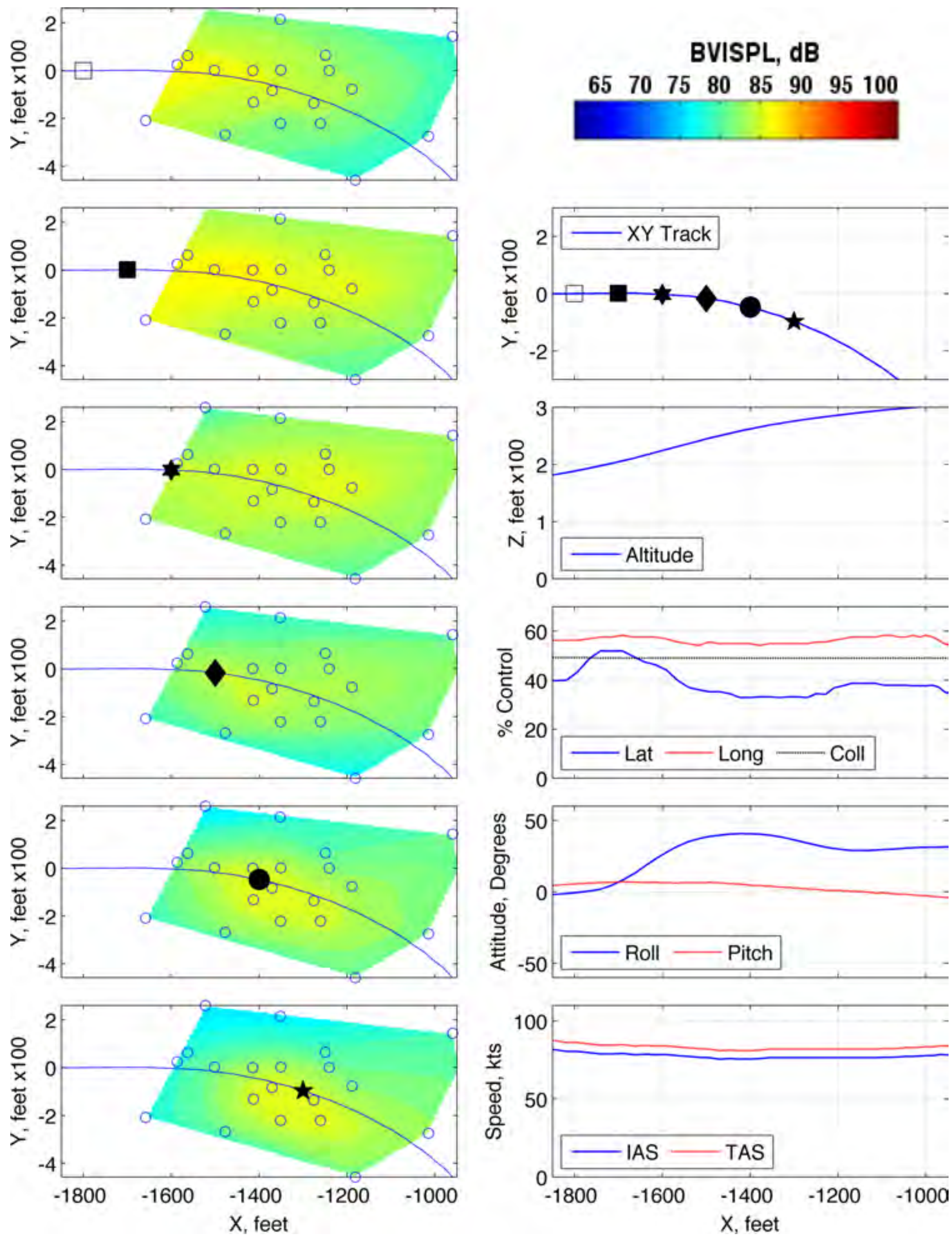

Figure 307: Maneuver condition Z15, 80 KIAS, 0° to 6° , roll right, run number 285515

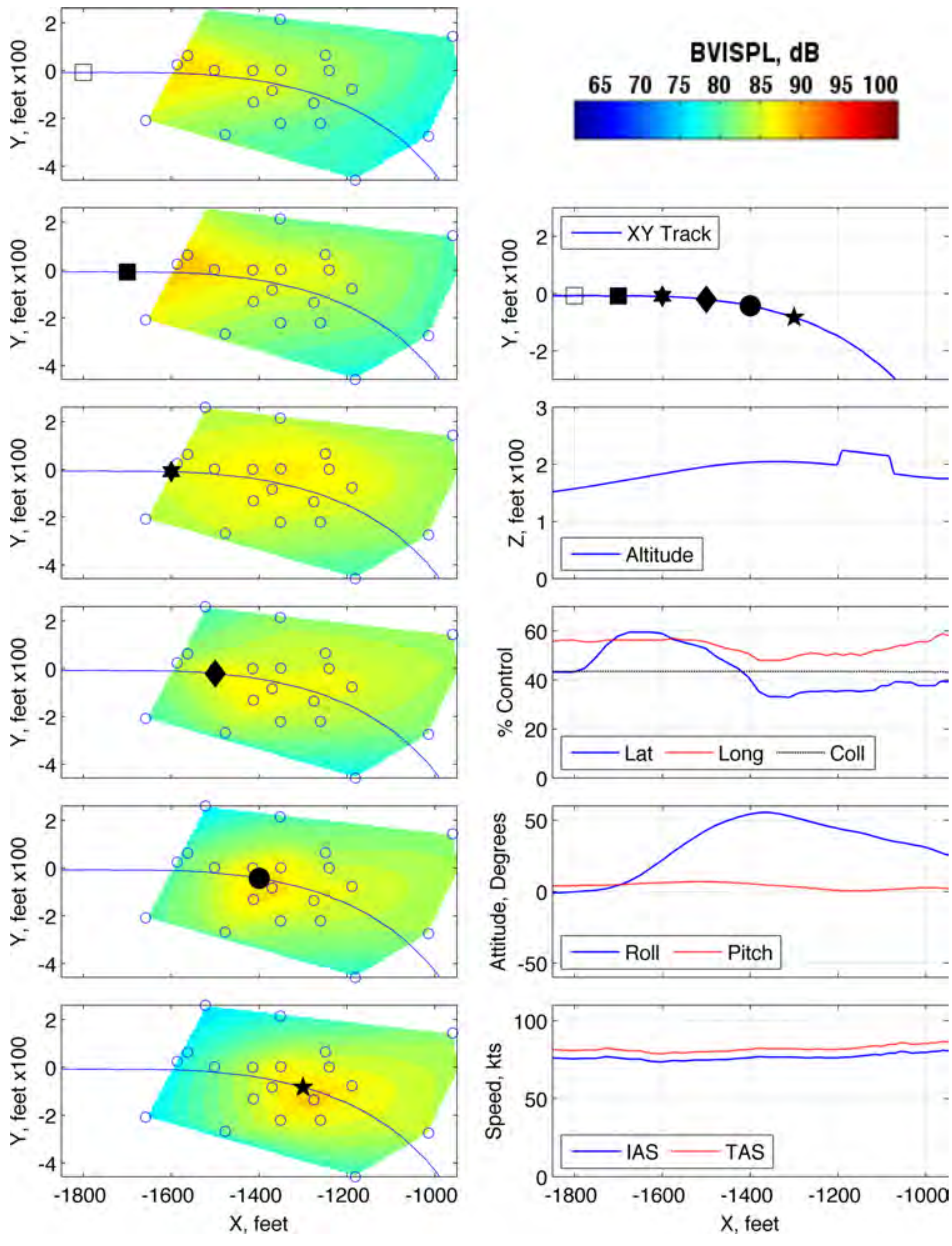

Figure 308: Maneuver condition Z15, 80 KIAS, 0° to 6° , roll right, run number 287548

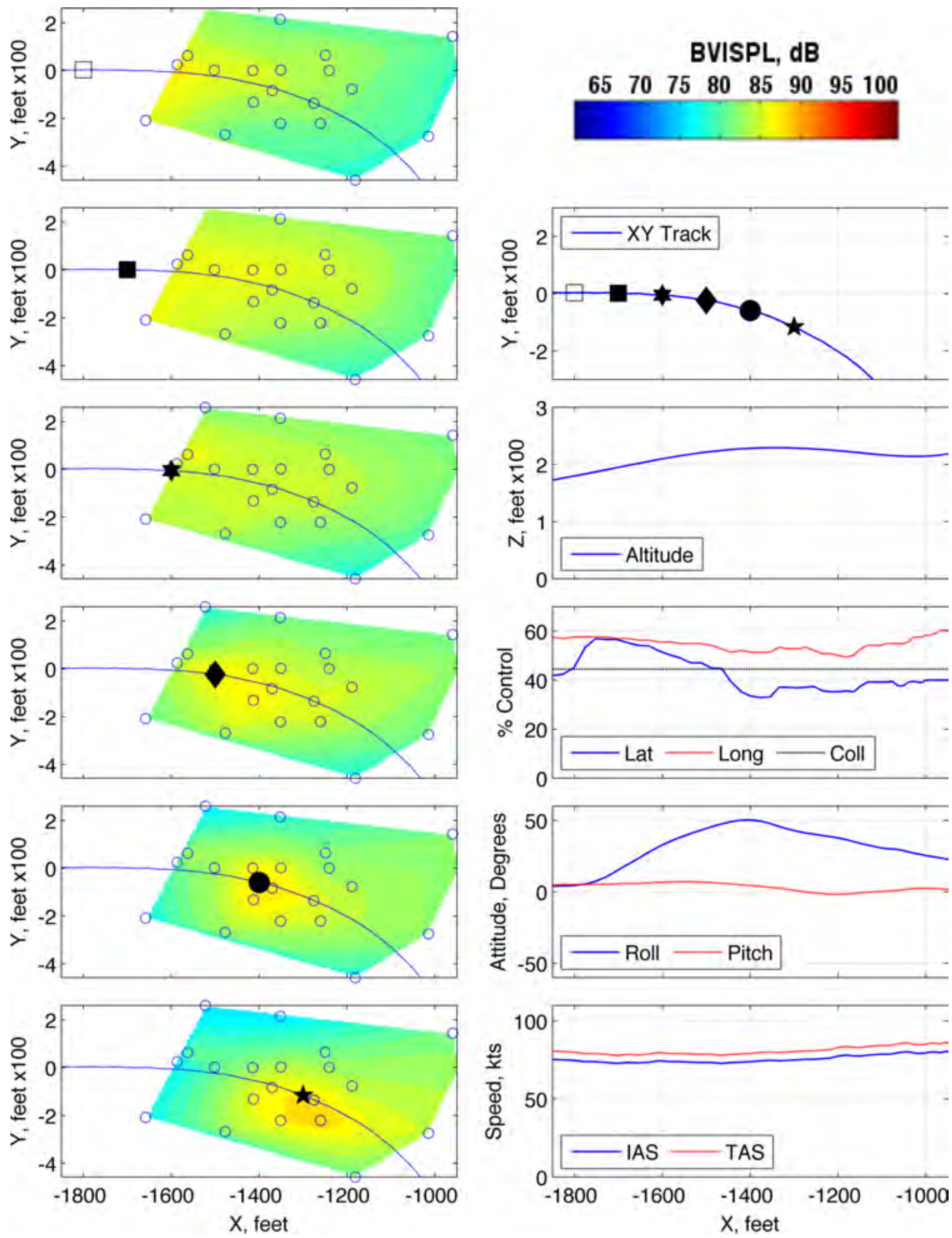

Figure 309: Maneuver condition Z15, 80 KIAS, 0° to 6° , roll right, run number 287549

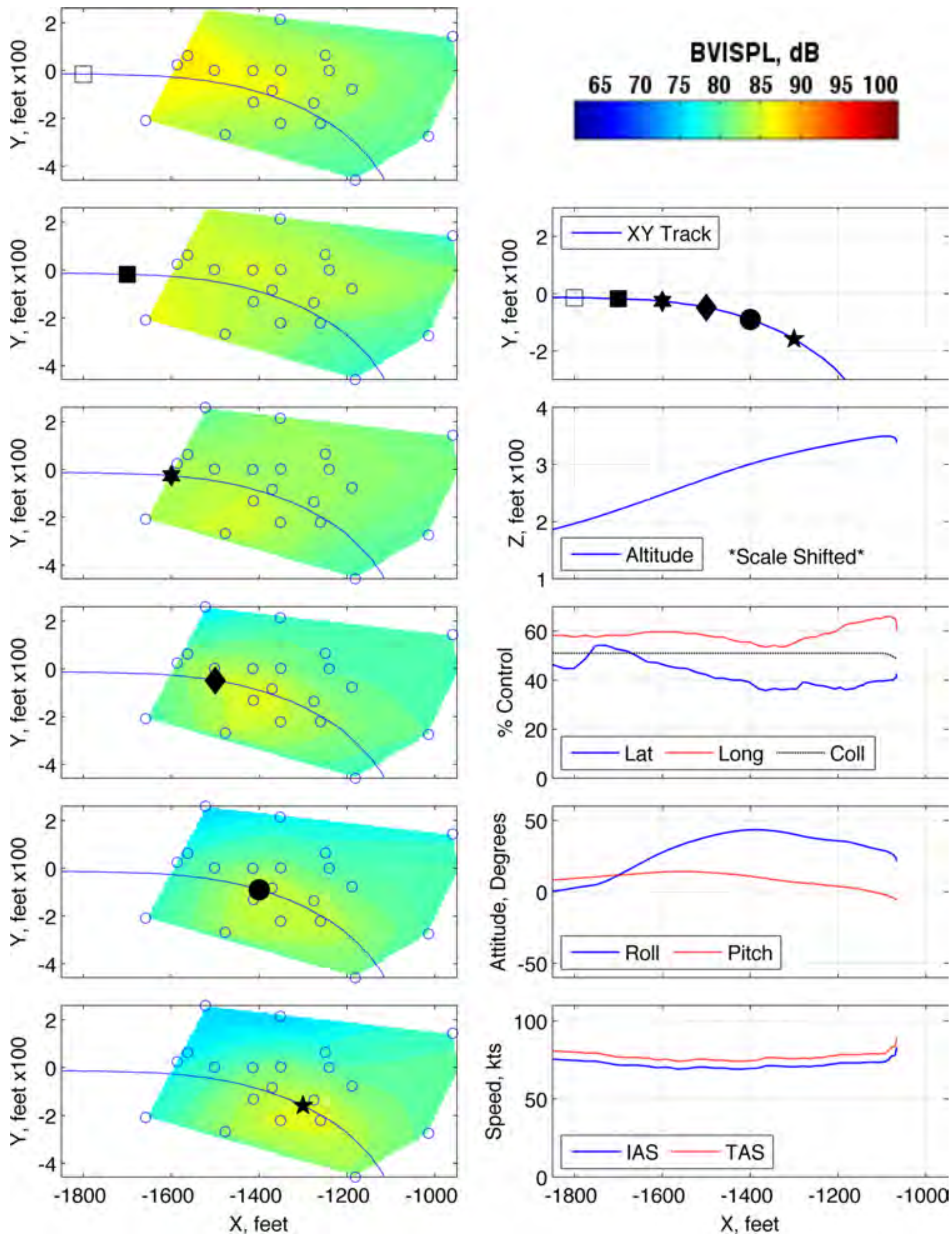

Figure 310: Maneuver condition Z18, 80 KIAS, 0° to 9° , roll right, run number 287552

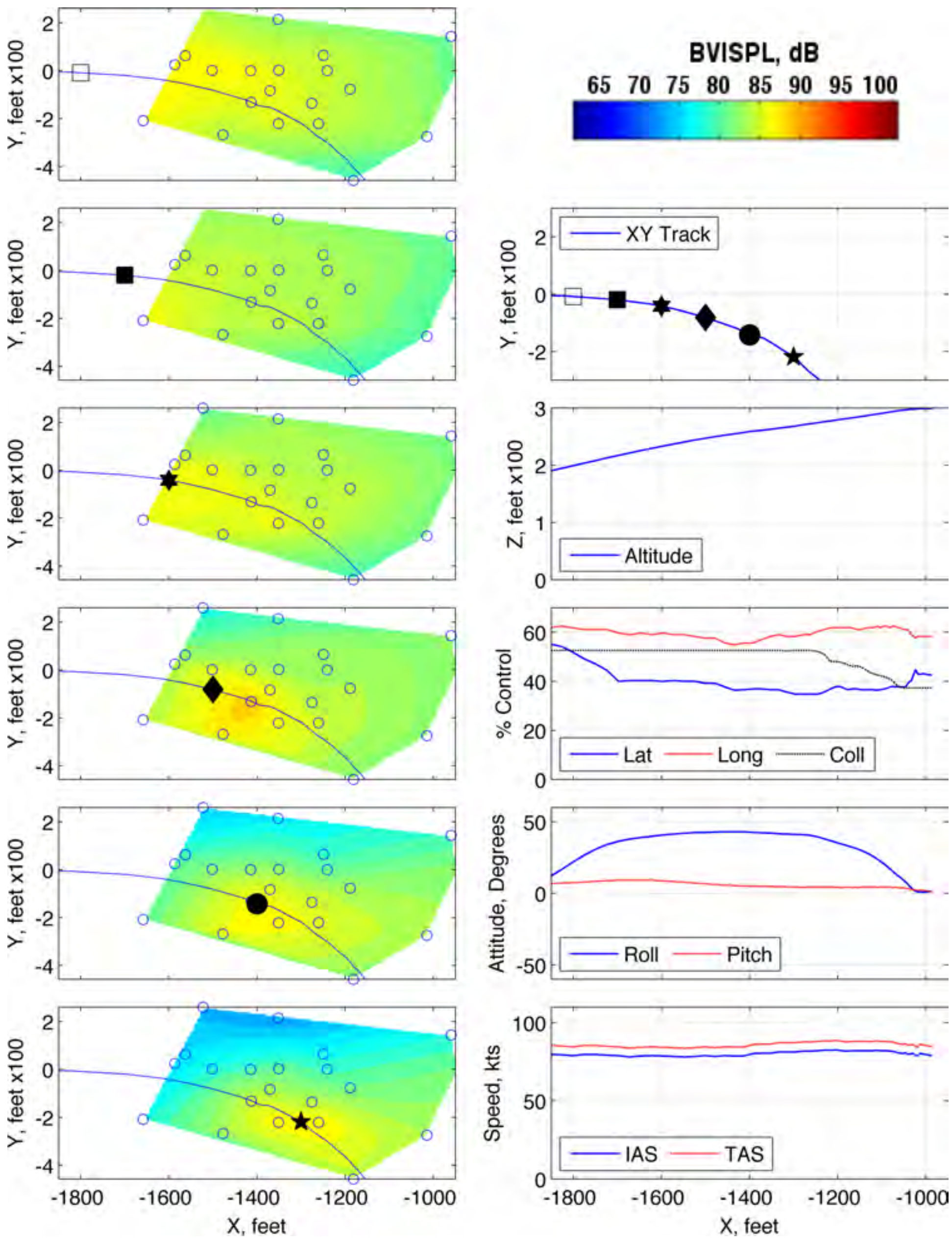

Figure 311: Maneuver condition Z18, 80 KIAS, 0° to 9° , roll right, run number 287553

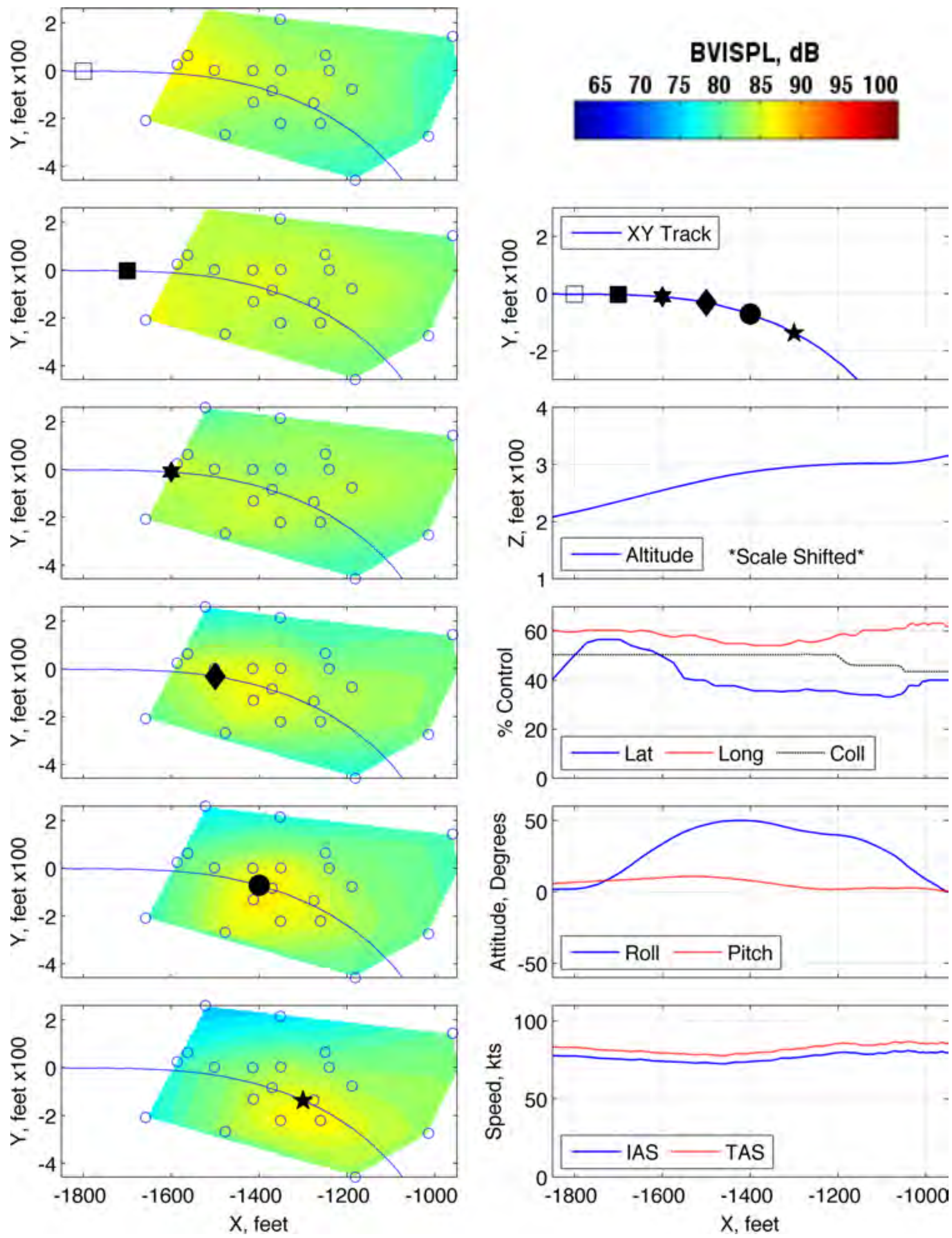

Figure 312: Maneuver condition Z18, 80 KIAS, 0° to 9° , roll right, run number 287554

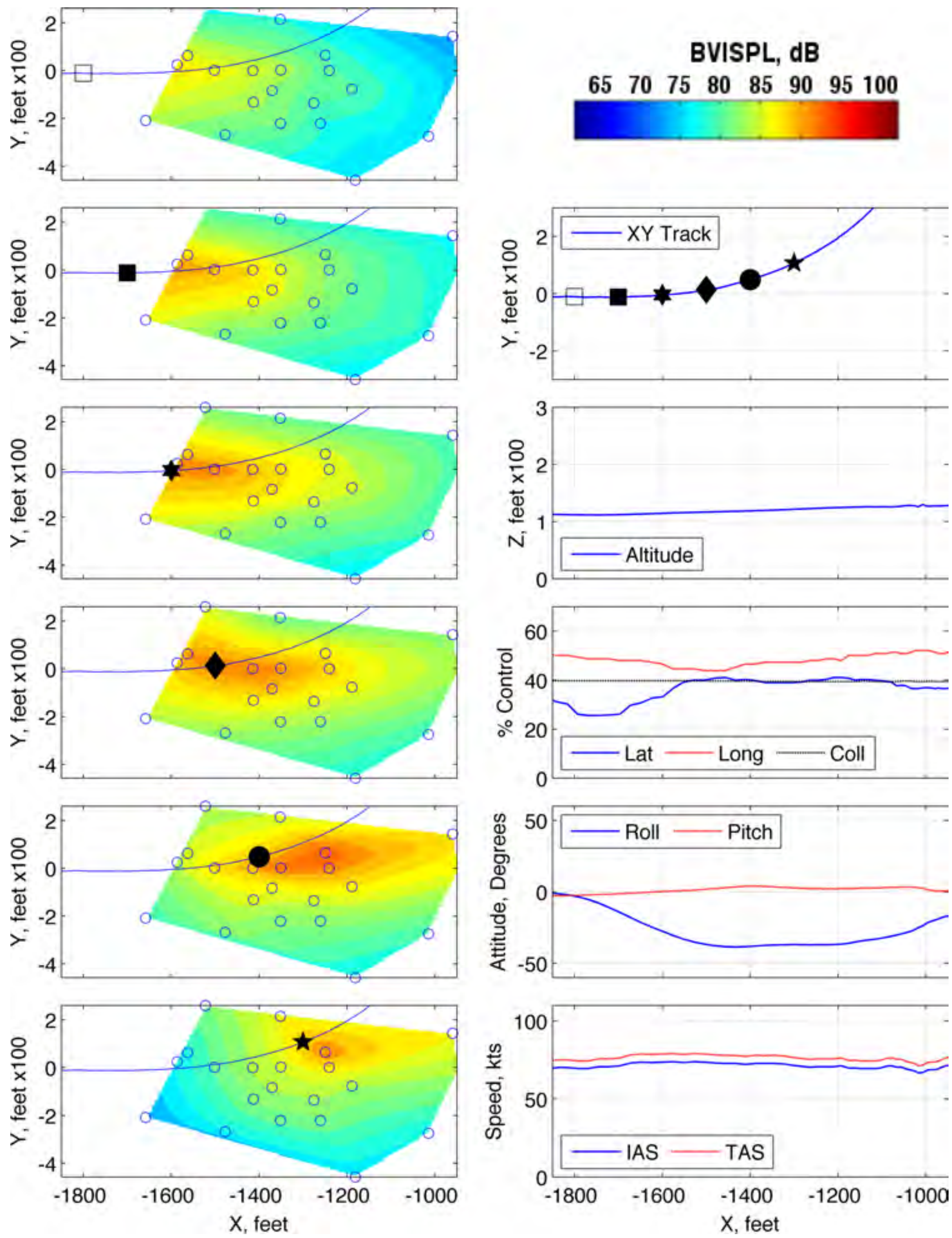

Figure 313: Maneuver condition Y3, 60 to 80 KIAS at 1 kt/s, level cyclic roll left, run number 287568

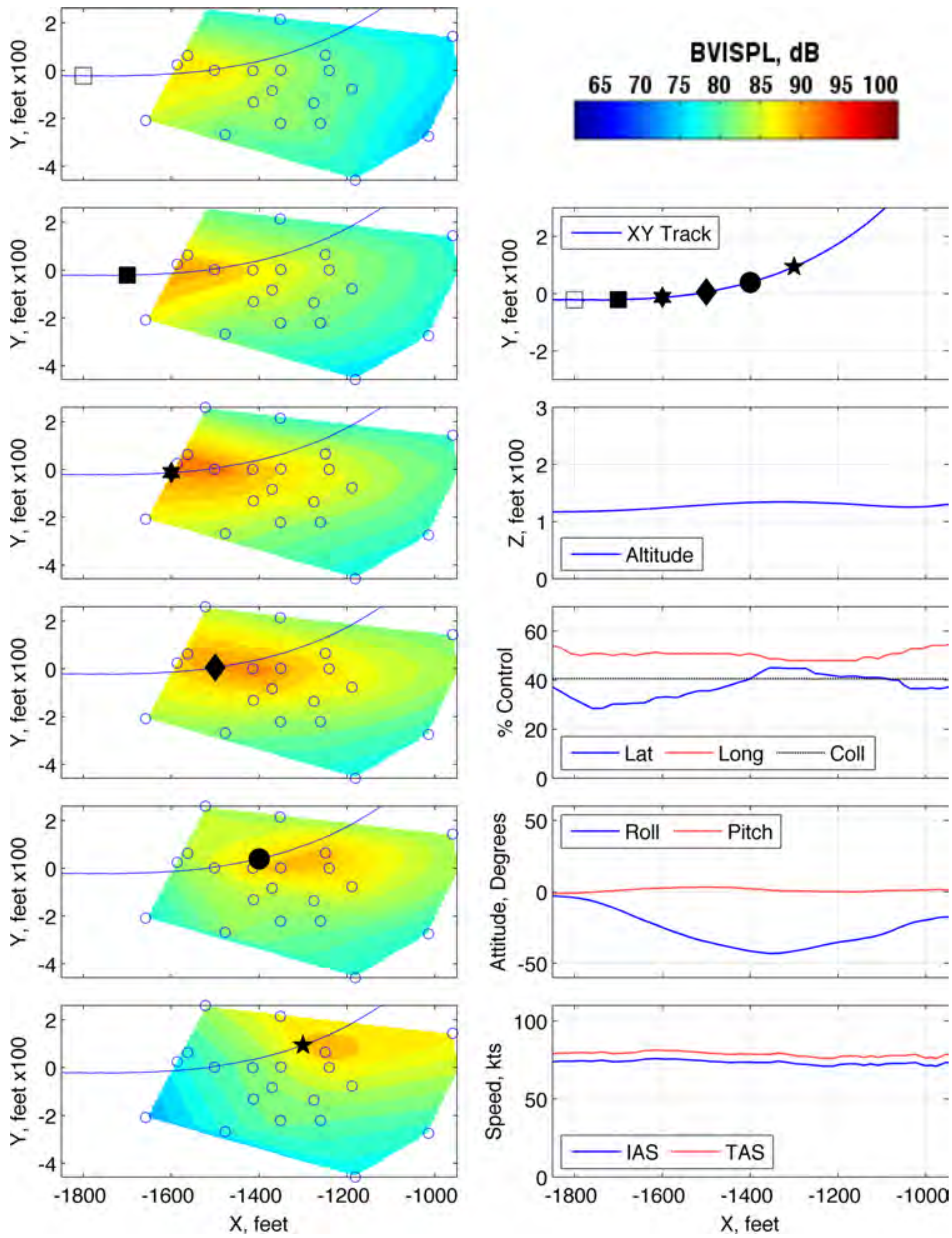

Figure 314: Maneuver condition Y3, 60 to 80 KIAS at 1 kt/s, level cyclic roll left, run number 287569

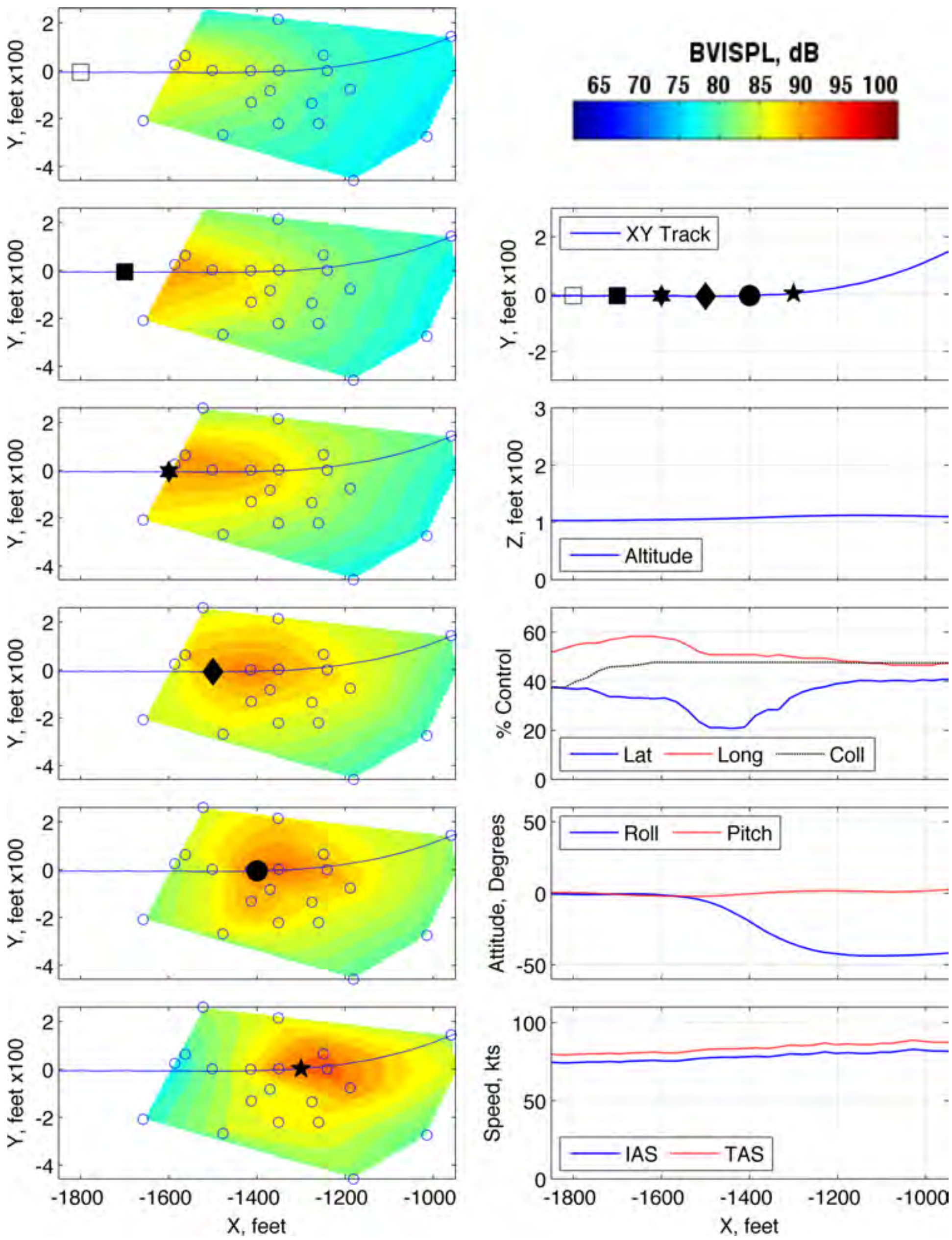

Figure 315: Maneuver condition Y6, 60 to 80 KIAS at 2 kt/s, level cyclic roll left, run number 285508

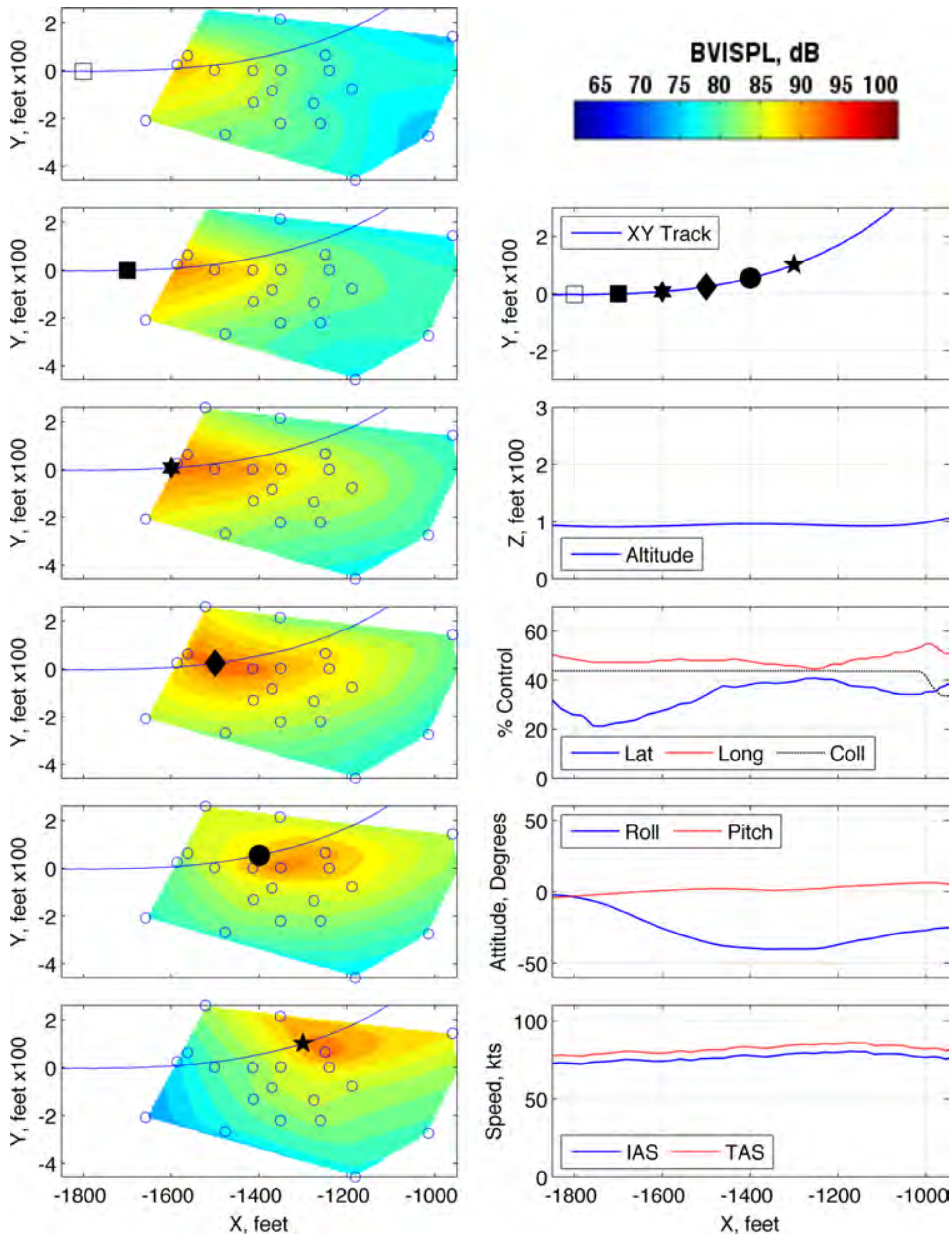

Figure 316: Maneuver condition Y6, 60 to 80 KIAS at 2 kt/s, level cyclic roll left, run number 285509

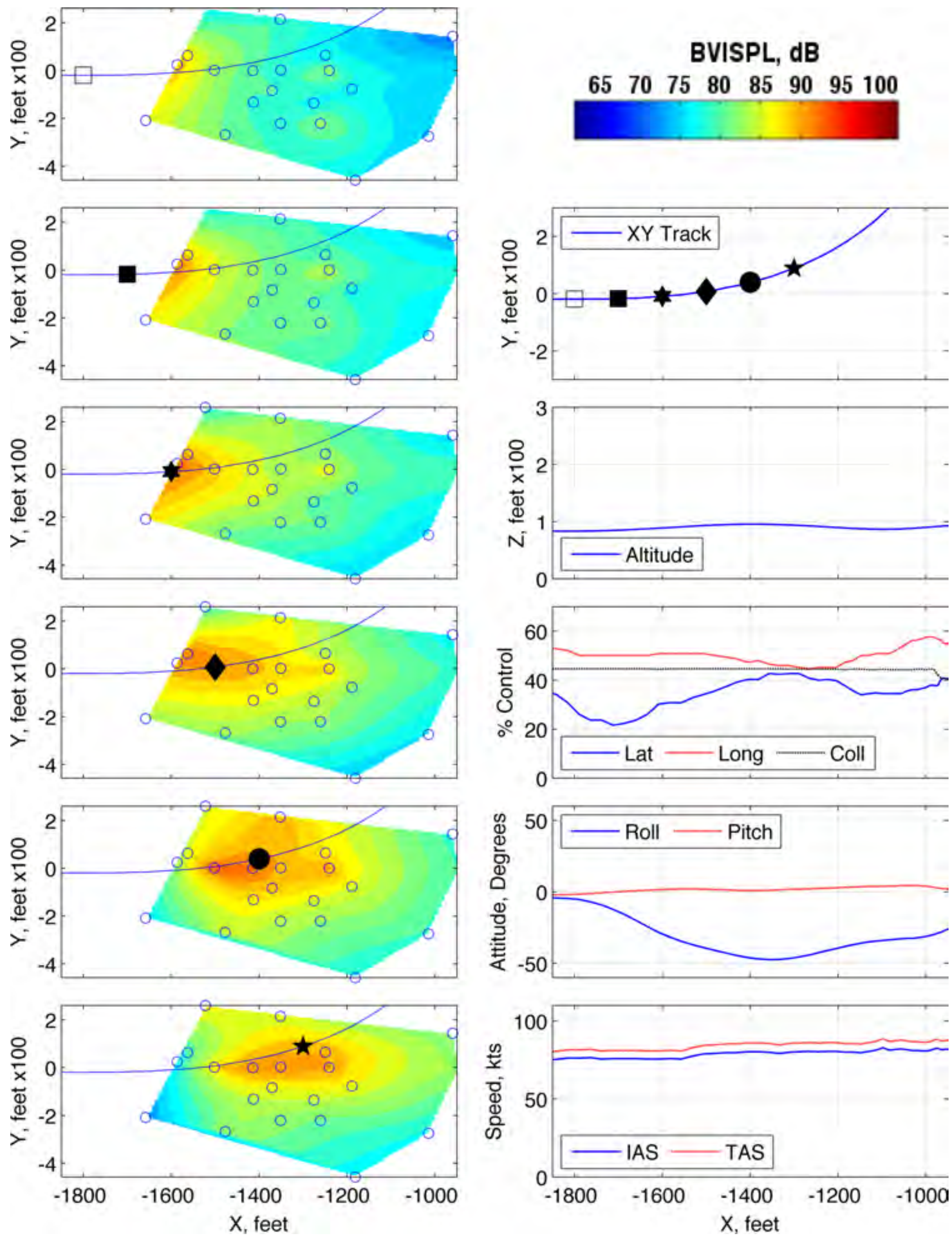

Figure 317: Maneuver condition Y6, 60 to 80 KIAS at 2 kt/s, level cyclic roll left, run number 285510

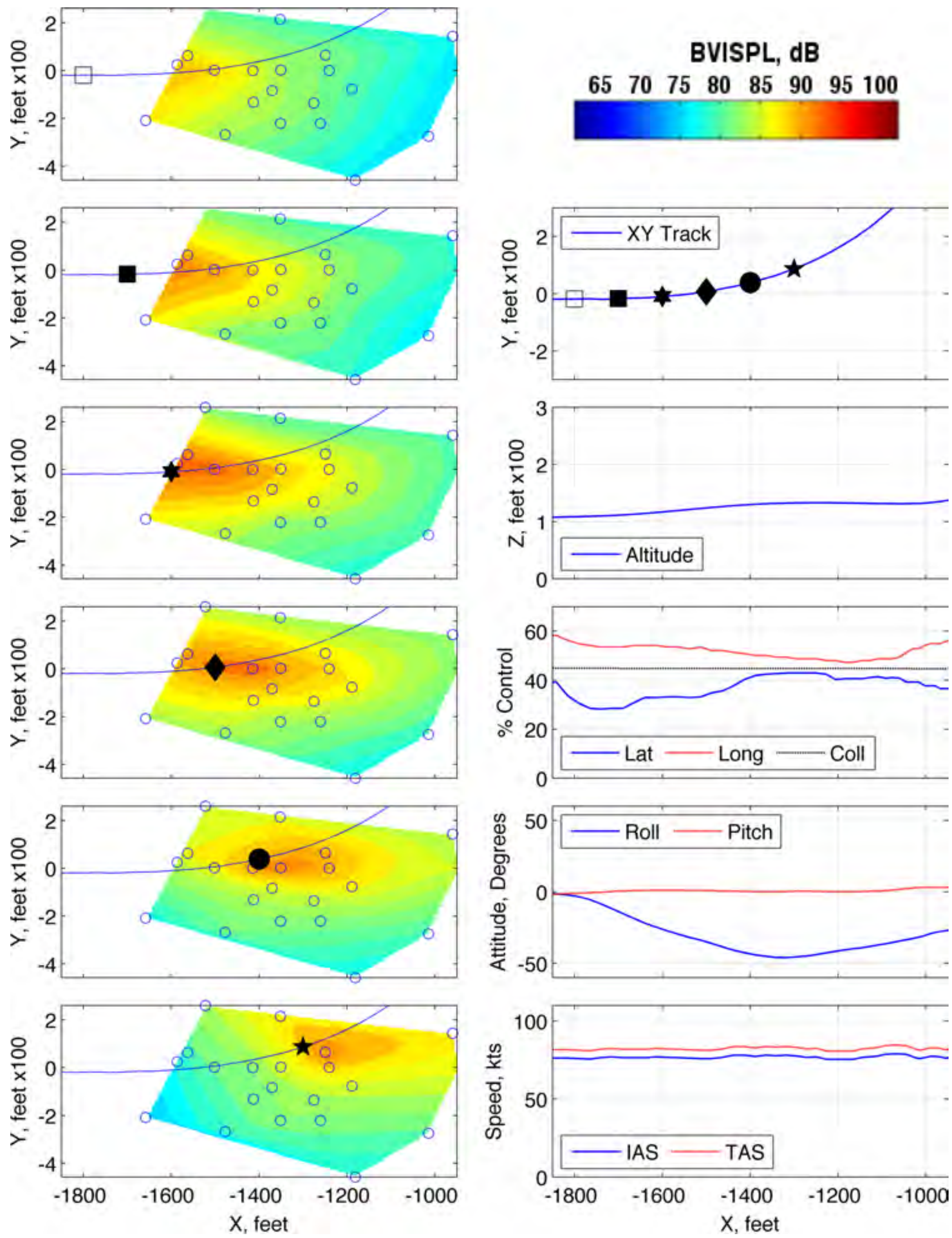

Figure 318: Maneuver condition Y6, 60 to 80 KIAS at 2 kt/s, level cyclic roll left, run number 287571

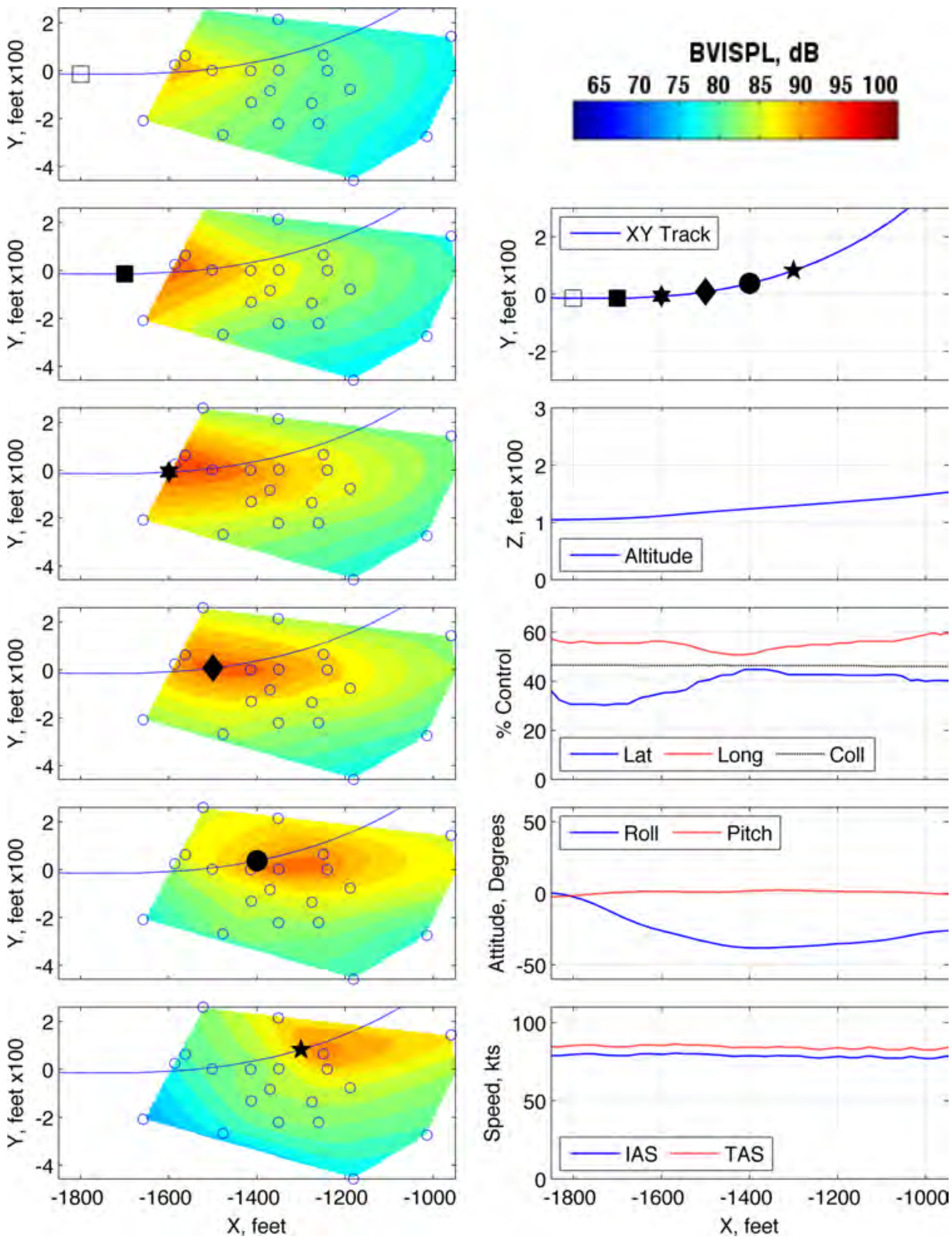

Figure 319: Maneuver condition Y6, 60 to 80 KIAS at 2 kt/s, level cyclic roll left, run number 287573

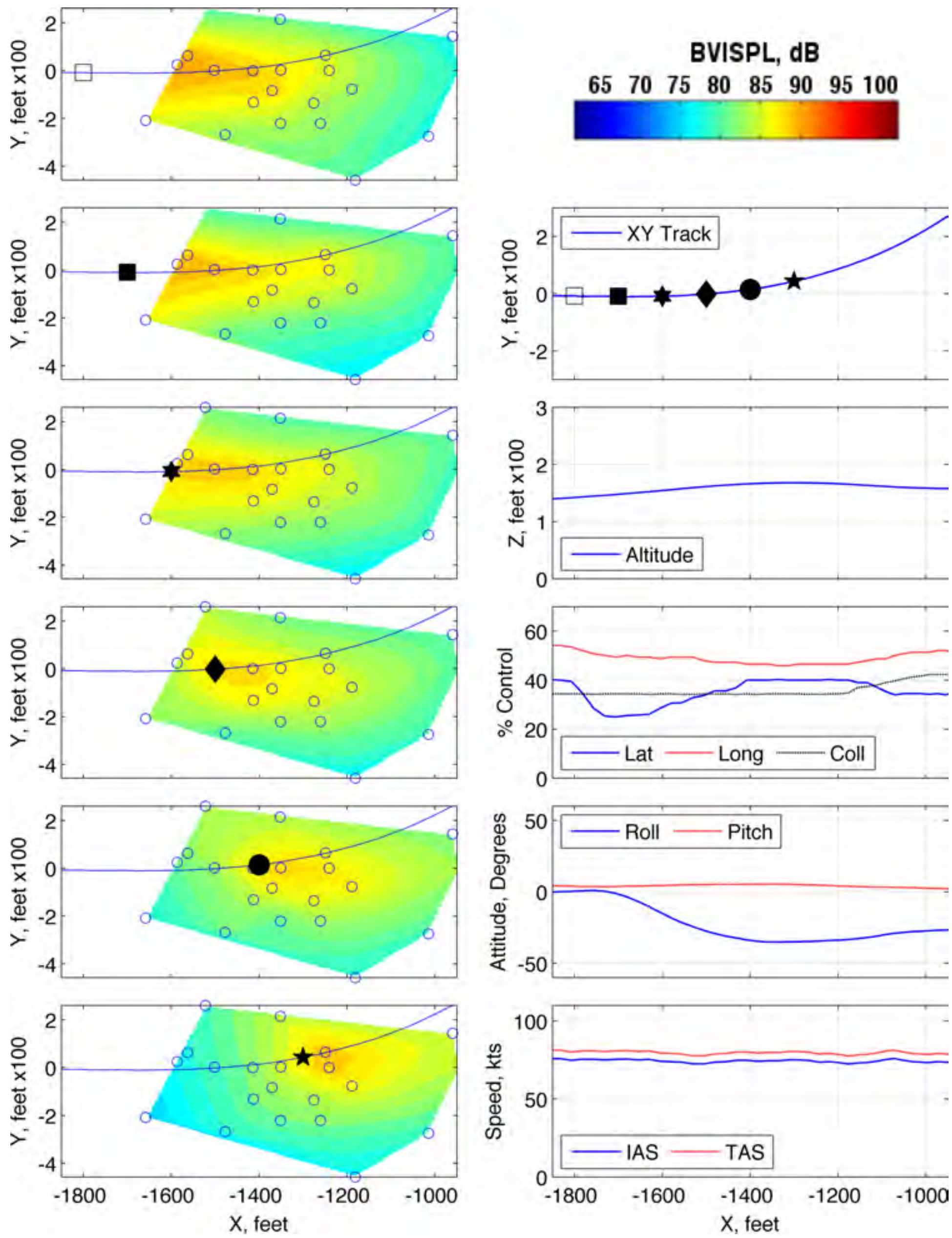

Figure 320: Maneuver condition Y12, 100 to 80 KIAS at 1 kt/s, level cyclic roll left, run number 287560

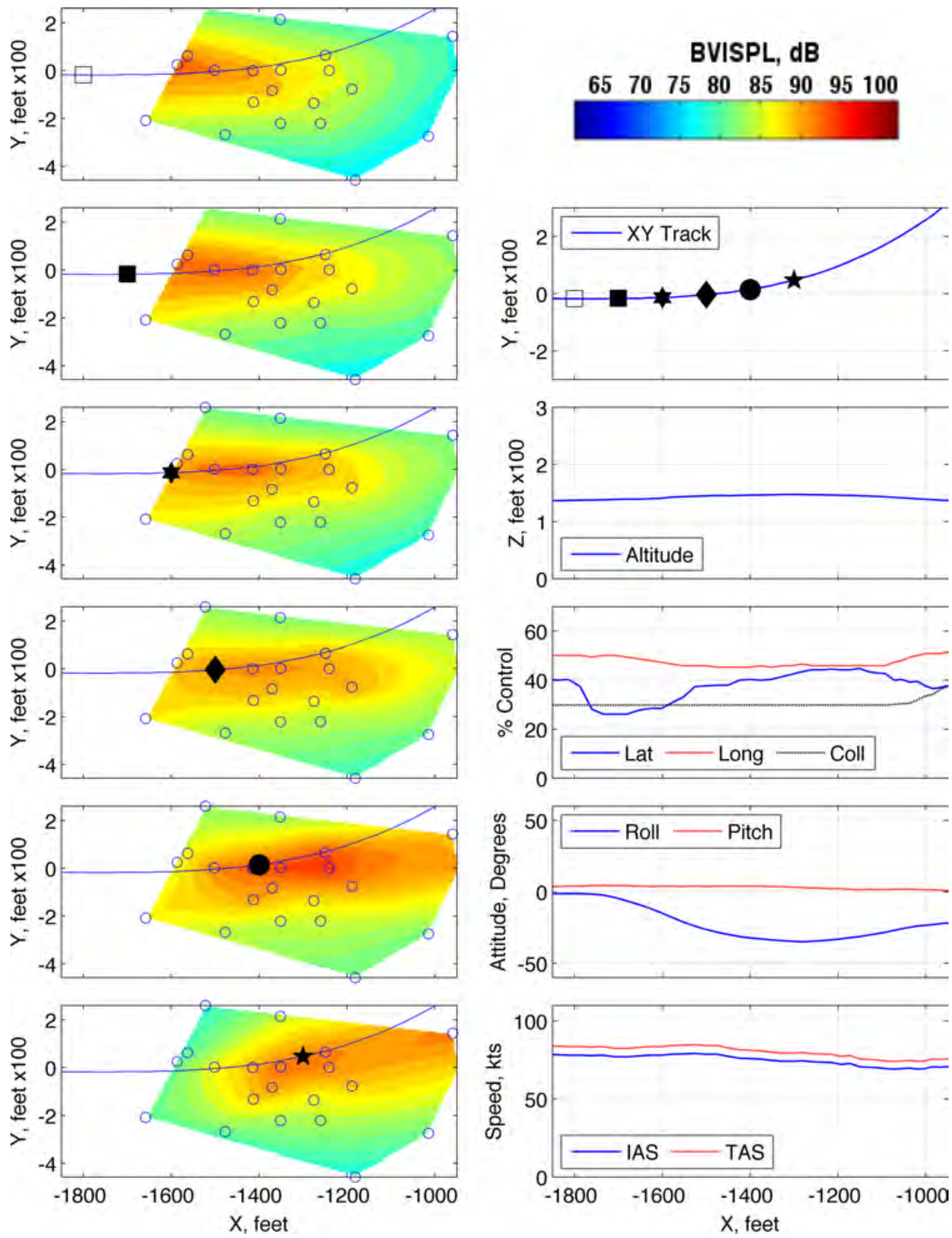

Figure 321: Maneuver condition Y12, 100 to 80 KIAS at 1 kt/s, level cyclic roll left, run number 287561

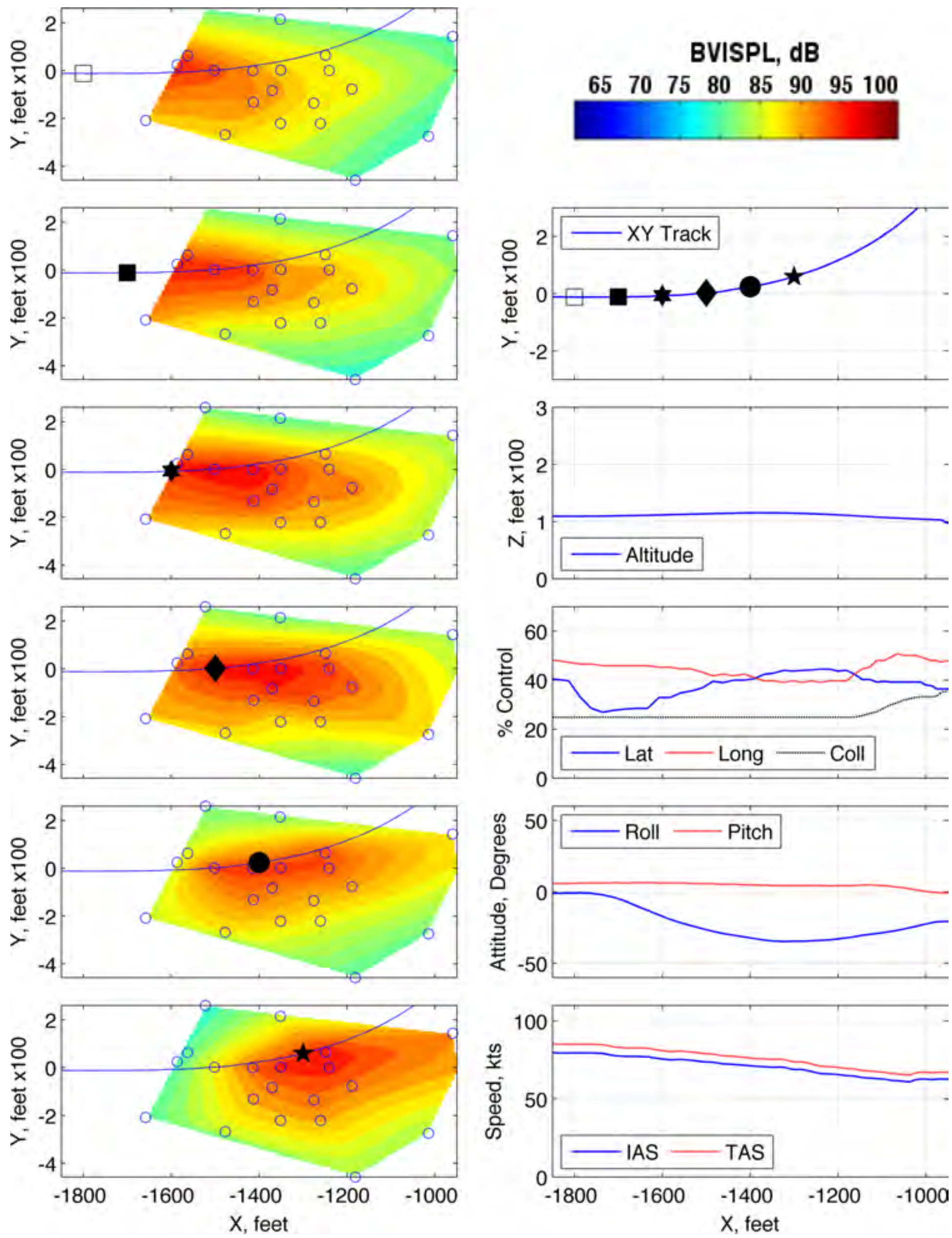

Figure 322: Maneuver condition Y15, 100 to 80 KIAS at 2 kt/s, level cyclic roll left, run number 287564

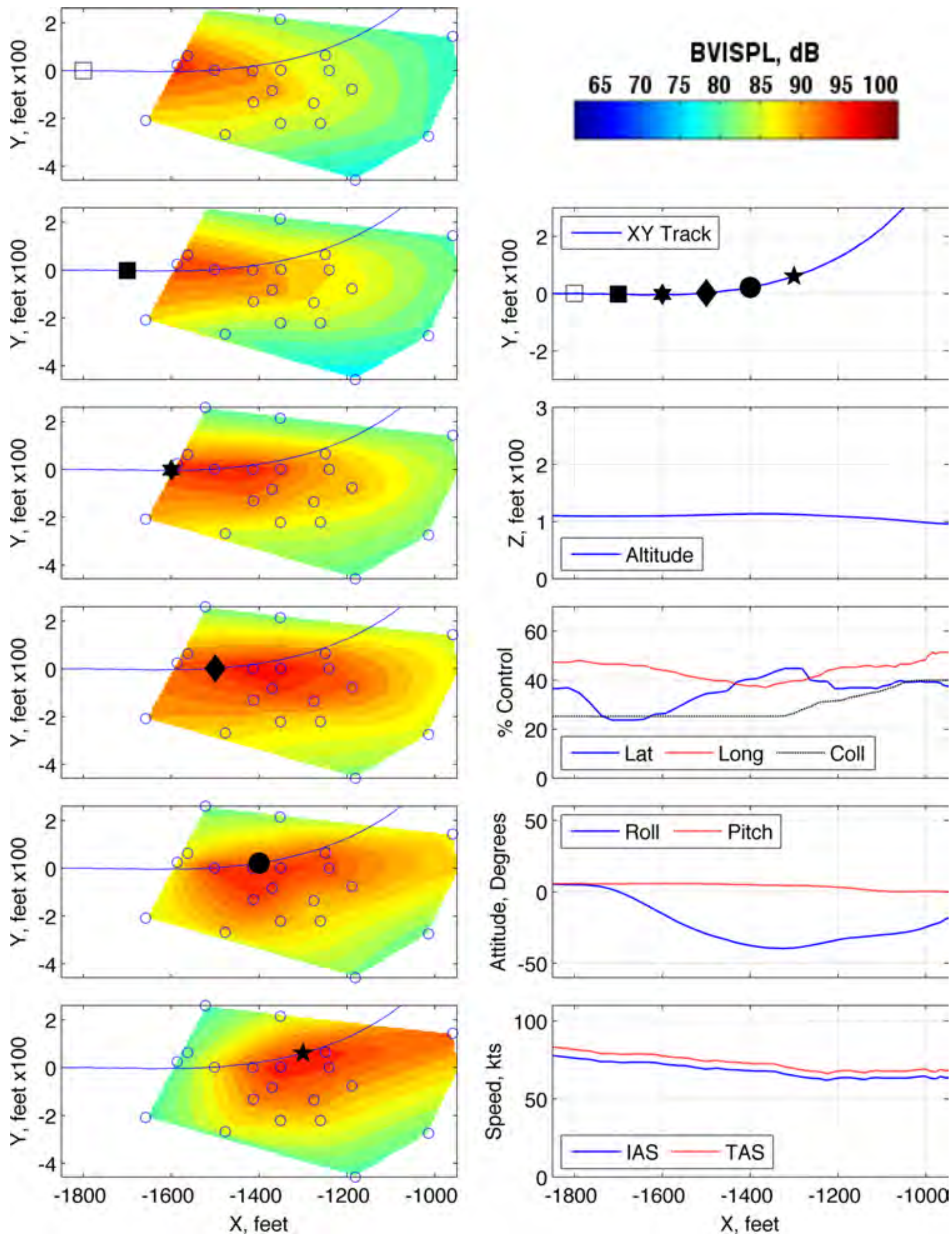

Figure 323: Maneuver condition Y15, 100 to 80 KIAS at 2 kt/s, level cyclic roll left, run number 287565

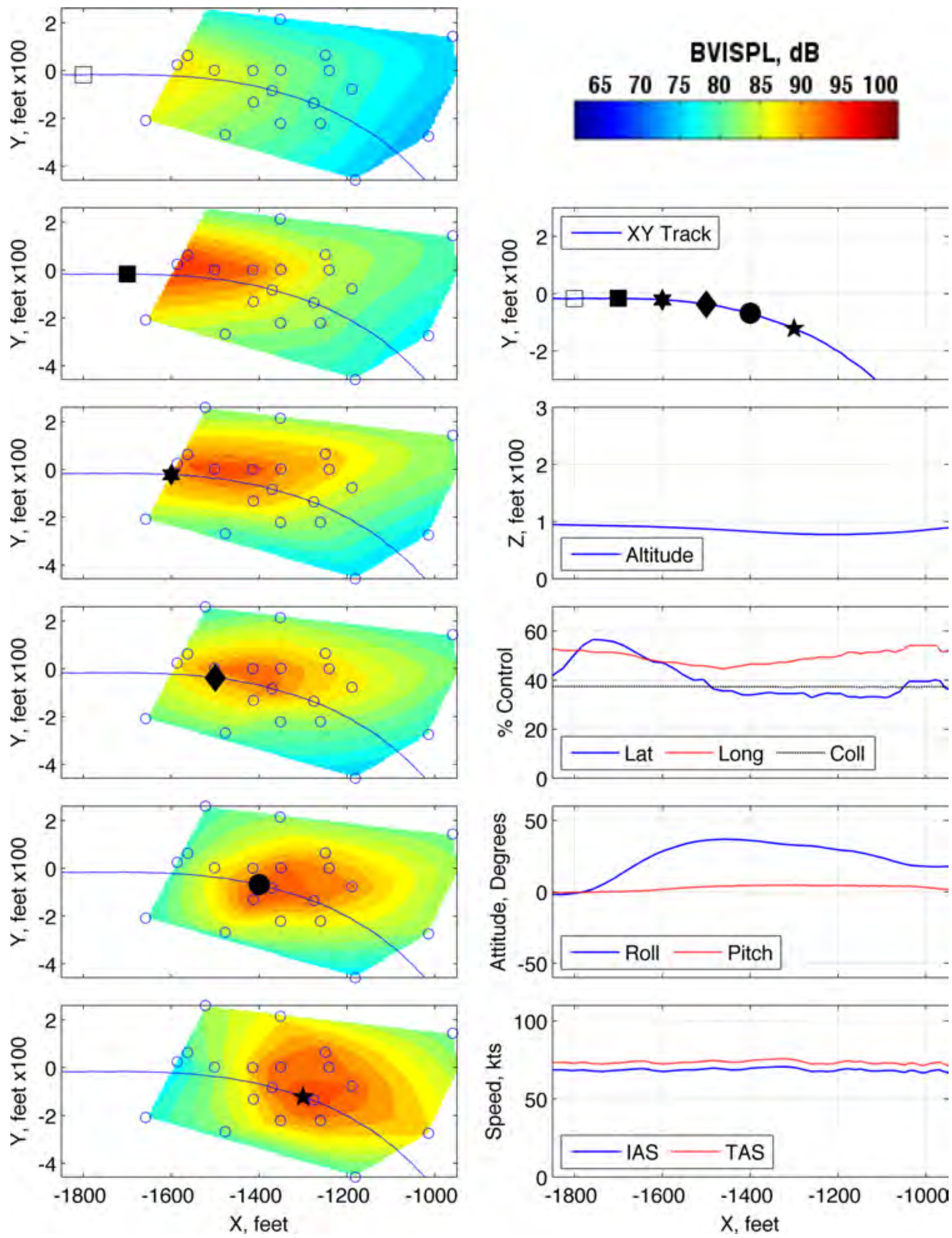

Figure 324: Maneuver condition Y21, 60 to 80 KIAS at 1 kt/s, level cyclic roll right, run number 287566

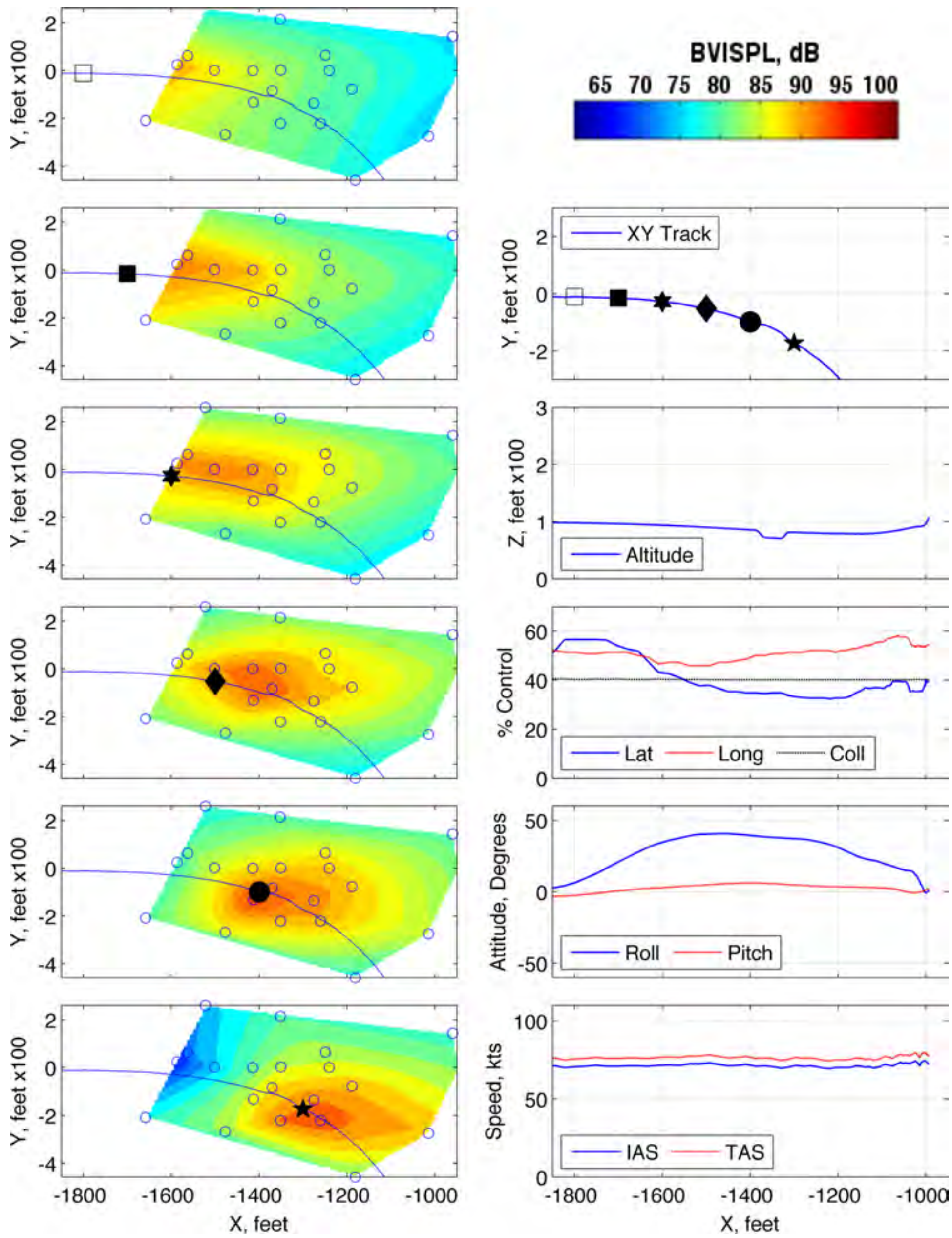

Figure 325: Maneuver condition Y21, 60 to 80 KIAS at 1 kt/s, level cyclic roll right, run number 287567

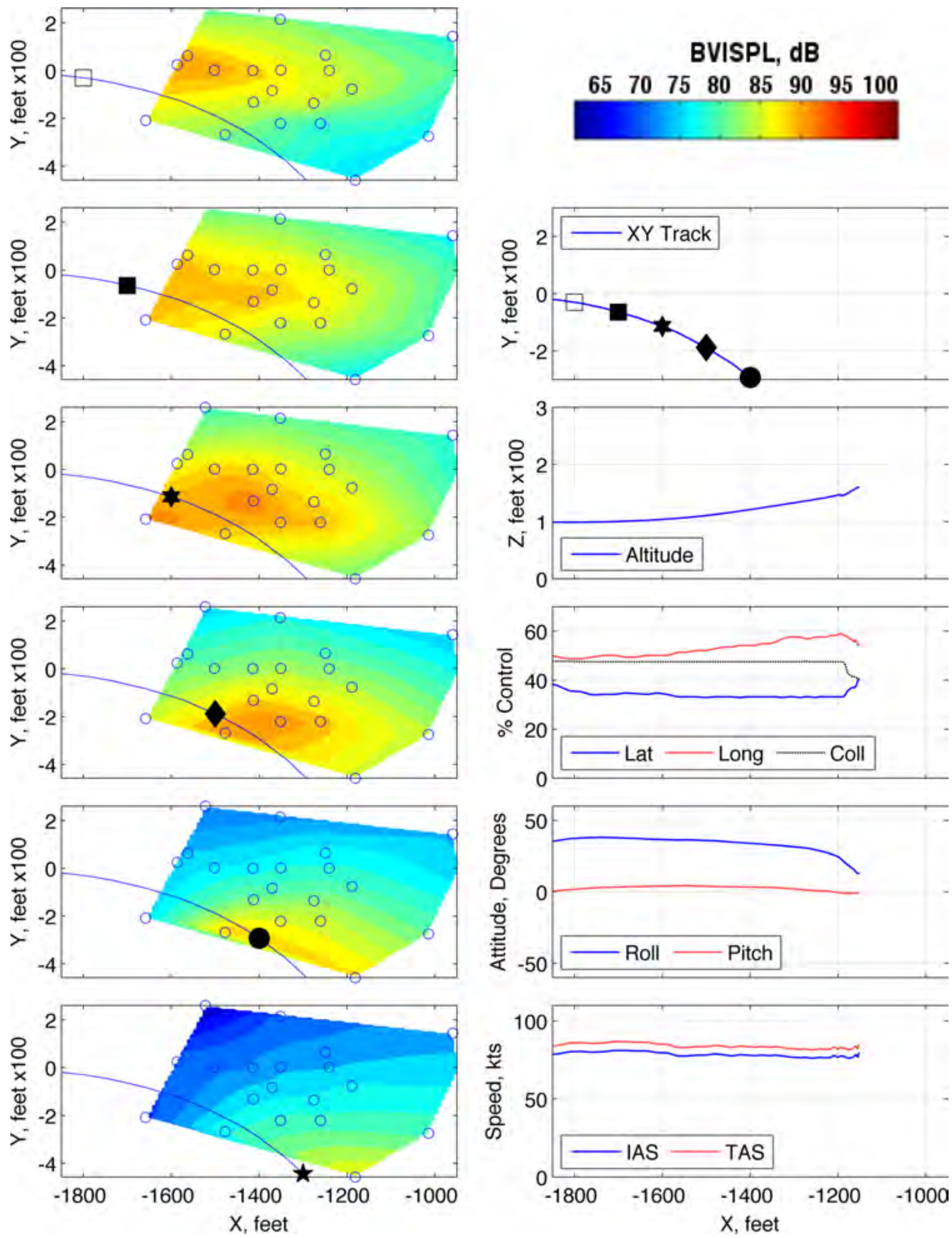

Figure 326: Maneuver condition Y24, 60 to 80 KIAS at 2 kt/s, level cyclic roll right, run number 285511

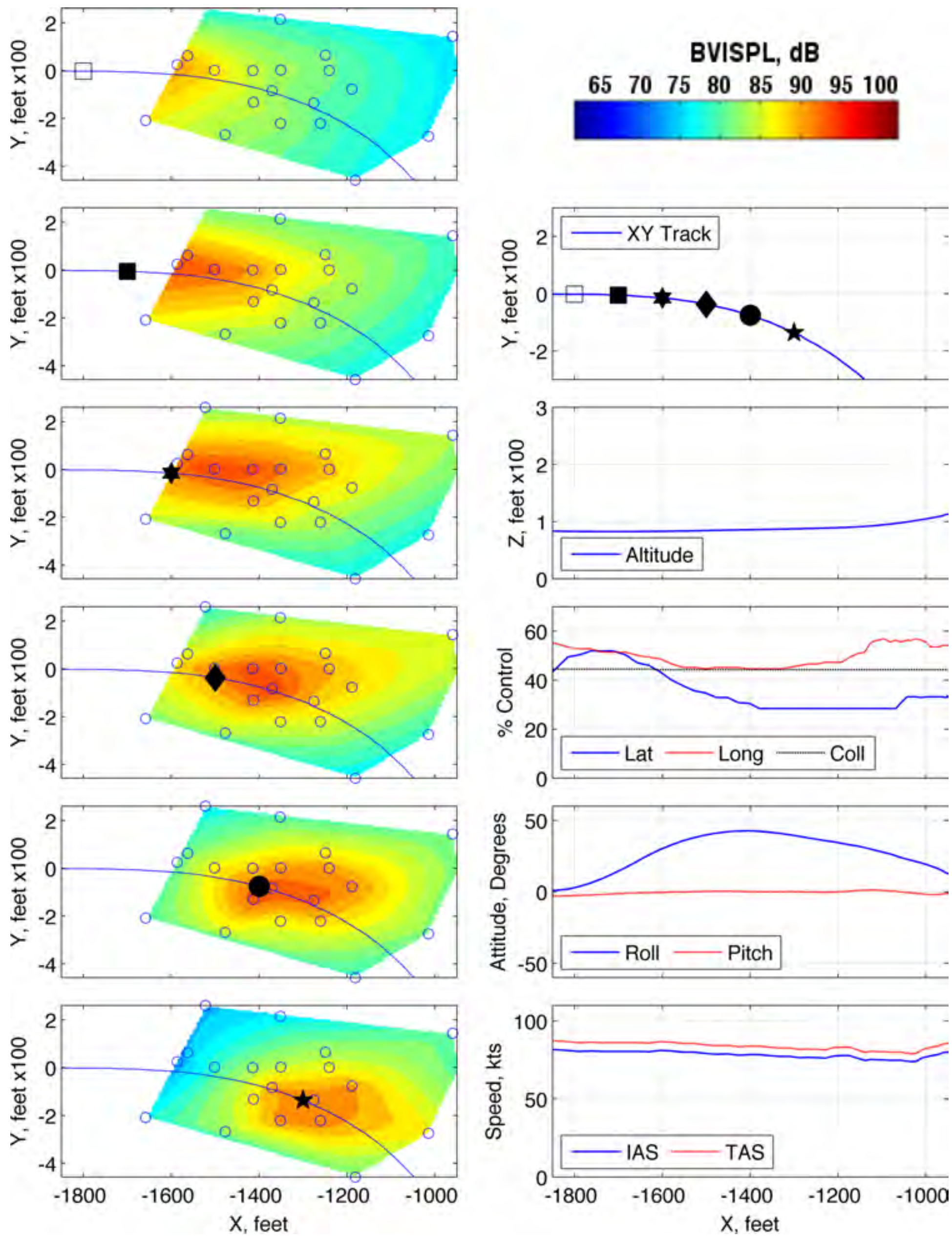

Figure 327: Maneuver condition Y24, 60 to 80 KIAS at 2 kt/s, level cyclic roll right, run number 285512

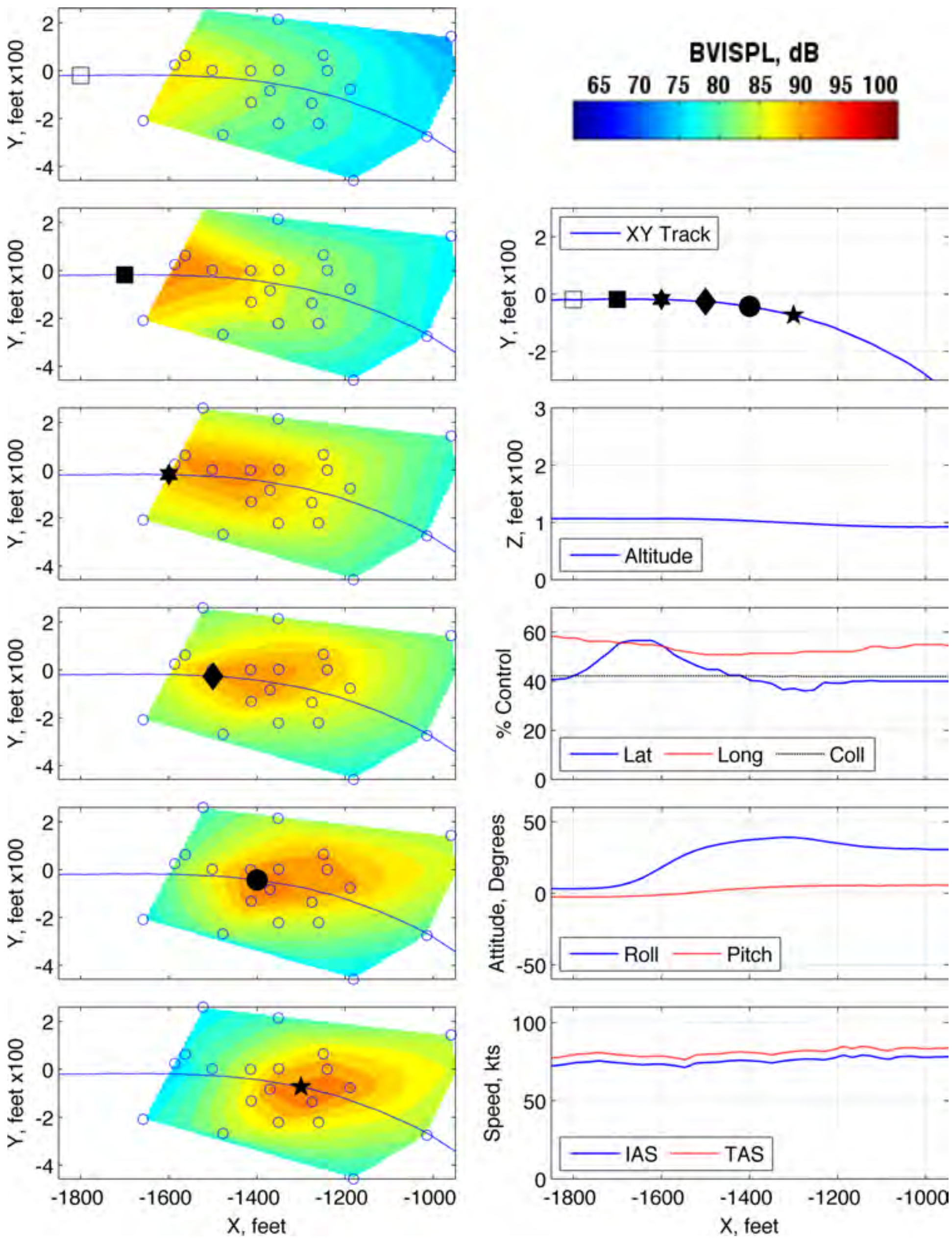

Figure 328: Maneuver condition Y24, 60 to 80 KIAS at 2 kt/s, level cyclic roll right, run number 287570

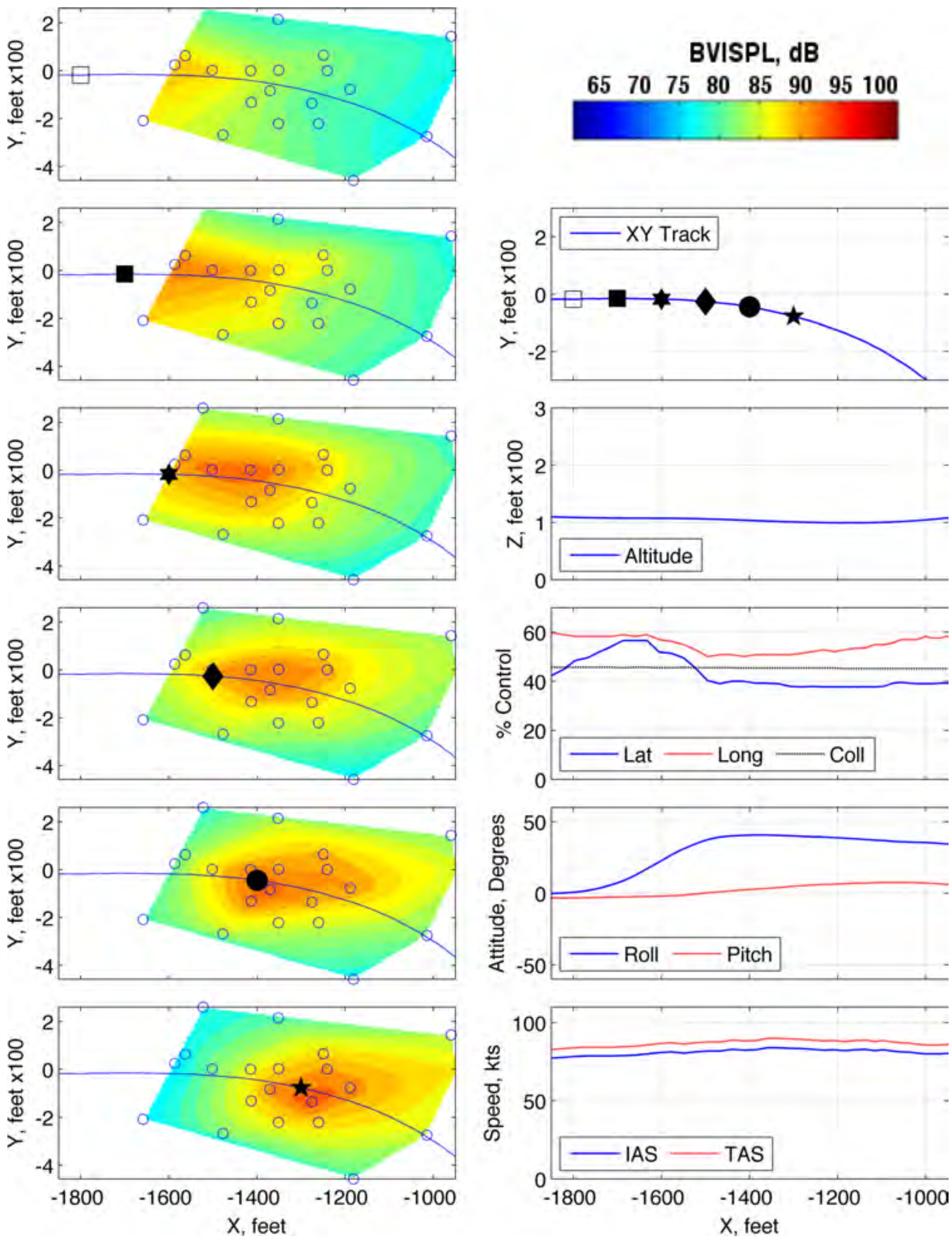

Figure 329: Maneuver condition Y24, 60 to 80 KIAS at 2 kt/s, level cyclic roll right, run number 287572

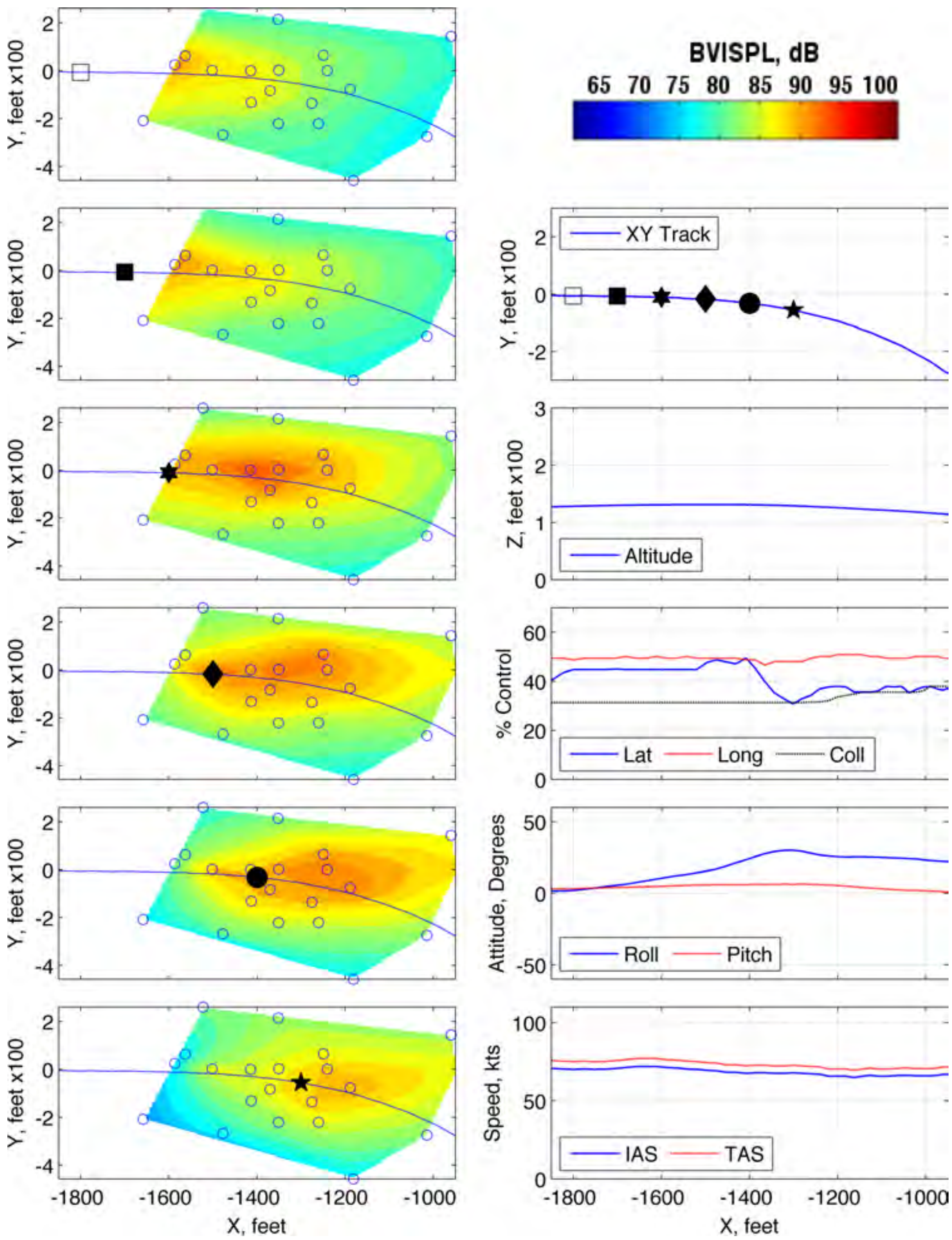

Figure 330: Maneuver condition Y30, 100 to 80 KIAS at 1 kt/s, level cyclic roll right, run number 287557

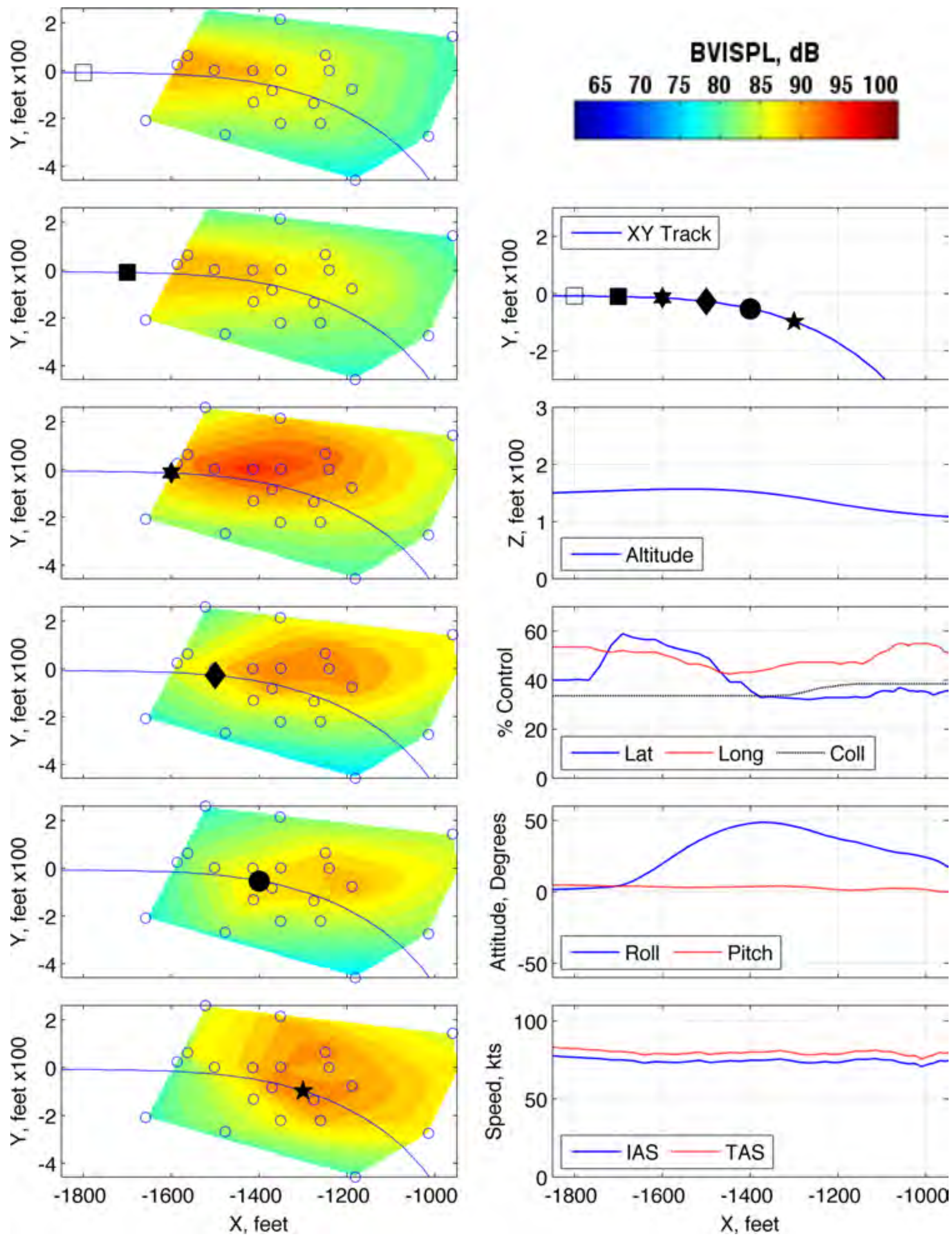

Figure 331: Maneuver condition Y30, 100 to 80 KIAS at 1 kt/s, level cyclic roll right, run number 287558

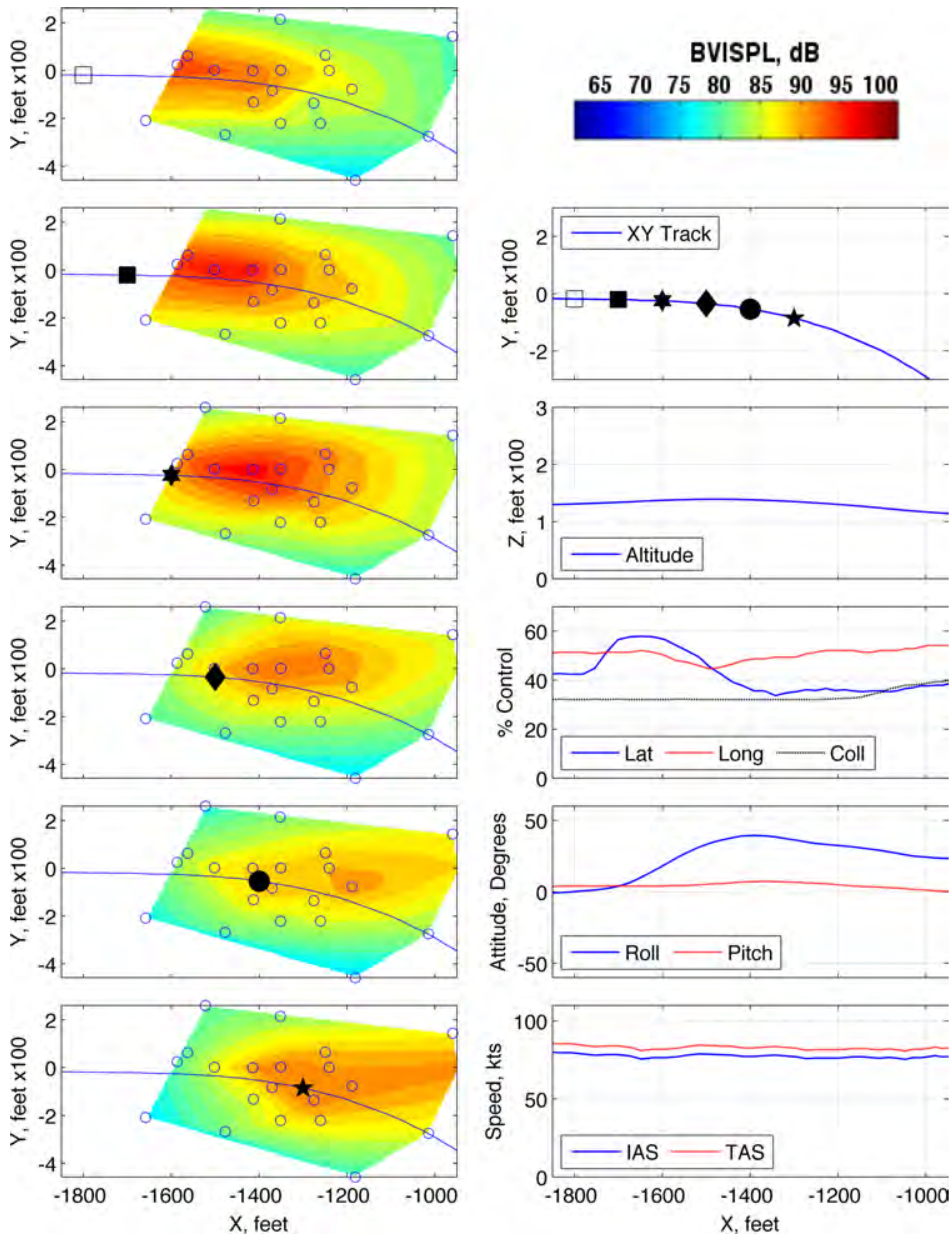

Figure 332: Maneuver condition Y30, 100 to 80 KIAS at 1 kt/s, level cyclic roll right, run number 287559

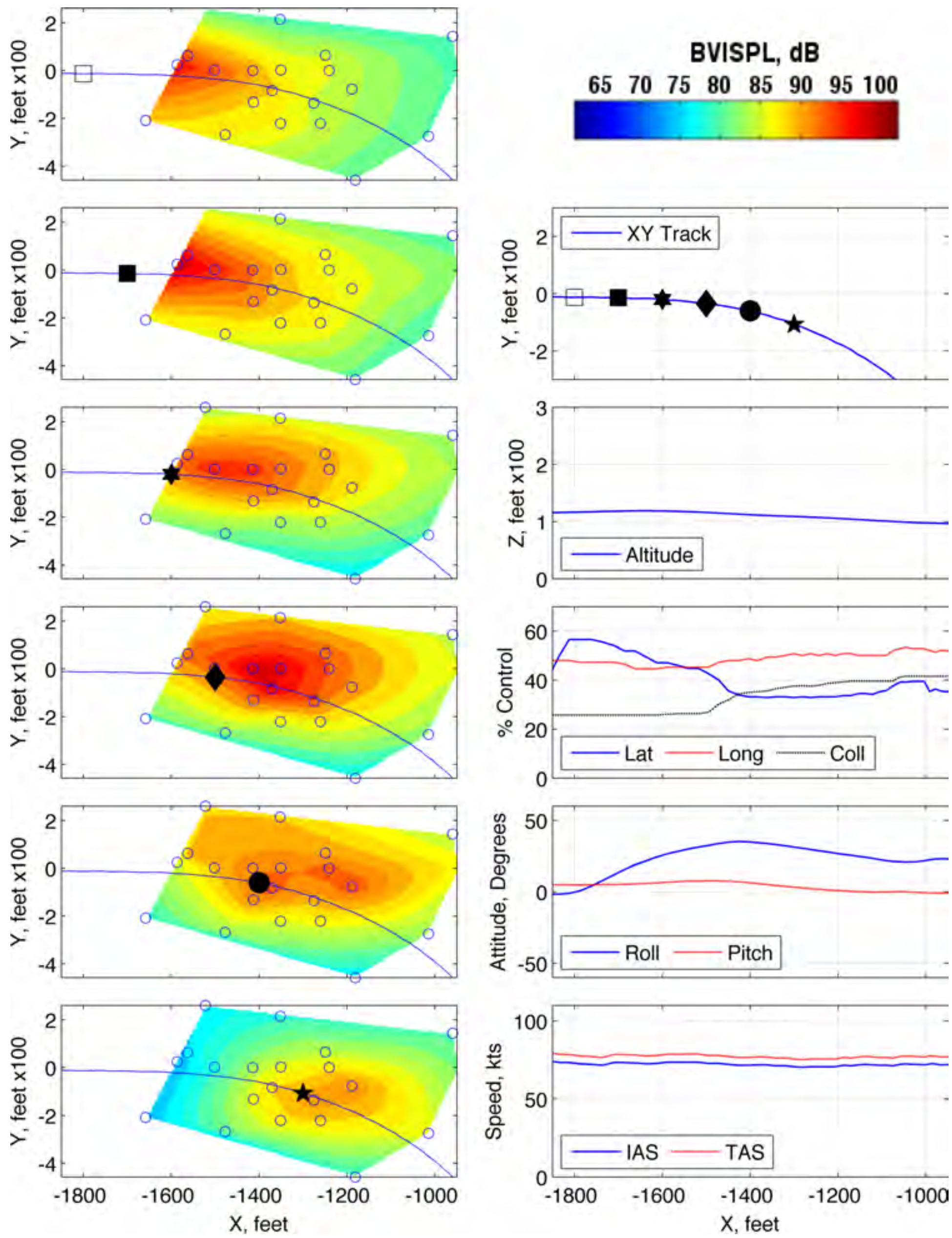

Figure 333: Maneuver condition Y33, 100 to 80 KIAS at 2 kt/s, level cyclic roll right, run number 287562

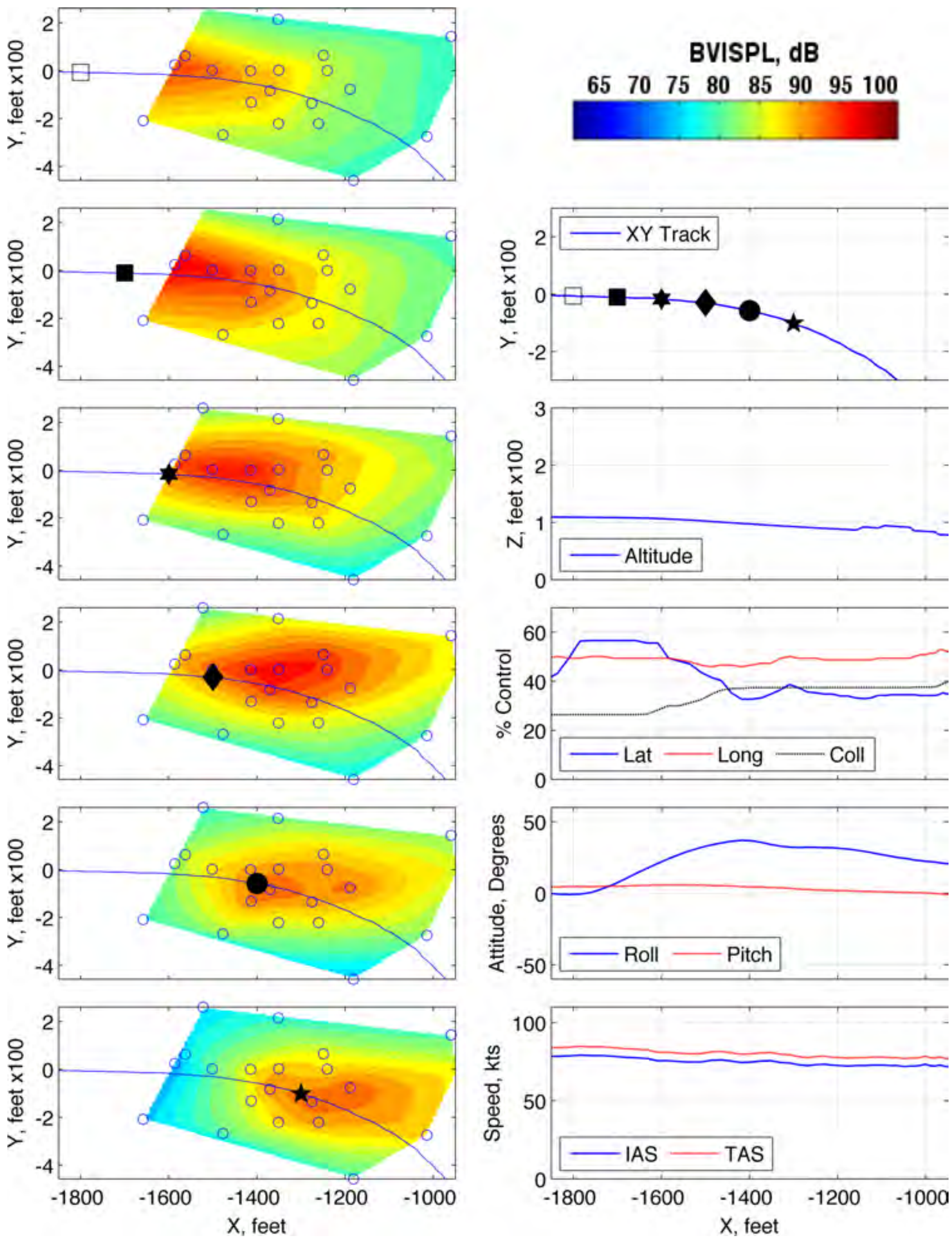

Figure 334: Maneuver condition Y33, 100 to 80 KIAS at 2 kt/s, level cyclic roll right, run number 287563

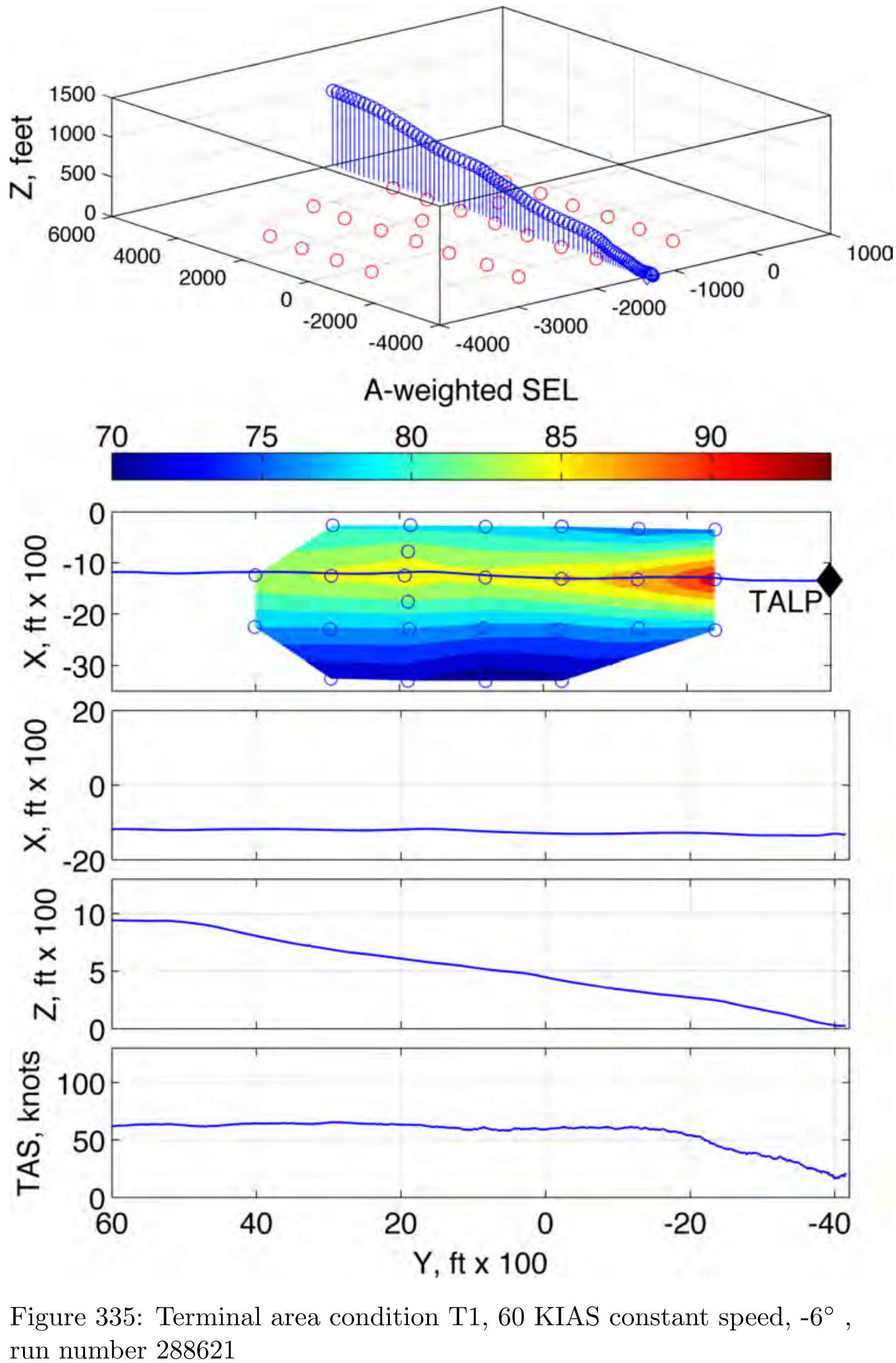

Figure 335: Terminal area condition T1, 60 KIAS constant speed, -6° , run number 288621

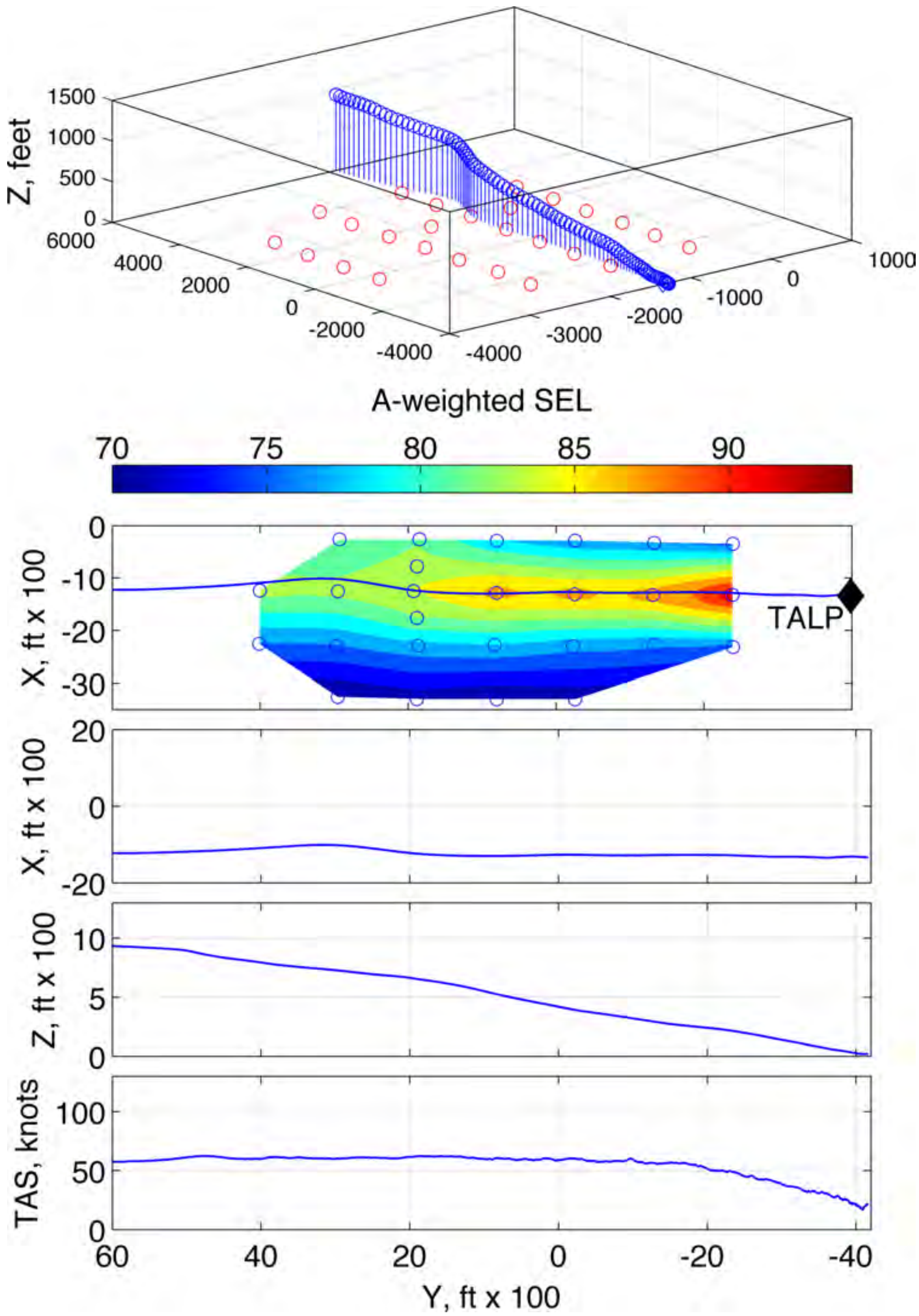

Figure 336: Terminal area condition T1, 60 KIAS constant speed, -6° , run number 288623

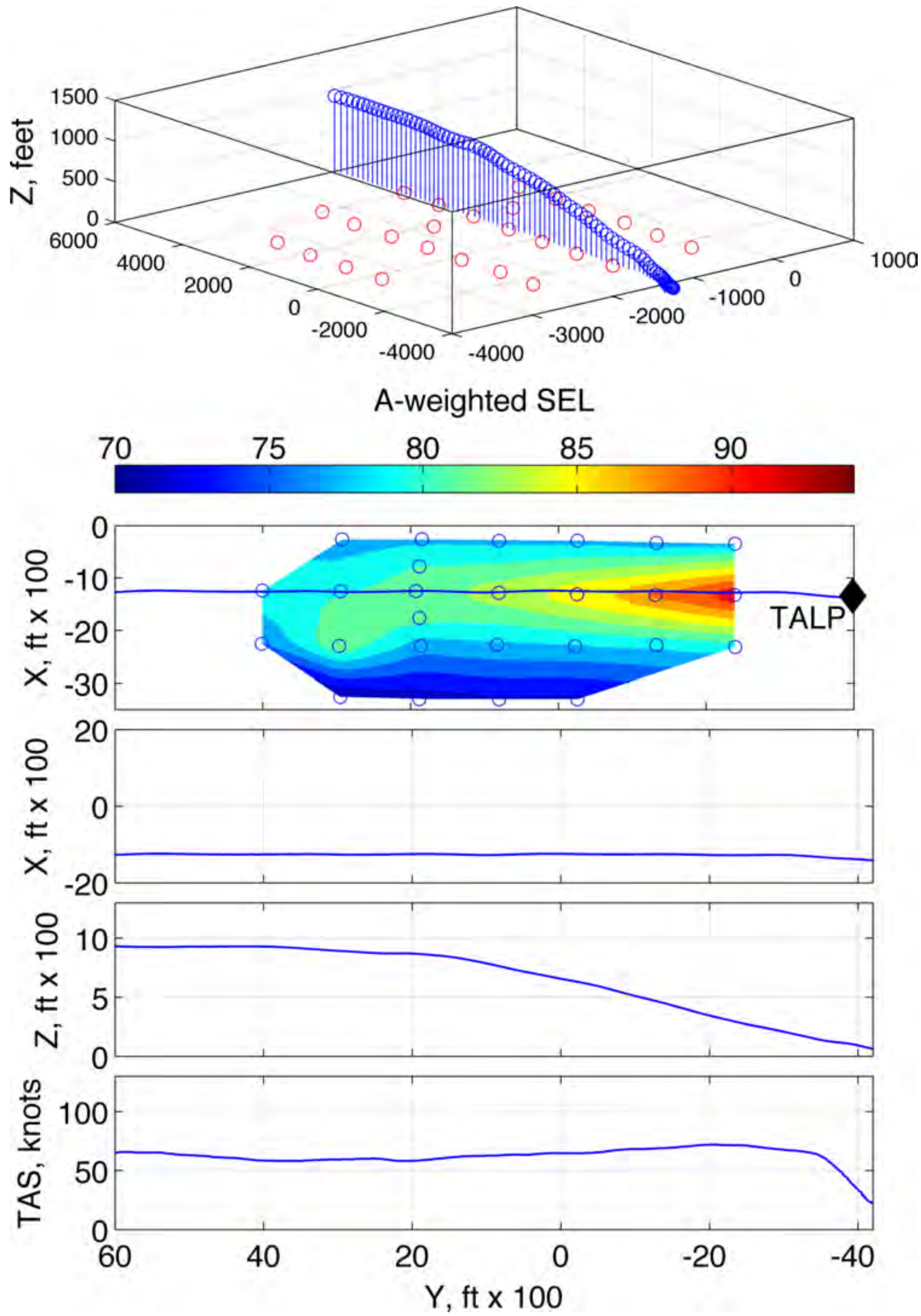

Figure 337: Terminal area condition T2, 60 KIAS constant speed, -9° , run number 288610

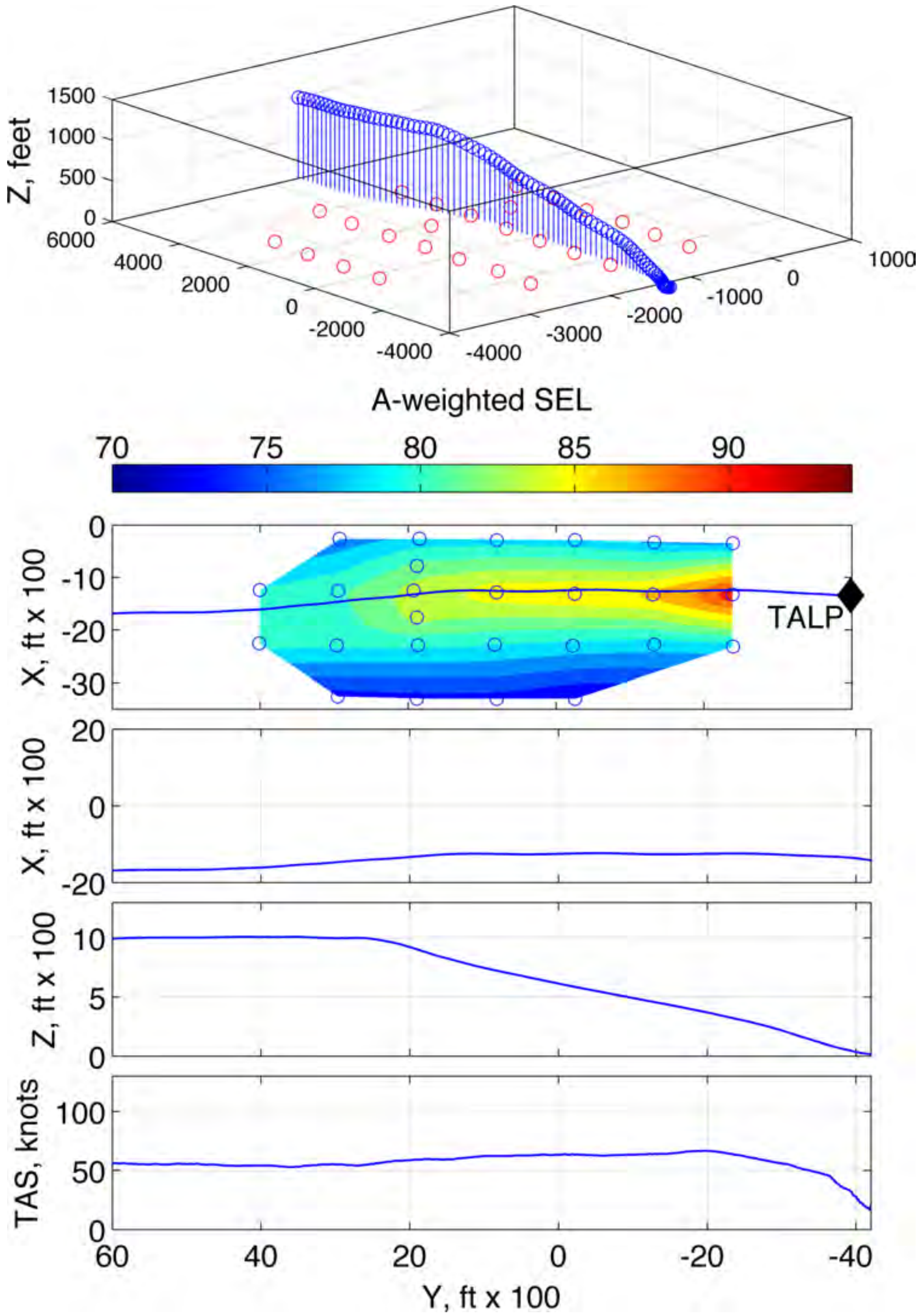

Figure 338: Terminal area condition T2, 60 KIAS constant speed, -9° , run number 288611

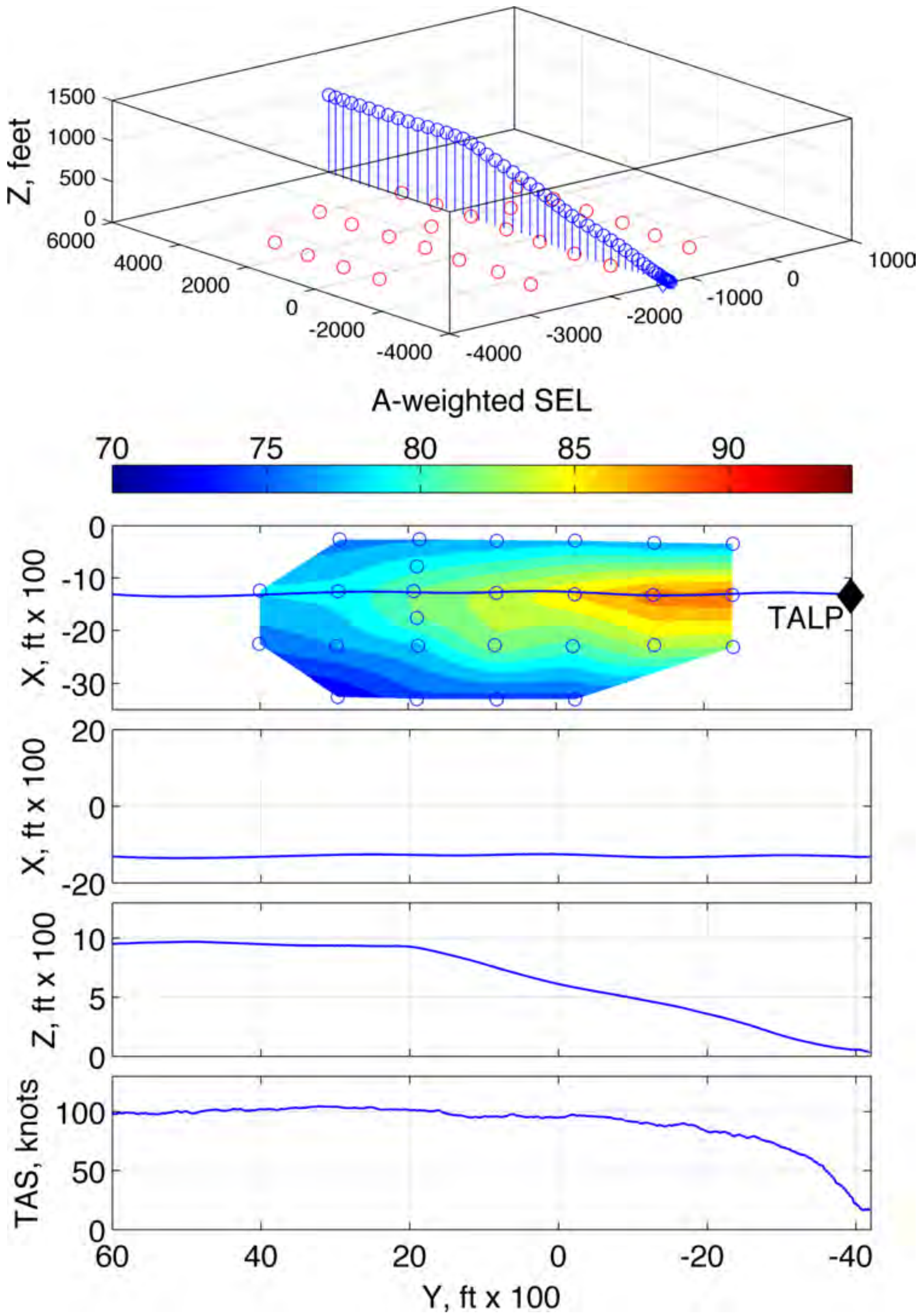

Figure 339: Terminal area condition T2, 60 KIAS constant speed, -9° , run number 288639

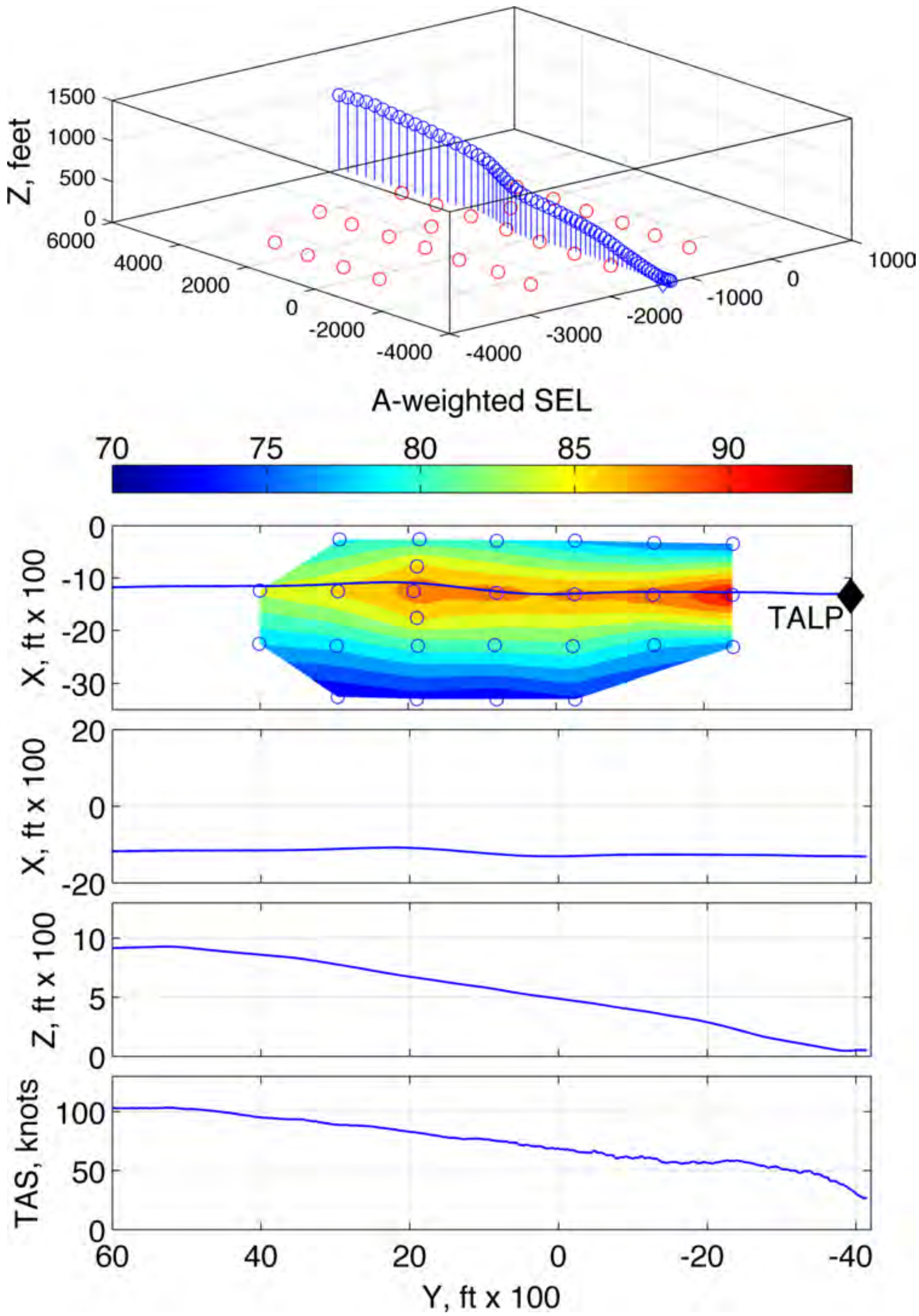

Figure 340: Terminal area condition T3, 100 KIAS decelerating, -6° , run number 288624

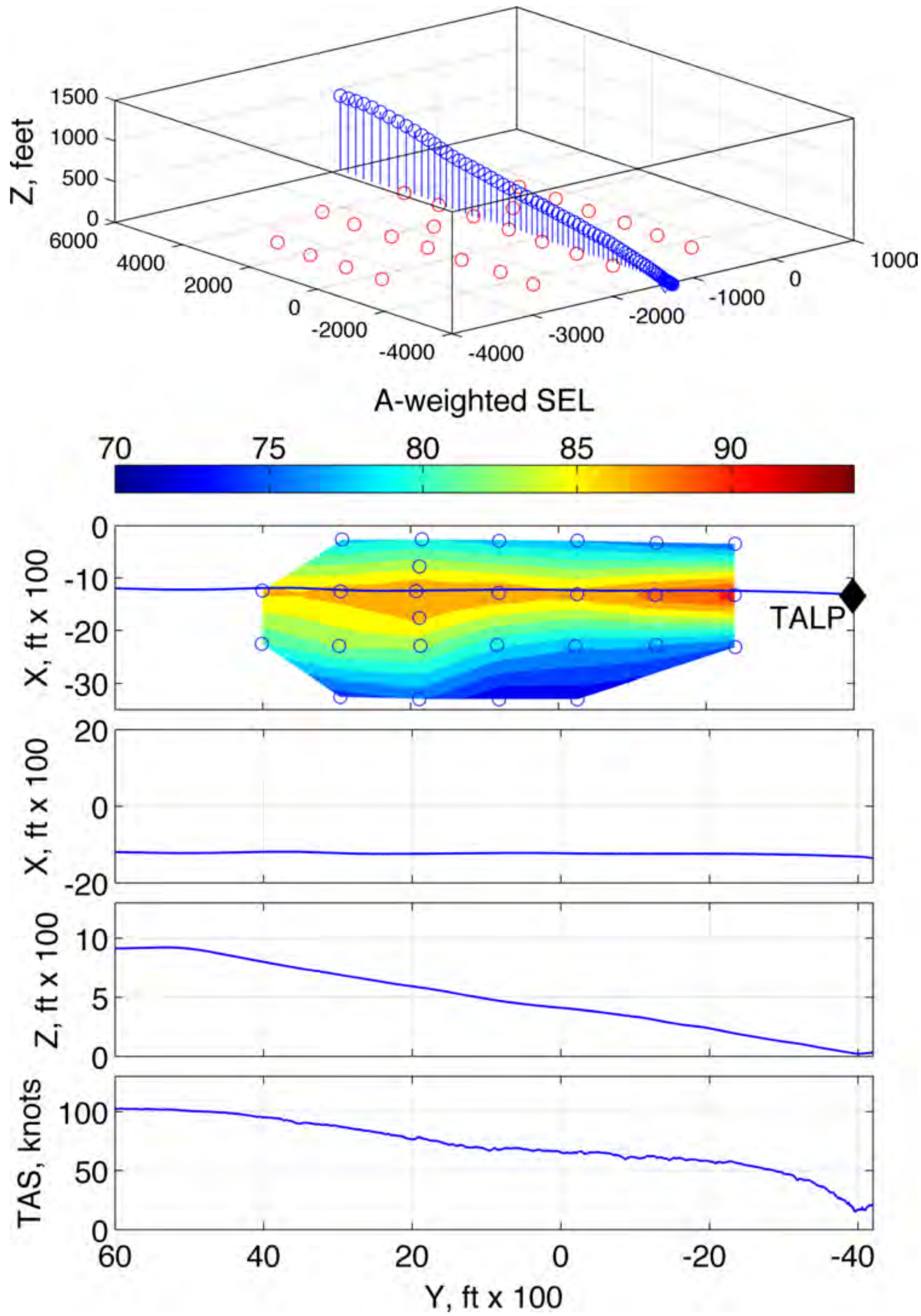

Figure 341: Terminal area condition T3, 100 KIAS decelerating, -6° , run number 288625

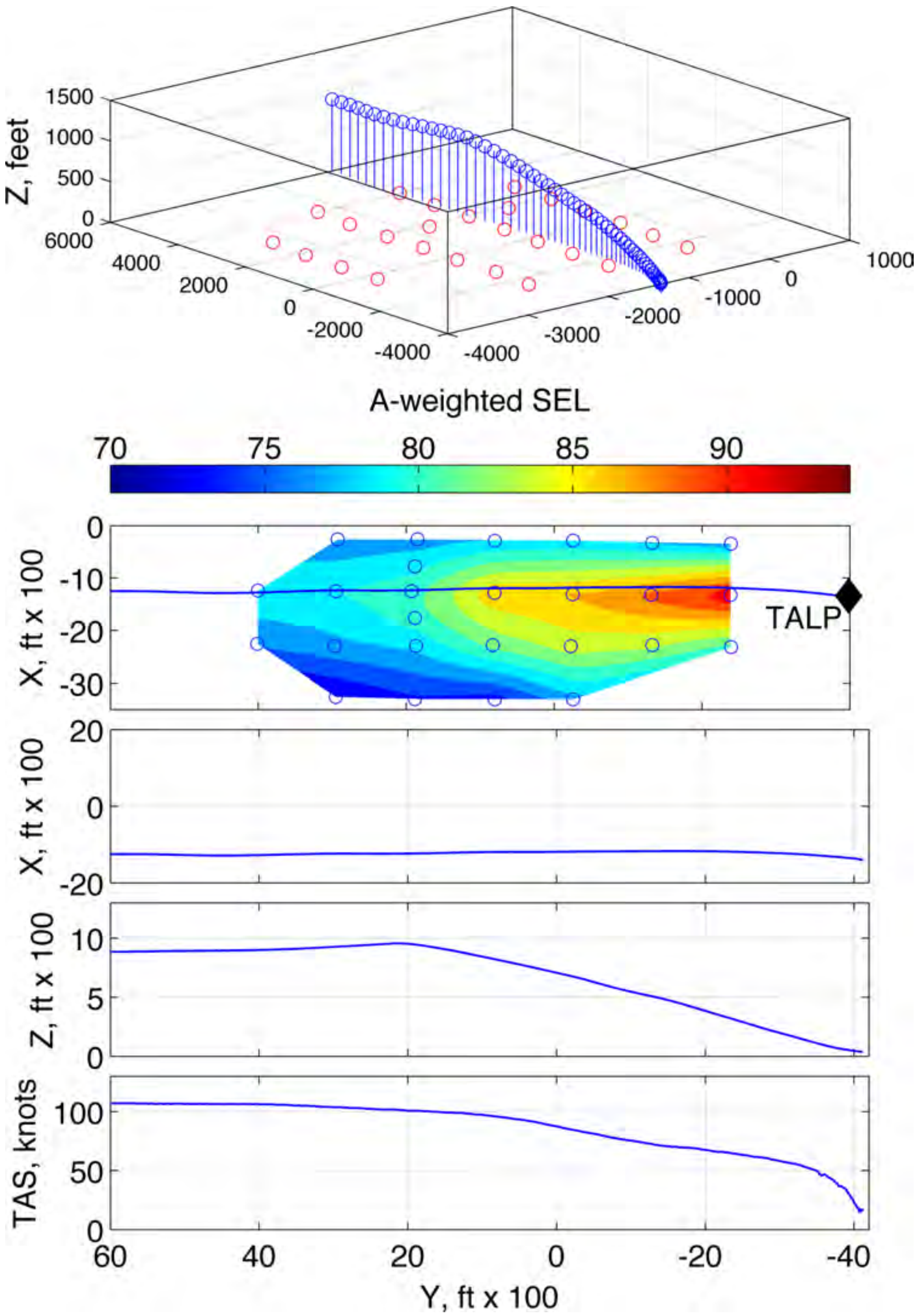

Figure 342: Terminal area condition T4, 100 KIAS decelerating, -9° , run number 288612

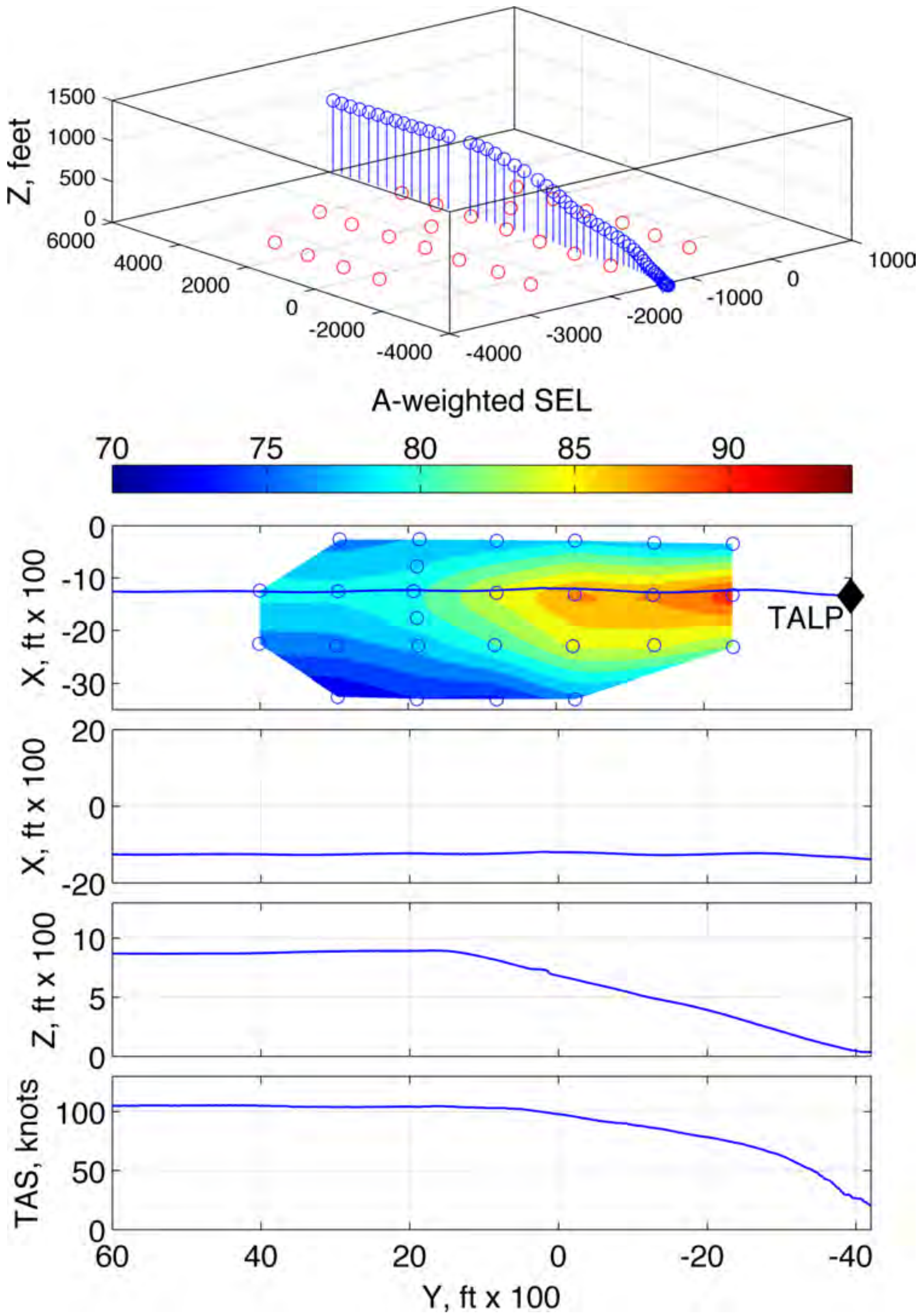

Figure 343: Terminal area condition T4, 100 KIAS decelerating, -9° , run number 288613

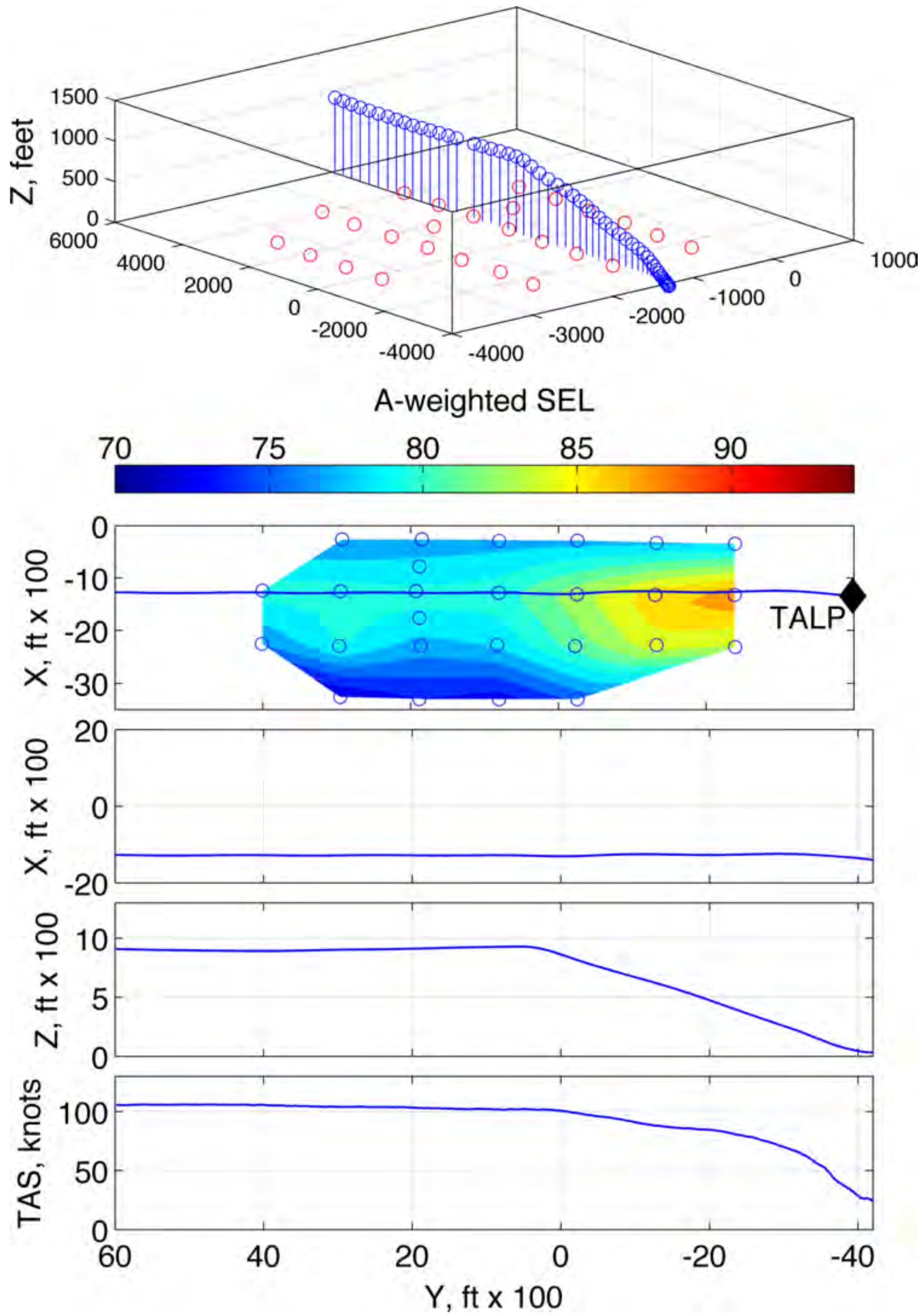

Figure 344: Terminal area condition T5, 100 KIAS decelerating, -12° , run number 288614

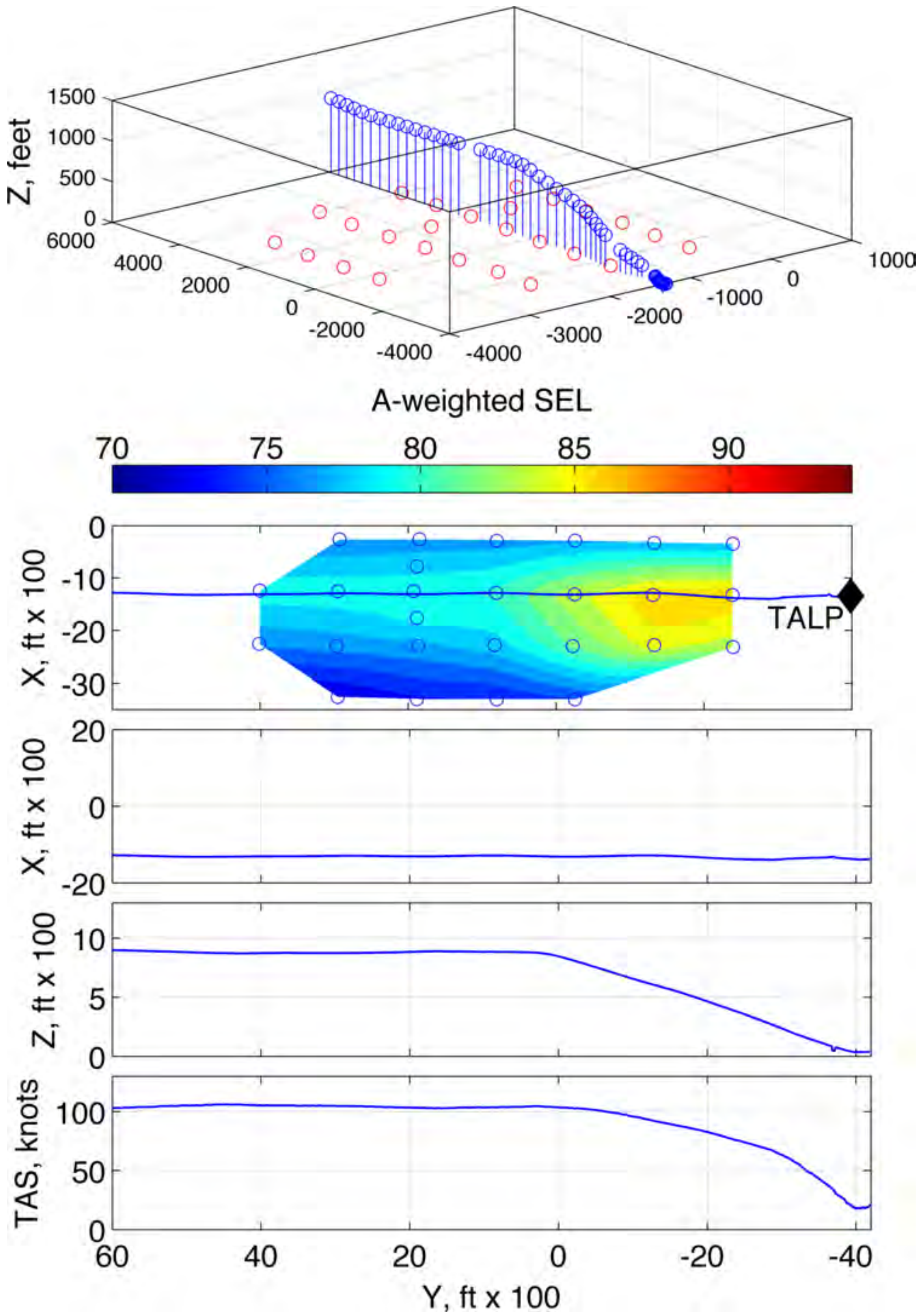

Figure 345: Terminal area condition T5, 100 KIAS decelerating, -12° , run number 288615. Quietest approach profile flown.

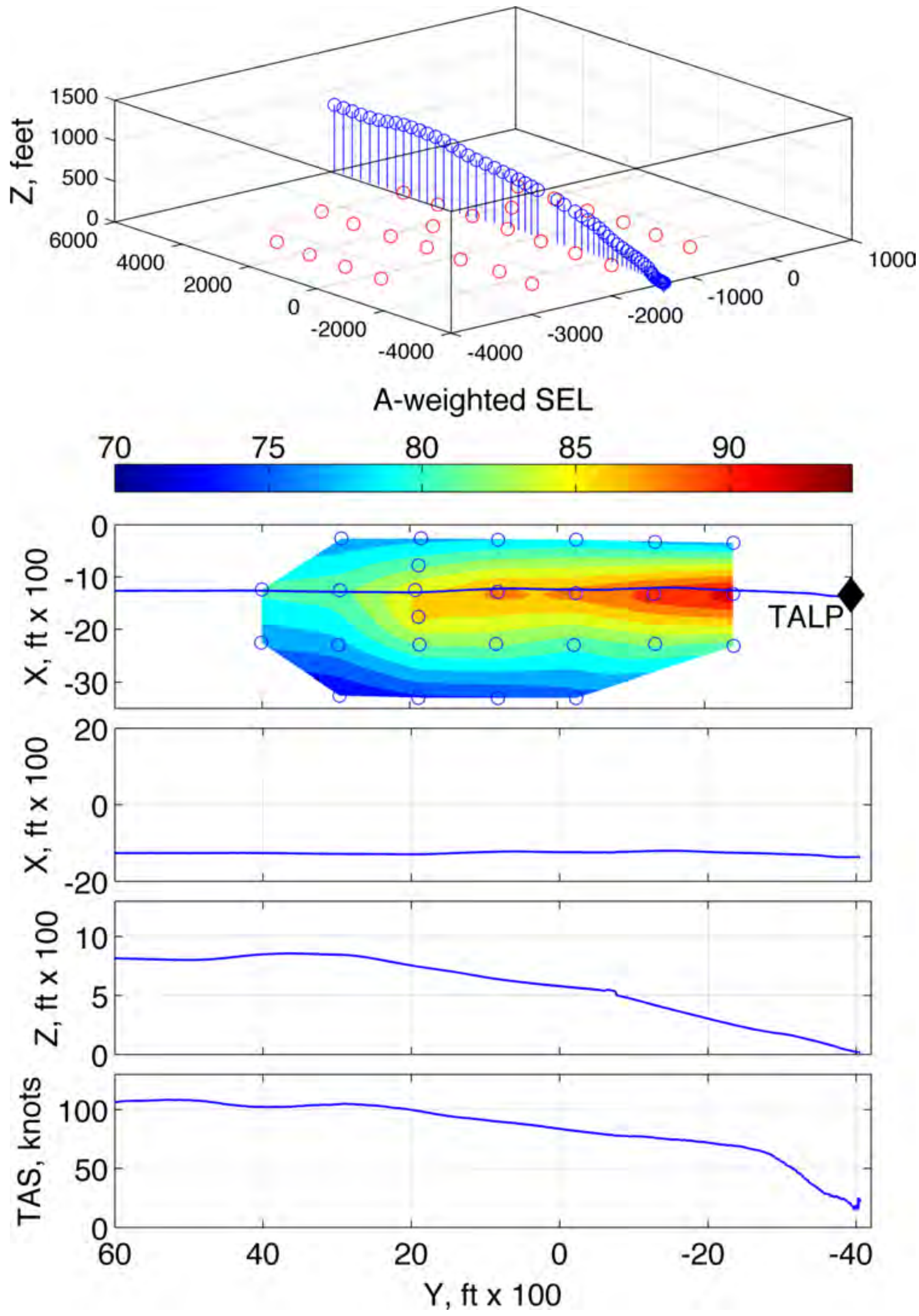

Figure 346: Terminal area condition T6, segmented 100 - 40 KIAS, -6° , 40 - 0 KIAS, -12° , run number 288616

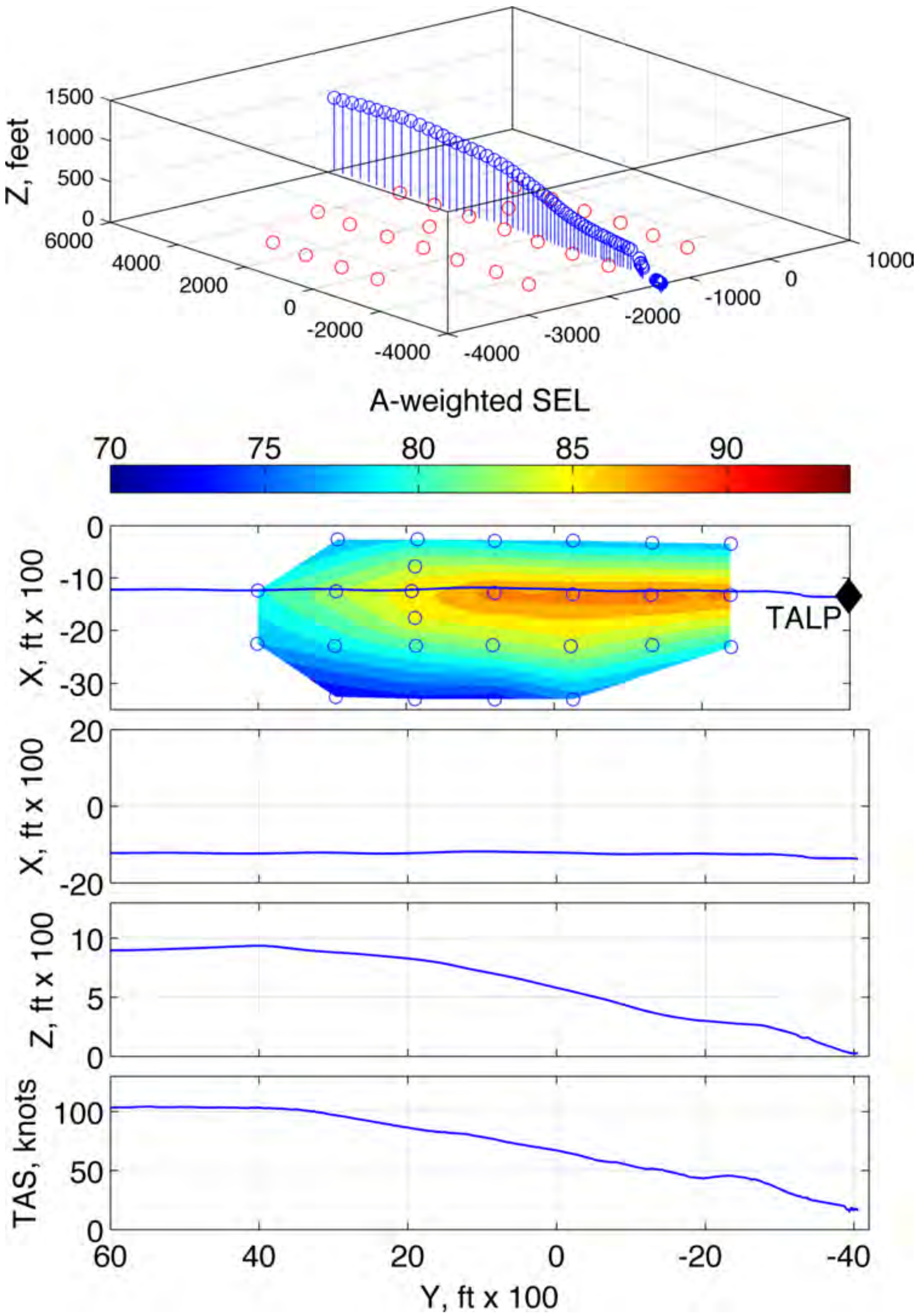

Figure 347: Terminal area condition T6, segmented 100 - 40 KIAS, -6° , 40 - 0 KIAS, -12° , run number 288617

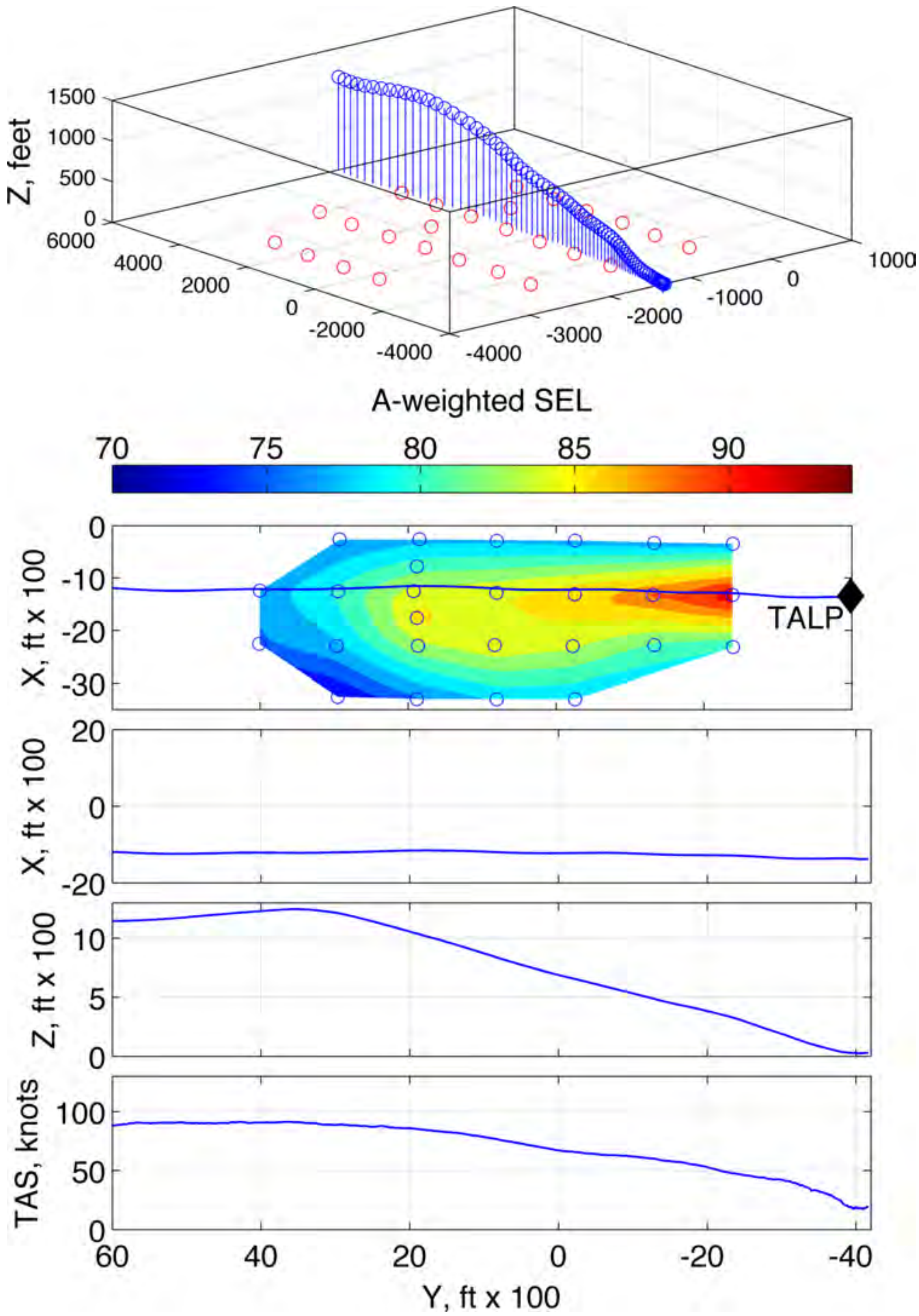

Figure 348: Terminal area condition T7, segmented 100 - 90 KIAS, 3° , 90 - 0 KIAS, -9.5° , run number 288618

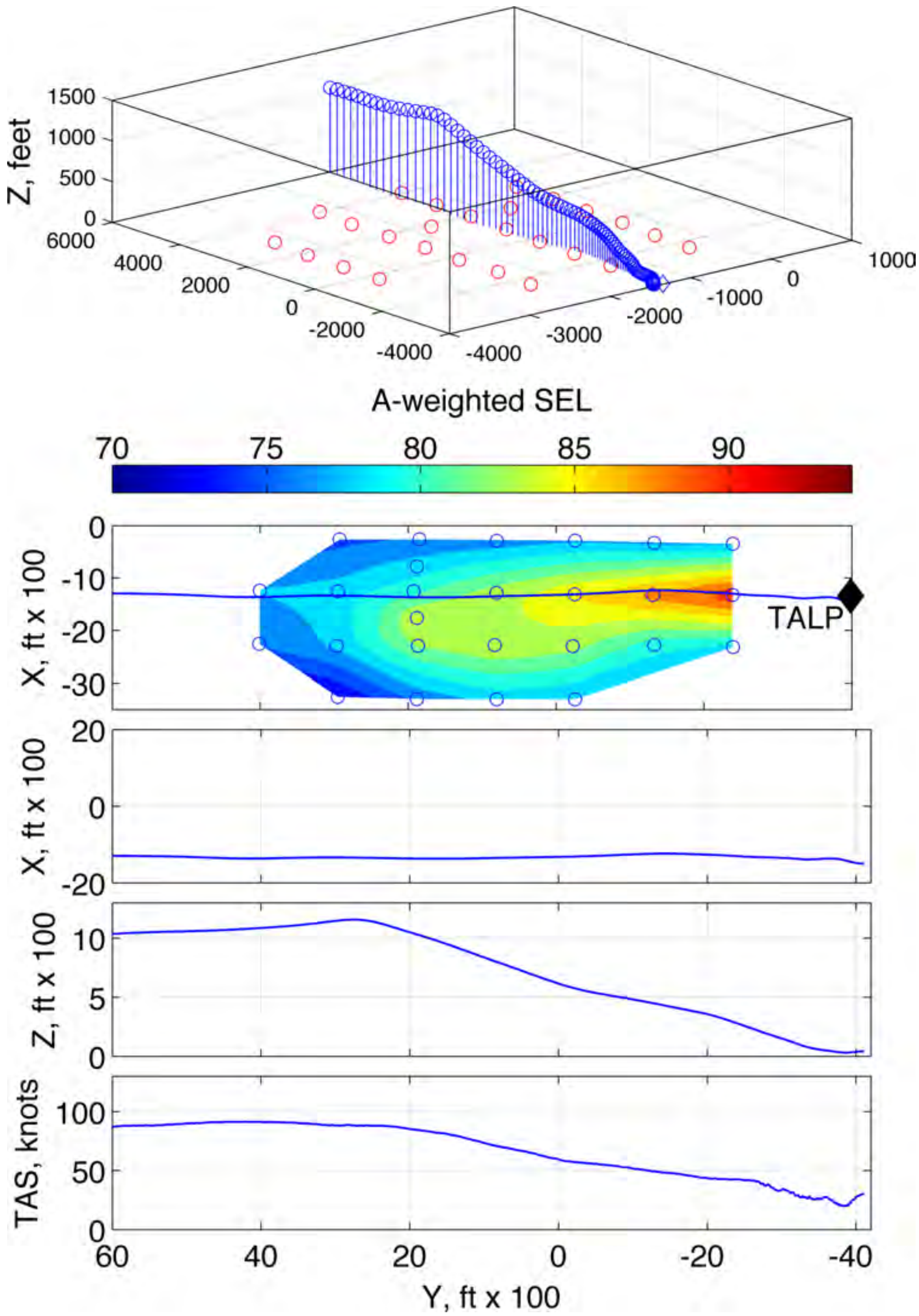

Figure 349: Terminal area condition T7, segmented 100 - 90 KIAS, 3° , 90 - 0 KIAS, -9.5° , run number 288619

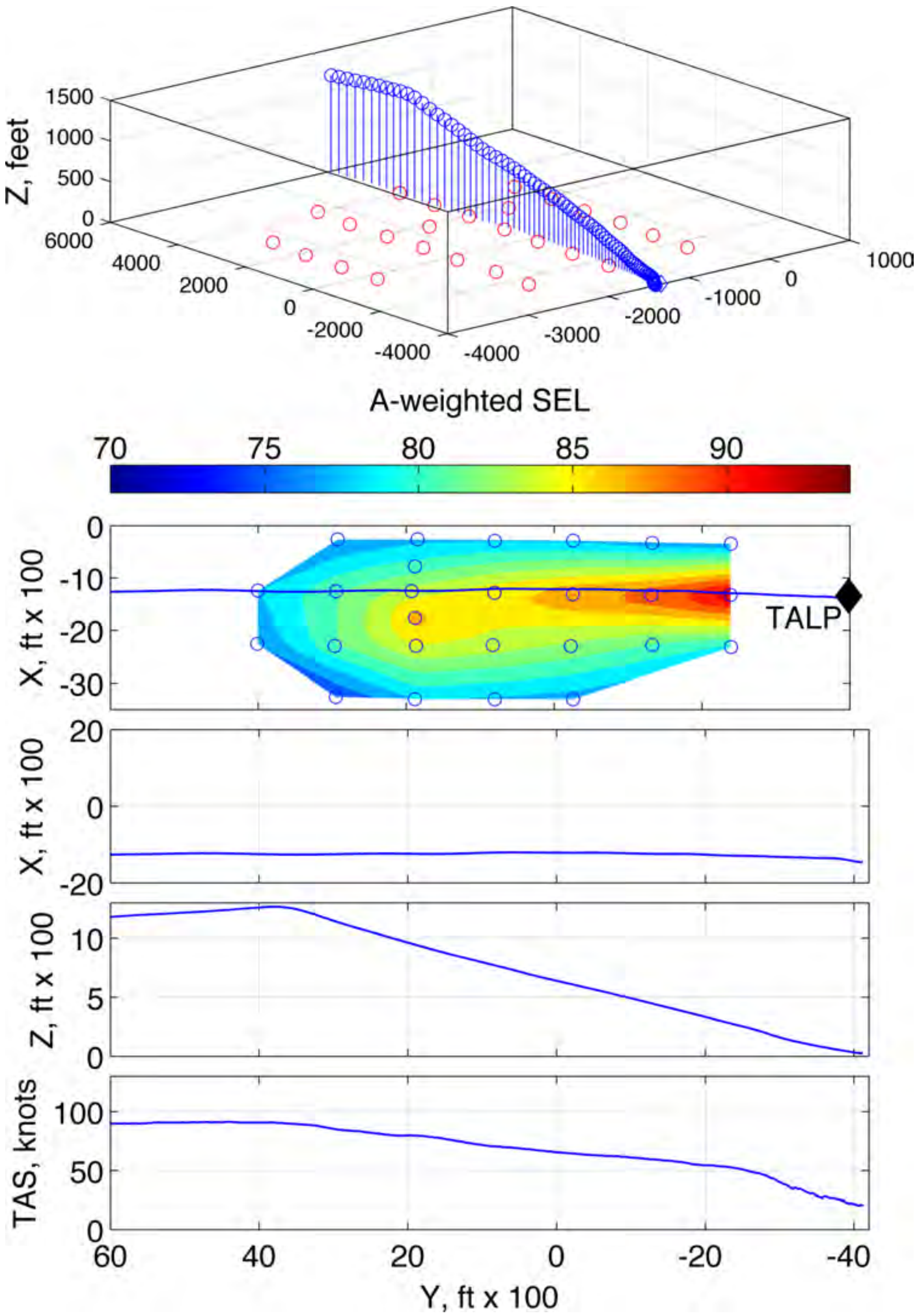

Figure 350: Terminal area condition T7, segmented 100 - 90 KIAS, 3° , 90 - 0 KIAS, -9.5° , run number 288620

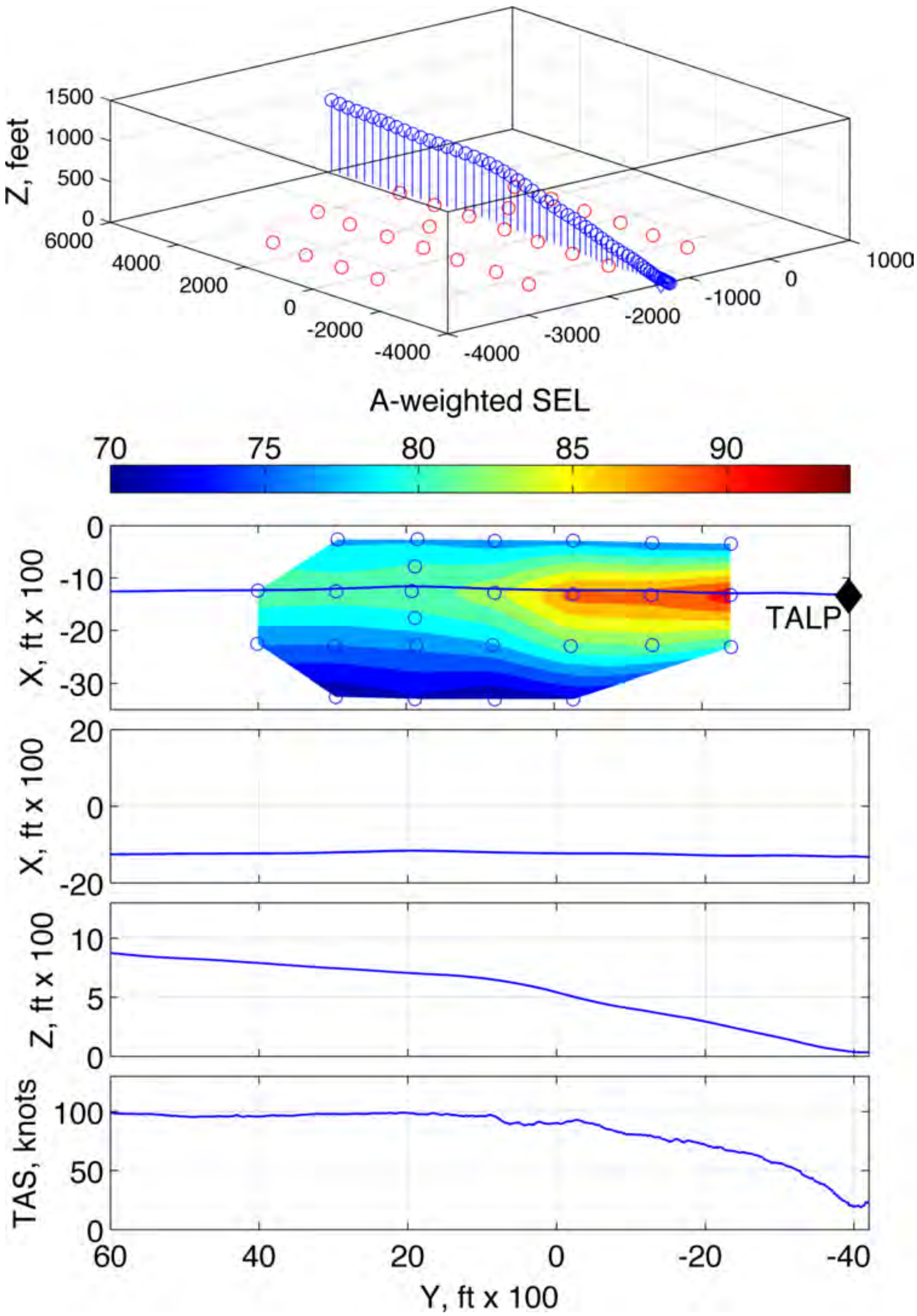

Figure 351: Terminal area condition T8, segmented 100 - 95 KIAS, -3° , 95 - 0 KIAS, -7.5° , run number 288626

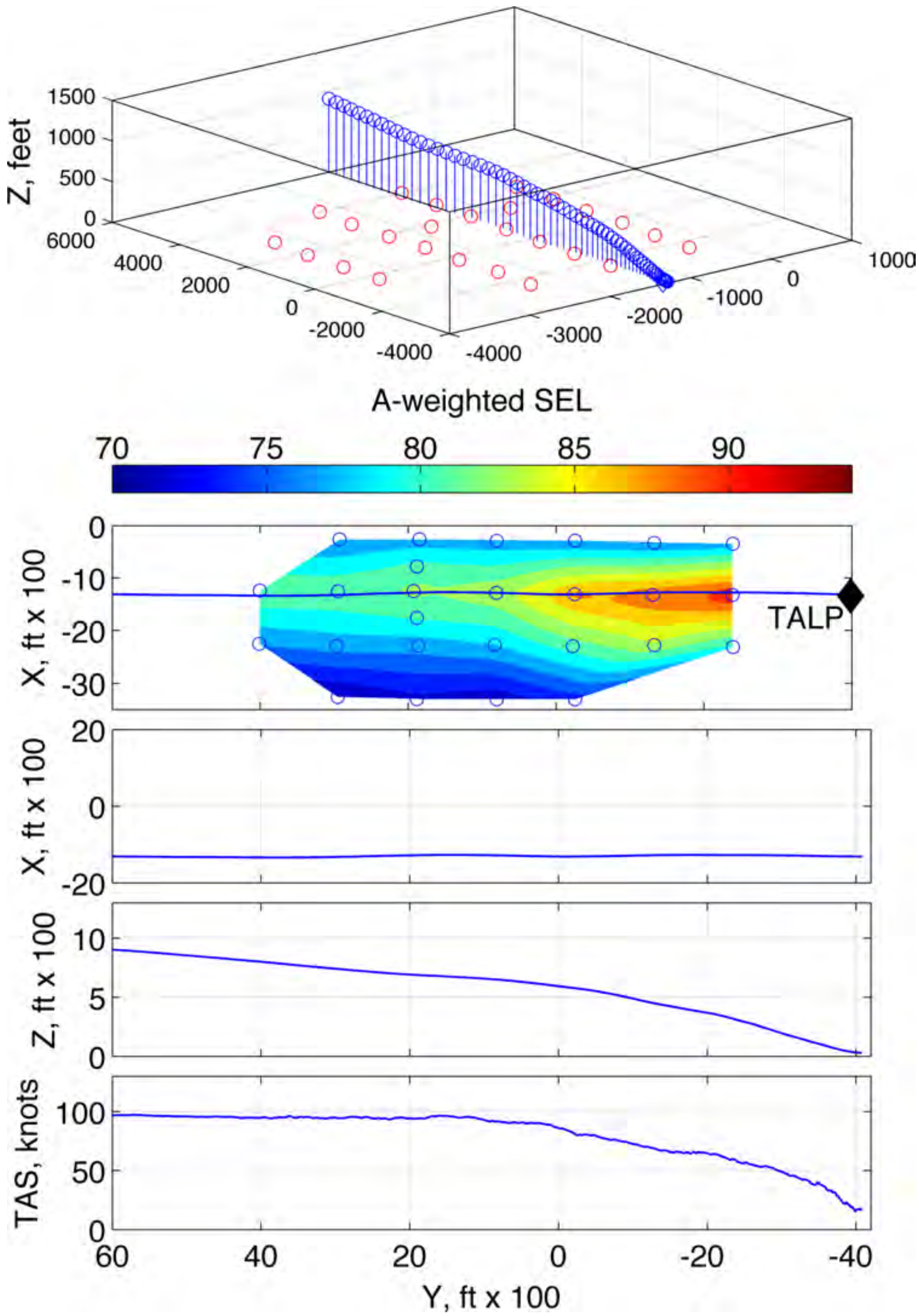

Figure 352: Terminal area condition T8, segmented 100 - 95 KIAS, -3° , 95 - 0 KIAS, -7.5° , run number 288627

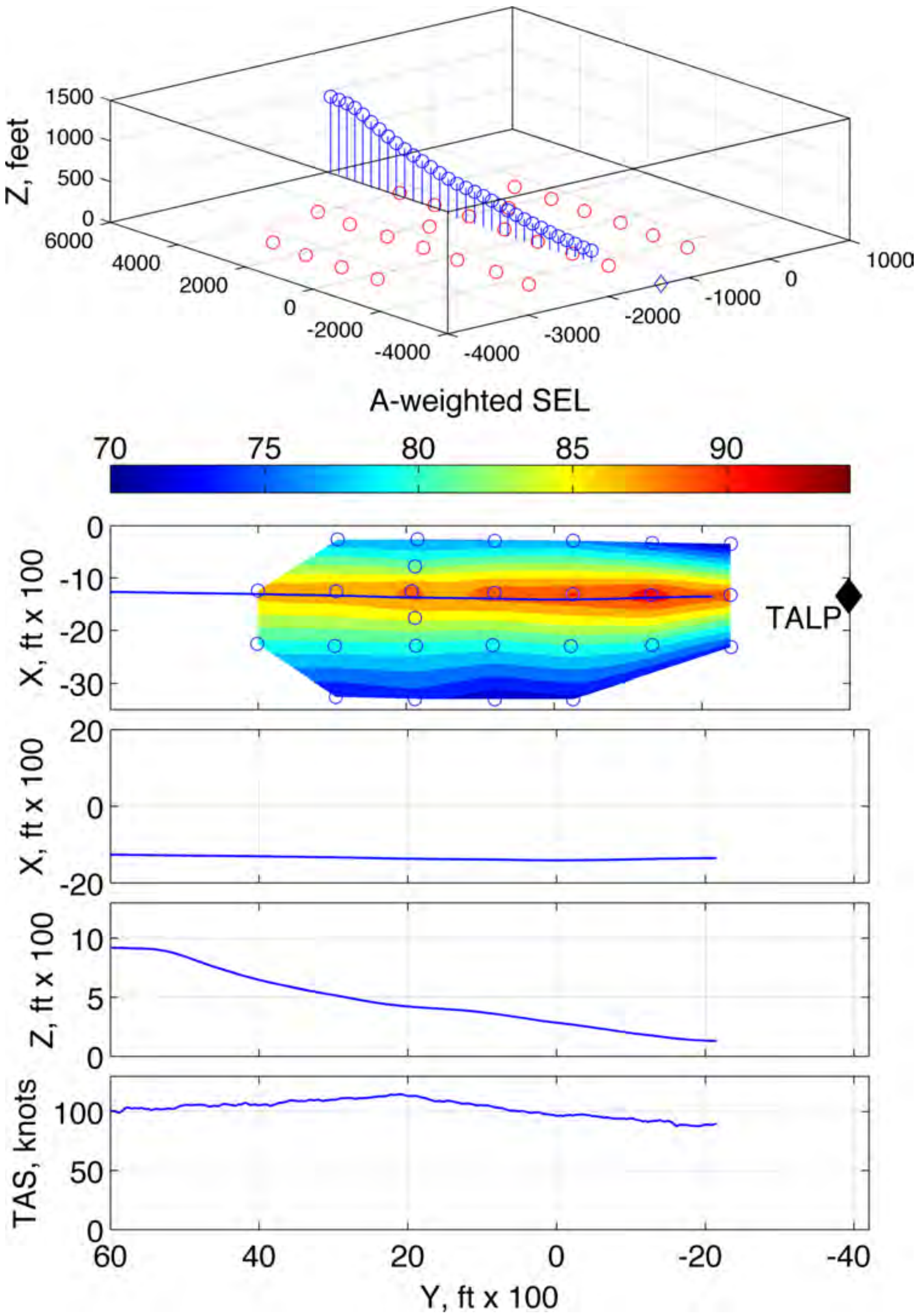

Figure 353: Terminal area condition T9, segmented 100 - 110 KIAS, -9° , 110 - 90 KIAS, -7.5° , 90 - 0 KIAS, -4° , run number 288629

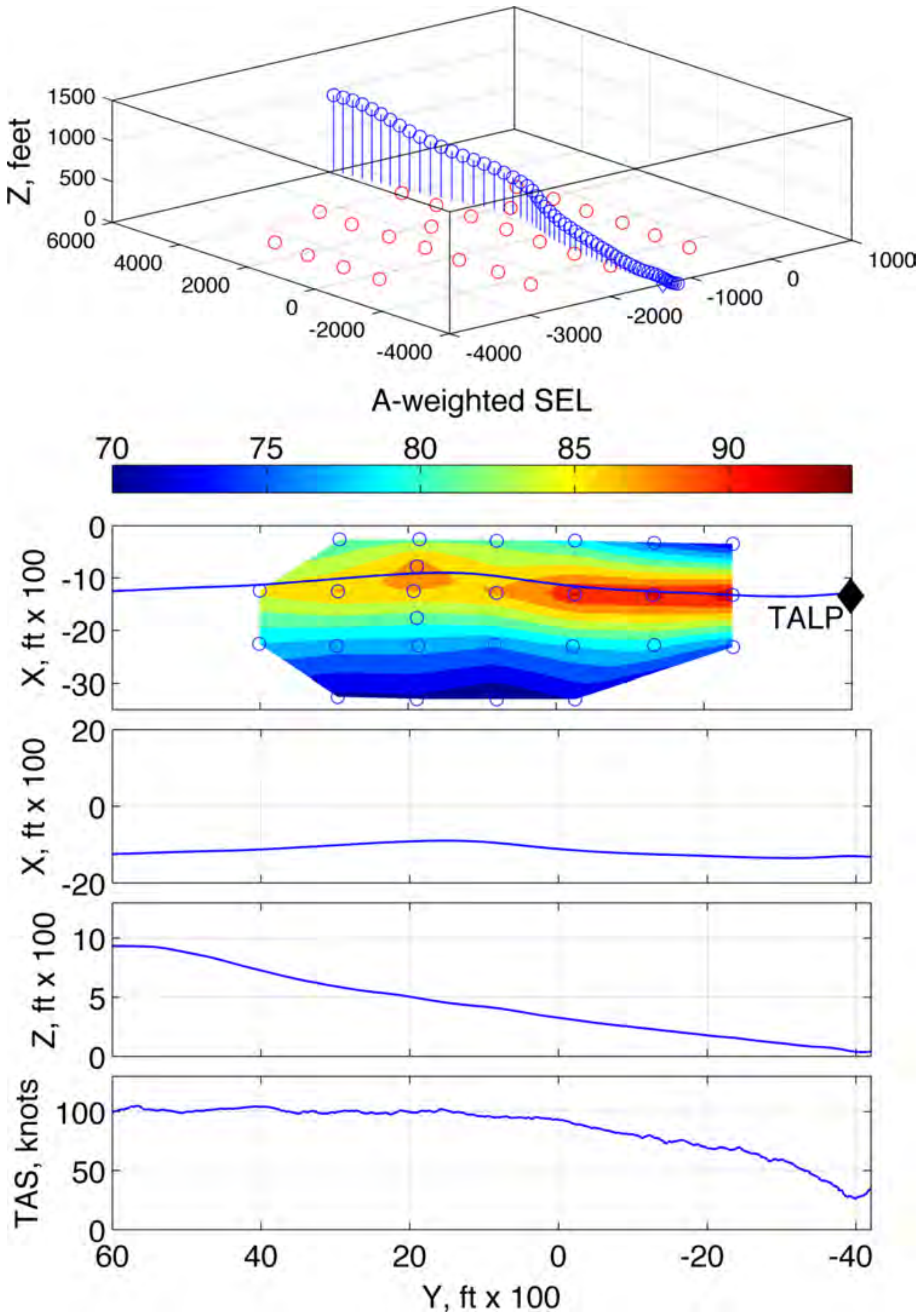

Figure 354: Terminal area condition T9, segmented 100 - 110 KIAS, -9° , 110 - 90 KIAS, -7.5° , 90 - 0 KIAS, -4° , run number 288630

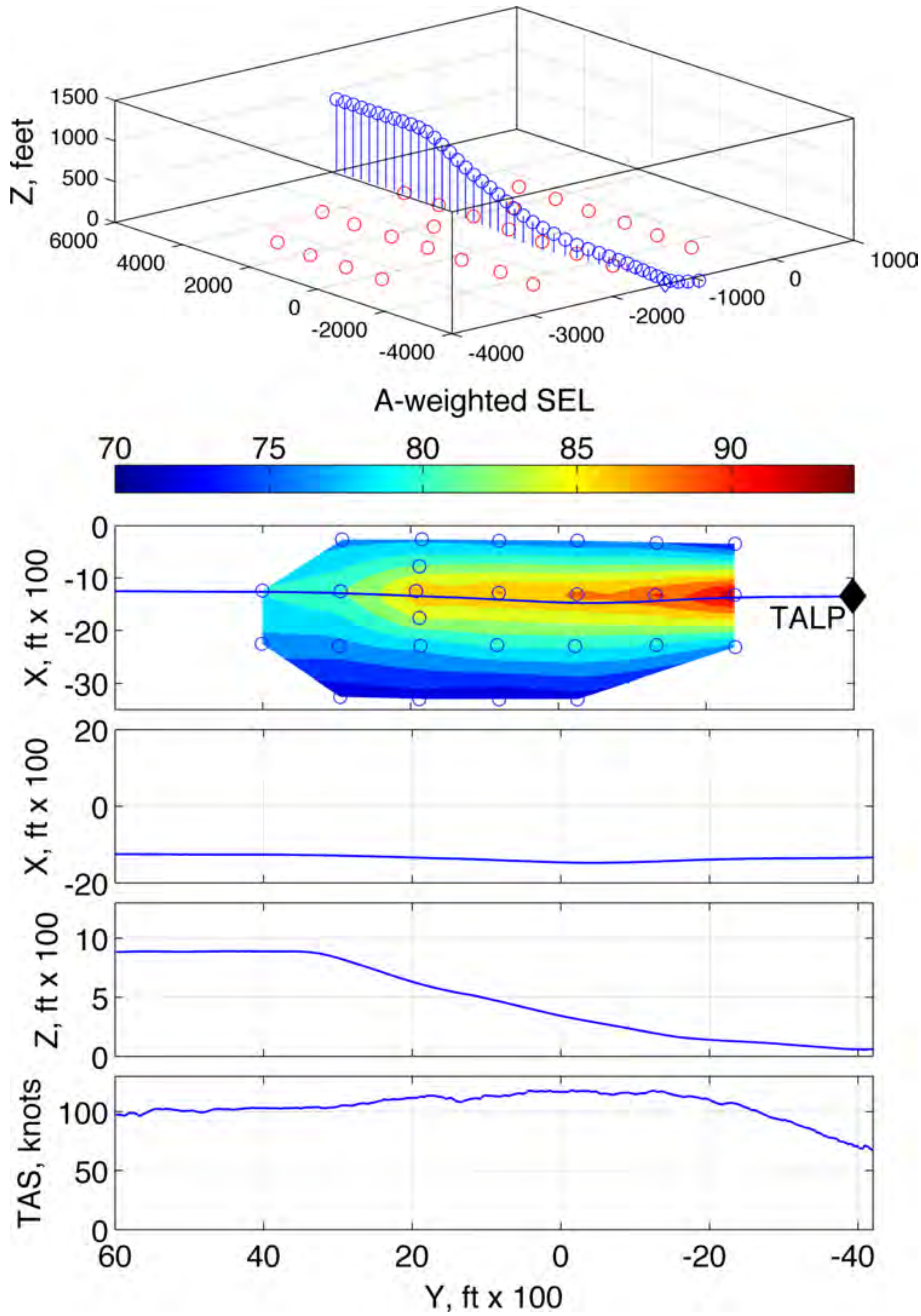

Figure 355: Terminal area condition T9A, segmented 100 - 110 KIAS, -9° , 110 - 90 KIAS, -7.5° , 90 - 0 KIAS, -4° , run number 288631

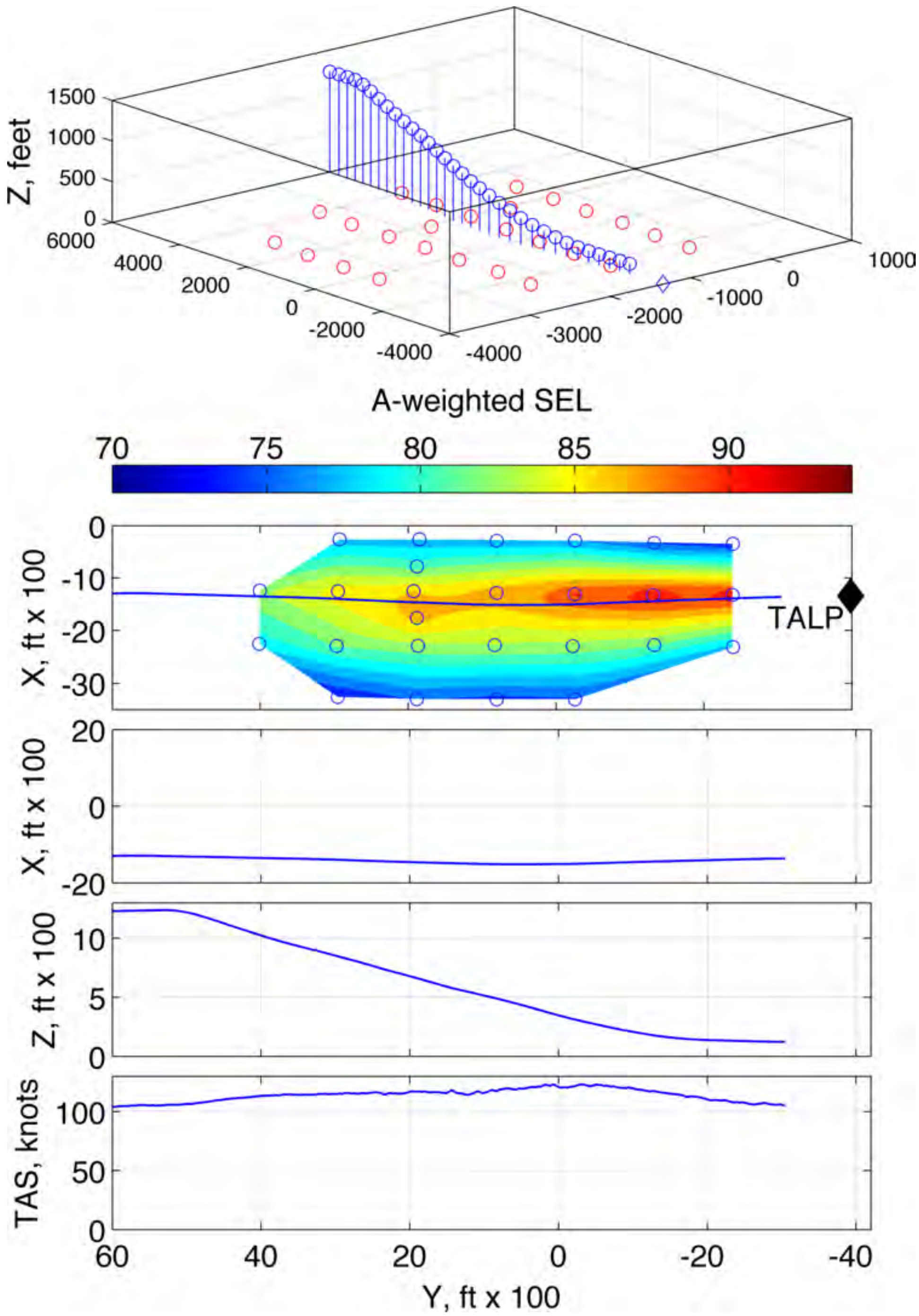

Figure 356: Terminal area condition T9A, segmented 100 - 110 KIAS, -9° , 110 - 90 KIAS, -7.5° , 90 - 0 KIAS, -4° , run number 288632

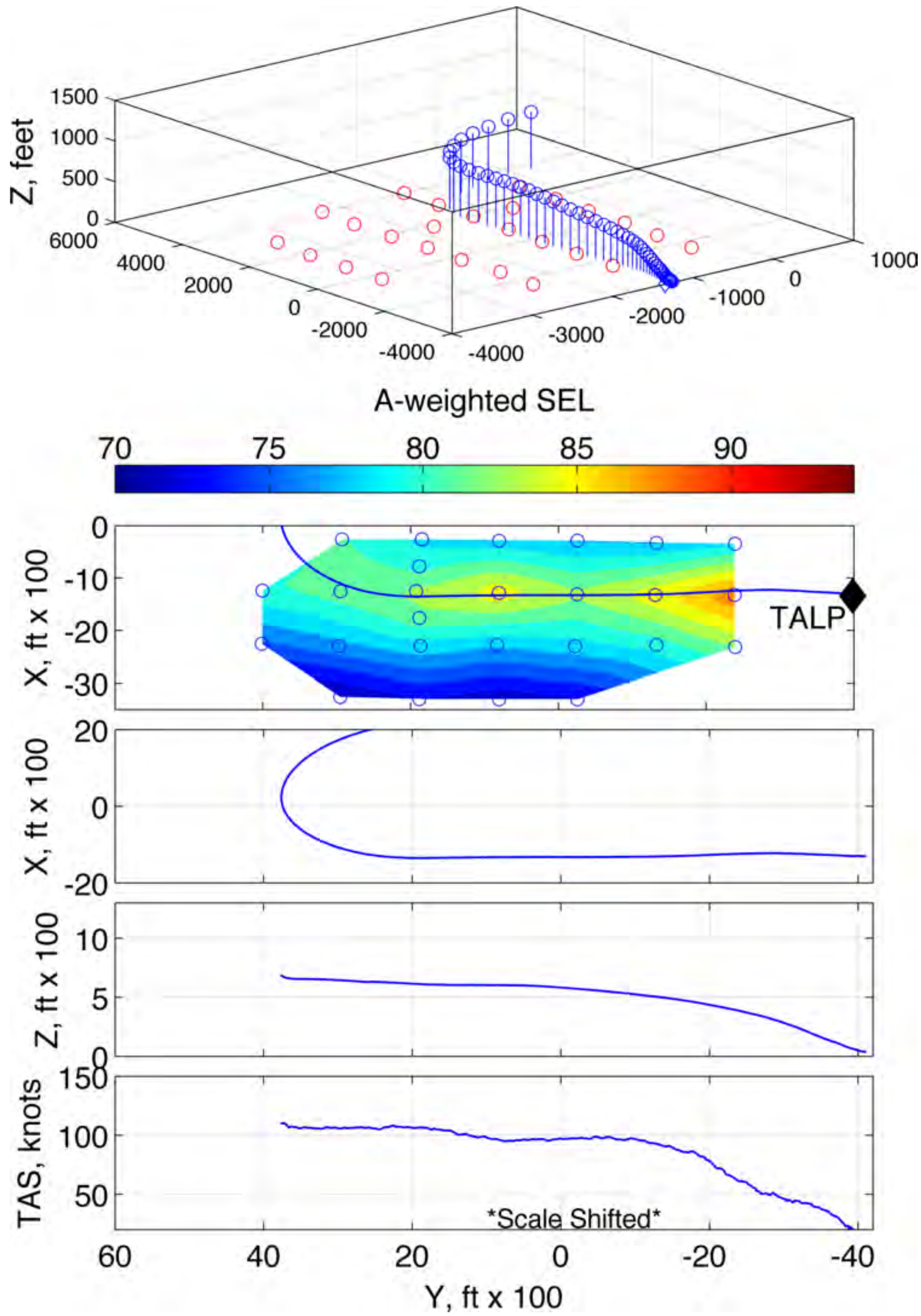

Figure 357: Terminal area condition T10A, U shaped, 100 KIAS, -9° , run number 288638

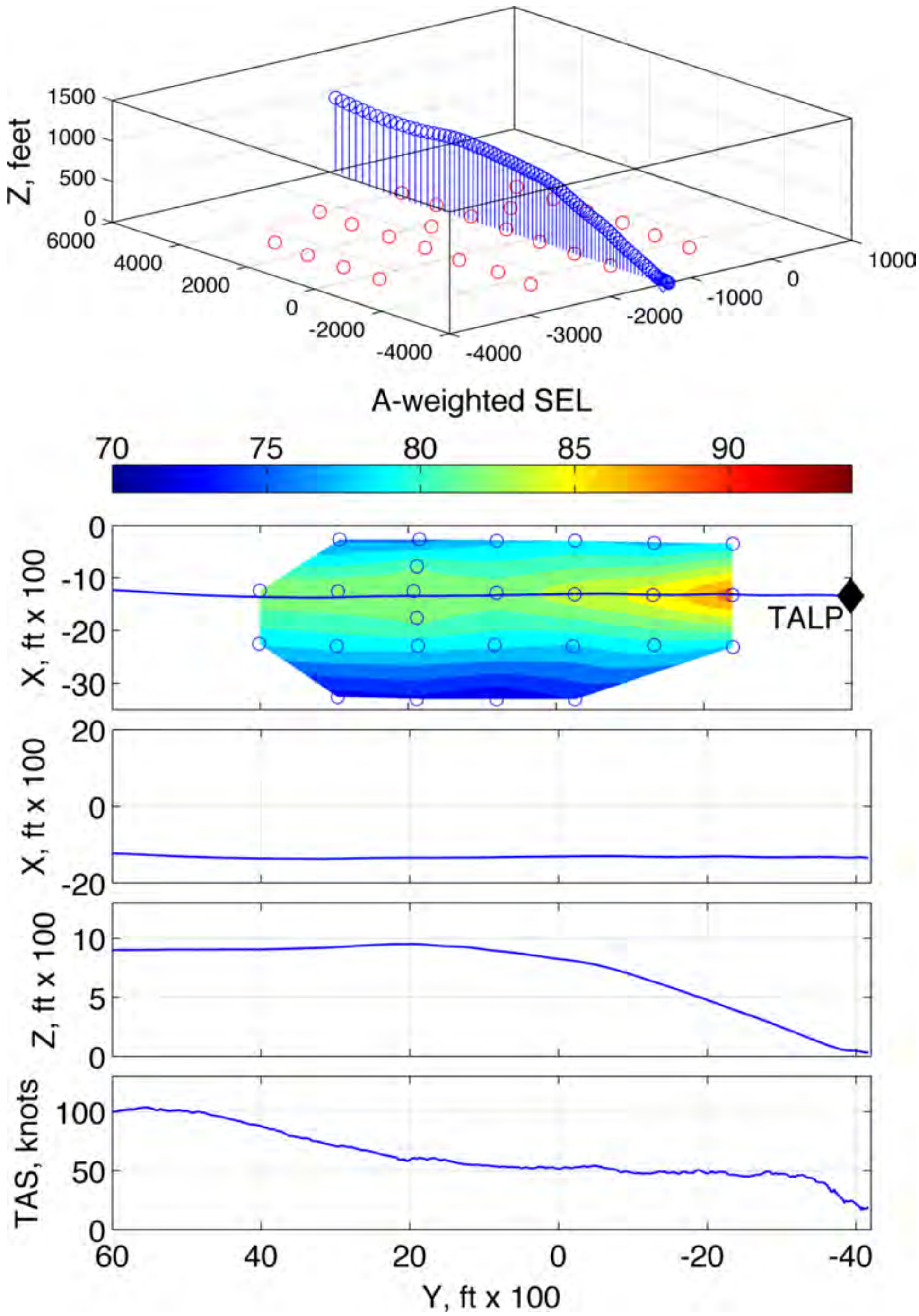

Figure 358: Terminal area condition T11, pilot discretion, run number 288633

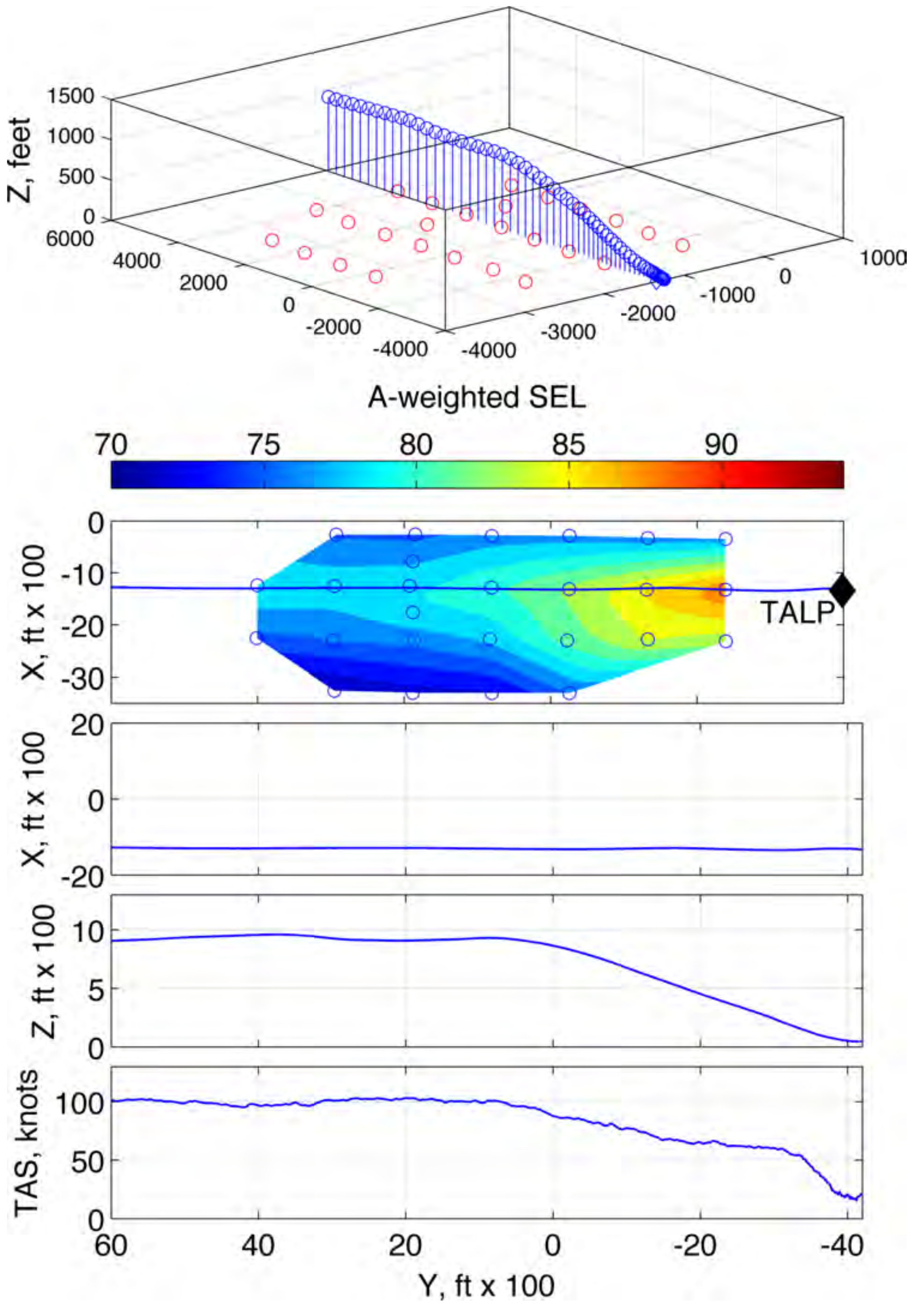

Figure 359: Terminal area condition T11, pilot discretion, run number 288634

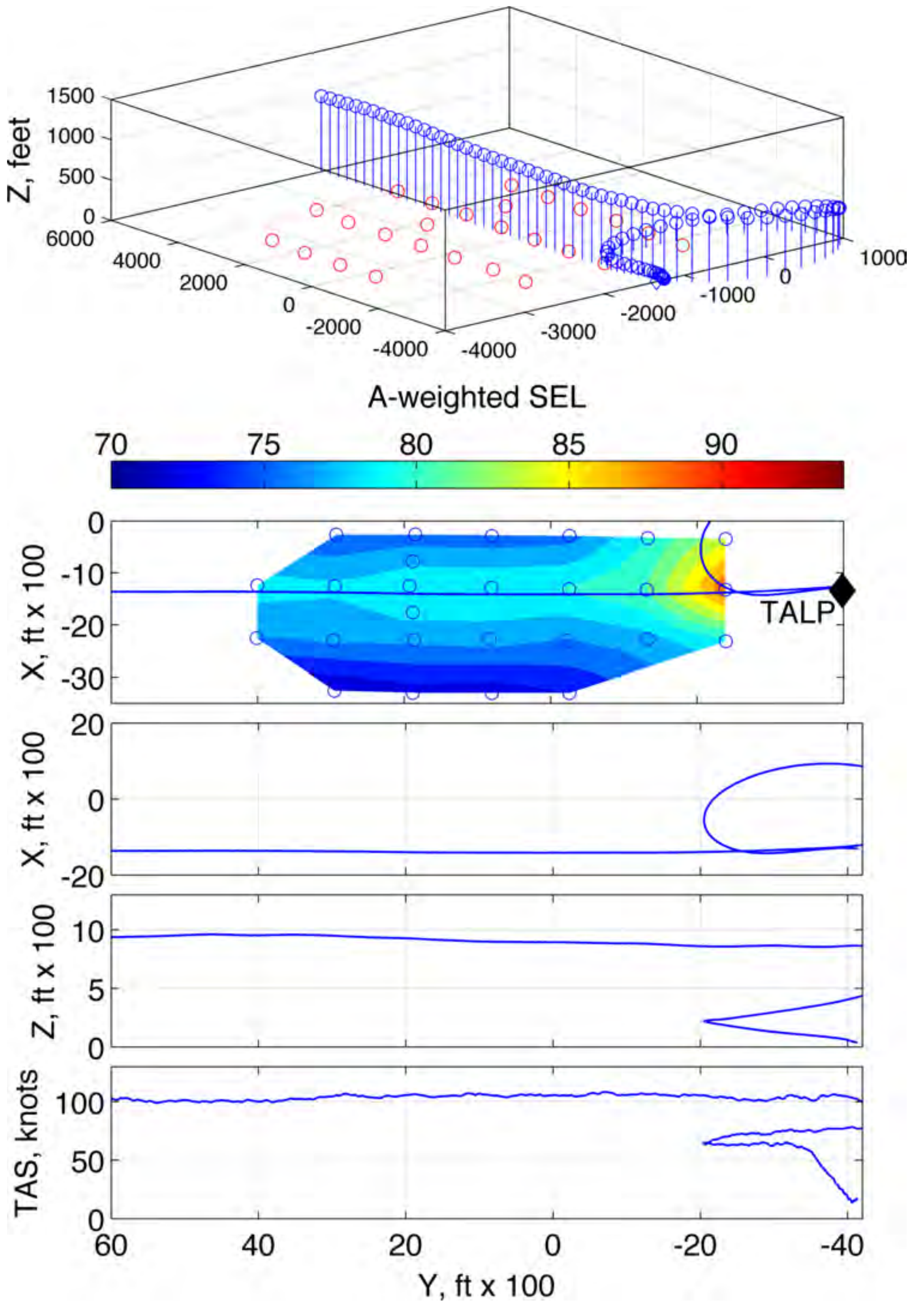

Figure 360: Terminal area condition T11A, pilot discretion, run number 288635

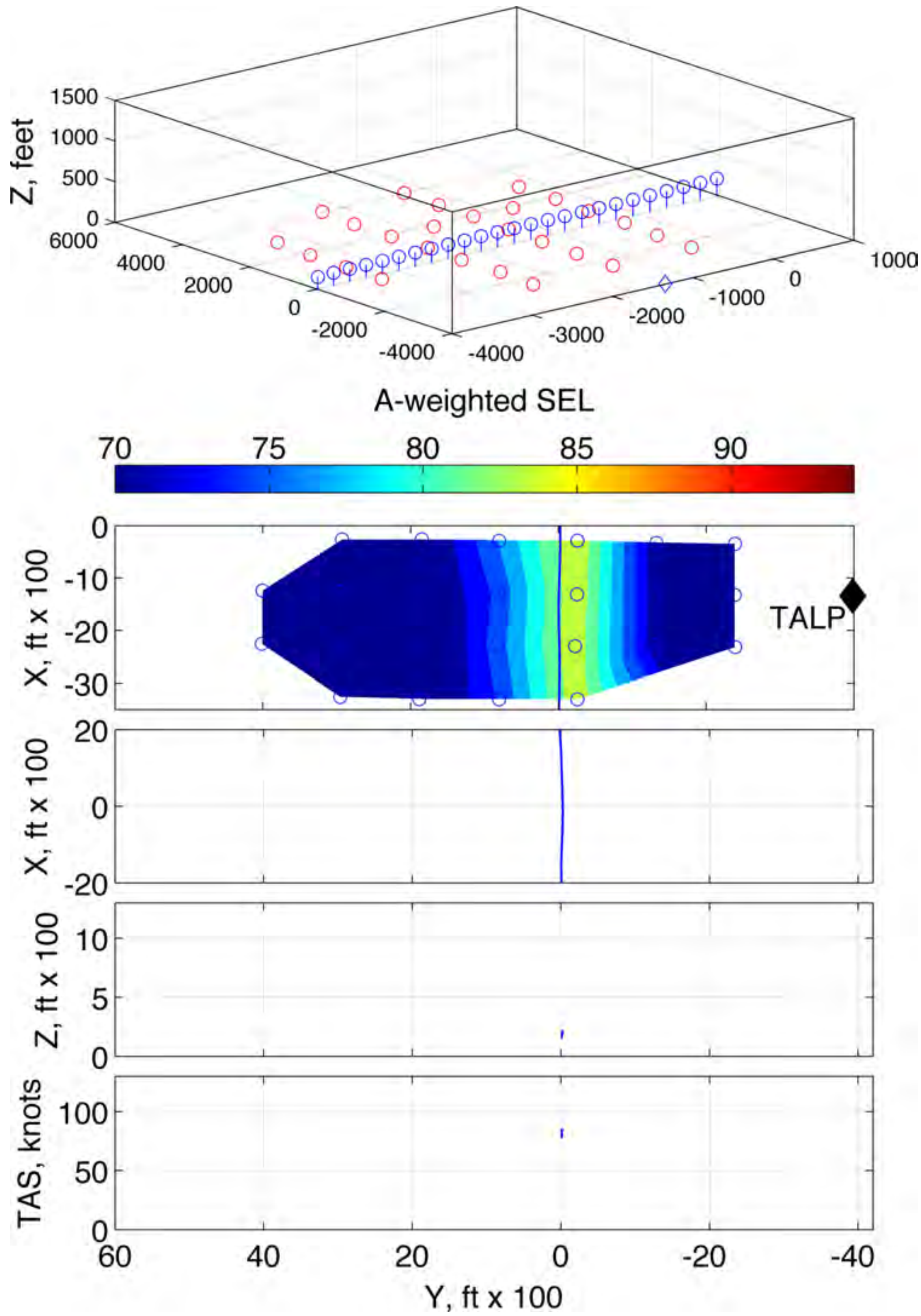

Figure 361: Terminal area condition L1, 80 KIAS, level, run number 288601

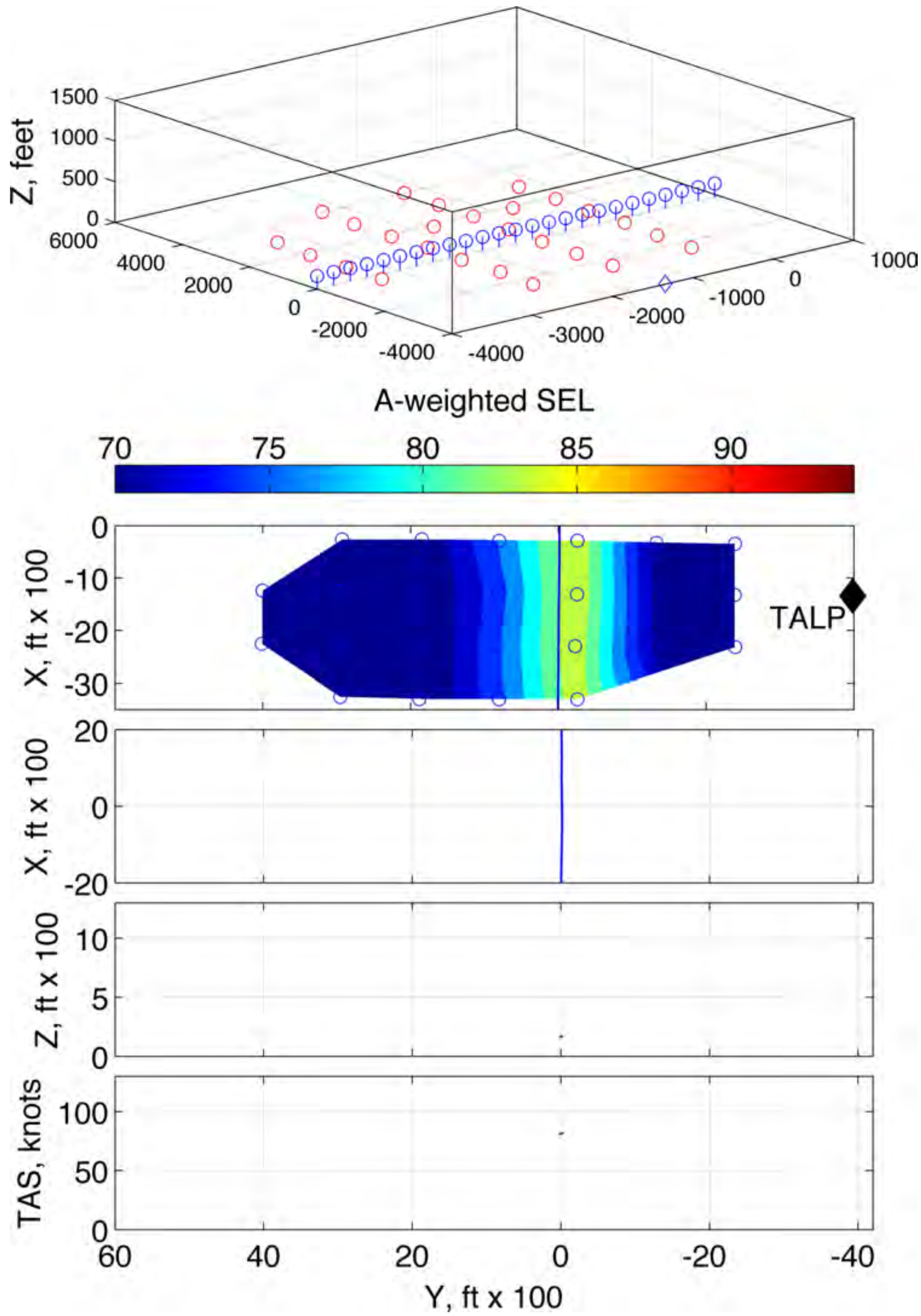

Figure 362: Terminal area condition L1, 80 KIAS, level, run number 288602

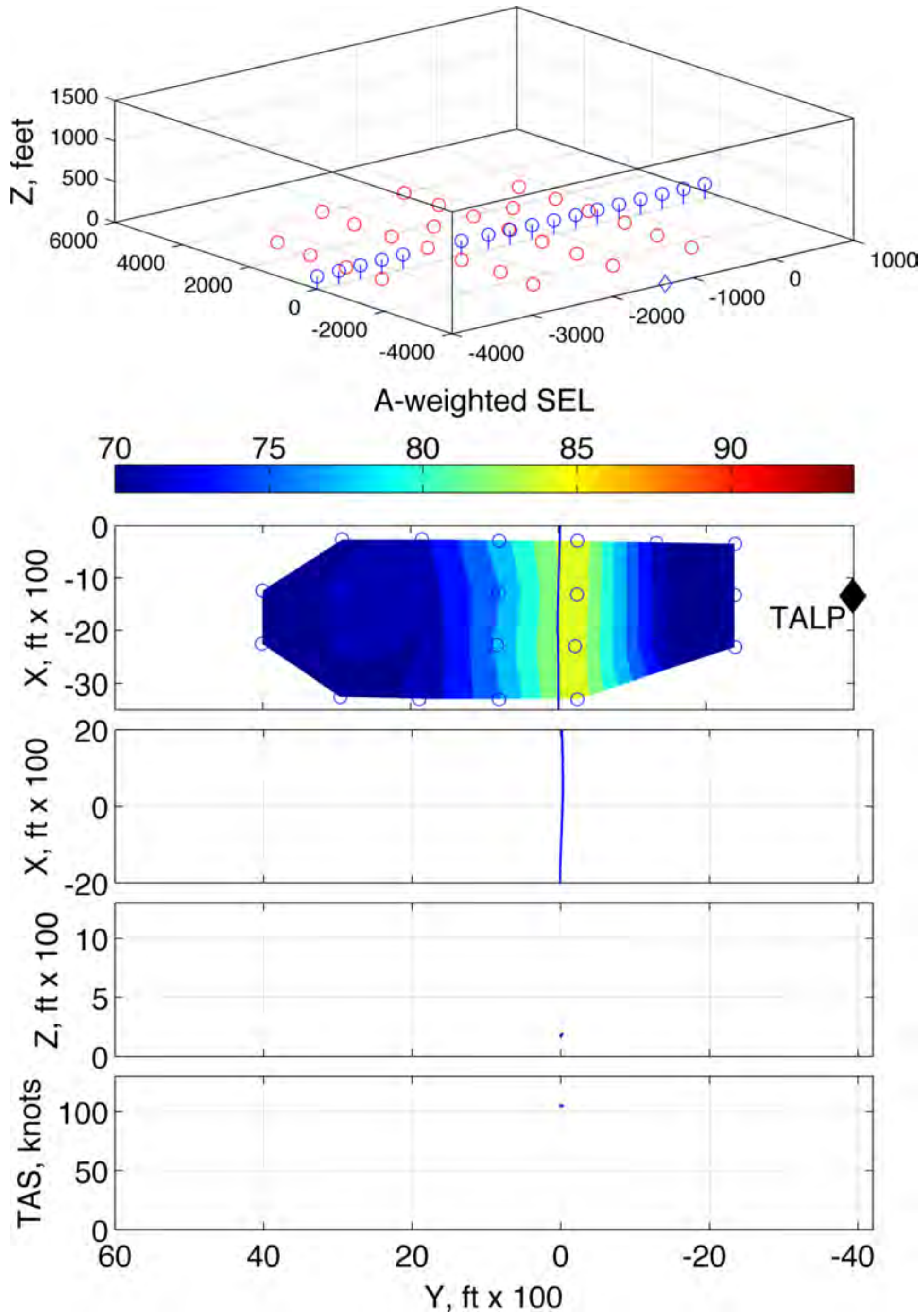

Figure 363: Terminal area condition L6, 100 KIAS, level, run number 288603

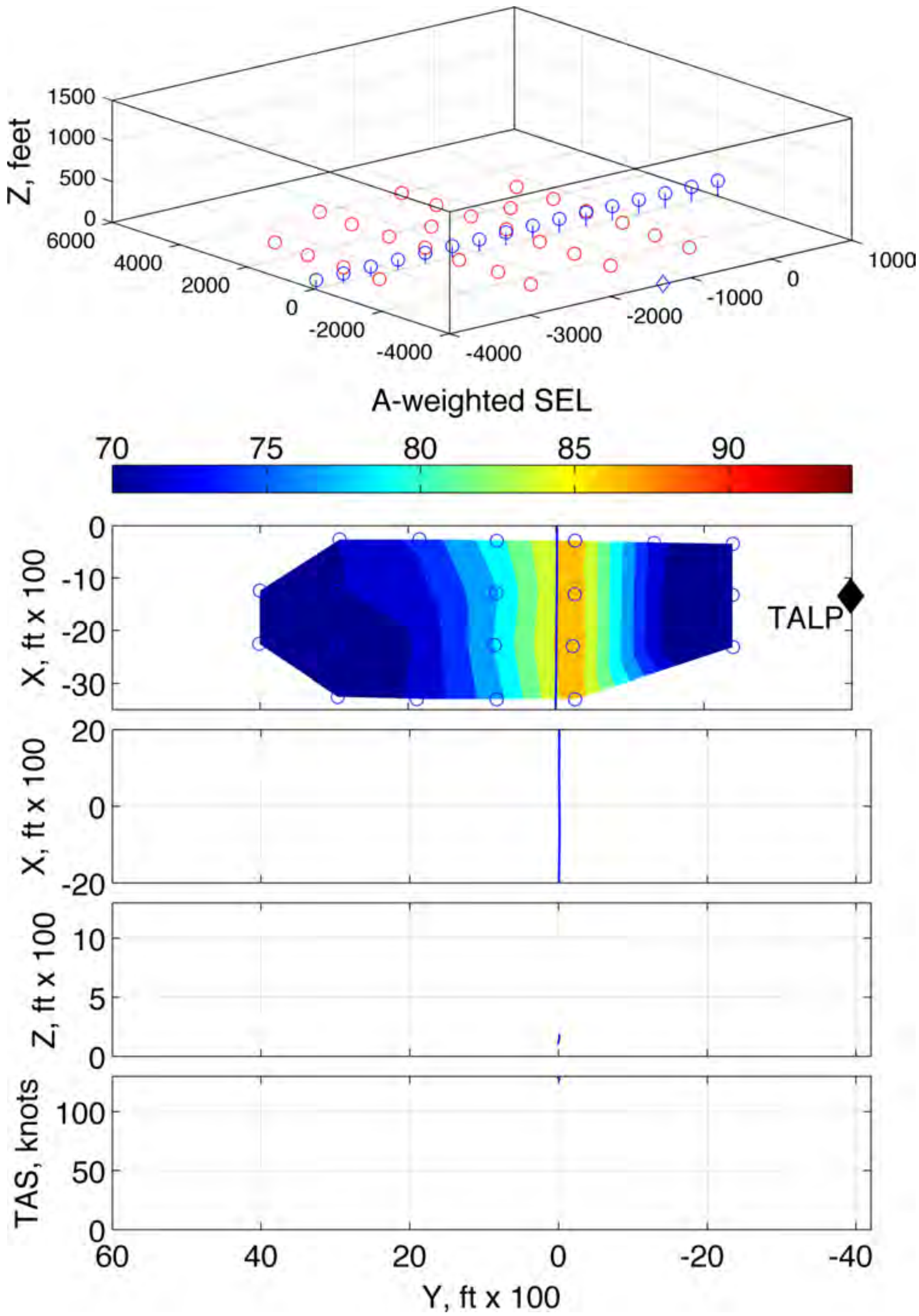

Figure 364: Terminal area condition L8, 120 KIAS, level, run number 288604

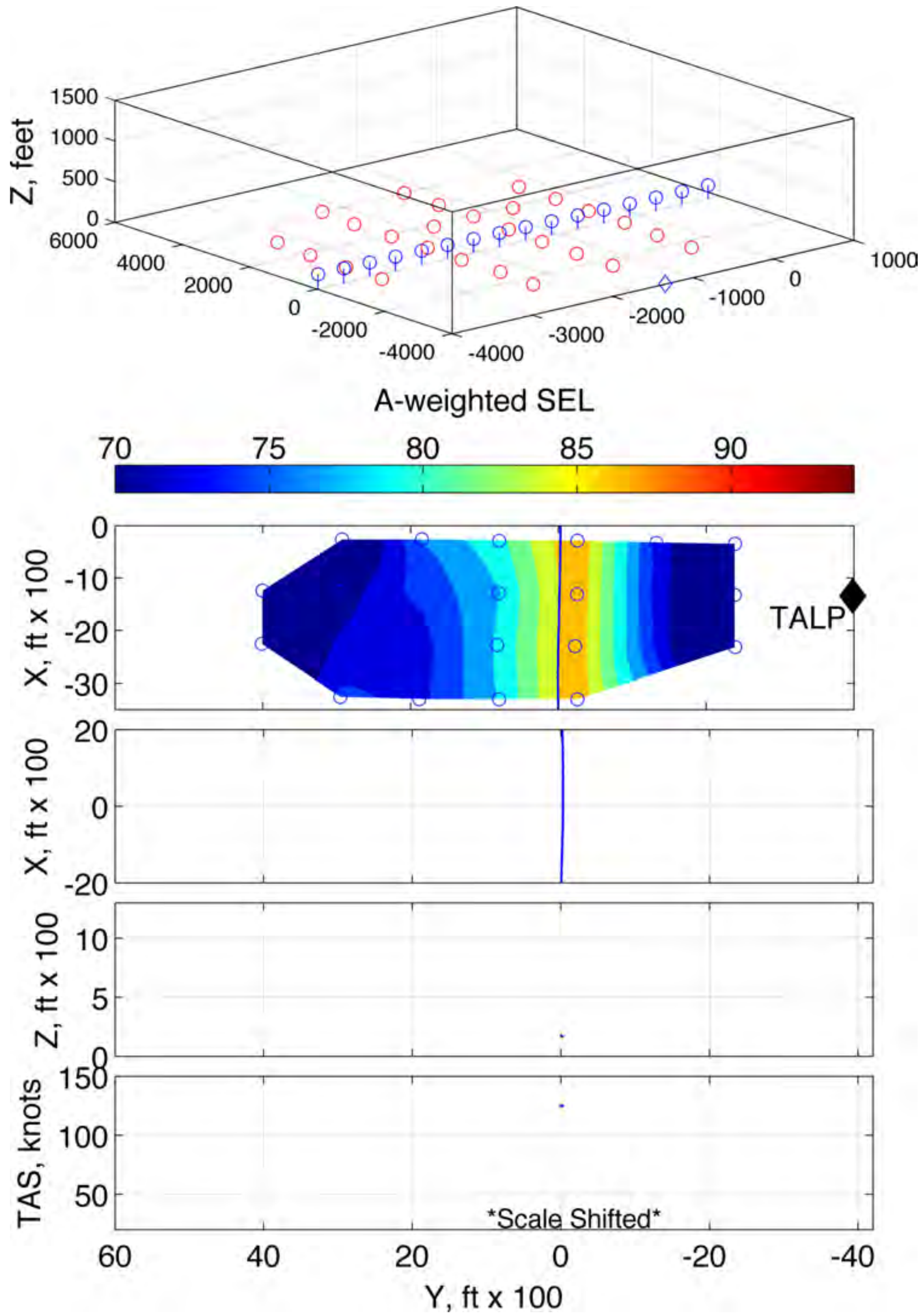

Figure 365: Terminal area condition L8, 120 KIAS, level, run number 288605

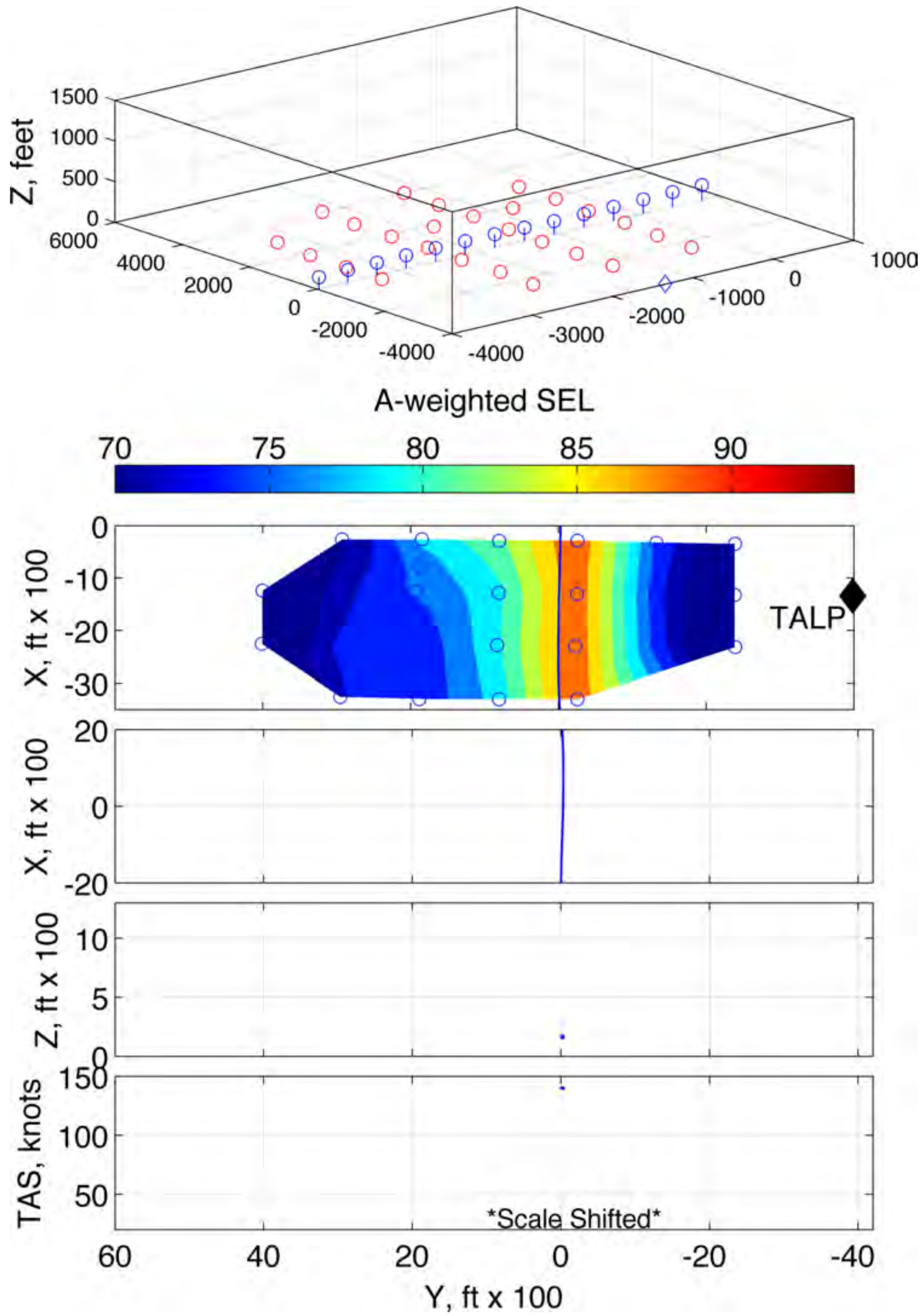

Figure 366: Terminal area condition L10, 140 KIAS, level, run number 288606

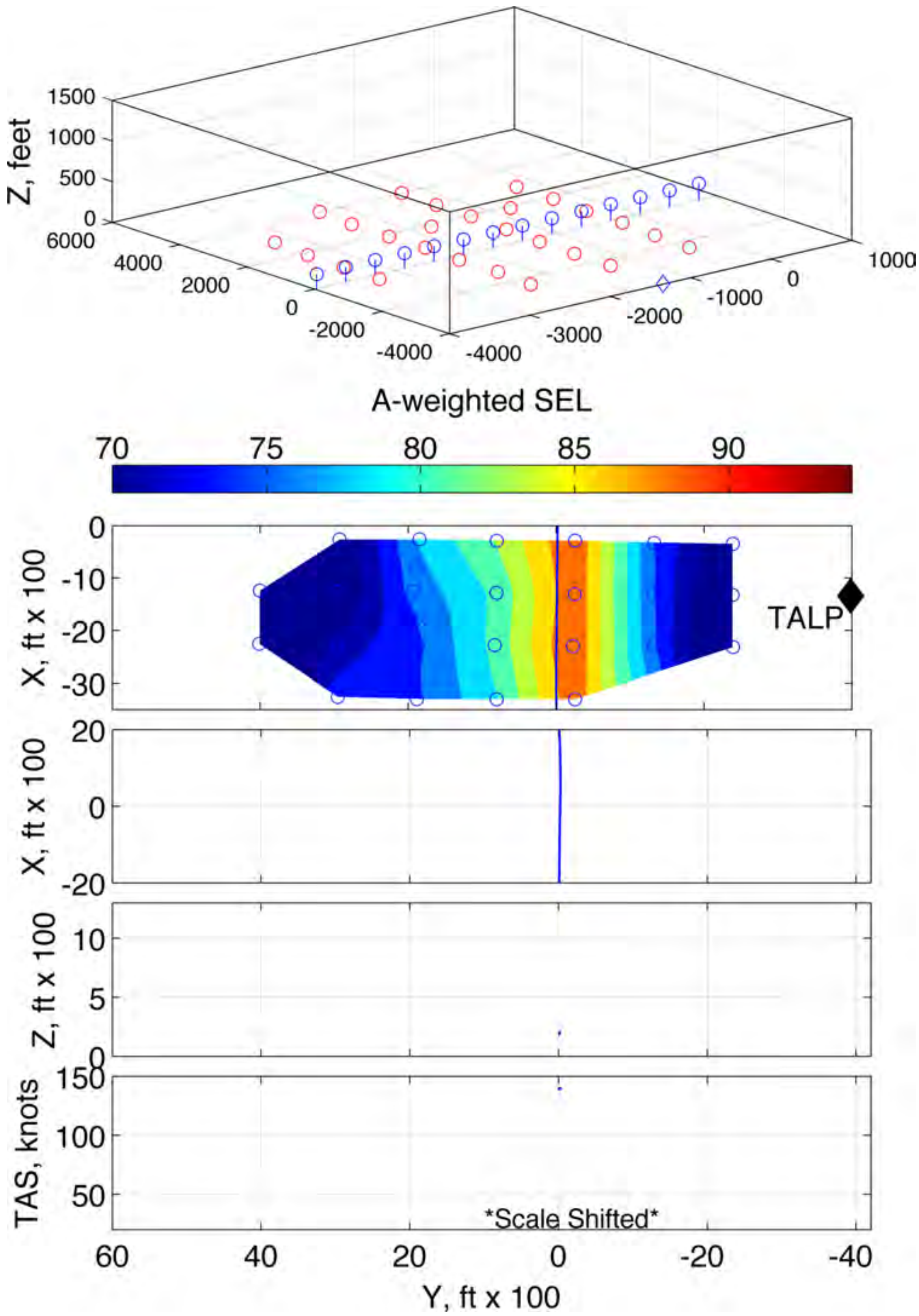

Figure 367: Terminal area condition L10, 140 KIAS, level, run number 288607

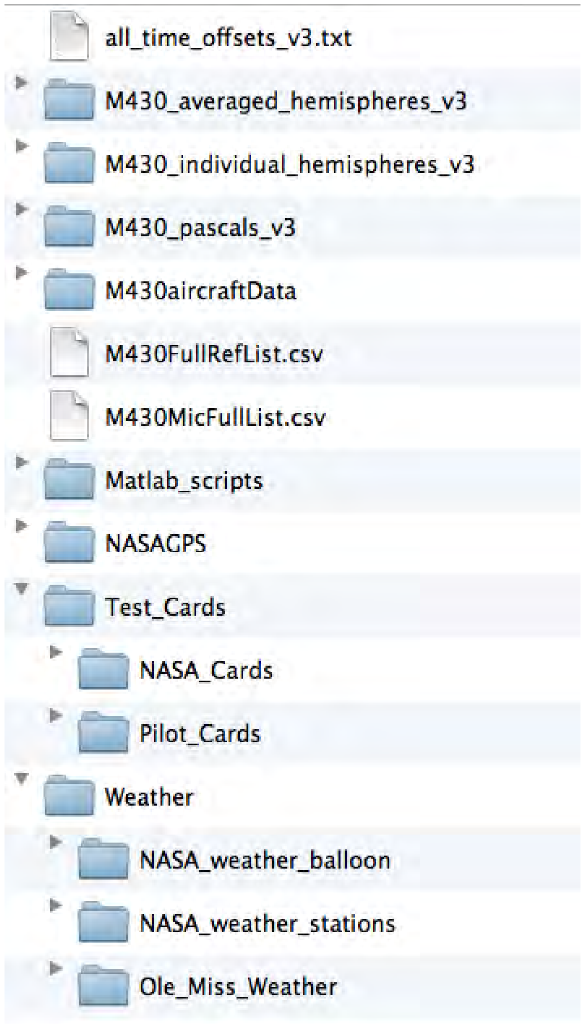

Figure 368: Electronic data file structure.

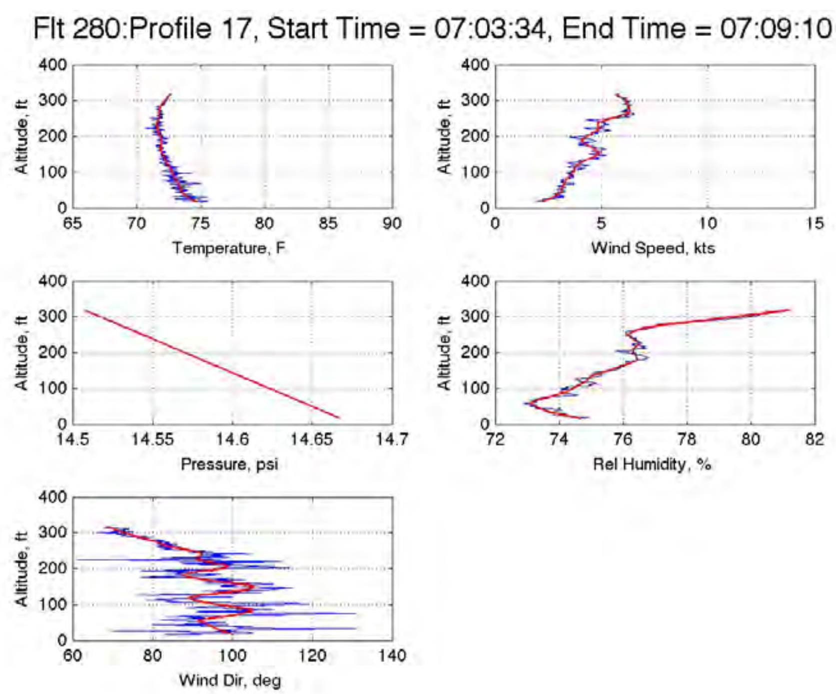

Figure 369: Flight 280, profile number 16.

REPORT DOCUMENTATION PAGE	*Form Approved OMB No. 0704-0188*

1. REPORT DATE *(DD-MM-YYYY)*
01- 05 - 2014

2. REPORT TYPE
Technical Memorandum

3. DATES COVERED *(From - To)*

4. TITLE AND SUBTITLE
Maneuver Acoustic Flight Test of the Bell 430 Helicopter Data Report

5a. CONTRACT NUMBER

5b. GRANT NUMBER

5c. PROGRAM ELEMENT NUMBER

6. AUTHOR(S)
Watts, Michael E.; Greenwood, Eric; Smith, Charles D.; Snider, Royce; Conner, David A.

5d. PROJECT NUMBER

5e. TASK NUMBER

5f. WORK UNIT NUMBER
380046.02.07.03.01.02

7. PERFORMING ORGANIZATION NAME(S) AND ADDRESS(ES)
NASA Langley Research Center
Hampton, VA 23681-2199

8. PERFORMING ORGANIZATION REPORT NUMBER
L-20367

9. SPONSORING/MONITORING AGENCY NAME(S) AND ADDRESS(ES)
National Aeronautics and Space Administration
Washington, DC 20546-0001

10. SPONSOR/MONITOR'S ACRONYM(S)
NASA

11. SPONSOR/MONITOR'S REPORT NUMBER(S)
NASA/TM-2014-218266

12. DISTRIBUTION/AVAILABILITY STATEMENT
Unclassified - Unlimited
Subject Category 71
Availability: NASA CASI (443) 757-5802

13. SUPPLEMENTARY NOTES

14. ABSTRACT
A cooperative flight test by NASA, Bell Helicopter and the U.S. Army to characterize the steady state acoustics and measure the maneuver noise of a Bell Helicopter 430 aircraft was accomplished. The test occurred during June/July 2011 at Eglin Air Force Base, Florida. This test gathered a total of 410 test points over 10 test days and compiled an extensive database of dynamic maneuver measurements. Three microphone arrays with up to 31 microphones in each were used to acquire acoustic data. Aircraft data included Differential Global Positioning System, aircraft state and rotor state information. This paper provides an overview of the test and documents the data acquired.

15. SUBJECT TERMS
Acoustics; Bell helicopter; Data base; Global positioning system; Helicopter; Rotors; Steady state

16. SECURITY CLASSIFICATION OF: a. REPORT	b. ABSTRACT	c. THIS PAGE	17. LIMITATION OF ABSTRACT	18. NUMBER OF PAGES	19a. NAME OF RESPONSIBLE PERSON
					STI Help Desk (email: help@sti.nasa.gov)
					19b. TELEPHONE NUMBER *(Include area code)*
U	U	U	UU	452	(443) 757-5802